iarigai
print and media research
www.iarigai.org

Advances in Printing and Media Technology

Vol. XXXVI

Edited by Nils Enlund and Mladen Lovreček

Darmstadt
MMIX

Advances in Printing and Media Technology

Proceedings of the 36th International Research Conference of iarigai

Stockholm, Sweden
September 2009

Published by the International Association
of Research Organizations for the Information,
Media and Graphic Arts Industries

Darmstadt, Germany 2009

Co-edited by

Nils Enlund, Stockholm, Sweden

Mladen Lovreček, Zagreb, Croatia

The facts published in this book are obtained from sources believed to be reliable. However, publishers can accept no legal liability for the contents of papers, nor for any information contained therein, nor for conclusions drawn by any party from it.

No part of this publication may be reproduced, stored in a retrieval system or transmitted in any form or by any means of eletronic, mechanical, photocopying, recording or otherwise without the prior written premission of the publisher.

ISBN 978-3-9812704-1-0

Printed in Croatia by Sveučilišna tiskara, Zagreb - December 2009

Contents

Introduction

Preface
Research for a sustainable print and media value chain 3
Nils Enlund

Research on media technology and its integration with
media research from other disciplinary perspectives 5
Pirkko Oittinen

1. Toward a sustainable value chain

Challenges in carbon footprint calculation and interpretation - Case Magazine 15
Tiina Pajula, Hanna Pihkola and Minna Nors

Environmental impact of printed and electronic teaching aids,
a screening study focusing on fossil carbon dioxide emissions 23
Maria Enroth

Print media trends in packaging as they pertain to corporate social
responsibility in the bottled water marketplace 31
Natalia Gilewicz and Chris Kular

Green packaging materials - implementation procedures
in the society and the Graphic Arts industry
- An empirical study of sustainability 41
Marios K. Tsigonias and Anastasios E. Politis

Graphic design and environmental sustainability 53
Ivana Bolanča Mirković, Zvjezdana Vukić and Zdenka Bolanča

iPhone 3G typography 61
Blaž Rat

Visualization of large font databases 67
Martin Solli and Reiner Lenz

A product semantic study of the influence of touch
and vision on the evaluation of different paper grades 75
Siv Lindberg and Annika Kihlstedt

Perception and measurement of the whiteness
of papers with different gloss and FWA amount 83
Ludovic Gustafsson Coppel

Perception of printed special effects 91
Janne Laine, Tapio Leppänen and Olli Nurmi

Perception of print quality as a function of level of experience
and as measured by eye movement and psychophysical scaling 99
Siv Lindberg and Annika Lindström

New business forms in e-Business and media - e-Media 107
Ulf Lindqvist, Niels Bjørn-Andersen, Örn S. Kaldalóns, Arne Krokan, Christian Persson, Leif Bloch Rasmussen and Soley Rasmussen

Open innovation process in graphic arts companies 113
Olli Nurmi

RIT Media independent news model for rapid publishing 119
Michael Riordan

Media organisations and local news in a new media environment: super local news - redefinition of news from a local perspective 125
Asta Cepaite and Elisabeth Stúr

Print media in everyday life - interview-based study on media use in Finland 137
Kirsti Arjas-Kauranen and Anu Seisto

2. Color and ink

A new approach to calculate colour values of halftone prints 147
Sasan Gooran, Mahziar Namedanian and Henrik Hedman

Predicting color of overprint solid 155
Robert Chung and Fred Hsu

Colour prediction model on basis of the wavelength dependent area coverage including the scattering of light and optical brightener 161
Michael Dattner, Heinz Mantler, Jorge Rodriguez-Giles and Peter Urban

How to apply Kubelka-Munk Model to media of partial diffuse-light distribution? 171
Li Yang

Chromatic adaptation models evaluation using principal components analysis 179
Dejana Đorđević, Aleš Hladnik, Andrej Javoršek

Assessment of the colorimetric behaviour of different spectrophotometers 185
Vicente de Garcia, Jesús Inarejos, Susana Otero, Esther Perales and Francisco Martínez-Verdú

Rotogravure spot color proofing for decorative laminates using SmartColour iVue software 193
Alexandra Pekarovicova, Veronika Chovancova-Lovell, Sangmeshwar. L. Sangmule, Paul D. Fleming, Yu Ju Wu and Bill Guillot

Electric field assisted ink lifting in gravure 201
Soile Passoja, Jorma Koskinen and Robert Roozeman

Spray inking unit for offset printing machines 207
Gert Schlegel, Arved Hübler, Robert Thieme, Alexander Böddicker, Thomas Hädrich and Günter Wozniak

Investigation of the influence of the composition and rheological characteristics of photopolymerized systems (vehicles) on the rheological behavior of the UV-curing inks for screen printing 217
Tatiana Sretentseva and Julia Timchenko

Ink formulation with the new multi-phase ink model 223
Juha Saari, Roger Bollström, Ken Mueller and Martti Toivakka

Nanopigments in offset printing inks 231
Verónica Marchante, Francisco Martínez-Verdú, Elena Marchante, Juan Antonio Maciá, Elisabeth Chorro, Esther Perales, Vicente de Garcia, Jesus Inarejos, Susana Otero

3. Printing and print quality

Pressroom draw variation and its impact on web breaks
Part II: Commercial pressroom trials 239
Nina Deng, Frédéric Parent, Tony Manfred, Joe Aspler and Jean Hamel

How to utilise improved newsprint - balancing image quality and set-off 247
Marianne Klaman, Per-Åke Johansson and Erik Blohm

Printing by the numbers on commercial paper grades 255
Petter Kolseth, Luc Lanat and Örjan Sävborg

Drying in heatset web offset printing 267
Kaisa Koivumäki and Erkki K. O. Hellén

Rubber blanket surface energy modification using
oxygen plasma treatment 273
Gorazd Golob, Miran Mozetič, Kristina Eleršič, Ita Junkar, Dejana Đorđević and Mladen Lovreček

Ink ribbing in printing nips 279
Tim C. Claypole, Georgios Vlachopoulos and David C. Bould

Dynamic evaluation of lint build-up during newspaper production 287
Miroslav Hoc

Methodology for identification of papers causing
critical lint issues on printing presses 295
Christine Canet, Michel Martineau and Valériane Vigne

Characterization and modelling of the effect of
calendering on coated polyester film 301
Erik Bohlin, Ludovic Coppel, Caisa Andersson, Per Edström

Estimation of rubber ink transfer effectivity in flexography
on the basis of laboratory studies 309
Marie Kaplanova, Jiri Hejduk, Ondrej Panak

Research of interaction on the border polymer film - ink 315
Evgeny Bablyuk and Konstantin Farenbrukh

Penetration of microscopic drops into paper structures 323
Martin Dube, Francois Drolet, Claude Daneault and Patrice Mangin

Printed interference effect colours - process control
and quality assurance 329
Katharina Kehren, Edgar Dörsam and Heike Hupp

Physical and optical dot gain: separation and relation to print resolution 337
Daniel Nyström and Li Yang

The effect of tone measure spatial dispersion on the fine detail
accuracy at the anew image encoding in the process of screening 345
Andrey Schadenkoand Yuri Kuznetsov

Water induced irregularity of halftone dots and its impact on print mottle 353
Göran Ström and Sandra Madstedt

Quality prediction of printed photographs using
computational and instrumental methods 363
Raisa Halonen, Tuomas Leisti and Pirkko Oittinen

4. Digital and special printing

Mechanisms involved in the optical interaction between ink and substrate for Home&Office inkjet printing 373
Nils Pauler, Ole Norberg and Per Edström

Methodology for evaluation of digital production printing 383
Abhay Sharma and Martin Habekost

Fusing of electrophotographic toner on thermally engineered coated paper 391
Philip Gerstner and Patrick A. C. Gane

Printing of inorganic conductive layers 401
Ulrike Herzau-Gerhardt, Frank Hilscher and Henning Nagel

Inkjet printing of electrically conducting carbon nanotubes/conductive polymer composite inks 407
Aurore Denneulin, Anne Blayo, Julien Bras and Charles Neuman

An investigation into the performance of biodegradable plastic electronics by flexography 415
David Bould, Tim Claypole and David Gethin

Electrical resistivity of screen printed conductive lines 421
Maša Žveglič, Valerija Demšar, Raša Urbas, Nina Hauptman, Marijan Maček and *Marta Klanjšek Gunde*

Colour changes of UV-curable thermochromic inks 429
Rahela Kulčar, Mojca Friškovec, Nina Knešaurek, Barbara Sušin and Marta Klanjšek Gunde

Colour changes due to UV-varnishing at the production of the paper-based cards 435
Erzsébet Novotny and Ildikó Endrédy

The print of the double picture and INFRAREDESIGN in the space of the security graphics 445
Ivana Žiljak, Klaudio Pap and Jana Žiljak Vujić

High volume security printing using sheet-fed offset press 449
Slavtcho Bonev

Index of authors **457**



Introduction

Research for a sustainable print and media value chain

Nils Enlund

Co-editor, Chairman of the Program Committee
KTH - Royal Institute of Technology
Media Technology and Graphic Arts
SE-10044 Stockholm, Sweden
E-mail: nilse@kth.se

Preface

Like a huge ocean liner trying to avoid an iceberg, research in the print and media field is slowly but steadily turning its attention toward the challenges of creating and maintaining sustainability in production, distribution and consumption of content and products. During the last three years there has been a dramatic increase in the number of reports on environment-related research presented at the annual iarigai conferences - the main international forum for scientific exchange in the print and media technology field.

This trend is especially visible in the volume that you now hold in your hand. This book contains the scientific and technical research contributions presented at the 36th International Research Conference of iarigai, the International Association of Research Organizations for the Information, Media and Graphic Arts Industries, held in Stockholm, Sweden, on September 13-16, 2009. The contributions for this conference were selected by a scientific committee of prominent international experts through a double-blind review process. At a very early stage in the selection process, it became obvious to the committee, of which I am also the chairman, that sustainability has risen to become a main research concern among scientists and organizations within the field. A large number of reseach papers, not only concerning environmental sustainability but also social and economic sustainability within the print and media value system. The best and most interesting work is presented in one of the main sections of this book.

A qualified presumption is that sustainability research will fill an even larger part of next year's proceedings. The research ship is making an important, strategic turn.

But research into quality and productivity issues still occupy many scientists and will continue to do so. In this book are included sections reporting on current research in color, ink, print quality, printing processes, digital printing, and special printing. I am convinced that you also here will find many results that will be of immediate use in your present activities, whether you are a researcher or a practitioner in our field.

I would especially like to draw your attention to the introductory invited paper by professor Pirkko Oittinen. It contains many insightful thoughts on the challenges of future media technology research. If research is an ocean liner, this paper provides us with a compass and directions for the exciting journey toward the future.

I wish you interesting, useful and stimulating reading in the many pages following!

Research on media technology and its integration with media research from other disciplinary perspectives

Pirkko Oittinen

Department of Media Technology, Helsinki University of Technology
P. O. Box 5500, FIN-02015 TKK, Finland
E-mail: pirkko.oittinen@tkk.fi

Abstract

Media technology is defined as the technologies of the content value chain. The paper has two purposes. First it surveys how media technology is framed in current European level research agendas. These are compared to the scope of the Finnish strategic research agenda for media. Against this background the paper discusses as its second topic forms of research collaboration in general and maps the principles to a research case. The case deals with collaboration on cross-media publishing between three research groups representing journalism and photography, marketing and media technology in a new university context.

Keywords: content value chain, creative content, science systems, multidisciplinary, transdisciplinary

1. Introduction

The speed of communication and the space of storage have increased tremendously while the ease of access of information has improved dramatically at the same time as the cost has gone down. This development has led to a disruptive phase in the media industry with new media forms challenging the conventional media [Jenkins, 2006], [Silverstone, 2003]. The situation raises the level of need and urgency for research - whether to create understanding of the ongoing phenomena, taking advantage of the new opportunities or managing the technological, process and organizational changes. The challenges touch most areas of media operations. At company level they call for activities which cross professional boundaries of technology, product and service development and marketing. An expression of the challenges at the research front is an increase in the type, number and volume of joint initiatives between industrial and research communities.

Media technology is defined here as the technologies of content value chains. Content is understood consistent with [Future Content Networks Group, 2009] as any type and volume of media. The term can also be extended to include not only the essence but also metadata, i.e. any data which describes the essence from some perspective whether it be creation, use, ownership or relation to other essence [NEM Networked & Electronic Media, 2008].

The definition includes content in the sectors of communication media (such as newspapers, broadcast television and magazines in different channels) and cultural media (such as books, music, audiovisual productions, digital games and cultural spaces) [Abadies, 2008]. According to [Abadies, 2008] the value of content in communication originates mainly from accuracy and timeliness. The value of cultural or creative content on the other hand lies in its intrinsic, cultural, aesthetic or entertaining properties. It has been identified in Europe as one of potential growth sectors facilitated by ICT [ISTAG, 2007].

The flow of content in the value chain takes place in many directions and in many time scales which makes linear thinking obsolete. Also feedforward and feedback mechanisms as illustrated in Figure 1 are important. The resources to make the chain functional include hardware, software and humanware components. The roles of the human actors have become more diversified as the producer and consumer roles are being increasingly intertwined. The generic activities in the content value chain are still the same: content creation and accessing, packaging, managing, publishing, delivery, retrieval, use and feedback. These have been combined and presented as content value chains with a varying number of nodes. The number is dependent on the aspects which are in focus in a particular case of study.

Media value chains often contain four nodes (content creation, content packaging, delivery and use). In the creative content context the delivery aspects are of paramount importance due to the many actors (publisher, distributor, retailer) in the delivery chain [Abadies, 2008]. The research case to be discussed later deals with cross-media publishing. In its context content management has high priority and it is raised as a node in a three phase model consistent with [Behrendt, 2003] (cf. Figure 5).

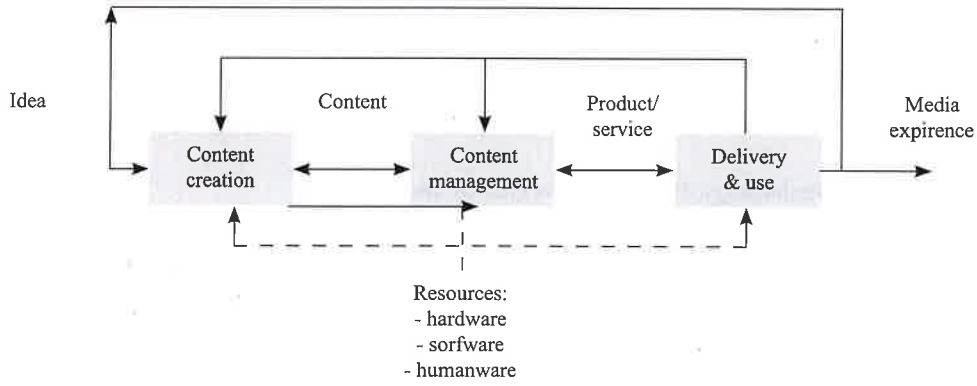

Figure 1: Illustration of a content value chain

The purpose of this paper is first to survey how media technology is framed in current research agendas on the European level and what the topics of interest are. It is evident that the interest on the media sector has grown. The agendas are compared to the scope of the Finnish strategic research agenda for media, called Next Media [Antikainen, 2009]. Against this background the paper discusses as its second topic forms of research collaboration and maps general principles to a research case. The case deals with collaboration on cross-media publishing between three research groups representing journalism and photography, marketing and media technology in a new university context.

2. Research on media technology

The scope of media technology as a discipline is still somewhat fuzzy. According to the definition above it includes both a process oriented holistic view as also specific views of any of the activities, inputs, outputs or resources in the content value chain. As the definition is fairly broad, it means that positioning of media technology in research contexts is not fully straightforward. A four field representation of the ICT sector [Houghton, 1999] consists of the horizontal axis which ranges from conduit (or form) to content (or substance) and the vertical axis which ranges from product to service. In this representation as shown in Figure 2 the media sector is characterized by its focus on value added content products and services. For reference the telecommunications sector draws its business from combining conduits and services. The internet industry becomes positioned in the lower left hand quadrant as a conduit provider and the software industry in between the internet and media industries as a supplier of programware products. Clearly the hardware and software resources which the media sector exploits need to be excluded from the definition of media technology. This means that the definition becomes narrowed to content and the value adding operations.

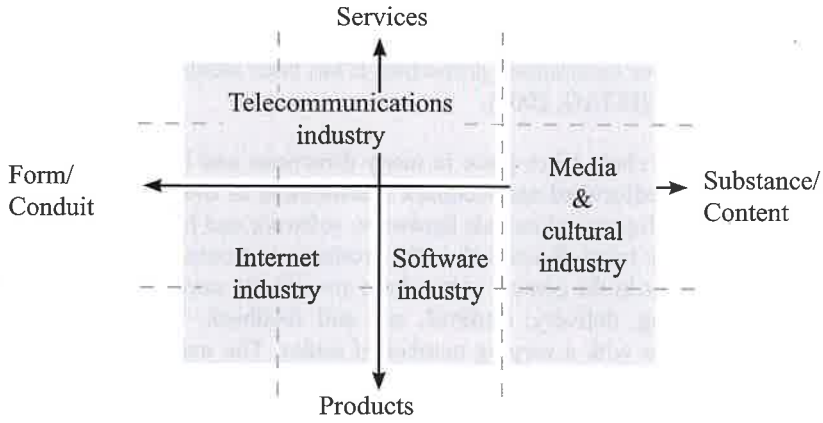

Figure 2: The media sector in the four field map of Houghton [Houghton, 1999]

In proposals for the future internet for instance in EU initiatives the role of mechanisms supporting content centred applications is prominent. This means that mechanisms to handle content related issues will become

more and more embedded in the infrastructure for media. These range [Future Content Networks Group, 2009] from network level mechanisms related to content transportation to content awareness and further to content use mechanisms such as subscription and payment mechanisms. The media operate at the application level of internet hierarchies taking advantage of the functionalities offered at the lower levels. The development of layered internet structures with content related functionalities leads to needs to intensify the collaboration between the internet and media communities. This is already true in European level research initiatives in the media domain which are closely coupled with the future internet.

The most extensive media related EU level initiative is the Networked and Electronic Media technology platform NEM [Networked & Electronic Media, 2008]. It has named content creation, delivery, media presentation, the underlying enabling technologies as also media applications and business models as the most important research topics. Research organization viewpoints collected by the Media Task Force [Rodríguez-Roselló, 2007] and the Future Media and 3D Internet Task Force [Future Media and 3D Internet Task force, 2008] emphasize similar themes. National needs for a strategic research agenda for the media sector are very similar across EU: the opportunities in the content sector have been recognized but the capability to capitalize on them has been found lacking. This is due to the complexity and scale of the ongoing phenomena of media creation and consumption.

Development of the Finnish Next Media SRA [Antikainen, 2009] was started as an extension to an existing SRA [Flexible Services Strategic Research Agenda, 2008] on networked services called Flexible Services. The work was hosted by the strategic centre for science, technology and innovation in the field of ICT (Tivit Ltd). The needs of the media sector, although they interface to those of the telecommunications and internet sectors, were considered to demand a separate SRA. The work progressed with discussions about the mission, vision, breakthrough targets and the scope.

At an initial stage a sketch was made for a research framework. It was refined in workshops and discussions between industrial and research partners. In its final form, as illustrated in Figure 3, the horizontal layers represent research themes and the verticals different media genres. In the first version the horizontal layers were research themes defined from a technological perspective. It became soon clear that a technologically-driven approach was too narrow and needed to be widened. In particular business, organizational, journalistic, creative and social issues were included. As for the verticals the cultural content viewpoint was mapped to "education and learning" and "entertainment and games" and social media viewpoint to "community media".

Co-creation was selected as the defining concept to describe the program. The term seeks to cause associations about the multitude of partnerships which are possible in content creation: professional-non-professional, private-public, local-global etc. Such partnerships are believed to be likely sources of new media genres.

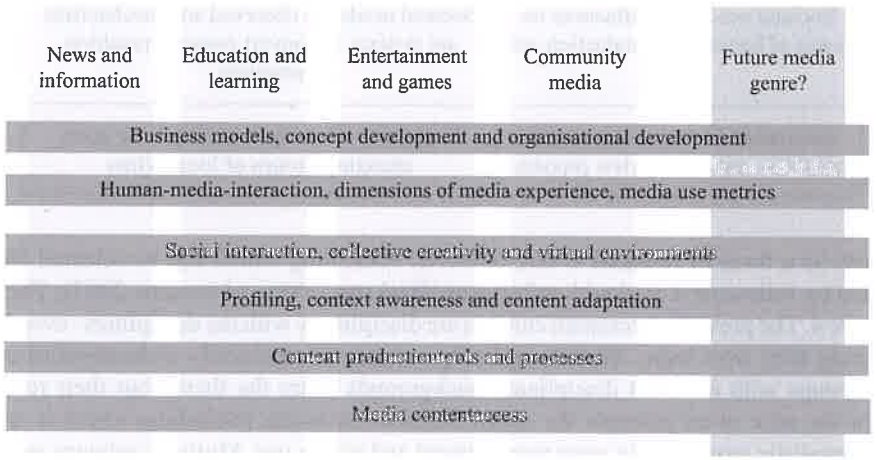

Figure 3: Scope of the Next Media SRA [Antikainen, 2009]

Comparison of Figure 3 with the European counterparts especially the NEM SRA reveals many similarities but also some noteworthy differences. The Next Media SRA is "channel-agnostic". This means that it is not restricted to networked, i.e. digital media. Printed media are included as one type of media serving the same functions as

networked media. The thinking behind the slogan of "co-creation" emphasizes the content aspect beyond content creation as a technological issue. In this sense the Next Media SRA has a slant towards the creative content sector [ISTAG, 2007] [Future Content Networks Group, 2009] which is not visible in the NEM-SRA.

The above means that in addition to the socio-economic dimension of research [Hausheer, 2008], evident in European internet related programs, also journalistic, design and artistic research approaches are included. Each of these has its own research tradition or the notion of research may still be in the infancy. Successful integration of the different disciplines needs to be considered to be a research objective as such. Traditional research partnerships in technologically-led research projects have typically been between engineering, psychology and economics. Social media phenomena have also created collaboration with journalistic studies.

3. Forms of research collaboration

The paradigm of innovation as the basis of competitiveness and economic growth of societies is widely accepted. It has led to examination and systematic development of innovation systems. Research of course is a basic component in the systems. Novel ideas of its organisation and funding have in many countries led to new structures such as academic centres of excellence and strategic centres of between industrial and research partners (such as Tivit Ltd.).

Also activities to restructure universities are ongoing. The principles applied for instance in the Aalto University case in Finland mean a shift from traditional disciplinary organized structures (called Mode 1) to transdisciplinary structures (Mode 2). The differences are elaborated in Table I based on original work by Gibbons et al [Gibbons, 1994].

Table I: Modes of scientific knowledge production [originally translated from Miettinen, 2006]

Mode 1	Mode 2
Research in academic context	Research in the context of application
Disciplinary approach	Transdisciplinary approach
Knowledge production in hierarchical organisations	Knowledge production in changing organisations and non-hierarchical cooperation networks
Societal needs and influences on ways of knowledge production are minor	Societal needs are observed and mechanisms are in place to convert research results to practices
Evaluation of research outcomes is by an academic review process	Evaluation of research quality is by many changing groups of local actors

Transdisciplinarity as a form of research is not, however, something which can be selected [Baker, 2006]. It needs to be earned by following a road with milestones [Wickson, 2006], [Aboelela, 2007]. The milestones are illustrated in Figure 4. The prevailing research cultures are disciplinary with the disciplines - even in collaborative projects - following their own logic. Multidisciplinary research is commonly understood as collaboration in which research groups with different disciplinary backgrounds share the theme but their research questions are different. For the sake of an example the theme could cross-media publishing which is studied from the standpoints of journalistic work, media asset management and media use. Multidisciplinary research is the first milestone.

An interdisciplinary approach takes collaboration one step further. The research groups share their understanding of the problem by defining a common framework and research questions. These are explored using methods characteristic of the disciplines. In cross-media publishing research the problem could be for instance how to meet the requirements for hyperlocality in web and print. The research framework would include all the relevant

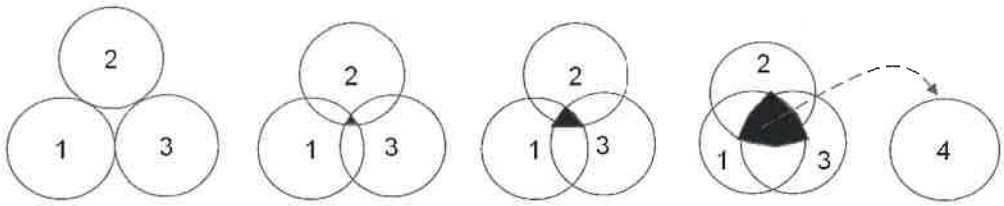

Disciplinary research: separate research themes and problems

Multidisciplinary research: common themes

Interdisciplinary research: common framework for problem solving

Transdisciplinary research: solution of large scale problems and fostering development of new disciplines

Figure 4: Forms of research collaboration. 1, 2, 3 and 4 refer to disciplines

Transdisciplinary research is the last milestone. Although the term is commonly used in a loose sense, transdisciplinary research is perceived as feasible in solving large scale problems with many stakeholders and societal impacts. Solution of the problems requires new methodologies, integration and long-term commitment. Over time the activities may lead to the build-up of new disciplines.

There are no doubt large scale problems in the media domain. The future of journalism, issues of intellectual property rights, the freedom to access information and the reliability of mediated information may be named as such. Some of these are included in the current research agendas. These examples suggest that transdisciplinary research groups are needed.

4. Research case

As part of the ongoing reorganisation of the university sector in Finland, a new university, Aalto University has been established. The university will start its operations officially in 2010. It has been created through a merger between three existing universities: the Helsinki School of Economics (HSE), the University of Art and Design Helsinki (TAIK) and the Helsinki University of Technology (TKK). In the planning stage Aalto University was widely called "the Innovation University". This expressed the expectations, trivialized as "engineers make inventions, artists make designs and business people market". Merging the universities is consistent with the transformations which are on-going in science systems [Hessels, 2008].

Media factory is one of the three spearhead initiatives of the Aalto University. Launched in 2008 the Media Factory brings together media related activities on education and research. When the Media Factory project was started the commission was to develop integrative structures. Doing Cross-Media is a start-up research project funded by the Media Factory. It brings together three research groups with backgrounds in journalism and photography, marketing and media technology. Figure 5 presents the high level framework of the project. The project focuses on the broad field of design, management, analysis and development of new cross-media research concepts. The term "media concepts" is understood in a wide sense, including brands, organizational models, products, new formats, technological innovations, new audiences and their changing media habits. The overall approach in the project is practice-based. In other words it collects its research material from the application context - consistent with the mode 2 model discussed above. The research group shares the experimental data collected by interviews, interventions, so called media concept laboratories [Helle, 2009] and behaviour logging. The research questions are related to the three areas defined in Figure 5.

With reference to Table I the context of the study is the application domain, i.e. media companies. The research can be labelled as multidisciplinary: the research groups share the theme of topic-based publishing in a cross-media context. Currently this is approached from different perspectives with disciplinary oriented research questions. In the start-up phase the shared research framework is that of the Media Concept Laboratory [Helle, 2009]. It can be considered to be a starting point for further development of joint research practices and consolidation of the research towards transdisciplinarity. The already established methodology in the Media Concept Laboratory context is action research which as such has transdisciplinary components [Stokols, 2006].

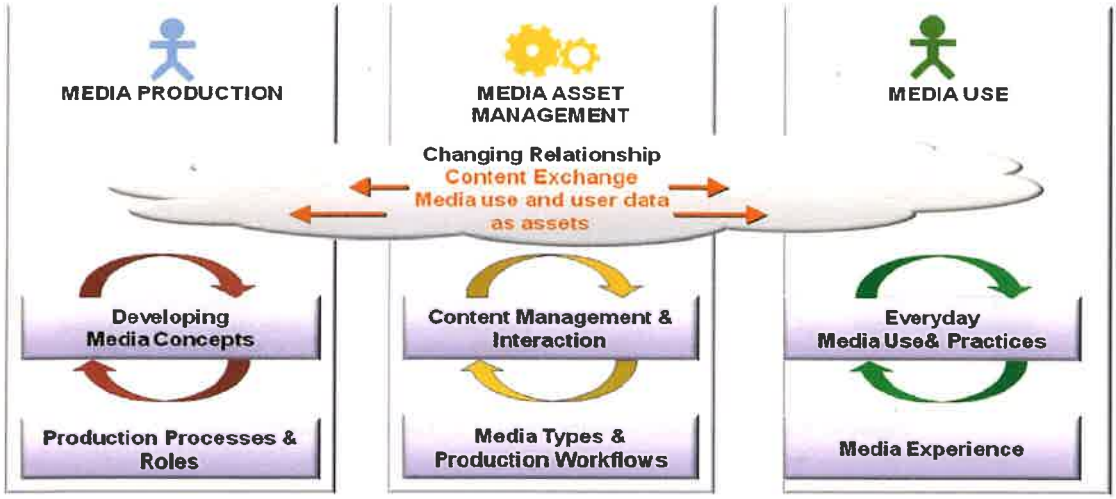

Figure 5: The research framework of the Doing Cross-Media project

In agreement with the features of Mode 2 type of research, the Doing Cross-Media project is run in a non-hierarchical manner. A project manager is the interface to the doctoral and master's students employed in the project. Involvement of media companies in the Media Concept Laboratory sessions guarantees that there is a direct link from research to the application context. Typically the case companies have active own projects in the problem area which is being researched by the academic group. This supports conversion of research outcomes to real-life practices. The last-named also functions as a measure of the success of the research.

5. Conclusions

The development of information and communication technologies has created a pressing need for the media sector to renew itself. New forms of collaboration and new structures of research have been built. These reflect expectations of the benefits of cross-disciplinary research and research collaboration between the academia and industry.

The paper discusses the position of different forms of cross-disciplinary research in media technology related initiatives on European, national and case level. Promising initiatives have been launched. Harvesting the benefits which are achievable clearly requires more competencies than research so far and long-term commitments.

Acknowledgements

The author would like to thank the project group of the Doing Cross-Media project for many fruitful discussions and cooperation, especially Professors Maija Töyry and Johanna Moisander and Project Manager Merja Helle, and Professor Hannu Saarelma for helpful comments on the manuscript.

References

1. Abadies, F., Maghiros, I., Pascu, C. (eds.). (2008). *The Future Evolution of the Creative Content Industries - Three Discussion Papers. European Commission, JRC Institute for Perspective Technological Studies, Scientific and Technical Reports*, 12, 2008. http://ftp.jrc.es/EURdoc/JRC47964.pdf
2. Aboelela, S. W., Larson, E., Bakken, S., et al. (2007). *Defining Interdisciplinary Research: Conclusions from a Critical Review of the Literature. I, Health Services Research,* 42(2007), 329-346
3. Antikainen, H., et al. (2009). *Proposal Next Media Strategic Research Agenda. Espoo: Tivit, May* 20, 2009. http://www.tivit.fi/fi/uudetohjelmat
4. Baker, L. A., (2006). *Perils and pleasures of multidisciplinary research. Urban Ecosystems.* 9(2006)45-47
5. Behrendt, W. et al. (2003). *EP2010 - The future of electronic publishing towards 2010. Salzburg: Salzburg Research,* September 2003. http://ep2010.salzburgresearch.at/dossiers/ep2010_summary-report.pdf

6. Flexible Services Strategic Research Agenda. (2008). *TIVIT, Espoo. May 16, 2008.* http://www.tivit.fi/fi/flexibleservices.
7. Future Content Networks Group. (2009). *Why do we need a Content-Centric Future Internet? Proposals towards Content-Centric Internet Architectures. Prague,* May 2009*: FIA-Future Content Networks Group* http://www.future-internet.eu/fileadmin/documents/prague_documents/FIA-FCN_Internet_Architecture_20090507.pdf.
8. Future Media and 3D Internet Task Force. (2008). *Research on Future Media and 3D Internet. Future Media and 3D Internet Task Force,* October 2008. ftp://ftp.cordis.europa.eu/pub/fp7/ict/docs/netmedia/fm3di-tf-white-paper_en.pdf
9. Hausheer, D., Nikander, P., Fogliati, V., et al. (2008). *Future Internet Socio-Economics - Challenges and perspectives.* 2008. http://www.future-internet.eu/fileadmin/documents/madrid_documents/FISE/FISE_position_paper_final.pdf
10. Gibbons, M. L. (1994). N*ew Production of Knowledge: The Dynamics of Science and Research in Contemporary Societies.* London: Sage Publishers
11. Helle, M., Töyry, M., (2009). *Media concepts as a tool for analysing changing media. Printed Media - Principles, Processes and Quality (Editors Pirkko Oittinen and Hannu Saarelma). Helsinki: Paperi-insinöörien yhdistys/Paperi ja Puu Oy*
12. Hessels, L. K., van Lente, H., (2008). *Re-thinking new knowledge production: A literature review and research agenda. Research Policy,* 37(2008), 740-760
13. Houghton, J. W., (1999). Mapping information industries and markets. Telecommunications Policy. 23(1999)10-11, 689-699
14. ISTAG. (2007). *New Business Sectors in Information and Communication Technologies. The content sector as a case study. 2007.* http://cordis.europa.eu/documents/documentlibrary/96255781EN6.pdf
15. Jenkins, H., (2006). *Convergence culture. Where old and new media collide. New York: NYU 2006*
16. Miettinen, R. T., (2006). *Tieteestä tuotteeksi? (From Science to Product?). Helsinki:* Yliopistopaino 2006
17. NEM Networked & Electronic Media. (2008). *Strategic Research Agenda "Networked and electronic Media" European Technology Platform. nem-initiative, September 2008.* http://www.nem-initiative.org/Documents/NEM-SRA-060.pdf
18. Rodríguez-Roselló, L., Ballesteros, I. L., (2007). *Networked Media of the Future. Brussels: DG Information Society and Media European Commission, October 2007.* ftp://ftp.cordis.europa.eu/pub/fp7/ict/docs/netmedia/networked-media-of-the-future_en.pdf
19. Silverstone, R., (2003). *The European Life and Technology in Everyday Life Network. London: London School of Economics and Political Science,* 2003
20. Stokols, D., (2006). *Toward a Science of Transdisciplinary Action Research. Am J Community Psychol ,* 38 (2006), 63-77
21. Wickson, F., Carew, A. L., Russel, A. W. (2006). Transdisciplinary research: characteristics, quandaries and quality. Futures, 38(2006), 1046-1059





1

Toward a sustainable value chain

Challenges in carbon footprint calculation and interpretation - Case Magazine

Tiina Pajula, Hanna Pihkola, Minna Nors

Technical Research Centre of Finland
P. O. Box 1000, FIN-02044 VTT, Finland
E-mails: tiina.pajula@vtt.fi, hanna.pihkola@vtt.fi, minna.nors@vtt.fi

Abstract

Carbon footprint has become a key element in evaluating the emissions of greenhouse gases related to manufacturing of print products. The study defines carbon footprint of a Finnish weekly magazine and discusses the significance of the results and ways to diminish greenhouse gas emissions occurred during the product's life cycle. Energy needed in the pulp, paper and printing processes creates the main part of the emissions. Furthermore, transporting the product to customer becomes a remarkable contributor. However, current methodology involves open questions and e.g. landfill data estimations bring in great variation. The calculations provide a baseline against which the development can be measured and communicated. Lots of emphasis should be given on the communication of the results and the carbon footprint should be expressed as a range of values rather than as a single figure.

Keywords: carbon footprint, life-cycle assessment (LCA), printing technology, environmental impact

1. Introduction

Due to concern over climate change and global warming, reducing greenhouse gas (GHG) emissions has become important topic in the sustainability discussion. The need for calculating GHG emissions has led to the development of the carbon footprint concept. Carbon footprint means the amount of greenhouse gases produced during a products' life cycle. It can be calculated for products, processes, companies, or persons. In each of these the scope and system boundaries of the calculation are different.

The concept of carbon footprint has been rapidly implemented in the business communication. During last two years several companies have announced their carbon footprint results. However, not many studies concerning print products and the end use phase of the product's life cycle are available. A study of Moberg et al. [2007] discusses the GHG emissions and the global warming potential of a Swedish newspaper, web based newspaper and electronic paper based on screening LCA. Carbon Trust [2006] presents the carbon footprint of a British newspaper.

There are issues specific for different product groups that cannot be easily dealt with in general level guidelines or standards that aim to cover all product categories. The interpretations of different calculations are demanding since a common calculation method has been lacking. With the help of a case study, the challenges related to carbon footprint for fibre based print products covering the whole life-cycle from cradle to grave are discussed.

The results are a part of a Finnish research project Lean Development with Renewable Resources [LEADER, 2007 - 2010]. It has been coordinated by KCL and is conducted in cooperation with the Finnish Environment Institute, Metropolia University of Applied Sciences, FinnMedia, several printing companies, suppliers, logistics and paper manufacturer's Stora Enso, UPM-Kymmene, Myllykoski and Metsäliitto. The project has been funded by StoraEnso, UPM-Kymmene, Myllykoski, Metsäliitto, Graphic industry research foundation and Finnish funding agency for Technology and Innovations.

In the study, results of a carbon footprint case study for a Finnish weekly magazine are presented. The main sources of GHG emissions are pointed out in the life cycle of a magazine, and possibilities for reducing the carbon footprint are evaluated. The carbon footprint of a magazine is utilized as an example, but many of the issues discussed are relevant for print products in general. In addition critical issues of carbon footprint calculation and usability of the results are discussed. Specific features of fibre based print products are highlighted (e.g. the ability of products to store biogenic carbon).

The aim is to analyze the usability of carbon footprint concept as a sustainability indicator for print products.

footprint calculation, communication and areas for further study. Including the whole life cycle creates new knowledge about the importance of the end use phase of the products. In addition, it provides a holistic view of the overall climate change impacts occurred during the value chain of products.

2. Methods

During last two years a few carbon footprint guidelines have been announced. Confederation of the European Paper Industries (CEPI) published a framework in 2007 concerning life cycle stages which to include in a carbon footprint calculation for paper products. British Standards Institute (BSI) published a PAS2050 on Specification for the assessment of the life cycle greenhouse gas emissions of goods and services. The International Standardization Organization ISO has started the development of a carbon footprint standard, which aims to be ready in 2011.

In the study, the carbon footprint of a magazine was calculated based on life cycle inventory (LCI) and according to the LCA principles of ISO 14040-44 standards. The life cycle of the magazine was covered from cradle to grave, i.e. from wood harvesting until the end use and disposal or recycling of the magazine. In the carbon footprint, GHG emissions (carbon dioxide CO_2, methane CH_4, and nitrous oxide N_20) from fossil sources are expressed as carbon dioxide equivalents (CO_2 eq.) according to the factors of Intergovernmental Panel on Climate Change [Forster et al., 2007]. It was assumed that the product is disposed within one year after production. Due to assumed short life span of the product, the bio based carbon stored in the product was not included in the carbon footprint. This approach is in accordance with the PAS 2050. However, some magazines are stored for years or even decades. To provide additional information, the carbon content of the product was calculated. Based on the furnish of the LWC paper it was assumed that 30 w-% (percentage by weight) of a magazine is carbon.

KCL-ECO software was applied for the calculations. The reliability of the LCI results is dependent on the data quality which can be considered high. Data was collected directly from corresponding industry and suppliers. For supplementary data KCL EcoData data base was used. This is a continuously updated leading data base covering pulp and paper industry related data from harvesting, chemicals production, energy production, transports and pulp, paper and converting processes.

2.1 Carbon footprint case definition

The scope of the study was a weekly magazine printed on 150 gsm coated fine paper (cover) and on 80 gsm LWC paper (inner sheets) by heatset offset printing process. 83% of the product was recycled, 16% was land filled and 1% was incinerated. In comparative scenarios 100% of the product was either landfilled or incinerated. The assumptions made are presented in more detail in Table I.

The product is assumed to be delivered to customers (households). This is a typical situation in Finland since magazines are commonly subscribed. In general, the case represents a typical situation that could take place in Finland. This also means that the fuel breakdown in energy production represents the Finnish situation which is presented in Table II.

Since it is a well known fact that energy production plays a key role in carbon footprint composition a sensitivity analysis was carried out applying Swedish electricity production profile in pulp and paper making. The Swedish profile consists of 50% nuclear power, 40% hydro power, 4% biomass and 3% of fossil fuels [OECD 2004].

Another area of importance is the emissions associated with landfilling. Current estimations for methane production and release of landfilled paper bring in large variation. In this study, data from different sources are applied to understand the influence this end-of-life stage can have to the results. The data comes from studies by IPCC and Danish University of Technology.

Currently available estimates of decomposition of carbon in wood products in landfills range from 0 - 3% up to 35% and to 56% of the total carbon in the wood products [Micales and Skog 1997, Mann and Spath 2001, Bingemar and Gratzen 1987]. In the case study, the IPCC recommendations [IPCC 2000] were considered to

provide the baseline for calculating the emissions from paper degradation in landfills. Landfill data module A was formed (according to the recommendations of the IPCC) to provide the baseline for the magazine case study. Comparative calculations were conducted using default values based on the model constructed for LCA on waste management by the Danish University of Technology [Kirkeby et al. 2007; Manfredi & Christensen 2009]. Comparative landfill module C was formed accordingly.

Table I: Case study assumptions

Print product	Weekly magazine
Life cycle stages included	Wood harvesting (incl. thinnings and final felling), manufacturing and transports of paper and paper raw materials (chemicals etc.), production of purchased energy, printing and manufacturing of main printing raw materials, distribution, end use (recycling, incineration and landfill) and all related transports.
Life cycle stages not included	Editorial work for the magazine, production of 98% pure aluminum for printing plate manufacturing, manufacturing of raw materials needed for printing ink manufacturing.
Printing	Heatset web offset (HSWO) 4- colour printed in Finland
Paper	Cover 150 gsm coated fine paper from Finland Inner sheets 80 gsm LWC paper from Finland
Distribution	All magazines distributed to households
End of life phase	Recycling 83% Landfill 16% Incineration 1%
End of life phase Comparative scenarios	Landfill 100% or Incineration 100%

Table II: Finnish average energy production profile [source: OECD 2004]

Fuel	Electricity production	Heat production
Coal	27.5 %	19.8%
Oil	0.7%	7.9%
Natural gas	14.9%	30.3%
Biomass	11.9%	18.9%
Waste	0.6%	1.6%
Nuclear	26.5%	0.0%
Hydro	17.6%	0.0%
Peat	0.4%	17.4%
Others	-	4.0%

Compared to module A, in module C, a lower value for the methane generation potential of paper is used. Additionally, both the share of recovered methane and the oxidation factor for methane released through the top layer of a landfill are higher in module C than in the module A. Module A can be considered giving maximum level of GHG emissions and Module C giving the minimum level of GHG emissions from paper disposed to landfill.

3. Results

Based on the case study, the carbon footprint for one ton of magazines varies between 1140-1350 kg CO_2 eq depending on the estimations related to landfilling. The biggest contributor to the footprint is the energy consumed in pulp and paper production (43 - 51%). This includes the production of all the paper needed for

one ton of magazines containing the maculature of approximately 270 kg. Although this maculature is recycled the corresponding load is a part of the footprint. Printing stage causes 14 - 17% of the greenhouse gases. This consists of the electricity and fuels (propane) demanded at the heatset printing facilities. Also transport plays significant role in this case due to the home delivery of the magazine (15 - 17%). Transport emissions coming from the home delivery of magazines is remarkable, 88% of all greenhouse gases originating from transport, even though the magazine is delivered to reader's home together with other mail. Other transport emissions include transportation of wood, chips, chemicals, paper and waste. The influence of landfilling varies between negligible and 15%. The distribution of the greenhouse gas sources are presented in Figure 1.

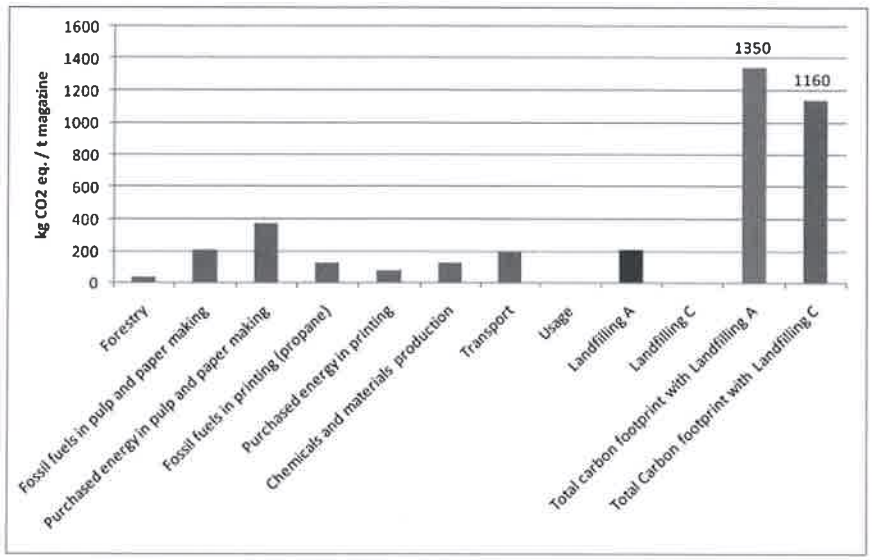

Figure 1: Greenhouse gases (as carbon dioxide equivalents) emitted during the life cycle of ton of magazines

When substituting the average Finnish electricity production profile in pulp and paper making for average Swedish profile the carbon footprint reduces by 23% and the contribution of pulp and paper manufacturing reduces from 43% to 16%. The remaining 16% comes mainly from the fuels used at the mill.

The influence of the end of life options was studied using two additional scenarios. In these extreme scenarios the magazine is either 100% incinerated or 100% landfilled. The electricity produced in the incineration is replacing the average Finnish electricity consumed in pulp and paper production. As a result the carbon footprint reduces by 27% when the magazine is incinerated (990 kg CO_2 eq). When landfilling the carbon footprint nearly doubles (2440 kg CO_2 eq.). In this case the IPCC estimate with high greenhouse gas emissions for landfilling is applied (landfill Module A). The recovered paper leaving the system decreases from 1100 kg to 270 kg (maculature from printing) in both cases.

When calculating the carbon footprint from cradle to the gate of the printing house, i.e. until the product is finished but not yet delivered to customer, the value is 974 kg CO_2 eq. When changing the boundaries of life-cycle stages to consist also the distribution of magazines to home, i.e calculating the carbon footprint from cradle to customer, the value is 1130 kg CO_2 eq.

Carbon content of the product is 1080 kg as CO_2/ ton of magazines. The share of wood fibres in a magazine (62%) is calculated based on the LWC and fine paper furnishes. The carbon content of wood is assumed to be 50%. The carbon is converted to CO_2 according to molecular masses. The carbon footprint values in different case set ups are presented in Table III together with the carbon content of the product.

4. Discussion

The case results presented in this paper point out that carbon footprint results are very sensitive for the chosen system boundaries and assumptions. One of the most important issues is the definition of the system boundaries

Table III: The carbon footprint results for ton of magazines with different assumptions

Assumptions		kg CO_2 eq/ ton of magazine
BASE CASE: 83% recycled, 16% landfilled, 1% incinerated	Landfill A	1350
	Landfill C	1140
	Swedish electricity in pulp and paper production (Landfill A)	1040
	Cradle to gate (printing house)	974
	Cradle to customer	1130
100% of Magazines incinerated		990
100% of Magazines landfilled (Landfill A)		2440
Bio based carbon stored in the product		1080

i.e. which stages of the product's life cycle are included in the carbon footprint. Especially the emissions occurring from the end use phase are difficult to evaluate but might contribute significantly to the total carbon footprint of the product. The carbon footprint for one ton of magazines varies between 1140 - 1350 kg CO_2 eq depending on the estimations related to landfilling. The difference between these two values is significant. Due to uncertainty related to emissions from the end use phase, it is recommended that the carbon footprint is expressed as a range of values rather than as a single figure, when the whole life cycle of a product is considered. Furthermore, the producer or publisher has a very limited potential to influence the final way of using the product. As a consequence, the cradle-to-gate or cradle-to-customer carbon footprint value is more reliable since it is based on data from the actual life cycle steps that have taken place. These system boundaries are widely used in business to business communication. However, in consumer communication, enough information about the possible impacts of the end use of the product should be available. Greenhouse gas emissions from the end-use of products are clearly an area that requires further study.

The biggest contribution to the carbon footprint comes from energy production and use of fossil fuels. Thus the energy production profile utilized for the production of purchased energy that is consumed in the paper mill and in the printing house has a great impact on the results. These indirect emissions from purchased energy cannot always be controlled by companies giving them unequal position to reduce their carbon footprint. For example, a paper mill in Sweden with a possibility to purchase renewable "green" electricity gets advantage to a German mill with only coal power at hand. In the worst case the carbon footprint can be even 10 times bigger in one country compared to another. Improving energy efficiency and investing in electricity saving equipment becomes important in these cases.

Another important factor is the choice of fuels that are utilized in the paper mill. As a consequence, improving energy efficiency and reducing the use of purchased electricity and heat is the most efficient way to reduce the carbon footprint. Moving over to renewable energy sources is another way of reducing carbon footprint. Additionally, improving material efficiency in the production process would have positive impacts to the carbon footprint. For example, if more web breaks occur or the amount of maculature during printing increases the carbon footprint increases directly.

Incinerating magazines and exploiting the corresponding energy reduces carbon footprint while landfilling increases it. The amount of this increase is dependent on the estimations used for landfill emissions and varies between nearly negligible to remarkable. However, one must keep in mind that the opportunity to recycle the recovered paper is wasted in these two cases. The magazines made of primary fibres contain excellent quality fibres from recycling point of view. Still it is clear that incineration is superior option to landfilling when fossil fuels can be substituted.

An interesting aspect related to carbon footprint of fibre based print products is that they are made from renewable raw material and the carbon sequestered in the forests remains stored in the products until they are

will be calculated, if the product exists for one year or more. The carbon storage impact shall be included as a negative value in the assessment of GHG emissions arising from the life cycle of the product. The maximum benefit is gained if the carbon is stored in the product for 100 years or more.

The aim of guidelines is to insure reliability and comparability of studies. Life cycle approach involves many aspects of choice, like data source, allocation methods, system boundaries etc. which affect the results. Even if detailed instructions are provided and followed, a possibility of different appliance remains. Transparency is important and enables experts to assess the uniformity of different studies. However, at least for the time being, before internationally accepted methods for the quantification and communication of carbon footprints are widely in use, general comparisons between different studies should be avoided.

5. Conclusions

Carbon footprint calculations provide useful information on the GHG emissions occurred during a products life cycle. The information can be used to find out hot spots in which most reduction potential exists and thus provide also economic benefits for the companies. The calculations provide a baseline against which the development can be measured and communicated. Reliable carbon footprint information can guide both producers and consumers towards less polluting actions and have a positive impact on the environment. However, many open questions remain and a lot of emphasis should be given on the communication of the results.

On many occasions, the system boundaries utilized in the calculations are not clearly stated and thus the evaluation of the results is difficult. If the calculations are not performed in identical ways the results cannot be compared. Among the most important system boundaries are whether the calculation included the end use and disposal of the product (cradle to grave) or whether the life cycle was followed until the manufacturer's gate or to customer's home. When paper products are considered, the calculation methods utilized when evaluating the environmental impact of recycling and use of recovered fibres can have a remarkable impact on the results and should be mentioned.

While carbon footprint can be a useful tool in evaluating and reducing the impact on global warming and climate change, it ignores all other environmental impacts. On some occasions the impacts (such as acidification or eutrophication) can be more severe that the ones reflected by the carbon footprint. As a consequence, the sustainability of a product should not be evaluated based on solely greenhouse gas emissions and carbon footprint, but other aspects should be considered. Therefore, further research to cover also other environmental aspects is important.

Acknowledgements

The authors would like to thank the companies that are participating in the research project and the Finnish Environment Institute for cooperation related to landfill emissions, as well as StoraEnso, UPM-Kymmene, Metsäliitto, Myllykoski, TEKES and the Graphic industry research foundation (GTTS) in Finland for financial support.

References

1. Bingemer, H. G., Crutzen, P. J., 1987. The production of methane from solid wastes. Journal of Geophysical Research 92, 2181-2187
2. British Standards Institute 2008, PAS 2050 - Specification for the assessment of the life cycle greenhouse gas emissions of goods and services
3. Carbon Trust 2006, Carbon footprints in the supply chain: the next step for business. Available at: www.carbontrust.co.uk
4. Confederation of the European Paper Industries 2007, Framework for the development of Carbon Footprints for paper and board products

5. Forster, P. V., Ramaswamy, P., Artaxo, T. Berntsen, R. Betts, D. W. Fahey, J. Haywood, J. Lean, D. C. Lowe, G. Myhre, J. Nganga, R. Prinn, G. Raga, M. Schulz and R. Van Dorland (2007): Changes in Atmospheric Constituents and in Radiative Forcing. In: Climate Change 2007: The Physical Science Basis. Contribution of Working Group I to the Fourth Assessment Report of the Intergovernmental Panel on Climate Change [Solomon, S., D. Qin, M. Manning, Z. Chen, M. Marquis, K.B. Averyt, M.Tignor and H.L. Miller (eds.)]. Cambridge University Press, Cambridge, United Kingdom and New York, NY, USA)
6. IPCC 2000. Intergovernmental Panel on Climate Change. Good Practice Guidance and Uncertainty Management in National Greenhouse Gas Inventories. Chapter 5: Waste
7. ISO (International Organization for Standardization). ISO 14040: Environmental management -- Life cycle assessment -- Principles and framework. Switzerland, Geneva: ISO, 2006
8. ISO (International Organization for Standardization). ISO 14044: Environmental management -- Life cycle assessment -- Requirements and guidelines. Switzerland, Geneva: ISO, 2006
9. ISO standardization organization on-going work of SC7 GHG WG2 Carbon Footprint for products
10. Kirkeby, J. T., Birgisdóttir, H., Bhander, G. S., Hauschild, M. Z. & Christensen, T. H. 2007: Modeling of environmental impacts of solid waste landfilling within the lifecycle analysis program EASEWASTE. Waste Management 27 (7), 961-970
11. Manfredi, S. & Christensen, T. H. 2009. Environmental assessment of solid waste landfilling technologies by means of LCA-modeling. Waste Management 29 (1), 32- 43
12. Mann, M. K., Spath, P. L., 2001. A life cycle assessment of biomass co-firing in a coal-fired power plant. Clean Products and Processes 3, 81-91
13. Micales, J. A., Skog, K.E., 1997. The decomposition of forest products in landfill. International Biodeterioration and Biodegradation 39 (2-3), 145-159
14. Moberg, Å.; Johansson, M.; Finnveden, G.; Jonsson, A. 2007. Screening environmental life cycle of printed web based and tablet e-paper newspaper. Reports from the KTH Center for Sustainable Communication, Stockholm. Royal Insitute of Technology. TRITA-SUS Report 2007:1. ISSN 1654-479X. Available at: http://www.csc.kth.se/sustain/publications/
15. Nors, M., Behm, K., Dahlbo, H., Pajula, T., Pihkola, H., Viluksela, P., Wessman, H., Carbon footprint of print products, KCL Carbon Footprint Publication, 23 April 2009

Environmental impact of printed and electronic teaching aids, a screening study focusing on fossil carbon dioxide emissions

Maria Enroth

MSG Management System Group AB
Vivstavarvsvägen 237, SE-122 64 Enskede, Sweden
E-mail: maria.enroth@msgab.se

Abstract

This study was initiated in order to clarify the environmental impact of different kinds of teaching aids easily available today. The aim of the study is to give a screening comparison of the environmental impact when it comes to the global warming potential of printed versus electronic teaching aids. A life cycle perspective is used in the study which means that the different specific life cycle steps of the media products are analysed. In the study, the environmental impact is limited to the impact category global warming. The study focuses on the emissions of fossil carbon dioxide which is the only climate gas included in the analysis.

The study shows that the impact on global warming of a web based electronic teaching aid is approximately 10 times higher than the environmental impact of a printed textbook, if a low energy computer equipment scenario is used. If a high energy computer equipment scenario is used, the impact is nearly 30 times higher for the web based electronic teaching aid compared with the impact of the printed textbook. A reason for this is that a textbook can be used for a long time by many users.

Keywords: environmental impact, printed textbooks, electronic teaching aids, media products

1. Introduction

This study was initiated in order to clarify the environmental impact of different kinds of teaching aids easily available today. The original study was financed by NHO Grafisk in Norway.

The aim of the study is to give a screening comparison of the environmental impact when it comes to the global warming potential of printed versus electronic teaching aids. For the electronic teaching aids, the study is focusing on electronic solutions that are available in practice today for teaching compulsory-school pupils, i.e. solutions using computer equipment for the use phase.

The number of published studies comparing the environmental impact of printed and electronic media products is quite low. Some of the more recent studies are focusing on media products with relatively short life time such as newspapers [Moberg et al 2007] and invoices [Moberg et al 2008] or automatically generated documents, e.g. monthly bank account statements [Schmidt and Kløverpris 2009]. This study compares the environmental impact of a media/information product with a long life time and many users.

2. Methods

A life cycle perspective is used in the study which means that the different specific life cycle steps of the media products are analysed. In Figure 1 and Figure 2 the life cycle steps of the respective media product are illustrated together with the system boundaries of the study. For the printed textbook the following steps are included; pulp and paper production, transportation of paper, prepress, printing, distribution of the books, use during studies and waste management of the books. For the web based electronic teaching aid the steps included are formatting the teaching material, use of internet infrastructure, production of computer equipment for users, distribution of computer equipment, use of electronics during studies and waste management of electronics. Editorial work is not included in the study, however, this work is assumed to be comparable for the two types of products. Details about the life cycle steps and the assumptions made are described in Table I and Table II.

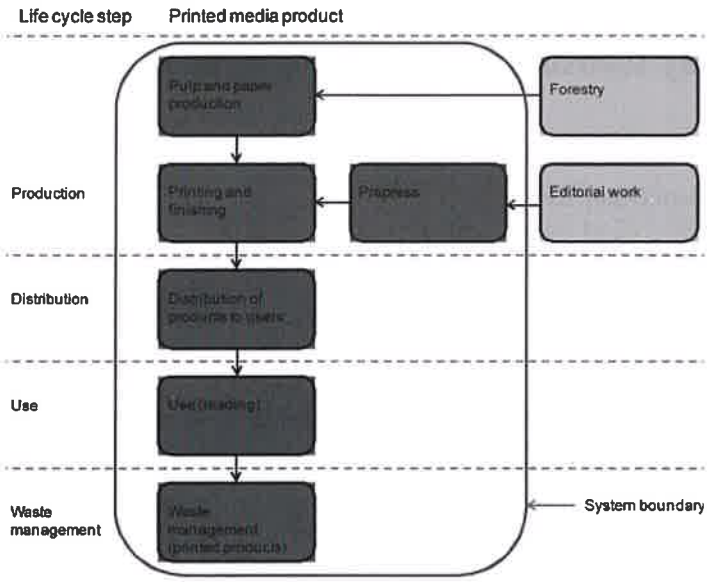

Figure 1: The life cycle steps of printed products and the system boundary for the studied printed textbook

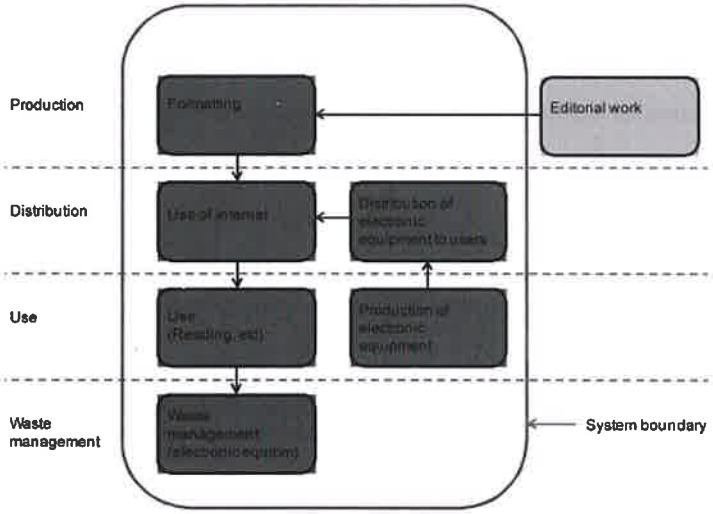

Figure 2: The life cycle steps of electronic media products and the system boundary for the studied electronic teaching aid

In the study, the environmental impact is limited to the impact category global warming. The study then focuses on the emissions of fossil carbon dioxide which is the only climate gas included in the analysis. This means that mainly the use of energy and transportation in the different product life cycles are taken into consideration in the study. For some processes, data on fossil carbon dioxide equivalents is used for the calculations due to availability of data.

The functional unit of the study is "Use of teaching aid during five years for 5,000 pupils per year (i.e. 25.000 pupil years). Each year the pupils use the teaching aid 2 hours per week for 40 weeks. The pupils reside in six different cities in Norway".

The studied printed product weighs 0.8 kg/book which corresponds a total weight of 4.8 tonnes of paper including 17% paper waste at the production. The total weight of the final product thus is 4.0 tonnes. A life time of 5 years is assumed for the textbooks. For the electronic teaching aid, the share of the total impact from the needed computer equipment for users is calculated to be 3.7%, based on a life time of 5 years and a total use of approximately 10.900 active hours during this life time. For both types of media products, low as well as high energy scenarios were studied. For the printed product this means that two different levels of energy use for the

printing process were studied. For the electronic product the low energy scenario included laptops for the users and the high energy scenario included desktops and LCD screens for the users.

Table I: Details about the life cycle steps of the studied printed text book and assumptions made

Process	Description
Pulp and paper production	Direct emissions of fossil carbon dioxide from the production of pulp and paper and indirect emissions as a consequence of bought electricity (Swedish average). Data for a specific paper produced in Sweden was used [Grycksbo Paper, 2008].
Transportation of paper	Emissions of fossil carbon dioxide from the transportation by truck of paper from the paper mill to an assumed printing company in Oslo. Emission data for a truck with draw bar trailer, long distance, was taken from Baumann and Tillman [2004]. The distance was estimated to 400 km.
Printing and finishing	Energy Two different scenarios for energy use at the printing company were used. In both cases the data include all type of energy used at the printing companies, i.e. not only electricity but also energy used for heating, etc. The low energy scenario with a use of 610 kWh/tonne product represents fairly large offset printing companies [Enroth 2006]. The high energy scenario with a use of 1590 kWh/tonne product represents rather small offset printing companies [Enroth et al., 2003]. For the calculation of emissions of fossil carbon dioxide, Nordel[1] was assumed for the printing process. Printing plate Data for use of plate in offset printing is found in Larsen [2004] where the figure 4.16 m^2/tonne printed product is reported as an average. With an assumed thickness of 0.3 mm, this results in a value of 3.37 kg/tonne offset product. Based on figures given by EAA [2008] for emissions of CO_2-equivalents from European production of primary aluminium, sheets and recycled aluminium, the emissions when producing the printing plate were estimated. Since 100% of the printing plates are recycled the calculation is based on 95% recycled and 5% primary aluminum in order to compensate for the EAA reported average loss of aluminum when recycling. Printing ink The use of ink for offset printing is reported in Larsen [2004] as 5.8 kg/tonne printed product. Data on fossil CO_2 emissions from the production of printing ink was calculated to 1180 kg/tonne printing ink, based on inventory data for mineral oil based black ink in Strömberg [1998].
Distribution of the books	The emissions arising from the distribution by truck of the books from the assumed printing company in Oslo to schools in six different cities in Norway (Oslo, Kristiansand, Stavanger, Bergen, Trondheim and Tromsø) were estimated. Emission data for a truck with draw bar trailer, long distance, was taken from Baumann and Tillman [2004]. The transport work was calculated to 1600 tonne*km.
Use	No emissions from the use of text books.
Waste management	For the waste management of paper 80% fiber recovery and 20% incineration with energy recovery were assumed based on the situation for newsprint in Sweden [Moberg et al., 2007]. This however does not fully represent the situation for fine paper. The impact of handling waste paper was estimated based on an emission of 0.06 kg CO_2-equivalents/kg paper calculated from data given in Moberg et al., [2007].

3. Results

The study describes the significant life cycle steps of each product type; see the illustrations in Figure 3 and Figure 4. The results show that the pulp and paper production as well as the printing process contribute significantly to the total impact on global warming of printed textbooks. In addition, it is indicated that the waste management step contributes in a considerable manner. The advantages of material recovery of fibres are not obvious when studying impact on global warming since energy requiring processes and lots of transportation are often used. For the web based electronic teaching aid, the production of computer equipment for the users and the use phase contribute in a significant way to the total impact on global warming of this type of product.

A relatively small contribution to global warming is seen from transportation activities for both types of products in the study.

The results of the calculations in the study are summarised in Table III for the printed textbook scenarios and in Table IV for the web based electronic teaching aid scenarios.

Table II: Details about the life cycle steps of the studied electronic teaching aid and assumptions made

Process	Description
Formatting	The time for formatting the editorial material for the electronic web based teaching aid was approximated to 50 hours. This only represents the assumed extra time compared with the printed textbook when a print original is produced based on the editorial material. A desktop computer and a screen were assumed for this process. The use of energy for the process was calculated based on the effect of 78 W for a desktop and 31 W for a LCD-screen during active use [Jönbrink and Zackrisson 2007]. For the calculation of emissions of fossil carbon dioxide, Nordel was assumed for the formatting process. The use of internet infrastructure for uploading the material is not taken into account in this process.
Use of internet	The energy need for the use of internet infrastructure is based on the estimated size of the downloaded material, in this case 1500 MB, and approximations of the energy required for using the internet backbone. The internet backbone was described by Taylor and Koomey [2008] as servers, data storage, hubs, routers, LAN[2] switches and WAN[3] switches. Data for the energy intensity of using the internet backbone, 3 Wh/MB, is given in Moberg et al., [2008], p 34, for the use of fixed networks and transport networks. This figure was extrapolated in order to approximately describe the situation 2007. In addition, the use of access technologies such as modem and DSLAM[4] is accounted for. In this case the use of energy was calculated based on the effect of 9 W for modem and 5 W for DSLAM. It is assumed that only ten different schools are downloading the teaching aid material from internet once a year during the period of five years which is studied.
Distribution of electronic equipment	The emissions arising from the distribution of the electronic equipment to the users in schools in the six different cities in Norway from the production in China were estimated. 3.7% of the environmental impact from the transportation was allocated to the functional unit of the study. Emission data for large ships >8,000 dwtonne and trucks with draw bar trailer, long distance, were taken from Baumann and Tillman [2004]. Data on weights of the computer equipment were found in Jönbrink and Zackrisson [2007].
Use	For the functional unit, the time for using the teaching aids was estimated to 2,000,000 hours (2 hours x 40 weeks x 5 years x 5,000 pupils). Two different scenarios for use of the electronic teaching aid were studied. The use of energy was calculated based on the effect during active use; 32 W for a laptop, 78 W for a desktop and 31 W for a LCD-screen [Jönbrink and Zackrisson 2007]. For the calculation of emissions of fossil carbon dioxide, Nordel was assumed for the use phase.
Production of computer	3.7% of the environmental impact from the production of electronic equipment was allocated to the functional unit of the study. For production of a laptop the emission of 81 kg CO_2-equivalents was used for the calculation, for production of a desktop the emission of 138 kg CO_2-equivalents was used based on data in Jönbrink and Zackrisson [2007].
Production of screen	3.7% of the environmental impact from the production of electronic equipment was allocated to the functional unit of the study. For production of a LCD-screen the emission of 55 kg CO_2-equivalents was used based on data in Jönbrink and Zackrisson [2007].
Waste management of electronics	For the waste management of electronics, 95% material and energy recovery and 5% landfill were assumed based on information in Jönbrink and Zackrisson [2007]. The impact of waste handling of electronics was estimated based on the following reported data; -1 kg CO_2-equivalents for a desktop or a laptop and 4 kg CO_2-equivalents for a LCD-screen.

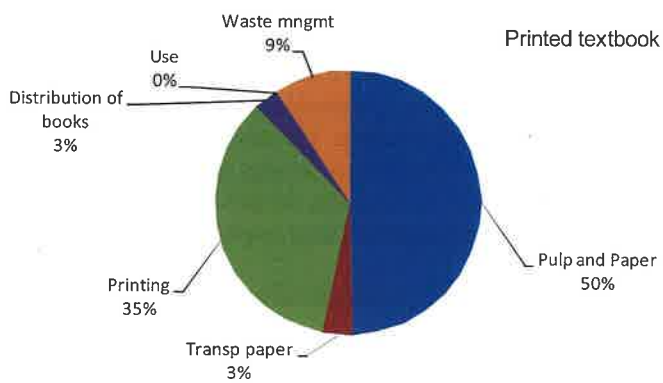

Figure 3: The contribution from the different life cycle steps of the studied printed textbook (high energy printing scenario) when it comes to fossil carbon dioxide emissions

[2] LAN, Local Area Network.
[3] WAN, Wide Area Network.
[4] DSLAM, Digital Subscriber Line Access Multiplexer. For consumers, there is one DSLAM per subscriber. In the case of business, internet connection is less energy demanding per computer [Moberg et al., 2008]. Here, one DSLAM per school is assumed.

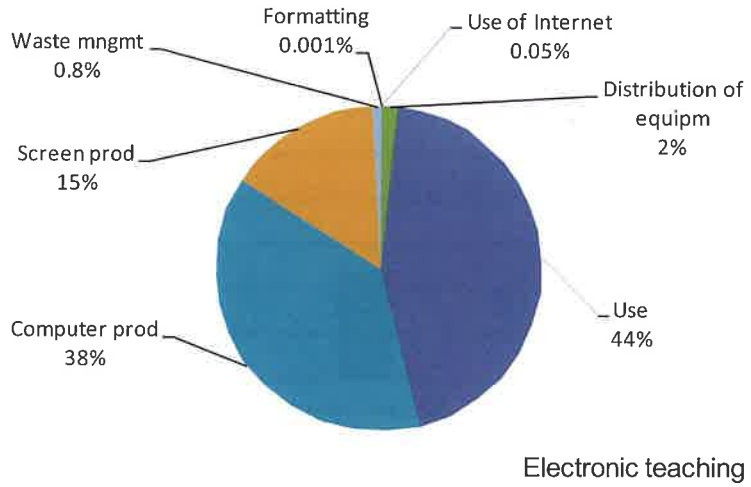

Figure 4: The contribution from the different life cycle steps of the studied web based electronic teaching aid (high energy scenario with desktops & screens) when it comes to fossil carbon dioxide emissions

Table III: Emissions of fossil carbon dioxide (in kg) from the studied printed textbook scenarios. The contributions from the different processes as well as the total amount are shown

	Pulp and Paper, Direct emissions	Pulp and Paper, Bought electricity	Transp, Paper	Printing, Energy	Printing, Plate	Printing, Ink	Distrib, Books	Use	Waste mngmt	Total
Printed textbook (low energy printing)	1170	129	91	334	13	27	77	0	240	2080
Printed textbook (high energy printing)	1170	129	91	871	13	27	77	0	240	2620

Table IV: Emissions of fossil carbon dioxide (in kg) from the studied web based electronic teaching aid scenarios. The contributions from the different processes as well as the total amount are shown

	Formatting	Use of internet, Backbone	Use of internet, Access Techn	Distrib, Equipm	Use	Computer prod	Screen prod	Waste mngmt	Total
Web based electronic teaching aid (laptops)	0.75	31	0.38	169	8770	14980	0	-185	23800
Web based electronic teaching aid (desktops & screens)	0.75	31	0.38	1070	29870	25530	10180	555	67200

The study shows that, with the given prerequisites, the impact on global warming of a web based electronic teaching aid is approximately 10 times higher than the environmental impact of a printed textbook, if a low energy computer equipment scenario (with lap tops) is used. If a high energy computer equipment scenario is used (with desktops and LCD screens), the impact is nearly 30 times higher for the web based electronic teaching aid compared with the impact of the printed textbook.

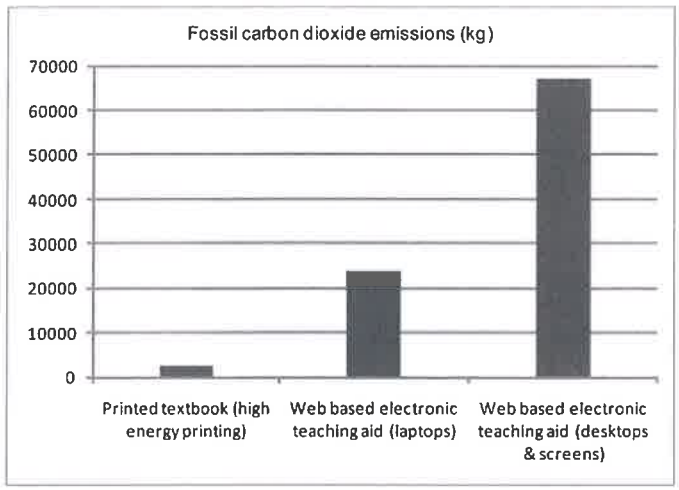

Figure 5: Total fossil carbon dioxide emissions (in kg) for the main alternatives of teaching aids studied

4. Discussion

In comparing studies like this it is always important to take the function of the products, in this case different types of teaching aids, into consideration. With different character of the products it can be difficult to find comparable functions. This study does not illustrate how the different teaching aids influence the study results of the pupils. It can be claimed that printed and electronic teaching aids have different strengths and therefore somewhat different use and target groups.

The study shows possible improvements within the different products systems. For the printed product it is important to choose environmentally adapted papers and to optimise the use of energy in the printing process. For the electronic information product, the study shows that the production of electronics and the use phase are comparatively energy intense. To develop and choose energy efficient equipment are therefore of great importance. In this case, so called e-book reader devices which need substantially lower energy during use, will therefore be of great interest in the future. Very promising results for e-book reader devices are for example described by Kozak [2003] and Moberg et al [2007]. Notable for all energy intense activities is that the mix of energy sources when producing electricity has a great influence on the global warming potential.

A limitation of the study is that it focuses on only one impact category, global warming. The reason for this is the large general interest in this environmental task and a possibility to delimit the screening study. Besides, global warming has earlier shown to be a significant aspect of media products and energy intense products. However, other environmental impacts have to be analysed as well, where toxicity is especially important to mention.

The biogenic carbon dioxide is defined as zero in this study, which means that no specific attention has been made to carbon sequestration in forests or carbon stored in forest products. With a life cycle perspective of products, these aspects are assumed to be of limited importance for this study.

The environmental effects of the use of internet infrastructure are not yet very much studied and data are scarce. There is a need for more studies in this field, especially since the development of techniques is intense. In this study energy intensity data from Moberg et al [2008] is used. These data can be compared with data given by Taylor and Koomey [2008] which is higher and data given by Schmidt and Kløverpris [2009] which is somewhat lower. There are still large uncertainties about the energy use of internet infrastructure and other networks as well as how to allocate the energy use between different services such as data, television and voice calling. Nevertheless, it is interesting to start estimating the environmental effects of information and communication technologies (ICT).

In this study, the use of internet is not so large since it is assumed that only ten different schools are downloading the teaching aid material from internet once a year during the period of five years which is studied. The picture

5. Conclusions

The study shows that the impact on global warming of a web based electronic teaching aid is approximately 10 times higher than the environmental impact of a printed textbook, if a low energy computer equipment scenario is used. If a high energy computer equipment scenario is used, the impact is nearly 30 times higher for the web based electronic teaching aid compared with the impact of the printed textbook.

A reason for this is that a textbook is used for a long time by many users. This makes this type of printed product relatively energy effective and therefore it has a fairly low impact on global warming.

Acknowledgements

The author would like to thank NHO Grafisk in Norway for an inspiring co-operation in the original study which comprises the basic part of this paper.

References

1. Baumann, H., Tillman, A.-M., (2004), The Hitch Hiker´s Guide to LCA, An orientation in life cycle assessment methodology and application. Studentlitteratur, Lund
2. Econ Pöyry AB, (2008), The Telephone directory - an evaluation of public benefit and environmental impact, Telefonkatalogen - en värdering av samhällsnytta och miljöpåverkan (in Swedish), Rapport R-2008-047
3. Enroth, M., (2006), Paper VI: Environmental data on gravure and offset printing. Published in Developing tools for sustainability management in the graphic arts industry, Doctoral Thesis, KTH Stockholm
4. Enroth, M., Moberg, Å., Johansson, M., (2003), Environmental indicators for newspaper industry - development of an industry specific data base, Miljönyckeltal för tidningsföretag - utveckling av en branschgemensam databas, STFI Report PUB 15
5. European Aluminium Association (EAA), (2008), Environmental Profile Report for the European Aluminium Industry, Life Cycle Inventory data for aluminium production and transformation processes in Europe
6. Grycksbo Paper, (2008), Paper Profile G-Print Smooth, Data 2007
7. Jönbrink, A. K., Zackrisson, (2007), M. Lot 3, Personal Computers (desktops and laptops) and Computer Monitors, EuP Preparatory study, TREN/D1/40-2005
8. Kozak, G., (2003), Printed Scholary Books and E-book Reading Devices: A Comparative Life Cycle Assessment of Two Book Options, Centre for Sustainable Systems, Report No. CSS03-04, University of Michigan
9. Larsen, H. F., (2004), Assessment of chemical emissions in life cycle impact assessment - focus on low substance data availability and ecotoxicity effect indicators, Chapter 2, p 67, Doctoral Thesis, Technical University of Denmark
10. Moberg, Å., Johansson, M., Finnveden, G., Jonsson, A., (2007), Screening environmental life cycle assessment of printed, web based and tablet e-paper newspaper. KTH Centre for Sustainable Communications, TRITA-SUS 2007:1
11. Moberg, Å., Borggren, C., Finnveden, G., Tyskeng, S., (2008), Effects of a total change from paper invoicing to electronic invoicing in Sweden, A screening life cycle assessment focusing on greenhouse gas emissions and cumulative energy demand, KTH Centre for Sustainable Communications, TRITA-SUS 2008:3
12. Schmidt, A., Kløverpris, N. H., (2009), Environmental impacts from digital solutions as an alternative to conventional paper-based solutions, FORCE Technology
13. Strömberg, A., (1998), Comparing life cycle analysis - vegetable oil and mineral oil based black newspaper inks (in Swedish). The Swedish paint and printing ink makers association, SVEFF
14. Taylor, C., Koomey, J., (2008), Estimating Energy Use and Greenhouse Gas Emissions of Internet Advertising, Working Paper. Available at www.imc2.com/csr/ClearSkyMediaTool.aspx (Oct 2008)

Print media trends in packaging as they pertain to corporate social responsibility in the bottled water marketplace

Natalia Gilewicz and Chris Kular

Ryerson University
350 Victoria St. Toronto, ON M5B 2K3, Canada
E-mails: ngilewic@ryerson.ca, ckular@ryerson.ca

Abstract

In an effort to respond to consumer demands for more sustainable products, the packaging industry is constantly updating what constitutes a sustainable package. One of the fastest growing segments of consumer packaging is the bottled water industry. This area of packaging is under heavy scrutiny from the public in North America - especially in areas where water is safe to drink from the tap. Part of the problem is that consumers do not have enough information to make sustainable choices. This research investigated the package from a consumer perspective. A sample of bottles was subjected to a visual inspection and content analysis of environmental information on the package and the corresponding company website. Environmental claims were gathered and categorized using a typology developed by Carlson [1993]. The results revealed physical characteristics that are identifiable to consumers (such as package weight or size of label). Further, it was found that very few packages carried any sustainable messages on the bottle but where they did, claims were supported with further information on the website. Lastly, the bottles that contained data on the package did not have the physical characteristics of a sustainable package. Thus, not only does the water bottle industry need to provide consumers with more information, package characteristics need to better showcase sustainability. This in turn will help consumers make educated and sustainable choices.

Keywords: bottled water, packaging, sustainability

1. CSR, environmental sustainability and the consumer

In an increasingly competitive corporate environment, Corporate Social Responsibility (CSR) initiatives and practices have been acknowledged as having strategic importance to the firm [Perry, 2008]. CSR allows companies to show concern for not only immediate consumers but also society as a whole. CSR is a broad concept, which is concerned with transparent business practices entrenched in good ethics, legal requirements, and respect for people, communities and the environment. Companies who consider CSR in their strategic goals are thinking beyond today's profits, to the impact they will have tomorrow, on themselves and their surroundings. [Chandler, 2001] Some scholars criticize the practice of CRS as simply being a smokescreen for the unsustainable business model underneath [Friedman, 1970]. Others see CSR as a positive and genuine practice to better our world [Mintzberg, 1983]. Whether one considers CSR as a positive or negative initiative, one thing is for sure - consumers are increasingly aware of its presence. [Crane, A. Matten, D. and Spence, L., 2008]

In order to standardize CSR initiatives and potentially improve their credibility, the ISO is developing Social Responsibility standards. While the standardization process is advantageous, today these principles are clearly broad and difficult to apply to a more specific context. In order to be able to draw some more practical conclusions, this research focuses on one specific aspect of CSR - environmental sustainability. The academic pursuit of CSR largely stems from research in ethics as well as the growing environmental concerns that began to rise in the early 1990's. Today, consideration for the environment is becoming a necessary part of doing business [Crane, A. Matten, D. and Spence, L., 2008].

Much like CSR, sustainability is also a term plagued with many definitions. Most generally it is the earth's ability to maintain itself in the long - term [Crane, A. Matten, D. and Spence, L., 2008]. Environmental sustainability is important to consumers. People look for products that not only work, but also carry ethical values [Jedlicka, 2008]. Pollution and waste reduction, the formation of sustainable business practices, and other environmental concerns are now a part of the buying decision. And while consumers expect that companies are responsible in this regard, some studies have identified that they are only willing to pay about a 5% premium for the efforts. [Davis, 1991] On the other hand, if two products are identical on every front except for eco - performance, the

consumer will choose the green product [Kardash, 1974]. As such companies need the ability to build strong CSR messages that consumers are able to understand and internalize.

There are several difficulties around building a strong environmental message. A study by Davis [1994] showed that 84% of adults believe it is the company that should do more, and 83% felt that companies are not worried enough about the environment. Thus, consumers perceive environmental issues largely as the responsibility of other actors such as corporations and government. [Niva & Timonen, 2001] This means that companies are expected to invest in these initiatives with little anticipated return. As such many companies have attempted to portray themselves as being environmentally friendly with as little investment as possible. This has spawned a second problem called *greenwashing*.

Greenwashing is another reason that formulating an effective corporate message has become difficult. The term greenwashing stems from the concept of whitewashing, described as a deliberate attempt to hide unpleasant facts, thus fueling consumer confusion. (greenwashingindex.com) Claiming you are environmentally friendly is a lot easier (and much cheaper) than actually *being* environmentally friendly. The result is that many initiatives are more symbolic than substantive in their environmental benefits. [Cowe, R., 1996] Further, claims that are vague, lack specific information, and can in fact be misleading are causing consumer doubt. [Gray, V., 1990] For example one study found that 60% of environmentally based advertisements featured unacceptable claims ranging from the ambiguous to the 'downright false'. [Carlson, 1993] Therefore not only do companies have to make very efficient investments in being green, they must also communicate with customers in a clear and trustworthy manner to avoid the effects of greenwashing.

In summary, given the smarter and more aware consumer of today, sound strategies around CSR have become increasingly important. Social responsibility is historically rooted within environmentalism. Studies have shown that while consumers feel that being green is important to them, they believe that it is ultimately the responsibility of the firm. In addition, consumers are not willing to pay much more for green products. This has perpetuated the problem of greenwashing-companies are using vague and even false environmental claims in an attempt to capture the consumer. As such, it has become difficult to know how to satisfy the pressures to be increasingly green, to communicate efforts effectively, and to ensure that those efforts are sustainable for all stakeholders.

2. Bottled water packaging: a sustainability problem and solution

Today, consumers and the general public are more aware of their personal impact on the environment. This in turn, has had an impact on the packaging industry. Packages symbolize immediate and visible waste created by consumer buying behaviours. The world packaging market in 2009 was worth $US 563.847 million, showing 34% growth from 1999 [WPO, 2008a]. Clearly a market of this size has the ability to have a significant impact on the environment.

For many products we consume, packaging is a "necessary evil". The purpose of packaging is to contain, preserve, protect, transport and communicate. A sustainable package must first satisfy these factors before it can then add value back to the consumer and the environment. By the given definition of sustainability, a sustainable package would meet our immediate needs without compromising the ability for future generations to meet theirs. [WPO, 2008b] Organizations such as the Sustainable Packaging Coalition have been working hard to understand what a sustainable package should be, providing guidelines (Table II) and resources to manufacturers.

Table II: Definition of sustainable according to the sustainable packaging coalition

Is beneficial, safe and healthy for individuals and communities throughout its lifecycle
Meets market criteria for performance and cost
Is sourced, manufactured, transported, and recycled using renewable energy
Maximizes the use of renewable or recycled source materials
Is manufactured using clean production technologies and best practices
Is made from materials healthy in all probable end of life scenarios
Is physically designed to optimize materials and energy
Is effectively recovered and utilized in biological and/or industrial cradle to cradle cycles

The ability to discuss the immediate cost and sustainability advantages has created the potential for a stronger bond between package manufacturers and the product companies themselves. Today when a company is planning to release a product they can discuss sustainability with their package suppliers during the packaging design phase. Thus, an understanding of what constitutes a sustainable package is being formulated between these two parties. The next important step is to be able to link the consumer into this discussion.

One can argue that there is a lack of connection between the concept of the package and consumer understanding. The result of this is that environmentally savvy consumers have been very vocal about the drawbacks of packaging. These same consumers need to be informed about the process behind the final product. Companies need to actively promote their green packaging initiatives so that consumers are aware of positive changes being made. In fact, lack of adequate information is claimed to be the most important obstacle for environmentally conscious product purchasing [Leire & Thidell, 2005]. The reality is that there is a trade - off between the volume of packaging materials and the need to identify brands and increase the attractiveness of a product. [Canadian Bottled Water Industry, 2009] An inappropriate balance of this equation has spawned consumer criticism. Today, consumer sites such as overpackaging.com are dedicated to exposing companies who over - package. They take pictures of the excess packaging, display them on the web, and then send emails to the companies responsible. The progress of the conversation and company action is tracked on the website. As such, now that we are beginning to successfully identify what a sustainable package looks like from a manufacturing perspective, there needs to be a shift toward translating this information to the consumer.

While in many cases packaging is necessary, consumers are requiring that corporations are more responsible with its use. Given that packaging is a large industry spanning across most consumable goods, this research focuses on one segment of the market-bottled water. There are several reasons why the bottled water industry was chosen for this research. Firstly, beverages constitute 14% of the packaging industry. Yearly beverage consumption is approximately 1.35 trillion liters worldwide. Within this, bottled water represents the fastest growing sector of the market with strong growth in both emerging markets and developed economies. [WPO, 2008b]. Though food packaging has an even larger portion of the market, there are too many types of food packages to be able to assess as a group. Thus, researching water bottles specifically has generalizable value allowing us to observe trends.

In addition to being the fastest growing sector of a large segment within packaging, as well as having characteristics across which one can generalize, the most important factor in deciding to research bottled water is the public scrutiny the industry has undergone. Environmental gurus from the likes of David Suzuki have voiced that bottling and selling a resource that is free from the tap in North America is irresponsible. The debate has spawned legislative action, resulting in water bottle bans in some areas of Canada. "Environmentalists have said they are concerned by the amount of energy it takes to transport the bottles, as well as the waste produced by them, particularly when most areas of Canada have safe water supplies," the CBC reports [CBC, 2008]. Studies have found that even in areas where tap water is safe to drink, demand for bottled water is increasing - producing unnecessary garbage and consuming vast quantities of energy. [Arnold & Larsen, 2006] It is no wonder that water bottles are under attack. At the same time however, there are companies who are responding to these pressures with better bottles. Thus it becomes clear that while stirring environmental concerns, water bottles can also stand to be a solution when companies consider sustainability.

From the perspective of the bottle as a problem, the media criticism and legislative action against water bottles is warranted. Firstly, there is a strong product focus when assessing environmental impact. The product and in effect the package, is seen as the carrier of pollution, energy and material waste. [Niva & Timonen, 2001] Even though the most common plastic bottle is highly recyclable, not all bottles make it down the recycling pipeline. One study has identified that in the US, the recycling rate for PET is only 23%, directly translating to 38 billion water bottles or $ 1 billion in plastic [Fishman, 2007]. Another researcher tabulated that 1.5 million barrels of oil are used to transport water bottles and that 2.7 million tons of plastics are used to bottle water each year [Arnold & Larsen, 2006]. In Canada, the recycling statistics are much less daunting, with recycling rates ranging from 60 - 85%. [Canadian Bottled Water Industry, 2009] Sadly, no matter how much plastic you recycle, the cost of producing it in the first place is unnecessary given that tap water is safe to drink in North America.

At the same time, the success and the growth of the bottled water industry is driven in part by the package. For one, consumers want convenience. In fact, consumers demand convenience over sustainability, avoiding choosing green products for reasons such as lack of time or convenience 33% of the time [Polonsky, 1994]. The

package is addressing those needs, and strategic companies should consider its sustainability to further create a competitive advantage. There are plenty of opportunities for the industry to respond to this challenge. For example, the amount of plastic in PET bottles is decreasing. [Canadian Bottled Water Industry, 2009] This has a domino effect as lighter bottles use fewer materials to produce and require less energy to transport [Fiksel, 2006]. The materials being used are also changing. As an example the negative image of plastic is creating more opportunities for the paper industry [Gray & Guthrie, 1990]. In response companies such as Tetra Pak are creating a package from over 60% renewable materials of which the majority is paper. Manufacturers have many opportunities to improve through cleaner processes, cleaner products or the use of more sustainable resources. [Fiksel, 2006]

As can be seen packaging can be portrayed as both a problem, causing waste and pollution, and a solution creating value for the customer because it is convenient. When manufacturers and packagers work together they create creative sustainable packaging solutions. The next necessary step is bridging the gap from corporate sustainability efforts to consumer understanding. Consumer vehicles to expose irresponsible packagers, such as overpackaging.com are already in place. Thus vehicles to promote packaging, convenience and sustainability are necessary to overcome the skepticism.

An information gap now exists between the impact of the improvements being made by packagers, and consumer's ability to understand that information. The purpose of this research is to assess the bottled water industry from within this consumer - packager gap. In order to achieve this the research is positioned from the point of view of a non - expert customer. The assessment will use the two access points that a consumer would most likely use to gather information about the sustainability of bottled water: the package and the company website. Next the research methodology for the research is discussed.

3. Research methodology and discussion of findings

Examples of prior research in this area have investigated environmental claims on dishwashing detergent packages, Polonsky et al. [1998] as well as ads in magazines, Kangun et al. [1991] and Carlson et al. [1993], using content analysis. This research also used content analysis. The analyses consisted of a visual inspection of the bottles and websites of a selected group of bottled water suppliers. The sample of bottles was strategically selected to reflect readily available brands to the average consumer (available in popular grocery chains and supermarkets in Toronto). Two groups of researchers investigated various bottled water containers to ensure strict objectivity, systemization, and quantification - three critical elements of content analysis.

The research was broken down into two portions: a physical assessment of the bottles, and an assessment of the sustainability information included on the package and website. For the physical characteristics of the bottle the criteria was based on characteristics of production noted to be important from an environmental perspective directly identifiable by the package. This data is presented here in the format of trends appearing in the sample. Secondly, the printed labels and containers were inspected for content that displayed environmental benefits. An assessment of the information available on the websites followed this inspection. Both the label and website data information was categorized using a typology of claims developed by Carlson et al. [1993] - originally used to assess printed advertisements. This typology was selected because it was successfully validated in previous research.

There are several reasons why a package is an important point of contact for the consumer. Gray [1990] identifies that 80% of purchases are made on impulse. This means that the package is the only information vehicle the consumer has while making the product purchase decision. Strengthening this importance, Gray also finds that 90% of women read food - packaging labels before they make a purchase. This translates to a captive audience exactly at the time of purchase. The package can also confirm core values, meaning that the inclusion of sustainability messages can attract new customers [Jedlicka, 2008]. Given that packaging is both necessary and the perpetrator of waste, on the package itself is the ideal location to effectively reassure the consumer that sustainability has been considered.

Even though the best place to identify packaging initiatives to a client is on the package itself, the package is limited by its size. Given that the brand is still important, and water requires specific labeling, there is not much space left for sustainable messages. As such, the savvy consumer can intuitively find out more on a company's website. Studies have identified that 95% of consumers use the Internet for finding information about goods and

services. [Liu, 2007] More importantly the way in which consumers perceive the content on the site is directly related to how informative the website appears. [Huizingh, 2000] Therefore content on the website needs to be carefully planned and useful for the consumer. One approach is to appeal to the consumer on multiple levels. A website can feature images, which appeal to the consumer's emotions and require his/her own social context, or it can feature information relevant to the product itself. [Hoffman & Novak, 1997]

The analysis of consumer website data for this research was appropriate because company websites hold product information that is accessible to the consumer. Thus, if not enough information exists on the bottle itself, the consumer's next natural point of information is the website. Originally, the CSR policies of the company were going to be the point of assessment. However that information was deemed difficult to access for a consumer. The research is addressing the gap of consumer understanding of the information from a non - expert perspective. In keeping with that theme, analysis of the website was more appropriate.

In summary, now that the landscape of the industry is understood, it has been identified why the bottled water industry is an appropriate choice for this research. This paper is situated in the information gap that potentially exists between the investments made by companies to be more environmentally friendly and the understanding of those investments by consumers. The focus of the research is the package, and the trends associated with the display of sustainable information on it, along with an interrogation of the website as a second point of contact. Thus, the research was broken down to first assess the physical sustainability trends on the bottle, followed by a content analysis of the environmental information available on the bottle, and lastly that same analysis was conducted on the company website.

4. Physical trends of the water bottle

The sample for assessment consisted of 22 water bottles found in local grocery stores in the Toronto area. The bottles varied in material, size and other characteristics. The characteristics were captured via a visual inspection and measurement. The traits were then categorized after the fact, thus making the initial approach to the assessment exploratory. This is extremely important, as consumers assessing the bottles are not likely to have the same consistent set of categories for assessment. Further, it ensures that the researches do not impose their own biases, and allow trends to emerge empirically. Table III shows a list of water bottle trends in the Toronto market.

Table III: Trend data for physical characteristics of water bottles

A majority (77%) are plastic
A majority weigh 3 - 9% of the total product weight
More than half (55%) have labels with more than 60% ink coverage
More than half (55%) have paper labels
Most labels use between 3 to 6 colours (1% with 6 or more colours and 9% with 3 or less colours)
Just less than half (43%) use a label with a surface area of less than 150 cm^2
A majority (62%) limit the amount of adhesive used
A majority (70%) have a cap that weighs less than 2 grams
A majority (59%) use a plain cap with no additional processes Examples of additional processes included embossing, printing, labeling, and added utility such as the sports cap pull top
All include some additional unique and non - essential process, with texture (embossing/debossing) being most popular (47%) Examples of additional process included, a unique bottle shape, shrink wrapping, die - cutting and special assembly (Tetra Pak containers or additional add on pieces)
More than half (54%) waste less than 15% of space when stacked

Using these categories, an ideal of the sample was drawn out in theory. Overlooking the benefits of different material types (given that they would be highly dependent on the recycling capabilities of a region) the following was discerned as having a high sustainability score within the sample:

- Lightweight bottle and cap;
- Minimal ink coverage and low number of inks;
- Smallest label;
- Minimal adhesive;

- A shape that reduces the amount of stack space wasted;
- No additional processes to the cap and bottle.

Given this ideal set of characteristics, the next phase of research will interrogate the weighted value of each of them in order to assign grades to the physical finished product. Thus these six characteristics will become the basis of an easy to apply weighted score system. The significance is that all of them are readily apparent on the bottle, and easily understood by the general public. In this phase the limitations will also be considered. Such a minimalist perspective has its drawbacks. For example, branding is important in a commodity market such as bottled water. Many implications of branding, for example a distinct shape or special metallic colour ink, will have a negative impact on the sustainability score. As such, a pilot study can test this sustainability/ branding threshold. A weighted score of characteristics that consumers identify as being sustainable will allow manufacturers to better connect with them.

The implication of these findings is that they are easily relatable to the consumer. The nature of the water bottle buyer is that he/she in not likely to be aware of the process involved to manufacture a sustainable bottle. If one reflects back to the considerations for sustainable packages listed in Table 2, it can be seen that most of them are not ascertainable from the package itself. Here the research is looking to identify a package that would "look" sustainable immediately, thus helping customers make environmentally friendly choices. It is the environmental claims on the website or the bottle that help relate the message of the sustainable package as understood by the manufacturer. As such the next portion of the research is an assessment of these claims. Together, with an understanding of a physical package, the two provide a complete explanation to the consumer.

5. Assessment of sustainable information

In the spirit of positioning the research from the consumers' point of view, in addition to identifying the physical characteristics of the bottles the second phase of the research was to identify any environmental information presented on the bottles themselves. This process was done using the typology developed by Carlson et al. [1993] defined in Table IV. The purpose of this paper was to first aggregate the claims. This aggregation allowed us to compare the information that exists on the bottle to the information provided on the website. Knowing that most purchases are impulse buys, and that the package represents an information point, being able to identify the trends associated with the types of claims being presented on the package and the website is quantifiable and valuable.

Table IV: Typology of Environmental Advertising Claims [Carlson, 1993]

1.	Product Orientation: The claim focuses on the environmentally friendly attributes that a product possesses. Example: "This product is biodegradable."
2.	Process Orientation: The claim deals with an organization's internal technology, production technique, and/or disposal method that yields environmental benefits. Example: "Twenty percent of the raw materials used in producing this good are recycled."
3.	Image Orientation: The claim associates an organization with an environmental cause or activity for which there is broad - based public support. Example: "We are committed to preserving our forests." Example: "We urge you to support the movement to preserve our wetlands."
4.	Environmental Fact: The claim involves an independent statement that is ostensibly factual in nature from an organization about the environment at large, or its condition. Example: ''The world's rain forests are being destroyed at the rate of two acres per second."
5.	Combination: The claim appears to have multiple facets, (i.e., it reflects a product orientation, process orientation, image orientation and/or an environmental fact).

While the first portion of the research was more exploratory in nature, the latter consisted of a set of three hypotheses:

H1: The website data will have a higher number of sustainability claims than the bottle/container data.
H2: Printed bottled water containers with high numbers of sustainability claims will also have a high number of website claims.
H3: Bottles with a high number of claims, both on the bottle and the site, will not necessarily appear sustainable from a physical perspective.

Given the scrutiny that the bottled water market has undergone, it was hypothesized that manufacturers would use the website as a vehicle for displaying improvements being made to help alleviate the public's concern. Secondly, where claims had made their way to the packages themselves, one would anticipate that additional claims would exist on the websites. This second hypothesis helped verify whether the claims on packages were substantiated with more information, given the package would be limited in size. The third conjecture combined the concept of the former physical assessment. Though bottles may make sustainability claims, it was hypothesized that manufacturers would not go the one step further and create a bottle that "looks" sustainable (particularly over looking attractive). Thus, even those bottles making claims would not appear sustainable from a physical perspective.

6. Claims on the bottle

An assessment of the bottle sample revealed and that a shockingly low amount of environmental claims exist on the package itself. Figure 1 identifies that while a majority of manufacturers displayed a recycling symbol, along with instructions for a bottle deposit, only 5 bottles of 21 (one bottle disqualified because the label was not in English) made claims in addition. Thus the customer had no facts regarding the package on purchase, outside of the physical appearance of the package. Given this set of circumstances, the characteristics an environmentally savvy consumer would use would be the physical characteristics identified in the first portion of the study. As such, if a manufacturer made special investments in machinery that used less energy for example, the consumer would not know given the package as an information vehicle alone. Furthering the issue, only two of the labels directed consumers to a point of contact such as a website or a customer care number. Thus, if an informative website exists, the company is leaving it up to the client to find it.

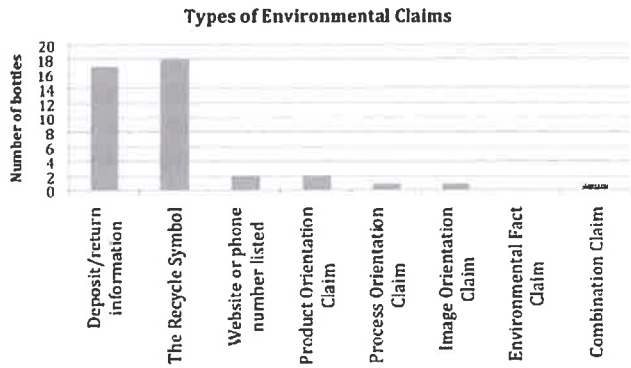

Figure 1:
Types of environmental claims on the water bottle

7. Claims on the Websites

After reviewing the lables of the bottles themselves, the same assesment was applied to the company websites. The website numbers improved only marginally. To begin with seven of the bottles either did not have a website, or were eliminated as a result of no English site being available. Thus the sample size was reduced to 14. In Figure 2 we saw that of the final sample, six websites (43%) made no environmental clamis whatsoever. Where claims were made, they tended to be combination claims. If counted out separately, the most popular claim types were Process (40%) and Product (30%) claims (Figure 3). Though not as substantially as had been anticipated, the research did endorse the first hypothesis, that the websites will house more environmental information, than the package.

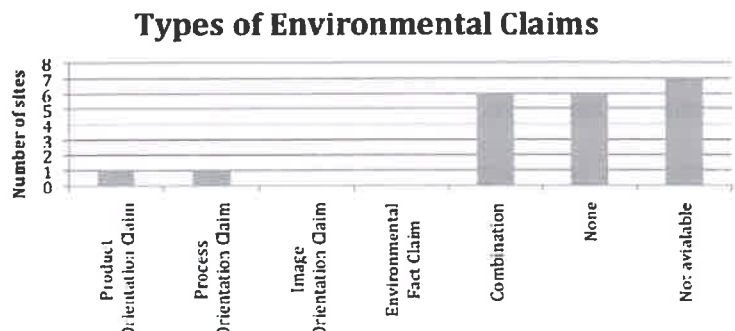

Figure 2:
Types of environmental claims on company websites

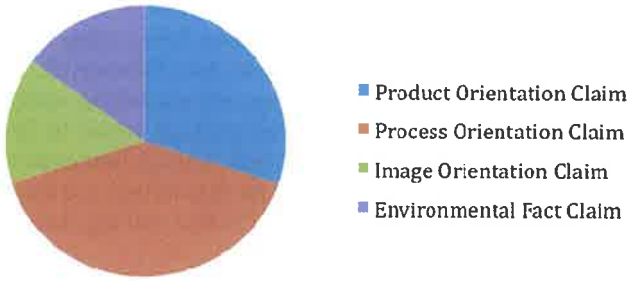

Figure 3: Types of claims most commonly appearing on the websites, including a breakout of the combination claims

8. Linking the bottles and websites

In addition to aggregating the number and types of claims that existed on the bottles and websites, it was valuable to understand if there is a link between the two media types. The second hypothesis conjectured that when the bottles have environmental messages on the package, companies would also include more information on their websites to formalize those claims. In all cases except one, if a claim existed on the bottle the company provided further claims on the website. Interestingly the outlier in this case was an image claim on the bottle, with no claims on the website - image claims being rather subjective. On the whole however, the assessment did confirm the second hypothesis, showing that where claims exist on the bottle, they are substantiated on the website.

The last portion of the research combined the physical appearance of the bottle and the environmental claims data in order to validate whether top performers appeared to be the same in both tests. The third hypothesis conjectured that those bottles with a high number of claims, both on the bottle and the website, would not necessarily appear as the ideal physical representations of a sustainable bottle. A selection of the top three bottles in the environmental claims assessment represented marginal physical appearance scores, thus confirming the hypothesis.

The scoring system was not weighted, thus each characteristic was given 2 points when appearing in the low range of the sample (i.e. 2 for light caps relative to the sample), 1 if it was in the mid range, and 0 if it was in the high range. The scores were totaled for a final percentage (with most sustainable having a 100% score). The three best performing bottles on the claims assessment were then scored using this system. Two bottles received equal scores of 43%, while the third scored only 18%. Thus the last hypothesis was confirmed: none of the best ranking bottles, physically represented sustainable characteristics as defined by this sample. The question then becomes whether the sustainability messages can stand to inform consumers, and create trustworthy messages that overpower the appearance of the bottle. The scoring system will be further defined in later research when a weight to each category is added, thus bringing the system closer to actual manufacturing sustainability.

9. Conclusions

Being environmentally friendly is increasingly important to today's consumers. However, studies have shown that consumers believe that it is the responsibility of the firm, and should not be an additional cost to them. This has in turn perpetuated the problem of greenwashing - companies are using vague and even false environmental claims in an attempt to capture the consumer. As such, it has become difficult to know how to satisfy the pressures to be increasingly green, to communicate efforts effectively, and to ensure that those efforts are sustainable for all stakeholders. It is particularly important in the packaging sector where consumers can make a direct connection between the package and waste. Within the bottled water marketplace, consumer criticism has increased the pressure to be accountable and innovative.

Companies need to actively promote their green packaging initiatives so that consumers are more aware of positive changes being made. One can argue that there is a lack of connection between the concept of the package and consumer understanding. The result of this is that environmentally savvy consumers have been very vocal about the drawbacks of packaging. These same consumers need to be informed about the process behind the final product. Companies need to invest in connecting all of their sustainability efforts back to the consumer. This can be done through the physical package and other information channels such as the company website.

This research investigated the bottled water marketplace, selecting a sample readily available to the Toronto consumer market. A visual inspection of the group of bottles, along with a content analysis of their sites and labels, supported all three research hypotheses. It was found that websites had more sustainability data then bottles, bottles with more sustainability data also had more informative websites, and finally, where the bottles and websites were environmentally friendly, the physical appearances of the bottles did not match up. The last hypothesis is where the consumer gap exists. It is currently difficult to recognize what an eco - friendly bottle looks like. While the packaging industry continues to develop definitions of a sustainable package, it is critically important for the consumers to recognize these efforts.

Future research in this area needs to include a pilot test, which would determine the types of environmental claims customers value the most within the typology used here. In addition, a weighted system for the physical characteristics of a bottle would provide more thorough sustainability scores for the bottles. As such this research agenda is founded in developing an understanding of sustainable packaging from a consumer perspective.

Acknowledgements

The researchers would first like to thank their research assistant Diane Ford for helping with this project. Thank you to the Faculty of Communication and Design and the School of Graphic Communications Management at Ryerson University, as well as IARIGAI for the opportunity to present the paper.

References

1. Arnold, E. & Larsen, J. (2006) *Bottled water: Pouring resources down the drain. Earth Policy,* 51, 1
2. Carlson, L., Grove, S. J. & Kangun, N. (1993) *A content analysis of environmental advertising claims: A matrix method approach. Journal of Advertising,* 22(3)
3. Chandler, S. G. (2001) *Introduction: Defining Corporate Social Responsibility, Ethical Performance Best Practices Quoted In Michael Stohl, Cynthia Stohl, And Nikki C. Townsley, 2007. A New Generation of Global Corporate Social Responsibility," in may, Cheney and Roper,* 30-44
4. Cowe, R, E. J. (1996). *Fair enough?*
5. Crane, A., Matten, D. and Spence, L., (2008) *Corporate social responsibility: Readings and cases in a global context Routledge*
6. Davis, J. J., (1991) *A blueprint for green marketing. Journal of Business Strategy,* 12(4), 14-17
7. Davis, J. J. (1994). *Consumer response to corporate environmental advertising. Journal of Consumer Marketing,* 11(2), 25-37
8. Fiksel, J., (2006) *Achieving eco - efficiency through design for environment. Environmental Quality Management,* 5(4), 47-54
9. Fishman, C., (2007) *Message in a bottle. Fast Company,* 117, 110
10. Friedman, M., (1970) *The social responsibility of business is to increase its profits. New York Times Magazine,* 32 (13), 122-126
11. Gray, V., & Guthrie, J., (1990) *Ethical issues of environmentally friendly packaging. International Journal of Physical Distribution & Logistics Management, 20(8), 31-36*
12. Hoffman, D. L. & Novak, T. P., (1997*) A new marketing paradigm for electronic commerce. Information Society,* 13, 43-54
13. Huizingh, E. K. R. E., (2000) *The content and design of web sites: An empirical study. Information & Management,* 37(3), 123-134
14. Jedlicka, W., (2008) *Packaging sustainability: Tools, systems and strategies for innovative package design John Wiley and Sons*
15. Kangun, N., Carlson, L. & Grove, S. J., (1991) *Environmental advertising claims: A preliminary investigation. Journal of Public Policy & Marketing,* 47-58
16. Kardash, W., (1974*) Corporate responsibility and the quality of life: Developing the ecologically concerned consumer. Chicago: American Marketing Association*
17. Leire, C. & Thidell, Å., (2005) *Product - related environmental information to guide consumer purchases - a review and analysis of research on perceptions, understanding and use among Nordic consumers. Journal of Cleaner Production,* 13(10 - 11), 1061-1070

18. Liu, H., (2007) *Social network profiles as taste performances. Journal of Computer - Mediated Communication,* 13(1), 252-275
19. Mintzberg, H., (1983) *The case for corporate social responsibility. Journal of Business Strategy,* 4(2), 3-15
20. Niva, M. & Timonen, P., (2001) *The role of consumers in product - oriented environmental policy: Can the consumer be the driving force for environmental improvements? International Journal of Consumer Studies,* 25(4), 331-338
21. Perry, W., (2008) *CSR as managing relationships in an increasingly complex world. Ryerson University*
22. Polonsky, M. J., (1994) An introduction to green marketing. *Electronic Green Journal*
23. World Packaging Organization. (2008a) *Market statistics and future trends in global packaging,* 1-45
24. World Packaging Organization. (2008b) *Position paper - sustainable packaging,* 1-2

Web sources

1. The Canadian Bottled Water Industry. (2009). *Retrieved 05/07, 2009, from http://www4.agr.gc.ca/AAFC - AAC/display - afficher.do?id=1171644581795&lang=eng*
2. CBC News. (2008). *Toronto may copy london, ont.'s ban on bottled water. Retrieved 05/07, 2009, from http://www.cbc.ca/consumer/story/2008/08/20/toronto - bottledwater.html*
3. Overpackaging.com. (2009). *Retrieved 06/22, 2009, from www.overpackaging.com*

Green packaging materials - implementation procedures in the society and the Graphic Arts industry - An empirical study of sustainability

Marios K. Tsigonias [1,2,3] *and Anastasios E. Politis* [1,2]

[1] Hellenic Open University, School of Applied Arts
[2] Athens Technological Educational Institute -TEI, Faculty of Graphic Arts Technology
[3] National Centre of Scientific Research Demokritos, Institute of Physical Chemistry

27 Ermou St,GR-16233, Byron, Athens Greece
E-mail: mtsigon@chem.demokritos.gr

Lefka, P. O. Box 6562, GR-19015 Oropos, Greece
E-mail: politisresearch@techlink.gr

Abstract

Environment and its protection, as well as increasing sustainability requirements from the society, "push" the industry to act towards new materials, production processes and management of industrial products. Printed matters and in particular packaging are among those industrial "products" which need to be designed, produced, distributed and recycled with the sustainable processes.

Printing substrates - in general materials used for printing and packaging, are among the important factors that influence sustainable concepts within the graphic arts and packaging printing industry. Sustainability within printing substrates as well as printing inks, concern mainly recycled or environmentally friendly materials, which are currently used by the graphic arts industry. Paper, board and vegetable-based inks are examples of such materials.

However, as the protection of the environment is becoming an increasingly demanding issue, new materials and in particular new printing substrates are being evolved. The most prominent development is naturally degradable materials, which do not affect the environment. There are also techniques used to convert common packaging materials (such as PE, PP, PVC, PS) into degradable ones. Another process is the transformation of degradable materials into composite degradable ones, with the addition of alginates -polymers produced by the sea algae- or other biomass materials.

The present study aims primarily to explore the behavior of the Greek consumers and their opinion on degradable materials future use and secondly, to investigate the processing of degradable materials and in particular the printing and finishing processes within the Greek graphic arts industry and production of these materials.

Keywords: degradable packaging materials, packaging industry, consumers' environmental attitude, green printing

1. Law and ethics issues

European Parliament and Council Directive 94/62/EC aims to harmonize national measures concerning the management of packaging and packaging waste in order, on the one hand, to prevent any impact thereof on the environment of all Member States as well as of third countries or to reduce such impact, thus providing a high level of environmental protection, and, on the other hand, to ensure the functioning of the internal market and to avoid obstacles to trade and distortion and restriction of competition within the Community [94/62/EC, 1994].

According to this Directive it is clearly clarified that all Member States shall ensure that, in addition to the measures to prevent the formation of packaging waste taken in accordance with Article 9, other preventive measures are implemented. Such other measures may consist of national programmes or similar actions adopted, if appropriate in consultation with economic operators, and designed to collect and take advantage of the many initiatives taken within Member States as regards prevention. They shall comply with the objectives of this Directive which are the reduction of the quantity and of the harmfulness for the environment of materials and substances contained in packaging and packaging waste, at production process level and at the marketing, distribution, utilization and elimination stages and in particular by developing 'clean' products and technology. In the Directive it is mentioned that Packaging shall be designed, produced and commercialized in such a way

as to permit its reuse or recovery, including recycling, and to minimize its impact on the environment when packaging waste or residues from packaging waste management operations are disposed of. There are many other environmental issues that are mentioned in this Directive such as the environmental requirements of the packaging that must be simultaneously satisfied. Material and energy recovery and composting are mentioned as critical factors of sustainable packaging and recycling and reuse of the packaging materials are mentioned as the most common ways to manage the packaging waste. There is also a statement that biodegradable packaging waste shall be of such a nature that it is capable of undergoing physical, chemical, thermal or biological decomposition such that most of the finished compost ultimately decomposes into carbon dioxide, biomass and water [PIRA International Ltd, ECOLAS N.V., 2005].

2. Degradable packaging materials - state of the art

Many solutions are suggested by the scientists in order to protect the environment against the packaging waste. The main object is to replace the common - non degradable packaging substrates (LDPE, HDPE, PP, PET, PS etc) with other environmentally friendly polymers. Some of them are currently accepted by the Industry and many degradable packaging substrates are used in a large scale [Andrady, 2003 & Graziani et al., 2007].

Some substrate materials, quite interesting for their characteristics and behavior that have been tested and are used in a small industrial scale are carbohydrates, starch, cellulose, chitosane, alginate and polylactide [Anshuman et al., 2007, Rindlav-Westling et al., 1998, Rhim et al., 1998, Remunan-Lopez et al., 1997 and Kale et al., 2007].

The most common degradable polymer is PLA (polylactide) that is used in a medium industrial scale and offers plenty other advantages besides degradability. PLA has very interesting characteristics for packaging purposes such as good thermal and barrier properties, mechanical strength, flexibility and printability [Davis et al., 2006, Lorcks, 1998, Balkcom et al., 2002 and Rothenberg et al., 2002].

The most serious problem of the degradable packaging materials is the large variety of the properties that is necessary to fulfill the demands of an industry. Packaging printing industry uses many types of polymers in order to adjust the characteristics of the produced materials. Now it has to do the same with only one polymer -PLA. To solve the problem researchers use blended degradable polymers and have achieved a large range of complex and degradable materials suitable for almost every packaging application [Tsigonias, 2005, Tsigonias et al., 2006 and Avella, 2005].

Another process is the transformation of degradable materials into composite degradable ones, with the addition of alginates - polymers produced by the sea algae. Algae constitute an environmental threat for the North Europe seas due to the eutrophication phenomenon and part of our future study will be to use them for the production of composite degradable materials [Tsigonias, 2005 & 2006 and Avella, 2005].

There are also techniques used to convert the common packaging materials (such as PE, PP, PET, PVC, PS) into degradable ones (eg. The "d2w" technology). This technology uses some additives in order to produce a large variety of oxo-degradable polymers that do not have significant differences (concerning thermal, barrier or mechanical properties) to the polymer materials that were used besides the very short time of degradation in the physical environment or the landfill [Plastic technologies PLC, 2006 & Symphony environmental technologies, 2007].

3. Study and methodology

The present study is twofold: Firstly, it aims to explore the use of degradable materials and the opinions and behavior of consumers. Secondly, it investigates the processing of degradable materials and in particular the printing and finishing processes within the graphic arts industry and production of these materials.

As it regards consumers' behavior, the study refers to social research that takes place in Greece and indicates the increased tendency of the Greek consumer and user of the packages not only to accept but also pursue the alternative degradable packaging materials that are produced nowadays. The informational level and the consumers' level of knowledge on environmental issues are studied. What is more, the will of the consumer to use the new degradable packaging materials is investigated, taking under consideration issues such as the cost of packaging (which is relatively increasing) and the price of the product that the consumer is going to pay.

Regarding the production and processing of degradable materials, the second part of the research refers to the awareness and readiness of the graphic arts and in particular the packaging printing companies to efficiently process these materials as printing substrates. The level of awareness and knowledge about degradable printing substrates is investigated, with the packaging printing companies in Greece [Politis et al, 2007]. Furthermore, the expediency of the degradable packaging materials use in the near future is a matter of investigation. The readiness degree of the Greek Graphic Arts industry to adapt the new production changes is also studied. Industrial changes that are necessary by the acceptance of the use of these new "green" products are clarified and the reflections of the graphic arts industry around the environmental issues are listed.

The study is based on field research related methodology. Within this framework, the research carried out is supported by the collection of data with the use of two separate questionnaires: One for the consumers and their behavior on degradable packaging materials and one for the packaging printing companies, regarding the level of awareness and knowledge on sustainability and in particular their concern regarding effective and efficient printing and finishing of degradable printing substrates.

3.1 Study on the consumers' attitude

The first questionnaire, that concerned the average Greek consumer of packaging, was designed to be simple but comprehensive and to be able to be answered in less than five minutes. The questionnaire is designed in such a way that it is easy to be used in crowded public places such as metro-railway stations, schools and shopping malls. The questions aim to identify the degree of awareness of the public/consumers about degradable packaging materials and to explore the attitude of the social community to these environmental proposals. Most of the questions that were used in this questionnaire were based on a 5 grade - Likert based scale [Likert , 1932 and Dawes, 2008].

The correlation factors that are studied are the region of residence, the gender, the age and the educative level of the participants."The demographic characteristics of the sample that was used in order to carry out this study (391 people from all over Greece) are represented in the following graphs.

Demographic characteristics of the sample

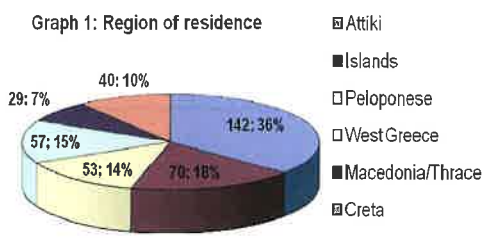

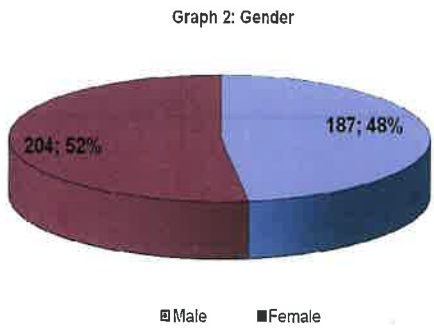

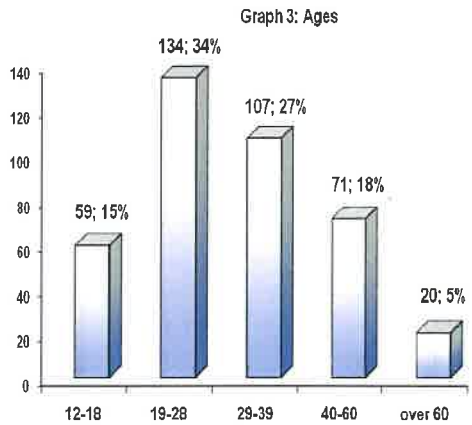

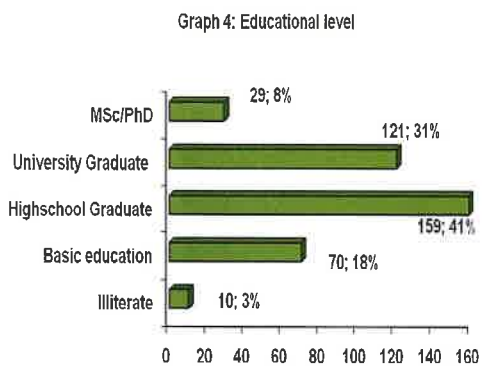

3.2 Study on packaging printing industry

The second part of the study is based on a structured questionnaire that concerned the Greek packaging printing companies, has been aimed at owners of the companies and the upper management. It is more complex however, it is comprehensive and it can be answered by the owners/managers of the companies. The questions aim to identify the awareness and knowledge degree of the managers about the degradable packaging materials and to investigate their attitude on adaptation of production and management operations towards the efficient production and processing of such printing materials. A vital question of the study is the will or expediency of the companies' owners/managers to incorporate the new degradable packaging materials into the workflow of their production.

The correlation factors that are studied are the structure and specialization of the companies, the existing production equipment and the range of substrates that they currently print, among the size of the companies, and the number of employees.

The study is resulting concrete data which show the behavior trends of the consumers towards degradable packaging materials and the degree of readiness of packaging printing companies to print and post-press processing of these materials. An important aspect of the results of the study is the match of the consumers' trends and will and the ability of the printing companies to adapt to these trends.

The sample of this research included 20 packaging printing companies from all over Greece. Their representative was called to answer a detailed questionnaire consisted by 2 preliminary and 12 basic questions, some of them being descriptive, aiming in collecting qualitative data. Our first approach was to correlate the size (number of employees) to the main activity field of the company.

Characteristics of the participated companies

*Table I: Company size (number of employees) * business activity - Crosstabulation*

Count

Q B. Company size (no of employees)		Question A: Which is your main business activity?					Total
		1-9	10-20	21-49	50-99	Above 100	
Business activity	Flexible packaging materials	0	0	0	0	4	4
	Paper and board packaging	5	6	3	0	1	15
	Multilayer materials	0	0	0	0	3	3
	Corrugated board packaging production	0	0	0	0	3	3
	Labels production	0	0	3	0	0	3
	Other	0	0	0	0	0	0

4. Results

Questionnaire 1: Data are analyzed with the assistance of the statistical program SPSS 14 for social sciences. Descriptive statistics (graphic and numerical techniques) were used for the presentation of the research data. Inductive statistics methods were developed in order to export conclusions and to organize of forecasts with regard to the characteristics of population, based on data of the present research. With regard to the investigation of characteristics of affinity between two variables, the correlation factor Pearson (r) was calculated.

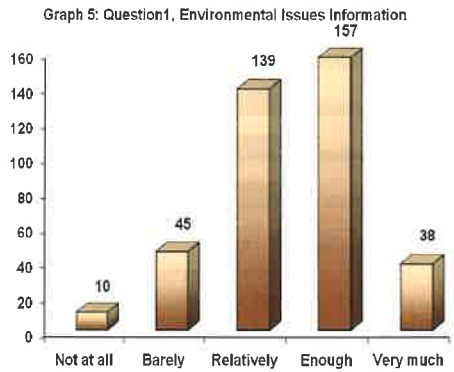

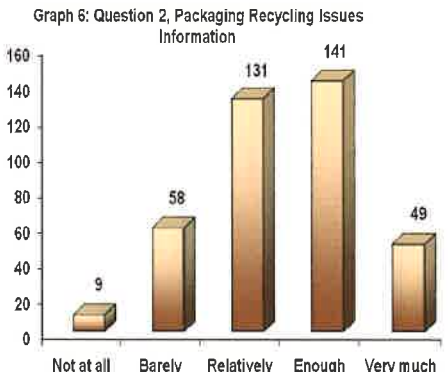

*Table II: Gender * 2nd Question Crosstabulation*

Count

		Question 2: How well informed are you on environmental subjects?					
		Not at all	Barely	Relatively	Enough	Very much	Total
Gender	Male	8	36	67	55	19	185
	Female	1	22	64	86	30	203
Total		9	58	131	141	49	388

Graph 7: Question 3, Basic information sources - 1st and 2nd choices & no choice at all

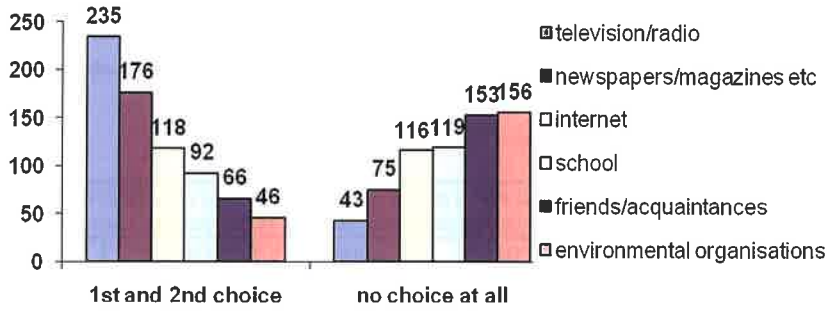

*Table III: Age * 3rd Question (school) - Crosstabulation*

Count

School		Question 3: How do you get your information regarding the environmental issues?									
		No choice	1st choice	2nd choice	3rd choice	4th choice	5th choice	6th choice	7th choice	Simple choice	Total
Age	12-18	10	22	11	4	5	6	1	0	0	59
	19-28	31	23	15	12	20	16	17	0	0	134
	29-39	55	4	9	7	5	8	17	1	1	107
	40-60	43	3	5	3	1	7	7	2	0	71
	Above 60	14	0	0	0	2	2	2	0	0	20
Total		153	52	40	26	33	39	44	3	1	391

*Table IV: Age * 3rd Question (printed media - newspapers/magazines) - Crosstabulation*

Count

Printed media		Question 3: How do you get your information regarding the environmental issues?								
		No choice	1st choice	2nd choice	3rd choice	4th choice	5th choice	6th choice	Simple choice	Total
Age	12-18	18	5	6	5	10	10	4	1	59
	19-28	23	21	37	27	7	12	5	2	134
	29-39	15	19	39	18	6	4	0	6	107
	40-60	12	14	25	12	4	1	1	2	71
	Above 60	7	3	7	3	0	0	0	0	20
Total		75	62	114	65	27	27	10	11	391

*Table V: Age * 3rd Question (the internet) - Crosstabulation*

Count

The Internet		Question 3: How do you get your information regarding the environmental issues?									
		No choice	1st choice	2nd choice	3rd choice	4th choice	5th choice	6th choice	7th choice	Simple choice	Total
Age	12-18	10	8	12	7	7	6	6	0	3	59
	19-28	17	25	27	24	21	11	4	1	4	134
	29-39	33	21	12	12	17	7	2	0	3	107
	40-60	41	2	10	8	5	3	2	0	0	71
	Above 60	15	0	1	0	0	2	1	1	0	20
Total		116	56	62	51	50	29	15	2	10	391

Graph 8: Question 4, Does Recycling contributes to the environmental problem solution?

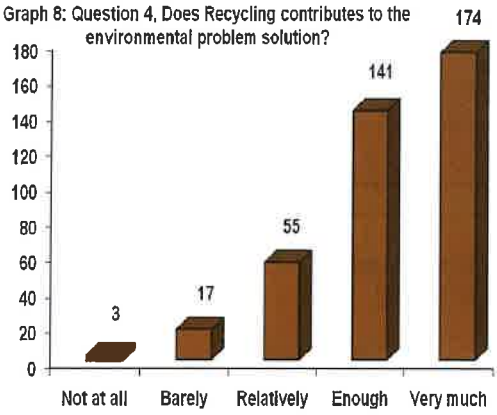

Graph 9: Question 5, How much are you informed on degradable packaging materials?

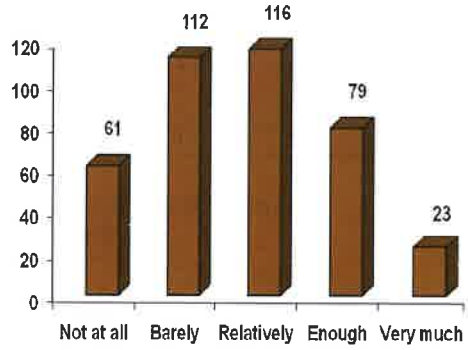

*Table VI: Gender * 4th Question - Crosstabulation*

Count

		Question 4: In what degree do you believe that recycling contributes in the solution of environmental problems, caused by plastic packing materials?					Total
		Not at all	Barely	Relatively	Enough	Very much	
Gender	Male	3	11	33	62	77	186
	Female	0	6	22	79	97	204
Total		3	17	55	141	174	390

*Table VII: Educational level * 5th Question - Crosstabulation*

Count

		Question 5: How well informed are you regarding recycled products/ materials/by-products;					Total
		Not at all	Barely	Relatively	Enough	Very much	
Educational level	Illiterate	4	3	2	1	0	10
	Basic Education	15	21	16	11	7	70
	Graduate	27	46	52	26	8	159
	University Degree	12	37	35	29	8	121
	Postgraduate Degree	3	5	11	10	0	29
Total		61	112	116	77	23	389

Graph 10: Question 6, Would you be allocated to buy products packed in degradable materials even if this increased the price of product?

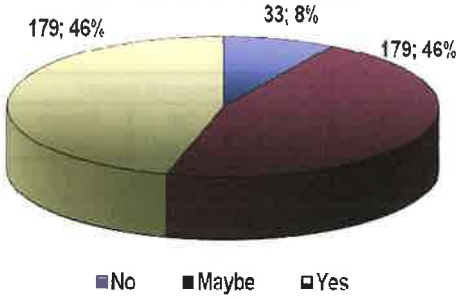

Graph 11: Question 7, Up to which percentage could/would you afford the increase of the products' price as a cause of the use of degradable packaging materials ?

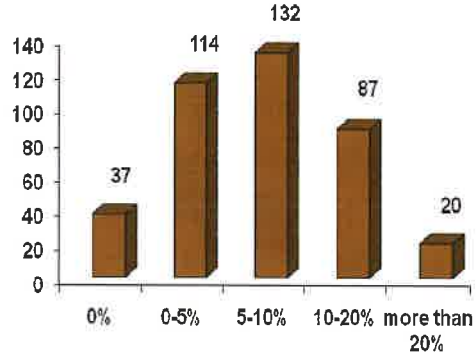

*Table VIII: Age * 7th Question - Crosstabulation*

Count

		Question 7: Up to which percentage could/would you afford the increase of the products' price, as a cause of the use of degradable packaging materials?					Total
		0%	0-5%	5-10%	10-20%	Above 20%	
Age	12-18	5	9	22	16	7	59
	19-28	11	39	48	31	5	134
	29-39	11	32	34	27	3	107
	40-60	6	27	23	11	3	70
	Above 60	4	7	5	2	2	20
Total		37	114	132	87	20	390

Questionnaire 2: Data are analyzed with the assistance of the statistical program SPSS 14 for social sciences. Descriptive statistics were used for the presentation of the research data.

*Table IX: Company size (number of employees) * Question 1, Printing method*

Company size (no of employees)		Question 1: Which of the following printing methods does your business incorporate?					Total
		1-9	10-20	21-49	50-99	Above 100	
Printing method	Gravure	0	0	0	0	4	4
	Flexography	0	3	3	0	5	11
	Offset - lithography	6	3	3	0	0	12
	Metal printing	0	3	0	0	0	3
	Silk screen printing	0	0	0	0	0	0
	Digital printing	6	3	3	0	1	13
	Other	0	0	0	0	0	0

*Table X: Company size (number of employees) * Question 2 & 3 (ISO 9001 & ISO 14001 or EMAS)*

Company size (no of employees)		Question 2: Does your company apply a quality management system - ISO 9001? Question 3: Does your company apply an environmental management system - ISO 14001 or EMAS?					Total
		1-9	10-20	21-49	50-99	Above 100	
ISO 9001	Companies with ISO 9001	3	3	3	0	5	14
	Companies without ISO 9001	3	3	0	0	0	6
ISO 14001 Or EMAS	Companies with EMS	0	0	3	0	5	8
	Companies without EMS	6	6	0	0	0	12

*Table XI: Company size (number of employees) * Question 4, Type of printing substrate*

Company size (no of employees)		Question 4: Which type of materials do you print at your company?					Total
		1-9	10-20	21-49	50-99	Above 100	
Printing substrate	Paper - Board	6	6	3	0	5	20
	Flexible materials -polymers	0	0	3	0	4	7
	Aluminum foil	0	0	3	0	4	7
	Other metalic substrates	0	0	0	0	0	0
	Other	0	0	0	0	0	0

*Table XII: Company size (number of employees) * Question 5, Type of recycled or reused materials*

Company size (no of employees)		Question 5: Which type of materials do you recycle or reuse at your company?					Total
		1-9	10-20	21-49	50-99	Above 100	
Recycled or reused materials	Paper - Board	3	6	3	0	5	17
	Polymers	0	0	3	0	4	7
	Solvents	3	3	3	0	5	14
	Metals	0	3	3	0	5	11
	Other	0	0	0	0	0	0

*Table XIII: Company size (number of employees) * Question 6 & 7 (Information on degradable materials and investigation of the potential to use them)*

Company size (no of employees)		Question 6: Do you know something about the degradable materials regarding their application in packaging? Question 7: Have you investigated the potential of changing the printing substrates you use with similar degradable ones?					Total
		1-9	10-20	21-49	50-99	Above 100	
Information on degradable materials	Informed Companies	0	3	3	0	5	11
	Uninformed Companies	6	3	0	0	0	9
Investigation of the potential to use degradable materials	Companies which have express interest	0	3	0	0	4	7
	Companies which haven't express interest	6	3	3	0	1	13

*Table XIV: Company size (number of employees) * Question 8, Investigation of changing the common substrates with the degradable materials schedule*

Company size (no of employees)		Question 8: In which time frame do you intend to investigate the change the printing substrates you use with similar degradable ones?					Total
		1-9	10-20	21-49	50-99	Above 100	
Investigation of changing to degradable materials schedule	It has been done	0	3	0	0	3	6
	Within next 12 months	0	0	0	0	0	0
	Within 1-2 years	0	0	3	0	0	3
	Within next 2-3 years	0	3	0	0	1	4
	It has not yet scheduled	6	0	0	0	1	7

*Table XV: Company size (number of employees) * Question 9, Information about the additional costs for replacing the common materials with the degradable ones*

Company size (no of employees)		Question 9: Do you have any idea on the additional cost for replacing the printing and production of traditional packaging substrates with similar degradable?					Total
		1-9	10-20	21-49	50-99	Above 100	
Degradable material cost information	Yes	0	0	0	0	2	2
	No	3	0	0	0	2	5
	No but I am interested to learn about	3	6	3	0	1	13

*Table XVI: Company size (number of employees) * Question 10, Possible Reaction Plans*

Company size (no of employees)		Question 10: Which will be your possible reactions based on the material characteristics and market potential of the degradable packaging?					Total
		1-9	10-20	21-49	50-99	Above 100	
Possible Reaction Plans	A. Investment	6	6	3	0	4	19
	A1. Same printing process	3	3	3	0	1	10
	A2. New printing process	3	3	3	0	3	12
	A3. Hybrid printing process	0	3	3	0	0	6
	B. Wait and see	3	3	0	0	5	11
	C. Subcontracting	3	3	0	0	0	6
	D. Not interested	0	0	0	0	0	0
	E. Don't Know	0	0	0	0	0	0

*Table XVII: Company size (number of employees) * Question 12, Training and Know-How development*

Company size (no of employees)		Question 12: Regardless of your intention on investing on the production of degradable packaging materials, do you think you should receive training, take part in seminars and generally develop your know-how on these subjects?					Total
		1-9	10-20	21-49	50-99	Above 100	
Should you receive training and develop your know-how on these subjects?	Yes, definitely	3	3	3	0	3	12
	Rather yes	0	3	0	0	2	5
	Maybe	3	0	0	0	0	3
	Rather not	0	0	0	0	0	0
	No	0	0	0	0	0	0

5. Discussion - conclusions

Regarding the first part of the study, it is obvious, that most Greeks think they have enough environmental information generally, and especially about packaging recycling (Graphs 5 & 6). Women state to be more informed on packaging recycling than men as it is shown on Table II.

On the other hand, most people do not seem to be satisfied about the information that school offers as it is described on Graph 7. This attitude seems to be more intense in the elderly ages (Table III) which means that environmental issues are concerning more and more the younger people in their school life. Elderly people seem to prefer newspapers and magazines as information sources about environmental issues than the internet (Tables IV & V) but this is not significant for our research as this is a general attitude of these age categories. We could say that internet is a choice of information on environmental issues especially for younger people but is still not an option for elderly.

The main sources of information on environmental issues for most people are television/radio and newspapers/ magazines. Environmental Organizations do not seem to be serious sources of information since only 46 people select them as 1st or 2nd choice and 156 people believe that Environmental Organizations are not a source of environmental information at all (Graph 7).

Many people (Graph 8) think that packaging recycling is a very good solution to the environmental problem, but most of them do not have enough information about degradable packaging materials (Graph 9). Men, on the other hand, do not seem to be that optimistic as women on the environmental results of the packaging recycling and this attitude is clearly clarified on Table VI. It is also obvious that the educational level of the participant is strongly connected to the degree of information on degradable packaging materials that is a normal phenomenon due to the high specification of the question (Table VII).

When people are informed about the characteristics of the degradable packaging materials most of them are shaping a positive idea about them in order to answer that they would or probably would pay more money to get a product that is packed in degradable materials as it is visualized on Graph 10. Regarding the cost most of them would accept an up to 10% increase. It is interesting that younger people tend to state that they would pay more money on products packaged in degradable materials than the elderly (Table VIII).

As it regards the second part of the study (packaging printing companies), it can be concluded (Table IX) that only bigger companies are printing with flexography and only industries with more than 100 employees are printing with the method of gravure.

Exclusively, medium and large companies apply both quality and environmental management systems. Some smaller companies apply quality but not environmental management systems. We could say that in Greece environment is an issue for the large industrial settlements whereas smaller companies ignore these parameters (Table X).

Smaller packaging printing companies manage to recycle or reuse materials such as paper, board and some solvents but only the large ones have the opportunity to apply a complete recycling program (Table XI).

All small companies that participate in this research seem to totally ignore the degradable printing substrates and only medium to large industries state to be well informed about those solutions (Table XIII). Most small companies express their will to get informed about the degradable materials and the additional cost for replacing the common substrates with the degradable ones in the printing production (Table XV).

Investments are the most popular reaction for all companies in order to satisfy the degradable materials potential market. Only smaller companies are seriously thinking subcontracting and most companies use the "wait and see" policy for the present time (Table XVI). The vast majority of the companies are positive to the training and developing their know-how on degradable materials issues (Table XVII).

In addition, as regards the second part of the study, some paper and board printing companies consider that paper and board substrates are environmentally friendly enough and they will keep their production volume in the future. As such, sheet-fed offset- lithography printing process on paper and board as well as flexographic printing on corrugated board will continue to serve these packaging printing segments. As a result someone might conclude that these companies are less interested in printing of degradable substrates as long as they are in the form of flexible packaging.

5.1 Final conclusions and future research

With the present study we stress our concern to investigate ways for the graphic arts and printing companies to expand their business and production into new products and markets and to secure their future viability.

Environment and its protection is becoming a first-class priority for everyone. Industry sectors - among them the printing industry should strategically orientate towards concrete actions implementing new production structures within this environmental strategic thinking. Such actions should include people, training, management, investments, processes and of course materials and printing substrates.

Degradable materials might be the solution for use in flexible packaging and labels, towards the potential replacement of plastics and oil-based polymers. Such replacement appears today as an option among others; however, degradable materials seem to have a good potential since, by their nature, eliminate up to a certain degree the recycling process applied for traditional materials. Packaging printing companies need to be thoroughly informed about the potential of degradable materials and their use for packaging.

A necessary action towards this direction is our orientation for future research, aiming in printing degradable materials at a pilot and experimental stage, by applying traditional printing processes and equipment (such as sheet-fed offset printing, flexography, gravure and narrow-web machines). The planned study will allow us to investigate further factors regarding printing of degradable substrates and in particular the ink and its correlation with the degradable substrate. Furthermore, an important part of our future study will be focused in printability, press run, the behavior of the substrate

Acknowledgements

We would like to express our grateful thanks to that entire people in Greece which helped us by spending their time to collect the questionnaires that were used in this study and are E. Ploumi, D. Michailidou, T. Kiritsis, P. Karamfillidi, A. Tatsiopoulos, M. Lili, X. Ntarlagiani, P. Andrianopoulos and Th. Mandila. We would also like to mention the great contribution of Elina Tsermidou on statistical analysis issues.

References

1. 94/62/EC (1994), *Europ. Parliam. and Council Directive of 20 Dec. 1994 on packaging and packaging waste*
2. Anastasios Politis and Spyridon Nomikos, (2007), *Smart packaging printing - what do packaging printers need to know?, Advances in Printing and Media Technology, IARIGAI, Vol. XXXIII, Acta Graphica Publishers, Zagreb, pp 19-33.*
3. Anshuman A. Khardenavis, M. Suresh Kumar, Sandeep N. Mudliar, Tapan Chakrabarti, (2007), *Biotechnological conversion of agro-industrial wastewaters into biodegradable plastic, poly β-hydroxybutyrate, Bioresource Technology 98, 3579-3584*
4. Anthony L. Andrady, (2003), *Plastics and the Environment, John Wiley & sons publications*
5. Asa Rindlav-Westling, Mats Stading, Anne-Marie Hermansson, Paul Gatenholm, (1998), *Structure, mechanical and barrier properties of amylase and amylopectin films, Carbohydrate Polymers 36, 217-224*
6. Carmen Remunan-Lopez, Roland Bodmeier, (1997), *Mechanical, water uptake and permeability properties of crosslinked chitosan glutamate and alginate films, Journal of Controlled Release 44, 215-225*
7. G. Davis, J. H. Song, (2006), *Biodegradable packaging based on raw materials from crops and their impact on waste management, Industrial Crops and Products 23, 147-161*
8. Gaurav Kale, Rafael Auras, Sher Paul Singh, Ramani Narayan, (2007), *Biodegradability of polylactide bottles in real and simulated composting conditions, Polymer Testing 26, 1049-1061*
9. John Dawes, (2008), *Do Data Characteristics Change According to the number of scale points used? An experiment using 5-point, 7-point and 10-point scales, International Journal of Market Research 50 (1): 61-77*
10. Jong-Whan Rhim, Aristippos Gennadios, Curtis L. Weller et al, (1998), *Soy protein isolate-dialdehyde starch films, Industrial Crops and Products 8, 195-203*
11. Jurgen Lorcks, (1998), *Properties and applications of compostable starch-based plastic material, Polymer Degradation and Stability 59, 245-249*
12. Marios Tsigonias, (2005), *Study of complex polymeric membranes with additional alginate materials aiming in their possible use as packaging materials, M.Sc. thesis, National and Kapodistrian University of Athens (In Greek)*
13. Marios Tsigonias, Tamara Travinskaya et al, (2006), *Preparation and characterization of polyurethane-alginate thin films, National Centre for Scientific Research, first international workshop of the European Network of excellence INSIDE POReS, Montpellier, France*
14. Maurizio Avella, Jan J. De Vlieger, Maria Emanuella Errico et al., (2005), *Biodegradable starch/clay nanocomposite films for food packaging applications, Food Chemistry 93, 467-474*
15. Mauro Graziani and Paolo Fornasiero, (2007), *Renewable Resources and Renewable Energy -a global challenge-, Taylor & Francis Group*
16. Melisa Balkcom, Bruce Welt, Kenneth Berger, (2002), *Notes from the packaging laboratory: Polylactic acid- An exciting new packaging material, Institute of Food and Agricultural Science, ABE339*
17. PIRA International Ltd, ECOLAS N.V., (2005) *Study on Implementation of Directive 94/62/EC on Packaging and Packaging Waste and Options to Strengthen Prevention and Re-use of Packaging, Final Report 21 February 2005*
18. Plastic technologies PLC, (2006), - *Caribbean Environmental Protection, D2W Totally Degradable Plastics, Antigua & Barbuda*
19. Rensis Likert, (1932), *A Technique for the Measurement of Attitudes, Archives of Psychology 140: 1-55*
20. Sandra Rothenberg, Rafael Toribio, Monica Becker, (2002), *Environmental Management in Lithographic Printing, Printing Industry Center*
21. Symphony environmental technologies, (2007), *Sao Paolo*

Graphic design and environmental sustainability

Ivana Bolanča Mirković, Zvjezdana Vukić, Zdenka Bolanča

Faculty of Graphic Arts, University of Zagreb
Getaldićeva 2, HR-10000 Zagreb, Croatia
E-mails: ibolanca@grf.hr , zvukic@grf.hr, zbolanca@grf.hr

Abstract

Design for environment sustainability is promoting new qualitative criteria that at the same time are environmentally sustainable, socially and economically acceptable and culturally attractive.

In this work the investigation results are presented, which comprise the ecological approach to creation of the graphic product - poster, which has the role of promotional activity of the environment. In addition the optical characteristics of the digital print, i.e. the reproduction with the ecological message in the function of printing substrate choice and in context of the design sustainability are discussed.

The obtained results have proved the possibility of appreciation of the compact approach of integration creativity by incorporating the elements of visual arts, graphic and textual expression in the phase of poster design and propositions of the life cycle of the graphic product, appreciating the ecological responsibility of the design in the system of the sustainable development.

Keywords: graphic design, environmental sustainability, substrate, poster, prints characteristics

1. Introduction

The development of the ecological favourableness and the terms connected with the industrial design can be followed from end–of–pipe policies which include pollution treatments, up to the clean technologies and further to the redesigned products in so called low impact products [McDonough, Braungart, 2002]. The clean technology is a conceptual and procedural approach to production which demands that all the phases of the life cycle should be the aim of prevention and minimize of risks for people and environment. These technologies can be presented as the reduction of the produced waste quantity, more effective energy and resource usage and the production of environmentally acceptable products and services. The basic principles of strategy of the clean technologies are the principle of caution (call for decreasing the input of the anthropogenic pollutants into environment) the principle of prevention (introduction of exchanges upstream in standard net of production and consumption) principle of integration (adoption of complete observation of the production flow including the life cycle analysis of the product) and the principle of democracy (including the people in the way the production is organized) [Marten, 2004].

The role of the industrial design can be understood as the activity which connects the technical possibilities with the ecological necessities and it aspires to the significant socio-cultural propositions [Manzini, Collina, Evans, 2004]. In this segment four different interventions are essential: ecological redesign of the existing systems by choosing the material and energy with lower influence on environment, design of the new products and services by the substitution of the system according to ecological sustainability, design of the new products - consumption of the systems and creation of the new scenarios for the sustainable life style [Vezzoli, Manzini 2008].

Design for environment sustainability is promoting new qualitative criteria that at the same time are environmentally sustainable, socially and economically acceptable and culturally attractive [Charter, Tischner, 2008].

The conception of the green design comes out from the domain of the mentioned. It consists in searching the ecologically more favourable materials and processes which will result with smaller quantity of waste. Except that, the designer has to be observed as creator, builder of brand and communication with the aimed population which has a positive influence on the world. Designer is initiator of changes according to sustainable solutions.

Graphic design can have the role of the promotional mean in the environment protection. From the domain of poster with ecological contents, the ones of informative character are most often present (Faster, 2008; Rivers, 2007).

Such posters are met on scientific conferences, exhibitions and public and cultural manifestations. Poster that informs is sometimes connected to the narrow thematic area such as ecological problems of air or waters of a local character or to particular endangered plant or animal kinds. However, recently, the more frequent are the posters which inform about the global problems of the environment such as the greenhouse effect or destroying of the ozone layer (De Jong Burger, Both, 2008; Weil, 2004).

The poster of ecological contents can be engaged; it can warn or condemn the polluters, because of the systematic influence on environment (Batory, 2004). Except the mentioned, the essential role of a poster with the ecological contents is in education, especially of young people.

In this work the investigation results are presented, which comprise the ecological approach to creation of the graphic product - poster, which has the role of promotional activity of the environment. In addition the optical characteristics of the digital print, i.e. the reproduction with the ecological message in the function of printing substrate choice and in context of the design sustainability are discussed.

2. Experimental

The prints made on the digital printing machine based on electrophotography Xerox DocuColor 5000 with the dry toner. The test form consisted of standard CMYK wedges in the range from 10-100% RTV, standard ISO illustration, textual positive and negative microelements and standard wedges for the production of ICC profiles and 3D gamut.

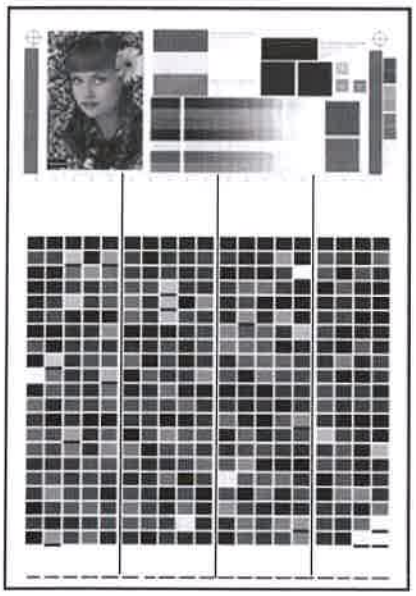

Figure1: Test form



Figure 2: Poster with the ecological message, author Z. Vukić

The presentation of the wedge containing 378 fields is important in printing form, which enables the getting of the ICC profile, i.e. 3D gamut. For measuring the spectrophotometer Xrite DTP-41, which works with the application Monaco profiler platinum was used.

Except the presented test form the poster with the ecological contents is printed on all mentioned substrates. It animates and incites to the concrete ecological action, forest protection by greater usage of waste papers with the application of recycling. Ecological message in this case is intentional, clear and unambiguous as it can be seen in figure 2.

The papers Flora (Gruppo cordenos) are used for printing. They are ones of most exclusive substrates containing the recycled fibers (composition: 50% of the recycled fibres, 40% of ECF cellulose and 10% of cotton). Flora Malto (sample 1), Flora Avorio (sample 2 and Flora Camoscio (sample 3) were used in investigations Looking at the paper surface one gets the impression that it was made from the recycled fibres, because the ink particles are visible on the surface, which are characteristics for the cases when they are not completely removed in the flotation process. The usage of paper is assigned for the production of prestigious editions, fine art reproduction, covers, greeting cards and luxurious packaging and similar. The application of such substrates is especially interesting in the case when the product has to be created in eco style. The surface of paper is treated with gelatine and it has high gloss.

The spectral reflectance curves in the area of the wavelengths from 390 to 710 nm as well as L*a*b* values are presented for the observed printing substrates.

Except the mentioned, the colorimetric difference ΔE was determined, which describes the reproduction quality and which shows deviation of the reproduction from the original. In indirect way, this value describes the loss and the deviation of the three stimulus information and the formula CIEDE2000 was used in the work for calculation [Luo, Cui, Rigg, 2001].

For determining the number, size and the surface of ink particles in the structure of paper samples were assessed with image analysis-based software systems: Spec*Scan (Apogee System). Spec*Scan system utilizes the flat-bed scanner Epson Perfection 2400 Photo to digitize image. Samples were scanned on both sides. Size intervals were defined according to TAPPI methods T 213 and T 437. Threshold value (100), white level (75) and black level (65) were chosen after comparing computer images to paper samples.

3. Results and discussion

In order to give the contribution to explanation of the composition influence and the surface properties of the printing substrate on the optical characteristic and print quality in figure 3, gamut of prints was presented. Gamut the whole information about colour, including the hue, saturation and lightness, which is possible to reproduce on the given medium are presented.

In figure 3, the gamuts of prints on the printing substrate with equal composition (50% of the recycled fibres, 40% ECF cellulose and 10% cotton) and different chromatic characteristic and different area the particles from paper structure (table I) are presented. The print on paper sample 2 has the greatest gamut, greater for 381,270 spatial units than the gamut of print on sample 1. Sample 1 contains the 220 times more ink particles on the substrate surface, which comprise the area for 71,049 mm^2 greater, in comparison with the sample 2. The mentioned samples differ sufficiently as well as in relation to the chromatic values a* and b*, as it is visible from the table II.

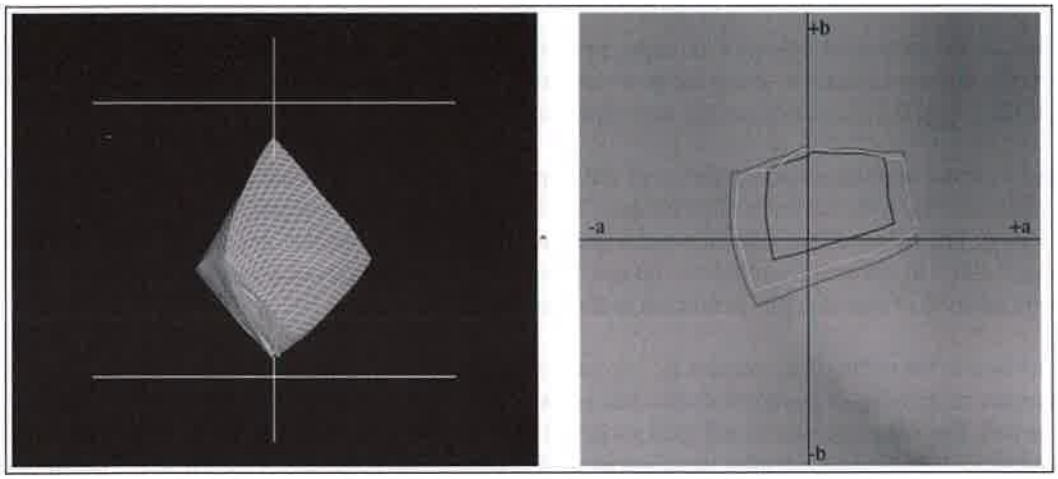

Table I: Results of image analysis

Sample	Total		Particles > 0,04 mm²		Particles < 0,04 mm²	
	Area/ mm²	Count of the particles	Area/ mm²	Count of the particles	Area/ mm²	Count of the particles
1	72,590	9246	30,032	270	42,599	8976
2	1,550	42	1,18	9	0,371	33
3	6,451	214	4.738	32	1.686	182

Table II: Characteristics of the printing substrates and prints gamut

Sample	Vol. of gamut	L*	a*	a*
1	244,155	81,431	10,275	29,192
2	625,525	94,535	1,058	13,12
3	503,358	93,29	3,161	23,677

In addition, the sample 1 shows extremely great decrease of the gamut surface in cyan towards red where the colours are near to achromatic point. In the area towards yellow the gamut of print corresponds approximately to other prints on the substrates 2 and 3 while in the area towards grebe and magenta it is decreased. On the prints on the substrates 2 and 3 the obtained gamut values are essentially more synchronized which means that the substrate has less influence on colour reproduction.

From the designer's point of view the presented data should mean that more saturated colours should be used and the tonality of the complementary ink area of that printing substrate (sample 1) should be avoided, if you want to achieve a good reproduction, as well as the illustrations with greater halftone values.

In the process of product creation, the ecological impact of the paper should be acknowledged which is essential for designers and which can be divided into three categories: fibre, water and energy issues.

Recent life cycle studies tend to favour recycling over both incineration and landfill [Villanueva, Wenzel, 2007]. The study compares the environmental impact of the system of disposing of paper and cardboard: recycling, incinerating and land filling, using of different impact categories for the environmental assessment (energy use, resource consumption, global warming, other energy related impacts, toxicity and waste generation). The results reflect that the environmental benefit of recycling is especially clear in the categories of energy use, waste generation, energy related impacts, waste water and importantly the reduction of carbon compounds emissions.

The recent report gives support to the economic benefit that paper recycling can provide. Effluents from recycled plants have less environmental impact than virgin pulp effluents. Heavy metals in the sludge have declined in line with a reduction in their use in inks and pigments.

In relation to the presented influence of paper production on the environment the designer can do things to minimize the negative impact by using the post-consumer recycled fibre, alternative fibres, totally chlorine free fibre and the use of the renewable energy sources in paper making.

In figures 4 - 6 the spectral reflection curves of different kinds of the non-printed paper as well as the reflection curves of the surface with full tones of particular CMYK colour separations of prints on the mentioned substrate are presented. The values of the reflection of the spectral curves point at similar optical properties of the printing substrates 2 and 3 in the area from 580 to 700 nm. The reflective properties of paper 1 are smaller in the whole measuring interval of wavelengths in relation to the samples 2 and 3.

On the surface of the paper of all samples the ink particles from the recycling process are noticed. In tables I and II the number of particles in paper structure, their surface, chromatic values a* and b* and the volume of gamut are presented. Optical properties in the contexts of the decreased reflection can be influenced by the surface of the ink particles which remained after recycling as well as colour characteristic of the surface. The investigation results show that the colour of the substrate and the presence of ink particles absorb the part of light and result

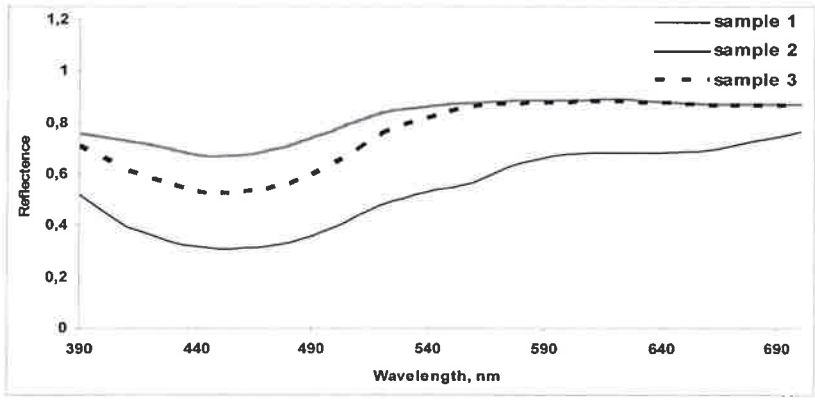

Figure 4: Spectral reflection curves of the printing substrates

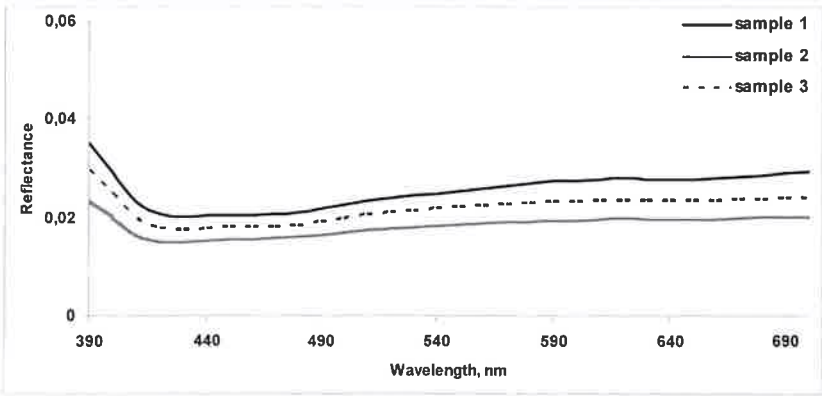

Figure 5: Spectral reflection curves of the prints for carbon

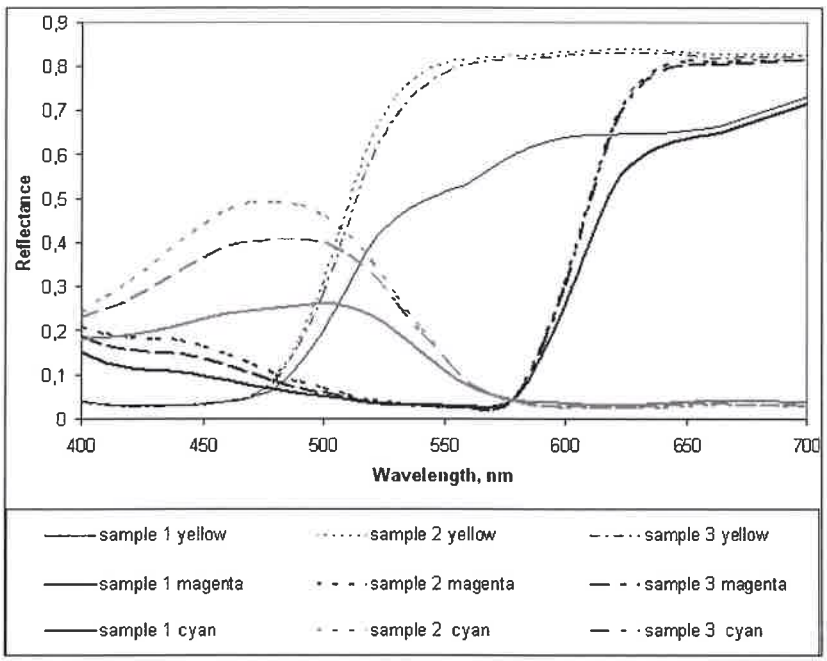

Figure 6: Spectral reflection curves of the prints for particular colours in CMY

The flows of the reflection curves for particular colours in CMY show the general characteristic property; they reflect only one part of radiation. When speaking about the print, the ink layer acts as filter where the radiation

The spectral reflection curve for cyan, because of the increased absorption of yellow and red light shows very small reflections in the area of wavelengths from 560 to 700 nm as well as for all the prints of almost the same values. The mild increase of reflection at shorter wavelengths in the area from 390 to 480 nm is most expressed for the print on the printing substrate 2. The smallest increase of reflection is noticed on prints on the substrate 1. Such result can be explained by greater number of the ink particles remained from the paper recycling process (9246), i.e. the surface they occupy (72,590 mm^2) in relation to other prints and mild decrease of surface property of the tested sample. The values of relative reflection can be influenced by the chromatic characteristics of the printing substrate. So the greatest reflection in the mentioned area of wavelengths has the print made on the substrate with the chromatic values a* = 1,056, b* = 13,12, and the smallest one has the print made on the substrate with a* 10,275 and b* 29,192.

The spectral curve for magenta is characteristic for the reflection of the long wave electromagnetic radiation over 600 nm and the absorption of green and blue light. In the area of shorter wavelengths 390 nm up to 500 nm there is a mild decrease of reflection with almost curve flows for all the samples. The arrangement of the reflection curves towards lower reflection values in relation to the samples has mutually similar value and the arrangement of curves is the same as in cyan. The increase of reflection appears above 580 nm and the samples on the printing substrates 2 and 3 have almost identical values different from the sample 5 which has smaller values especially in the area from 610 to 700 nm.

Contrary to that, the yellow colour reflects already from 500 nm and it absorbs only blue light and the reflection curve in the area from 390 to 480 nm has almost equal values for all the samples. The continuation of the reflection curves through all areas of the wavelengths for samples 2 and 3 differ very little in the area 500 - 540 nm. In this case it is again recognizable because of lower values of reflection at the wavelengths 480 - 700 nm, sample 1.

The reflection curves for black differ from other CMY colours because it absorbs almost completely electromagnetic radiation in the tested area of the wavelengths. The reflection curves presented in figure, as it can be seen, have the same flow for the investigated samples, and the samples mutually differ for similar value. The arrangement of samples is the same, as it was discussed earlier.

Chromatic differences appeared by using the different printing substrates can be determined by calculating the colour difference ΔE* among the prints of optimal reproduction and print sample which is chosen for analysis (Table III).

Table III: Colour differences for prints on the substrates 1 and 2 according to the print of optimal reproduction

	dE_{00} print with optimal reproduction vs. sample1	dE_{00} print with optimal reproduction vs. sample 2
C 100%	11,05	3,75
C 50%	22,31	7,43
M 100%	8,07	2,83
M 50%	16,98	7,02
Y 100%	10,94	1,70
Y 50%	12,41	2,79
K 100%	4,73	2,06
K 50%	14,35	7,21

From the point of view of graphic reproduction the colour difference ΔE* describes the deviation of three stimulus information and it gives the information about the print quality[12]. The evaluation of prints is performed according to the given criteria. The marks are from ΔE* between 0 and 1 - the deviation cannot be perceived to ΔE* exceeding 5 - massive deviation.

If the print with the optimal reproduction is compared with the print on the substrate 1 greater difference in colours with 50% coverage can be noticed than with colours with 100% coverage. The colour differences are greater than those on substrates 2 (table III). Such results mean that the printing substrate - sample 1 from the colour reproduction aspect is less favourable and that the change in colours will be greater on illustrations based on lighter and middle tones in regard to the darker tones. The colour differences are expressively great, so ΔE* is greater than 16 for magenta and cyan at 50% tone value. Such results confirm that at smaller surface coverage

4. Conclusion

With regard to the investigation results the following conclusions can be made:

- the smallest gamut is obtained for the print on paper with the following characteristics (sample 1): composition 50% recycled fibres, 40% ECF cellulose, 10% cotton; number of particles from recycling 9246, surface 72,590 mm^2; chromatic values: a* 10,257, b*13.12

- the greatest gamut is obtained for the print on paper with the following characteristics (sample 2): composition 50% recycled fibres, 40% ECF cellulose, 10% cotton; number of particles from recycling 42, surface 1,550 mm^2; chromatic values: a* 1,058, b*13.12

Sample 1 shows extremely great decrease of the gamut surface in cyan towards red where the colours are near to achromatic point. In the area towards yellow the gamut of print corresponds approximately to other prints on the substrates 2 and 3 while in the area towards green and magenta it is decreased.

The mentioned conclusions are confirmed with other investigation results. It was estimated that the sample 1 has great colour differences ΔE* especially for magenta and then for cyan (greater than 16 at 50% tone value). This paper is less favourable for reproduction in relation to other papers used in investigations. In application of this substrate the change in colours will be greater in illustrations based on lighter and medium tones in regard to the dark ones.

From the designer's point of view the presented data should mean that more saturated colours should be used if you want to achieve a good reproduction, as well as the illustrations with greater halftone values. Form the aspect of the design very effective particles of inks from recycling in paper structure give to that substrate advantage in the creation of the defined products. When the aim is to emphasize the mentioned facts, the investigation results confirm that in the case of less surface coverage, essentially greater influence of the substrate is achieved.

In the phase of the product creation, by choosing the right printing substrate the designer can contribute: to the attractiveness and message emphasis when speaking about the graphic promotional mean, to the quality of the technological product making as well as to the environment quality through the phases of the product life cycle.

The obtained results have proved the possibility of appreciation of the compact approach of integration creativity by incorporating the elements of visual arts, graphic and textual expression in the phase of poster design and propositions of the life cycle of the graphic product, appreciating the ecological responsibility of the design in the system of the sustainable development.

Acknowledgment

The work has been supported by the Ministry of Science, Education and Sports of the Republic of Croatia under grant 128-1281955-1953.

References

1. Batory, M., (2004). *Posters and Graphic Works*, S. Malik ID Pablishing, Foenix, Arizona
2. Charter, M., Tischner, U., (Ed.) (2008). *Sustainable solutions:developing products and services for the future,* Greenleaf, Sheffield
3. De Jong Burger, C. S., Both, J., (2008). *New Poster Art,* Thames & Hudson, New York
4. Faster, J., (2008). *Poster Design for the Next Century*, Rockport, USA
5. Luo, M. R., Cui, G., Rigg, B., (2001). *The development of the CIE 2000 colour-difference, Formula: CIEDE2000, Colour Research and Application, 26(5)340*
6. Manzini, E., Collina, E., Evans, E., (Eds.), (2004). *Solutions oriented partnership, how to design industrialised sustainable solutions,* Cranfield University, Cranfield
7. Marten, G. G., (2001). *Human ecology, Basic concept for sustainable development*, Earthscan, London

8. McDonough, W., Braungart, M., (2002). *Cradle to cradle. Remaking the way we make things,* North Point, New York
9. Rivers, C., (2007). *Poster Art: Innovation in Poster Design*, Rotovision, Swizerland
10. Thomson, B., (2002). *Printing materials*, PIRA Leatherhead
11. Vezzoli, C., Manzini, E., (2008). *Design for environmental sustainability*, Springer Verlag, London
12. Weil, A., (2004). *Graphics*, *A Century of Poster and Adverting Design*, Thames and Hudson, New York
13. Villanueva, A., Wenzel, H., (2007) Paper waste-Recycling, Incineration or Landfilling? A Reviev of Existing Life Cycle Assessments, *Weste Management* 27, 29-46

iPhone 3G typography

Blaž Rat

University of Ljubljana, Faculty of Natural Sciences and Engineering
Chair of Information and Graphic Technology
Snežniška 5, SI-1000 Ljubljana, Slovenia
E-mail: blaz.rat@ntf.uni-lj.si

Abstract

Using different mobile devices, we often come across the function anti-aliasing, which makes our typography look blurred, as we would be looking at a badly taken photo. The problem appears because of using fonts that were designed for printing and are not optimized for screen display. These are two different types of media and despite the fact we can find a compromise, the best screen fonts (used in small size) are created pixel by pixel.

iPhone 3G is an electronical device with, according to its size, a quite high screen resolution; nevertheless, the producer decided not to use pixel fonts as a device system font. They decided to use font Helvetica and hereby another question appears: Why not use Myriad Set, especially developed for them and which they use in all screen and print applications, instead of Helvetica?

Therefore, the purpose of this research was to define Helvetica as the system font of iPhone 3G, describe its advantages and weaknesses in comparison with Myriad Set font. We decided to check the suitability of individual font regarding device, screen and shown contents.

Keywords: iPhone 3G, Helvetica, Myriad Set, legibility, typography

1. Introduction

The company Apple has in the recent years also entered the telephony, music and video industry area. Their wide offer includes iPod players and a multimedia mobile phone iPhone 3G. The latter is the newest technological achievement of mobile technology and was introduced in the middle of the last year [Apple, 2009]. The device enables presentation of information and contents in a special way; it is not only about the visual appearance of the applications, usage of colours and animations, but also about the selection of typography.

The purpose of the research was to analyze why Apple decided to use Helvetica as the system font for iPhone 3G. The question is connected to the fact that Apple uses Myriad Set font as a standard, because it was developed (from Myriad font) especially for them and because it meets the criteria for on-screen display; and so does Helvetica.

The purpose of this research was therefore to define Helvetica as the system font of iPhone 3G, describe its advantages and weaknesses in comparison with Myriad Set font. We decided to check the suitability of individual fonts regarding the device, screen and shown contents. A special part was devoted to display and readability of fonts regarding phone position (horizontal or vertical). We wanted to find out whether Myriad Set could replace Helvetica and what factors influenced that decision. A research was carried out for this purpose, asking the interviewees about their opinion regarding fonts and readability in view of usability.

2. Anti-aliasing

Anti-aliasing makes possible that a user or reader gets the same feeling by looking at a screen as he would by looking at a printed page. This method is based on the description of the font outline, considering repeated colour shades that appear against background colour. Parts where font outline united with the background were united using middle hue values. In this way, we can create more smooth looking fonts, especially when using bigger font sizes. When working with smaller font sizes, anti-aliasing influences the entire letter, which makes

When horizontal and vertical lines align with the pixel frame, font looks sharp and solid, but if deviation from the pixel frame occurs and the font stretches over two or more lines, it looks foggy. In practice, a larger amount of text rarely aligns with the pixel frame in more than just a few parts, therefore, the rest of the text looks blurred.

The quality of anti-aliasing depends on numerous factors. Software developers use different technologies, techniques and algorithms which calculate optimal hue values for middle colour values of anti-aliased font outlines.

Due to conformity with pixel frame, made by screen pixels, pixel fonts adjust to the screen, there are no anomalies or worse readability of the text, respectively. With other fonts, namely with Helvetica, it is just the opposite; letters are made of lines different from angles 0°, 45° or 90° and additional adjustment is therefore needed.

Letters whose parts do not align with pixel frame require processes taking time and additional capacity of the device. Helvetica is a part of so-called "smartly designed fonts" as its lines mostly stick to or adjust to the frame and thus its display is satisfactory. Adjustment is mostly made with the use of colour and shade that make the edges appear smooth. Therefore, for the black letter on white background between 16 to 20 intermediate shades of grey colour is used for such smoothing, which gives the letter the right image for viewing from a normal distance. The process is the same for colour versions of font and background. This way is possible only if the screen of the device supports 16-byte colour display. If the screen shows 8-byte display or only 256 colours, all intermediate shades are lost and are replaced by colours that correspond to the so-called web palette. Figure 1 shows how individual pixels pixelized in an 8-byte display.

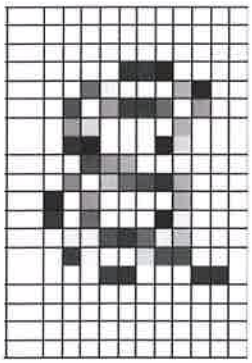

Figure 1:
Magnified view of the arrangement of individual pixels on the pixel frame for the sign »&« [Joe Gillespie, 2009]

This way is completely acceptable for larger fonts and bold versions; the problem between the pixel frame and font increases with decreasing the font size. Helvetica avoids this problem in two ways. In the first way, the basic line is levelled with the pixel frame (on account of the sign proportionality) and it is called 'hinting'. In the second way, the actual position of the basic line is simulated, where again shade illusion is used for edge smoothing. To achieve the impression of a line positioned precisely between two pixels, brighter shades of colours, used in neighbouring pixel lines, are used [Joe Gillespie, 2009]. To show smaller font sizes, it is thus better to use well designed screen fonts or pixel fonts, respectively. Apple was also aware of this fact and did not use Helvetica is smaller size than 8. With this size anti-aliasing still does its job satisfactory and shows the user a font sharp and recognizable enough.

3. Methods

The research was done in the form of anonymous questionnaire that referred to the photographs of iPhone 3G screen which showed the same contents with help of two different fonts: Helvetica and Myriad Set. The comparison of fonts on screens of iPhone 3G was projected to a larger screen via beamer. The distance between interviewees and the screen was calculated according to the ratio as if they were holding the iPhone 3G in their hands. While using iPhone 3G, the average distance between the device and the eye is 50 cm (the device measures 11.5 x 6.2 cm). When projecting the contents on the screen, the distance between the observer and the contents was 375 cm (the size of the projected device amounted to 86.2 x 46.5 cm). The research was carried out among a group of students, working in the field of graphic technology at the Textile department of the Faculty of Natural Sciences and Engineering in Ljubljana. The group is confronted with this technology on a daily basis, they are familiar with iPhone 3G device and the Apple (and Mac family) environment. They are also familiar

A pilot study was done first, including 10 interviewees. No problems were noticed during the pilot testing, the testing therefore continued. 50 people participated in the research (n=50), all of them completed the whole questionnaire and were thus included into further analysis. Collected data was statistically processed and a thorough analysis, explanation and formulation of gathered data was made. A combination of suitable scientific methods was used, including the most important such as the inductive method, the analysis and synthesis method and the statistic method. A statistic analysis was performed with help of questionnaire program tools.



Figure 2: Example of the projected photograph of iPhone 3G screen showing the same contents with help of two different fonts: Helvetica (example A) and Myriad Set (example B)

4. Results and discussion

Analysis showed that the interviewees were mainly female (72%); only 28% were male. In a more detailed way: 50% of the interviewees were between 19 and 21 years old, 44% were between 22 and 24, 4% between 25 and 27 and 2% 27 years or older.

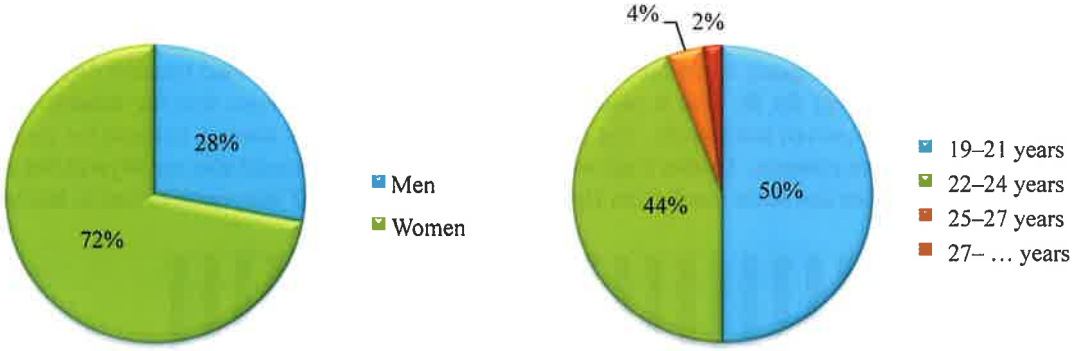

Figure 3 and 4: Gender and age analysis of the interviewees

Results confirmed our expectations that the majority of interviewees were familiar with iPhone 3G device, because 92% responded positively to that question. Additional confirmation was presented through results of questions related to familiarity with functions that the device offers. Most frequent answers: telephony (46 interviewees), internet (45 interviewees), SMS (43 interviewees), audio contents (41 interviewees), e-mail (38 interviewees) and playing video contents (36 interviewees). The same number of people thought that taking photos and multi-touch screen can also be found among the basic functions (36 interviewees). A slightly lower number stated Wi-Fi and GPS (28 interviewees), Bluetooth (27 interviewees), voice call (23 interviewees) and EDGE technology (12 interviewees). While 4 interviewees also knew some other functions beside the above

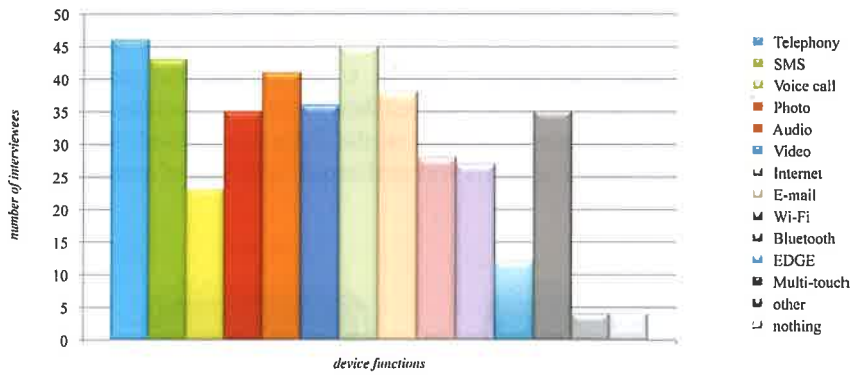

Figure 5: Familiarity with iPhone functions

The next set of questions referred to general knowledge and opinion of used fonts. Results show that the selection of font types for electronical devices is a well thought-out decision, based on many tries and research. The number of mobile phone devices grows daily; the number of font types is also increasing. As a rule, it is the use of pixel fonts that enable a clear display and are adjusted to the screen frame composed by pixels. But there are also more and more devices that are trying to break away from pixel fonts; new and powerful high-resolution screens enable users to use more than one type of fonts. We can thus show the contents in a different and more attractive way, which is very important for the user. 92% of all interviewees believe that the selection of font type matters, only 8% did not pay a lot of attention to it. The same percentage also responded to the question on suitability of the font type that is used as the system font at iPhone 3G. The research results thus prove that the selection was appropriate and that experience and opinions of users were considered.

The results show that Apple also landed an important coup with the selection of font colour compared to its background; 100% of the interviewees believed the combination of letters and the background to be just right and that it considerably influenced the readability of the text.

What followed was a group of 25 questions which referred to the comparison between examples A and B. They differed regarding the used font, but the contents were the same in both. Example A used Helvetica (Apple iPhone 3G system font), example B used Myriad Set, which is used by Apple in its corporate identity.

Research showed that the company made the right decision when choosing Helvetica because 54% opted for example A, while 46% went for B. This is also confirmed by t-test which shows that the relation between examples A and B can be proven statistically. The percentage differed, which is normal, because the readability also depends on the shown contents. To sum it up; we can conclude that Apple could also use Myriad Set as their system font because it does not differ much from Helvetica and a large share of interviewees was in favour of it.

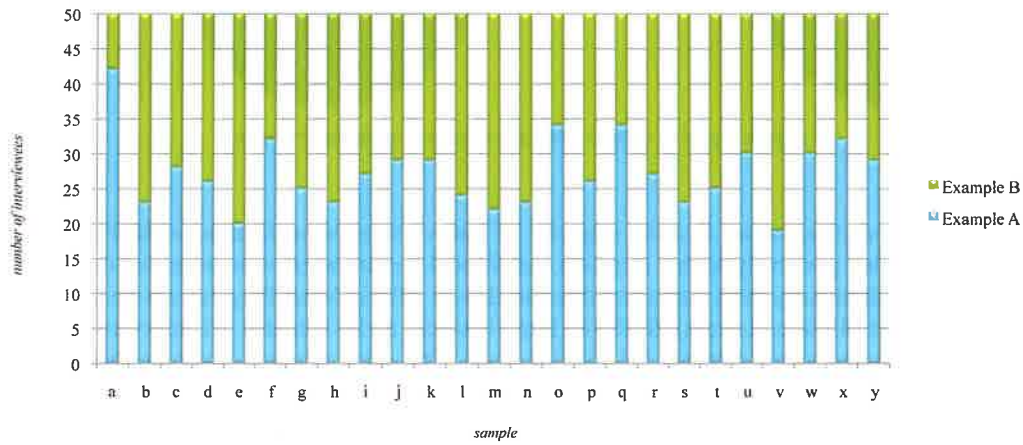

This thesis is even further supported by results that refer to the question of contents and used fonts regarding the positioning of iPhone 3G. Certain contents can be viewed in 2 ways; vertically (example A) and horizontally (example B). 61% of interviewees chose example B, 39% went for example A.

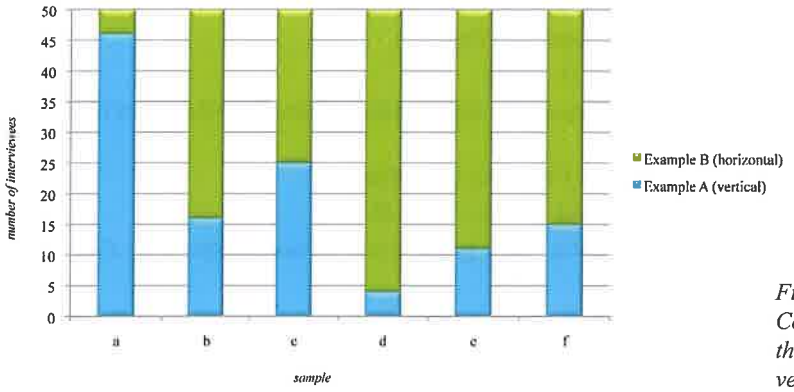

Figure 7:
Contents and used fonts regarding the positioning (horizontal or vertical) of iPhone 3G

The reason might be in general recognition of the font, which is also shown in this research, where 32% of all interviewees recognized Helvetica. 20% opted for Arial, 8% for Verdana, 2% for Myriad Set, 12% for none of the above, 26% did not know which font was used in example A.

Myriad Set showed even worse results in example B because only 4% recognized it. A larger share again opted for Verdana (12%), Arial (10%) and Helvetica (6%). The largest share shows those who opted for a different font type or did not know what font was used (68% in total).

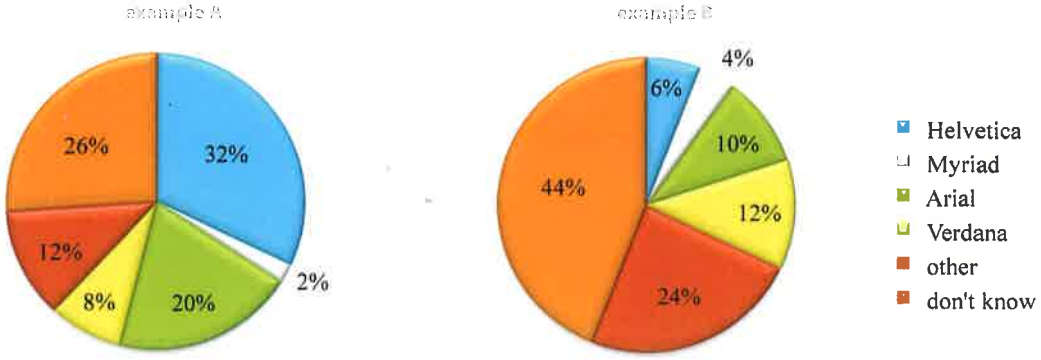

Figure 8 and 9: Recognition of the font in example A and example B

5. Conclusion

This research work tackles a concrete question and respective answers that offer interesting results. It is not only about analysis of the current situation but also about the analysis of the situation and events that will occur in the future.

It was proven that Apple's decision about using Helvetica is right and wrong at the same time. The font looks professional, it is readable and emphasizes the quality of user interface. However, we always have the same question: Why have they not used the Myriad Set? This font works well on the screen (depending on the contents); much better than Helvetica in the horizontal position. An additional argument is that this is also the primary font of Apple which should be used in all areas.

This did not happen with a brand new iPhone 3GS that came out this June, but it might happen with the next product coming out of Apple and results of this research might be valuable while planning it.

References

Printed sources

1. Buckley, P. 2007. *The rough guide to the iPhone.* London: Penguin Books
2. Götz, V. 1998. *Color and type for the screen.* Crans: RotoVision SA
3. Horvat, M. 2007. *iPhone.* Monitor, Vol. 17, No. 11, pp. 22
4. Kommer, I., Mersin, T. 2002. *Typografie und Layout für digitale Medien.* München Wien: Carl Hanser Verlag, pp. 109-143
5. Možina, K. 2003. *Knjižna tipografija.* Ljubljana: University of Ljubljana
6. Robar, V. 2007. *iPhone brez telefona.* Monitor, Vol. 17, No. 12, pp. 36
7. Robar, V. 2007. *Hello, iPhone - What You Need to Know about Apple's Groundbreaking New Gadget.* Macworld, Vol. 3, pp. 54-61
8. Zwick, C., Schmitz, B. 2003. *Digital Color for the Internet and other Media.* Crans-pres-Celigny: AVA Publishnig

Web sources

1. Apple. *iPhone.* January 2009 <*http://www.apple.com/iphone/*>
2. Gillespie, Joe. *Pixel Fonts Explained.* December 2008 <*http://www.bestflashanimationsite.com/tutorials/2*>
3. Gillespie, Joe. *Typography.* January 2009 <*http://www.wpdfd.com/issues/23/typography/*>

Visualization of large font databases

Martin Solli and Reiner Lenz

Linköping University, Sweden
ITN, Campus Norrköping, Linköping University, SE-60174 Norrköping, Sweden
E-mails: Martin.Solli@itn.liu.se, Reiner.Lenz@itn.liu.se

Abstract

We describe a novel system for interaction with large font databases. The system is an efficient tool for browsing in large font databases and as such it can be used by people in the Graphic Arts industry. The proposed approach is based on shape descriptors developed for visual characterization of character images rendered from different fonts. Here the descriptors are used in a visualization of a large font database containing more than 2700 fonts. By applying geometry preserving linear- and non-linear manifold learning methods, in combination with a refinement process, character images of different fonts are organized on a two-dimensional grid, where fonts are positioned based on visual similarity.

Keywords: font selection, visualization, dimensionality reduction, image analysis

1. Introduction

Selecting an appropriate font for a print job, or some other Graphic Arts application, can be a difficult and time consuming process. With the number of available fonts increasing, the task will become even more demanding. Consequently, we need to find new ways of finding and selecting fonts in large font databases. One solution is to visualize the entire font collection in a transparent way, where the user easily can locate fonts with a desired appearance. Such visual overview of all fonts in the database might be helpful for various persons who are employed in the Graphic Arts industry, both those who are managing and selecting fonts in their daily work, and temporary users. The visualization is a challenging task, especially if the size of the database is large. We describe how to use the findings from the font recognition study presented in Solli and Lenz [2007], in the design of a visualization tool for large font databases. The basic idea with the method is to order all images of a given character in the different fonts in a transparent way, giving the user an opportunity to effectively interact with the database. As starting point we use the high-dimensional vectors (41 dimensions) obtained from Solli and Lenz [2007]. Then linear and non-linear mappings are used to project the 41-D space of all images of a given letter to a two-dimensional manifold. Using a two-dimensional representation is rather natural since we want to use a conventional monitor as display device. Finally we describe a refinement process that maps these raw two-dimensional representations to a regular two-dimensional grid to avoid overlapping images and provide a better overview for the user. The performance is illustrated with a large database consisting of 2755 fonts for the English alphabet.

Font selection in general seems to be forgotten by the research community. With this work we intend to initiate a discussion on how to simplify font selection. The proposed method should be interpreted as a pilot study and inspiration for future research. As a complementary tool to the earlier developed font recognition system, the visualization system will be implemented on our publicly available website: http://media-vibrance.itn.liu.se/fyfont.

The paper is organized as follows. In Section 2 we give a brief overview of some previous attempts in font recognition and image database visualization. In Section 3 we describe the database used, the shape descriptors, and the method for calculating similarity between different fonts. Section 4 contains a description of dimensionality reduction methods used to obtain a two-dimensional representation of the characters, and Section 5 describes how coordinates are mapped to a two-dimensional grid. The results obtained from the experiments are illustrated in Section 6. We discuss the results and give some conclusions in Section 7.

2. Related work

Research in font recognition used mainly two strategies: a local approach based on features for individual characters or words, and a global approach using features for blocks of text. An example of the local approach

describing font clustering and cluster identification in document images can be found in Östürk et al. [2001]. Four different methods (bitmaps, DCT coefficients, eigencharacters, and Fourier descriptors) are evaluated on 65 fonts. All tested methods resulted in adequate clustering performance, but the eigenfeatures result provided the most compact representation. Another contribution to font recognition is Morris [1992], considering classification of typefaces using spectral signatures. A classifier capable of recognizing 100 typefaces is described by Baird and Nagy [1994], resulting in significant improvements in OCR-systems. In Cooperman [1997] font attributes such as "serifness" and "boldness" where estimated in an OCR-system. In a global approach by Zhu et al. [2001], text blocks are considered as images containing specific textures, and Gabor filters are used for texture recognition. The authors conclude that their method is able to identify more global font attributes, such as weight and slope, but less appropriate to distinguish finer typographical attributes. Similar approaches with Gabor filters can be found in Ha et al. [2005] and Yang et al. [2002]. Also Avilés-Cruz et al. [2005] describes an approach based on global texture analysis. Features are extracted using third and fourth order moments.

To our knowledge, only one commercial search engine is available for font recognition or selection: WhatTheFont. The engine is operated by MyFonts.com. An early description of the method can be found in Sexton et al. [2000]. Fonts are identified by comparing features obtained from a hierarchical abstraction of binary character images at different resolutions. We are not aware of newer, publicly available, descriptions of improvements that are probably included in the commercial system. A competitor is TypeDNA [http://www.typedna.com]. They are developing tools that can be used for recognising and finding fonts, and also for visualising a collection of fonts. However, their products have not yet reached a public release.

As mentioned in the previous section, the font selection task in general received little attention from the research community. Here we mention a few examples regarding visualization of image database content, not particularly focusing on font databases. Nguyen and Worring [2004] present a method for similarity based visualization based on three criteria: 1) The displayed images should show a general overview of the whole dataset, 2) the original structure of the data should be preserved, and 3) reduce image overlap as much as possible. They use the SNE (Stochastic Neighbour Embedding) and the ISOMAP method for preserving neighbour identities. Moghaddam et al. [2001] visualize retrieved images on a 2-D screen not only in order of their decreasing similarities, but also according to their mutual similarities. Images are converted to feature vectors based on color moments, wavelet based textures, and water-filling edge features. They use PCA for reducing the dimensionality of the feature space to only two dimensions (using the two eigenvectors corresponding to the two largest eigenvalues), and then, to minimize the overlap between images, a constrained nonlinear optimization approach is used.

For non-conventional browsing in image databases we mention Torres et al. [2003], where images are placed on concentric rings or spirals. The motivation for using such shapes is that they make it easier to keep user focus on both the query image, and the most similar retrieved images. The query image is placed in the centre of the spiral or rings, and retrieved images are placed on surrounding rings depending on similarity (images with high similarity close to the centre). In Heesch and Rüger [2004] three different interfaces are presented and evaluated. First an interface where images are displayed in the form of a spiral, with image distances from the centre being proportional to the distance to the query image in feature space. The second interface uses basically the same approach, but images in the periphery are displayed at a smaller size. By placing images from the centre and outwards, the method avoids overlapping images. In the final approach a pre-selection task is utilized where the user is shown a set of nodes (images) that are representative for different collections of images. Clicking on one of the nodes recovers the set of nearest neighbours from the database, which are then displayed such that their distances to the centre are proportional to their dissimilarity to the selected node. Within a query the user can easily move between interfaces for a better understanding of the search result.

3. Font recognition

This section contains a brief summary of the font recognition method presented in Solli and Lenz [2007]. The findings are used as input to the dimensionality reduction procedure described in the next section. We will use a database containing 2755 different fonts, where every character in a font is represented by an image. A few examples of character 'a' can be seen in Figure 1. We choose to represent each image by a coordinate vector based on principal component analysis, an approach frequently used in other applications. This method was popularized by Turk and Pentland in [1991] where they applied it on face images, and called it the eigenface approach. In our application we will call it the eigenfont representation, and use it as follows. All characters in

the database are in a given orientation and are given by gray value images. They are however of different sizes and in a first step all images of a given character are therefore resized to a fixed image size.



Figure 1: Examples of character a

Images of characters from different fonts are quite similar in general; therefore images can be described in a lower dimensional subspace. The principal component analysis (or Karhunen-Loéve expansion) reduces the number of dimensions, leaving only the features that are most important for font classification. Eigenvectors and eigenvalues are computed from the covariance matrix of each character in the original database. The eigenvectors corresponding to the K highest eigenvalues describe a K-dimensional subspace on which the original images are projected. The coordinates in this low-dimensional space are stored as the new descriptors. The first five eigenimages for character 'a' can be seen in Figure 2.



Figure 2: First five eigenimages for character a (normalized gray values)

The shape of a character can obviously be described by its contour. We use this observation and filter the character images with different edge filters before calculating eigenimages. We applied several filters and found that a combination of a horizontal and two diagonal filters resulted in the best recognition results. Vertical filtering did not improve the performance, probably because many characters contain almost the same vertical lines. Summarizing the results of these experiments we decided to represent characters by vectors in a 41-dimensional feature space, where the distance between two points describes the similarity between those fonts. Table I provides an overview of the final combination of different parameters and settings included in the recognition method. Details can be found in Solli and Lenz [2007].

Table I: An overview of the final combination of different parameters and settings included in the recognition method

Image scaling:	Square images, size 24x24 pixels, for "square characters" like a, e, and o, and rectangular images, for instance 24x20 pixels, for "rectangular characters" like l, i, and t. Characters are aligned and scaled to fill the whole image. We use bilinear interpolation for scaling.
Edge filtering:	Three Sobel filters, one horizontal and two diagonal
Number of eigenimages:	40
Extra feature:	Ratio between character height and width before scaling

4. Dimensionality reduction

After the process of feature extraction described in the previous section, every character in the font database is represented by a 41-dimensional feature vector, which will be mapped to a two-dimensional surface. To be meaningful this mapping must preserve the intrinsic geometrical structure (visual similarity) of the original representation space. In the following we will illustrate two examples of such mappings, one linear, and the other non-linear. The linear mapping is simply a selection of the second and third component in the PCA coordinate space (the first coordinate has very little visual information related to font appearance). In many applications linear mappings are too restrictive since they cannot take into account that the actual data vectors may be located on a lower dimensional manifold embedded into a higher dimensional space. In the simplest example of such a situation the data vectors are all located on a two-dimensional circle. Traditional PCA will always indicate that the data is two-dimensional and will need two principal components to represent the data. These two-dimensions are, however, only a consequence of the coordinate system used to describe the data. Selecting a polar coordinate system with origin at the centre of the circle will reveal that the radial value for all data vectors is constant and that the data can be represented by the angle without information loss. In this simple example it is clear how to choose the coordinate system in which the lower-dimensionality of the data becomes obvious. In the general case it is however very difficult to estimate the intrinsic dimensionality of the data and to construct non-linear mappings to achieve this reduction. This problem is known as manifold

learning in the machine learning community [see http://www.math.umn.edu/~wittman/mani/ for an overview of different methods].

In our experiments we mainly worked with the ISOMAP algorithm described in Tenenbaum et al. [2000]. The ISOMAP (isometric feature mapping) estimates the true distance between two data points by first linearly fitting neighbouring points. Then these local approximations are patched together and the shortest paths connecting any two points is computed. In the final step this table of approximations of the geodesic distances between point pairs is used to embed the data points into a low-dimensional subspace such that the intrinsic geometry is preserved as much as possible.

Many powerful tools for both linear and non-linear dimensionality reduction have been presented in the past. Well-known examples are SOM, or Self-Organizing Maps, also known as the Kohonen Maps [see http://www.cis.hut.fi/projects/somtoolbox/], Locally Linear Embedding (LLE) by Saul and Rowels [2004], and Laplacian Eigenmaps by Belkin and Niyogi [2002]. Preliminary experiments with Self-Organizing Maps gave no improvements compared to the PCA or ISOMAP approach. However, the performance of the SOM algorithm seems to improve if rather few of the dimensions included in the original dataset (totally 41 dimensions) are used as input. Possibly, the explanation is related to the conclusion made by De Backer et al. [1998], that SOM performs better for very low number of dimensions. The method might be more suitable in a classification task, where the obtained code vectors (also known as model vectors or prototype vectors) provide the classes. In general, the use of different dimensionality reduction methods should be investigated further in future research.

5. Grid representation

The dimensionality reduction technique (both PCA and ISOMAP) results in a visualization in which large parts of the space are relatively empty while others are crowded. For many purposes a more ordered presentation will provide a better overview of the font database. Our solution is to evenly distribute images on a square grid, while at the same time trying to maintain mutual relations. The following algorithm was used to compute such an ordered display.

Let M be the matrix containing the font indices: $k = M(r,c)$ means that font number k is presented at position (r,c) in the display. We use an almost square-formed display leading to a matrix of size $52x53$ for the 2755 fonts. The matrix P contains the coordinates of the characters as computed by PCA or ISOMAP: the vector $(P(i,1),P(i,2))$ contains the coordinates for character images i in the two-dimensional space obtained by the PCA or ISOMAP transformation. The coordinates in P are first scaled to fit the size of M. Each element in M will be assigned an image index i corresponding to the nearest neighbour in P. The algorithm used is as follows:

Starting with the top row, for every position (r, c) we do the following:

I. Find the index i giving the minimum Euclidean distance between $M(r,c)$ and $P(i)$, where $i=1,...,2755$.
II. Move the image at coordinates $P(i)$ to $M(r,c)$.
III. Mark the index $P(i)$, so it can not be relocated.
IV. If we have not reached the end of the row increase the column index by one and go to step I, if we have reached the end of the row, reset the column index to 1 and go to the next row.

6. Results

In Figure 3 and Figure 4 we show all the font images for character 'a' (for 2755 fonts) at coordinates obtained from the PCA respectively ISOMAP representation. It can be seen that the ISOMAP reduction seems to better divide different types of fonts into different clusters, and fewer images are overlapping. In Figure 5 and Figure 6 PCA and ISOMAP results for character 'a' are converted to grid representations, as described in Section 5.

We also tested if the ordered representations could be improved by further optimizations. For this purpose we selected two points in an ordered representation described above. If we could improve the presentation by swapping these two points then the accumulated distances between these two points and their neighbours would decrease after the swapping compared to the same accumulated distance before the swapping. We created

a large number of random pairs for swapping and systematically tested swapping points located near each other. In none of the cases we could observe a reduction of the distances after swapping. This indicates an optimal local solution of the selected ordering method. An optimal global solution, which can be searched for in upcoming research, would require for instance a more exhaustive swapping method where accumulated distances are calculated over the entire grid.

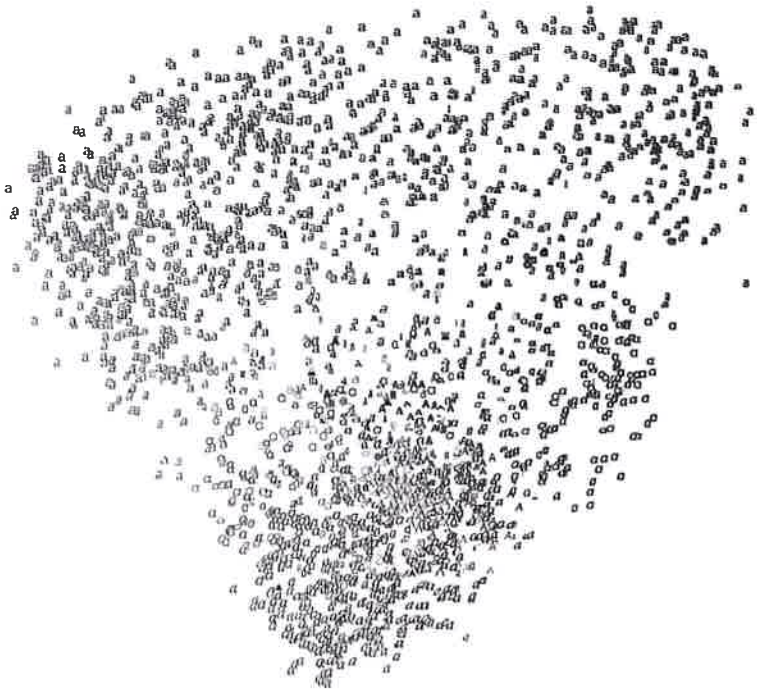

Figure 3: A visualization of all characters 'a' in the database based on the second and third PCA coefficients



Figure 4: A visualization of all characters 'a' in the database based on ISOMAP manifold learning

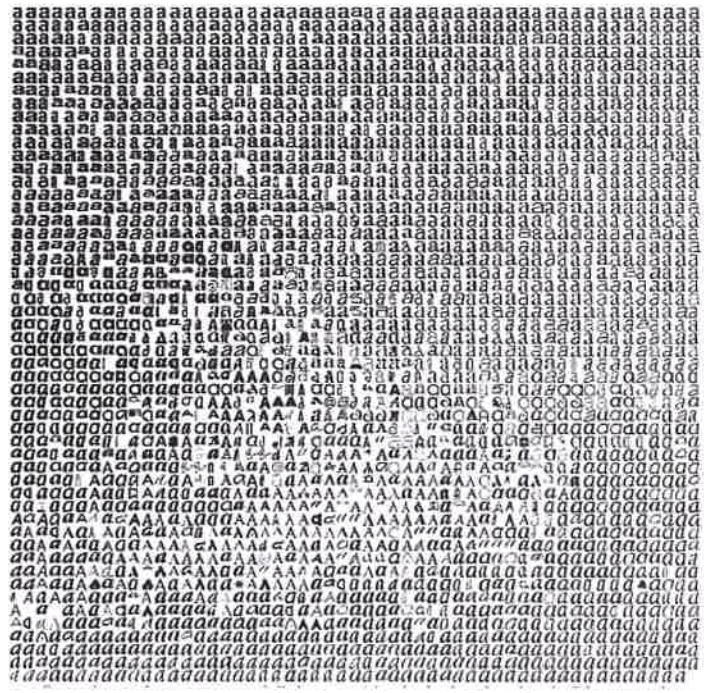

Figure 5: A grid representation of all characters 'a' in the database based on the PCA approach

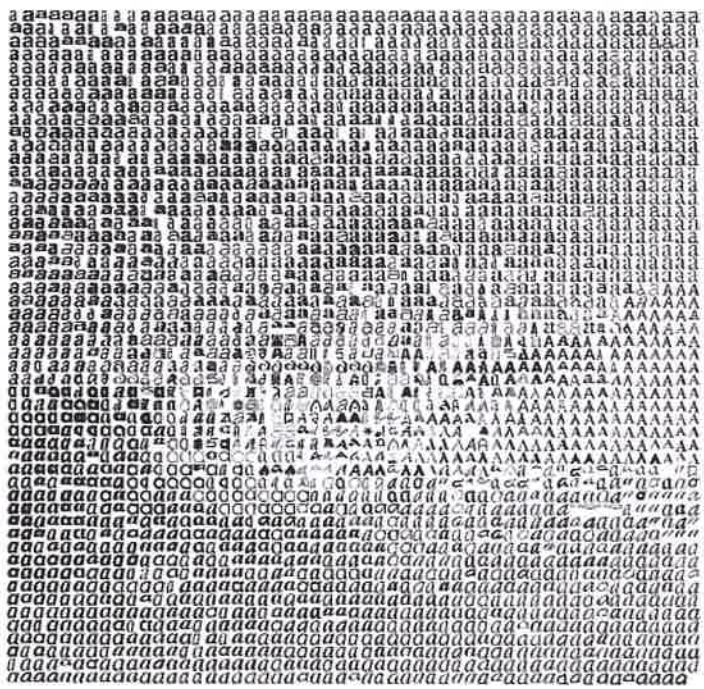

Figure 6: A grid representation of all characters 'a' in the database based on the ISOMAP representation

7. Discussion and conclusions

A novel system for interaction with large font databases has been described. Shape descriptors obtained from related research have been applied in the visualization of a large font database containing 2755 fonts. It was shown that geometry preserving linear- and non-linear manifold learning methods can be used for mapping the structure of the high-dimensional feature space to a two-dimensional manifold. To avoid overlapping font images and provide a better overview for the user, a refinement process is utilized, where the raw two-dimensional representation is mapped to a regular 2-D grid. A visual evaluation of the image grid obtained from

the ISOMAP reduction, shown in Figure 6, reveals that different font styles are clearly separated. In the upper left corner mainly bold characters are located. The upper right corner is dominated by the regular style. Similar regions can be found for italic, "small caps", etc. We believe the proposed method can be implemented in an interface used by, for instance, people in the Graphic Arts industry, as an efficient tool for browsing in large font databases. The user can relatively quick find a group of interesting fonts, and study these in more detail. In the final application, the idea is that the user can zoom in on parts of the space for studying a few fonts more closely, and then obtain names, and possibly more characters, for specific fonts. An example is illustrated in Figure 7.



Figure 7: An illustration of the intended usage of the visualization method. The user can zoom in on a selected area of the grid, and by clicking on a font image, the user will obtain the name of the font together with a few more characters

A topic for further research is to extend the method to utilize more than one character in the visualization. Moreover, the proposed method should be evaluated in user tests to clarify if people find the system useful, and how they interact with it. Another topic do be dealt with in future work is the method for dimensionality reduction. There are many tools for both linear and non-linear dimensionality reduction and our preliminary experiments with Self-Organizing Maps reveal no improvements compared to the PCA or ISOMAP approach. Nevertheless, the use of different dimensionality reduction tools should be investigated further. One can also think of using other methods as a pre-classifier, and then for instance apply ISOMAP on individual classes to obtain a final visualization grid.

References

1. Avilés-Cruz, C., Rangel-Kuoppa, R., Reyes-Ayala, M., Andrade-Gonzalez, A. and Escarela-Perez R., (2005), *"High-order statistical texture analysis - font recognition applied", Pattern Recognition Letters,* 26(2), 135-145
2. Baird, H. S. and Nagy, G., (1994), *"Self-correcting 100-font classifier", in Proceedings of SPIE,* 2181, 106-115
3. Belkin, M. and Niyogi, P., (2002), *"Laplacian eigenmaps and spectral techniques for embedding and clustering", in Advances in Neural Information Processing Systems* 14, 585-591
4. Cooperman, R., (1997), *"Producing good font attribute determination using error-prone information",* in SPIE, 3027, 50-57
5. De Backer, S., Naud, A. and Scheunders, P., *"Non-linear dimensionality reduction techniques for unsupervised feature extraction", Pattern Recognition Letters* 19, 8, 711-720
6. Ha, M. H., Tian, X. D. and Zhang, Z. R., (2005), *"Optical font recognition based on Gabor filter", in Proc. 4th Int. Conf. on Machine Learning and Cybernetics,* 8, 4864-4869
7. Heesch, D. and Rüger, S., (2004), *"Three interfaces for content-based access to image collections", Lect. Notes Comput. Sci.,* 3115 LNCS, 2067
8. Nguyen, G. and Worring, M., (2004), *"Optimizing similarity based visualization in content based image retrieval", in 2004 IEEE International Conference on Multimedia and Expo, ICME04,* 2, 759-762

9. Moghaddam, B., Tian, Q. and T.S., Huang, (2001), *"Spatial visualization for content-based image retrieval", in 2001 IEEE International Conference on Multimedia and Expo,* ICME01, 22-25
10. Morris, R. A., (1992), *"Classification of digital typefaces using spectral signatures", Pattern Recognition,* 25(8), 869-876
11. Saul, L. and Rowels, S., (2004), *"Think globally, fit locally: Unsupervised learning of low dimensional manifolds", J. Mach. Learn. Res.,* 4, 119-155
12. Sexton, A., Todman, A. and Woodward, K., (2000), *"Font recognition using shape-based quad-tree and kd-tree decomposition", in Proceedings of the Fifth Joint Conference on Information Sciences, JCIS 2000,* 2, 212-215
13. Solli, M. and Lenz, R., (2007), *"FyFont: Find-your-font in large font databases", 15th Scandinavian Conference on Image Analysis, SCIA 2007, Lect. Notes Comput. Sci.,* 4522 LNCS, 432-441
14. Tenenbaum, J., De Silva, V. and Langford, J., (2000), *"A global geometric framework for nonlinear dimensionality reduction", Science,* 290, 2319-2323
15. Torres, R., Silva, C., Medeiros, C. and Rocha, H., (2003), *"Visual structures for image browsing", in Proceedings of the 12th ACM International Conference on Information and Knowledge Management,* CIKM 2003, 49-55
16. Turk, M. and Pentland, A., (1991), *"Eigenfaces for recognition", Journal of Cognitive Neuroscience,* 3(1), 71-86
17. Yang, F., Tian X. D. and Guo B.L., (2002), *"An improved font recognition method based on texture analysis", in Proc. 1st Int. Conf. on Machine Learning and Cybernetics,* 4, 1726-1729
18. Zhu, Y., Tan, T. N. and Wang, Y. H., (2001), *"Font recognition based on global texture analysis", IEEE T-PAMI,* 23(10), 1192-1200
19. Östürk, S., Sankur, B. and Abak, A. T., (2001), *"Font clustering and cluster identification in document images", Journal of Electronic Imaging,* 10(2), 418-430

A product semantic study of the influence of touch and vision on the evaluation of different paper grades

Siv Lindberg and Annika Kihlstedt

Innventia AB
P. O. Box 5604, SE-114 86 Stockholm, Sweden
E-mails: siv.lindberg@innventia.com; annika.kihlstedt@innventia.com

Abstract

There is a growing awareness in marketing today of the importance of sensory information in the evaluation of products. Functional attributes and product benefits are no longer enough in order to attract and commit the consumers. In the paper industry this translates to explore in which way the consumer perceives added value and how smelling, hearing, seeing, tasting or touching can enhance the interaction with printed products. The objective of present study was to create an inventory of the haptic and visual sensory impressions for different paper grades. Unimodal tactile and visual exploration of LWC, MWC, SC, copy paper, newsprint and book paper was performed. Paper grades were rated on seven point semantic scales consisting of the attributes Elegant, Exciting, Masculine, Modern, Feminine, Smooth, Brittle, Ecological, Warm and Cheap. The results show that for the five attributes Feminine, Modern, Cheap, Elegant and Exciting there are no significant differences in ratings between the tactile and visual condition, i.e. the perceptual differences between paper grades are stable over the two different senses. For Ecological, Brittle, Smooth, and Warm there are statistical differences between the senses for some paper grades. In particular the SC paper looks more ecological than it feels. Copy paper and newsprint feel smoother than they look. Paper nuances were measured instrumentally using an X-rite and correlated to the psychological measurements. The b* values are had a significant impact on attributes such as: Warm (0.97), Ecological (0.79), and Modern (-0.79). The lightness values of the samples, L* correlated to Feminine (0.63) and to Elegant (0.61), and negatively to Ecological (-0.72 and Brittle (-0.67).

Keywords: paper quality, tactile perception, visual perception

1. Introduction

The competitive market rising from the increase in product consumption has led to an increased awareness of the role of the senses in human-product appraisal and interaction. When users interact with products they create meaning from what the different senses perceive. Thus, it is important in product design to ensure that the product message is conveyed congruently between the senses. For example, humans infer material properties using all senses. Paper has a certain feel, and a certain sound. Wool has a certain look, a certain feel, and a certain smell when wet. To find out if a wall is solid wood we can knock on it and listen to the sound. A whole new field relating design to emotions has emerged which draws on methods from experimental psychology and marketing research methods. The aim of such research is to unravel how design features (colour, shape, etc.) and material characteristics (roughness, thermal properties, etc), integrated through our senses, form intangible attributes of perception (warmth, smoothness etc) and create feelings and emotions.

Assessing what consumers see is important in market research. Visual properties of paper and print have a long standing history of research in the field of graphic arts and paper making [Attridge, Leverton, Pointer & Jacobson, 1996; Hunt, 1987; Lyne, 1979; Stokes, Fairchild & Berns, 1992]. Improving visual quality, i.e., paper whiteness, gloss, colour rendition, print mottle etc., has received much attention [Béland & Bennett, 2000; Johansson, 1999; Klahman, 2002; Norberg, 2006]. While these parameters remain highly important to consider, impressions mediated through other senses, i.e. touch, may give additional insights for product development and marketing.

Tactile input provides unique information about a product's geometrical properties (shape, size) and material properties (texture, hardness, roughness, temperature and weight) [Klatzky, Lederman & Matula, 1991; Klatzky, Lederman, Pellegrino, Doherty & McCloskey, 1990; Lederman & Klatzky, 1987]. The importance of tactile input during evaluation of products with primarily material properties has been demonstrated in a couple of

[Peck & Childers, 2003] consumers differ in their motivation to obtain haptic information ("need for touch", NTF), and consumers high in NTF are more frustrated and less confident in their product judgements when touch is unavailable. In other words, those who like to touch products are more influenced by the sense of touch. The salience of tactile input differs thus across products, consumers and situations.

Tactile properties of tissue paper, i.e. softness have been studied since the 1960ies. From around 1980, tissue paper producers began to apply the sensory evaluation methods used by the food, textile and cosmetics industry [Hollmark, 2004; Kawabata, 2001]. However, only few studies have been published on tactile, aural or olfactory qualities papers. Forsell and colleagues assessed touch and feel properties of publication papers by means of descriptive panels and psychometric methods. Four categories of descriptors were used; structural, surface, handling and sound properties and they concluded that even within fairly similar samples (LWC grades for offset and gravure), significant differences could be noted on noisiness and rigidity, [Aikala, Nieminen, Poropudas & Seisto, 2003; Forsell, Aikala, Seisto & Nieminen, 2004]. In a study performed by the authors, four subjective dimensionality of tactile perception of paper and board surfaces were identified. Salient groupings on the dimension were Ordinary papers", "Rough papers", "Old-fashioned papers" (fine structured) and "Smooth papers" (gloss coated) Verbal descriptors given by 20 end users were predominately related to material properties such as smoothness-roughness and hard-soft, but also evaluative descriptors were given such as quality, luxury and natural [Lindberg & Kihlsted, 2008].

There is research extensive on the integration of sensory information and on which modality is more accurate or dominant in perceiving object/material characteristics. The interrelation among senses in general has been studied by Marks [Marks, 1978]. Several researchers have focused on the interaction of two specific sense modalities, e.g. vision and touch [Martino & Marks, 2000] vision and audition [Vroomen & de Gelder, 2000], vision and olfaction [Blackwell, 1995; Fiore, 1993], and audition and touch [Zampini, Guest & Spence, 2003]. Also, the effects of different sensory information on people's perception of objects have been studied, e.g. the effect of sound on the identification of material [R. Klatzky, Pai & Krotkov, 2000].

The objective of present study was to create an inventory of the haptic and visual sensory impressions for different paper grades. To assess each modality's potential contribution to overall product experiences, a split-modality approaches was used [Schifferstein & Cleiren, 2005], in which subjects experienced different paper grades through only one modality at the time.

2. Method and materials

Ten different paper grades were used, LWC gloss and 60 g/m^2 (offset and gravure), LWC silk 60 g/m^2 (offset and gravure), Copy paper, Newsprint 45 g/m^2, Book paper 70 g, SC 52 g/m^2, MWC matt 80 g/m^2 and MWC gloss 100 g/m^2. Each grade was evaluated as 20 sheets of the same paper stapled together to form a booklet-like stack (Figure 1).



Figure 1:
The papers used in the visual and tactile tests

2.1 Tactile method

Thirty respondents, 18 women and 12 men, all naive to the purpose of the study, were recruited and paid a fee for their participation. The paper grades were presented in random order, one at a time. The respondents were allowed to freely handle the paper sets (Figure 2) but vision and hearing were blocked by black painted goggles

(UVEX) and hearing protection (PELTOR Optime III headset with audio input). Nine adjectives that constituted the semantic scales were read one at a time in random order by the test leader through a telephone connected to the headset. The respondent then gave an integer between 1 and 7, where 1 meant that the word was not associated with the sample and 7 that the word was strongly associated with the sample. The respondents were thereafter asked to freely associate the paper set with a paper product at a newsstand, and finally to estimate its price between 10 and 100 SEK.



Figure 2: For each paper grade, the respondents could flip through the pages and handle the paper set like a magazine

2.2 Visual procedure

Thirty new respondents, 17 women and 13 men, all naïve t the purpose of the study, were recruited and paid a fee for their participation.

The paper sets were presented as open magazines, one at a time in random order. The respondents were only allowed to look at the paper sets. When the test leader switched between paper sets, the respondents put on hearing protection to prevent any acoustic cues about the papers. A grey pad was used on the table to avoid colour influences from the wooden table, see figure 3. The same evaluation procedure as in the tactile task was used except that this time the adjectives were read out loud directly to the respondent, not through the headset.



Figure 3: Between the visual evaluations of each paper grade, the respondents wore hearing protection. Respondents wore no hearing protection while performing the visual evaluation

3. Results

3.1 Semantic scales

Semantic profiles were calculated as an average score for each paper grade on the nine adjectives in the tactile (Figure 4) and visual (Figure 5) conditions separately. Analysis of variance (ANOVA) was performed in order

Using the tactile sense only with vision and hearing and blocked the following significant differences were found ($p < 0.05$): MWC gloss and matte feels more Elegant and Modern than newsprint, copy paper and book paper. MWC gloss feels more Exciting than newsprint, copy paper and book paper. LWC and SC feels significantly more Feminine than Masculine. LWC, SC, MWC matt & gloss feels more Feminine than book paper. MWC gloss feels more Masculine than SC, LWC and newsprint. Book paper and newsprint feels more Ecological than all others. Copy paper also feels significantly more Ecological than SC and MWC matt. The coated grades (LWC, MWC gloss and matt) and SC feels more Smooth than the others. MWC gloss and matte feels less Brittle than newsprint and SC. The semantic profiles are shown in Figure 4.

Using the visual sense only, the following significant differences were found ($p < 0.05$): The MWC gloss and matte are perceived the most Elegant but significantly different only to newsprint and book paper. MWC gloss and matte are judged to be the most modern looking and significantly more modern than book and newsprint. Exciting, Feminine and Masculine did not significantly differentiate between the grades in the visual condition newsprint and book paper are perceived to be more Ecological than the other paper grades Coated grades (LWC, MWCs) and SC looks significantly Smoother than copy paper, newsprint and book paper. Newsprint, book and SC are Warm looking. MWCs look the least Brittle and MWC glossy looks significantly less Brittle than LWC, newsprint, book and copy. The semantic profiles are shown in Figure 5.

Some paper grades, for example MWC gloss and matt were perceived very consistently in the two sense modalities whereas others, like SC paper, gave different impressions in different sense modalities. A comparison of the semantic profiles between the visual and tactile conditions reveals that for the five adjectives: Feminine, Modern, Cheap, Elegant and Exciting there are no significant differences in ratings between the tactile and visual condition, i.e. the perceptual differences between paper grades are stable over the two different senses. For Ecological, Brittle, Smooth, and Warm there are statistical differences between the senses for some paper grades. In particular the SC paper looks more Ecological than it feels. Copy paper, and newsprint feel more Smooth than they look.

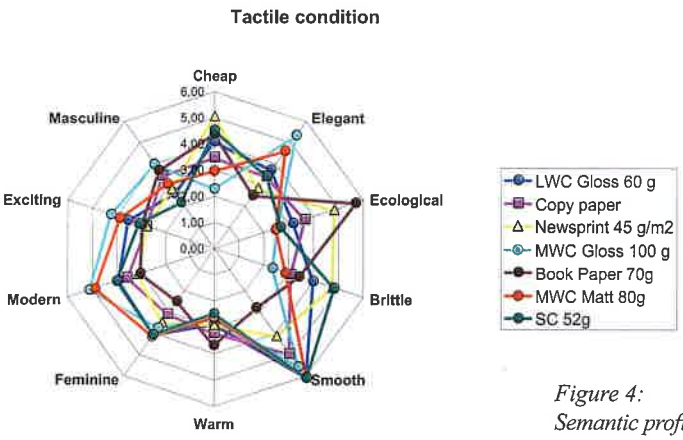

Figure 4:
Semantic profiles for different paper grades, tactile condition

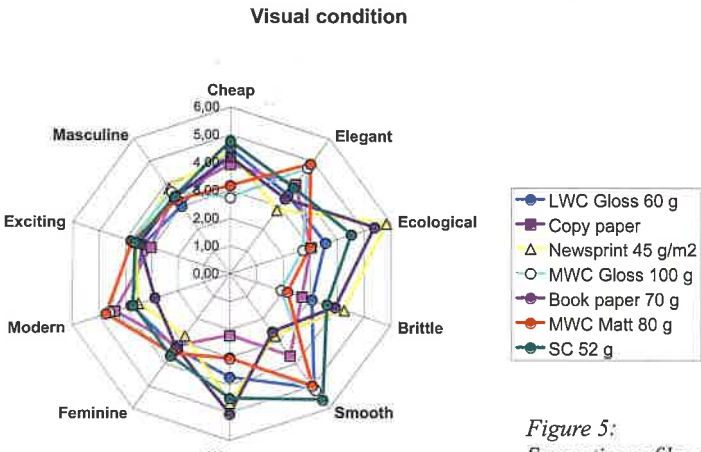

Figure 5:

3.2 Quality space

A Factor Analysis (FA) with a principal axis extraction was carried out on n (samples) x m (adjectives) matrix of average ratings for each of tactile and visual data sets. The FA derived two factors with eigenvalues >1.0 for both sets. Figure 6 show the sample score in the semantic space for the tactile evaluation and Figure 7 the sample space for the visual evaluation. The factor loadings of the adjectives are illustrated as arrows and the samples by their factor scores. Factor 1 discriminates between the MWC grades on one hand and newsprint and book paper on the other. The corresponding semantic dimension for the tactile impressions is Modern and Elegant on one hand and Warm and Ecological on the other. Book paper and MWC gloss are each others opposites on the Modern-Ecological dimension but they booth score high on the second factor which is determined by the adjective Masculine; thus book paper can be perceived as Ecological, Warm and Masculine whereas MWC is perceived as Elegant, Exciting and Masculine. Using the same reasoning, SC paper and to some degree LWC, can be said to be perceived as both as Feminine and Brittle. SC and LWC are the opposite of Masculine and in particular the LWC is associated with femininity. Interestingly, Masculine and Feminine are not exact opposite perceptions (only ~ 115 deg apart), because Feminine is also correlated to the Modern-Elegant variable cluster.

Data from the visual condition exhibit a similar pattern (Figure 7). However some difference can be noted. Perceptually, Factor 1 discriminates between the Modern and Elegant Cluster on the one hand, and the Warm and Ecological on the other. Factor 2 is defined by the adjective Masculine. However, the correlation structure between variables is slightly different and Modern and Brittle are direct opposites now. Exciting is highly correlated to Masculine whereas in the tactile evaluation Exciting is correlated to Elegant. In the visual

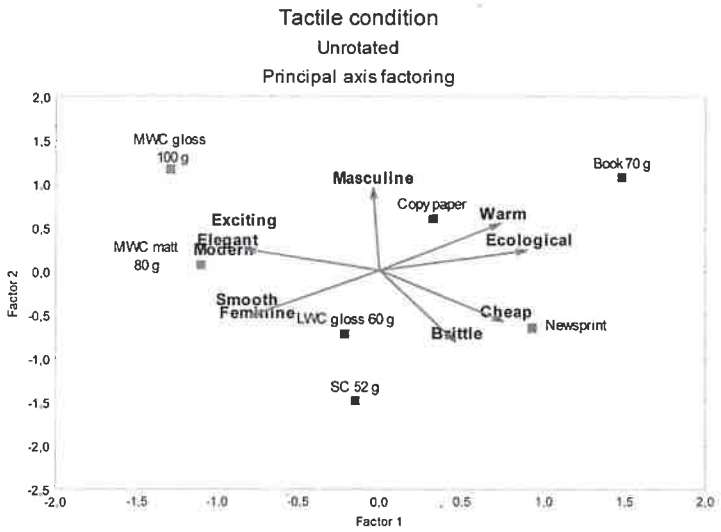

Figure 6:
Factor loadings (variables) and factor scores (samples) for the tactile condition. Unrotated factor solution in order to provide easy comparison between visual and tactile conditions

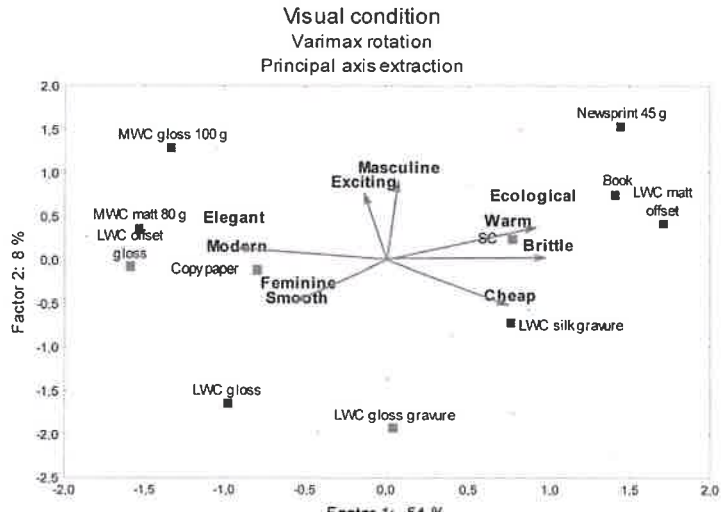

Figure 7:
Factor loadings (variables) and factor scores (samples) for the

evaluation four additional LWC grades, manufactured for offset and gravure, were added. All LWCs exhibit similar profiles on the semantic scales and differences between them are not statistically significant. LWC Offset Gloss was rated to be the most modern and Elegant among the LWC grades and the least Cheap, Brittle and Ecological. All LWCs scored high on Smooth and to some Extent on Cheap which positions them rather low on Factor 2. However, being highly inter-correlated the exact location of the LWCs in the spatial map should be taken with caution. The most notable difference between tactile and visual condition can be seen for SC and copy paper. The SC paper is perceived smooth and brittle through tactile inspection but looks warm and ecological through visual inspection. The copy paper feels warm and slightly masculine but looks modern and slightly feminine.

Paper nuances were measured instrumentally using an X-rite with no polarization filter D50 Illumination and a 2° observer. Five measurements were taken on each sheet and average CIE Lab value for each paper grade was calculated and the product-moment correlation was calculated to the average scale values for each adjective. For the visual evaluation the b* values are correlated (> 0.05) to Warm (0.97), Ecological (0.79), Brittle (0.67) and to Modern (- 0.79). The lightness values of the samples, L* correlated to Feminine (0.63) and to Elegant (0.61), and negatively to Ecological (- 0.72) and Brittle (- 0.67).

3.3 Perceived value: Price estimation

In order to make data comparable between individuals and groups the price estimation data were converted to standardized scores (0, 1). Price estimation (Figure 8) follows the same general trend in the tactile and visual conditions. However, LWC, copy and book paper together with MWC Gloss feels more expensive in the tactile condition.

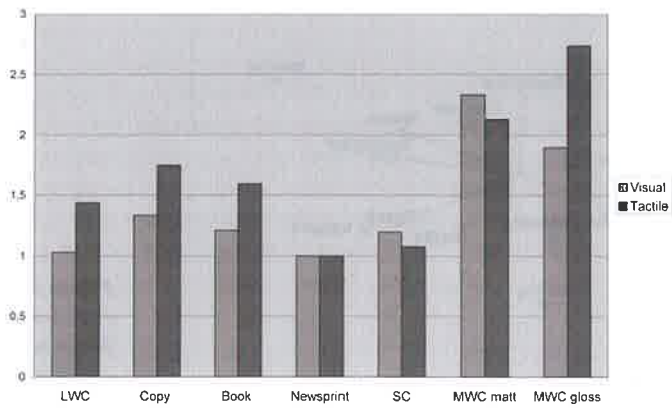

Figure 8: Estimated price of paper grades in both the visual and tactile conditions. Standardized data

3.4 Categorization of paper product associations

The paper product associations were categorized into 15 categories for each of the tactile and visual conditions: cartoons, daily papers, weekly magazine, monthly magazine, supplement, book, art supplies, brochure & advertisements, office paper, packaging & wrapping, domestic supplies (e.g. oven paper, toilet paper, table cloth), drawing pad, money (incl. pools coupon, receipt etc.), ecological and miscellaneous. The respondents were allowed to give several examples of paper products, however, each category was allowed to have only one contribution from each respondent, but each respondent could give contributions to several categories.

MWC gloss was associated with monthly magazines in both conditions whereas MWC matt in addition was also associated with weekly magazines in the visual condition. SC paper was predominately associated with weekly magazines in both conditions and to some degree with supplements in the tactile condition. Newsprint was associated with newspaper in the tactile condition but with packaging and wrapping in the visual mode.

4. Conclusions

For certain paper grades like MWC and LWC, the product message in terms of semantic profiles is conveyed congruently between the senses. However some qualities give a stronger association with touch, like 'ecological', than with vision, which can lead to an incongruent perception of the paper grade.

People have a fairly good sense of a paper's quality in terms of estimated price and suitable product type for a specific paper. The associations made by the respondents were fairly correct in terms of how different paper grades are used in the marketplace.

Significant differences in the ratings on the semantic scales could be noted between different grades. These differences can be quantified and evaluated for different paper grades. Being able to assess these differences will allow us to evaluate how different grades can perform in selected market segments.

Acknowledgement

Financial support from the Innventia Research Cluster "HPI - Core Values of Paper" and from Vinnova is greatfully acknowledged.

References

1. Aikala, M., Nieminen, S., Poropudas, L., Seisto, A. (2003). *The end user aspect in print product development*. Paper presented at the 30th IARIGAI Conference
2. Attridge, G. G., Leverton, C., Pointer, M. R., Jacobson, R. E. (1996). Measured colour difference and the acceptability of colour prints. *Journal of Photographic Science, 44*, 14-17
3. Béland, M. C., Bennett, J. M. (2000). Effect of local microroughness on the gloss uniformity of printed paper surfaces. *Applied Optics,* 39(15), 2719-2726
4. Blackwell, L. (1995). Visual cues and their effect on odour assessment. *Nutrition and Food Science, 5*, 24-28
5. Design, & Emotion; from http://www.designandemotion.org/
6. Fiore, A. M. (1993). Multisensory integration of visual, tactile, and olfactory aesthetic cues of appearance *Clothing and Textiles Research Journal.,* 11(3), 45-52
7. Forsell, M., Aikala, M., Seisto, A., Nieminen, S. (2004). *End users' perception of printed products.* Paper presented at the Pulp and Paper Research Conference, Helsinki
8. Grohmann, B., Spangenberg, E. R., Sprott, D. E. (2007). The influence of tactile input on the evaluation of retail product offerings. *Journal of Retailing,* 83(2), 237-245
9. Hollmark, H. (2004). Measurement of tissue paper softness: A litterature review. *Nordic Pulp and Paper Research Journal,* 19(3), 345-353
10. Hunt, R. W. G. (1987). *The Reproduction of Color in Photography, Printing and Television.* Tolworth: Fountain
11. Johansson, P. Å. (1999). *Optical Homogeneity of Prints.* Unpublished Doctorial Thesis, Royal Institute of Technology, Stockholm, Sweden
12. Kawabata, S. (2001). Testing the tactile properties of tissue and nonwovens. In J. M. Borch, B. Lyne, R. E. Mark & C. C. Habeger Jr. (Eds.), *Handbook of physical testing of paper* (Vol. 2, pp. 505-530): Marcel Dekker
13. Klahman, M. (2002). *Aspects of Colour Rendering, Colour Prediciton and Colour Control in Printed Media.* Royal Institute of Technology, Stockholm
14. Klatzky, R., Pai, D. K., Krotkov, E. P. (2000). Perception of material from contact sound. *Presence,* 9, 399-410
15. Klatzky, R. L., Lederman, S. J., Matula, D. (1991). Imagined haptic exploration in judgments of object properties. *Journal of Experimental Psychology,* 17(2), 314-322
16. Klatzky, R. L., Lederman, S. J., Pellegrino, J., Doherty, S., McCloskey, B. (Eds.). (1990). *Procedures for haptic object exploration vs. manipulation.* New Jersey: Albex
17. Lederman, S. J., Klatzky, R. (1987). Hand movements: A window into haptic object recognition. *Cognitive Psychology,* 19(3), 342-368

18. Lindberg, S., Kihlsted, A. (2008). *Analysis of tactual perception of paper and board materials*. Paper presented at the Materials & Sensations
19. Lyne, M. B. (1979). Multidimensional scaling of print quality. *Tappi Journal,* 68(11), 103-107
20. Marks, L. E. (1978). *The unity of the senses: Interrelations among the modalities*. New York: Academic Press
21. Martino, G., Marks, L. E. (2000). Cross-modal interaction between vision and touch: the role of syesthetic correspondence. *Perception*, 29, 745-754
22. McCabe, D. B., Nowlis, S. M. (2003). The Effect of Examining Actual Products or Product Descriptions on Consumer Preference. *Journal of Consumer Psychology,* 13(4), 431-439
23. Norberg, O. (2006). *The Importance of Paper Properties in Digital Colour Printing*. Linköping Univeristy, Linköping
24. Peck, J., Childers, T. L. (2003). To have and to hold: The influence of haptic information on product judgemnets. *Journal of Marketing,* 67, 35-48
25. Schifferstein, H. N., Cleiren, M. P. H. D. (2005). Capturing product experiences: a split modality approach. *Acta Psychologica* (118), 293-318
26. Stokes, M., Fairchild, M. D., Berns, R. S. (1992). *Colorimetrically quantified visual tolerances for pictorial images.* Paper presented at the TAGA Conference
27. Vroomen, J., de Gelder, B. (2000). Sound enhances visual perception: Cross-modal effects on auditory organization of vision. *Journal of Experimental Psychology,* 26, 1583-1590
28. Zampini, M., Guest, S., Spence, C. (2003). The role of auditory cues in modulating the perception of electric toothbrushes. *Journal of Dental Research,* 82(11), 929-932

Perception and measurement of the whiteness of papers with different gloss and FWA amount

Ludovic Gustafsson Coppel

Innventia AB
Drottning Kristinas väg 61, P. O. Box 5604, SE-114 86 Stockholm, Sweden
E-mail: ludovic.coppel@innventia.com

Abstract

The effect of mean gloss level on perceived whiteness was evaluated by magnitude estimation and pair wise comparison of papers with varying shades and gloss levels. The samples were printed on substrates of different gloss to target $L^*a^*b^*$ values measured under a light booth illumination having a 5000 K correlated colour temperature. Observers were able to rate the whiteness of the samples with large mean gloss differences in the 5000 K illumination and in the same illumination with an additional UV lamp. The CIE whiteness equation predicted well the perceived whiteness in both illuminations and the mean gloss level had no significant effect on perceived whiteness. This means that the CIE whiteness equation can be used to compare the perceived whiteness of papers having very different mean gloss levels. However, due to the different amount of fluorescent whiteness agents (FWA) in the papers, the perceived whiteness prediction was only valid when the measurement was performed under the same illumination as for the visual evaluations. Typical indoor illumination with florescent light tubes contains much less UV than the D50 or C illuminants. The instrumental whiteness differences due to mean gloss and instrument geometry were negligible compared to the effect of the UV content of the illumination.

Keywords: whiteness, gloss, perception, fluorescence

1. Introduction

The gloss of an object has a significant effect on its perceived colour. Matte surfaces appear less intensely coloured with lower chroma and higher lightness than glossy surfaces, all else being equal, and the perceived or measured colour depends on how much of the light reflected at the surface is detected [Dalal, 1999]. Makarenko and Shaykevich [2000] studied theoretically the dependence of measured paper whiteness on the surface roughness and proposed a numerical model taking the measurement geometry of a d/0° instrument and surface roughness into account. Although the effect is stronger for saturated colours, they found that measured whiteness depends on both surface roughness and instrument geometry. The appearance of unprinted paper or board is strongly influenced by the mean gloss level, especially if one looks at it from different angles. Two papers judged as equally white and tinted will still appear different if the gloss is different, which raises the question if the glossy appearance affects the perception and judgement of whiteness.

The aim of this study was to investigate the effect of mean gloss level on the perceived and measured whiteness of paper samples. For this purpose, it was required to produce samples with different mean gloss levels and with all other optical properties being equal. Dalal et al. proposed a model that describes the influence of gloss on the measured colours of xerographic prints and tested the model on prints fused to different gloss levels on a off-line fuser [Dalal, 1999]. Ariño et al. applied the same model to injection-moulded pigmented plastics and varied the surface gloss by using plaques with different structures [Ariño, 2005]. Unprinted paper surfaces are more difficult to control without changing the other optical properties such as bulk scattering. Coated surfaces can for instance be modified by the choice of pigment size and shape. Calendering can be used to make the surface smoother but the process will also change the inner structure of the paper and hence its scattering properties.

2. Method

By printing the paper samples, it was possible to produce samples with different gloss but with nearly identical colour in one instrument geometry. Commercial inkjet papers are available with a wide span in gloss and were suitable for this study. However, one problem in measuring the shade of high whiteness paper was fluorescence

Commercial papers have different amounts of fluorescent whitening agents (FWA) and their appearance depends of the UV content of the illumination. By measuring the whiteness of the samples in the same illumination and approximately the same geometry as in the visual evaluations with real observers, the influence of mean gloss level on perceived whiteness could be evaluated. This was done by having a panel of observers perform a magnitude estimation of perceived whiteness in two illuminations with different UV content. The results were then compared to the instrumental whiteness of the samples in the specific illumination. The samples with different gloss levels were also evaluated pair-wise by the observers.

In order to quantify the effect of measurement geometry on the measured whiteness, the samples were measured with three instruments: the spectroradiometer used as a reference measurement for the visual evaluations, a d/0° spectrophotometer, and a 45/0° densitometer. To avoid the effect of the different UV contents in the measuring devices, two substrates were modified so that their FWA content remained the same but their mean gloss varied.

2.1 Paper samples

Six paper samples were printed with a Canon BJC-8200 photo inkjet printer at 4 different $L^*a^*b^*$ target values measured with a Photo Research PR-650 spectroradiometer under an overhead illumination with a correlated colour temperature (CCT) of 5000 K. The instrument was calibrated with a non-fluorescing Spectralon white tile. The reflectance of the tile was measured with a calibrated Technidyne ColourTouch spectrophotometer. The samples consisted of three inkjet photo papers (matte, semi-glossy, and glossy) and a copy paper. The glossy inkjet photo paper was used with and without a taped transparent film on top of it and the copy paper was used with and without extra calendering.

The spectral radiance factor of the samples was measured under the 5000 K illumination with and without an additional UV lamp. The spectral radiance factor was also measured with a TechKon spectro-densitometer (with and without polarisation filter), and with a Technidyne ColourTouch 2 spectrophometer with the UV settings UV(D65), UV(C), and UVex. The mean gloss level was measured with a Zehntner ZLR 1050M gloss meter at 75° angle of incidence (Table I).

Table I: Mean gloss levels of the printed paper samples

Substrate	Type	Gloss 75° (%)
1	Copy Paper	11
2	Calendered Copy	18
3	Canon SG-201	50
4	Canon GP-501	79
5	Epson S041256	3
6	Canon GP-501 + transparent film	95

2.2 Visual evaluations

Four experiments were performed by a total of 43 observers with no previous experience in psychophysical scaling or paper related issues. All the observers had an average colour discrimination in the Farnsworth Munsell 100 hue test [Farnsworth, 1943].

1) The 24 samples (4 shades and 6 gloss levels) were presented one by one to 12 observers. The samples were attached to a grey background and laid on the grey table (Figure 1, left). The observers were instructed to report their perceived whiteness of the sample in relation to a reference sample, which was always present on the table. The reference was one of the printed Epson Matte samples. If the observers perceived the sample to be half as white as the reference they had to report the value 50, if they perceived it to be twice as white they should report 200 Each observer gave three individual estimates of their perceived whiteness. The individual response was taken as the geometric mean of the three observations. The mean rating was calculated as the geometric mean of the individual mean responses. The samples were evaluated in a perception laboratory with homogeneous overhead illumination having a correlated colour temperature about 5000 K. The observers

2) The next 12 observers performed the same experiment holding the samples in their hands, free to look in any direction.

3) All the previous 24 observers participated also in a pair-wise comparison experiment. Samples from substrates 3, 4 and 5 were evaluated pair-wise. A pair of samples attached to a grey background were presented on top of a grey table (Figure 1, right). The observers were asked which sample they experienced as the whitest. In order to reduce the number of observer evaluations, the samples were not compared to themselves (same gloss and shade) and each pair was evaluated only once at random, but constant for all observers, left/right positions. This resulted in 66 evaluations from each observer.

4) 19 observers who did not participate in the previous experiments performed the same evaluation as in experiment 1 but under illumination with an additional UV lamp.

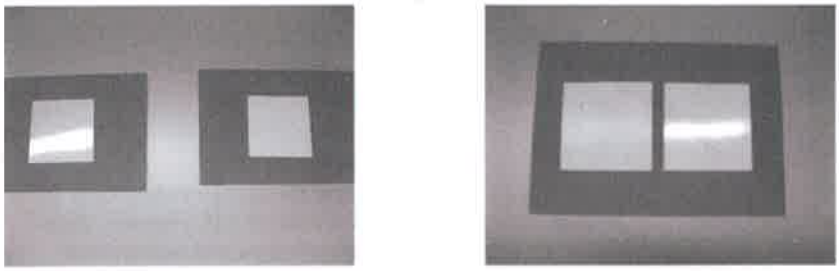

Figure 1: Samples in the visual evaluations. Left: Magnitude estimation of the sample to the left compared to the right reference white (experiments 1 and 4). In experiment 2, the observers were holding the sample to be evaluated in their hands and compared to the reference on the table. Right: Pair wise comparison in experiment 3

3. Results

3.1 Magnitude estimation

The rating of the 24 samples on the table is plotted versus the CIE whiteness measured in the overhead 5000 K illumination, W_{CIE}*, in Figure 2 (left) and the rating of the held samples is plotted in Figure 2 (right). The rating correlated highly with the measured CIE whiteness, irrespective of the mean gloss level of the samples, both when the samples were laid on the table and when the observers had the sample to be rated in their hands. The perceived whiteness of the samples having 50% mean gloss level was higher than the perceived whiteness of the copy papers having 11% mean gloss level, when the samples were evaluated on the table. However, samples with a 2% mean gloss level were judged as white as glossier samples, and some of the glossiest samples (95%) were judged less white than matter samples.

The rating of the 24 samples under an overhead 5000 K illumination with additional UV illumination versus CIE whiteness applied to that illumination is shown in Figure 3. Since the illumination was different, the reference sample's appearance changed when the UV lamp was turned off. Therefore, the rating of the samples with additional UV should not be compared to the rating obtained in the illumination without additional UV.

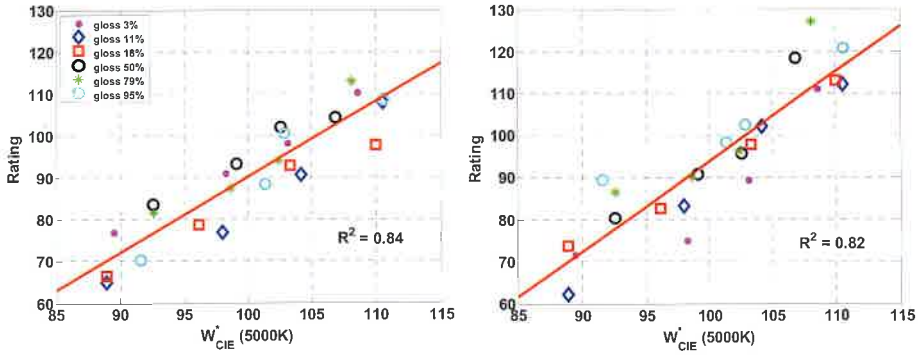

Figure 2: Rating of the samples compared to the reference versus CIE whiteness measured under the overhead illumination with correlated colour temperature of 5000 K. Left: samples on table. Right: observers having

However, since the matte sample used as a reference white was compared to itself, it is expected that observers should report 100 for that sample. The mean rating for that sample was 99 (Figure 3) in the illumination with additional UV and 98 in the illumination without additional UV (Figure 2, left). On the other hand, the measured whiteness was 125 with additional UV but only 103 without additional UV.

A high correlation was obtained between the rating in the illumination with additional UV and the measured whiteness in that illumination ($R^2 = 0.87$). All the samples but the printed Canon SG-201 inkjet papers (gloss 50%) had a significantly larger instrumental whiteness with the UV lamp on. The SG-201 samples exhibited very little fluorescence and their instrumental whiteness was not much affected by the UV content of the illumination. These samples were also judged less white than the other samples under illumination with additional UV.

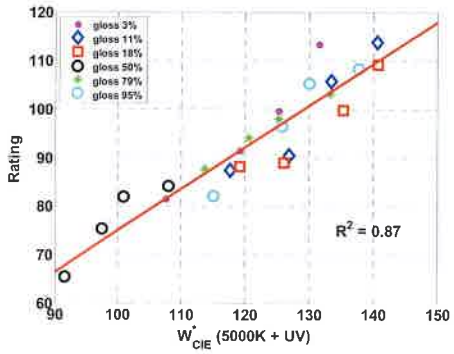

Figure 3:
Rating of the samples compared to the reference versus CIE whiteness. Both visual evaluation and measurement were made under the 5000 K overhead illumination with an additional UV lamp. The line shows the linear fit for all points

3.2 Pair-wise comparison

In experiment 3, the observers were asked which sample they experienced as the whitest in each pair of samples. The value 0 was assigned to pairs for which an observer judged the left sample as the whitest and the value 1 was assigned to pairs for which an observer judged the right sample as the whitest. The mean response of the 20 observers was then computed to give the proportion, p, of whiteness judgement for each pair and the Just-Noticeable Difference (JND) was calculated with (ISO 20462-3, 2003)

$$\text{JNDs} = \frac{12}{\pi}\sin^{-1}\left(\sqrt{p}\right) - 3 \qquad [1]$$

The JNDs are plotted versus the difference in CIE whiteness measured under the overhead illumination with a correlated colour temperature of about 5000 K in Figure 4. The JNDs are highly correlated to the CIE whiteness ($R^2 = 0.84$), despite the fact that the samples had different mean gloss levels. This confirms the results from the magnitude estimation experiments and suggests that the mean gloss level has a negligible effect on the perceived whiteness. The CIE whiteness equation is suitable for comparing these samples when applied to tristimulus values measured in the illumination used for the visual evaluation. From the figure, one JND can be determined to be 4 whiteness values.

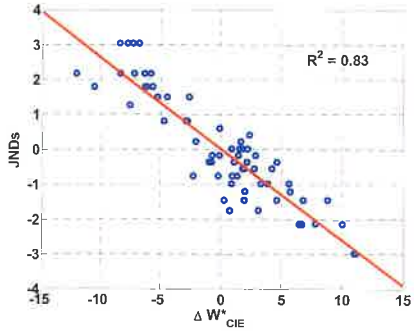

Figure 4:
JNDs versus the difference in CIE whiteness measured in the real illumination for the samples in the pair-wise comparison. The line shows the linear fit

3.3 Instrumental prediction of perceived whiteness

The CIE recommends two illuminants and standard observers for the determination of whiteness, D65/10°

the defined illuminant. Measurement instruments on the other hand use real illuminations designed to fit the standard illuminant. Spectrophometers with a d/0° geometry used in the paper industry are UV calibrated to get the same amount of UV as in the D65 or C illuminant but the power spectral distribution of the illumination is not well defined. Densitometers used in the graphical industry lack UV calibration methods although they report values as being measured with e.g. a D50 illuminant.

Moreover, real office illuminations such as the fluorescence light tubes in the overhead illumination used in the visual evaluations have spectral power distributions that differ much from the C or D65 illuminants. The typical spiky spectral power distribution of the light tubes with a 5000 K correlated colour temperature is compared to standard illuminants in Figure 5. Besides their spiky nature, common 5000 K or 6500 K fluorescent light tubes illumination have much lower UV content than the D65 or C illuminants. It is important to note that the C illuminant used for predicting indoor whiteness contains much more UV than typical indoor illuminations (outdoor through-window light excluded). The addition of a UV fluorescent light tube increased the UV content to a level close to that of C or D50 illuminants.

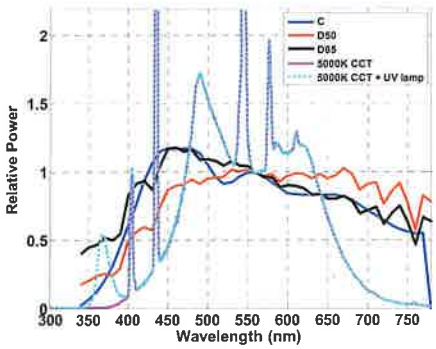

Figure 5:
Spectral power distribution of the overhead illuminations used compared to standard illuminants

Because the samples in this study had different amounts of fluorescent whitening agents (FWA), the differences in their measured whiteness was strongly dependent on the UV amount of the illumination. Figure 6 shows the perceived whiteness rating of the samples under the overhead illuminations with and without additional lamp versus CIE indoor whiteness. There are clearly three groups of samples, with low, medium, and high FWA content. Compared to Figure 2 (left), where the whiteness was measured under the real illumination, the indoor whiteness fails totally in predicting the perceived whiteness under 5000 K CCT light tube illumination. Clearly, the higher UV amount in the measurement overestimates the perceived whiteness of the samples under the illumination without additional UV lamp. On the other hand, the correlation between indoor whiteness and perceived whiteness was high (R^2 = 0.85) when the visual evaluations were made under 5000 K CCT illumination with additional UV lamp (Figure 6, right).

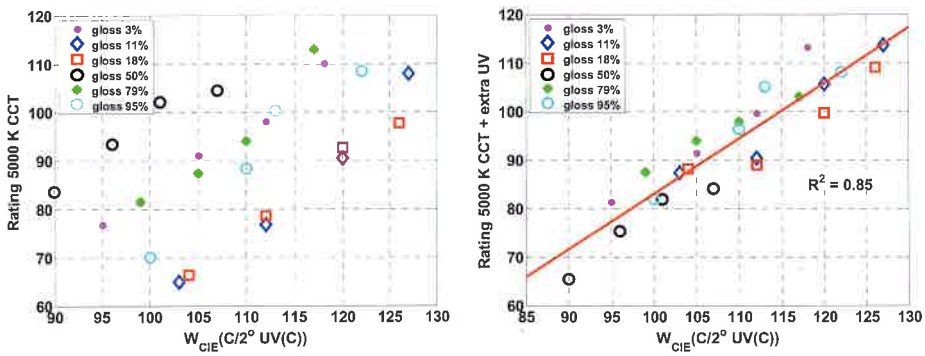

Figure 6: Rating of the samples compared to the reference versus indoor CIE whiteness measured with a ColourTouch spectrophotometer. Left: Visual evaluation made under the 5000 K overhead illumination. Right: Visual evaluation made under the 5000 K overhead illumination with additional UV lamp

The results obtained with other instrument/illuminations are summarised in Table II. Non surprisingly, the outdoor whiteness performs even worse than the indoor whiteness for the visual evaluation without additional

UV lamp, due to the higher UV content in the measuring illumination. The densitometer, with unknown UV content in the illumination, gave similar results, meaning that the UV content in the densitometer is much higher than that of common overhead light tube illumination.

Table II: Correlation coefficients (R2) between visual evaluation of perceived whiteness under the two real illuminations and the measured whiteness from different instruments and illumination/standard observer conditions

Instrument, illumination, and standard observer	R^2 Rating under 5000K	R^2 Rating under 5000K + UV
Spectroradiometer 5000K/10° UV(5000K CCT tube)	0.84	0.54
Spectroradiometer 5000K/10° UV(5000K CCT tube) + UV (UV tube)	0.12	0.87
ColourTouch, outdoor whiteness (ISO 11475, 2004) D65/10° UV(D65)	0.05	0.80
ColourTouch D50/2° UV(C)	0.33	0.84
ColourTouch, indoor whiteness (ISO 11476, 2000) C/2° UV(C)	0.31	0.85
ColourTouch C/2° UV_{ex}(420nm)	0.83	0.14
TechKon Densitometer D50/2° no pol. filter	0.53	0.80
TechKon Densitometer D50/2° with pol. filter	0.29	0.72

4. Conclusions

Commercial paper samples with mean gloss levels ranging from 11 to 95% were printed to target $L^*a^*b^*$ values in order to study the effect of mean gloss level on perceived whiteness. The D65/10° CIE whiteness of the samples varied from 120 to 155. The samples varied not only in gloss but also in their amount of fluorescence whitening agents (FWA). Thus, the instrumental whiteness of the samples, and their relative whiteness difference varied greatly depending on the measurement illumination.

The copy paper substrate was calendered to raise the mean gloss level while keeping the FWA amount constant. The gloss increased only from 11% to 18%. Another way of increasing gloss was to laminate an inkjet paper with a transparent film but UV absorption in the transparent film prevented a thorough analysis of the effect of measurement geometry and gloss trap on the measurement of whiteness from samples with different mean gloss levels. It is very difficult to produce samples with different gloss levels and keep all other optical properties constant. Nevertheless, this study suggests that instrumental whiteness is not significantly affected by the measurement geometry and sample gloss, unlike for saturated colours where larger effects would be expected.

Densitometers and spectrophotometers with different UV contents in the illumination will on the other hand rank samples with different FWA amounts differently. The CIE whiteness stipulates a D65 (outdoor) or C (indoor) illuminant. These theoretical illuminations are difficult to generate in measuring instruments, and impossible to produce in a viewing environment large enough for visual evaluation of large sample sets. Moreover, paper and prints are often inspected and used in an office environment under light tube illuminations far from the theoretical C or D65 illuminants. Common overhead illumination with 5000 K correlated colour temperature was revealed to contain much less UV than the D50 illuminant and most office environments are likely to have less UV than the "indoor" C illuminant. Defining the right choice of illuminant for the measurement of whiteness is out of the scope of this report but it is crucial to use the same (real) illumination in the measurement and visual evaluation when comparing the perceived whiteness of samples with different amounts of FWA. Previous ranking of commercial copy papers was not affected by the illumination [Coppel, 2007] because all samples had a relatively high FWA content. Predicting the perceived whiteness from samples with different amounts of FWA requires the illumination to be the same in both prediction (measurement) and visual evaluation (from real observers).

Using the same illumination in both measurement and visual evaluation, a high correlation was obtained

CCT and additional UV lamp). The CIE whiteness equation applied to the real illumination predicted well the perceived whiteness of samples having a large difference in mean gloss level, both when the samples were laid on the table and when the observers had the samples in their hands and were free to look at tem in any direction. This reveals that the mean gloss level does not have a significant impact on the perceived whiteness. This result was confirmed by a pair-wise experiment, from which the whiteness just-noticeable difference (JND) of a group of observers was determined to be 4 whiteness values with whiteness ranging from 90 to 110 under the 5000 K CCT illumination.

This work shows that the CIE whiteness equation can predict well the perceived whiteness of samples with different amount of FWA when the same illumination is used in the measurement and the visual evaluation. Observers were able to rate the whiteness of papers with very different mean gloss levels and their response was well predicted by the CIE equation.

Acknowledgements

This work is part of a consortium project on the appearance of paper and on print quality. Financial support from Holmen, M-real, Norske Skog and Stora Enso is gratefully acknowledged. Siv Lindberg, Innventia, is acknowledged for numerous discussions. Per Edström, Mid Sweden University and Caisa Andersson, Karlstad University are thanked for comments on the manuscript.

References

1. Ariño, I. and Kleist, U., (2005), *Effect of Gloss and Texture on the Color of Injection-Molded Pigmented Plastics. Polymer Engineering and Science, 45(5),* p. 733-743
2. Coppel, L., Lindberg, S. and Rydefalk, S., (2007), *Whiteness Assessment of Paper Samples at the Vicinity of the Upper CIE Whiteness Limit, in Proc. 26th session of the CIE, Beijing, China,* p. D1-10
3. Dalal, E. N. and Natale-Hoffman K. M., (1999), *The Effect of Gloss on Color, Color Research and Application,* 24(5), p. 369-376
4. Farnsworth, D., (1943), *The Farnsworth-Munsell 100 hue and dichotomous tests for color vison, Journal of the Optical Society of America,* 33, p. 568-578
5. ISO 11475, (2004), *Paper and board - Determination of CIE whiteness, D65/10° (outdoor daylight)*
6. ISO 11476, (2000), *Paper and board - Determination of CIE whiteness, C/2° (indoor illumination conditions)*
7. ISO 20462-3, (2003) *Photography - Psychophysical experimental methods to estimate image quality - Part 3: Quality ruler method*
8. Makarenko, A. V. and Shaykevich, I. A., (2000), *Dependence of the whiteness of paper on surface roughness and illumination conditions. Color Research & Application,* 25(3), p. 170-175

Perception of printed special effects

Janne Laine, Tapio Leppänen, Olli Nurmi

VTT Technical Research Centre of Finland
P. O. Box 1000, FIN-02044 V TT, Espoo, Finland
E-mail: janne.laine@vtt.fi

Abstract

Psychometric experiments were carried out in order to increase the understanding of how special effects influence the consumer perception of printed products. Seven different contents ranging from advertisements to covers of packages and annual reports were chosen and different special effect versions of each were created. The following types of special effects were used: metallic inks, selective gloss or pearlescent varnishing, and scented varnish. Conventional CMYK samples without special effects were also included in the sample set for reference. A total of 49 observers participated in the subjective assessment of the special effect print samples. An assessment session with a single observer consisted of a number of different assessment tasks and lasted for approximately 1.5 hours. Especially the gloss and pearlescent varnish effects were seen to increase the effectiveness of a printed product in attracting the viewers' attention, compared to samples with no special effects. In some cases a significant improvement in the preference assessments was also achieved with the use special effects, particularly the two varnish effects mentioned above. Principal component analysis (PCA) was applied to distil from the large data set of subjective assessments (50 attributes of 12 print samples assessed by 49 observers, for a total of 29.400 observations) the essential perceptual shifts caused by the printed special effects. The first two principal components explained the majority of perceived differences between the special effect print samples, and were interpreted to correspond to perceptual dimensions that were termed Noteworthiness and Aesthetic Value.

Keywords: special effects, printing, perception, user experience, psychometry

1. Introduction

Special effects such as metallic inks, spot gloss varnishing, or scented inks can be used to enhance a printed product. The assumption when using and the argument for selling special effects to a buyer of a print job is usually that the effects make the product stand out from the mass of ordinary printed products, making the product better at catching the attention of the consumer, more effective in shaping their mental impressions in order to deliver the desired message, and more memorable. This heightened user experience is then expected to result in the increase of the sales of the product.

Increased sales provide a direct indication of a success of a marketing campaign involving printed special effects. In this work, instead of looking at possible economic benefits directly, the consumer perception and mental impressions associated with printed special effects were examined (Figure 1). Such studies are not known to have been published before.



Figure 1: The expected result of using special effects in printed products, and the scope of the study (encircled)

It is clear that the perception of a special effect in a printed product and the mental impressions associated with it are highly context-dependent, involving a perceptual process the outcome of which is affected by complex interactions between the interpretation of the content by the consumer, viewing environment, consumer expectations, and things like colour reproduction. Furthermore, there can be variation in the specific aims of using special effects, and a given effect can be used in a number of different ways. Clarifying the contribution of printed special effects to the consumer's perception of printed products is therefore a very challenging research task, and due to the case-by-case variations it is not considered reasonable to look for categorical rules of how any given special effect is perceived.

The overall goal of the study described in this paper was to increase the understanding of how printed special effects are perceived by the users of printed products. Seven different contents ranging from advertisements to covers of packages and annual reports were chosen and different special effect versions of each were created. The print samples were then assessed in a set of psychometric experiments that were designed to yield data from which perceptual scales could be constructed, showing how the effects had modified the mental impressions of the printed products in each case, possibly revealing trends in the perception of certain special effects. A further goal was to find the perceptual dimensions that best reflected the use of special effects; this information would facilitate more efficient psychometric tests in future studies of the printed special effects.

2. Print samples

Seven different contents were chosen. The following labels are used to identify the samples of different content when the results of the psychometric experiments are presented later in the text: *Magazine* (a cover of a graphic arts magazine), *Car* (a car advertisement), *Perfume* (a perfume advertisement), *Lipstick* (a lipstick advertisement), *SunLotion* (a sun lotion advertisement), *Chocolate* (the cover of a chocolate box) and *Report* (the cover of an annual report of a technical research centre).

Different print sample versions of each content were made with different special effects:

- Conventional CMYK printing (as a reference),
- Metallic ink (silver or gold, sample label *Silver* or *Gold*),
- Gloss varnish (sample label *Gloss*),
- Pearlescent varnish (sample label *Pearl*),
- Scented varnish (sample label *Scent*).

The effect labels listed above identify the different effect versions later in the report. Thus *ReportGloss*, for instance, refers to the version of the annual report that has a gloss varnish effect. No samples with two or more special effects were made.

In the metallic ink samples either a gold or silver ink was printed to certain areas of the page under the CMYK inks. This adds to those areas a metallic sheen, which is especially evident when the print sample is seen from a certain angle relative to the light source. Figure 2 shows an example of silver ink separation. In that case two versions were made, one with compact silver layer below the CMYK inks (*CarSilver1*), the other with varying halftone percentages of silver (*CarSilver2*). The CMYK separations of the original image were also opened up to reveal the silver colour underneath.



Figure 2: Silver ink separations for the special effect print samples CarSilver1 and CarSilver2

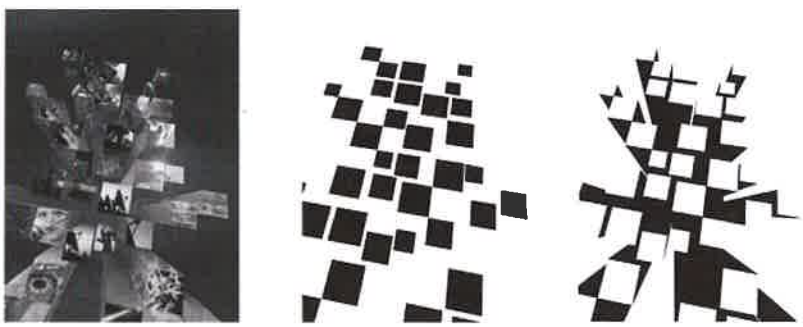

Figure 3: An example of the masks for the gloss varnish (center) and pearlescent varnish (right)

Varnish was applied to the print samples afterwards at a silk screen printing press. Gloss varnish and pearlescent varnish was applied to parts of the samples to emphasize certain objects, as in the case shown in Figure 3.

Gloss varnish was used to give a glossy appearance to selected objects in the images or to add decorative shapes that stand out from the background image especially when the print sample is viewed in certain angle relative to the light source. Pearlescent varnish containing glittering flakes was used in a similar manner.

3. Experiments

The psychometric experiments described in this section were designed to yield data from which perceptual scales could be constructed, showing how the effects had modified the mental impressions of the printed products in each case.

A total of 49 observers participated in the experiments. An assessment session with a single observer consisted of a number of different assessment tasks and lasted for approximately 1.5 hours. The first two experiments in each experimental session sought to provide data for analyzing the performance of special effects in catching the observer's attention and increasing the overall pleasantness of printed products. Both of these seem to be assumptions that are often made, but hardly any published results are known to be available to support or refute such claims.

In the first experiment the special effect samples and the reference CMYK sample without any special effects that were made from a single content were laid out simultaneously on the table in random order. The contents used in this experiment were the car advertisement, chocolate box, lipstick advertisement, sun lotion advertisement, and the annual report. The special effect versions were the metallic ink, the gloss varnish, and the pearlescent ink varnish sample. In the case of the car and lipstick advertisements two metallic ink versions, with different metallic ink and CMYK separations for different visual effects, were used. These two contents thus had five different samples, including the reference sample, while the four other contents had four different samples.

The observer was instructed to keep her eyes closed until the samples were ready, then to look at the samples on the table for approximately 3 seconds and then point to the sample that first caught her attention. After pointing at the sample the observer again closed her eyes and the instructor removed the chosen sample. The task of choosing the sample that most attracted the observer's attention was repeated with the remaining samples, until only one sample remained.

The data from this experiment thus consisted of ranking of the samples by each observer. The data was analyzed to build scales showing which samples most strongly attracted the initial attention of the observers, as described in the next section.

In the second experiment the same set of print samples as in the first experiment were used. Now the observer was allowed to view the samples, again presented simultaneously on the table in random order, at length. This time the observer was instructed to choose the sample that she preferred:

"A set of print samples, some of which include different special effects, are placed in front of you. Choose the sample that you prefer. You can imagine that you are choosing which one of these different versions of brochure, magazine, packaged product, or other printed product you would like to have for yourself. Point your choice to the instructor, who will remove the chosen sample. Then point the most preferable of the remaining samples. This will be repeated until all the samples are chosen."

This experiment thus resulted in ranking of the samples according to the preference by each observer.

The third experiment was the main part of the experimental session and provided the data for identifying the main perceptual attributes that are typically affected by the use of printed special effects. In the third experiment the observers assessed 50 different perceptual attributes of each print sample. The observers made their assessments by marking their level of agreement to statements concerning the perceived attributes on visual rulers such as

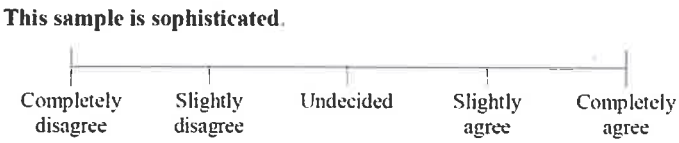

Figure 4: The visual ruler used in evaluating the print samples

The answers were converted into integer numbers from 0 (mark on the extreme left of the ruler) to 100 (mark on the extreme right). The data from this experiment thus consisted of what can be understood as the assessment of the magnitude 50 perceptual attributes of each of the 12 samples by each of the 49 observers.

Based on the data from this experiment the samples could be placed on 50 different univariate scales corresponding to the 50 perceptual attributes. The main point of this experiment, however, was to apply multivariate statistical methods to the combined data to find the principal perceptual dimensions affected by the use of special effects.

4. Results

The (inverse) correlate for the effectiveness of each sample in attracting the viewers' attention was calculated simply as the average rank over the rankings of all the 49 observers obtained by that sample in the experiment. The results are presented in the Figures 5, 6 and 7 for some of the tested contents. The possible range for the values is from 1 (sample always chosen first) to 4 or 5 (sample always chosen as the last one), depending on the number of the samples. Smaller value (point higher in the graph) therefore indicates better performance in attracting the observers' attention. The error bars indicate the 95% confidence intervals of the mean values.

Considering the results for all contents, a trend was obvious in the results: the gloss varnish and pearlescent varnish versions attracted the observers' attention significantly better than the reference sample. The metallic ink versions, on the other hand, did not significantly improve the noticeability in these cases. The case of the car advertisement shows how the way a special effect is applied can have a considerable effect on how the printed product is noticed. In this case the metallic ink version *CarSilver2*, in which the separation of metallic ink was modified and the CMYK separations were opened up in an effort to more strongly reproduce the play of shadows and highlights on the car, caught the observers' attention significantly better than *CarSilver1*. In *CarSilver1* a compact metallic ink layer was used under the CMYK inks, which resulted in a decrease in the visual contrast and actually made the sample fare worse than the reference sample in this experiment.

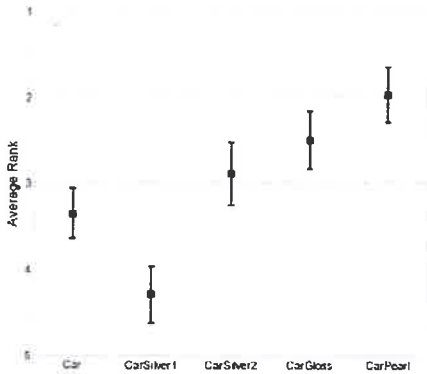

Figure 5:
Average ranks for attracting the observers' attention for the reference sample and four special effect versions of the car advertisement

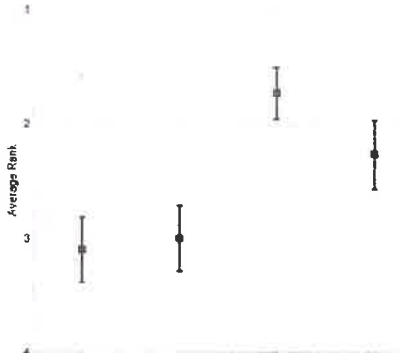

Figure 6:
Average ranks for attracting the observers' attention for the reference sample and three special effect versions of the chocolate box cover

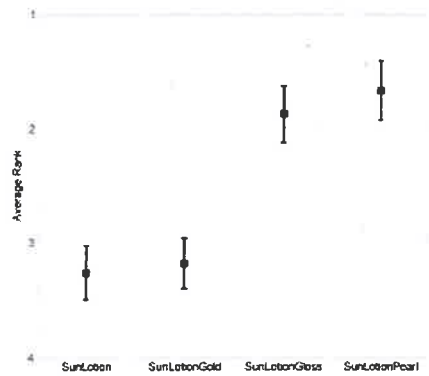

Figure 7:
Average ranks for attracting the observers' attention for the reference sample and three special effect versions of the sun lotion advertisement

In Figures 8, 9 and 10 the results of the preference judgments for some contents are presented as the average ranks in the same manner as the results for attracting attention above. Thus smaller values (points higher in the graph) again indicate samples that were, on average, preferred over the samples with higher average ranks. Error bars indicate 95% confidence intervals of the average ranks.

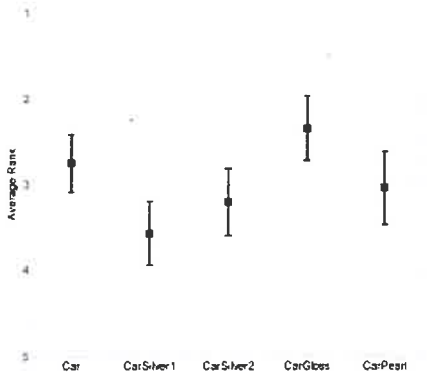

Figure 8:
Average ranks of preference for the reference sample and four special effect versions of the car advertisement

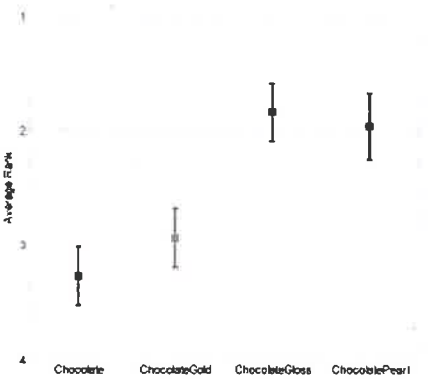

Figure 9:
Average ranks of preference for the reference sample and three special effect versions of the chocolate box cover

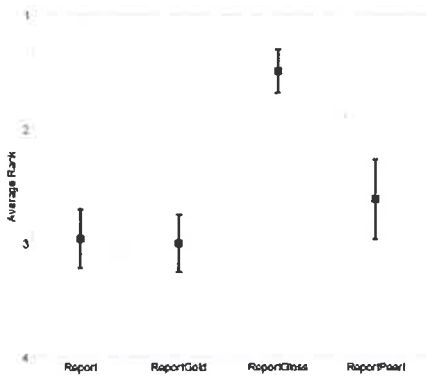

Figure 10:
Average ranks of preference for the reference sample and three special effect versions of the annual report

Compared to the results of the previous experiment, there is more variation in the results here. This is an expected result, since when making judgments of preference the observers have to judge the effects and other characteristics of the samples in the context of the content, presumably making higher-level semantic interpretations of what they are seeing than when just quickly directing their attention to the most prevalent

version alone or both gloss varnish and pearlescent varnish versions were considerably preferred over the reference (chocolate box, sun lotion advertisement, and the annual report). In the case of the car advertisement both metallic ink versions were less preferred than the reference sample. As will be discussed in more detail later, the case by case variations seen here are likely related to the success, or lack of it, in designing the samples so as to form an aesthetically pleasing image.

A multivariate statistical method known as principal component analysis (PCA) was used in the analysis of the results of the third experiment, in which multiple perceptual attributes of the special effect print samples was evaluated. PCA was applied in order to distil from the large data set of subjective assessments (50 attributes of 12 print samples assessed by 49 observers, for a total of 29400 observations) the essential perceptual shifts caused by the printed special effects. PCA reduces the redundancy in the original data by replacing a group of original variables with a single new variable. The new variables generated by the method are called the principal components. Each principal component is a linear combination of the original variables. [Jackson, 2003]

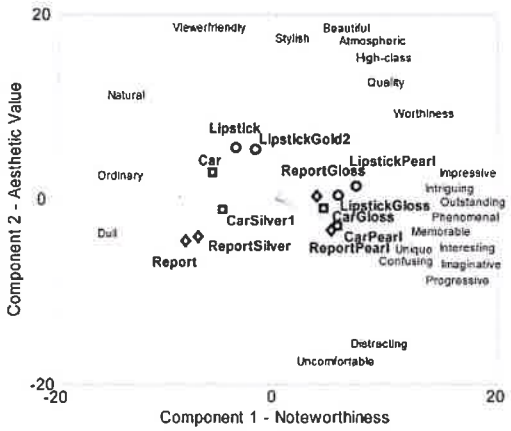

Figure 11:
The average observations for 12 special effect print samples in the plane defined by the first two principal component axes. Also shown is a selection of the original attribute vectors

In this case the first two principal components together explained approximately 90% of the variance between the samples, as assessed on the 50 separate perceptual attribute scales. Figure 11 shows the locations of 12 print samples, mapped from the 50 original attribute scales to the plane defined by the first two principal components. *Lipstick*, *Car*, and *Report* refer to conventional CMYK versions (without special effects) of three different contents (a lipstick advertisement, a car advertisement, and a cover of an annual report, respectively), which served as references to the special effects samples. The suffixes *-Gold* and *-Silver* denote the metallic ink versions of the same three contents while *-Gloss* and *-Pearl* mark the print samples in which gloss or pearlescent varnish, respectively, had been used.

Also shown is a set of vectors corresponding to a selection of the original attributes (dotted lines in the graph). The lengths and directions of the vectors indicate their relative contributions to the first two principal components. For example, it can be seen that "stylishness" correlates highly with the component 2 but has an almost negligible correlation with component 1, while "ordinariness" has a strong negative correlation with component 1. The original attribute vectors were used in interpreting the latent perceptual dimensions represented by the principal components.

The first principal component was labelled Noteworthiness (comprised of such perceptual attributes as "uniqueness", "interestingness", and "memorableness") and the second principal component was labelled Aesthetic Value (comprised of such attributes as "stylishness", "beauty", and "viewerfriendliness"). These perceptual dimensions best captured the perceptual shifts caused by the use of special effects in the studied cases.

The above interpretation also facilitates a rather straightforward explanation of the perceptual effects of printed special effects, as found in these cases. By applying special effects the noteworthiness of the printed products can be increased, as evidenced by the special effect samples moving to the right, in the direction of the Noteworthiness axis. Depending on the sense of style with which the effects have been applied they can also affect the Aesthetic Value of the samples in either a positive or negative manner, as indicated by vertical shifts of the special effect samples relative to the reference samples. The fact that there are a number of negative shifts in the Aesthetic Value in these samples is not surprising considering the fact that most of the effects were applied to contents that were not originally designed to have any special effects, and that the design of these

and Aesthetic Value, going toward the top right-hand corner in the graph, when using printed special effects. This was achieved with the gloss varnish version of the sample labelled *Report*, for example.

Finally, as an example of the variation in the expectations and preferences of different groups of people, Figure 12 shows the locations of the samples calculated separately from the assessments of the female and male observers. All samples considered, the special effect samples tended to be more positively perceived by the female observers, the shifts produced by the effects being toward right or top right in the graph, indicating increase in the Noteworthiness or both Noteworthiness and Aesthetic Value. In the case of male observers the shifts were mainly towards right or bottom right, indicating increase in Noteworthiness but often accompanied by decrease in Aesthetic Value.

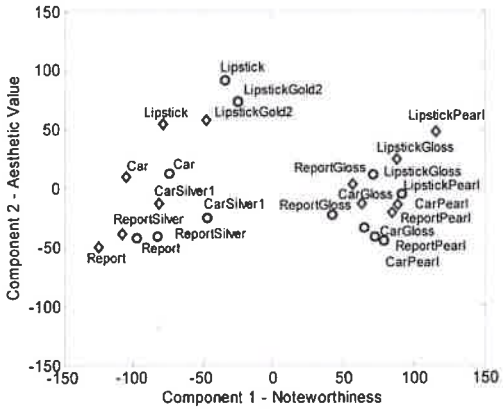

Figure 12:
The average observations of female and male observers for the 12 special effect print samples in the plane defined by the first two principal component axes. The average locations of the samples based on the assessments by female observers are marked by diamonds, while the sample locations based on the assessments by male observers are marked by circles

5. Conclusions

Especially the gloss and pearlescent varnish effects were seen to increase the effectiveness of a printed product in attracting the viewers' attention, compared to samples with no special effects. In some cases a significant improvement in the preference assessments was also achieved with the use special effects, particularly the two varnish effects mentioned above. The perceptual shifts relative to the reference sample with no effects was generally smaller for the samples in which metallic inks had been used.

Noteworthiness (comprised of such perceptual attributes as uniqueness, interestingness, and memorableness) and Aesthetic Value (comprised of such attributes as stylishness, beauty, and viewerfriendliness) were identified as the perceptual dimensions that best captured the perceptual shifts caused by the use of special effects in the studied cases. This information can be used for more effective measurement of the perception of printed special effects in the future. Noteworthiness was found to be relatively easy to increase with the application of special effects, but increases in Aesthetic Value were seen to require a sense of style in the design of the special effects. The current study was done with a relatively small set of print samples. Considering this and the numerous ways in which any of the special effect types could be used within the context of the given advertisement (or other content) and numerous other factors affecting the mental impressions of a printed product, one should be careful not to make too far-reaching generalizations about the perceptual effect of any given special effect based on these results. Still, the results of the study showed significant trends in all the cases that were examined, and provided a sensible interpretation of the perceptual effects.

More studies with a larger sample set representative of a wider range of applications of printed effects would be needed in order to make more general statements of the perceptual effects of printed special effects. As mentioned above, no categorical statements of the perceived effect of any given special effect can be made, due to the unpredictable case by case variations in the complex perceptual process involved in forming an impression of a printed product. What could reasonably be sought are significant perceptual trends in larger populations. A follow-up study concentrating on efficiently measuring Noteworthiness and Aesthetic Value of a considerably larger set of special effect print samples, and using a considerably larger group of observers, will be carried out during 2009.

References

Perception of print quality as a function of level of experience and as measured by eye movement and psychophysical scaling

Siv Lindberg and Annika Lindström

Innventia AB
Box 5604, SE-114 86 Stockholm, Sweden
E-mail: siv.lindberg@innventia.com; annika.lindstrom@innventia.com

Abstract

This study investigates the perception of print quality in printed images using eye movement recordings and psychophysical scaling. Further, the relation between the perceptual criteria: print quality, colour accuracy, sharpness, and print mottle are investigated. Eye-movement patterns were compared during evaluation. Results show that although average perceptual scales show a good agreement between experts and laymen, eye-tracking data show that different visual strategies are adopted in certain cases. In particular, experts have significantly fewer fixation counts and longer average fixation duration during all assessment criteria, compared to laymen. This may indicate that experts have a more focused way of evaluating print quality criteria, that they have a strategy about where to look in an image when assessing a specific criterion.

Keywords: print quality, eye-tracking, colour accuracy, sharpness

1. Introduction

The perception of quality in printed images in relation to eye-movements has not received much attention so far. This is mainly due to the difficulty in setting up well controlled eye-tracking studies using printed materials as stimuli so that the viewing area can be properly calibrated in a plane and thus analyzed with quantitative methods. However, new technical solutions open up the possibility for eye-tracking studies on printed materials and packaging.

Few studies have focused on eye movements in relation to digital image quality perception. Vuori et al [2004] investigated perceived image quality on CRT-screens and in particular whether perceived image quality can be associated to eye movements. Their result showed that eye movement parameters change depending on the instructions given to the viewer and, importantly, to physical image quality. Further, their results indicate that recording eye movements can be used to differentiate image quality evaluation strategies used by the viewers. They used saccade duration as the test parameter and showed a significant effect of image quality, i.e. mages with added blur and images with low or too high contrast caused longer saccade duration.

Buswell 1935 [in Babcock, Pelz and Fairchild 2002] indicate that level of training, type of instruction, and observer's background has influence on the viewing strategies adopted. Yarbus [1967] showed that type of instruction has an influence on the eye movement patterns when viewing a picture. Yarbus also suggest that the eyes tend to land on regions in the picture that contains information that is for the viewer "useful or essential for perception".

This study investigates the perception of print quality in printed images using eye movement recordings and psychophysical scaling. Further, the relation between the perceptual criteria: print quality, colour accuracy, sharpness, and print mottle are investigated. Eye-movement patterns are compared during the assessment of these criteria.

2. Method

A non-intrusive (remote) eye-tracker (Tobii x50) was used. This is a binocular eye-tracker and analyses may be based on monocular or binocular data. The accuracy is 0, 5 degrees and the spatial resolution 0, 25 degrees. Drift errors are less than 1 degree. Effective freedom of head- movement is about 30 x 15 x 20 cm at 60 cm from the eye-

A scene camera was positioned behind and slightly above the observer's head. The eye tracker was placed directly underneath the slanted plane used for sample presentations. A calibration grid with 9 fixation marks was used to calibrate the eye gaze to the physical area in the plane and for the gaze overlay in the recorded video sequences. The calibration routine allows for viewing of physical objects, for example a print and obtaining absolute coordinates for fixations and gaze paths.

Eye movement data collected in the experiments are locus of fixation (gaze point), which indicates which points received the most foveal attention, number of fixations, duration of fixations, order of fixations and time in milliseconds to fixations. In addition, recordings of gaze paths are collected.

The viewing room was equipped with standard illumination and viewing conditions within the graphic arts industry [ISO, 2000]. Overhead illumination was used (D50) on a slanted plane to avoid glare effects. The viewing angle was approximately 35 degrees. Participants wore gray lab coats in order to avoid influence of different colour in clothing.

2.1 Stimuli

A printed advertisement for children's clothing, approximately 188 mm × 247 mm, was used as stimulus. Twelve different versions from different newspapers, varying widely in quality but with the same motif, were presented to the observers. Each print was evaluated against a reference print, a proof that represented the reproduction goal for the process.



Figure 1: Left: Test image used. Right: View of experimental set up. A scene camera is mounted behind the observer that captures a video on which gaze data is overlaid

2.2 Subjects

Laymen: A group of 24 observers with no previous experience of print quality scaling was selected. They were students, recruited from the Royal Institute of Technology and they were paid approximately $35 for their participation. Experts: a group of 12 experienced print quality graders was recruited from the in-house panel and from professionals within the field.

2.3 Procedure

The participants first read written instructions about the experiment. Each observer then briefly viewed all 12 samples in order to familiarize themselves with the range of variation, as well as to provide data for a 'base line'. In order to get an assessment of overall print quality that was not biased by the assessment of other quality criteria, all observers started by assessing the 'print quality' for all samples. After that, the observers assessed the 3 specific print quality criteria: sharpness, colour accuracy and mottle, each in separate trials. This was done in order to obtain independent assessments of the respective criteria. The presentation order of the samples, as well as the assessment order of the criteria, were randomized and balanced between the observers.

The twelve printouts were presented to the observers by the experimenter. The samples were always placed in a fixed position on the slanted plane. The observers were asked to assess the criteria on a 9 point scale in

comparison to the reference proof print. A scale number of 1 denoted much worse print than the proof and 9 denoted the same quality as the proof. The scale could be extended to 10 in cases where the observers felt that a sample might be better than the proof. The observers were instructed to view the printouts for a maximum15 seconds.

2.4 Colour measurements

The prints had no control strips and thus L*, a*, b* measurements were performed directly in the image using a GretagMachbeth Spectrolino with and x,y SpectroScan table, and adopting a procedure suggested by Leeming [2004].

Eighteen areas were chosen to represent the image content. These were areas located within the areas that received a lot of foveal attention during assessment of colour reproduction according to the hot spot map in figure 2 a. For all samples, ΔE to the reference was calculated as the average 18 measurement areas. A positioning and repeatability tests was performed (on the reference sample).

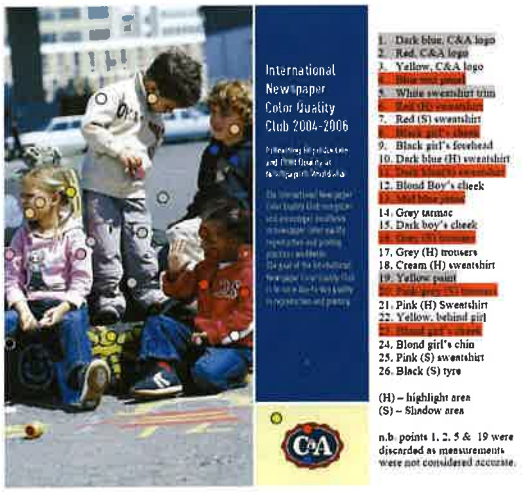

Figure 2:
Areas selected for colorimetric measurements (L, a*, b*).*
Areas 4, 6, 8, 11, 13, 16, 20 and 23 were used to define image colour

3. Results

3.1 Consistency of data

Inter-observer agreement was analyzed in terms of correlation coefficients between the observer's ratings of 12 samples. A moderate within-group agreement was found for both experts and laymen and the internal agreement was slightly higher for the expert group (Table I).

Table I: Inter-observer agreement for the different quality criteria

	Laymen	Experts
Print quality	0,61	0,65
Sharpnes	0,55	0,68
Colour	0,72	0,72
Mottle	0,36	0,43

The agreement between average scale values for experts and laymen was high: 0.96 for print quality 0.97 for Sharpness, 0.98 for colour accuracy and 0.82 for mottle. A multiple regression analysis using the three criteria variables 'sharpness', 'colour accuracy' and 'mottle' account for 89% of the variance in "overall quality" ($F(3,8)=284,8$ $p < ,00000$). The significant βweights are 0.5 for 'colour accuracy', 0.4 for 'sharpness'. These results are in agreement with earlier findings that stress the importance of colour [c.f. Montag, 2001, Green &

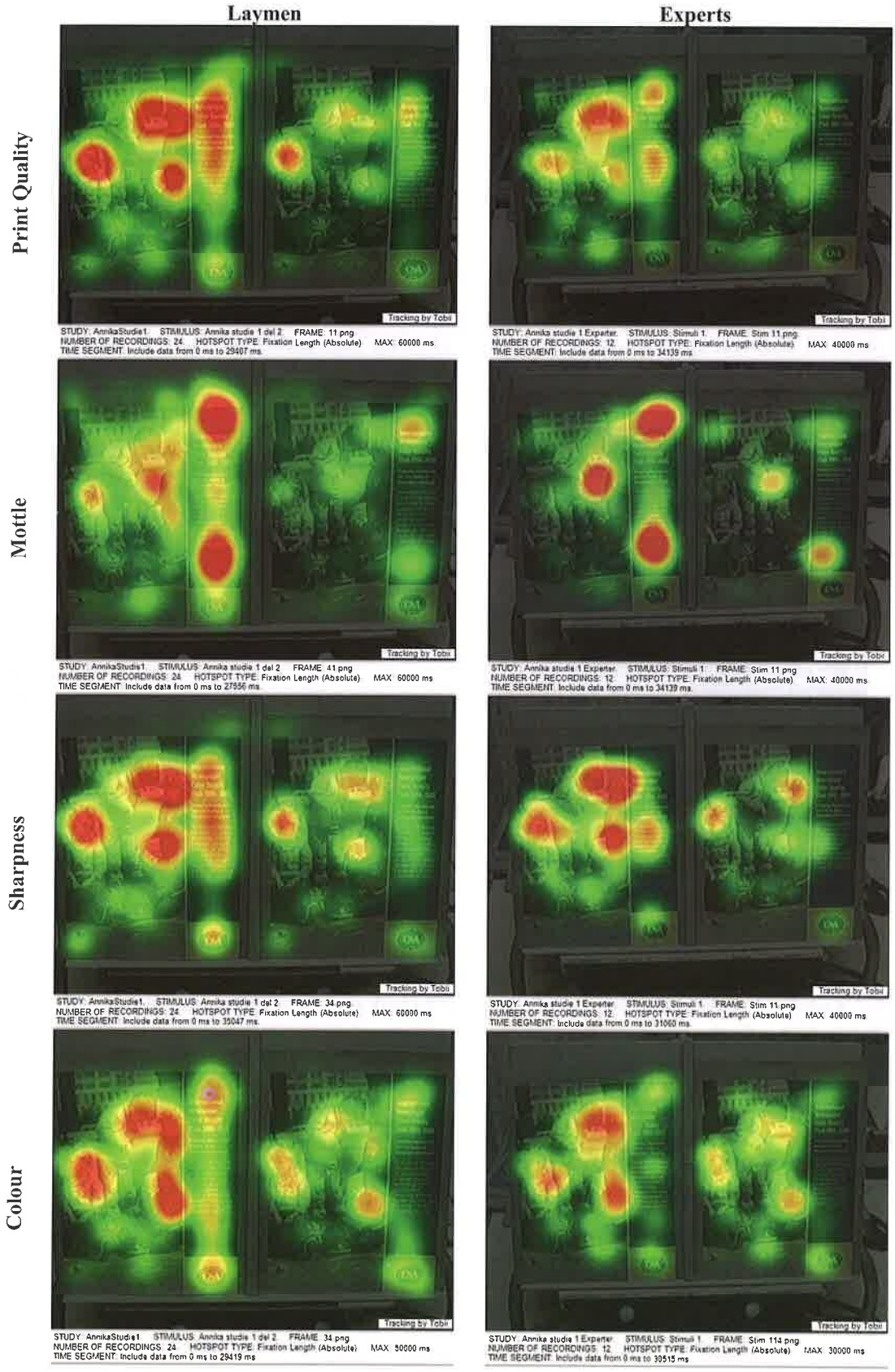

Figure 3: Average fixation duration for laymen (left) and experts (right). Reference sample is always placed to the left in the sample holder

3.2 Fixation density maps

Fixation density maps, so called hot-spot plots, were analyzed. Fixation density plots serve to visualize gaze behavior. The hot-spot plots separated for experts and laymen for the four different judgment criteria show similarities and differences, see Figure 3. There is a tendency for the expert group to have their fixations concentrated to a smaller area of the image this being particularly evident in the mottle and colour accuracy evaluation. The mottle criteria reveal a slightly different visual strategy in that fewer fixations are on the persons in the image and more fixations are found in the homogene blue areas. For the sharpness evaluation, laymen rely more on text areas and both groups focus on fine detail in the faces. The print quality and colour accuracy evaluation appears to give similar gaze pattern for both groups.

3.3 Fixation data

A 2 (level of expertise) x 4 (rating criteria) repeated measures analysis of variance (ANOVA) was conducted in order to get a general impression of differences between laymen and experts. The two within-subjects factors were level of expertise (laymen or experts), and assessment criteria (print quality, sharpness, colour accuracy, mottle). The ANOVA results are given in Tables II-V. There is a significant difference in gaze pattern for level of expertise and for the interaction between level of expertise and assessment criteria. Experts have significantly fewer fixation counts and longer average fixation durations during all assessment criteria, see Figure 4. Furthermore there is a significant difference between gaze patterns for different evaluation criteria. For experts, colour assessment requires shorter average fixation than mottle and sharpness criteria (Figure 4, right panel) and for laymen fixation count is higher for the print quality criterion than for the mottle criterion (Figure 4, right panel).

Table II: ANOVA results for fixation count

Sources of variation	df	F	p	MS
Main effects				
level of expertise	1	1859,790	<0,001	1328,834
criteria	3	5,750	<0,001	4,108
Interaction				
level of expertise X criteria	3	2,784	<0,001	1,989

Table III: ANOVA results for average fixation duration

Sources of variation	df	F	p	MS
Main effects				
level of expertise	1	3177,25	<0,001	1328,834
criteria	3		<0,001	4,108
Interaction		29,07		
level of expertise X criteria	3	3,38	<0,05	1,989

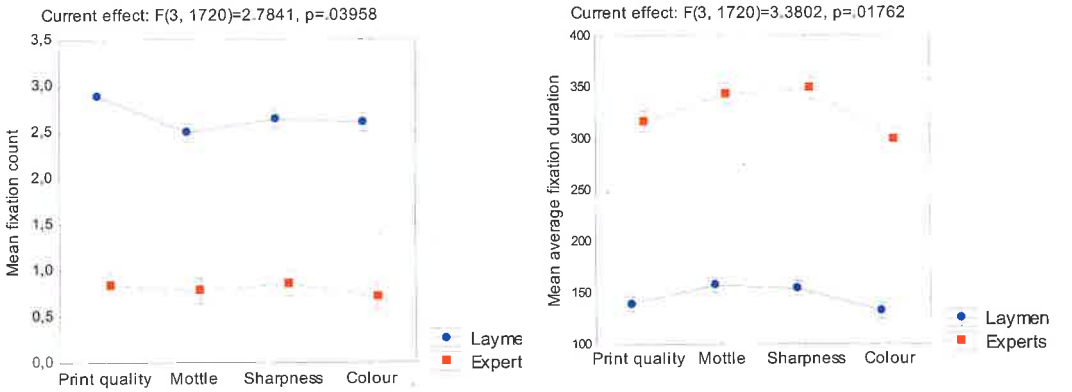

Figure 4: Average fixation count (left) and average fixation duration (right) for each assessment criteria plotted for

The data was further analysed in terms of Areas Of Interest (AOI) in order to see if there are statistical differences between different areas of the image and between with respect to assessment criteria. Ten AOIs were defined in the test image. For the ANOVA, the AOI:s were merged into five areas based on general content and the hot spot analysis. The merged AOIs were 1) Faces, 2) Blue (homogeneous area), 3) Text, 4) Clothes, and 5) Background. AOIs are shown in Figure 5.



Figure 5:
Areas if interest used for statistical analysis: 1 = faces, 2 = blue, 3 = text, 4 = clothes and 5 = back(ground)

For all the assessment criteria print quality, sharpness, and colour accuracy, the faces in the image received significantly higher fixation count compared to other areas. Experts had fever average fixation counts than laymen relatively less differences in attention diverted to the different AOIs, see Figure 6. For the mottle criterion the homogeneous blue areas received more fixation counts. A visual inspection of Figure 6 and 7 indicates that there is a possible significant interaction effect between level of expertise and AOI for mottle assessment.

Table IV: ANOVA results for fixation count

Sources of variation	df	F	p	MS
Main effects				
level of expertise	1	1752,064	<0,001	36757,3
criteria	1	8,432	<0,001	176,9
Interaction				
level of expertise X criteria	3	2,185	<0,05	45,8

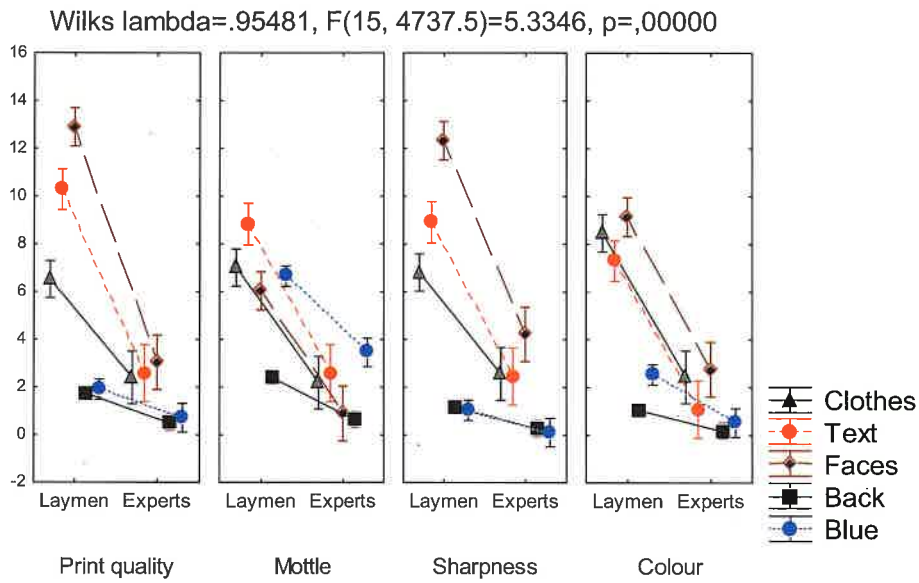

Figure 6: ANOVA results for numbers of fixations in different areas of interest. Average fixation counts for each AOI is plotted against level of expertise for the different assessment criteria

Table V: ANOVA results for average fixation duration

Sources of variation	df	F	p	MS
Main effects				
level of expertise	1	404,388	<0,001	350430
criteria	3	11,697	<0,001	93433
Interaction				
level of expertise X criteria	3	3,119	<0,05	29958

For all the assessment criteria print quality, sharpness, and colour accuracy, the faces in the image received significantly longer average fixation duration compared to other areas. For the mottle criterion the homogeneous blue areas received longer average fixation duration,

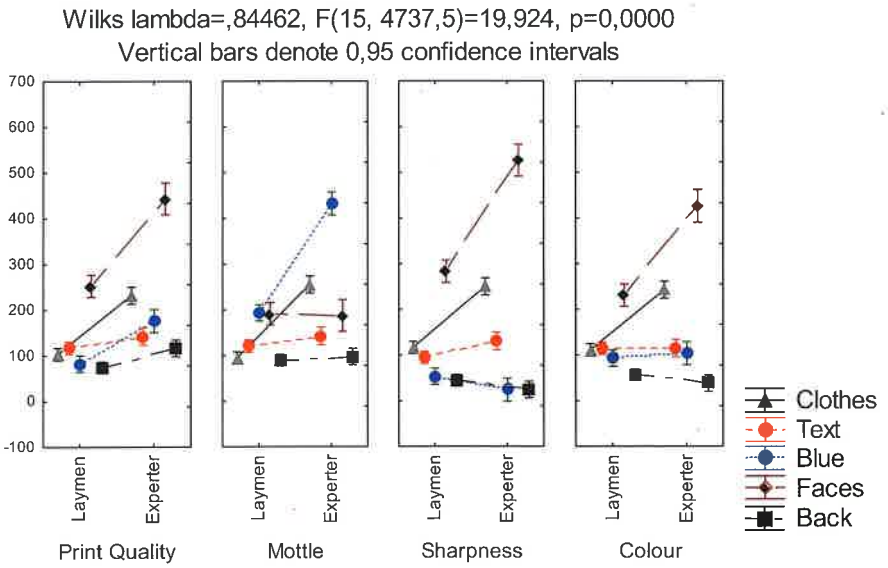

Figure 7: ANOVA results for numbers of fixation length in different areas of interest. Average fixation duration for each AOI is plotted against level of expertise for the different assessment criteria

3.4 Psychophysical scales

The average scale values for colour reproduction were plotted against colour deviations between reference and test samples, expressed as ΔE averaged over several measurement areas (see Figure 2). The correlation was r = 0.90 for experts and 0.87 for laymen. Interestingly, no individual measurement area in the image showed good correlation to the assessed colour reproduction.

4. Conclusions

The inter-observer agreement within the laymen and expert groups were moderate for print quality, colour accuracy and sharpness. For mottle agreement was poor in both groups indicating that this criterion was most difficult to assess. The agreement between expert and laymen groups was excellent for all criteria but mottle showed a slightly lower agreement.

Multiple regression analysis shows that the colour accuracy criterion adds substantially to the prediction of the perception of overall print quality. Average colour deviation from the proof measured as ΔE CIE Lab in selected image areas gave a good prediction of the colour accuracy assessment.

The gaze patterns from the sharpness and mottle assessments show that there were fewer fixations on the persons in the image and more fixations in the slowly varying areas and the text areas.

Laymen and experts use similar strategies depending on the criteria they are asked to evaluate, but experts have a more focused gaze pattern on slowly varying areas in the mottle assessment. Experts have significantly fewer

fixation counts and longer average fixation duration during all assessment criteria, compared to laymen. It is believed that longer fixations is associated with cognitive demand and fixation duration has been correlated with the amount of information being processed during foveal analysis [Mofitt 1980; Duchowski, 2007].This may indicate that experts have a more focused way of evaluating print quality criteria and a strategy about where to look in an image when assessing a specific criterion.

Eye-tracking in image quality assessment and in particular in print quality assessment is still a relatively new field and different ways of making use of such information is currently being investigated. Some authors have tried to use visual eye-movement information to improve the prediction capabilities of the image quality metrics, frequently used in digital video quality prediction. Image quality metrics are a set of equations that predict perceived image quality from its physical descriptors and weighted by some model of the human visual system, e.g. the contrast sensitivity function [c.f. Barten, 1999]. By adding the visual attention as quantified by eye-movements to such metrics, Ninassi, Callet and Barbara [2007] have investigated different approaches to how to weigh an image distortion map with a human saliency map obtained from eye tracking recordings. Although, their results could not clearly establish a prediction improvement, it still indicates a promising direction for image quality research.

References

1. Babcock, J. S., Pelz, J. B., Fairchild, M. D (2003) *Eye Tracking Observers During Color Image Evaluation Tasks Proceedings of SPIE, Human Vision and Electronic Imaging.* San Clara, 2003. Vol. 5007 -20
2. Barten, P. G. (1999). Contrast Sensitivity of the Human Eye and its Effect on Image Quality. Bellinghamn, WA: SPIE Optical Engineering Press
3. Duchowski, A. (2007). Eye Tracking Methodology. Theory and Practice. London: Springer. information processing. *Cognitive Psychology, 1*, 225-241
4. Green, P., & Lindberg, S. (2004). *Methods of quality assessment for large sample sets.* Proceedings of the CGIV 2004. Second European Conference on Colour in Graphics, Imaging, and Vision, Aachen, Germany 201-206
5. ISO. (2000). *ISO 3664:2000 Viewing conditions - Prints, transparencies and substrates for graphic arts technology and photography.* Geneva: ISO
6. Leeming, K. J. (2004). *A model of the relationship between image colour and visual assessment score.*, Univeristy of Arts/London College of Communication, London
7. Montag, (2001) Multidimensional analysis reveals importance of color for image quality. Proc. 9th IS&T/ SID Color Imaging Conference. 17-21
8. Moffit, K. (1980). Evaluation of fixation during visual search. *Journal of Perception & Psychphysics.*2743: 370-372
9. Ninassi, A., Le Meur, O., & Le Callet, D. B. (2007). Does where you gaze on an image affect your perception of quality? Applying visual attention to image quality metric. Paper presented at the IEEE International Conference on Image Processing, San Antonio, USA
10. Vuori, T., Olkkonen, M., Pölönen, M., Siren, A. & Häkkinen, J. (2004). *Can eye movements be quantitatively applied to image quality studies?* Paper presented at the Proceedings of the third Nordic conference on Human-computer interaction

New business forms in e-Business and media - e-Media

Ulf Lindqvist[1], Niels Bjørn-Andersen[2], Örn S. Kaldalóns[3], Arne Krokan[4], Christian Persson[5], Leif Bloch Rasmussen[2] and Soley Rasmussen[2]

[1] VTT Technical Research Centre of Finland
P. O. Box 1000, FIN-02044 VTT, Finland
E-mail: ulf.lindqvist@vtt.fi

[2] CBS Copenhagen Business School
Njalsgade 80 bld. 16, DK-2300 Copenhagen, Denmark
E-mail: nba@cbs.dk

[3] ICEPRO
Kringlunni 7, IS-103 Reykjavik, Iceland
E-mail: icepro@icepro.is

[4] NTNU
Høgdaveien 44, NO-1482 Nittedal, Norway
E-mail: arne@krokan.com

[5] INNVENTIA AB
P. O. Box 5604, SE-114 86 Stockholm, Sweden
E-mail: christian.persson@stfi.se

Abstract

It has been the scope of this study to create new service forms and business models for the border area between e-Business and Media (e-Media). The project was carried out by a Nordic consortium consisting of five research organisations and eight companies with financial support from the Nordic Innovation Centre (NICe).

The study first analyses the structural changes in the media and allied industries, i.e. content creation and advertising. Thereafter, a framework for innovations in e-Media is built up, together with a variety of business models. The framework is used to identify new, innovative service embryos for the e-Media sector. Finally eight new services are developed in industrial case studies.

The project has been carried out by a consortium consisting of five Nordic research organisations, which have relations to e-Business and the media sector, together with eight industrial partners from the media sector, software companies, and service providers.

The outcome of the project is an extensive description of innovation methods and business models for Nordic companies working in the media or e-Business sector or offering services over the net. The report also gives eight examples of more or less successfully exploited e-Media pilot cases.

Keywords: e-Business, e-Media, business models, value chain

1. The objectives of the research

e-Media refers to the boarder area between e-Business and media, where the Nordic countries have the opportunity to create new business thanks to its strength in both the ICT and media sectors. In a preliminary study a Nordic network for e-Business was established between the media industry, software vendors, service providers and scientists. It was also stated that new service forms were needed for this boarder are together with new business models.

It has been the scope of this project to create new service forms and business models for the e-Media market exploitable to Nordic media companies, service providers and software vendors on a global market. The project

To reach the goal the study first had to analyse the structural changes in the media and allied industries, i.e. content creation and advertising. Thereafter, a framework for innovations in e-Media had to be built together with a variety of business models. The framework was then used to identify new innovative service embryos for e-Media. Finally some of the new services should be exploited in industrial case studies.

The outcome of the project should be an extensive description of innovation methods, business models, a number of innovation embryos for exploitation and a number of more or less successfully exploited e-Media pilot cases. The project should also elucidate the business potential of e-Media.

2. Research methods

The future position of the media industry was first evaluated. The media sector faces increasing competition from network operators, software and hardware providers and new service providers turning into content providers. At the same time advertising is searching new channels like search engines, social media and virtual networks. Also the boarder between content providers and consumers is blurred up as consumers become producers. The conclusion is that the media company can be successful only, if innovation becomes an integrated part of its strategy.

Therefore, a framework for innovation in e-Media was developed. This included a general innovation methodology of both technological and non-technological innovation methods in combination with a permanent, comprehensive and systematic (TRIZ) approach.

An essential part of the innovation framework consists of new business models. A variety of business models were outlined. These are either marked based industrial business models or informal business models focusing on transaction costs or values, norms and belief systems.

The innovation framework was applied to brainstorming in the e-Media area resulting in 63 innovation embryos. The innovation embryos were further analysed using the TRIZ problem solving methodology. Since the e-Media service forms usually requires new business models, where the earning logics go beyond the traditional media models based on subscription or ad selling. Therefore, a variety of business models were analysed.

Finally, eight new specific e-Media services were specified and developed. Each service was analysed and the contradictions related to their realisation were estimated together with their business potential. The degree of maturation varied between the different pilots: some of them were fully developed and exploited during the project, whereas some of them were only planned and analysed.

3. Results

The media industry is facing a lot of new challenges at the moment:

The traditional position of the media industry as content provider is weakened by competition from network operators, software and hardware providers and new service providers like retailers, finance houses etc. The media companies can enlarge their position in the value chain and become service providers.

The media industry strongly depends on advertising, which is going through a dramatic evolution process. The consumer's freedom of choice regarding media and time of consume it increases, which makes the traditional media less attractive to the brand owners. New effective channels appear like search engines, social media, virtual networks, which can reach specific target groups in specific decision making moments.

The boarders between content providers and consumers are blurred up, as are the boarders between the driving forces of media: advertising, entertainment and information. Consumers turn into content providers and the driving forces overlap each other more and more in infotainment and edutainment.

The success of e-Media requires innovation to become a part of the strategy of the media company. This process has been facilitated in this project in several ways:

A framework for innovation in e-Media has been presented. The framework includes technical innovations in the media sector, non-technological innovations in the media sector, permanent innovations, comprehensive innovations and systematic approach using TRIZ' problem solving methodology.

The methods have been applied in brainstorming meetings with nine experts resulting in 63 new innovation embryos for new service products for e-Media. Of these embryos 28 were media applications, 18 technology applications and 19 general new service forms. The experts considered the following technologies to be most important: high speed broadband, on-line mobile technology, hybrid media and codes, AD-search, visual and audial.

Table I: A summary of the most important technology and market trends and contradictions for e-Media

TECHNOLOGY	MARKET	CONTRADICTIONS
• High speed broad-band • Displays: Flexibility, ePaper etc • Integration of infra-structures • Distributed systems • 2-D/3-D codes, RFID • Pier-to-pier • Health monitoring media • Deep web/links • Online via mobile phone • Visuality/audio • Web 3.0 • Hybrid media • Blogs • sms • Podcasting • Advertising: Search, Video, Mobile	• Mobility • Interactivity • Integration of media into everyday life • Self service culture • Personalisation, customization • User generated content • Visuality/audio - Less textual • Work/leisure/social/political space --- Individual consumer value • Age: Digital natives/ immigrants • Gender • Income • National characteristics • Online (always "wired"/never "wired")	• Publish first in print / online • Trust / cynisism • Pro-am / Ingrained standards • Cooperate / compete • Global / local • Diversify / focus • More visual / less textual • "Digital natives"/ " Digital immigrants" • Subscription / CoD – Micropayments / Free content --- Future contradictions ?

The Gartner Hype Cycle is a technology forecasting tool. A comparison of the curves published in 2006 and 2008 [Gartner 2006, Gartner 2008] in Figures 1 and 2 illustrates the rapid changes in expectations to for example Web 2.0 and 3.0 technologies.

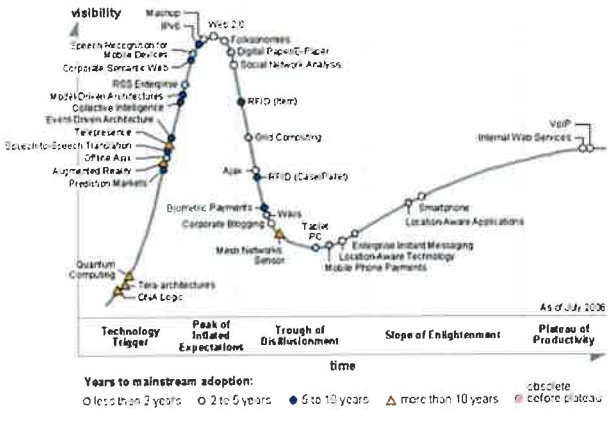

Figure 1: Gartner Hype Cycle 2006

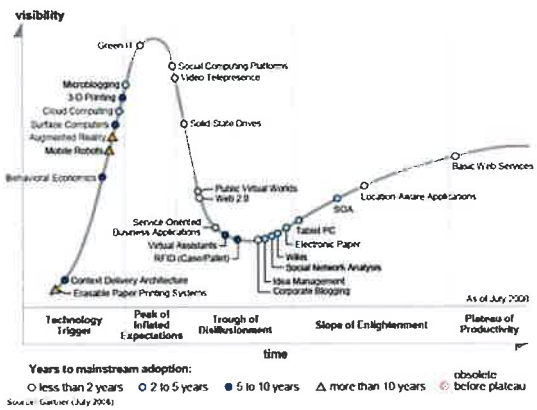

Figure 2: Gartner Hype Cycle 2008

The e-Media service forms usually requires new business models, where the earning logics go beyond the traditional media models based on subscription or ad selling. Therefore, a variety of business models have been analysed, the most important ones are:

- Industrial business models, which are either market based and focusing on positioning the innovation in a market chain, or resource based focusing on core competencies and organizational cultures.

- Informal business models, which are either transaction cost models focusing on handling the transaction costs related to information and knowledge, or new institutional models focusing on values, norms and belief systems.

Finally, eight new specific e-Media services were specified and developed, one by each industrial company in the consortium in co-operation wit the national research partner. Each service form was described in detail, its relation to e-Media analysed and the key contradictions for realisation were described according to the TRIZ method. Thereafter, technical solutions were searched for to overcome the contradictions and the ideal final result specified. The case was studied from a technological and a business perspective and the business potential evaluated. Finally each case was reported. The eight e-Media service cases were:

- The use of 2D barcodes in lottery business for playing on-line and receive latest information and statistics about games and teams,
- Design your own shoe on-line via the Internet or Facebook and become designer for the shoe collection,
- Personalised ads on the Internet based on individual profiles,
- Coffee AdInfo, hot spot media application in a coffee machine for the personnel in a company,
- Quattro – an application of e-Learning for publishing in mobile and conventional media,
- Business News – a value model for Facebook,
- FM957 – make the income match the popularity of radio FM957,
- Funding Model for Media and IT Consulting.

The pilots are described in Table II. For each pilot the research organisation responsible for its evaluation and the company responsible for its exploitation have been given together with an estimation of the maturity degree of the pilot.

Table II: Pilots for e-Media developed in the project and their degree of maturity

PILOT	NAME	EXPLOITER	RESEARCHER	MATURITY
1	2D barcodes in lottery online	Veikkaus Oy (FI)	VTT (FI)	Ready to take into use
2	Shoe design on Internet	Kesko Oyj	VTT (FI)	Commercially exploited
3	Personal ads based on profiles	Adaptlogic Intressenter AB (SE)	STFI-Packforsk AB (SE)	Commercially exploited
4	Coffee AdInfo, Hot Spot Media	Edita Sverige AB (SE)	STFI-Packforsk AB (SE)	Theoretical planning
5	Quattro e-Learning in media	07-Gruppen (NO)	NTNU (NO)	Ready to take into use
6	Facebook business model	Jyllands-Posten (DK)	CBS (DK)	Ready to exploit
7	Case FM957	Radio station FM957 (IS)	ICEPRO (IS)	Ready to take into use
8	Consultations in e-Media business	IT/Media Consultant (IS)	ICEPRO (IS)	Unfinished

The degree of maturation varied between the different e-Media service pilots. The shoe design and the profile based personal ads were fully produced and applied during the project. The Coffee AdInfo, the value model for Facebook and the Funding Model were partly tested during the project. The remaining pilots were only analysed and planned. For each pilot the business potential was estimated.

Two pilots utilized social media like Facebook. Examles of their applications are illustrated in Figure 3 and 4, i.e. the winning shoes collection of Kesko Oyj designed by a reader and the Facebook business model built around user generated content based on the e3-value ontology developed by Gordijn and Akkermans [2001].



Figure 3: The winning shoes collection "Andiamo by Sonja"

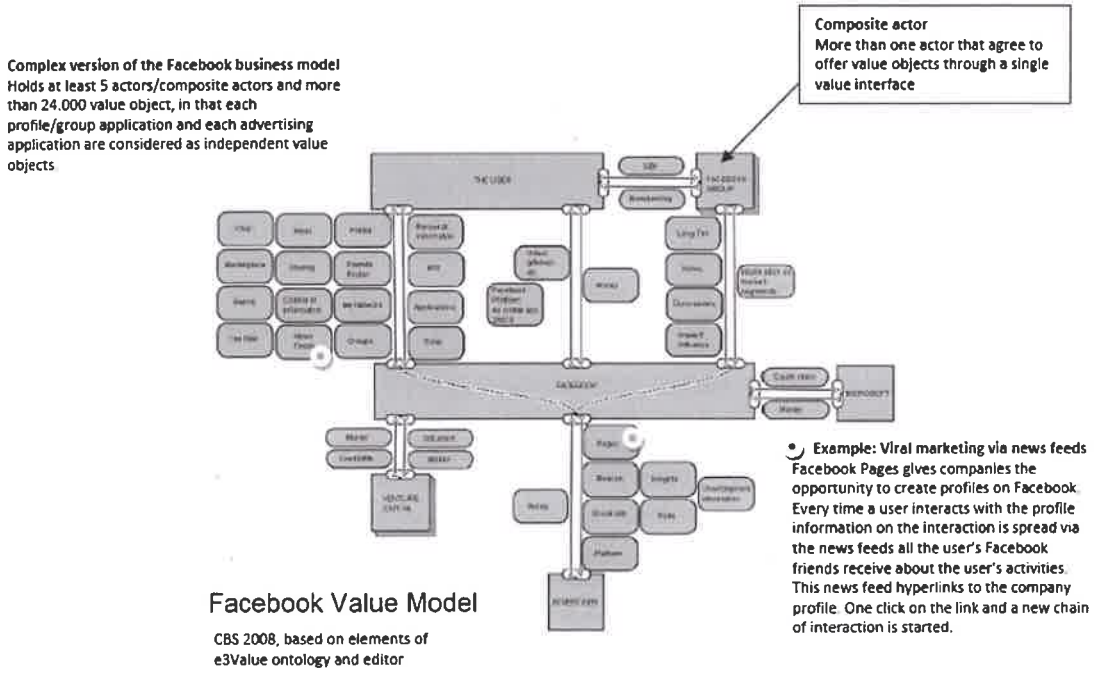

Figure 4: Facebook business model applied in the pilot of Jyllands-Posten

4. Conclusions

As a general conclusion it has been shown that e-Media, i.e. the integration of e-Business in media, offers a huge potential for both Nordic media companies, service providers and software vendors. The applications always require innovative new services and innovation must, therefore, become an integrated part of the co-operation between service providers, vendors and media. For these applications, the project leaves behind an extensive description of innovation methods, business models, more than sixty innovation embryos for exploitation and eight examples of more or less successfully exploited e-Media pilot cases.

Essential questions for both the future of the media industry, e-Business and the advertisement business are how to create diversified and high quality content the consumers are willing to pay for, and how media shall meet the new requirements of advertising in the future. These questions are logical continuations of the work done so far for e-Media.

References

1. Lindqvist, U., Bjørn-Andersen, N., Kaldalóns, Ö. S., Krokan, A., Persson, C., (2008), *New Business Forms in e-Business and Media "e-Media", Final Report of NICe Project 06212, VTT Working Papers, Espoo 2008, 150 p. To be published by Nordic Innovation Centre (NICe)*
2. Gartner (2006), *Hype cycle for emerging technologies, 2006*
3. Gartner (2006), *Hype cycle for emerging technologies, 2006*
4. Gordijn, J., Akkermans, H., (2001), *Designing and evaluating e-Business models, IEEE Intelligent Systems, July-August,* 2001



Open innovation process in graphic arts companies

Olli Nurmi

VTT Technical research centre of Finland, Media technologies
P. O. Box 1000, FIN-02044 VTT, Finland
E-mail: Olli.Nurmi@vtt.fi

Abstract

Development of new business opportunities and new products and services has traditionally taken place within one company. Several factors have however contributed that this closed innovation process has become in functional and open innovation process has been developed to enhance the innovation process. The open innovation process includes active idea generation and seeking technology outside the company borders and co-operation with the suppliers and competitors to generate added value for the customers.

The purpose of this project was to define and implement the open innovation process in several graphic arts companies. The project generated networks, innovations and more specifically three development projects.

The open innovation process works best in the so called precompetitive stage where the time to market is relatively long. Additionally it was found out that the best result was achieved when the customers are involved into to the innovation process.

Keywords: Open Innovation implementation, graphic arts companies

1. Introduction

Finland has consistently ranked at the forefront of innovation investment and performance, and innovation policy is at the heart of public policy. Finland ranks second in the OECD in terms of R&D intensity (at 3.45% of GDP) and aims at 4% of GDP by 2010. Business R&D stood at 2.44% of GDP in 2007 and the intensity of higher education R&D has doubled over the past 15 years. The largest investments into the R&D are within ICT-, electronic- and medical industries.

In the media industry the R&D intensity is low compared to the other industries in Finland. It has been argued that the media industry belongs to the creative and knowledge intensive industries and the innovation intensity metrics should cover not only the product, but also the production, user experience, communications and even the internal organisation, business model and the location in the value chain.

It can be argued that the print media industry has reached mature state which can be characterised by overcapacity and heavy competition based primary on product pricing. In order to find growth and economic viability the companies should increase their efforts on developing new services and innovations that give added value to the customers compared to the ordinary four colour standard printing service.

This innovation process can be speeded up by applying open innovation process. The central idea behind open innovation is that in a world of widely distributed knowledge, companies cannot afford to rely entirely on their own research, but should instead buy or license processes or inventions (e.g. patents) from other companies. In addition, internal inventions not being used in a firm's business should be taken outside the company (e.g., through licensing, joint ventures, spin-offs). In contrast, closed innovation refers to processes that limit the use of internal knowledge within a company and make little or no use of external knowledge.

The objective of this research was to define and apply open innovation process in the graphic arts companies. The study involved in nine companies working in different market segments. The research focused on identifying:

- new customer segments or current segments that were underestimated
- new customer needs or needs those were currently underestimated.
- new ways to create, produce or deliver current or future products or services to the new or existing customer segments.

The innovation process was implemented into the companies and it resulted into several research ideas. Some of the ideas were later realised as development projects.

2. Open Innovation process

A recently proposed and popularized model for the management of innovation is based on the need for companies to open up their innovation processes and combine internally and externally developed technologies to create business value. This notion of open innovation was first proposed by Chesbrough. [Chesbrough 2003].

Changes in society and industry has led to an increased mobility of knowledge workers and the development of new financial structures such as venture capital - forces that have caused the boundaries of innovation processes to start breaking up. Chesbrough defines open innovation as:

"the use of purposive inflows and outflows of knowledge to accelerate internal innovation, and expand the markets for external use of innovation, respectively. Open Innovation is a paradigm that assumes that firms can and should use external ideas as well as internal ideas, and internal and external paths to market, as the firms look to advance their technology". [Chesbrough, 2006]

Open innovation has emerged as a model where firms commercialize both external and internal ideas/technologies and use both external and internal resources. In an open innovation process, projects can be launched from internal or external sources and new technology can enter at various stages. Projects can also go to market in many ways, such as out-licensing or a spin-off venture in addition to traditional sales channels.

There are many ways of practicing open innovation. Enkel and Gassmann [2007] suggest some examples:

- customer and supplier integration,
- applying innovation across industries,
- buying intellectual properties,
- investing in global knowledge creation.

The focus lies on the transformation of the previously solid boundaries of the company to a semi-permeable membrane to enable innovation to move more easily between the external environment and the internal R&D processes. A central part of innovation process is also to organize search for new ideas that have commercial potential.

The research field is expanding in many directions and the ongoing debates cover a multitude of areas connected through the overall aim of understanding how firms can become more innovative.

An organisation that promotes innovation as a key output must couple creativity, calculated risk, and entrepreneurial spirit with business and project delivery disciplines. An innovative organisation is, therefore always a subtle and shifting balance between the two different cultures of creativity/freedom (inspiration) and control/delivery (perspiration).

3. Methodology

In this study the open innovation model was defined and applied for the graphic arts companies. The purpose was to generate innovation networks where the connections with between the different actors were loose. New ideas were gathered outside the companies from the related universities and colleges and the ideas were innovatively combined and refined. The project used common wiki-based knowledge store and blogs were used to inform different parties.

The practical work was carried out within the companies in several workshops. The idea generation was carried out both inside the companies and together with the project group. Several material and press suppliers, research organisations, universities and college of media technology were involved in this idea generation stage.

Following methods were applied:

- customer/product segmentation,
- mapping of the company innovation capacity,
- identification of the new business opportunities by analysis of the solutions that the customers were looking for,
- identification of the common business practices and opportune for new solutions,
- identification of new and developing customer or service segments,
- identification of the new value chains between different actors,
- analysis of the actions that led to the buying decision of the customer.

After this first stage the ideas were analysed and evaluated within one company by mapping the potential of the idea against the strategy and possibilities of the specific company. This stage was carried out confidentially. After selecting the most potential ideas a specific project was defined to develop the idea further after evaluation and possible implementation.

4. Implementing open innovation process

Generally the innovation activity breaks down into discrete linear units. Progression only occurs after satisfying certain criteria, designed to ensure that the investment is minimised in the early stages and if necessary the project abandoned sooner rather than later. In this way a portfolio of projects in an "innovation pipeline" (sometimes called the innovation funnel because many initial ideas are refined down to only a few market entry projects), can be created, with their progress matched to suit the available funding, resources and desired entry time into the market place.

The generic stages of the innovation process are presented in the picture 1 and the stages were:

1. **Idea generation**
   A very large number of ideas are considered against strategic fit, market need, impact on the company and the chances of technical success, to decide which are worth exploring further.
2. **Proof of concept/principle**
   Projects to go into development are selected on the basis of market acceptability, achievability of technical requirements, risk/reward criteria, and the availability of the required resources (people, facilities and money).
3. **Development, prototyping and testing**
   Progress to market is dependent on satisfactory feedback on the prototype, an assessment of the competitive response, and deliverable strategies on sourcing, marketing and pricing/ margins.
4. **Marketing and launch**

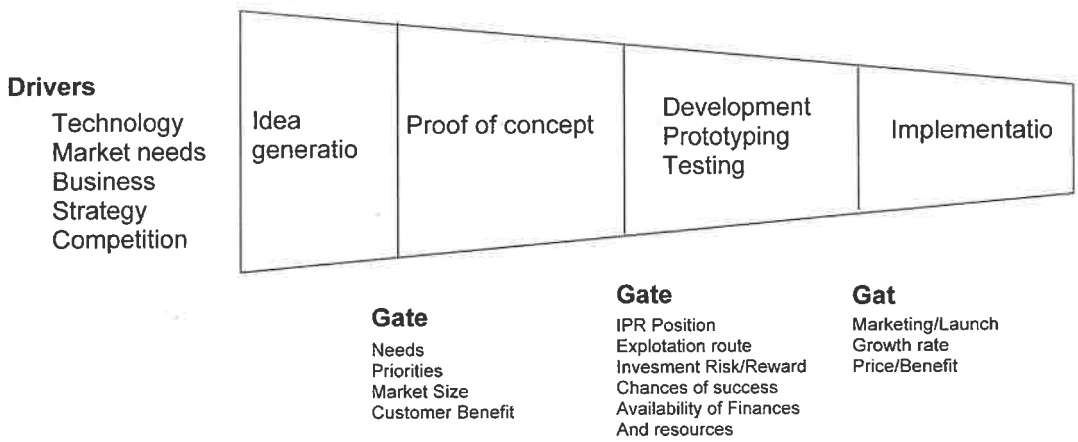

Figure 1: Generic innovation process in the graphic arts SME

In the workshops within one company the generic open innovation process was adapted and applied to the needs of the specific company. Typically the innovation process was organized as part of the steering group meetings of the company. The themes of the meetings ranged from idea generation, idea evaluation and ranking, selection of the ideas to concept creation. The customer involvement was carried out in many different ways including direct discussions, workshops and thematic days.

5. Results of the open innovation process

At the end of the project the first results of the innovation process were gathered. In the following list some of the published results are described.

5.1 Ecocalculator for book printer

The printing of books is impacted by growing competition from Asian "low cost" countries, to which some of the printing of books has been relocated. Especially relocation from Europe to Far East countries is occurring in the educational and consumer book segment.

This market pressure and discussions with the book publishers lead to the idea of ecobalance calculator for the book printing process where the effect of the different manufacturing parameters on the ecobalance can be seen. These ecobalance calculations were seen as a possibility to differ from the printers in the Far East countries. The book publishers can also be assisted to do more environment friendly material and process choices.

The ecobalance calculator is software that can be run over the internet by standard browser. Several factors during the lifecycle of the book are taken into the account to optimise the material consumption, waste, energy and transport emissions.

The key factors in the printing process are energy consumption, heat generation, material consumption, paper and material waste. The wood harvesting, pulp and paper production, chemicals, energy consumption and material transports are included into the paper ecobalance data. The transport of the printed books to the storage of the client is also taken into the account. The basic data is collected from the statistics of the printer and from the material suppliers.

The user interface of the calculator is rather simple. First the basic information including the format and the number of pages are feed. After selecting the paper type with the grammage and the bulk, the binding type and the number of colour are selected. The cover type, special treatments, packaging methods and transport destinations are also feed in.

The result of the ecobalance calculation is shown as emissions on air and on waters on total level and on separated process stages.

5.2 Scented inks for gravure printer

The starting point for the innovation was the recognition that print is the only media that offers an infinitive combination of colours, surface treatments, shapes substrates and smells to address all of the human senses to emphasise the value of a product.

This observation lead to the selection of the scent inks as the key differentiating factor for the gravure printer. The idea behind this concept is that scents can evoke powerful memories and emotions. Scent inks enable brand owners to capture that emotional connection to promote their products. It was also noticed that the market demand for the luxurious catalogues in Russian market is growing and the scented inks could bring added value for the customers.

The innovation in the gravure printer was to modify the flexo printing unit in the gravure printing machine in a way that it is possible to print five scented ink segments on one paper web. This gives the opportunity for the customers to use several different scents in the same product.

The printer uses scented inks which can be formulated with stock scents, like lemon, or custom fragrances for unique cosmetics, personal care and other consumer brands. The scented inks are applied directly over printed graphics and activate only when gently rubbed. The inks contain fragrance oils that use a state of the art form of microencapsulation. The rubbing action shears the capsules embedded on the surface of the varnish, releasing the fragrance oil. The net result is a release of scent, which dissipates after a short while, until rubbed again.

5.3 New services for commercial printing company

The starting point for the innovation was the printers thrive to build stronger customer-relationship and generate more value added services. In order to increase the flexibility and quality level this printer decided also to invest new printing presses with the JDF-based workflow.

Following service models were identified as having high potential: special effects printing, logistics and mailing services and hybrid media services. One quite interesting service offering possibility was movable digital printing press service. This idea was not however realised.

5.4 Innovation process in Graphic Arts College

As a part of the innovation process the idea generation and documentation took also place in the graphic arts college. The process was implemented by giving a lecture of different idea generating techniques and giving the preliminary ideas for potential new products as a starting point for the students. The different preliminary ideas were: mini sized magazine, hybrid media products using 2D-optical codes, lenticular printing products and Post It-sticker advertisement in the newspaper. Several different product options were identified and some of them were tested in the participating companies.

6. Speeding innovations by innovation competition

In is known that the innovations activity can be enhances by innovation competition. This is why innovation competition was launched during the project. The purpose of the completion was to encourage the Finnish companies in the graphic arts domain to generate new products and services, increase the knowledge on open innovation process and show their innovation capability to the customers. The competition has following three categories:

1. Innovative use of special print techniques in the print products. This category includes magazines, newspapers, books, promotional print products, annual reports, packages and direct mail. The evaluation criteria were technical realization, design and functionality.
2. Innovative network to produce print products and services. This category includes new and innovative combination of different actors which can deliver unique products and services in the graphic arts domain. The evaluation criteria were the clarity of the roles of the different actors and the quality and innovativeness of the end product or service.
3. Innovative technology. This category includes excellent technical solutions or materials which are used to manufacture the print products. The category covers all of the process stages including prepress, printing and post press. The evaluation criteria were the benefit that the solution brings to the companies.

6.1 The result of the competition

The number of valid applications to the competition was relatively small. The reason for this is probably the fact that in many graphic arts companies the innovation process is relatively new concept which has not been applied effectively. Following two applicants were rewarded:

TagAge
This innovation offers an easy way to create RFID/NFC-integrated printed products for your needs. It is a web-driven application, which helps the end consumers and businesses easily create their own smart products. This is done by combining web-to-print functionality with web-to-encode ability.

First the user creates a layout she wants by importing the image and text. After this a hotspot tool is used to create NFC-enabled tag positions and the information for the tag is uploaded. The typical products include posters and photos.

This innovation includes new kind of network with actors from different industries, which have created together a new type of service and products. The innovation network includes digital printer, advertising company and NFC-tag suppliers.

Stafix
This innovation is a statically charged, printable polypropylene film that adheres quickly and easily to virtually any clean, dry surface without any adhesives. The film has a permanent static charge stored inside. The electric field contained inside the film produces an adhesion force, which makes the film adhere to almost any surface.

The installation of the film is fast and trouble-free because no adhesive substances, tape, pins or blue tack are needed. The film can be removed easily and repositioned on another surface.
The film will adhere, on average, three months to a surface, depending on the conditions.

This innovation generates new business for the graphic arts domain and the material can be applied in many different products.

7. Discussion and conclusions

In this project an open innovation process were defined for graphic arts companies and it consisted of following modules: data gathering, idea creation, idea evaluation and concept creation and commercial application. When applying this process in the companies it turned out that the best results were gained when the customers were involved into the innovation process.

The ability to create new ideas, to evaluate them and to access and use knowledge and skill to develop them is fundamental to business innovative success. Business networks, whether local, sector or technology based are excellent sources of ideas, knowledge, support and encouragement, and possible collaborators or partners.

One of the main challenges for a company is to find the right people and to have a larger set included rather than only a group of individuals and firms with which the company already is in contact.

Effective innovation process required vast source of information to generate potential ideas. This was the challenge in several SMEs because the limited resources.

One of the interesting aspects in implemented innovation process was to analyse the source of ideas. It was noted the ideas arise mainly from:

- Customer intimacy, immersion, and interaction,
- Employee involvement, in an open and receptive organisation,
- Networking, with exposure to other businesses, and technologies,
- Research and technology development.

It can be estimated that about 60% of good ideas arise from the first two areas. Idea generation is facilitated by inspirational leadership and an open listening culture, with good feedback.

It was also noticed that the open innovation process works best in so called pre-competitive stages (time to market quite long). This is typically the stage where the commercial interests of the companies are not too high to prevent the open information flow.

One publicly reported outcome of the applied open innovation process was the initiation of the development work for the web-based software to calculate the ecobalance of books. With this software it is possible to calculate how different book production options impact on the ecobalance of a book.

References

1. Chesbrough, H. W. 2003. Open innovation : the new imperative forcreating and profiting from technology, Boston, MA: Harvard Business School Press.
2. Chesbrough, H. W. 2006b. New puzzles and new findings. In H. W. Chesbrough & W. Vanhaverbeke & J. West (Eds.), Open innovation: Researching a new paradigm: 15-33. Oxford: Oxford University Press. p.1
3. Enkel E. & Gassmann O. 2007. Driving Open Innovation in the Front End:the IBM Case, the EURAM Conference, May 16-19, Paris

RIT Media independent news model for rapid publishing

Michael Riordan

Rochester Institute of Technology, School of Print Media
69 Lo mb Memorial Drive, Rochester, NY 14623 USA
E-mail: michael.riordan@rit.edu

Abstract

This paper presents a model for a news production system optimized for multi-channel publishing outcomes, including a nearly instantaneous newspaper, website and GPS-synchronized publishing feed displayed via Google Earth. Customized modules of open-source software were created to bridge between proprietary hardware and software commonly used in publishing.

Keywords: newspaper, open-source, XML, metadata, GPS

1. Introduction

The challenge of both authoring and publishing news content live during one-day event created the impetus for developing a publishing system that leveraged metadata and automation to create a web-to-publishing model for multi-channel publishing. The model was designed to publish content to a website that would subsequently export structured document content to publish the same stories to a Google Earth display and to print. The goal was to publish stories to the web and Google Earth immediately and to a new print edition approximately every hour.

The activities of the one-day event being were scheduled in a manner that required news to be gathered simultaneously at multiple locations throughout the day. In total, nearly 100 potential news items were identified as being worthy of being covered as a written story, a photograph or both. By necessity, all reporters being assigned to cover these stories were students.

After assessment of the technical and human variables, the folowing objectives were identified to guide the development of a publishing system for this event:

- The use of open-source software was of high priority.
- The interface for all participants must remain simple and intuitive.
- Anything that could be automated should be.
- Maintaining quality between platforms and devices was expected.

The emphasis on open-source was became a priority as this project was an outgrowth of the efforts of RIT's Open Publishing Lab (OPL). The OPL is a cross-disciplinary undergraduate research lab dedicated to creating publishing solutions and releasing them in an open-source environment.

It was decided that the optimum workflow solution would be robust behind-the-scenes but very simple to the end-user. This approach would allow writers, photographers and editors to concentrate on their assigned tasks without the overhead of a complex interface or decision-making process to follow. By design, this approach would also minimize the need for training.

The focus on automation was emphasized to help address the speed requirement for processing as well as to insure the entire workflow system was architected in a manner that fully exploited the possibilities of automation. By extension, an emphasis on standards and standardization carried through all phases of project development.

After much discussion about the trade-offs associated with speed versus quality, it was agreed that workflow innovation should enable both. As a result, the emphasis on open-source solutions was balanced with an acceptance of proprietary solutions to insure good typography and the color fidelity and consistency of all images.

2. Methods

The methodology developed and implemented divided the publishing production process into seven basic functions:

- Image Workflow;
- Text Workflow;
- Editing;
- Publishing to the web;
- Publishing to Google Earth;
- Publishing to print;
- Distribution.

2.1 Image workflow

Image capture for all stories was handled by students enrolled in RIT's Photojournalism program. Each student was assigned a "photographer ID number" and specific stories to cover. They were encouraged to concentrate on getting the best image(s) possible for their assigned story and limited only by two technical restrictions: all images must be captured as JPEG files and all captured with sRGB as the color profile. Additionally, each photographer was required to provide description information for the captions for their photographs.

The uploading of image files was distributed among "field editors" assigned to various areas of the campus. As each photographer competed his/her assignment(s), they would drop off their CF cards with caption notes to the field editor and then continue on to shoot their next assignment. The field editor would review the images on a laptop and wirelessly upload only the best 3 - 6 images per story. The uploading of images to the server was accomplished using a customized implementation of Xinet's Upload tool. The Xinet uploader was configured to insure that only JPEGs would be accepted and that no file could be uploaded without the required metadata fields filled in. Required fields included the photographer ID number and story ID number. Both of these fields were filled in via a drop-down-menus. Description data (for captions) and keywords (for searching) were also filled in by field editors but could be edited later in the newsroom. All fields could be filled in to one or more images at a time.

The uploading process utilized the metadata fields containing the story and photographer ID to automatically rename all files as they were uploaded to the server. A naming convention of *storyID_ photographerID_ original_filename.jpg* was implemented via a custom script as each image file was processed to be saved to the server. The keywords and description data were also written directly into each file during this process.

All image files uploaded were saved to a web-accessible server location for the newsroom to access for image editing. The editors in the newsroom determined final selections for publication and made any crops or adjustments to tone and color for the images selected. Once editing was complete, final image files were uploaded to a separate server volume that sent images to a DALiM TWiST workflow that created two versions of all image assets: one high resolution CMYK file for print and one display resolution sRGB for web publishing. The CMYK files generated were then automatically saved to a server volume for later retrieval while the sRGB files were placed in a server volume that published then to the web immediately.

The bulk of images collected during the event were processed through the workflow described above. However, an additional workflow to allow the use of two wireless cameras in the field was developed in parallel. The JPEG and sRGB restrictions for these two photographers were the same but, instead of utilizing a field editor for file uploading, all images recorded were transmitted directly to a dedicated server volume for that camera. For captions, each photographer utilized the built-in microphone on their camera to record an audio file describing the images. These audio files were passed along in-sequence with the image files. All image and audio files were then reviewed by the photo editors in the newsroom where image selections were made and the audio files transcribed to create the caption information for each image file.

2.2 Text workflow

The open-source software Drupal was selected as the platform to handle all text content. Drupal is a content management software for web publishing that is module-based and very extendible. Text for stories was handled

effectively as a series of blog posts where authors would log into the system through the web and then fill in the title and body of their story. Every story submitted was then reviewed by an editor prior to publishing.

As with the photographers, student writers were assigned specific stories and encouraged to create the best work possible. Story length was to be 300-500 words and authors were to submit their stories directly into Drupal. To do this, each author was issued a unique ID to log-in to the Drupal install for the project. Stories could be written directly into the simple blog interface or, if another software tool (e.g. MS Word) was used for authoring, content could be copy/pasted into the Drupal interface. As with the photographers, a unique story ID was assigned to each story covered and it was the responsibility of the writers to insure they selected the correct story ID from the drop-down menu in Drupal.

A simple database in the back-end of Drupal synchronized each author's log-in with their name for the byline for their published story. Similarly, the use of the story ID number allowed stories covered independently by a writer and photographer to be brought back together automatically during publishing. Additionally, for every story assigned, a metadata field for the GPS coordinates of that story had been previously created and saved in a simple database. By selecting a specific story ID, the associated GPS coordinates were relinked with the story and written into the story file's metadata in Drupal.

2.3 Editing

The photo editors in the newsroom worked directly off a Xinet server for all image editing tasks. Images uploaded by the field editors were evaluated and edited locally using Adobe Photoshop and then resaved and transferred to a separate volume on the server. This triggered a series of automated actions utilizing DALiM TWiST and a custom Perl script to create the secondary assets required for print and web publishing.

Text editing was done on a rolling basis as each story came in directly in the Drupal interface on the web. For stories that needed extensive editing, text could be copy/pasted into MS Word, edited, and then copy/pasted back into Drupal. Once editing was complete, each story was "published," an action that made it immediately available on the website and Google Earth.

2.4 Publishing to the web

Publishing the text content of stories was accomplished automatically as soon as an editor approved content. The Drupal module created "tagged" the title and body content fields so that the style sheets for the webpage template could apply formatting specific to each. The byline for each article received a similar treatment except that the author's name was generated dynamically based on the associated author ID number.

Images were associated with each article based on the story ID number that was included as part of the image naming convention. Each web article pointed to a separate volume on the server containing all images that had been resized for the web. Images associated to that story were displayed in alphabetical order based on file name as they came in.

2.5 Publishing to Google Earth

The customized Drupal module created used for web publishing created a structured (e.g. XML) document that could be exported via RSS or similar means. The individual tags for content types created to enable web publishing included title, body, author, story ID and, based on the story ID, the GPS coordinates of each story location. As a feed from the story published on the web, all associated images could also be included.

Publishing to Google Earth requires that any feed content be transformed to a Google KML file. Effectively, a KML file is a modified XML file and, based on the XML feed already being generated from the web published stories, a custom KML feed was created. When installed, stories would appear dynamically in a Google Earth display in the location specified by the GPS coordinates.

2.6 Publishing to print

For print publishing, it was determined that coupling Drupal's XML export with Adobe InDesign's XML import options would provide the highest quality publication. To do this, an InDesign template was designed for the print editions and, based on testing, a custom JavaScript developed to add functionality to page layout and to better synchronize the association of the high resolution images with the structured text content of each story.

The page template was designed with minimal master page elements and very strict definitions for paragraph and character styles. In addition to the article content, a QR code (2D barcode) containing the http address for the web editions was included on the front page for web-enabled phones to utilize. A page size of 12 x 18 inches was determined based on the maximum size of the printers being used for production. Similarly, to avoid any need for finishing, an "edition" was defined as one 12 x 18 form, printed both sides.

The specific content for each print edition was decided on-the-fly based on the amount of story and image content available. To help determine how much content was available for a potential print edition, a custom Drupal module was written to display the character count of each article published on the web. When the minimum number of characters needed to filled an edition was reached, the page layout artist would download the content as an XML file containing just those articles directly from Drupal. Combined with the JavaScript written for this process, all text content for the edition would arrive pre-formatted (e.g. font, style, point size) on the desktop in the area outside the page margins. The artist would then "drag and drop" content into the page layout, manually arranging articles to establish a best fit.

The CMYK images prepared by DALiM for each article were downloaded in parallel and each was placed and then resized in InDesign as necessary for fit. Captions for each image were generated dynamically based on the Description field in the metadata of the image file and a photo credit generated automatically from the content in Author field.

Once page layout was complete, the file was exported as a PDF-X1a file and placed on a central server accessible on the web. From here, print production of each edition would begin on five different digital printers at five locations on campus. A run lengths of 1000 sheets (two reams of paper) for each device was decided upon to reach a goal of 5000 copies of each edition to be distributed to the estimated 20,000 attendees at the event.

2.7 Distribution

The distribution of each edition was done by newspaper carriers, each outfitted with a traditional carrier's bag. The inclusion of the carrier bag was done in part to help reinforce the idea that each full-color 2-page was a newspaper. The bags were very practical as well, and each carrier hand-delivered several hundred copies of each edition to drop-off points and directly to the hands of attendees.

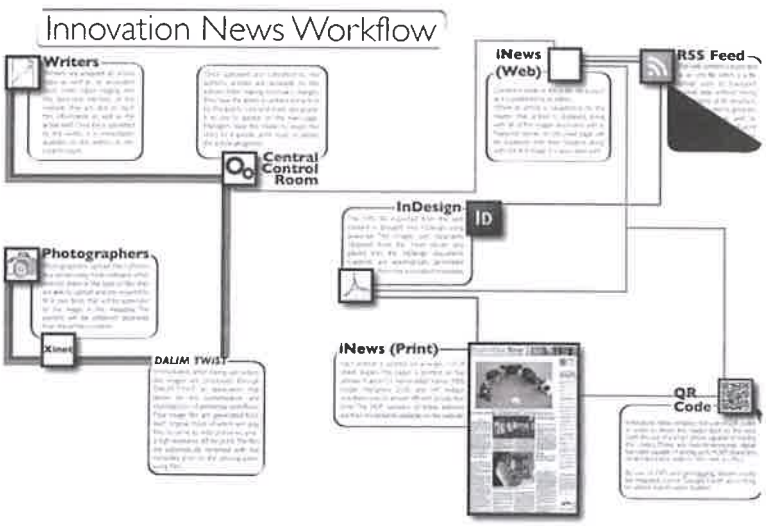

Figure 1:
A workflow diagram of the proposed publishing system

3. Results

While several technical challenges appeared during the course of the production, the overall production system developed worked as intended. Al image uploads from the field came in as sRGB JPEG files, renamed and containing all required metadata. Text files came in as expected as well. Editing for both text and images proved to be a bottleneck in the newsroom in several instances, but editing for both averaged less than five minutes per story.

Publishing to the web went as planned with the exception occasional issues with lines breaks and text flow that were attributed to the template used for the webpage. Additionally, for one story, there were problems rendering several characters. Investigation showed this to be a problem in font encoding and converting to Unicode corrected the issue.

Publishing to Google Earth went exactly as planned and all stories published to the web were successfully publishing in Google Earth as well. The font issue noted above carried through to Google Earth as well but was corrected immediately after the web edition.

Four print editions were successfully produced and distributed inside four hours. The first edition took nearly 1.5 hours to produce as content was slow to come in. A corrupt font problem further delayed production of the first edition. The page layout process for all four editions proved to be the pressure point as the single page layout artist had to make many design and some editorial decisions under relatively intense pressure. Each edition became easier than the previous to layout and, by the fourth edition, the process was down to approximately ten minutes from the time the content was available to the time that edition was on press.

The decision to go with PDF-X1a as the standard for production did result in color inconsistencies between devices, despite each being set to simulate SWOP.

The distributed print model made delivery of each edition relatively efficient but, as most attendees were congregated in a central area on campus, nearly all news carriers ended up converging in this location regardless of where their delivery route had begun. There was also some confusion among some attendees when the second and third editions of the newspaper came out. Many attendees informed the carriers that they had already received the paper only to have the carriers have to explain that there were multiple editions throughout the day.

4. Discussion

The model presented was designed as a proof of concept of a multi-channel publishing system based on a web-to-publishing system model. In terms of testing and implementation, the implementation of the model described served as the alpha test of the entire system. Three other instances followed in later months to allow the application of the learning from this test and resulted in several refinements of the model, inclusion of other publishing software for editing (*e.g.* Adobe Bridge, PhotoMechanic), other content feeds (*e.g.* Twitter) and a switch to a PDF/X3-based RGB workflow for print more predictable color output in print. Additionally, several changes were made in the visual appearance of the page templates and to the JavaScript used to aid the formatting of XML content in InDesign.

The open-source portion of the project was released to the Drupal community in 2008 and the feedback from other open-source developers has been informative. In addition to changes in the Drupal code already implemented, future stages of development for the publishing system will include the migration away from proprietary systems for the image processing and page layout tasks to allow more users to be able to fully implement and test and the system.

5. Conclusions

The success of the alpha test was the result of two key factors: 1) the collaborative and diverse nature of the project team designing the system, and 2) the modular approach to tasks necessitated by the emphasis on both automation and the integration of open-source and proprietary tools.

The project team was comprised of students and faculty that had expertise ranging from print, publishing, photography, software engineering, computer science and design. The total development cycle was only about eight weeks, forcing the team to work fast and debate openly about the pros and cons of suggested approaches. Multiple solutions to specific tasks were developed, tested and presented to the group to deliberate on.

Development and integration of the specific components of the workflow was further enabled by the emphasis on standards and the modularization of the core publishing elements of text, image, formatting (styles) and metadata. This allowed multiple approaches to specific phases and sub-phases of the workflow and, by extension, the integration of the full publishing system tested.

Acknowledgements

The project described in this paper was made possible through the collaborative efforts of the extended team at the Open Publishing Lab at RIT. Specifically, the leadership of Professors Matthew Bernius, Doug Rea, William Synder and undergraduate students John Karahalis, Mark Newell, Michael Ricciardi, Micah Stupak and Robert Whitney were critical to the development and implementation of the model described.

Media organisations and local news in a new media environment: super local news - redefinition of news from a local perspective

Asta Cepaite and Elisabeth Stúr

Department of Information Technology and Media
Mid Sweden University, SE-851 70 Sundsvall
E-mails: asta.cepaite@mah.se, elisabeth.stur@miun.se

Abstract

New forms of media have produced opportunities for a new kind of journalism. The technological changes have transformed the content, how it is created, the methods of news work, how news companies are organized, and the ways in which individuals use and interact with content.

The objective of this paper is to discuss the phenomena of super local news in perspective of the recent changes in local media organisations in a context of a transformed media environment. This is exemplified by the development on the Swedish local media market with focus on the role of local news in media organisations. In this paper three research questions are selected from the research field: First, what kind of changes in the organization structure and the news production has the local media organization to face? Secondly, how has the form and content of local news changed? Last, what will be the future role of the local news?

The study is based on qualitative methods. The majority of the material for the study is collected from selected Swedish local papers.

Some results of the study concerns changing procedures in content production and distribution, which require restructuring of journalists' working methods. Production of the news becomes more rapid which can have an effect on the quality of the content. Reduction of local news offices at the same time as production of the local content is preferred influence likely who is producing the content and controlling its quality.

Keywords: super local news, media organization strategy, local newspapers

1. Introduction

The last two decades of changes on the media market have had impact on form, appearance and content of the newspapers. It has also created new conditions for consuming news. The development of new technical ways of getting information together with changed economical conditions on the media market has affected the form and content of news. [Castells, 2000] New forms of media have produced opportunities for a new kind of journalism. [Nygren, 2008; Carroll, 2006; Maier, 2007].

In the new media landscape the local newspaper are trying to adjust to the development. In embracing instead of fearing the changes the editors-in-chief, senior news executives and reporters are remaking the local newspapers. There are several tendencies looking at both form and content as in the media organisations.

Changes in media market, including new conditions for news production and growing different habits of media consumption, require innovations and re-structuring of media organizations. The changes affect the employees in media organizations, their working conditions and patterns, responsibilities and professional values. Development in media market has forced newspapers to respond to and manage changes at the organisational level. Managers and journalists in media companies have to think differently, decision-making process has to be examined and restructured.

The role of the readers has changed during the last years. As a consumer the reader of local news has become much more active today, they even participates in the production of the local newspapers through the on-line sites. They can on-line participate actively with giving direct comments on the news in the paper and at the same time write their own articles and get them published on local on-line sites. The readers can also decide and chose out of interest what they want to read and it will be served on-line by the paper [Hvitfelt & Nygren, 2008; Maier,

2007]. This means that the media organizations have to become more specialized in their content providing. The newspapers have to move away from the unfocused, one-size products and increase their differentiation - which is necessary for their competitiveness and creation of economic value. The most effective way to it is localization, creation of value for readers and advertisers through local coverage [Picard, 2006].

A tendency towards a sort of super local news can be noticed. Even though the local editorial offices are closing down and the local reporters are getting more and more rare there are more local news in the paper today, mostly found on the on-line sites. In the paper there are instead tendencies of covering bigger events, news that are making headlines [Sternvik, 2007; Carroll, 2006].

Others trends are connected with the many ways news are published in. As a result the amount of news has increased and from the same paper the readers can get news in many ways and places. The same local news can be found in the paper, on-line, on the local paper TV-station and so on. There also are tendencies of convergences between the different medias, in reporting, and journalistic forms as genre and content [Castells, 2000; Hvitfelt & Nygren, 2008].

1.1 Objectives of the paper

The objective of this paper is to discuss the phenomena of super local news in a perspective of the recent changes in local media organisations. This is exemplified by the development on the Swedish local media market with focus on the role of local news in media organisations in a context of the transformed media environment.

The trend towards super local news and super local journalism in local papers raises several questions. In this paper three research questions are selected from the research field:

First, what kind of changes in the organization structure and the news production has the local media organization to face? Secondly, how has the form and content of local news changed? Last, what will be the future role of the local news?

2. Methods

This study is based on qualitative methods. The majority of the material for the study is collected from some selected Swedish local papers (notice references in appendix). The papers in the study represent local papers in Sweden that have the last years undergone vast changes regarding organisation, form and content.

The study is made in three levels concerning three different kinds of materials and the results are at the end put to gather for an analysis and discussion. First: In the study local news published both in the paper as on their online-paper during autumn 2008 were closely followed and examples were selected for qualitative content analysis. Secondly: There was a review made on recent research both concerning the media development global as on the Swedish local media market and Swedish local news. Thirdly: There was a review of events and data on how the Swedish local media organisations are adapting to the development in perspective of the transformation of local news. Examples of material in this part of the study are published interviews with editors-in-chief and news journalists of the local papers in the study.

The paper begins with a review of the development within media organisations and discusses how local papers in the study have adapted new forms of news covering. Secondly, the paper discusses the theoretical frames and practises of local journalism and super local news with examples from Swedish local papers in autumn 2008. Put together the two parts will give a context for a discussion about the future role of local news in Swedish local papers.

3. Results

3.1 The local media world in transformation - Sweden as an example

The last ten years development on the media market has been revolutionary in many ways. Its affects on media organisations and content of media have been vast. Today its possible to summoned up some of the results of the progresses, how it has influenced media and the way we communicate. One outstanding outcome of

the development is how the Internet have created various ways to get information on; it has also opened up new arenas for debate and exchanging opinions. As the well-known media researcher Manuel Castells puts it in words, we are nowadays living on "the internet Galaxy" and we have to deal with new ways to act and correspondent with each other in our society [Castells, 2001].

The development of Internet has influenced the content of media on several levels, global as a national, and not at least on a local level when it comes to spreading information and covering local news. The local papers owners, editors in chief and journalists are confronted by a new media world with new expectations and demands from consumers and advertisers. The Swedish local media market is one example of how the development has progressed. During the last years most of the Swedish local media companies and papers have undergone great changes concerning organisation, distribution of the news, and in the journalistic work with local coverage of news and information. Also the way the paper communicates with its readers has changed dramatically [Nygren, 2008; Nygren & Hvitfelt, 2008].

3.2 Development of products and services

The Newsroom Barometer survey reveals an industry ready and willing to change [Trends in newsrooms, 2008]. The changes include development of the news production and distribution of the local content in supplementary channels. The newspapers offer a range of new services, primarily based on online-solutions and available for free.

An example of the activity for strengthen position on the media market can be an establishing of new products on free basis, as Östersunds Posten does [Medievärlden, 18. 9. 2008]. The media companies' two free newspapers are produced of its own editorial staff. These free newspapers content a local material, and in that way the media company covers its positions on the local media market. One of the expected effects is to attract advertisers both to established newspaper and to the new free newspapers.

Development of online services continues in a number of newspapers. Online editions of daily newspaper have become the norm and new services on web arise. Such services constitute usually a part of online newspaper, where the readers are offered a possibility to interact and publish some material. Web services can also be arranged in addition to the regular online newspapers, as Allehanda Media and Västerbottens-Kuriren do in a joint project [Medievärlden, 18. 9. 2008].

3.3 Rationalisation as strategy for increasing profitability

A number of media organisations meet requirements from the owners to be so efficient as possible. One method to increase efficiency is to rationalise the production, using new technological solutions and restructuring organisation. Another way to better efficiency is consolidation between newspapers and their cooperation at different levels. Apart from synergy effects of rationalisation that diminish costs and enable new methods of production organising, a range of jobs disappears or decrease.

There is no clear tendency for what kind of jobs reduces when the newspapers consolidate. Administrative ant technical, as well as editorial posts can be drawn back. A planned fusion of tree newspapers included in the media group Skånska Dagbladet implies a reduction of approximately 100 posts [Skånska Dagbladet 3.12. 2008]. The same amount of posts will be drawn back in the media group Promedia, with intension to save money.

In addition to savings and rationalisation, a number of the newspapers attempt to increase their sales or develop new products. For example, Helsingborgs Dagblad slims down the organisation, while focusing on the investments on the new channels and production of a free newspaper Helsingborg City [Helsingborgs Dagblad, 18. 9. 2008]. Technological and organisational development allows in many cases to do the same tasks with less employees involved. The question is if organisations are capable to adapt to changing working conditions so quickly as an ongoing re-structuring of media production and distribution requires. The media organisations, in particular those that experience consolidation, faces extensive changes in organisation culture, working methods and routines. It requires maturity in innovativeness of organisation members for being ready for changes.

Another reason for rationalisation, usually related to insufficient profitability, is the media users' diminishing interest for subscription of newspapers. The local newspaper Norra Skåne recede an amount of editorial posts

due to falling circulation [Norra Skåne, 20. 3. 2008]. The newspaper public is growing older, readers become fewer, and new readers are difficult to attract which is the common problem for the most newspapers.

3.4 Integration of print and online newsroom

A study of trends of Swedish media development [Sternvik et al., 2008] has shown that around two-thirds of Swedish newspapers in 2007 have online editions. Technical reorganizations in the production process and increased coordination as a consequence of the establishment of bigger newspaper groups have resulted in a more efficient production.

A number of Swedish newspapers follow the global trend in increasing integration of print and online newsrooms. For example, the local newspaper Sundsvalls Tidning is undergoing an organisational change [Sundsvalls Tidning, 22. 1. 2008]. The newspaper has developed new distribution channels: web-TV and news for the mobile phones. An old organisation was not really suitable for new methods of news production and distribution, and required changes in the working routines. The reorganisation of the newsroom supposes to adapt production the news 24-hours daily.

Increasing amount of distribution channels requires restructuring of working methods. A need for a better overview of daily routines of production, planning and coordination between different departments comes up. A national daily Dagens Nyheter is reorganizing the structure of work [DN, 1. 10. 2008]. Some chief posts has been taken away, while some new posts that suit better the changing needs, become established. A number of positive effects of reorganisation are expected, as fewer chiefs, more clearly divided areas of responsibility and an improved contact between every department and the news production on web.

Another media company, Sydsvenskan, is also planning reorganization due to the old-fashioned way to organize its activity. Structure of the organisation has not changed noticeably the past twenty years - with the exception that a web department has been built up. The integration of web and print is the focus of reorganisation.

An integrated organization requires work across traditional barriers. Different departments need to communicate and coordinate well. Survey from 2008 of more than 700 editors and senior news executives, presented in Newsroom Barometer-08, shows that newspapers are ready to change. Many editors see neither their newsroom nor journalists as being "print-only", having clearly accepted the multimedia revolution. Integrated print and online newsrooms will become the norm and journalists will be expected to be able to produce contents for all media within five years.

3.5 Getting local - with reducing local news offices

Increasing interest of local contents production can be noticed internationally, as well as on the Swedish media market. In the context of rise of online news, a number of newspapers consider the increasing local coverage being more a necessity than a choice [Chainon, 2008]. The decrease in circulation affected all types of traditional daily newspapers, especially papers with national or regional circulation, whereas the local newspapers have kept their positions [Sternvik et al., 2008]. In some extent it can explain the newspapers intentions to focus on the local content production.

Free newspapers also focus on the local news. Whereas free newspapers make a loss on national media markets, they are still successful on local market. The local free newspapers as Xtra Östergötland and City Helsingborg (former Xtra Helsingborg) is pushing out more established free dailies as Metro from the local market.

Rationalisation of media companies has affected the amount of local news offices. The newspaper Sydsvenskan closes its local news office in Eslöv [Sydsvenskan, 12. 03. 2008], as a part of an extensive reorganization. It does not mean that the local covering becomes missing - the local content is available both in print and online editions - but a question about quality of the news can be raised. Another newspaper that closes the local news offices, Norra Skåne, intends to replace these offices with mobile teams. It will require new methods of working, news reporting and managing.

Two-thirds of participants in the survey by Newsroom Barometer - 08 believe some editorial functions will be outsourced in the future. A survey by Polopoly reports that European newspaper executives believe that within three years 40% of their content will be user generated. The blogs will become more important, personalized advertising will be more possible.

Internationally, many newspapers are opting for relatively cheap and staff-light online sites, relying on the public to produce content. Some executives of media companies are sceptical about participation of the public in content production, such as blogs [Chainon, 2008]. The opinion is that the content produced by the public, on one hand do not attract potential advertisers, on the other can hardly offer a well-worked up, analytical content. The importance of analysis is perceived to be increasing, as well as the need of journalists training. Editorial quality is in many cases a priority for investments.

3.6 Social media and the local papers

Today nearly all-local papers in Sweden provide their readers with news and information on-line. The on-line editions have become an important part of the local papers [Karlsson, 2006]. From the beginning the Webb-sites of the local papers were static - giving one-way information to the readers. Nowadays they have become interactive, readers can in different ways react on what is written on-line and also write their own comments, and on some on-line papers even their own news. This has opened up for a direct contact - conversation between journalists on the papers and their readers. This has been one approach of the local media companies to keep their appearance on the media market up-dated.

Through the interactivity on the on-line editions the local papers also have become a part of what today is known as "social media". Internet phenomena as blogs and twitters are examples of how social media works. Every one in the society can through own created blogs on Internet make their voices heard and give comments on events. This has opened up for new possibilities for communication and created new arenas for political debate and discussions between people [Mikael Karlsson, 2006; Våge et al 2005].

The local papers have to deal with the development of blogs and twitters. Social media provides new arenas for spreading news and information on, which affect the traditional media. It is a dilemma for the media companies how to act and face this development - also how to value the impact and importance of the new media in the future. [Hvitfelt & Nygren, 2008; Schulman, DN 4. 7. 2009]

3.7 Redefinition of local news

The last years there has been a serious discussion if the traditional newspaper will survive the fast development of media. Media researchers, journalists and other people involved in the production of newspapers have drastically prophesied the death of the newspaper.

In an inquiry made by Newsroom Barometer [2008] 85 percent of the editors-in-chief who participated were quite positive about the future of the newspaper. 435 editors worldwide participated. All respondents were editor-in-chief or senior news executives. Half of the respondent believed that the journalistic quality would improve over the next ten years, versus one quarter who thought it would worsen. The respondents also looked positive upon new forms of media such as free paper, citizen journalism and online news. They were defined as challenges and opportunities for positive changes: "Far from resenting these forms, senior news executives embraced them" [Newsroom Barometer, 2008].

This can be put in relation to what is happening on the Swedish media market. Also the Swedish local papers have to adapt to a new media environment. And there are many challenges as new strategies for the media organisations and production of news, new forms of media and ways of consuming news, and not at least new forms of journalism: "Fifteen years ago, selling newspapers was simply a matter of marketing. But editors-in-chief realize that content matters more than ever and cutting newsroom resources is not an effective solution: the redefinition of news will take place with the journalists, not against them" [Newsroom Barometer, 2008].

3.8 Change of form and content

Basically there are several main tendencies in the development of local news. One is about the tabloidization of the papers, and this is not just about the form but also concerning the content [Sternvik, 2007]. Others are how the papers are getting more and more local in their content. There are also tendencies of convergence both when it comes to the ways of working with the news as to the form and content. [Nygren, et al., 2008] Different

materials, texts and genre tend to become more and more mixed, together with how news are reproduced and recycled in different media forms of the paper. Then there is an increasing interactivity with the readers - the possibilities for the readers to participate in the paper and influence the content through the on line sites [Storsul & Stuedal et al. 2007; Våge, et al 2005; Maier, 2007].

During the last ten years most of the local papers in Sweden has changed size, from broadsheet to tabloid. In 1984 was 35 percent of the Swedish daily press printed in broadsheet, 22 berliner and 42 tabloids. In 2005 the figures had changed into 9 percent broadsheet, 9 berliner and 78 percent tabloids. [Nordicom. gu .se October 2008] One of many is Gefle Dagblad who turned into a tabloid in November 2003. Other examples that followed GD the next year were Upsala Nya Tidning, Sundsvalls Tidning and Västerbottens-Kuriren. The decision to change size was based on several factors.

The editor in chief of Sundsvall Tidning Kjell Carnbro has emphasised the urge to become more modern and at the same time give the readers better service. The smaller tabloid would be more comfortable to read he thought. The new size made it possibly to use new ways of editing the paper. Articles and not least pictures could be presented in new forms. It was the whole formula of changing the paper into something that felt more modern and trendy that influenced the decision for a change. One hope was also to catch the attention of younger readers with being trendier as a tabloid [Interview, September 2008].

Another not so outspoken factor by the owners and managers of the local press was connected with economy. The figures of the circulations were slowly sinking and the traditional local press seemed to lose position on the media market, at the same time the advertiser demanded a more unified form so it would be easier to advertise all over Sweden. Changing into tabloid was one of many ways in the effort to become economically stronger and uphold the leading position of the local press on the market in the future. [Sternvik, 2007]

3.9 Super local news as phenomena

Citizen journalism is another new type of journalism that has been tried out by the local papers as one way to reach the readers and make the readers participants in the news production [Kolodzy, 2006]. Citizen journalism depends on the interest of the readers of getting engaged in the news covering of their local community and also great support of the local papers and their journalists otherwise the idée tend to stay as a good idée and nothing more. So its success has therefore varied, also the quality of the content. In the Swedish examples there are a mixtures between citizen journalism and a sort of blog-journalism. Sometimes the papers, as in the case of VK.se and "allehanda nära" - the on-line paper of Västerbottens-Kuriren och Ångermanland/ Örnsköldsviks Allehanda - are letting the readers ether directly comment the local news or write them themselves. The key question is what kind of news are the readers actually delivering? Looking on the local sites of VK.se and "allehanda nära" - the on-line paper of Västerbottens-Kuriren and Ångermanland/ Örnsköldsviks Allehanda - during the autumn of 2008 one can summon that a lot of the news have a strong local connection.

Taking examples from the 14 of October 2008 from *allehanda nära* there were news as "A food culture day in Hoting". The text was about how some classes from the school in the region visited Hoting and learned how to bake special Swedish bread, tunnbröd. Together with the text there was a picture showing the school class and their teachers. A bit further down on the site there was a text about a local scooter club: "The Scooters on Rossön are standing ready waiting for the snow". Together with the text there was a small picture from Rossön. Some of the news from the local web sites is published during the week on a special page in the paper, Ångermanland/ Örnsköldsviks Allehanda.

The outcome of the reader's participation is several. First the paper can offer a lot more news to its readers. It is information that concerns specific regions, groups and communities. The readers can immediately respond, comment the news and give new information on the subject. In the case with the school class baking bread in Hoting the event were commented by several readers, as for example, one parent thanking the teachers, or friends of the pupils writing things like: "Yeeah, what an excursion!" The news is more connected to individuals than before due to the near correlation with a singular person sending in her or his own news.

The content mostly concerns only small groups in the community, the closest related people to the event. There are clear tendencies of what is called "return information" in Swedish journalism. A school class on an excursion learning how to bake bread is only interesting for those how participate. It is exciting to be able to

point out your self on a picture on the local on-line paper and show your parents and buddies that you were there. Other news on the local site can be referred to as gossip, internal information only interesting for a small circle of persons, those who know the codes involved in the message.

It is interesting to notice that these were the presumptions for local news a long way back, a couple of hundred years. In the 18 century when the periodical press started most of the information spread at that time had the character of being super local. It was information and gossip from the little community, mostly interesting only for those who lived there. [Leth, 1996; Holmberg, Oscarsson, Torbacke, 2000, Lundell, 2002]

4. Discussion

4.1 Trends in media organisation strategies

The media structure and the news production in Sweden are changing dramatically. Standard procedures in newsroom culture such as once-a-day deadline structure, content production for a sole and print platform have been overturned. Instead of them, continuous news operations, multimedia content distribution and rapid publishing with minimal editorial oversight are developing [Trends in newsrooms, 2008]. The past years has also been characterized of fall in circulation and advertising on one hand, increasing costs of distribution, competition with new media actors and media forms and changing patterns of media use on the other. Several researchers [Alström and Hedman, 2002; Fee, 2007] means that changes in media market forces media companies to form new strategies for performance, to develop new supply of production and to create new forms of organizing. The strategies that the media companies choose become decisive to future decisions regarding production and distribution, and thereby affect companies' economical development and organizing.

It is common to media landscape's features that they represent convergence of processes and entities in the newsroom. Newspapers that previously competed on the media market, seek new ways for continued existence, usually by different kinds of cooperation, consolidation and building of economical alliances. Media companies that are growing as a result of fusions or cooperation as well as smaller newspapers, need to be flexible and innovative. Newspapers face the owner requirements to be profitable whereas the advertisers look for new advertising channels, and the readers' interest to pay for the news diminishes. Knowledge growth, flexibility and new way of thinking are decisive for media companies' success [Cepaite, 2006].

There has been a substantial upswing in the news production for different channels. The possibility to publish the news on different channels has been used a while ago but it has faced some concerns. Simultaneous publishing for different channels requires adaptation of organisational structures. Working routines in many newspaper organisations has not been suited for integrated, 24-hour production. There has also been a discussion about what material, when and on which channel should be published, in purpose to attract larger audience but also avoid internal competition within a media company. New services that allow better contact between readers and between media organization and its readers require rethinking about the communication process. In the past, media organizations directed the flow of communication and dictated consumption choices. Today, much of that control has shifted to audiences and they have created a demand market in which the traditional ways that media organizations have selected and supplied news are less effective. [Picard, 2006]. That development lead to changes in journalists role as news producers and a need of discussions in the newsroom about news value appear.

4.2 New reporters - new journalism

The old classic local journalist who was assigned to cover a district, working from a smaller editorial office on the countryside has slowly disappeared. He or she who worked alone collecting information directly from the people on the streets and who everybody in the community knew and often had personal relation to is hard to find today [Nygren, 2008].

During the last ten years many of the small editorial offices has been shut down. Instead the news covering is managed from one central editorial office, mostly placed in the biggest city in the area. As a result of the development the reporters must cover huge areas, and it takes time to travel from one part to another. In purpose not to loose much time the reporters tends to stay in editorial office and do their interviews and researches over phone from there. One could fear that the intimate contact with the readers in this way would get lost also

important local knowledge and information. It can be noticed that the news coverage is concentrated to the main area. Other news further away from the main area tends to get smaller exposure in the papers [Västerbottens-Kuriren & Västerbottens Folkblad, September 2008].

4.3 The impact of super local journalism

The local on-line sites offer the readers great possibility to express their opinions on local political issues. Here they can actively get into political debates and pursue different political questions on a local level. As their own made journalist reporting their own news out of interest there is possibilities to start debates outside the common political sphere [Karlsson, 2006; Habermas, 2006].

In autumn 2008 there was a referendum over a projecting of a watercourse, a river in the north of Sweden called Vojmån. The people of the community and village Vilhelmina - about 8 500 inhabits - were supposed to chose whether the watercourse should be changed or not. In the two local newspapers, Västerbottens-Kuriren and Västerbottens Folkblad a lively debate took place about the projecting though out the whole year [Johansson & Stúr, 2009].

The no-voters criticised sharply the project and wrote many angry debate articles in the paper. They were campaigning under slogans as "Save the river" and their voices were heard not just in the papers but also on the local on-line sites. Especially in Västerbottens-Kuriren, on the on-line paper VK.se there was a very active debate due to the new super local journalism. The readers could them selves go in and discuss the projecting of the river. They could write articles were they brought up different perspectives of a change of the watercourse. And each article would get several comments with new opinions from other readers. On the on-line site of VK.se there were room for both those who looked positive on a change and those who were negative.

The whole discussion took place outside the common political arena and as result a new meeting place - community was created over this unique political issue. It was the on-line papers and blogs that made this possible. The outcome of super local journalism and super local news reporting produced new ways of communicating in political debates, also new ways of exercising democracy. It was very evident at an early stage that the opposition - the River savers - had the strongest voices in the debate that took place outside the common political arena - on the on-line sites and blog communities. On the common political arena it was the opposite - here the majority of the politicians were positive towards a change of the watercourse, Vojmån [Johansson & Stúr, 2009].

5. Conclusions

There is apparently a need and interest for local information, to know what your neighbours are doing, what is happening in the nearest community. This classic role of the local papers is still very much alive - that shows the development - and definitely the local papers are not dead. They have only restarted.

There are many aspects on the development of media. The changes we as consumers are facing today are fast and profound. We have got so many different ways of getting information on that its become difficult to sort out what's important or not. This makes it to a question of practise of democracy in our society; were do we get information, how and about what? This used to be an important task for the local press; will it continue to be so?

5.1 Major changes of local media organisations and local press in Sweden

Different forms of collaboration show the ways newspapers attempt to be more profitable and keep or strengthen the present position on the media market. Alström and Nord [2003] in their study of newspaper fusions have noticed that collaboration tends to be something more than ad hoc solution for non-profitable newspapers. Historically, the newspapers with economical problems usually had been liquidated or consolidated into bigger and more profitable companies. The ongoing development on Swedish media market shows that collaboration is an attractive alternative even for newspapers with strong positions. Collaboration or fusions between the newspapers are of long-term character. The newspapers become more competitive and less sensitive to threats on the market, as for example being purchased of bigger companies. They have discovered that cooperation in

different ways is useful for all parts involved. Cooperation allows relatively rapid development of new services and models of distribution.

Understanding the changing patterns in media organisations and in content itself cannot be achieved looking at the organisation and the content separately. Organising of production and distribution in the media companies is a condition for the content characteristics, and vice versa, the certain content can be produced only if the organisational structure allows it.

Some of organisational changes that deal with working routines, ways of production and distribution, and that in some extent affect the content, are following:

Building of alliances with other media actors, or consolidation of the organisations has an impact on decisions about what content and where will be published. New forms of organizing media production involve employees in all departments of media organizations. Involvement of the staff into the change processes and relevant communication between executives and employees is vital for successful cooperation.

The content has to be adapted for the publishing conditions on the different channels. Each channel has specific characteristics that influence how the content will be formed. Employees in media companies need a knowledge and experience in producing the news for the different media forms. Training of the staff is important for both the quality of news and the organizational climate in the working place.

Changing procedures in content production and distribution requires restructuring of working methods that journalists are used to. Production of the news becomes more rapid which can have an effect on the quality of the content. Reduction of local news offices at the same time as production of the local content is preferred influence likely who is producing the content and controlling its quality.

5.2 The local press and a new content

Loosing contact with the readers is a central issue for the local papers. The whole idea with being a *local* paper providing its readers with *local* news is to have a near contact with the readers in the region. One way to solve this problem has been to develop the possibilities the web sites of the papers offers: to extend the interactivity with the readers via the web paper. Several local papers around Sweden have during this last year started local sites were the readers can communicate directly with a web editor. In this way the readers can deliver their own news and also comment them on the web site. This is a form of citizen journalism that has been established in some local papers and become important in the daily work with covering local news [Nygren, 2008].

Västerbottens-Kuriren is one example. The paper hired an editor who together with the editors from the web paper, VK.se, came to the conclusion that eleven different local sites would cover the area of the papers circulation. The web editor on VK.se, who also calls him self "web publisher", Ingvar Näslund meant that this was an important way of getting in touch with readers where local offices had been closed: "The intention was to take back the positions we had lost. But it couldn't cost a lot of money. Maybe because we were unsure how big the income would be. First we should get the readers, then the money" [Medie Världen, 24. 9 2008].

And Näslund is today satisfied with the result. After eight months 20 percent of the visitors on VK.se are also visiting the local sites. About sex percent of the income of the web paper comes from the local sites on the on-line paper. Another paper that has taken the interactivity one step further is Ångermanland/Örnsköldsviks Allehanda. In 2008 the paper started a writing school for the readers to teach them how to write their own news. Now the readers are participating in the local news production, and the result is published on the papers on-line sites in short written articles: allehanda.nära.

References

1. Alström, B. & Nord, L., (2000), *Två små ger mer än en stor - en studie av tidningsfusionen I Ådalen*, Stockholm: Kunskapsförlaget
2. Alström, B. & Hedman, L., (2002), Dagens medieföretag - morgondagens affärsidé. FSCN-rapport R-02-41, Sundsvall
3. Alström, B. & Nord, L., (2003), *Den skånska modellen*, Sundsvall: Demokratinstitutet, Mittuniversitetet
4. Carroll, J. S, (2006), *What Will Become of Newspapers?* Harvard University: Joan Shorenstein Center / Press Politics Public Policy
5. Castells, M., (2000), *The rise of the Network Society*, Volym I: *The information Age - Economy, Society and Culture*, London: Blackwell Publishers
6. Castells, M., (2001), *Internetgalaxen, reflektioner om internet, ekonomi och samhälle,* Stockholm/ Uddevalla: MediaPrint AB
7. Cepaite, A., (2006), *Medieproducenter och mediekonsumenter i otakt,* Stockholm: KTH
8. Chainon, J. Y., (2008), Newsroom Barometer: threats to newspapers, areas of investment, more results. Http://www.editorsweblog.org/analysis/2008
9. Engström, C. & Nilsson, K., (2004), *Nytt format - nytt innehåll? - en studie av Gefle Dagblads lokala nyhetsmaterial fore och efter övergången till tabloid*, C-uppsats, Sundsvall: Mittuniversitetet - MKV
10. Habermas, J., (2006),"Political Communication in Media Society: Does Democracy Still Enjoy an Epistemic Dimension? The Impact of Normative Theory on Empirical Research", *Communication Theory*
11. Holmberg, C. G., Oscarsson, I., Torbacke, J., (2000), *Den svenska pressens historia 1: I begynnelsen* (tiden fore 1830), Stockholm:Ekerlid
12. Hvitfelt, H. & Nygren, G., eds. (2008), *På väg mot medievärlden 2020. Journalistik, teknik och marknad,* Lund; Studentlitteratur
13. Johansson, C. & Stúr, E., (2009), *Vojmån - En studie av kommunikation och demokrati,* Sundsvall: Mittuniversitetet
14. Karlsson, M., (2006), *Nätjournalistik - en explorativ fallstudie av digitala mediers karaktärsdrag I fyra svenska nyhetssajter,* Lund universitet: Avdelningen för medier och kommunikationsvetenskap
15. Kolodzy, J., (2006), *Convergence Journalism - Writing and Reporting Across the News Media*, Lanham, Md: Rowman & Littlefield
16. Leth, G., (1996), *Brasständaren och Iakttagaren,* Stockholm: Symposion
17. Lundell, P., (2002), *Pressen I provinsen: från medborgerliga samtal till modern opinionsbildning 1750 - 1850,* Lund: Nordic Academic Press
18. Maier, M., (2007), *Journalism whitout Journalists: Vision or Caricature?* Harvard University: Joan Sherenstein Center/ Press Politics Public Policy
19. Nord, L. & Stúr, E. (2009), *Tyckandets tid - Journalistik, kommentar och valrörelse*, Stockholm: Mediestudier (SIM)O
20. Nygren, G., ed. (2008), *Nyhetsfabriken - Journalistiska yrkesroller i en förändrad medievärld*, Lund: Studentlitteratur
21. Nygren, G., (2008), *Yrke på glid*, Stockholm: Sim(o)
22. Sternvik, J., (2007), *I krymt kostym: Morgontidningarnas formatförändring och dess konsekvenser*, JMG: Göteborgs universitet
23. Sternvik, J., Wadbring, I., Weibull, L., (2008), *Newspaper in changing media world: Swedish trends*, Götebrorgs universitet: JMG
24. Storsul, T. & Stuedal, D., eds. (2007), *Ambivalence towards convergence - digitalization and media change*, Götebrogs universitet: Nordicom
25. Stur, E., (2005), *Politisk journalistic - sju dagar I tabloidformat*, paper - Aalborg:17:e Nordiska medieforskningskonferensen 2005
26. Våge, L., Stattin, E., Nygren, G., (2005), *Bloggtider,* Stockholm: Institutet för mediestudier

Materials from local News Papers collected in September 2008:
Gefle Dagblad
Norrtelje Tidning
Skånska Dagbladet
Sundsvalls Tidning
Sydsvenska Dagbladet
Södermanlands Nyheter
Västerbottens-Kuriren / VK.se
Västerbottens Folkblad
Ångermanlands/Örnsköldsviks Allehanda / allehanda nära
Östersunds Posten

Other materials and sources
Aftonbladet and Dagens Nyheter 7. 9. 2008
Dagens Media.se september 08
Journalisten.se: September 2008
Media Världen, TU, September 2008
Newsroom Barometer, 2008: editorsweblog.org/analysis
Nordicom.gu.se: Nordicoms pressdatabas, Nya Lundstedt, Tidningsutgivarna, 2008/10
Resumé: *Turbolent på skånska tidningsmarknaden*, 18/ 30 .42008

Print media in everyday life - interview - based study on media use in Finland

Kirsti Arjas-Kauranen[1] and Anu Seisto[2]

[1] TKK
Forsellesintie 2 B, FIN-02700 Kauniainen
E-mail: kirsti.arjas-kauranen@tkk.fi

[2] VTT
Tekniikantie 2, FIN-02150 Espoo
E-mail: anu.seisto@vtt.fi

Abstract

The public discourse often promotes the idea that new forms of media will eventually replace older forms of media. What clearly appears to be happening today is that people are becoming more conscious of what is special in different forms of media. It is clear that various media are an essential part of everyday life. They belong to the routines that give the rhythm to the days but they are also used to counter-balance the work and the free time as well as the time the family spends together. According to the interviews those media that dominate time-wise were not the necessarily emotionally the most important ones. The interviews clearly showed the importance of emotional attachment especially to books but in some extent also to other print material. It is possible that the digital natives do not have an equally positive attitude towards the print media as the interviewees in this study. However it is very interesting to see the future influence of observational learning, media education and the home-based appreciation of different media on how today's children use media as adults.

Keywords: media use, print media

1. Introduction

Our relationship with time defines our lives, [Jönsson, 2000,]. There are two kinds of time, personal time and clock time. Not much similarity can be found between them, [Jönsson, 2000]. Time is also often a determining factor in research concerning both the everyday life and the media, [e.g. KMT Kuluttaja, 2008; TNS Gallup, 2009]. When assessing how successfully one can combine work and family in everyday life, the question about time comes again up as an important factor. The transition from work (Fast element) to home with the children-in, or something else that counter-balances the working life (Slow element), depends much on our ability to adapt to the speed of this change. Studies about how people use their time have focused specifically to how much time one spends with various types of media. When we consider which types of media take up much of our time and which are emotionally the most meaningful ones, the results are not necessarily identical. Here our definition of measuring time becomes a relevant factor.

Many of today's problems derive from our relationship with time - excessive speed, which itself is detrimental. [Jönsson, 2000] As reaction to this, several alternative responses have come up, such as slow food, the various mind and body-hours instead of the traditional aerobic, the popularity of horticulture and knitting, etc. [Honore, 2006]. It is interesting to examine the meanings of various media in people's everyday life. What are the roles of different types of media in this context? What do people use for working - that belongs predominantly to the fast-element - and what for private use - that, in particular with children, should bring the slow-element to the life? What types of media are used for uniting these two worlds together, which ones for the transition from everyday life to other fields, and which ones to balance the work and the leisure time? It is also interesting to examine how successful this transition is. Studies have shown that especially women with family normally have to be able to adapt at least at some level, because they still carry the majority of caring responsibilities, [Parkins, 2004]. This also reflects into the ways, how they use media.

The media use projects carried out at KCL in 2004-2008 drew from an idea that in order to understand the significance of print media one must consider the whole media environment. Thus, we have analysed the relations between different media technologies, concentrating on the specific significance and uses that print

the everyday life. They belong to the routines that give the rhythm to our days but they are also used to balance the work and the free time as well as the time the family spends together.

2. Methods

The aim of this research is to describe, how print media appear in the life of the interviewees and how they explain their ways of using the media.

The research material of this study comprises interviews of Finnish working men (15) and women (16), 27 - 42 years of age and with a university degree. Half of them had families with children and half were single (men: 7 + 8, women: 8 + 8). To the study were selected such individuals, who either had the financial ability to acquire the selected media for themselves, or who had access to it otherwise. Therefore those who were chosen had a university degree, were in work life (i.e. economic factors do not restrict the acquisition of media), and used media in their work. The potential impact of the family situation was examined by selecting both those living alone (eight women and eight men) and those living with a family (eight women and seven men). The minimum age was defined on the basis that the interviewee would have been able to complete their university degree and get the children. The upper age limit was set at 42 years, so that the interviewees' children would be in an age, in which their use of media is not yet completely independent.

The interviewees come from different parts of the country, but all of them live and work currently in the metropolitan area or in other larger cities. The reason for this is that such changes in the underlying factors that might affect their media behaviour would not take place (such as physically long distances, functionality of internet connections, availability of newspapers, etc.). The selection of the interviewees was based on the principles that Patton [1990] calls the "intensity sampling method". There the material must be rich enough (versatile use of media) to form a clear picture of the phenomenon. However, it should not represent extreme cases, such as information technology pioneers, or anti-technology users. The interviewees filled a media diary on two working days and on both of the weekend days. The purpose of the diaries was to activate the people to follow their media use before the interview. They served also as reference material for the case that people would have an unconscious tendency to deliver a picture that is more in harmony with their ideals than with the reality.

The main data of the study was collected through interviews, which were made between May 2004 and June 2006. It must be noted that since then, the media field has changed and especially the difficult economic situation at the time of writing this article may have had some effect on the everyday media use of this age group. However, it is justified to assume that no drastic changes in the values and attitudes of the interviewees regarding print media have taken place. Hence, the data was not updated. For data collecting method I chose interviews because of the following reasons, which also Hirsjärvi & Remes & Sajavaara [1997] present in their book as advantages of interviews.

- To emphasise the fact that the human being can be seen as a subject in the research. One gets the opportunity to express oneself on personal matters as freely as possible. One plays in the study an active part and can create different meanings.
- To set the result (talk) to a broader context. In an interview it is possible to see the interviewee, his / her face and gestures. One can also tell about oneself and about the topic in a broader context than the researcher can predict.
- An in-advance-known fact is that the research topic produces answers that are complex and contain many dimensions.
- The opportunity to clarify responses to questions.
- To deepen the assertions. It is possible, for example, to request explanations on the expressed views. Additional questions can be used when needed.

The base of this research was to examine people's overall media use that includes both work and private usage. Furthermore, the aim was to find out, whether the understanding of different situations in life helps us to comprehend the possible changes in the media use. I selected following themes to be the frame of the interviews: current media use, childhood, studying time, establishing the family and as additional themes the usage of media in ones work (work history and details of current use), and future prospects.

During the work it became increasingly obvious that research into the use of media using a qualitative method requires full familiarity with the cultural environment and the language. The interviewer must be familiar with

the environment in which the informant/interviewee lives. Traditionally the ways of using media have been different in different countries (such as newspapers in Finland) and also this affects the results. This gives specific characteristic features to the ways of using media, to its significance as well as to the future expectations. Based on a recent study [Leinonen, 2009], it seems that internet, as a global medium, is also experienced more universally than magazines. Cultural factors appear to have a more significant role in the attitudes towards the print media, and therefore the strengths of magazines are also regarded differently in different cultures.

3. Results

In this report I shall concentrate on the ways Finnish people use print media nowadays. Firstly I'll present the results on the use of print media at work. After that follows a short review on how newspapers, magazines and books are used among the research group. Interviewees spoke a little about observational learning and about media education, which I shall present from the viewpoint of print media. One striking element that I found during the text reading and encoding - process was the interviewees' opinion on the control or freedom that different types of media had. In their work the imposing element was the nature of a specific task or the organizational culture. In contrast to this, daily routines were part of transition from one phase to another (morning, commuting from home to work and back with public transportation and evening). The usage of media during one's leisure time was explained by one's vigour, how active one wants to be and by reflecting it to the situation in working life.

3.1 Print media in work

In this chapter the term 'print media in work' refers to professional literature and professional journals. The interviewees gave information also about the amount of material they print from the computer or from the internet, and what is the reason of doing so.

Almost all interviewees worked in such positions, in which reading professional literature was important. However, they did often not have enough time for reading during the working day. Some of them used the commuting time from work back home for this, but many of them said that they unfortunately bring this material home with them, even though they wished they did not have to.

The research group divided into two categories, when the question about printing the material was taken into focus. The first category consists of those who printed almost everything, because they did not want to read from the screen. They printed e-mails with the attachments, articles they had found, and their own concepts. The reasons for this were better readability, ease to take along and archiving. The second category were those, who could read long passages from the screen as well, and who claimed that they wanted to avoid printing because of paper piles or for ecological reasons. Printed material had several benefits: it gives an opportunity to underline the references and to make other markings into them; it gives in general a better perception of the entity and eased the distribution. Almost all interviewees printed materials that require engagement and good concerntration from the reader. *"If I have something that I want to reflect upon or to which I want to revert... I read it from the paper, I like to underline... write my ideas in the margins." (single man, 29 y.)*

3.2 Printed newspaper

The printed newspaper has still maintains its position among morning routines. Approximately one out of two of the interviewees in each group (women with children, single women, men with children, single men) reads or at least browses the newspaper during breakfast. *"I have the Helsingin Sanomat, it's a Must in the morning, I mean I can't start the day without it, it's like a habit." (Single woman, 30 y.). "Yes, it can take 45 minutes to read the Helsingin Sanomat in the morning." (Man with children, 34 y.)* On weekends the newspaper is an even more remarkable starter in the mornings.

For some people a newspaper (subscribed or free) was the first medium of the day although it was not a part of the morning routines. The interviewees claimed to read newspapers always on their way to the work in the

(Woman with children, 36 y.) Some of the interviewees pick up the newspaper again after work or in the evening. Two of the interviewees, who did not have time for the paper in the morning, had reading as an evening routine. *Around nine o'clock in the evening I usually read the newspaper of the day, I might watch the news at the same time... it's like a way to relax. (Woman with children, 34 y.)*

Only one interviewee (a single man) mentioned an internet version as part of morning routines. Online-newspapers did not belong to the morning routines of the other interviewees. They might browse them anyway during the working day for instance at the lunch break. Two interviewees didn't read newspapers at all and two only on weekends while visiting their parents. Some men and women with children claimed that they had dropped reading because of family reasons (small children) but believed they would revert to it when the children grow. One of the interviewees supposed he would abandon reading the newspapers totally in the future.

Besides reading being a habit, the reasons for reading newspapers were good user interface and a moment of private time. *"In the morning I usually wake up little earlier just because it is the time when you have some peaceful time with yourself... this reading in the morning while eating some the breakfast is such a routine" (woman with children, 42 y.), "Relates to certain kind of enjoying of your own time with a cup of coffee in front of you" (woman with children, 37 y.)* It was mentioned also to be a good way to orientate to the coming day during the transition from home to work. *"... I arrive by underground to work and there I take a free newspaper... actually I get pretty well into what is happening." (Woman with children, 34 y.)*

While talking about newspapers, some interviewees emphasized the fact that although they could find the actual news from other media as well, it was only the newspaper that gave a proper editorial background to the news. *"There is this analysis...somehow they go into the contexts" (man with children, 35 y.), "...you know that if you have seen something in the evening...that in the morning in the Helsingin Sanomat there will certainly be some more information about the background..."(single man, 32 y.)* Also the editorial content was regarded to be one of newspapers' strengths. *"Somehow it fits to print better that there is some kind of editorial vision to some news..."(man with children, 36 y.)*

Letters to the editor are something people often seemed to talk about with colleagues and friends. *"I like to reserve enough time for that, so that I could read more than just the headings, something from letters to the editor so that I know what the others are talking about and what kind of topics there are in the air..."(single woman, 27 y.)*Two interviewees mentioned also that they have less to discuss with such people who don't read newspapers. *"...We have noticed that with them (friends who don't prescribe to newspapers) you can't discuss about any current topics... you can't even talk about comic strips." (Woman with children, 37 y.)*

Some of the interviewees believe, that they will read traditional newspapers still in ten years' time. The reasoning for this was for instance the value of the newspaper as a morning routine. Some people, who expect the online media to replace other types of media as a means to report news in the future, supposed *"the traditional newspaper role to become more like a forum for good, deep analysis" (single man, 37 y.)*

3.3 Magazine

Magazines belonged clearly to relaxing, a moment for oneself, of the interviewees. Another typical situation to read a magazine is just before bedtime (evening routine). The majority of these people read business journals, as well as magazines related to their hobbies. Since the interviewees had a university degree and generally were members of some union, the membership brought them technical or business journals. Usually people read or at least browse such journals.

Six women with families had prescribed to magazines. They read some traditional women's magazines, family magazines, specialized magazines and magazines about well-being or about interior decoration. The idea of marking one's own time by reading magazines was characteristic for this group. *"If you do not have much time but would like to get a moment for yourself, it's nice to rest a little and browse through those things" (woman with children, 42 y.)* For four persons of the group of single women, magazines were an important way to relax after work or before bedtime. *"I find it wonderful when I come from work and look through it. I don't necessarily read it carefully, but browse" (single woman, 30 y.) "When I go to bed, then I usually read something.... some magazine "(single woman, 31 y.).* They also prescribed to magazines. Others read the journals they got through memberships but otherwise only occasionally.

Only two of the men with a family prescribed to hobby journals. Otherwise, they bought some news-stand copies when they saw an interesting headline. Business magazines they read to some extent. This was the group reading the lowest number of magazines. *"For some reason reading magazines has remained quite minimal" (man with children, 34 y.)* Six of the single men read magazines quite frequently. These included in particular business-related magazines and hobby magazines, both prescribed ones and news-stand copies. *"I'm reading a lot photography journals" (single man, 29 y.) "I buy now and then news-stand copies, mainly those about computer games, or this kind of popular science -magazines, sometimes a bike magazine" (single man, 32 y.)*

The content of specialized magazines was regarded as interesting. When talking about magazines as part of the everyday life people felt that they were suitable because of their short articles and because they gave the possibility to sit down for a moment to browse them. For this reason magazines could substitute books that otherwise were regarded as relaxing reading. *"I'm usually so tired and so stressed out that I rather read something from magazines and especially shorter articles in them" (woman with children, 34 y.)*

3.4 Book

Besides magazines, also books are part of the evening routines in all four groups. It is an appropriate transition and a way to calm down to sleep. *"Always some book... that is a pretty good way to calm down a little in the evening before going to bed" (single woman, 37 y.) "If work matters don't leave my mind, so by reading, even a couple of pages, I forget them and tend to sleep better '(single woman, 35 y.) "I often fall asleep with a book" (man with children, 36 y.)*

The best aspects of books were that they were least bound to any location or reading position, one could read at one's own pace and stop whenever one wished to ponder. Books were considered the best media to isolate one from everyday life because reading requires concentration and personal imagination. There were a couple of eager readers in both of the men's groups, but otherwise the habit of isolating from daily life was more a topic typical of women. *"If I have more time, then a book is the best thing, so it's a good way to get rid of the everyday, but what it requires is that you have a little more time." (Woman with children 42 y.), "somehow it is the best way to get beyond everyday life, so for me it is a way to break away." (Woman with children 39 y.)*

Many interviewees regarded tiredness and lack of time as reasons to lessening reading of books. *"Mostly it is because of looking after the children that I don't have that much time to read." (Woman with children, 36 y.) " a book requires such concentration that if you're tired, you don't necessarily find the energy to read" (single woman, 40 y.) "Yes I could read, but somehow now I imagine I am so busy, and don't always have the intiative... "(Man with children, 36 y.)"However, reading a good book requires a suitable moment, and you shouldn't be too tired. Reading a good book is maximizing relaxation; the other media are almost only some sort of ways of spending time. (Single man, 30 y.)* For some of the interviewees reading books was seasonal and often focused on holidays. *"On holidays, yes I read a lot of books, it is a quite clear change to my normal habits" (single woman, 27 y.) "Like many others,I read during Christmas-time and summer holidays, otherwise less" (Man with children, 36 y.)* It was typical also, that during studying years people tended to reduce other reading. The reason was often, that they no longer found reading relaxing, because studying was mainly reading. Again some of them felt guilty if they read other books than those belonging to their studies. However, some did this anyway. (T. Kuula has studied students' media use in his Master's Thesis, IARIGAI Paper 2005)

Interviewees who had reduced their reading because of lack of time, told that they missed it. *"I wish I could read more, but I know I won't make it" (Woman with children, 34 y.) "I miss the books, but in fact my life is such that I won't manage to" (Woman with family, 34 y.) "I would like to read more books... feel like I don't have time for it." (Man with children, 34 y.)* These interviewees were among those, who had been active readers already in their childhood. Books were either bought from book-stores or borrowed from friends. There were fewer of those, who would use libraries. Many interviewees mentioned that they read popular literature. Only two women and three men said that they read books very little or not at all. The interviewees looked upon the future of the books as positive. *"I would imagine that some traditional media, such as a book would become more present again." (Man with children, 36 y.) 'I would see it so that the book should maintain its position "(single man, 32 y.)* Electronic books were not considered as a liable threat to the printed ones.

3.5 Observational learning and media

Almost all women and men with children said that a bedtime story is an evening routine in their families or was when the children were small. It was considered to be a good method to help the children calm down before going to bed. *"We read a bedtime story almost every night ... even if the day would have been long anyway we usually read it '(Woman with children, 36 y.)*

Even if the children are born into a different media atmosphere than their parents, the interviews pointed out the importance of observational learning. At the infant stage, this type of modelling still has an important role, and parents seem to be aware of it. *"... The younger one, who is four years old, he reads the books and then the books are upside down and he reads stories aloud, clearly imitating" (Woman with children, 34 y.)* For example, a few of the boys' mothers pointed out the importance of the father's reading hobby as a good model for their sons. *"We have talked little about it... what kind of a role model it is... that the boy sees the father reading a book, my opinion is that it is extremely important" (Woman with children, 36 y.)* Some interviewees explained that their older children are already interested in reading newspapers, if it belonged to the parents' morning routines. *"Our eleven-year-old... when he sees that his father is reading, he can take a short look as well... somehow you start thinking that you could somehow be a model yourself..." (Family with children, 37 y.)*

Reading of books was something the parents deliberately encouraged their children to do. *"Yes, reading is something that I emphasize to my own children." (Woman with children, 36 y.)* This could be seen from examples, in which the parents urge their youngsters to calm down by reading something. *"Pretty often I tell them to go and calm down little bit and for example to take a book for that. (Woman with children, 36 y.)* Some visit actively a library with the children. *"We go to the library quite frequently, weekly, so that they would learn to read and to find books as well..." (Woman with children, 34 y.)* One way to encourage children to read is, of course, to get books for them. *"Mika has been such a book-worm that he values reading and we have bought the boys loads of booksas gifts..." (Woman with children, 42 y.)*

4. Conclusions

Print media have still a clear position in people's everyday life in Finland. They are routinely used in transitions from one phase to another, e.g., in the morning from home to the surrounding world, and in the evening from the day's activities into sleep. Even when the use is of routine nature, it should not be underestimated. This becomes obvious in situations when one has to diverge from the routine. When e.g. the newspaper has not been delivered, active readers feel that the day does not begin in the right way or they browse through an old newspaper. Many of the interviewees highlighted the value of the newspapers editorial content. They felt that they could not find such content in other types of media. Is it conceivable that with age people become more interested in material that gives information about contexts and analyses the background of current news? What would replace this task of the newspapers in the future, if printed papers disappeared?

Newspapers, magazines and books are also important in influencing the life while people decide the pace themselves. Printed media is used to get distance from the everyday life, to counter-balance the work and to mark one's time and space territory that others are not allowed to disturb. According to some other studies made at KCL [e.g. Leinonen, 2009] it seems that the usage of printed media is strongly culture-related, and that's why differences in the ways of using such media are bigger than those with electronic media.

Based on this investigation, youth and studying years are a more homogeneous period with regard to the use of media but after about thirty years of age the individually characteristic ways of using media begin to influence the choice of media. This became obvious e.g. in that persons who had read much as children consciously strived to read more as they got an opportunity to do so, say after studying years or as soon as the children had grown older. It will therefore be very interesting to see the future influence of observational learning, media education and the home-based appreciation of different media on how today's children use media as adults.

According to the interviews those media that dominate time-wise were not necessarily emotionally the most important ones. An interesting fact is that the basis for using print media is principally different from that of many electronic ones. They require being active oneself, imagination (particularly books), and concentration. When using them our relationship with time is different. Does this increase the sense of a personal and intensive

experience? Did this make the interviewees highlight the importance of printed media as the emotionally important ones? And what is the significance of childhood media memories and emotional experiences later in life, when one selects a way to relax and seeks counter-balance to the pressure of everyday life?

The high level of education of the interviewees may at least partly explain the positive attitude towards print media in this study. In addition, the interviewees belong to an age group that has not grown up surrounded by digital media. It is possible that the digital natives do not have an equally positive attitude towards print media as the interviewees in this study. However, the future does not just happen, and attitudes do not just change. As adults and parents, we have great responsibility in giving the younger generations unforgettable and good memories of reading, either together or alone. In addition, the wonders and joys of reading could very well emphasized in campaigns for large masses of people.

References

1. Hirsjärvi, S., Remes, P. & Sajavaara, P., (1997), *Tutki ja kirjoita. Kirjayhtymä Oy*
2. Honore, C., (2006), *Slow - Elä hitaammin! (In praise of Slow) Bazar. Uddevalla*
3. Jönsson, B., (2000), *10 Ajatusta ajasta. (Tio tankar om tid) Tammi. Helsinki*
4. Kuula, T., Seisto, A. & Nieminen, S., (2005), Media Use of Young University Students in Helsinki Area. In proceedings of 32nd International Iarigai Research Conference. Haikko Manor, Porvoo, Finland, 4-7 Sept. 2005
5. Leinonen A., (2009), *Content, concepts and portability. KCL Link 1/2009,* pp. 24-26
6. KMT Kuluttaja, (2008), TNS Gallup, (2009) referred to in e.g. http://www.digipaper.fi/aikakauslehtienliitto/29796/
7. Parkins, W., (2004), *Out of Time. Fast Subjects and Slow Living. Time & Society no. 2/3,* vol. 13, 363-382
8. Patton, M. Q., (1990), *Qualitative Evaluation and Research Methods. SAGE Publications*





2

Color and ink

A new approach to calculate colour values of halftone prints

Sasan Gooran, Mahziar Namedanian and Henrik Hedman

Department of Science and Technology, Linköping University
Campus Norrköping, SE-601 74 Norrköping, Sweden
E-mail: sasgo@itn.liu.se

Abstract

Printed dots appear bigger than their reference size in the original bitmap. This is because of the physical and optical dot gain. In order to overcome the problem original images are compensated for dot gain. The compensation is usually done by using a dot gain curve for each colour separation. In this paper we firstly show that using only one dot gain curve works well for black, but not for any of the other three colours, i.e. cyan, magenta or yellow. We also present a new approach to calculate colour values where three different curves are used for each colour separation. In order to evaluate the proposed approach we compare the results of our method with the results when only one dot gain curve is used for each colour, both for Murray-Davies and Yule-Nielsen models. In the case of only one dot gain curve for each separation we use the curve that gives a minimized ΔELab using least squares method. The experiments and calculations show that our approach gives a better approximation of the resulting colour coordinates.

Keywords: dot gain, colour calculation, halftone print

1. Introduction

One of the most famous and simplest models to predict the reflectance of a halftone print is Murray-Davies (MD) model, (Murray, 1936):

$$R(\lambda) = aR_i(\lambda) + (1-a)R_p(\lambda) \tag{1}$$

where $R(\lambda)$ is the predicted spectral reflectance, a is the fractional area of the ink, $R_i(\lambda)$ is the spectral reflectance of the ink at full coverage and $R_p(\lambda)$ is the spectral reflectance of the substrate (paper). Because of the linear relationship between CIEXYZ values and the spectral reflectance Equation 1 can be extended to an equation based on CIEXYZ values, which is called Neugebauer's equations [Neugebauer, 1937]:

$$\begin{bmatrix} X_{ave} \\ Y_{ave} \\ Z_{ave} \end{bmatrix} = a_i \begin{bmatrix} X_i \\ Y_i \\ Z_i \end{bmatrix} + (1-a_i) \begin{bmatrix} X_p \\ Y_p \\ Z_p \end{bmatrix} \tag{2}$$

where a_i is the fractional area covered by the ink with CIEXYZ values (X_i, Y_i, Z_i) and $\sum_i a_i = 1$.

The coverage of each ink in this equation is actually supposed to be the physical coverage after print. Hence, the optical dot gain is not included in this equation. These equations are, however, often used to find dot gain for process colours, Cyan, Magenta, Yellow and Black. The equations become then:

$$\begin{bmatrix} X_{ave} \\ Y_{ave} \\ Z_{ave} \end{bmatrix} = a_i \begin{bmatrix} X_i \\ Y_i \\ Z_i \end{bmatrix} + (1-a_i) \begin{bmatrix} X_p \\ Y_p \\ Z_p \end{bmatrix} \tag{3}$$

where (X_i, Y_i, Z_i) denote the CIEXYZ values for the full-tone ink (Cyan, Magenta, Yellow or Black) and (X_p, Y_p, Z_p) denote the same values for paper. In order to find dot gain, a number of test patches with different coverage are printed and their CIEXYZ values are measured by a Spectrophotometer. Then the measured XYZ values are put in the left hand side of Equation 3 and the effective coverage is calculated thereby. For instance Equation 4 finds the effective dot coverage after print for a cyan patch using CIEX,

$$a_{c-eff} = \frac{X_{c-mea} - X_p}{X_c - X_p} \tag{4}$$

where $X_{c\text{-}mea}$, X_c and X_p denote the X-value of the measured cyan patch, the full-tone cyan and the paper, respectively. Since the measurement has been carried out for a number of patches with different nominal (reference) coverage this equation gives a curve that defines the relationship between the nominal and the effective dot coverage. Dot gain can then be calculated by subtracting the reference dot coverage from the effective dot coverage.

Yule and Nielsen (YN) showed that the nonlinear relationship between predicted and measured reflectance spectra can be described with a power function [Yule, 1951].

$$R^{1/n}(\lambda) = aR_i^{1/n}(\lambda) + (1-a)R_p^{1/n}(\lambda) \tag{5}$$

where n, which is referred to as the n-factor, is a parameter accounting for light scattering in paper and all other variables are as in Equation 1. Fitting the n-factor requires nonlinear optimization (Wyble, 2000). Although the relationship between the reflectance spectra and the CIEXYZ is not linear any longer, a modified version of Equation 2 is commonly used to predict the CIEXYZ colour values using n-factor.

$$\begin{bmatrix} X_{ave} \\ Y_{ave} \\ Z_{ave} \end{bmatrix}^{1/n} = \sum_i a_i \begin{bmatrix} X_i \\ Y_i \\ Z_i \end{bmatrix}^{1/n} \tag{6}$$

Many prediction models have been discussed and examined in literatures during recent years [Gerhardt, 2007], [Hersch, 2005], [Wyble, 2000]. Most of them are complicated, require nonlinear optimization and need a training set of patches to predict the colour values. In this paper we present a simple approach that predicts the colour values very well when one or two colours are involved. The results of this model are compared with those of MD and YN models. First in Section 2 we describe how we use the MD and YN models to predict the colour values. This is followed by the description of our model. In Section 3 the results of all three models are presented. Finally, in Section 4 discussions and conclusions are given.

2. Our approach

As mentioned in Section 1, although MD model is commonly used to obtain dot gain curves there are some issues that have to be observed. In Equation 3 the optical dot gain is neglected. Since the measurements are done by optical devices, the effect of optical dot gain is reflected in the measurement results. Therefore, the effective dot coverage is actually used to represent both physical and optical dot gain. According to Equation

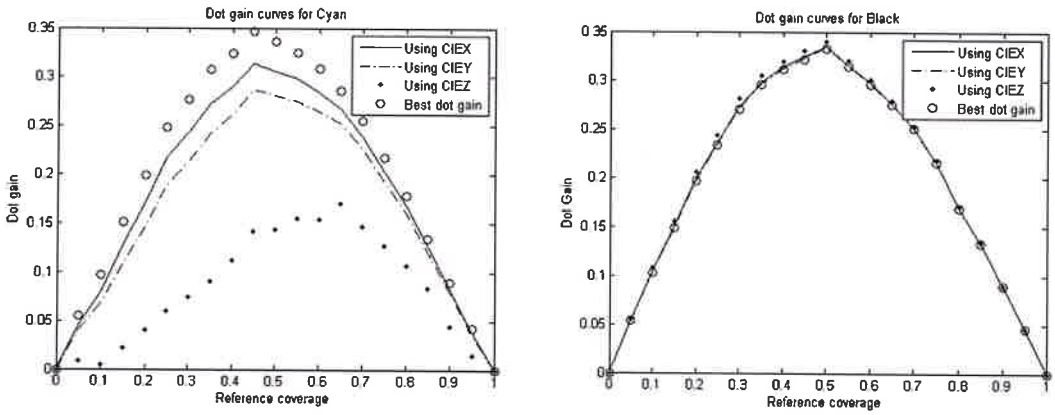

Figure 1: Dot gain curves using CIEX, CIEY and CIEZ and the best dot gain curve for a laser printer at 300 dpi. a) for cyan b) for black

3, the effective dot coverage should be the same if $X_{c\text{-}mea}$, X_c and X_p are replaced by $Y_{c\text{-}mea}$, Y_c and Y_p (or: $Z_{c\text{-}mea}$, Z_c and Z_p) in Equation 4, respectively. Figure 1 shows the dot gain curves for cyan and black printed at 300 dpi by a laser printer (Xerox, Phaser 6180), using CIEX, Y and Z, respectively. This figure depicts that different dot gain curves are obtained for cyan using CIEX, Y and Z. For black the dot gain curves are almost the same, as expected. It must be observed that if the cyan ink and the paper were both ideal then it would only be possible to find the effective dot coverage by using the reflectance spectra in longer wavelength, which corresponds to CIEX values. According to our measurements these three dot gain curves for yellow and magenta also differ. This experiment clearly shows that it is not completely correct to only define one dot gain curve for each process colour, which has been done in many studies [Gerhardt, 2007], [Hersch, 2005], [Wyble, 2000]. Let us now assume that we want to only use one of the three dot gain curves shown in Figure 1 for cyan.

According to our discussion above the most suitable choice would be the dot gain curve obtained by CIEX. With the same reasoning, the dot gain curve obtained by CIEY is most suitable for magenta and the one obtained by CIEZ for yellow. It is obvious that even if we use the most suitable dot gain curve for each ink, the predicted colour values will differ quite much from the measured values, see Figure 1 again. If we now want to use one dot gain curve it is probably better not to use any of these three curves. Instead, it is better to use a dot gain curve that gives the smallest ΔELab difference between the predicted and the measured colour values. In order to do that we use the least squares method and find the best dot gain curve, denoted by *dg_best_MD*, which gives the smallest ΔELab. The predicted colour values are calculated by:

$$\begin{cases} X_{calc} = (a_{ref} + dg\_best\_MD(a_{ref}))X_c + (1 - a_{ref} - dg\_best\_MD(a_{ref}))X_p \\ Y_{calc} = (a_{ref} + dg\_best\_MD(a_{ref}))Y_c + (1 - a_{ref} - dg\_best\_MD(a_{ref}))Y_p \\ Z_{calc} = (a_{ref} + dg\_best\_MD(a_{ref}))Z_c + (1 - a_{ref} - dg\_best\_MD(a_{ref}))Z_p \end{cases} \quad (7)$$

where a_{ref} denotes the reference (nominal) dot coverage and $dg\_best\_MD(a_{ref})$ gives the effective dot gain at the reference coverage, a_{ref}. (X_c, Y_c, Z_c) and (X_p, Y_p, Z_p) denote the CIEXYZ values for full-tone cyan and paper, respectively. The colour values of full-tone cyan and paper are measured. Besides those we have measured the colour values of nineteen other patches with reference coverage 5%, 10%, 15% ..., 90% and 95%. For each of these reference dot coverages the XYZ values are calculated by Equation 7 and then converted to CIELab values. The *dg_best_MD* is then found at each reference coverage by minimizing the ΔELab between the calculated and measured CIELab values for that coverage, see Figure 1 (circles). In a similar way the best dot gain curve can be found for magenta and yellow. Our calculations and measurements show that even this best dot gain curve gives a relatively big ΔELab, see Section 3. Since one dot gain curve does not even work well for one colour it will definitely not work when few colours are involved in the calculations, see next section.

Since the results using MD model, as expected, are not satisfactory we also use YN model to predict the colour values. For each measured reference coverage we calculate the XYZ values by:

$$\begin{cases} X_{calc} = ((a_{ref} + dg\_best\_YN(a_{ref}))X_c^{1/n} + (1 - a_{ref} - dg\_best\_YN(a_{ref}))X_p^{1/n})^n \\ Y_{calc} = ((a_{ref} + dg\_best\_YN(a_{ref}))Y_c^{1/n} + (1 - a_{ref} - dg\_best\_YN(a_{ref}))Y_p^{1/n})^n \\ Z_{calc} = ((a_{ref} + dg\_best\_YN(a_{ref}))Z_c^{1/n} + (1 - a_{ref} - dg\_best\_YN(a_{ref}))Z_p^{1/n})^n \end{cases} \quad (8)$$

Then we find the best *n*-factor and dot gain (i.e. *dg_best_YN*) that gives the smallest average ΔELab between the calculated and measured CIELab values. We do that by starting with $n = 1$ and find the best dot gain curve for this *n* and notice the average ΔELab value. We then increase the value of *n* with a small number, which is 0.1 in our calculations, and find the best dot gain curve for each *n* and calculate the average ΔELab value between the predicted and the measured colour values. The best *n* and dot gain curve are obtained when the difference is minimized. In our calculations we never let the dot gain values be less than zero for any reference dot coverage. The best *n*-factor and dot gain curve are found in the same way for magenta and yellow. Since the *n*-factor has no real physical description it is really hard to describe what the best dot gain curves represent [Ruckdeschel, 1978]. If the found *n*-factor was between 1 and 2, then one could probably describe the best dot gain curve to represent the physical dot gain. In our approximations, like many others, however, *n*-factor can be bigger than 2. It must be mentioned that in our calculations we never let *n* be bigger than a value that makes the dot gain be negative.

As illustrated earlier in this section using CIEX, CIEY and CIEZ gives three different curves showing the fact that MD cannot be used similarly for all visible wavelengths. The main idea behind our approach is to use three different dot gain curves, obtained by CIEX, Y and Z, respectively, see equations 9 - 11.

$$dg\_Xc(a_{ref}) = \frac{X_{c-mea}(a_{ref}) - X_p}{X_c - X_p} - a_{ref} \tag{9}$$

$$dg\_Yc(a_{ref}) = \frac{Y_{c-mea}(a_{ref}) - Y_p}{Y_c - Y_p} - a_{ref} \tag{10}$$

$$dg\_Zc(a_{ref}) = \frac{Z_{c-mea}(a_{ref}) - Z_p}{Z_c - Z_p} - a_{ref} \tag{11}$$

In Equations 9 - 11, *dg_Xc*, *dg_Yc* and *dg_Zc* denote the dot gain curve for cyan obtained by CIEX, CIEY and CIEZ, respectively. The dot gain curves for magenta and yellow are correspondingly found. Now in order to predict the colour values for cyan Equation 12 is used.

$$\begin{cases} X_{calc} = (a_{ref} + dg\_Xc(a_{ref}))X_c + (1 - a_{ref} - dg\_Xc(a_{ref}))X_p \\ Y_{calc} = (a_{ref} + dg\_Yc(a_{ref}))Y_c + (1 - a_{ref} - dg\_Yc(a_{ref}))Y_p \\ Z_{calc} = (a_{ref} + dg\_Zc(a_{ref}))Z_c + (1 - a_{ref} - dg\_Zc(a_{ref}))Z_p \end{cases} \tag{12}$$

The difference between Equation 12 and 7 is that in Equation 12 the coefficients of X_c and X_p are different from those of Y_c and Y_p (or: Z_c and Z_p), which actually makes the calculated XYZ values be exactly the same as the measured ones for all measured one colour patches. Observe that none of the other two approaches, i.e. MD and YN, give the exact XYZ values as the measured ones for one colour.

When two or more colours are involved, the effective dot coverage is first found for all reference coverages by the dot gain curves. Then Demichel's equations are used [Demichel, 1924]. Let us now illustrate that with an example. Assume that the reference coverage for cyan and magenta are denoted by *c* and *m* and these channels are halftoned independently and then printed. Now we want to calculate (or predict) the colour values using the three models discussed in this paper.

For the MD model we have one dot gain curve for cyan and one for magenta. By using those we get the effective dot coverage for cyan and magenta, denoted by $c_{eff\text{-}MD}$ and $m_{eff\text{-}MD}$. Now by using Demichel's equations we can find the effective coverage for cyan, magenta, blue and paper after print, see Equation 13.

$$\begin{cases} c_{MD} = (c_{eff\_MD})(1 - m_{eff\_MD}) \\ m_{MD} = (1 - c_{eff\_MD})(m_{eff\_MD}) \\ b_{MD} = (c_{eff\_MD})(m_{eff\_MD}) \\ p_{MD} = (1 - c_{eff\_MD})(1 - m_{eff\_MD}) \end{cases} \tag{13}$$

Now the Neugebauer's equations, Equation 2, are used to predict the resulting CIEXYZ values.

For the YN model the best *n*-factors are found for cyan, magenta and blue, denoted by n_c, n_m and n_b, respectively. Since n_c, n_m and n_b are most probably not equal, the main question is what *n* should be used in Equation 6 (modified Neugebauer's equations) to calculate the resulting colour values. Since our calculations are only based on the measurements carried out for the primary and secondary colours (in this example cyan, magenta and blue) there is no way to know what *n* is best when the colours are randomly printed. Therefore we use the average of n_c, n_m and n_b, i.e. $n_{YN}=(n_c + n_m+n_b)/3$. Using this new *n* (i.e. n_{YN}) we find the best dot gain curve for cyan and magenta as described before, see Equation 8. Assume that these dot gain curves give the effective dot coverage for cyan and magenta, denoted by $c_{eff\text{-}YN}$ and $m_{eff\text{-}YN}$. The Demichel's equations are used to find the coverage for cyan, magenta, blue and paper, see Equation 13. Then the resulting colour values are calculated by Equation 6 with $n=n_{YN}$.

Since in our approach three dot gain curves are used, three dot coverages are found for cyan and three for magenta, denoted by $c_{eff\text{-}X}$, $c_{eff\text{-}Y}$, $c_{eff\text{-}Z}$, $m_{eff\text{-}X}$, $m_{eff\text{-}Y}$ and $m_{eff\text{-}Z}$. For instance $c_{eff\text{-}X}$ is calculated by,

$$c_{eff\_X} = c + dg\_Xc(c) \tag{14}$$

dg_Xc is the dot gain curve for cyan obtained by CIEX values, see Equation 9. The other five effective areas are correspondingly calculated. Now when we have found these six effective coverages we use Demichel's equations to find the coverage for cyan, magenta, blue and paper. Observe now that, even here you get three different coverages for each of these four colours, see Equation 15 to see how these three coverages are calculated for cyan.

$$\begin{cases} c_{our\_X} = (c_{eff\_X})(1 - m_{eff\_X}) \\ c_{our\_Y} = (c_{eff\_Y})(1 - m_{eff\_Y}) \\ c_{our\_Z} = (c_{eff\_Z})(1 - m_{eff\_Z}) \end{cases} \tag{15}$$

With corresponding equations one can find the three coverages for magenta, blue and paper. The predicted colour values are now calculated by:

$$\begin{cases} X_{calc} = c_{our\_X} X_c + m_{our\_X} X_m + b_{our\_X} X_b + p_{our\_X} X_p \\ Y_{calc} = c_{our\_Y} Y_c + m_{our\_Y} Y_m + b_{our\_Y} Y_b + p_{our\_Y} Y_p \\ Z_{calc} = c_{our\_Z} Z_c + m_{our\_Z} Z_m + b_{our\_Z} Z_b + p_{our\_Z} Z_p \end{cases} \tag{16}$$

Notice that although Equation 16 is similar to Neugebauer's equation, they are not exactly the same.

3. Results

In order to compare our approach with MD and YN we first created a number of patches. The colour channels of the patches were then halftoned independently by a first generation Frequency Modulated (FM) technique, IMCDP [Gooran, 2004]. They were then printed at two different resolutions, 150 dpi and 300 dpi, using a laser printer (Xerox, Phaser 6180). CIEXYZ and CIELab coordinates of the printed patches were then measured by a Spectrophotometer (Gretag Macbeth Spectrolino) using *d50* light source for a 2° observer. The colour differences between the predicted and measured values were calculated using two CIELab colour differences, ΔE_{ab} and ΔE_{94}. ΔE_{ab} denotes the CIELab colour difference recommended in 1976, which is the Euclidean distance between the coordinates for the two stimuli. ΔE_{94} denotes the CIELab colour difference that was recommended for industrial use and was introduced in 1994 [Fairchild, 1997]. Here follow the results of our calculations for one colour, two colours and three colours using MD, YN and our model.

3.1 One colour

One colour patches with the reference coverage 0%, 5%, 10%, ..., 90%, 95% and 100% were created and halftoned with a FM method and printed in both 150 dpi and 300 dpi. The colour difference between the calculated and measured stimuli for these twenty one cyan, magenta and blue patches are illustrated in Table I. With blue we mean cyan printed on top of magenta, i.e. dot-on-dot.

In this table (Table I) the average colour difference (ave), the maximum colour difference (max) and the standard deviation (std) are shown. As can be seen the colour differences are very high for MD model, especially for blue. These differences in colour are less for YN but still high, especially for magenta. The colour differences are zero using our approach, which was expected.

3.2 Two colours

We created 180 different two colour patches using cyan and magenta. Hundred and eighty different coverages between 0% and 100% were randomly chosen for cyan and magenta, respectively. The cyan and magenta channels were halftoned independently by a FM method and printed in 150 dpi and 300 dpi. Table II shows the colour differences between the measured and calculated colour values for these hundred and eighty patches using MD, YN and our proposed model. As can be seen our approach predicts the colour values much more accurately than the other two models.

Table I: The CIELab ΔEab and ΔE94 colour differences between measured and calculated one colour patches (cyan, magenta and blue)

One Colour C, M and B			ΔE_{ab}			ΔE_{94}		
			MD	Y	Our approach	MD	Y	Our approach
150dpi	C	std	1.0550	0.1869	0.0000	1.0122	0.1744	0.0000
		ave	1.6298	0.2925 (n_{YN}=1.80)	0.0000	1.5670	0.2775 (n_{YN}=1.80)	0.0000
		max	2.9546	0.8806	0.0000	2.8263	0.8207	0.0000
	M	std	1.2534	0.9967	0.0000	1.1817	0.9428	0.0000
		ave	2.1434	1.7626 (n_{YN}=1.50)	0.0000	2.0237	1.6727 (n_{YN}=1.50)	0.0000
		max	3.7188	3.0373	0.0000	3.5006	2.8761	0.0000
	B	std	3.1521	0.5528	0.0000	2.8898	0.5044	0.0000
		ave	5.3910	0.9397 (n_{YN}=2.90)	0.0000	5.0131	0.8772 (n_{YN}=2.90)	0.0000
		max	9.7128	1.9505	0.0000	8.9014	1.7419	0.0000
300dpi	C	std	1.8834	0.2565	0.0000	1.7951	0.2388	0.0000
		ave	2.9692	0.5850 (n_{YN}=6.90)	0.0000	2.8421	0.5469 (n_{YN}=6.80)	0.0000
		max	5.3077	0.9124	0.0000	5.0737	0.8567	0.0000
	M	std	2.0501	1.6507	0.0000	1.9158	1.5477	0.0000
		ave	3.3308	2.7462 (n_{YN}=2.40)	0.0000	3.1141	2.5737 (n_{YN}=2.40)	0.0000
		max	5.8631	4.8377	0.0000	5.5032	4.5070	0.0000
	B	std	4.5906	1.0201	0.0000	4.1775	0.8824	0.0000
		ave	6.7796	1.8587 (n_{YN}=6.60)	0.0000	6.2603	1.6562 (n_{YN}=6.60)	0.0000
		max	13.1927	3.4608	0.0000	11.9915	3.0264	0.0000

3.3 Three colours

We created 120 different three colour patches using cyan, magenta and yellow. Hundred and twenty different coverages between 0% and 100% were randomly chosen for cyan, magenta and yellow, respectively. The colour channels were halftoned independently by a FM method and printed in 150 dpi and 300 dpi. Table III shows the colour difference between the measured and calculated colour values for these hundred and twenty patches using MD, YN and our proposed model. As can be seen our approach predicts the colour values much more accurately than MD model and a bit more accurately than YN.

Table II: The CIELab ΔE_{ab} and ΔE_{94} colour differences between measured and calculated two colour patches (cyan and magenta)

Two Colours CM		ΔE_{ab}			ΔE_{94}		
		MD	YN	Our approach	MD	YN	Our approach
150dpi	std	0.8776	0.9302	0.7835	0.8084	0.8589	0.7238
	ave	2.6913	2.2865 (n_{YN}=2.07)	1.3659	2.4690	2.0833 (n_{YN}=2.07)	1.2755
	max	4.4441	5.0025	3.7716	4.1827	4.6685	3.4814
300dpi	std	1.5299	1.4093	1.1637	1.3805	1.2568	1.0735
	ave	3.7703	3.2595 (n_{YN}=5.30)	1.9737	3.4372	2.9569 (n_{YN}=5.27)	1.8335
	max	7.2026	7.3331	5.4152	6.4057	6.4966	4.7948

It must be mentioned that in the case of 150 dpi all three models give their maximum colour difference at reference coverages c = 46%, m = 89%, y = 89%. For 300 dpi all three methods give the maximum at c = 53%, m = 55% and y = 95%. The expectation would be that the maximum colour difference occurs for the same set

of coverages for both 150 dpi and 300 dpi, which is not the case. For instance, in our approach ΔE_{ab} is 19.1679 for c = 46%, m = 89%, y = 89% at 150 dpi but for the same coverages ΔE_{ab} is 7.8295 at 300 dpi. The same big difference was noticed for MD and YN models. This indicates that error might have occurred when printing the patches or measuring them. These errors, however, could occur due to many reasons and are not possible to easily track or avoid, see next section.

Table III: The CIELabΔE_{ab} and ΔE_{94} colour differences between measured and calculated three colour patches (cyan, magenta and yellow)

Three Colours CMY		ΔE_{ab}			ΔE_{94}		
		MD	YN	Our approach	MD	YN	Our approach
150dpi	std	4.3668	4.0896	4.6990	4.2748	3.9913	4.5466
	ave	7.2950	6.0669 (n_{YN}=1.71)	5.9530	6.9476	5.7425 (n_{YN}=1.71)	5.6333
	max	20.1225	17.2756	19.1679	19.2404	16.6045	18.1809
300dpi	std	3.5818	2.9187	3.4492	3.4737	2.8835	3.3826
	ave	7.6264	5.4999 (n_{YN}=2.69)	5.2384	7.1912	5.2065 (n_{YN}=2.67)	4.9571
	max	20.9899	15.5084	15.7247	19.3766	14.5015	14.8894

4. Discussions and conclusions

Our experiments clearly show that using only one dot gain curve, even the best dot gain curve, doesn't provide a good approximation, even when only one colour is printed. In our approach we use three curves for each process colour, being obtained by CIEX, Y and Z. The experiment results clearly verify that our simple approach gives a much better approximation of the resulting colour values than MD and YN models for one and two colours. The prediction is slightly better than YN even when three colours are printed. It must also be noticed that YN model requires a lot of nonlinear optimizations to find the best *n*-factor and dot gain curve. In the case of three colours the best *n*-factor has to be found for seven colours, namely cyan, magenta, yellow, red, green, blue and black. The final *n*-factor that is used is the average of these seven *n*-factors, as discussed earlier. YN model is therefore very time consuming compared to our approach, which is very simple and fast and doesn't require any optimization. Notice also that in the YN model we need to measure the colour values for red, green, blue and black patches to find the best *n*-factor, but we only need the colour values for full-tone red, green, blue and black in MD and our approach. Another important point is that YN model doesn't really give a physical description of the *n*-factor and the best dot gain curve. Our approach, on the other hand, explains that different wavelength intervals have different impact on the effective dot gain and therefore should be taken into account in different ways.

The present paper also shows that more than one dot gain curve have to be used to characterize dot gain. It also provides a better understanding of optical dot gain and its wavelength dependency.

The results of our approach, though better than the other two, are not satisfying when three inks are involved. An average ΔE_{ab} around 5 when three colours are involved cannot be considered as a good approximation. However, the measurement errors that might occur shall not be disregarded. In our experiments we noticed that two exactly similar patches (even with only one colour), printed on the same sheet of paper, and sometimes next to each other, gave different measurement results. The ΔE_{ab} difference could sometimes be around 1.5. One of the reasons could be the fact that the paper structure is not homogenous, hence giving different measurement results. Another reason could be that the printer does not print homogeneously over the entire sheet. Therefore, due to circumstances, we believe an average ΔE_{ab} of around 2 when two colours are involved is a really good prediction made by our approach. Therefore, although ΔE_{ab} around 5 is not a good approximation, one should notice that parts of the colour differences between the predicted and measured stimuli could have been caused by the printer or measurement errors.

However, our current approach has to be modified to better predict the resulting colour coordinates. One idea is to use different curves in different cases. For instance, when all three colours are involved, probably the curves should be different from the case where only two colours were used. Another idea is to divide the visible

wavelength interval into more than three subintervals. For each subinterval one effective dot gain curve is then defined. This latter idea will most probably result in better approximations than the one discussed in this paper, but requires the spectral reflectance of printed patches and not only CIEXYZ values.

Acknowledgements

The financial support of Vinnova is gratefully acknowledged.

References

1. Demichel, M., 1924, *Proce'de', 26:* page 17-21, 26-27
2. Fairchild, M. D., 1997, *Color Appearance Models, ADDISON-WESLEY,* ISBN: 0-201-63464-3
3. Gerhardt, J., 2007, *Spectral Color Reproduction: Model Based and Vector Error Diffusion Approaches, PhD thesis signal et images, ENST, TSI, ENST,* page 209
4. Gooran, S., 2004, *Dependent Color Halftoning, Better Quality with Less Ink, Journal of Imaging Science & Technology, Vol. 48, Nr 4,* page 354-362
5. Hersch, R. D., Crété, F., 2005, *Improving the Yule-Nielsen modified spectral Neugebauer model by dot surface coverages depending on the ink superposition conditions, IS&T/SPIE Electronic Imaging Symposium, Conf. Imaging X: Processing, Hardcopy and Applications, SPIE* Vol. 5667, page 434-445
6. Murray, A., 1936, *Monochrome reproduction in photoengraving, J. Franklin Institute (Philadelphia),* Vol. 221, page 721
7. Neugebauer, H., 1937, *Die theoretischen grundlagen des mehrfarbendrucks, Zeitscrift fur wissenschaftliche Photographie,* page 73-89
8. Ruckdeschel, F. R., Hauser O. G., 1978, *Yule-Nielsen effect on printing: aphysical analysis. Appl Opt, 17,* page 3376 -3383
9. Wyble, D., Berns, R., 2000, *A Critical Review of Spectral Models Applied to Binary Color Printing, Journal of color research and application,* Volume 25, Number 1, page 4-19
10. Yule, J. A. C., Nielsen, W. J., 1951, *The penetration of light into paper and its effect on halftone reproductions. TAGA Proc 1951;* page 65-76

Predicting color of overprint solid

Robert Chung and Fred Hsu

Rochester Institute of Technology, Rochester, NY 14623, USA
E-mail: rycppr@rit.edu, cyhter@rit.edu

Abstract

Process color printing has three chromatic inks (C, M and Y). Colorimetric properties of the two-color overprint solids (R, G and B) are measured to determine the color gamut of the process ink set. Non-process colors, as defined by the Pantone Color Library, have more than a thousand ink formulations. There are too many possible two-color overprint solids to be measured. Colors of non-process color overprints are unknown until they are printed. While 'Overprint Fill' is available in Adobe Creative Suites that allows one spot color overprinting to the other, there is no color management solution to ensure that the overprint solids, as displayed, correctly matched that as printed. This paper describes a spectral-based solution based on paper, 1st ink, 2nd ink and a generalized ink trapping factor, t, using uni-tack inks, to predict color of overprint solid. Color differences between predicted and printed two-color overprint solids, resulted from wet-on-wet (offset) ink transfer are discussed.

Keyword: color, overprint, spectrophotometry, ink trapping

1. Introduction

In traditional process color printing, only four primaries, CMYK inks, are used. Colorimetric properties of two-color overprints are measured as a part of the color characterization task. These colorimetric measurements provide look-up tables for color display and color conversion in a color-managed workflow. There was no need to predict two-color overprints.

In spot color printing, the Pantone Color Library defines more than a thousand unique ink formulations. Today, "Overprint Fill" of any two spot colors is permitted in Adobe Creative Suites software. While spot color solid by itself is displayed accurately with the use of Pantone supplied look-up tables, display of spot color overprint is incorrect [Chung, Riordan & Prakhya, 2008]. No one knows what the color of the two-color overprint would look like until printed. In other words, the spot color management infrastructure is lacking in the current version of the Adobe Creative Suites software.

The key questions in this research are, "What is the color difference of overprint due to ink sequence change in wet-on-wet printing?" and "Can the color of the two-color overprint be predicted accurately with a spectral-based model?" By answering the first question, we identify a critical gap in current color management infrastructure. If we are able to devise a solution, it will enhance color communication of spot color applications between designers and printers.

2. Literature review

The term, overprint, means "image elements that are either solids or tints applied over a previously applied colorant or colorants" [CGATS.4, 2006]. In this research, the scope of overprint is limited to overprint solids only.

The relationship between color of the overprint, the first ink, and the second ink had been studied in the past. CGATS.4 documents a number of ink trap formulas, i.e., Brunner, Hamilton, and Preucil. These formulas are density-based and intended to express ink trapping (t) as a function of overprint (D_{op}), paper (D_0), first ink (D_1), and second ink (D_2). In other words, ink trapping (t) is calculated when all four of the quantities (D_0, D_1, D_2, and D_{op}) are known. Equation (1) depicts the Preucil trap formula [CGATS.4, 2006].

$$t = \frac{D_{op} - D_1}{D_2 - D_0} \tag{1}$$

To predict overprint color, Viggiano and Prakhya [2008] explored the use of a spectral-based model by adopting various ink trapping formulas (pp. 112-133). A fundamental obstacle in this pursuit is that there are two unknowns (t and D_{op}) in a single equation. The best they could do was to iterate ink trapping (t) until a minimum ΔE is calculated for a given ink-paper-printing condition.

Holub, Pearson and Kearsley [1986] reported the use of a reflectance-based spectral model to predict overprint colors (pp. 166-196). As shown in Eq. (2), spectral reflectance of the overprint at a given wavelength ($R_{op\lambda}$) is equal to the product of the reflectance of the first ink ($R_{1(\lambda)}$) and the second ink ($R_{2(\lambda)}$) at that wavelength. Upon testing and analyses, they concluded that the model did not perform well.

$$R_{op(\lambda)} = R_{1(\lambda)} \times R_{2(\lambda)} \tag{2}$$

In an earlier study, we found that ink trapping is a function of ink tack difference between the two inks, and gravimetric ink trapping, t, of uni-tack inks is 0.7 in wet-on-wet printing, and 1.0 in wet-on-dry printing [Chung, Hsu, Clark and Husain, 2009]. In other words, it may be possible to predict two-color overprint with a modification of Eq. (2) if we constrain the two overprinting inks with the same ink tack. If and when ink trapping of uni-tack inks converges to a constant, we will be able to predict overprint color because there is only one unknown, i.e., overprint, left in Eq. (1).

3. Methodology

This research has the following objectives: (1) conduct press runs using two inks in two sequences to find out the color difference of overprint due to ink sequence change in wet-on-wet printing; (2) develop the spectral-based overprint model by modifying the Holub equation with all variables in the Preucil equation; (3) test the performance of the spectral-based model by conducting offset press runs to simulate wet-on-wet ink transfer using inks with the same tack and in different ink sequences; and (4) test the performance of the spectral-based model by conducting digital printing to simulate dry-on-dry ink transfer.

3.1 Developing spectral-based overprint model

To begin with, we can re-write Eq. (2) by substituting $R_{2(\lambda)}$ in density term and including the ink trapping value (t) as a multiplier or factor to account for ink trapping of the second ink, as shown in Eq. (3). In order to solve for the reflectance of the overprint, all quantities, including the ink trapping (t), to the right of the equal sign, must be known.

$$R_{op(\lambda)} = R_{1(\lambda)} \times 10^{-D_{2(\lambda)} \times t} \tag{3}$$

The influence of paper in the spectral measurement of Ink 2, $D_{2(\lambda)}$, should be subtracted because the paper factor is already accounted for by the spectral measurement of Ink 1. Thus, Eq. (4) represents the spectral model that accounts for the influence of both trapping and paper substrate.

$$R_{op(\lambda)} = R_{1(\lambda)} \times 10^{-[D_{2(\lambda)} - D_{0(\lambda)}] \times t} \tag{4}$$

We can re-write all density variables in Eq. (4) in terms of reflectance, as shown in Eq. (5). Expressing overprint in spectral reflectance is necessary for CIELAB computation by means of tristimulus integration. Note that Eq. (5) is the same as Eq. (2) when both R_0 and t are equal to 1.

$$R_{op(\lambda)} = R_{1(\lambda)} \times 10^{-\log\left(\frac{R_{0(\lambda)}}{R_{2(\lambda)}}\right) \times t} \tag{5}$$

A Microsoft Excel spread sheet was devised to perform the following computational tasks: (a) accept spectral reflectance data for paper, ink 1, ink 2, and overprint solid; (b) compute the overprint spectra for a number of ink trapping values using Eq. (5); (c) perform tristimulus integration of these overprint spectra; and (d) compute ΔE_{ab} between predicted overprint color and the printed overprint.

3.2 Testing spectral-based overprint model

To test the performance of the spectral-model in predicting overprint color, a step-by-step procedure is shown below:

a. Collect overprint samples from spot color press runs. The Heidelberg Speedmaster sheet-fed offset press run represents wet-on-wet ink transfer using uni-tack inks.
b. Measure spectral reflectance values of paper, first- ink solid, second- ink solid, and their overprint. The measured overprint color is the reference.
c. Predict the spectral reflectance curve of the overprint by means of Eq. (5) and compute its CIELAB value (D50, 2° observer). The predicted overprint color is the sample.
d. Compare the color difference between the sample and the reference.
e. The HP Indigo 5500 digital press run represents dry-on-dry ink transfer.

4. Results and discussion

The prediction of the color of overprint solid requires that spectral characteristics of the paper, the two inks, ink sequence, and ink trapping be known. In wet-on-wet ink transfer, ink trapping can be approximated if uni-tack inks are used [Chung, Hsu, Clark and Husain, 2009]. In dry-on-dry ink transfer, ink trapping approaches unity. This section describes specific findings from the experiment.

4.1 Color difference of overprint due to ink sequence change

By changing the ink sequence of the two spot color inks in the Heidelberg Speedmaster 74 (SM74) sheet-fed offset press run, the color difference between the two spot color overprints, as shown in Table I, is very different (22.8 ΔE). This points out the influence of ink sequence on the overprint color in wet-on-wet ink transfer. This finding also confirms the fact that pre-media display of overprint color is incorrect due to the lack of an overprint prediction model.

Table I: Color difference due to ink sequence change in offset printing

Uni-tack 11	SM74_1788 (1st)			SM74_7466 (1st)			ΔE
	L*	a*	b*	L*	a*	b*	
Paper	95.5	1.9	-7.4	95.7	1.8	-7.5	0.2
PMS 1788	54.4	71.8	40.7	54.7	70.5	38.0	3.1
PMS 7466	64.1	-51.7	-23.7	64.8	-51.0	-23.6	0.9
Overprint	27.0	28.8	0.2	32.2	10.5	-12.2	**22.8**

4.2 Overprint solid prediction in wet-on-wet ink transfer

This section summarizes results of overprint prediction based on wet-on-wet ink transfer using the Heidelberg Speedmaster 74 (SM74) sheet-fed offset press. Two inks of the same tack (Tack 11) were printed in two ink sequences. Figure 1 shows the spectral reflectance curves (SRCs) of the paper (in gray), first-down ink (Pantone 1788), and second-down ink (Pantone 7466) and the overprint color (in black).

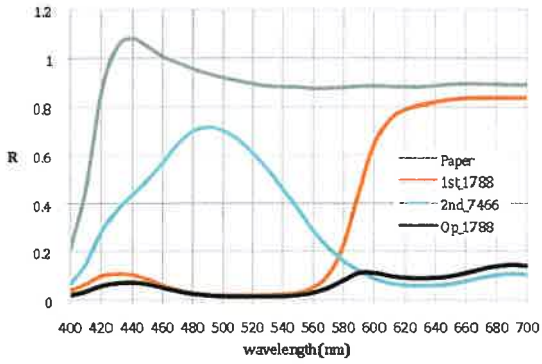

Figure 1:
SRCs of paper, Pantone 1788 (1st), Pantone 7466 (2nd), and overprint color

Figure 2 shows SRCs of the predicted spot color overprints with a range of ink trapping, t, from 0.7 to 1 with an increment of 0.1. Color differences (ΔE) between predicted overprint colors and the actual overprint color are also shown. As the ink trapping (t) assumes a larger value, i.e., more transfer of the second-down ink on top of the first-down ink, the overall reflectance of SRCs decreases (indicated by the dash arrow).

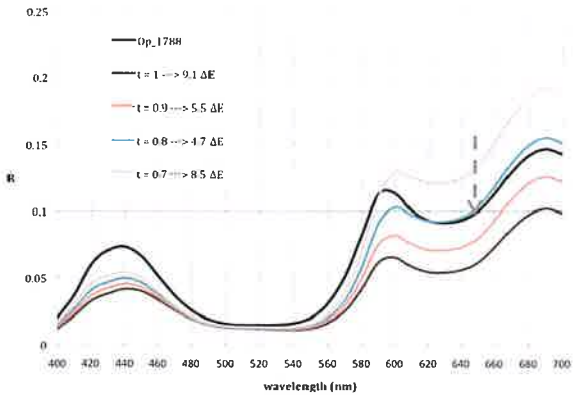

Figure 2:
Spectral prediction and color difference of SM_1788 (1st ink) overprint

Figure 3 compares predicted overprint colors with the reference print in a*b* diagram. We can see that as ink trapping assumes a larger value, the hue of predicted overprint shifts toward the chromaticity of the second-down ink (indicated by the dash arrow). It is also true that by decreasing the ink trapping (t), the L* increases and the hue of the overprint shifts toward the chromaticity of the first-down ink. While the color difference between the actual and predicted color with ink trapping value of 1.0 is 9.1, the best color match between the predicted and the actual overprint color is 4.7 ΔE at the ink trapping (t) of 0.8.

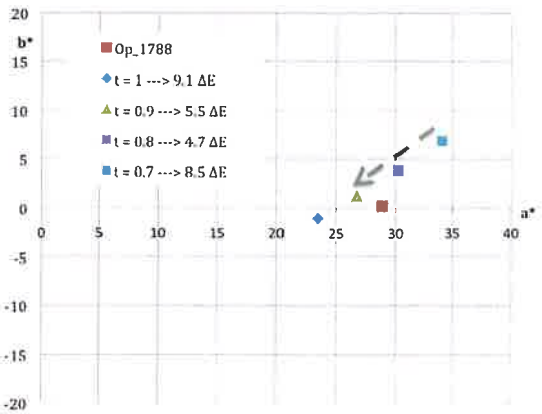

Figure 3:
Predicted vs. the actual spot color overprint by offset (1788 as 1st ink)

Figure 4 shows SRCs of the predicted spot color overprints with a range of ink trapping, t, from 0.6 to 1 with an increment of 0.1. Color differences (ΔE) between predicted overprint colors and the reference are also shown. In this case, as ink trapping (t) assumes a smaller value, overall reflectance of the SRC increases; so is the higher reflectance value of the overprint in the spectral region where the second-down ink absorbs.

As shown in Figure 5, the hue of the overprint is quite off when ink trapping is 1. As ink trapping assumes a smaller value, differences in hue, chroma, and lightness are all decreased. While the color difference between the actual and predicted color with ink trapping value of 1.0 is 19.9, the best color match between the predicted and the actual overprint color is 3 ΔE at the ink trapping (t) of 0.6.

Regarding two-color overprints in two ink sequences using uni-tack inks by offset printing, we conclude that colorimetric aim point of the overprint depends on the ink sequence. The ink trapping (t) in the spectral model alters lightness, hue, and chroma of the overprint color. As the ink trapping decreases, the hue of the overprint solid bears more influence of the hue of the first-down ink with lighter tonality.

Table II summarizes how the spectral model predicts the overprint color in wet-on-wet printing using uni-tack inks. The color difference is minimized, i.e., about 6 ΔE, when the ink tack is between 0.6 and 0.8.

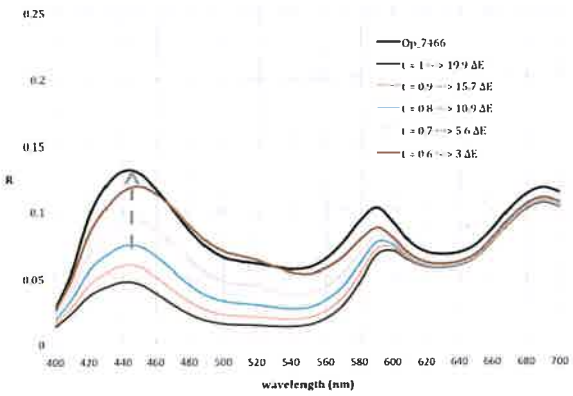

Figure 4:
Spectral prediction and color difference of SM_7466 (1st ink) overprint

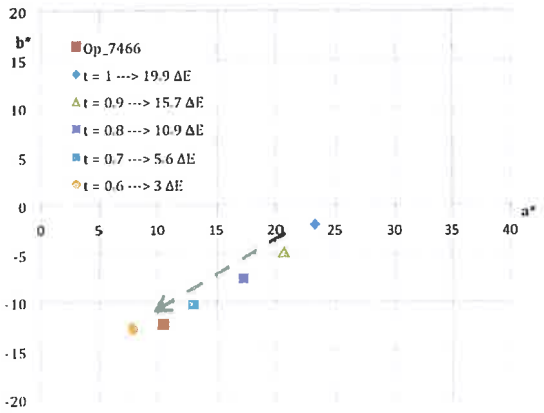

Figure 5:
Predicted vs. the actual spot color overprint by offset (7466 as 1st ink)

Table II: Effect of ink trapping on color difference in wet-on-wet printing

SM74	t	ΔE	SM74	t	ΔE
PMS 1788 (1st) Tack 11	1.0	9.1	PMS 7466 (1st) Tack 11	1.0	19.9
	0.9	5.5		0.9	15.7
	0.8	**4.7**		0.8	10.9
	0.7	8.5		0.7	5.6
	0.6	14.1		**0.6**	**3.0**

The same was concluded when we replicated the printing experiment using tack 14 inks. This finding is in reasonable agreement with the gravimetric ink trapping average of 0.7, as reported in a previous study [Chung, Hsu, Clark and Husain, 2009]. In other words, by providing two input conditions, i.e., wet-on-wet printing and ink sequence, the spectral-model with an ink trap constant of 0.7 serves as a first-order approximation of overprint color in pre-media software.

4.3 Overprint solid prediction in dry-on-dry ink transfer

This section summarizes results of the overprint prediction based on dry-on-dry ink transfer using the HP Indigo 5500 digital press. Two Pantone colors were printed in two ink sequences. As shown in Table III, the color difference (5.5 ΔE) due to ink sequence is quite small in comparison to wet-on-wet printing (22.8 ΔE).

Table III: Effect of ink sequence on overprint color difference in dry-on-dry printing

Dry-on-Dry	HP_1788 (1st)			HP_7466 (1st)			ΔE
	L*	a*	b*	L*	a*	b*	
Paper	94.1	2.2	-7.7	94.3	2.4	-7.6	0.3
PMS 1788	50.7	70.5	43.2	62.6	-50.3	-26.3	3.3
PMS 7466	62.5	-50.3	-26.3	50.6	71.4	46.3	0.1
Overprint	20.5	16.2	-0.5	22.2	17.0	4.6	**5.5**

By definition, the gravimetric ink trapping of dry-on-dry ink transfer is one. By specifying dry-on-dry printing, the spectral-model with an ink trap constant of one will do a good job to approximate the overprint color in either ink sequence with a color difference, as shown in Table IV, of less than 6 ΔE.

Table IV: Effect of ink trapping on color difference in dry-on-dry print

HP	t	ΔE	HP	t	ΔE
PMS 1788 (1st)	**1.0**	**3.4**	PMS 7466 (1st)	**1.0**	**5.4**
	0.9	6.5		0.9	5.4
	0.8	11.3		0.8	9.2
	0.7	16.9		0.7	14.9
	0.6	23.2		0.6	21.6

5. Conclusions and further research

A technology gap of current pre-media software is its inability to predict spot color overprint. While current pre-media software has no solution in predicting spot color overprint solid, this research shows that it is feasible to predict the color of the overprint solid by means of a spectral model and ink sequence to account for color characteristics of the ink, paper, and how the two inks interact during printing.

To implement the overprint prediction feature, consumable suppliers should standardize spectral characteristics of paper and inks. Inks of the same tack should be used to increase the prediction accuracy. Pre-media software needs to include the printing process and ink sequence as part of the 'advanced' output preview preferences. Ink sequence is required in wet-on-wet printing, e.g., offset printing, and a trap value of 0.7 is used to compute the overprint color. If dry-on-dry (electro-photographic) or wet-on-dry (conventional printing using inter-drying station) printing applies, ink sequence is not required and a trap value of 1.0 is used to compute the overprint color.

The spot color overprint solution, discussed in the paper, should be considered as a first approximation. To further improve the prediction of overprint color, additional spectral-based corrections may include first-surface reflection and ink transparency. Once two-color overprint solids can be predicted with higher accuracy, the next step is to predict the color of any tint combination of two spot colors.

Acknowledgments

This has been a journey of discovery and problem solving with regard to the prediction of overprint color in wet-on-wet printing. While the solution is still in the making, the authors wish to recognize their colleagues (Michael Riordan and Daniel Clark) as well as their students (Sri Prakhya and Khalid Husain) who had collaborated with them on the subject in previous publications.

References

1. ANSI CGATS.4, 2006 Graphic technology - Graphic arts reflection densitometry measurements - Terminology, equations, image elements and procedures
2. Chung, R., Hsu, F., (2008) A Study of Ink Trapping and Ink Trapping Ratio, *Test Targets 8.0*, pp. 33-39. May be retrieved at http://cias.rit.edu/~gravure//tt/index.html
3. Chung, R., Hsu, F., Clark, Husain, K., (2009) Weight-based Ink Trapping Assessment, *2009 TAGA Proceedings* (in press)
4. Chung, R., Riordan, M., Prakhya, S., (2008) Predictability of Spot Color Overprints. *Advances in Printing and Media Technology*, Vol. XXXV, pp. 373-380
5. Holub, R., Pearson, C., Kearsley, W., (1986) Spectral Measurement of Overprints on Press Sheets and Proofs, *1986 TAGA Proceedings*, pp. 166-196
6. Viggiano, J. A., Prakhya, S., (2008) Prediction of Overprint Spectra Using Trapping Models: A Feasibility Study, *Rochester Institute of Technology TAGA 2008*. Rochester, NY: 2008 TAGA Student Chapter

Colour prediction model on basis of the wavelength dependent area coverage including the scattering of light and optical brightener

Michael Dattner, Heinz Mantler, Jorge Rodriguez-Giles, Peter Urban

Bergische Universität Wuppertal
Rainer Gruenter Straße 21, D-42119 Wuppertal, Germany
E-mails: MDattner@uni-wuppertal.de, mantler@uni-wuppertal.de, rodrigez@uni-wuppertal.de, PUrban@uni-wuppertal.de

Abstract

We propose an application oriented colour prediction model for offset, which considers the effects of light scattering and optical brightener on the perception of printed colour. This model considers all underlying physical phenomena nearly without empirical parameters. It is based on the new developed wavelengths-dependent-area-coverage approach, which considers every current process specific parameter by considering the complete spectral information in an extended area coverage approach. This effective wavelengths-dependent-area-coverage (*wda-coverage*) is directly related to the constant nominal area coverage and allows the calculation of excellent spectral predictions for colour halftone prints. Optical brightener and the super positioning of inks are considered in the calculation of the reproducible colour space.

Keywords: offset, spectral colour prediction model, light scattering, wavelength dependent area coverage, brightener

1. Introduction

While plenty of models describe the autotypic printing process, the consideration of light scattering effects is attended by multiple and often empirical parameters. These parameters are difficult to estimate or associated with a high generation effort. In order to simplify these approaches and to consider all relevant printing process parameters in parallel, the *wda-coverage* with only one empirical parameter will be introduced. Typically, only a single value is in use as area coverage in existing colour prediction models, hence no spectral information is considered in this parameter. The new vectorial, wavelength dependent area coverage comprehends for every single wavelength an individual effective area coverage. Therefore, the whole spectral information is considered in the proposed *wda-coverage* approach for colour prediction. The well-defined relation to the nominal area coverage enables a straight forward calculation and keeps the model practicable and physically founded.

2. Existing approaches to spectral colour prediction

Colours reproduced by halftone prints are perceived as a combination of subtractive and additive colour mixing processes. In this context, the Murray Davis model and the Kubelka Munk model are two substantial theories for several colour prediction approaches.

2.1 Murray Davis

The most popular prediction model of monochrome halftone prints is the Murray Davis model, which is a direct application of the additive colour mixing theory [Murray, 1936]. The estimated spectral reflectance $\beta_a(\lambda)$ of a printed monochrome halftone is given by the weighted sum of the respective reflectances. Smooth inked areas and an ideal and smooth substrate are presumed in the Murray Davis model. Under these assumptions, the predicting equation can be considered as a linear interpolation between the substrate reflectance $\beta_{pw}(\lambda)$ and the reflectance of the printed full tone patch $\beta_{100\%}(\lambda)$. Equation 1 shows this interpolation formula concerning the nominal area coverage a.

$$\beta_a(\lambda) = a \cdot \beta_{100\%}(\lambda) + (1-a) \cdot \beta_{pw}(\lambda) \tag{1}$$

Given a statistical independent halftone colour dot placement, the corresponding area coverage factors are calculated by applying DEMICHEL's equation [Demichel, 1924] (equation 2)

$$
\begin{aligned}
f_{pw} &= (1-A_c)\cdot(1-A_m)\cdot(1-A_y),\\
f_c &= A_c\cdot(1-A_m)\cdot(1-A_y),\\
f_m &= (1-A_c)\cdot A_m\cdot(1-A_y),\\
f_y &= (1-A_c)\cdot(1-A_m)\cdot A_y,\\
f_r &= (1-A_c)\cdot A_m\cdot A_y,\\
f_g &= A_c\cdot(1-A_m)\cdot A_y,\\
f_b &= A_c\cdot A_m\cdot(1-A_y) \quad \text{and}\\
f_k &= A_c\cdot A_m\cdot A_y
\end{aligned}
\tag{2}
$$

with A_c, A_m and A_y as the area coverage for cyan, magenta and yellow respectively.

According to this statistical colour dot placement, the reflectance of a composed colour is estimated by the sum of all included full tone reflectances weighted by their area coverage in the NEUGEBAUER equation [Neugebauer, 1937] (equation 3):

$$\beta_{cmy}(\lambda) = \sum_{i\in\Psi} f_i\cdot\beta_i(\lambda) \tag{3}$$

with $\Psi = \{pw, c, m, y, r, g, b, k\}$ and f_i the respective fractional areas of the full tone reflectances $\beta_i(\lambda)$ for substrate, cyan, magenta, yellow, red (superposition of magenta and yellow), green (superposition of yellow and cyan), blue (superposition of magenta and cyan) and black (superposition of cyan, magenta and yellow) shown in equation 2.

Current offset printing cannot be sufficiently described by the NEUGEBAUER equation, because actual printed dots are less perfect than in the model presumed and the effects of interaction of light with dots and substrate are not considered, so far. In this context, the YULE NIELSEN correction is proposed for substrates with a large light diffusion length. In order to improve fits of experimental data, YULE NIELSEN introduced an adjustment parameter n, as an exponent in the NEUGEBAUER equation [Yule, 1951] (equation 4).

$$\beta_{cmy}(\lambda) = \left(\sum_{i\in\Psi} f_i\cdot\beta_i(\lambda)^{1/n}\right)^n \tag{4}$$

This adjustment leads to improvements, but it is only of empirical quality.

A further correction, which shows a progressively more thorough consideration of the halftone printing process, is the CLAPPER YULE approach. It includes the analytical analysis of multiple scattering, internal reflection and ink transmission by estimating the total reflected radiation as a sum of radiation fractions that emerge back from the chart [Clapper, 1953].

The spectral reflectance model of HERSCH enhances this CLAPPER YULE model by taking into account the fact that proportionally more incident light through a given colorant surface is reflected back onto the same colorant surface than onto other colorant surfaces. This model combined with a model that takes ink spreading into account, includes additional nominal-to-effective surface coverage functions for each of the different ink superposition conditions. In order to predict the reflectance spectrum of prints, HERSCH et al. use a spectral prediction model in which each ink is characterised by its spectral transmittance. For the model calibration measurements of 44 patches are required in case of the super positioning of cyan, magenta and yellow. This model fits the effective area coverage when printed alone or in combination with other inks (physical dot gain, ink spreading) and predicts reflectances. All internal spectra are calculated from measured reflectances, according to the model. Therefore, the model reflects at least to a certain extent the underlying physical phenomena [Hersch, 2004 and 2007].

Furthermore, optical brighteners are considered for inkjet prints in this kind of colour prediction model, which requires additional measurements [Hersch, 2008]. This model is state of the art if the CLAPPER YULE model and ink spreading functions are used as the initial point of a model.

2.2 Kubelka Munk

In contrast to MURRAY DAVIS, the KUBELKA MUNK theory describes the reflection and transmission characteristics of opaque and transparent - but infinitely wide - layers [Kubelka, 1954]. The concept is shown in the simplified figure of two diffuse light fluxes through the layer, one proceeding downward and the other simultaneously upward (i(x), i(x+dx) and j(x), j(x+dx) respectively in figure I).

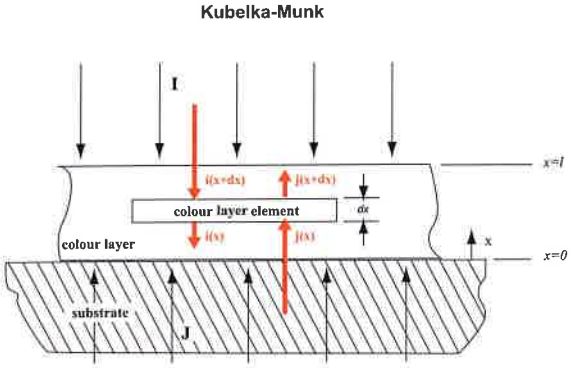

Figure I:
Kubelka Munk: Two light fluxes through a colour layer

The formulas that describe these two light fluxes concerning the infinitesimal thin colour layer element are shown in equation 5

$$\begin{aligned} i(x) &= i(x+dx) - (s+k)\cdot i(x+dx)\cdot dx + s\cdot j(x)\cdot dx \\ j(x+dx) &= j(x) - (s+k)\cdot j(x)\cdot dx + s\cdot i(x+dx)\cdot dx \end{aligned} \tag{5}$$

with s as the scattering coefficient and k as the absorption coefficient of the colour layer.

The LAMBERT BEER's law describes the same causal interrelation for ideal, non-scattering transparent layers (scattering coefficient $s = 0$) on substrate and can be written with reflectances instead of light fluxes (equation 6)

$$\frac{\beta_2(\lambda)}{\beta_1(\lambda)} = e^{-2k\delta} \tag{6}$$

with $\beta_1(\lambda)$ and $\beta_2(\lambda)$ reflectances of two individual printed layers of the same ink but different thickness, δ as the difference between the layer thicknesses and k as the common absorption coefficient of the single ink [Beer, 1852]. This correlation posted to autotypic printing dots has a main relevance for the *wda-coverage* model consolidation in chapter 3.3.

2.3 The initial model

Beside a couple of models, which describe the autotypic print process including the light scattering effects, the printed-dot-border model of PAUL gains also very convincing results. It considers next to an ideal centre of a printed dot, an additional brighter dot border to describe the dot gain appearances at the edgings of the printed elements. This dot border consists of the same ink but has a lower ink film thickness [Paul, 1994] (figure VII, down to the left). According to MURRAY DAVIS (c.f. equation 1) for monochrome halftone prints, equation 8 shows the extensions of PAUL

$$\beta_a(\lambda) = a_1\cdot\beta_1(\lambda) + a_2\cdot\beta_2(\lambda) + (1-(a_1+a_2))\cdot\beta_{pm}(\lambda) \tag{7}$$

with the nominal area coverage a and the related area coverage fractions a_1 and a_2 for the dot centre and the dot border respectively. $\beta_1(\lambda)$ and $\beta_2(\lambda)$ are, similar to equation 6, reflectances of two layers of the same ink but different thickness.

Unfortunately, PAUL's model does not allow a well-defined interrelation between model parameters and the effective area coverage. Furthermore, microdensitometer measurements are required to achieve the density of the centre and the border of printed dots on several patches with the known extra effort.

3. The new and application oriented colour prediction model for offset

The *wda-coverage* model, as an extension to the MURRAY DAVIS theory for monochromatic printing and an implementation of the KUBELKA MUNK theory, will be introduced after a specification of the effective area coverage, in this chapter. The corresponding model consolidation, the introduction of a brightener factor and the final extension to the modulation of the super positioning of several inks on substrate will also be presented.

3.1 Optical effective area coverage

In the context of area coverage, it is important to distinguish between the nominal or geometrical coverage and the optical effective coverage. One approach to evaluate the effective coverage is for example publicized in the ISO 12647-1, where chromaticity values are in use. Another approach is based on MURRAY DAVIS, where - due to the required density measurements - the wavelengths around the main absorption of the inks (figure II left) are considered [DIN 16536 - 2].

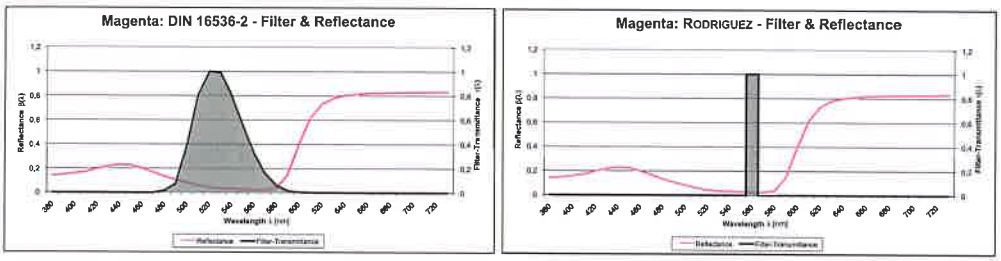

Figure II: Relevant filter transmittance around the main absorption for the calculation of the effective area coverage for magenta on basis of DIN 16536 – 2 (left) and RODRIGUEZ (right)

An adaptation of DIN 16536 - 2 considers only a single wavelength band at the main absorption of used inks for the calculation of the effective area coverage A_{eff} as shown in equation 8

$$A_{eff} = \frac{\beta_{pw}(\lambda_r) - \beta_a(\lambda_r)}{\beta_{pw}(\lambda_r) - \beta_{100\%}(\lambda_r)} \tag{8}$$

with the relevant wavelength λ_r at 635nm, 555nm and 425nm for typical offset inks cyan, magenta and yellow respectively [Rodriguez, 2006] (figure II right). Hence, $\beta_a(\lambda_r)$ is e.g. the reflectance value measured on a test patch with the nominal area coverage a at the corresponding wavelength λ_r. Exactly this effective area coverage A_{eff} according to RODRIGUEZ is the starting point for the development of the *wda-coverage* model.

3.2 Wavelength dependent area coverage

While PAUL uses microscopic measurements, the *wda-coverage* model has a macroscopic approach: The whole information of spectral measurements is considered to describe all process influences, including machine, ink and substrate specific parameters. All process parameters of a monochrome printing are included in the *wda-coverage* without any empirical parameters. Furthermore, the *wda-coverage* is directly related to the corresponding nominal area coverage.

The mentioned *wda-coverage* is based on a vectorial A_{eff}, which components have to be calculated individually for each wavelength λ. Thus, the single wavelength band, considered in RODRIGUEZ's approach, is not just extended to the remaining wavelengths to calculate a single value. It is utilised to calculate for every single wavelength band an individual $A_{eff,i}$ (figure III) which is directly related to the corresponding wavelength and can be written as $A_{eff}(\lambda)$.

Measurements of a full tone patch $\beta_{100\%}(\lambda)$, of a halftone patch $\beta_a(\lambda)$ with nominal area coverage a as well as of uncovered substrate $\beta_{pw}(\lambda)$ are required for calculating this $A_{eff}(\lambda)$ (equation 9).

$$A_{eff}(\lambda) = \frac{\beta_{pw}(\lambda) - \beta_a(\lambda)}{\beta_{pw}(\lambda) - \beta_{100\%}(\lambda)} \qquad \text{for all } \lambda \in [380\text{nm}, 730\text{nm}] \tag{9}$$

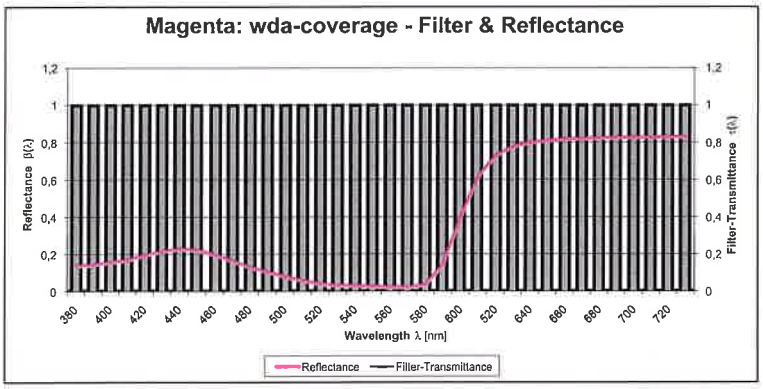

Figure III: Relevant filter transmittance over the whole spectrum for the calculation of the effective area coverage for magenta on basis of the wda-coverage approach

Figure IV shows the main characteristic spectral appearances of the *wda-coverage* $A_{50\%}(\lambda)$ related to the nominal 50% area coverage. This characteristic course of the funktion appears similarly but attenuated at the remaining courses while tending to full tone or unprinted substrate respectively.

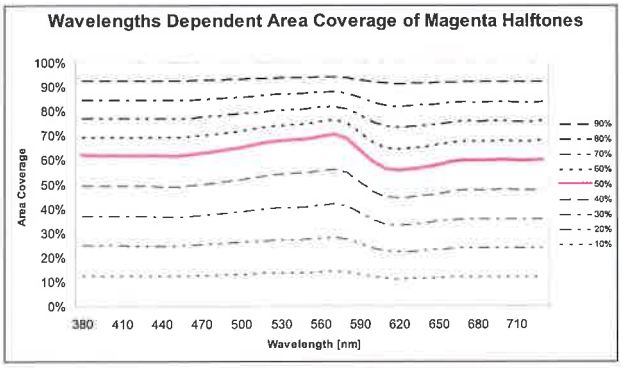

Figure IV: The effective wavelength dependent area coverage referring to the corresponding nominal area coverage shown in the legend

This strong interrelation between any effective area coverage and this *wda-coverage* $A_{50\%}(\lambda)$ enables the inclusion of spectral information in a improved colour prediction model based on the classical additive colour mixing approach.

For the calculation of the *wda-coverage* $A_a(\lambda)$ concerning any desired nominal area coverage a, the characteristic *wda-coverage* $A_{50\%}(\lambda)$ has to be calculated in advance (equation 10: directly linked to equation 9).

$$A_{50\%}(\lambda) = \frac{\beta_{pw}(\lambda) - \beta_{50\%}(\lambda)}{\beta_{pw}(\lambda) - \beta_{100\%}(\lambda)} \qquad \text{for all } \lambda \in [380\text{ nm}, 730\text{ nm}] \qquad (10)$$

By using only two more measurements of nominal 30% and 80% patches, the fit of the calculation of the *wda-coverage* $A_a(\lambda)$ concerning any desired nominal area coverage a becomes very accurate (figure V) with equation 11.

$$A_a(\lambda) = Z(a) \cdot A_{50\%}(\lambda) \qquad (11)$$

$Z(a)$ is the only weighting factor and depends on $|a - 50\%|$ to consider the attenuation of the characteristic $A_{50\%}(\lambda)$-course at any nominal area coverage.

The profound improvement of this approach is the concrete measurability and the explicit allocation of the *wda-coverage* to the process specific parameters (figure VI, top left and top right).

It is a very practical possibility to predict $A_a(\lambda)$ and subsequent the requested spectral reflectance $\beta_a(\lambda)$ for any desired nominal area coverage a on basis of $A_{\dots}(\lambda)$, $\beta_{\dots}(\lambda)$ and $\beta_{\dots}(\lambda)$ with $Z(a)$ as the only weighting factor.

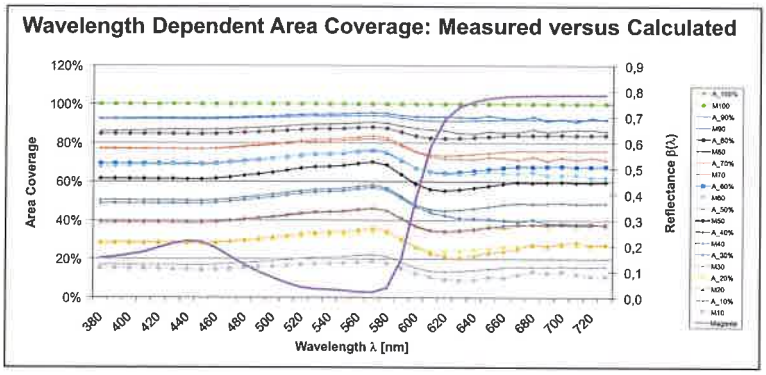

Figure V: wda-coverage: calculated values shown next to measured values; differences at wavelengths λ > 600nm are negligible because magenta is nearly transparent at these wavelengths

3.3 Consolidation

For the consolidation, the initial model (figure VI, down to the left) will be mathematically transformed to a formula, in which the constant nominal area coverage a_1 is not complemented by an additional area coverage a_2 for border appearances to estimate the corresponding spectral reflectance $\beta_a(\lambda)$. These constant nominal area coverages a_1 and a_2 will be transformed into the introduced *wda-coverage* $A_a(\lambda)$ and extended to any number of printed-sub-dot-areas with respective ink film thicknesses (figure VII, down to the right).

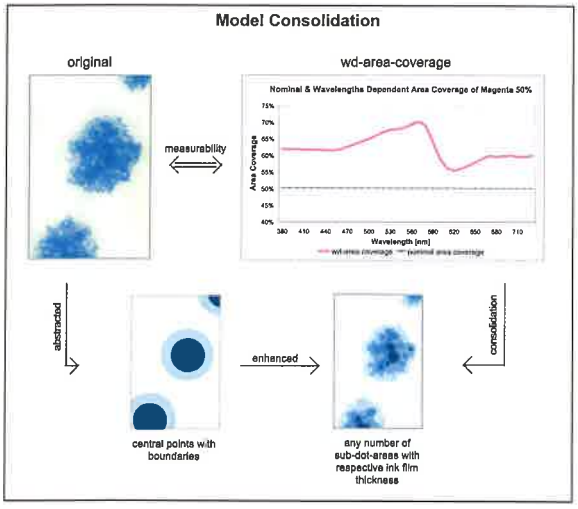

Figure VI: Model consolidation and interrelations

The concrete consolidation of the *wda-coverage* model to PAUL's one is shown in the equations 12 - 15. It considers, as mentioned at equation 7, a_1 and a_2 as the theoretical area coverage of the central point and the boundary respectively, $\beta_{pw}(\lambda)$ and $\beta_1(\lambda)$ as the spectral reflectance of substrate and a full tone patch respectively and finally $\beta_2(\lambda)$, which stands for the reflectance of the brighter dot border. This border is characterised by the same ink but a lower ink film thickness.

Consequently, $\beta_2(\lambda)$ can be written in dependency of $\beta_1(\lambda)$ as $\beta_2(\lambda) = \beta_1(\lambda)\, e^{-2k\delta}$ with δ considering the lower ink film thickness of the dot border and k as the common absorption coefficient according to LAMBERT BEER' law (equations of EQ 12 and c.f. equation 6).

$$\begin{aligned}\beta_a(\lambda) &= a_1 \cdot \beta_1(\lambda) + a_2 \cdot \beta_2(\lambda) + (1-(a_1+a_2)) \cdot \beta_{pw}(\lambda) \\ &= a_1 \cdot \beta_1(\lambda) + a_2 \cdot \beta_1(\lambda) \cdot e^{-2k\delta} + \left(1-\left(a_1 + a_2 \cdot e^{-2k\delta}\right)\right) \cdot \beta_{pw}(\lambda)\end{aligned} \tag{12}$$

Combining all coefficients of $\beta_1(\lambda)$ in equation 12 leads to equation 13:

$$\beta_a(\lambda) = \left(a_1 + a_2 \cdot e^{-2k\delta}\right) \cdot \beta_1(\lambda) + \left(1-\left(a_1 + a_2 \cdot e^{-2k\delta}\right)\right) \cdot \beta_{pw}(\lambda) \tag{13}$$

setting $A_a(\lambda) := a_1 + a_2 \cdot e^{-2k\delta}$ (the *wda-coverage*) leads finally to

$$\beta_a(\lambda) = A_a(\lambda) \cdot \beta_1(\lambda) + (1 - A_a(\lambda)) \cdot \beta_0(\lambda) \tag{14}$$

which again refers directly to MURRAY DAVIS model (c.f. equation 1) and describes the wavelength dependency of $A_a(\lambda)$, due to the wavelength dependent absorption coefficient k.

The final step of this consolidation is the mathematical extension of $A_a(\lambda)$ to any number m of printed-sub-dot-areas with the corresponding ink film thickness (equations in EQ 15 & figure VI, down to the right):

$$\begin{aligned}
\beta_a(\lambda) &= \sum_{i=1}^{m} a_i \cdot \beta_i(\lambda) + (1 - \sum_{i=1}^{m} a_i) \cdot \beta_{pw} \\
&= \sum_{i=1}^{m} a_i \cdot \beta_1(\lambda) \cdot e^{-2k \cdot \delta_i} + \left(1 - \left(\sum_{i=1}^{m} a_i \cdot e^{-2k \cdot \delta_i}\right)\right) \cdot \beta_{pw} \\
&= \left(\sum_{i=1}^{m} a_i \cdot e^{-2k \cdot \delta_i}\right) \cdot \beta_1(\lambda) + \left(1 - \left(\sum_{i=1}^{m} a_i \cdot e^{-2k \cdot \delta_i}\right)\right) \cdot \beta_{pw} \\
&= A_a(\lambda) \cdot \beta_1(\lambda) + (1 - A_a(\lambda)) \cdot \beta_{pw}(\lambda)
\end{aligned} \tag{15}$$

Please notice that these more general formulas show the validation of cases shown in figure VI, down to the right. Mainly, the equations of EQ 14 & 15 teach us the significance of the *wda-coverage*. The improvement of this approach is the concrete measurability and the explicit allocation of the *wda-coverage* to all process specific parameters with the very practical way to predict the spectral reflectance for any desired nominal area coverage on basis of three measurements and one weighting factor.

4. Brightener

The *wda-coverage* model on the shown level leads to excellent results if the focus is solely on substrates without brighteners or measurements with UVcut-filter. However, to describe printings on commonly-used brightened substrates, the calculation of halftone spectral reflectance $\beta_a^{oB}(\lambda)$ considering the consequences of the interaction of light, ink dots and substrate with optical brightener is introduced in equation 16

$$\beta_a^{oB}(\lambda) = B(\lambda) \cdot \beta_a(\lambda) \tag{16}$$

with $B(\lambda) = 1 + [\beta_0(\lambda) - \beta_0^{UV}(\lambda)]$ as the wavelength dependent brightener factor. Only the used substrate has to be measured once again without UVcut-filter to get the unfiltered spectral reflectance $\beta_0^{UV}(\lambda)$, which is essential to calculate this brightener factor. Figure VII shows the quality of computed values contrasted to the reflectance measured without UVcut-filter of offset printings concerning offset halftoning with magenta on brightened substrate:

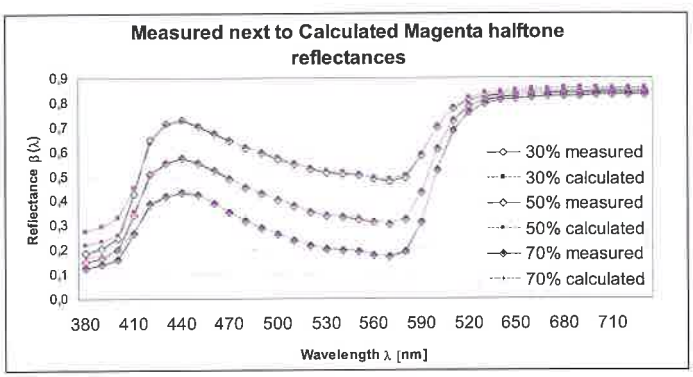

Figure VII:
Measured magenta halftone reflectances shown next to the calculated reflectances using the wd-area-coverage & brightener model

The small maximum prediction error of 0.6 ΔE units that appears in case of calculating the reflectance of monochrome halftones (e.g. at 30% nominal area coverage with magenta), attests that the complete colour prediction model is not endangered.

5. Super positioning model

So far, the presentation of the *wda-coverage & brightener* model refers solely to monochrome halftoning based on the MURRAY DAVIS THEORY and KUBELKA MUNK theory. In order to modulate the super positioning of several inks on brightened substrate, all parameters of the ink transfer onto already covered areas (figure VIII_right) and the resulting influence on the optical brightener effects have to be considered. Furthermore, the various scattering behaviour of used inks has to be considered in this super positioning model based on NEUGEBAUER and DEMICHEL.

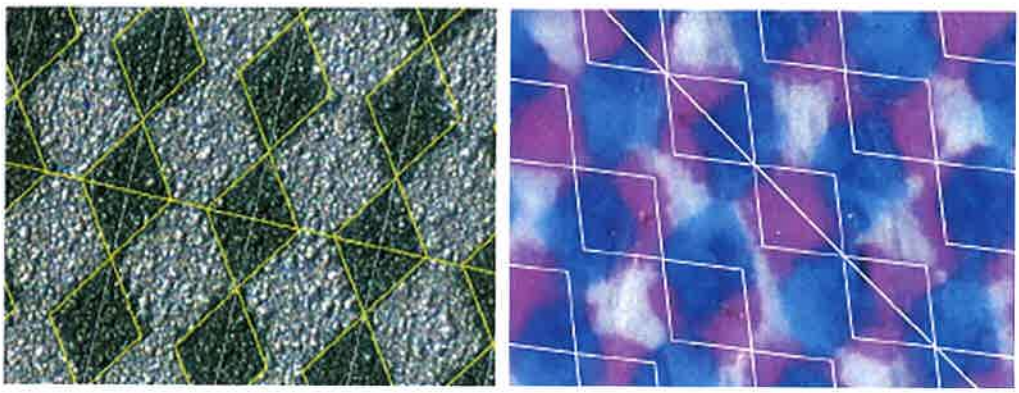

Figure VIII_left: 40% area coverage on plate in cyan-angle; right: Print of 40% magenta on 40% cyan with magenta-plate-mask, to show the effects of super positioning two inks [Riedl, 2008]

Therefore, the NEUGEBAUER equation has to be adjusted by the introduced brightener factor $B(\lambda)$ and a combined ink transfer and screening factor $TS_i(\lambda)$ to calculate $\beta^{oB}_{cmyk}(\lambda)$ in equation 17

$$\beta^{oB}_{cmyk}(\lambda) = \sum_{i \in \Psi} B(\lambda) \cdot f_i(\lambda) \cdot \beta_i(\lambda) \cdot TS_i(\lambda) \tag{17}$$

with

- $\Psi = \{pw, c, m, y, r, g, b, k\}$,
- the corresponding coverage factors that are calculated by applying DEMICHEL's equation (now of course with the *wda-coverage* $A_i(\lambda)$; c.f. equation 2 & 11),
- the full tone reflectances $\beta_i(\lambda)$ with $\beta_{pw}(\lambda)$, $\beta_c(\lambda)$, $\beta_m(\lambda)$, $\beta_y(\lambda)$, $\beta_k(\lambda)$ measured and
- the remaining reflectances calculated by the equations in EQ 18

$$\begin{aligned} \beta_r(\lambda) &= \beta_m(\lambda) \cdot \beta_y(\lambda), \\ \beta_g(\lambda) &= \beta_c(\lambda) \cdot \beta_y(\lambda) \quad \text{and} \\ \beta_b(\lambda) &= \beta_c(\lambda) \cdot \beta_m(\lambda). \end{aligned} \tag{18}$$

At last, the combined ink transfer and screening factor $TS_i(\lambda)$, which depends directly on $f_i(\lambda)$, is derived from two additional measurements for each ink: Reflectances of 100% and 50% nominal area coverage printed in each case onto 100% black and measured with UVcut-filter.

Finally, all model parameters for calculating the reproducible colour space are now introduced. Note that this approach holds true for several autotypic screenings (150 lpi, 200 lpi, 250 lpi, 300 lpi) including FM versions. The differences between the calculated and the measured CIE-Lab values are about 4 ΔE units or lower for particularly adjusted test charts (figure IX). For the colour prediction concerning regular test charts, additional test patches are required for the consideration of density fluctuations in and across printing direction, respectively.

6. Conclusions

For the model calibration, all variables are fitted by minimizing the sum of square differences between measured and predicted spectral reflectances. In the case of four inks (cyan, magenta, yellow and black), the calibration

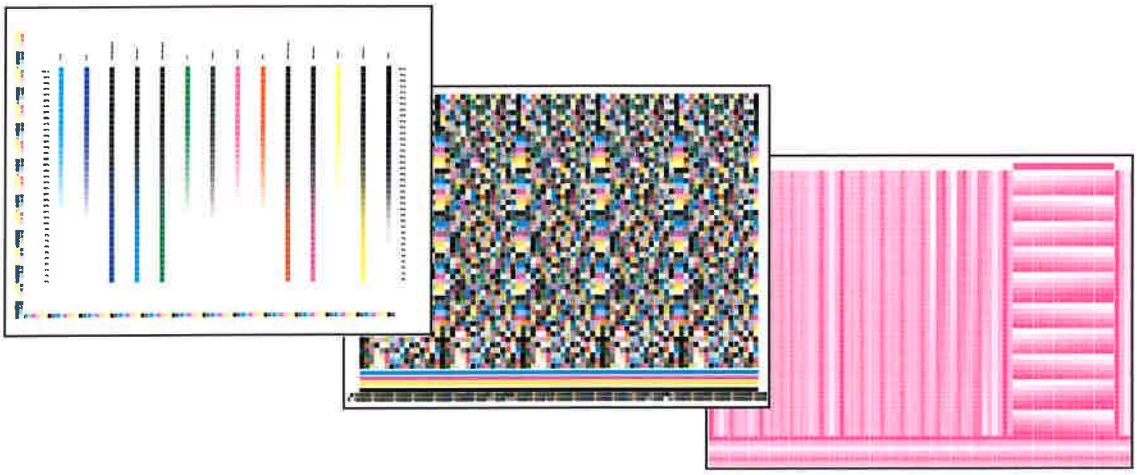

Figure IX: Particularly adjusted test charts

set can be as small as 24 samples for the *wda-coverage & brightener* model. This set comprises the data of the substrate measured twice - once with and once without UVcut-filter - and full tone as well as 80%, 50% and 30% halftone patches measured solely with UVcut-filter for each ink. Also included in this sample are measurements of 100% and 50% area coverage of cyan, magenta and yellow printed in each case onto 100% black to derive the combined ink transfer and screening factor. The differences between the calculated and the measured CIE-Lab values are about 4 ΔE units or lower.

References

1. Beer, August 1852, Ann. Physik 2, pp. 78-86
2. Clapper, F. R. & Yule, J. A. C. 1953 "The effect of multiple internal reflections on the densities of halftone prints on paper", Journal of the Optical Society of America, Vol. 43, pp. 600-603
3. Demichel, M. E. 1924 Procédé, Vol. 26, pp. 17-21
4. Hersch, R. 2008 "Spectral prediction model for color prints on paper with fluorescent additives" Applied Optics, vol. 47, No. 36
5. Hersch, R. & Hébert, M. 2007 "Deducing ink-transmittance spectra from reflectance and transmittance measurements of prints" IS&T/SPIE Electronic Imaging Symposium, (Spie) vol. 6493, pp. 649314-1 - 13
6. Hersch, R. & Emmel, P. & Collaud, F. 2004 "Spectral reflexion and dot surface prediction models for color halftone prints", Journal of Electronic Imaging, 14(3), 033001
7. Kubelka, P. 1954 "New contributions to the optics of intensely light-scattering material, part II: Non-homogeneous layers", Journal of the Optical Society of America, Vol. 44, pp. 330-335
8. Murray, A. 1936 „Monochrome reproduction in photoengraving", J. Franklin Institute, Vol. 221, pp. 721-724
9. Neugebauer, H. E. J. 1937 „Die theoretischen Grundlagen des Mehrfarbendrucks". Zeitschrift fuer wissenschaftliche Photographie,Vol. 36, pp. 36-73
10. Paul, Dr. Andreas 1994 "Steigerung der Druckqualität durch Variation des Offsetfarbenraums", FOGRA Forschungsbericht (München) no. 52.026
11. Riedl, R. 2008 „WK47 - Farbannahme im Offsetdruck – experimentelle Untersuchungen in Labor und Praxis", Wissenschaftliches Kolloquium der Bergischen Universität Wuppertal, vol. 47
12. Rodriguez, G. J. & Mantler, H. 2006 „WK35 - Eine Brücke zwischen Farbwerten und Prozessgrößen im autotypischen Druck", Wissenschaftliches Kolloquium der Bergischen Universität Wuppertal, vol. 35
13. Yule, J. A. C. & Nielsen, W. J. 1951 "The penetration of light into paper and its effect on halftone reproductions", Proc. TAGA, Vol. 3, pp. 65-76

How to apply Kubelka-Munk Model to media of partial diffuse-light distribution?

Li Yang

Holmen Paper Development Center, Holmen Paper
Vattengränden 2, SE-60188 Norrköping, Sweden
E-mail: li.yang@holmenpaper.com

Abstract

Perfect light diffuseness inside the medium, such as a paper sheet, is the fundamental assumption when applying the Kubelka-Munk (K-M) model. In reality, this pre-condition is seldom fulfilled, which is unfortunately either not well noticed or ignored by users. Nevertheless, this is little troublesome as long as it is applied to media of similar light diffuseness. When applied to media of significantly different light diffuseness great discrepancies between theoretical predictions and measurements may occur. Besides the intrinsic optical properties, there are other factors that affect light diffuseness inside the medium, such as illumination geometries, medium thickness, etc. In this work, we proposed a solution that enables the K-M model to be applicable across media of different light diffuseness. In the proposed model, the light distribution is explicitly expressed with a parameter, b, whose value equals to unity ($b = 1$) for a perfect diffuse light and zero ($b = 0$) for a collimated light distribution, respectively. The proposed model was verified by applying to papers of different light diffuseness, caused by different illumination geometries and different thickness. The spectra of light reflection as well as light transmission predicted with this model agree very well with measurements.

Keywords: Extended Kubelka Munk model, light scattering & absorption, partial light distribution.

1. Introduction

The Kubelka-Munk (K-M) model is a two-flux simplified approach of the radiation transfer theory. It was originally developed for light propagation in parallel colorant layers of infinite xy-extension [Kubelka and Munk, 1931]. The K-M theory assumes that light scattering in the sample is isotropic and that the light distribution inside the medium layer is perfectly diffused. Relying on these assumptions, light propagation in the layer is modelled by two simultaneous light fluxes traversing the layers. It is worthy of noticing that the upward-going flux does not represent any real light ray propagation rather it is an average representation of all light rays whose propagation vectors have a $+z$ component. Similar applies to the downward-going flux.

The perfectly diffuse light distribution is one of the most fundamental assumptions of the K-M model, which is also the crucial limitation, as in reality this presumption is seldom fulfilled. In practices, this pre-condition is either consciously or non-consciously ignored by users as this is little troublesome so long as it is applied to media of similar light diffuseness, such as white paper. When applied to media of significantly modified light diffuseness, such as dyed-sheet, great discrepancies between theoretical predictions and measurements occur [Foote, 1939; Granberg and Enström, 2003; Love et al., 1965; van den Akker, 1949]. In literature this has frequently been the topic of discussion [Billmeyer et al., 1968, 1985; Bloch and Sève, 2003; Koukoulas and Jordan, 1997; Maheu et al., 1984, 1989; Nobbs, 1985; Philips-Invernizzi et al., 2001; van den Akker, 1949; Rundlöf and Bristow, 1997; Vargas, 2002; Yang and Miklavcic, 2005].

There have been plenty of modifications of the K-M model, whose success has been modest [Philips-Invernizzi et al., 2001]. In the textile industry, Preston and Tsien [1946] proposed a modified model for stock-dyed fibers. They reasoned as if everything took place with fibers likened to plates and used Stock's work on transmission and reflection by a pile of plates. Being less intuitive and laborious in application, this model was not much used. In the paint industry, some modifications have also been carried out [Billmeyer et al., 1968]. Among others, Beasley et al., [1967] have proposed a generalization of the K-M model: they allow for the presence of parallel light in addition to diffuse light and the adjustment of the ratio of forward to backward scattering, and they add various reflection coefficients to consider the change in refraction index at the interface between color matter and air. But again, their equations have the major drawback that their application is delicate due to the numerous additional parameters that are included and then need to be determined.

In the present paper, we offer an alternative solution, without supplanting the K-M model, which is still much used because of its simplicity and effectiveness. For illustration purpose, without losing the generality, the proposed method is applied to weakly absorbing media, multiple paper-sheets. Potential influences of light scattering and light absorption are through discussed.

2. Experiments

Spectral reflectance- and transmittance values of paper (Biotop 3 from Neusiedler, 80 g/m^2, without fluorescent brighteners) have been measured with $45^0/0^0$ and $D/0^0$ measurement geometries in reflection and transmission modes, respectively. The different illumination geometries result in different light distributions inside the paper sample. It is diffuse for transmittance as a consequence of diffuse illumination used but it is only partial diffuse for reflectance measurement because of collimated light illuminated at 45^0 incident angle and also because of light scattering inside the paper.

The measurements include reflection and transmission spectra of single-, double-, and triple-paper sheets. The multiple sheets are simply laid out on top of one another. As it is well known that the refraction index of uncoated paper is close to unity, the two-sheet (multiple-sheet) system mimics very well a single paper sheet of twice (multiple) thickness. For simplicity, the spectra are denoted as R_1, T_1, R_2, T_2, R_3 and T_3, with the numbers in the subscript corresponding to the number of stacked paper sheets. The reflectance of many stacked paper sheets R_∞ is also measured.

3. Theoretical considerations and equations

To promote the understanding of the extended model proposed , the fundamentals of the original K-M model are briefly reviewed. Since, we are working with uncoated paper, whose refraction indices are close to unity, the Fresnel reflections from media-air interfaces or the so-called Saunderson Correction [Saunderson, 1942] are not included. A general expression for reflectance, including the Fresnel reflection, may be found in the recent publication [Yang and Hersch, 2008].

3.1 K-M model for medium of perfect diffuse-light distribution

According to the K-M model, light propagation in a medium layer is governed by the phenomenal coefficients of absorption K and of scattering S,

$$-\frac{dI}{dz} = -(S+K)I + SJ, \quad \frac{dJ}{dz} = -(S+K)J + SI. \tag{1}$$

For a paper sheet of thickness, D, the reflectance value is expressed by [9],

$$R = \frac{R_\infty \exp(-2\sqrt{K^2+2KS}D) - R_\infty}{R_\infty^2 \exp(-2\sqrt{K^2+2KS}D) - 1} \tag{2}$$

In the equation, R_∞ is the reflectance of a semi-infinitely thick medium which is expressed by

$$R_\infty = 1 + \frac{K}{S} - \sqrt{\left(\frac{K}{S}\right)^2 + 2\frac{K}{S}} \tag{3}$$

Similarly, the transmittance of the medium layer is [9]

$$T = \frac{(1-R_\infty^2)\exp(-\sqrt{K^2+2KS}D)}{1-R_\infty^2 \exp(-2\sqrt{K^2+2KS}D)} \tag{4}$$

In paper-making industry, it is the paper grammage (g/m^2) often used instead of paper thickness. In such a case, K and S have the dimension of m^2/g, instead of $1/m$. With this in mind the Eqs. (1)-(4) can directly be applied.

In the K-M model, the phenomenal coefficients of absorption and scattering, K and S, are linear functions of the intrinsic coefficients of absorption and scattering of the medium, a and s, according

$$K = 2a, \quad S = S \tag{5}$$

Hence, in the conventional K-m model, K and S are independent quantities, or there are no inter-dependence between light scattering and light absorption.

3.2 The extended K-M model for medium of various light distribution

One has to bear in mind that Eq. (5) holds only when it is perfectly diffuse light distribution in the medium layer. In case of non-perfect diffuse light distribution, Eq. (5) does not apply and modifications are needed. Following the derivation procedures for the Eq. (5) [Wedlandt and Hecht, 1966], we reformulate the equation into,

$$K = (\beta + 1)a, \quad S = \frac{(\beta + 1)}{2}s, \tag{6}$$

with b being a quantity and describing the degree of light diffuseness. The quantity, b, depends solely on light distribution in the medium. The general expression for b, for an arbitrary angular light distribution $\partial J/\partial\phi$ is (Wedlandt and Hecht, 1966),

$$\beta = \int_0^{\pi/2} \frac{1}{J}\frac{\partial J}{\partial \phi}\frac{d\phi}{\cos\phi} - 1. \tag{7}$$

For an ideal diffuses light-distribution, the angular distribution is

$$\frac{\partial J}{\partial \phi} = J\delta(0) \quad ,$$

while for a collimated light-distribution, the angular distribution is a d-function,

$$\frac{\partial J}{\partial \phi} = J \sin 2\phi \quad .$$

Therefore, the b factor equals to zero for a collimated light distribution (zero diffuseness) and it equals to unity when the light distribution is perfectly diffuse (100% diffuseness) as is required by the the original K-M model [Kubelka and Munk, 1931]. For other types of light distributions, b takes a value between 0 and 1, depending on their respective diffuseness grade.

Equation (6) is the principle modification/extension to the conventional K-M model. With this extension, one is allowed to directly apply the equations obtained from the K-M model, Eqs. (2-4), to a medium of arbitrary light distribution.

There are a few factors that affect the light distribution or quantity b: the angular distribution of the incident light (the optical geometry of the illuminating source), the intrinsic light properties of the medium, and the thickness (grammage) of the medium. When the medium is illuminated by perfectly diffuse light, the light distribution in the medium will also be well diffused provided the medium is little absorptive. In this perspective, the optical geometry of a measurement apparatus plays an important roll, for example, the light distribution in a sheet of paper, when measured with spectrophotometer of diffuse illumination (say D/0°), is different from that with a collimate light illumination (say 45/0°). The second factor is the intrinsic optical properties of the medium, namely the coefficients of light scattering and light absorption. By definition a strong light scatting means a short free-path length between two sequential scattering events or more frequent light scattering when passing through a certain path length. In consequence, the light diffuseness increases with increasing light scattering. Even with a collimated incident light (illumination), light distribution can still be partial or even perfect diffuse due to light scattering in the medium. On the contrary, light absorption impacts negatively on the light diffuseness as it limits the number of scattering events before absorption occurs. Consequently, light absorption reduces light diffuseness even if the incident light is perfectly diffused, because of different path-lengths along different propagation directions when passing through an identical thickness of the medium. The third factor that is often overlooked is the thickness effect of the medium layer. Since light may exit the medium at the medium-air interfaces, the average number of events of scattering or absorption depends on the thickness of the medium. As a result, with a collimated incident light, the light distribution in the double-stacked paper (little absorption) becomes more diffused than in the single paper sheet, and the triple-stacked is even more diffused. Hence, we will have, $b_3 > b_2 > b_1$, for the triple-, double-, and single- sheet systems, as is the case of the

reflectance measurements. But for transmittance measurements, light distributions in all systems are identical (diffuse), because the diffuse illumination is used (here we assume the light absorption is negligible).

4. Results: comparative calculations with conventional K-M model and the extended model

It is a common practice to obtain the phenomenal coefficients K and S of a medium from two measured reflection spectra (training set), namely, the reflectance values of a single paper sheet, R_1, and a semi-infinitely thick layer, R_∞. We denote these deduced coefficients as K_1 and S_1. According to Eq. (6), these coefficients are related to the intrinsic absorption and scattering coefficients a and s of the medium by the diffuseness factor b_1: $K_1 = (b_1 + 1)\, a$ and $S_1 = (b_1 + 1)\, s\, /2$. The reflectance of a semi-infinitely thick layer R_∞ depends only on the ratio of K_1/S_1 (see Eq. 3) and is therefore independent of b_1.

To better appreciate the effectiveness of the proposed model, comparative studies are shown. We begin with calculating the spectra of reflection and transmission with the conventional K-M model then follow with computations employing the modified model.

4.1 Spectral calculation with the K-M model

Traditionally, the deduced S_1 and K_1 coefficients are practically treated as the characteristics of the paper materials, irrelevant to the paper thickness or grammage. Hence, these coefficients are directly employed, using Eqs. (2) and (4), to predict the spectra of papers made of the same materials (as the training set), regardless their thicknesses.

Figure 1 depicts the calculated spectra of light reflection as well as light transmission, employing Eqs. (2) and (4) with the same S_1 and K_1 coefficients in all of the calculations. In the figure also show the corresponding experimental measurements. Clearly, the calculated reflectance values (the subfigure on the left) of the double- and triple-sheet system exhibit systematic derivations from the experimental vales: the computations are smaller than the experimental values in the wavelengths of low light absorption. At the first glance, one may overlook the discrepancies as they are not significant in quantity or attribute them to the inaccurate S_1 and K_1 values used in the calculations. However, the systematic behaviour of the discrepancies is troublesome.

When the S_1 and K_1 coefficients are used for computing the spectra of light transmission, the derivations between the calculated spectra and the measurements become much more severe. And again, the discrepancies are systematic, namely the calculated values are bigger than the measured ones.

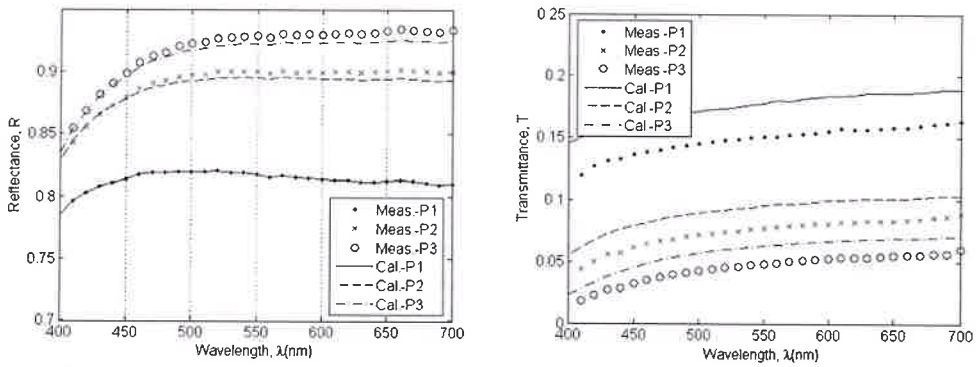

Figure 1: The calculated (Cal.) and measured (Meas.) spectral reflectance values of single (solid line), double (dashed line), and triple (dash-dotted line) sheet layers of paper. The spectra are calculated by directly using the identical phenomenal coefficients, K_1 and S_1 in all of the calculations. Left: the reflectance values; right: the transmittance values [from Yang and Hersch, 2008]

The discrepancies for both reflection- and transmission spectra can be attributed to different light diffuseness inside the paper sheets. Remember that the reflection-spectra were measured with a collimated light source (45°/0°). According to the discussions in the proceeding section (Sec. 3), the grads of the light diffuseness increase with the increasing thickness (or the number of paper sheets). Consequently, the phenomenal coefficients of

the scattering and absorption, S_1 and K_1, derived from the reflection-spectrum of the single paper sheet, can not directly be used for computing/predicting the reflection-spectra of the multiple-sheet, because of different light-diffuseness (thickness-effect) in the multiple-sheet from that in the single sheet. Naturally, the differences with respect to the light diffuseness are slightly greater in the wavelengths (longer wavelengths) of less light absorption. As shown later on, the degrees of the light diffuseness of the single, double and triple sheets, are $b = [0.65, 0.75, 0.88]$, respectively.

Different from the reflection spectra, the much severer differences of the transmission-spectra are primarily caused by the different illuminating geometries used for the measurements: reflection, respectively, transmission. In the transmission measurement, a diffuse light source was used. The light distributions in the paper sheets are therefore also diffuse ($b_T = 1$) for all of the sheets, which differ significantly from the one ($b_1 = 0.65$) used in calculation.

By data fitting, we obtain the following expression for the diffuseness of a multiple-sheet system, when measured with 45°/0° optical geometry.

$$\beta_n = 1 - \exp(-0.88n), \quad (n=1, 2, 3, \ldots) \tag{8}$$

Figure 2 is the plot of this expression.

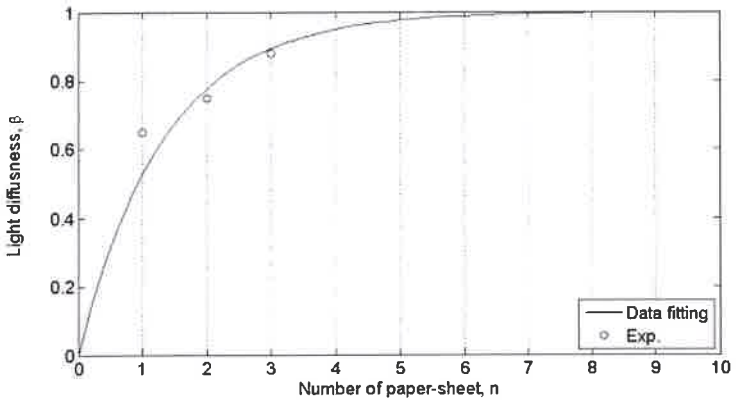

Figure 2:
The light diffuseness in the multiple sheet systems, plotted according to Eq. (8)

4.2 Spectral calculation with the extended model

As argued in Sec. 3, for the reflection spectra, measured with collimated illuminating light, the light distributions are more diffuse in the double- and triple sheets than that in the single (the training set) due to the thickness effect, i.e., $b_3 > b_2 > b_1$. This means we should use different phenomenal coefficients for calculations instead the ones derived from the reflection spectrum of the single sheet, K_1 and S_1, namely,

$$\begin{aligned} K_2 &= (\beta_2 + 1)a = \frac{(\beta_2 + 1)}{(\beta_1 + 1)} K_1, \quad S_2 = (\beta_2 + 1)s = \frac{(\beta_2 + 1)}{(\beta_1 + 1)} S_1 \\ K_3 &= (\beta_3 + 1)a = \frac{(\beta_3 + 1)}{(\beta_1 + 1)} K_1, \quad S_3 = (\beta_3 + 1)s = \frac{(\beta_3 + 1)}{(\beta_1 + 1)} S_1 \end{aligned} \tag{9}$$

By fitting to the reflection spectra of the double- and triple-sheet (see Fig. 3), we received that $(b_2+1)/(b_1+1)=1.06$ and $(b_3+1)/(b_1+1)=1.14$, respectively. This indicates that the degree of light diffuseness indeed grows with the medium-thickness (or grammage).

As a further confirmation, the spectra of light transmission are calculated with the same phenomenal coefficients of scattering and absorption for all the systems (single, double and triple sheet), namely,

$$K_T = (\beta_T + 1)a = \frac{2}{(\beta_1 + 1)} K_1, \quad S_T = (\beta_T + 1)s = \frac{2}{(\beta_1 + 1)} S_1 \tag{10}$$

In Eqs. (10), we have utilized the fact that the light distributions are perfectly diffuse ($b_T=1$) in the paper sheets due to the D/0° optical geometry of the measurements.

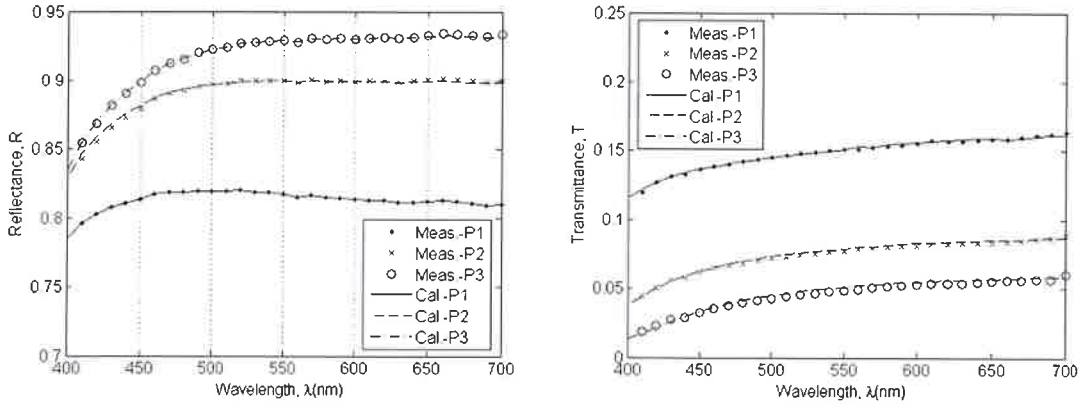

Figure 3: The spectral reflectance values of single (solid), double (dashed), and triple (dash-dotted) sheet layers. Left: the reflection spectra are calculated with $(b_2+1)/(b_1+1)=1.06$ and $(b_3+1)/(b_1+1)=1.14$ for the double- and triple-sheet layers; right: the transmission spectra of single (solid), double (dashed), and triple (dash-dotted) sheet layers, with $2/(b_1+1)=1.21$ for all [from Yang and Hersch, 2008]

By fitting to the spectrum of light transmission, we found that, the ratio $2/(b_1+1)=1.21$ provides the best to the single sheet (T_1, see Fig. 3). From this we obtain $b_1 = 0.65$. As a further test (confirmation) to the proposed model, the same K_T and S_T coefficients are then used to predict the spectra of the double- and triple-sheet systems.

Figure 3 depicts the calculated spectra of reflection (left) and transmission (right), with the proposed model. Clearly, the computed spectra are in excellent agreements with the experimental values.

5. Discussions

In this report we presented the method that extends the K-M model to media systems of arbitrary light distributions, from perfectly diffused to collimated. The extended model keeps the advantages of the conventional K-M model, namely the simplicity and physical intuitiveness. The major difference between the conventional K-M model and the extended one is the relationships between the phenomenal coefficients of light scattering and absorption, S and K, and the intrinsic optical properties, s and a, given in Eqs. (6). In this expression, the phenomenal coefficients of light scattering and absorption, S and K, depend even on the light distribution, characterized by the parameter, *b*.

There are probably three factors that affect the light distribution: the angular distribution of the incident light, the intrinsic light properties of the medium, and the thickness (grammage) of the medium. It is demonstrated that the proposed model applies well to the medium of low light absorption but strong light scattering. In such case, the parameter *b* is spectral independent and depends only on two of the three factors, namely the optical geometry of the illumination and the thickness of the medium (the light diffuseness increases with increasing medium-thickness in case of low light absorption).

It is worth to notice the intrinsic optical properties, *a* and *s*, can have significant influences on light distribution inside the medium. For an illumination of partial light diffuseness, say $b = 0.5$. The light distribution becomes more diffused in a medium due to strong light scattering provided the medium is of weak light absorption. On the contrary, it will be less diffused if the medium is strong absorptive (weak scattering). For a medium, whose optical properties are strongly wavelength-dependent, for example a cyan-dyed paper sheet, the light diffuseness in the paper will also be wavelength-dependent: higher light diffuseness (*b* close to 1) in the wavelengths of weak light absorption but lower light diffuseness (*b* close to zero) in the wavelengths of strong light absorption. The dependence of the light diffuse on the intrinsic optical properties, *a* and *s*, makes the quantity, *b*, a function of the coefficients of scattering and absorption, i.e., $b = b(a,s)$. From this point of view, it is easy to understand why the conventional K-M model failed when applied to such medium as dyed-sheet [Billmeyer, 1985; Foote, 1939; van den Akker, 1949] because of the presumption of ideal diffuse is not fulfilled. Along the line, one can easily understand why the additive principle breaks down for the phenomenal coefficients. Because of the dramatic modification upon dying, the light distribution in the absorption band of the dye becomes much less

diffused compared to that in the white sheet. Consequently, the phenomenal scattering coefficient of the dyed sheet becomes significantly smaller, in the absorption band of the dye, than that of the white paper sheet.

The dependence of the b parameter on the intrinsic optical properties, leads the nonlinear relationships between the phenomenal coefficients and intrinsic ones. This nonlinearity has been recognized as the vital cause for the failure of the conventional K-M model [Nobbs, 1985; Philips-Invernizzi et al., 2001]. Such non-linearity contributes also to the inter-dependency between S and K, which have been observed and reported by many researchers [Bloch and Sève, 2003; Granberg and Enström, 2003; Koukoulas and Jordan, 1997; Rundlöf and Bristow, 1997].

6. Summary

The conventional K-M model has limited applicability due to the pre-condition of perfectly diffused light distribution. This limitation has been believed to be the major cause to the failure of the model when applied to such medium as dyed paper sheet of strong light absorption because the light distribution of the light in the absorption band is far from diffuse.

The proposed method offers a solution to remove the limitation and enables the model to be applicable to media of various light distributions, from collimated light to perfectly diffused light. In the extended model, the relationships between the phenomenal coefficients of light scattering and light absorption, S and K, and the intrinsic optical properties, s and a, are regulated by the light distribution inside the media through the parameter, b. Through the physical analysis and the application to the multiple-sheet medium systems, it was identified that the light distribution in the medium depends on three factors: the angular distribution of the incident light (the optical geometry of the illuminating source), the intrinsic light properties of the medium, and the thickness (grammage) of the medium.

Acknowledgement

Many thanks to Prof. Hersch for providing me with measurements and fruitful discussions.

References

1. Beasley, J. K., Atkins, J. T. and Billmeyer, F. W. Jr. (1967), *Electromagnetic scattering, Gordon &Breach, New York*
2. Billmeyer, F. W. Jr., Abrams, R. L. and Davidson, J. L. (1968), *Color and appearance properties of paint film, J. Paint Technol. 40, pp. 143-149*
3. Billmeyer, F. W. Jr. (1985), *Color and appearance characterization for the coating industry, J. Coatings Technol. 57, pp. 47-53*
4. Bloch, J. and Sève, R. (2003), *About the theoretical aspect of multiple light scattering: Sivy's theory, Color Res. Appl., 28, pp. 227-228*
5. Foote, W. J. (1939), *An investigation of the fundamental scattering and absorption coefficients of dyes handsheets, Paper Trade J. 109, pp. 333-340*
6. Granberg, H. and Edström, P. (2003), *Quantification of the intrinsic error of the Kubelka-Munk model caused by strong light absorption, J. Pulp Paper Sci. 29, pp. 386-390*
7. Koukoulas, A. A. and Jordan, B. D. (1997), *Effect of strong absorption on the Kubelka-Munk scattering coefficients, J. Pulp Pap. Sci., 23, pp. 224-232*
8. Kubelka, P. and Munk, F. (1931), *Ein Beitrag zur Optik der Farbanstriche, Z. Tech. Phys., 12, pp. 593-601*
9. Love, R. B., Oglesby, S. and Gailey, I., (1965), *The relationship between dye concentration and reflectance - amendments to the Kubelka-Munk equation, J. Soc. Dyers Color 81, pp. 609-614*
10. Maheu, B., Letoulouzan, J. N. and Gouesbet, G. (1984), *Four-flux models to solve the scattering transfer equation in terms of Lorenz-Mie parameters, Appl. Opt. 23, pp. 3353-3362*
11. Maheu, B., Briton, J. P. and Gouesbet, G. (1989), *Four-flux model and a Monte Carlo code: comparisons between two simple, complementary tools for multiple scattering calculations, Appl. Opt. 28, pp. 22-24*

12. Nobbs, J. H., (1985), *Kubelka-Munk theory and the prediction of reflectance, Rev. Prog. Coloration 15, pp. 66-75 and references therein*
13. Philips-Invernizzi, B., Dupont, D. and Caze, C., (2001), *Bibliographical review for reflectance of diffusing media, Optical Engineering 40, pp. 1082-1092, and references therein*
14. Rundlöf, M. and Bristow, J. A. (1997), *A note concerning the interaction between light scattering and light absorption in the application of the Kulbelka-Munk equations, J. Pulp. & Pap. Sci., 23, pp. 220-223*
15. Saunderson, J. L., (1942), *Calculation of color pigmented plastics, J. Opt. Soc. Am. 32, pp. 727-736*
16. van den Akker, J. A., (1949), *Scattering and absorption of light in paper and other diffusing Media, Tappi 32, pp. 498-501*
17. Vargas, W. E. (2002), *Inversion methods from Kulbelka-Munk analysis, J. Opt. A, Pure Opt. 4, pp. 452-456*
18. Wendlandt, W. and Hecht, H. (1966), *Reflectance Spectroscopy, Ch. 3, Interscience Publishers (John Wiley& Sons), London*
19. Yang, L. and Miklavcic, S. J., (2005), *"Revised Kubelka-Munk theory. III. A general theory of light propagation in scattering and absorptive media", J. Optical Society of America A 22, pp. 1866-1873*
20. Yang, L. and Hersch, R. D., (2008) *"Kubelka-Munk model for non perfectly diffuse light distribution in paper", J. Imaging Sci. Techno. 52, pp. 201-207*

Chromatic adaptation models evaluation using principal components analysis

Dejana Đorđević, Aleš Hladnik, Andrej Javoršek

Chair of Information and Graphic Arts Technology, Department of Textiles
Faculty of Natural Sciences and Engineering, University of Ljubljana
Snežniška 5, SI-1000 Ljubljana, Slovenia
E-mails: dejana.djordjevic@ntf.uni-lj.si, ales.hladnik@ntf.uni-lj.si, andrej.javorsek@ntf.uni-lj.si

Abstract

Unlike human visual system, image-capturing devices, such as scanners and digital cameras, are unable to accommodate to different light sources. As a consequence, in color acquisition, display and rendering processes a number of chromatic adaptation transforms (CATs) are being used. In our study, a comparison among 15 models consisting of five CATs - Bradford, von Kries, XYZ Scaling, CMCCAT97 and CMCCAT00 - and three illuminant source pairs - D50-A, D50-D65 and D65-A - was made using 8190 color patches. Results showed that colour differences obtained with the Bradford method were the lowest regardless of the implemented illuminant source pair.

Keywords: chromatic adaptation models, color differences, principal components analysis

1. Introduction

Colour is the result of human perception of light reflected from the surface in visible spectrum between 380 nm and 780 nm. Unlike human visual system, which is capable of color adaptation to a wide range of lighting conditions, image-capturing devices, such as scanners or digital cameras, in general do not have the ability to adapt to the light source. Scanners usually use fluorescent light sources with color temperature between 4.200 and 4.800 K [Süsstrunk et al., 2001]. White point of displays is usually set to either CIE standard illuminant D50 (5.000 K), which is warmer white, or to D65 (6.500 K), which is cooler (i.e. more blue) white. D50 is appropriate for displays that are used for professional corrections of images prepared for printing process, according to standard ISO 12646 [ISO 12646, 2004]. D65 is suitable for preparing photos intended to be published on Internet according to standard ISO 3664 [ISO 3664, 2000]. For evaluation of prints (hardcopy), CIE standard illuminant D50 is also used [ISO 3664, 2000]. White point (D50) of Profile Connection Space (PCS) is defined by ICC specification.

Transforms between colours captured under certain lighting conditions (source colours) and colours displayed under different viewing conditions (destination colours) therefore play an important role both in colour appearance models and in colour reproduction. Such transformations from source to destination colours are called chromatic adaptation transforms (CATs). The most widely used CATs are based on a modified form of the von Kries model [von Kries, 1970; Luo and Hunt, 1998; Süsstrunk et al., 2001], which is a simple linear transform between CIE tristimulus values (XYZ) of colours observed under different light sources. A variety of other linear- or more complex, nonlinear models have been investigated, including XYZ Scaling [Lindbloom, 2009], Bradford [Finlayson et al., 2009], CMCCAT97 [Luo and Hunt, 1998], CMCCAT2000 [Li et al., 2000] and others.

The aim of our research was to evaluate the above mentioned five CATs based on three illuminant pairs by comparing color differences on prints using two delta E calculation equations as described below. No visual assessment of color patches by human observers was made. A multivariate statistical method - Principal components analysis (PCA) - was used to interpret the results. PCA is based on the linear transformation of original multivariate data into a lower dimensional space of new variables, so called principal components (PC), where the most important information, such as relationships among original variables or (dis)similarities among samples, becomes more obvious [Massart et al., 1997].

2. Methods

Test chart with 8190 color patches was prepared in Argyll, an open source, ICC-compatible color management system. Prints were made using inkjet printer Canon W8400pg and Heavy Weight Semi Glossy Photo Paper.

After a few days of colour stabilization, measurements with instrument GretagMacbeth Spectrolino Spectroscan were performed. CIE standard tristimulus values (XYZ) were then calculated from equations (1) to (3):

$$X = k\sum_{340}^{780} S(\lambda)R(\lambda)\bar{x}(\lambda) \quad (1)$$

$$Y = k\sum_{340}^{780} S(\lambda)R(\lambda)\bar{y}(\lambda) \quad (2)$$

$$Z = k\sum_{340}^{780} S(\lambda)R(\lambda)\bar{z}(\lambda) \quad (3),$$

where:

$S(\lambda)$ ... relative spectral power distribution

$R(\lambda)$ ... spectral reflectance

$\bar{x}(\lambda),\bar{y}(\lambda),\bar{z}(\lambda)$ ... red, green and blue color-matching functions

k... normalizing factor; for perfect white reflector (Y = 100), k can be calculated from equation (4):

$$k = \frac{100}{\sum_{340}^{780} S(\lambda)\bar{y}(\lambda)} \quad (4)$$

In addition, three different CIE standard illuminants - A, D50 and D65 - and CIE standard colorimetric observer (2°) were used in XYZ calculations.

Transformation from an XYZ source color $[X_s\ Y_s\ Z_s]$ to a destination color $[X_D\ Y_D\ Z_D]$ was accomplished according to equation (5):

$$[X_D\ Y_D\ Z_D] = [X_s\ Y_s\ Z_s]\ [M] \quad (5)$$

Matrix [M] coefficients depend on the implemented CAT. Matrices for five studied transforms are displayed in Table I. Note that [M] for CMCCAT97 and Bradford model are identical, however CMCCAT97, in addition to [M], also includes some nonlinear transformation factors.

Scheme of work is outlined in Figure 1. To calculate color differences (delta E) between the reference (XYZ values generated directly from the measured spectral data) and the chromatic adaptation-transformed values, the established ΔE_{ab} [Golob and Golob, 2001] as well as more recent ΔE_{00} [Sharma et al., 2004] formulas were implemented. All calculations were performed using program Octave 3.0 [Octave, 2009].

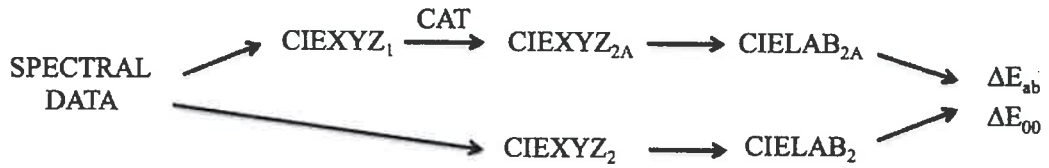

Figure 1: Scheme of work

3. Results and discussion

To visualize relationships that exist in a large results database consisting of color differences (delta E) values for 8190 samples - color patches - and 15 variables - combinations of five CATs and three illuminant pairs - PCA was implemented. Prior to the analysis, each sample was categorized according to the magnitude of its delta E value into one of the four groups: 0 - 1 (color difference undetectable by a human eye), 1 - 3 (small

color difference between two patches), 3 - 6 (perceivable difference) or >6 (large difference). The number of patches belonging to each group was a direct indication of the »quality« of the corresponding CAT/illuminant pair combination: the higher the number of low delta E (0 - 1, 1 - 3) patches, the better the performance of that model. PCA results are displayed in Figs. 2 and 3.

Table I: Matrix coefficients for the five chromatic adaptation transforms used in the study

CAT	[M]
XYZ Scaling	$\begin{bmatrix} 1.0 & 0.0 & 0.0 \\ 0.0 & 1.0 & 0.0 \\ 0.0 & 0.0 & 1.0 \end{bmatrix}$
Bradford	$\begin{bmatrix} 0.8951 & -0.7502 & 0.0389 \\ 0.2664 & 1.7135 & 0.0685 \\ -0.1614 & 0.0367 & 1.0296 \end{bmatrix}$
Von Kries	$\begin{bmatrix} 0.4002 & -0.2263 & 0.0000 \\ 0.7076 & 1.1653 & 0.0000 \\ -0.0808 & 0.0457 & 0.9182 \end{bmatrix}$
CMCCAT97	$\begin{bmatrix} 0.8951 & -0.7502 & 0.0389 \\ 0.2664 & 1.7135 & 0.0685 \\ -0.1614 & 0.0367 & 1.0296 \end{bmatrix}$
CMCCAT2000	$\begin{bmatrix} 0.7982 & 0.3389 & -0.1371 \\ -0.5918 & 1.5512 & 0.0406 \\ 0.0008 & 0.0239 & 0.9753 \end{bmatrix}$

Fig. 2 shows a clock-wise pattern of increased delta E values of investigated samples according to ΔE_{ab} formula. Superposition of this diagram with that in Fig. 3 reveals that D50-D65 illuminant pair generates by far the smallest color differences as all five corresponding CATs »samples« in Fig. 3 - Bradford (D50_D65_bfd), von Kries (D50_D65_vk), CMCCAT97 (D50_D65_cat97) CMCCAT00 (D50_D65_cat00) and XYZ Scaling (D50_D65_sc) - are located in the same (i.e. bottom-left) relative position as the »variable« point 0 - 1 in Fig. 2. Larger color differences - typically within 1 - 3 or 3 - 6 delta E classes - were found in case of D50-A models while samples that underwent one of the D65-A illuminant pair transforms were generally characterized by the largest (>6) differences. For instance, with D65_A_sc transform combination, as much as 20 patches exhibited delta E values larger than 30 units, while with D65_A_cat00 combination, 2 samples were found to have delta E values between 22 and 23 units.

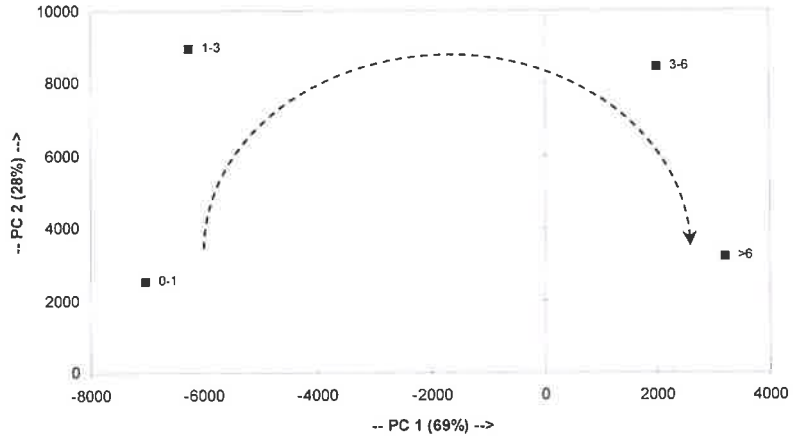

Figure 2: Groups of ΔE_{ab} values in PC1-PC2 coordinate system

PCA treatment of ΔE_{00} results (Figs. 4 and 5) leads to conclusions similar to those described above. Again, most of the relevant information (53% (PC1) + 42% (PC2) = 95%) is represented by the first two PCs. Although positions of individual data points are somewhat different when compared to those located in Figs. 2 and 3, the same clock-wise pattern of samples (0 - 1 followed by 1 - 3, 3 - 6 and >6) and ranking of variables (D50_D65_ xx model followed by D50_A_xx and D65_A_xx) is evident.

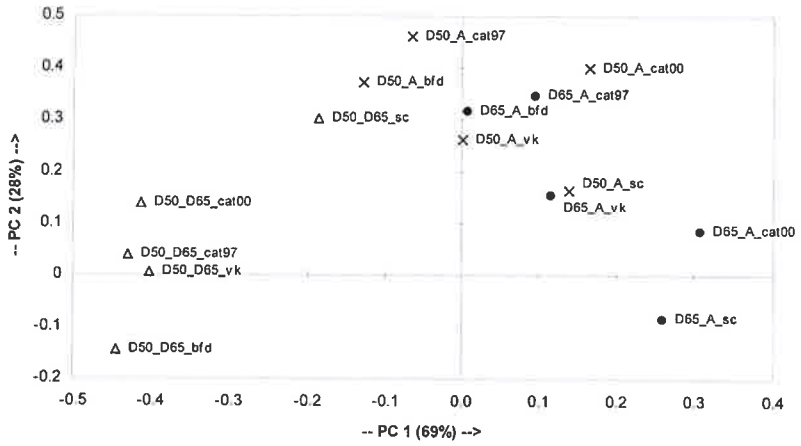

Figure 3: CAT/illuminant pair combinations for ΔE_{ab} formula in PC1-PC2 coordinate system

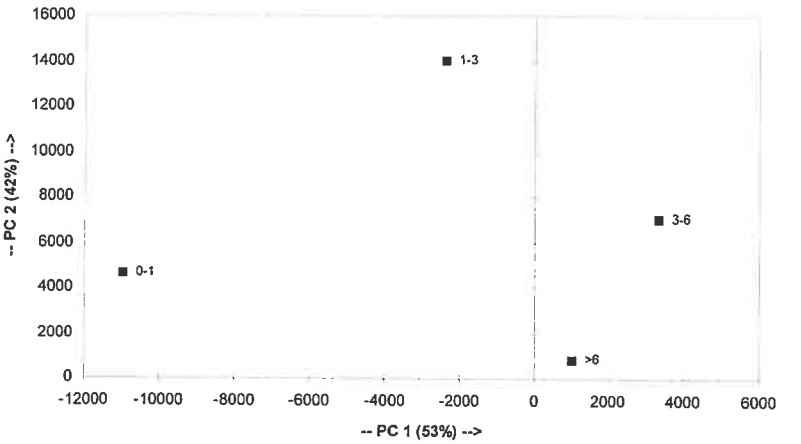

Figure 4: Groups of ΔE_{00} values in PC1-PC2 coordinate system

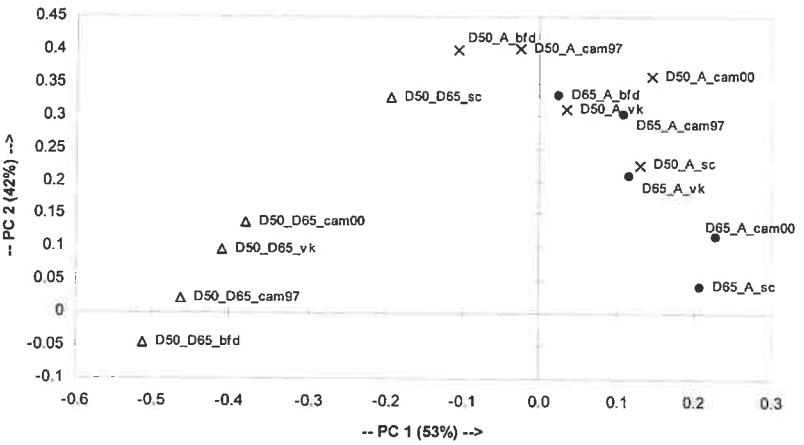

Figure 5: CAT/illuminant pair combinations for ΔE_{00} formula in PC1-PC2 coordinate system

In addition, individual CATs and the three implemented illuminant pairs - D50-A, D50-D65 and D65-A - were studied separately.

Fig. 6 (top) shows mean color differences (ΔE_{ab} and ΔE_{00}) obtained with D50-A illuminant pair and various CATs. Bradford CAT produces the smallest color differences, followed by CMCCAT97, von Kries, CMCCAT00 and XYZ Scaling model which generates the biggest ones.

Fig. 6 (middle) shows mean color differences obtained with D50-D65 illuminant pair and various CATs. Color differences are here much smaller than in the previous case; the biggest delta E values for D50-D65 pair (XYZ Scaling: ΔE_{ab} is 2.27 and ΔE_{00} is 1.50) are approximately the same as the smallest delta E for D50-A pair (Bradford: ΔE_{ab} is 2.57 and ΔE_{00} is 1.78). Note that the performance ranking of individual CATs is the same as with D50-A pair.

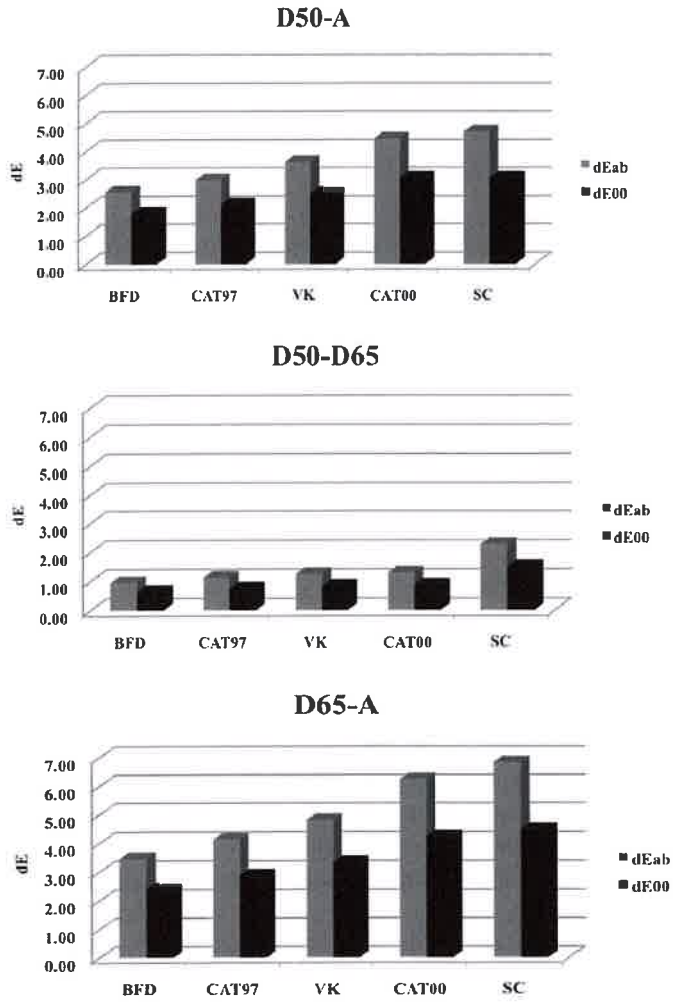

Figure 6: Mean color differences of patches obtained with D50-A (top), D50-D65 (middle) and D65-A (bottom) illuminant pairs and various CATs

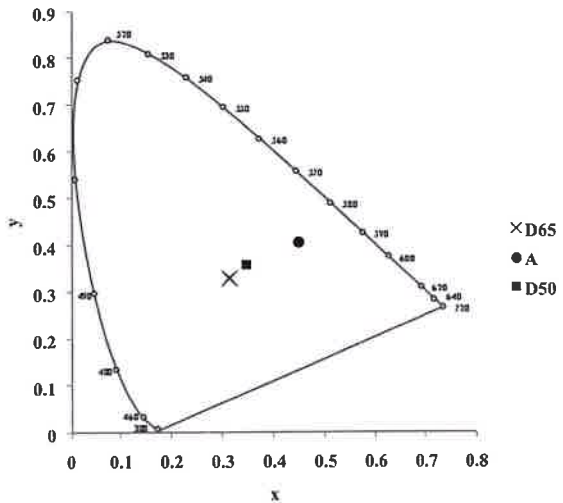

Figure 7: CIE x, y 1931 diagram (CIE Chromaticity diagram)

These findings can be explained by referring to the well-known CIE chromaticity diagram (Fig. 7). For example, illuminants D50 and D65 are both very close to each other in this diagram and also have a similar spectral power distribution, which explains the lowest delta E values obtained with this combination of illuminants. Illuminant A is closer to D50 than to D65, therefore delta E values for pair D50-A are smaller than in the case of D65-A illuminant pair.

Fig. 8 shows average color differences obtained with D65-A illuminant pair and various CATs. In this case color differences are the biggest of all three examined illuminant pairs, but ranking of the implemented CATs remains unchanged.

4. Conclusions

Raw spectral data make it possible to calculate CIE tristimulus values (XYZ) under various illumination sources. One of the major advantages of using CATs is their ability to transform CIE tristimulus values obtained under one illumination source into XYZ values related to a different illumination source in cases when spectral data are unavailable. Of all five examined models, the observed color differences were found to be the lowest in case of the Bradford CAT regardless of the illuminant pair used. PCA proved useful in detecting differences among individual CATs.

In the future we plan to perform psychophysiological experiments using a limited number of color patches and human observers to compare the results obtained in the study with those acquired by a visual assessment.

References

1. Finlayson, G. D., Süsstrunk, S.: Spectral Sharpening and the Bradford Transform [online]. http://infoscience.epfl.ch/getfile.py?docid=2373&name=FinlaysonS00&format=pdf&version=1; Accessed June 2009
2. Golob, V., Golob, D.: Teorija barvne metrike. (in Slovene) In: Interdisciplinarnost barve. Del 1. v znanosti. Maribor, Slovenian Association of Colorists, 2001
3. ISO 3664: Viewing conditions - Graphics technology and photography International Organization for Standardization, 2000 (Revision of ISO 3664-1975, Photography - Illumination conditions for viewing colour transparencies and their reproductions). ISO 2000, 20 p
4. ISO 12646: Graphic technology - Displays for colour proofing - Characteristics and viewing conditions. ISO 2004, 12 p
5. Li, C. J., Luo, M. R., Hunt, R. W. G.: Revision of the CIECAM97s model. *Colour Research and Application*, 23: 260-266, 2000
6. Lindbloom, B.: Chromatic Adaptation [online]. http://www.brucelindbloom.com/index.html?Eqn_ChromAdapt.html; Accessed June 2009
7. Luo, M. R. and Hunt, R. W. G.: A chromatic adaptation transform and a colour inconstancy index. *Color Reearch and Application*, 23:154-158, 1998
8. Massart, D. L., Vandeginste, B. G. M., Buydens, L. M. C., DeJong, S., Lewi, P. J., Smeyers-Verbeke, J.: Principal Components. In: D. L. Massart (Editor): Handbook of chemometrics and qualimetrics: part A, p. 520-535. Elsevier, Amsterdam, 1997
9. Octave [online]. http://www.gnu.org/software/octave/; Accessed June 2009
10. Sharma, G., Wu, W., Dalal, E. N.: The CIEDE2000 Color-Difference Formula: Implementation Notes, Supplementary Test Data, and Mathematical Observation. Submitted to *Color Research and Applications*, 2004 [online]. http://www.ece.rochester.edu/~gsharma/ciede2000/ciede2000noteCRNA.pdf; Accessed June 2009
11. Süsstrunk, S., Holm, J., Finlayson, G. D.: Chromatic Adaptation Performance of Different RGB Sensors. *IS&T/SPIE Electronic Imaging, SPIE* Vol. 4300, January 2001
12. von Kries, J.: Influence of adaptation on the effects produced by luminous stimuli. In: D. L. MacAdam (Editor): Sources of Color Science, p. 109-119. The MIT Press, Cambridge MA, 1970

Assessment of the colorimetric behaviour of different spectrophotometers

Vicente de Garcia[1], Jesús Inarejos[1], Susana Otero[1], Esther Perales[2], Francisco Martínez-Verdú[2]

[1] Graphic Arts Department, Technological Institute of Optics, Colour and Imaging (AIDO)
C/ Nicolás Copérnico, 7-13 Parque Tecnológico, S-46980 Paterna, Spain
E-mail: aagg@aido.es

[2] Departamento de Óptica, Farmacología y Anatomía, University of Alicante
Carretera de San Vicente del Raspeig, s/n, S-03690 San Vicente del Raspeig, Spain
E-mail: esther.perales@ua.es

Abstract

Colour reproduction is based on the ability to communicate colour information accurately. The different instrument manufacturers, models and conditions result in difficult colour communication due to the loose or inexistent inter-instrumental agreement between them.

With this study we have tried to develop an application to correct colour instruments by software by applying multi-dimensional polynomial transformations between pairs of instruments. This application will filter one spectrophotometer measurement, and apply a correcting factor to emulate the colorimetric response of any other spectrophotometer.

Keywords: colorimetry, spectrophotometer, measurement

1. Introduction

This study is part of a two year project whose aim is to develop an application able to do software-driven instrument correction. This application will filter one spectrophotometer measurement and apply a correcting factor to emulate the colorimetric response of any other spectrophotometer.

There is different instrument correction software in the market such as the X-Rite Net Profiler, but this has the problem that it only can be used in X-Rite Instruments. By developing this application we want to make instrument correction as universal a possible by using as many different instruments as possible.

With this application we will be able of improve the accuracy of colour measurement devices and this way help colour communication in all the industries that measure colour.

During this project we have studied the differences between the spectrophotometers and collected colorimetric data to evaluate the main differences in their behaviour, characterize the colorimetric response of these instruments and developed mathematical algorithms to emulate the response of a spectrophotometer in any other colour measurement instrument.

These algorithms perform mathematical transformations between various colour data (mainly type - CIE L*a*b*) from the different spectrophotometers in order to get a numeric dictionary to improve inter-instrument matching of Colorimetric data.

2. Methods

This research is divided in two parts:

Part one: Analysis of the behaviour of the different instruments.

We have selected seven spectrophotometers and nine ceramic plates as target and measured them every week during a year. We have chosen 45°/0° or 0°/45° geometry spectrophotometers, made by different manufacturers, of different models, conditions, etc.

Then we have determined the deviation in the measurement of the different instruments.

The information compiled was used for the calculation of the deviation in the measurement of the different spectrophotometers for every ceramic tile; the average values obtained were used as standard values to compare the behaviour of the different spectrophotometers.

- Measurement of the different areas of the visible spectrum

In this part of the study we have widened the areas of the spectrum to be studied, so instead of the 9 patches, we have printed two colour-charts with 513 and 619 patches respectively. We expected to represent the whole space of reproducible colour and receive sufficient information to characterize the instruments' colorimetric response in all the areas.

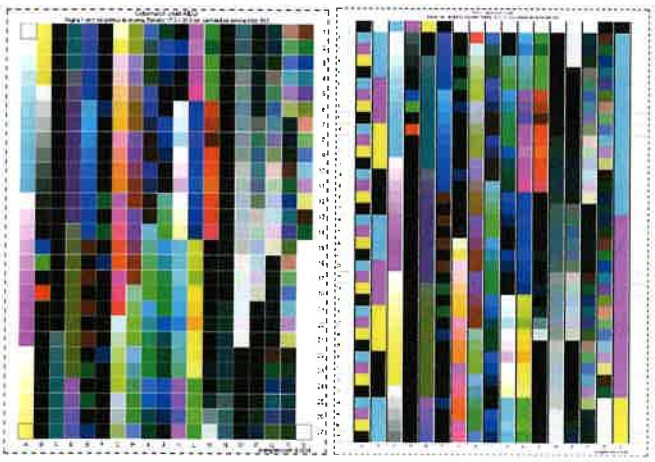

Figure 1:
Colour charts used

We printed four copies of the same colour chart, measured every patch of the four copies with each instrument, and calculated the average measure for every patch and instrument in order to minimize the possible effects that paper and small printing flaws could have on the measurement.

To analyze the difference between the spectrophotometers, we did measurements on the four copies with all the instruments, calculated the average of all the measurements for every patch, and chose this measurement as the standard value for each patch.

This standard value was compared with the mean value of the instruments for every patch to obtain more accurate information about the instruments' behaviour in the different zones of the visible spectrum.

We studied the different measurements of the spectrophotometers and compared them with the values taken as reference. We calculated the average and the standard deviation of the differences, (in ΔE^*, Absolute, best 90% and worst 10%), as well as the maximum value of ΔE^*, (for the Absolute and for the best 90%).

Part two: Development of the mathematical algorithms.

From the colorimetric database (CIE-L*, a*, b*) obtained from the comprehensive set of samples obtained in part one, multi-dimensional polynomial transformations between pairs of instruments have been performed.

The same database has been used as training dataset, and the efficiency of the polynomial transformations (statistical colour differences) has been tested with a verification set from this database.

To find the mathematical function, an application called "ColorMatch" has been designed in Matlab software. To carry out this work, the measurements made in the different colour charts have been used as a training dataset, this allows us to assess the differences between instruments and determine the correction factor to adjust the data to a reference spectrophotometer.

The application allows us to select the database associated with the reference and the test instrument; the test instrument is the one you want to obtain the correction factor.

To obtain the correction factor, an adjustment method that doesn't need more information than that obtained in the previous series of measurements (training set) is used.

To emulate the reference instrument with the test instrument, the colour data obtained with the test instrument was adjusted to the colour values obtained with the reference instrument [Kang, 1997]. This model attempts to find the mathematical function that best fit these training colours.

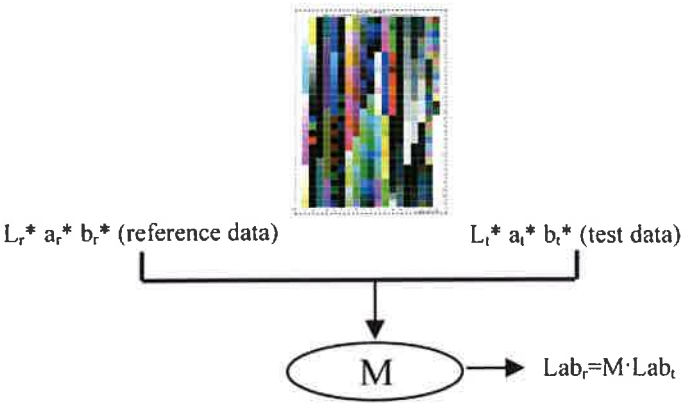

Figure 2: Steps followed in this process

To perform this transformation is assumed that as L* a* b* fit as a polynomial-type function dependent of the colorimetric data associated with the reference instrument as in Figure 3.

$$
\begin{aligned}
L_r^* &= f(L_t^*, a_t^*, b_t^*) = m_{11} + m_{12}L_t^* + m_{13}a_t^* + m_{14}b_t^* + \\
&+ m_{15}L_t^*a_t^* + m_{16}L_t^*b_t^* + m_{17}a_t^*b_t^* + \\
&+ m_{18}L_t^{*2} + m_{19}a_t^{*2} + m_{110}b_t^{*2} + \\
&+ m_{111}L_t^{*2}a_t^* + m_{112}L_t^{*2}b_t^* + m_{113}a_t^{*2}L_t^* + m_{114}a_t^{*2}b_t^* + m_{115}b_t^{*2}L_t^* + m_{116}b_t^{*2}a_t^* + \\
&+ m_{117}L_t^*a_t^*b_t^* + mt_{118}L_t^{*3} + m_{119}a_t^{*3} + m_{120}b_t^{*3}
\end{aligned}
$$

$$
\begin{aligned}
a_r^* &= g(L_t^*, a_t^*, b_t^*) = m_{21} + m_{22}L_t^* + m_{23}a_t^* + m_{24}b_t^* + \\
&+ m_{25}L_t^*a_t^* + m_{26}L_t^*b_t^* + m_{27}a_t^*b_t^* + \\
&+ m_{28}L_t^{*2} + m_{29}a_t^{*2} + m_{210}b_t^{*2} + \\
&+ m_{211}L_t^{*2}a_t^* + m_{212}L_t^{*2}b_t^* + m_{213}a_t^{*2}L_t^* + m_{214}a_t^{*2}b_t^* + m_{215}b_t^{*2}L_t^* + m_{216}b_t^{*2}a_t^* + \\
&+ m_{217}L_t^*a_t^*b_t^* + m_{218}L_t^{*3} + m_{219}a_t^{*3} + m_{220}b_t^{*3}
\end{aligned}
$$

$$
\begin{aligned}
b_r^* &= h(L_t^*, a_t^*, b_t^*) = m_{31} + m_{32}L_t^* + m_{33}a_t^* + m_{34}b_t^* + \\
&+ m_{35}L_t^*a_t^* + m_{36}L_t^*b_t^* + m_{37}a_t^*b_t^* + \\
&+ m_{38}L_t^{*2} + m_{39}a_t^{*2} + m_{310}b_t^{*2} + \\
&+ m_{311}L_t^{*2}a_t^* + m_{312}L_t^{*2}b_t^* + m_{313}a_t^{*2}L_t^* + m_{314}a_t^{*2}b_t^* + m_{315}b_t^{*2}L_t^* + m_{316}b_t^{*2}a_t^* + \\
&+ m_{317}L_t^*a_t^*b_t^* + m_{318}L_t^{*3} + m_{319}a_t^{*3} + m_{320}b_t^{*3}
\end{aligned}
$$

Figure 3: Polynomial function used to emulate the reference instrument

These equations can be written in matrix form as shown in Figure 4:

$$\begin{bmatrix} L'^* \\ a'^* \\ b'^* \end{bmatrix} = [m_{ij}]_{3x20} \cdot \begin{bmatrix} 1 \\ L_t^* \\ a_t^* \\ b_t^* \\ L_t^* a_t^* \\ \dots \\ b_t^{*3} \end{bmatrix}_{20x1}$$

Figure 4

Where "M" matrix is the coefficient matrix we want to calculate.

The "M" matrix could be calculated by obtaining the pseudoinverse matrix because it is not a square matrix and the inverse matrix cannot be obtained directly. But in this study we have used a minimization routine from Matlab software called "lsqlin". This routine solves problems by using a linear least squares adjustment with constraints. Although in this case, we do not work with any restriction.

3. Results

Part one:

- Results of the measurements made in the ceramic tiles

We have obtained two different sets of results, the measurements made in the nine ceramic tiles and the ones in the colour charts.

The measurement made to the ceramic tiles are presented in tables that include the average values of L*, a*, b* for each instrument obtained in the nine tiles of the following colours; White, Black, Red, Blue, Green, Yellow, Cyan, Gray and Pink.

In each table are presented the L*, a*, b* values for each instrument, the difference of all the L*, a*, b* values expressed as ΔE*, the mean ΔE*, and the average L*, a* and b* obtained.

The ΔE* values for each instrument have a colour code that indicates if this value is:
Acceptable: Green; ΔE* <1
Average: Yellow; 1 <ΔE* <1.5
Unacceptable: Red; ΔE*> 1.5

In addition, the instrument that gives a higher ΔE* value is highlighted in red; this is used to know if there is one that always gives different results from the others. The following table is an example of the results obtained when a tile is measured with the different instruments.

Table I

	White Tile			
	L*	a*	b*	ΔE*
DAE0009-964	95,91	-0,12	3,15	0,24
DAE0024-530	95,83	-0,06	3,01	0,17
DAE0026-530	95,51	-0,14	3,03	0,41
PE0049-Espectrolino	95,88	-0,21	2,67	0,26
PE0089-530	96,14	0,02	3,19	0,41
DAE0019-i1	96,15	-0,42	2,63	0,45
DAE0042-i1	95,89	-0,36	2,78	0,23
Mean	**95,90**	**-0,19**	**2,92**	**0,31**
Standard deviation	**0,22**	**0,16**	**0,23**	**0,11**

- Results of the measurements made in the colour charts

To analyze the different areas of the visible spectrum a representation of all the measured patches was made. The ones with the higher deviation were highlighted in yellow. This allows us to quickly visualize if there is any area in which the instrument is behaving in a different way from the others, or if the differences are present throughout the entire spectrum.

In the results we have included the average and the standard deviation of the differences, (in ΔE^*, absolute, best 90% and worst 10%), as well as the maximum value of ΔE^*, (for the Absolute and for the best 90%).

Here is an example of the results obtained. In this case we haven't found big differences between the instruments' behaviour and the average behaviour, and there isn't any spectral area that gives different values.

Table II: ΔE^* results of instrument "DAE0009"

	Mean	Standard Deviation	Maximum
Total	0.46	0.16	1.26
Best 90%	0.42	0.12	0.64
Worst 10%	0.77	0.15	

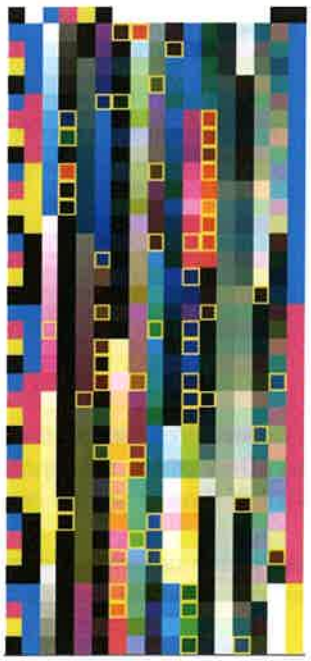

Figure 5:
Representation of the results of the instrument "DAE0009"

Figure 5 is a Graphic representation of the differences found in the measurements made in the colour chart with the instrument "DAE0009".

Part Two:

The "M" Matrix obtained to emulate the instrument "DAE0009" with the instrument "DAE0019" is shown in Table III:

Table III

M=	-4.9e-03	9.8e-01	8.1e-03	7.2e-03	4.3e-04	-1.1e+09	-7.6e+09	8.2e+09	-1.7e+09	-5.4e+09	...
	2.9e-02	7.7e-03	1.0e+14	-1.2e-02	6.5e+09	-3.6e-04	-4.4e+09	-9.3e+08	6.6e-04	2.3e-04	
	-4.8e-01	4.9e-02	1.9e-02	1.0e+14	-1.0e-03	3.2e-04	-2.6e-04	-1.9e+09	-2.6e-04	-1.7e-04	
		-2.4e+08	4.2e+07	7.3e+07	-1.3e+08	5.0e+06	1.5e+07	1.3e+07	1.8e+07	-9.3e+06	-3.1e+06
	...	-1.1e+08	4.4e+08	1.5e+08	-1.5e+07	-7.3e+08	-2.0e+08	-6.1e+07	-1.1e+08	-1.5e+08	-1.1e+08
		6.5e+08	-3.3e+08	1.2e+08	1.3e+08	4.0e+08	1.2e+08	5.2e+07	-1.4e+08	6.3e+07	3.0e+07

Once the "M" matrix is calculated, its adequacy (or performance) is evaluated by calculating the colour difference in ΔE_{ab} between the predicted colour after applying the correction factor, and the colour reference value. This difference is then compared with the initially calculated colour difference between the data and the colour reference value. Some of the results can be seen in Figure 6.

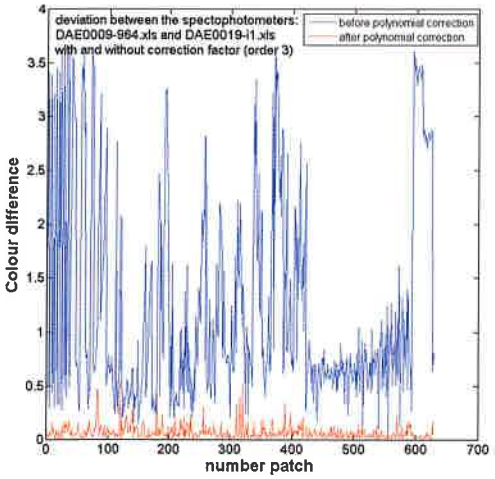

Figure 6

Some samples of the data set presented a not acceptable colour difference, even higher than before the correction factor was applied. This not occurred in a lot of patches, so it doesn't seem a problem related with the way the correction factors were calculated.

Therefore we cannot conclude that it is necessary to apply different correction factors depending on the colour we are measuring because it would lead us to find more samples with unacceptable colour differences. These differences in the calculation are more probably caused by flaws in the samples used in the exercise.

Table IV

$$M = \begin{vmatrix} 1.8e\text{-}02 & 1.0e{+}14 & -8.0e\text{-}03 & -6.3e\text{-}03 & -3.7e\text{-}04 & 1.0e{+}09 & 5.3e{+}09 & -7.4e{+}09 & 1.9e{+}09 & 7.7e{+}09 & \\ -2.4e\text{-}02 & -8.2e\text{-}03 & 9.9e\text{-}01 & 1.2e\text{-}02 & -5.4e{+}09 & 3.7e\text{-}04 & 5.1e{+}09 & 2.4e{+}09 & -6.6e\text{-}04 & -2.3e\text{-}04 & \cdots \\ 4.5e\text{-}01 & -4.5e\text{-}02 & -1.8e\text{-}02 & 9.8e\text{-}01 & 9.3e\text{-}04 & -3.3e\text{-}04 & 4.9e\text{-}04 & -6.1e{+}08 & 3.0e\text{-}04 & 1.0e\text{-}04 & \\ & 2.0e{+}08 & -3.7e{+}07 & -5.1e{+}07 & 1.2e{+}08 & -6.4{+}06 & -5.9e{+}07 & -1.2e{+}07 & -2.6e{+}07 & 7.1e{+}06 & 2.0e{+}06 \\ \cdots & 1.0e{+}08 & -4.5e{+}08 & -1.6e{+}08 & 1.5e{+}06 & 7.4e{+}08 & 1.8e{+}08 & 5.6e{+}07 & 9.7e{+}07 & 1.2e{+}08 & 1.2e{+}08 \\ & -5.9e{+}08 & 3.5e{+}08 & -3.4e{+}08 & -7.3e{+}07 & -4.9e{+}08 & 2.7e{+}07 & -6.1e{+}07 & 1.2e{+}08 & -8.3e{+}06 & -1.1e{+}08 \end{vmatrix}$$

4. Conclusions

Part one

After analyzing the results we reach some conclusions:

- We have found differences of more than 2 ΔE* between instruments when we measured the ceramic tiles.
- We haven't found any instrument that behaves in an especially different way from others, not depending of the spectrophotometer brand, model or condition. Nevertheless almost all of them in at least one tile have shown differences with the reference values of more than 1.5 ΔE*.
- After completing more than 20.000 measurements of the different colour patches covering almost the entire visible spectrum with eight very different spectrophotometers, we can conclude that we have enough data to characterize these instruments.
- We have found differences above 5ΔE*, which is over the tolerance specified in different colour standards. Differences like this make colour communication impossible.
- Nearly all the instruments show differences in specific areas of the visible spectrum, which may indicate differences in the manufacture of these instruments.
- After analyzing the results we can conclude that this is a correct way to assess the behaviour of the different instruments.
- We have found much bigger differences when comparing the measurements made with the colour charts than the ones found in the measurements done on the nine tiles which indicate that the standard 12 BCRA tiles are insufficient to evaluate how the spectrophotometers perform.
- Instruments of the same make and model behave in a different way, so we need to monitor these instruments and try to emulate them.
- Following the results obtained in the reproducibility study of the different instruments, and the differences found between them, it is necessary to obtain a mathematical function that performs the appropriate correction on the measurements made by the different colour measurement devices in order to obtain colorimetric data corrected and adjusted to a reference spectrophotometer.

Part two

The results obtained after applying the correction factor based on an order three polynomial adjustment are satisfactory and suggest that it can be used throughout the entire visible spectrum, as can be seen by the fact that the obtained difference in colour after the application of the polynomial adjustment in the whole training set is under the established tolerances $\Delta E_{ab} < 1$.

But the used algorithm doesn't work so well for all instruments. In particular, when we tried to emulate the behaviour of the Gretag Magbeth "i1" (DAE0042) with the "X-Rite 964" (DAE0009), the results weren't entirely satisfactory as can be seen in Figure 7.

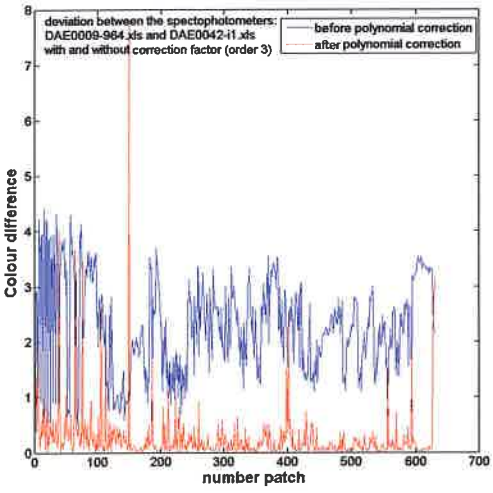

Figure 7

As an example, in Table IV we also present the results considering the two instruments of Table III, but reversing the roles. In other words we have changed which acts as reference instrument and which acts as a test instrument.

It's easy to see that a new "M" matrix obtained now coincides with the inverse matrix of the first "M" matrix, as expected.

Despite this, it can be concluded that this mathematical tool is useful but could be improved to make the appropriate correction between different instruments.

In particular, Table V summarizes some statistics on the results of the two previous examples.

Table V

	Mean	Standard deviation	Maximum	Minimum
DAE0019-i1→ DAE0009-964	0.0601	0.0653	0.5292	2.3599e-027
DAE0009-964 → DAE0019-i1	0.0650	0.0755	0.6476	2.9188e-029
DAE0042-i1 → DAE0009-964	0.2480	0.5181	7.7886	7.0220e-027

From these results, it can be concluded that we can achieve big improvements in reducing inter-instrumental differences by using polynomial-type function adjustments to colour measurements.

Further research in this study will include a set of test data to ensure that this matrix provides colour differences regardless of the data set considered.

To verify these results, we will evaluate the matrix with another set of different data from the training data set.

Acknowledgements

This research was financed by the Generalitat Valenciana, through IMPIVA by means of the grant number IMIDIN/2008/46 and co-financed by the ERDF: European Regional Development Fund.

References

1. Andrew Williams, 2008, IFRA "Improving inter-instrument agreement in colour and density measurement" in Advances In Printing And Media Technology Vol. XXXV
2. Schanda, János D., 1997, AIP-Press "Colorimetry". Handbook of Applied Photometry
3. Bala, Raja, 2003, CRC Press, "Device Characterization". Digital Color Imaging Handbook
4. Bruce Fraser, Fred Bunting, Chris Murphy, 2003, Peachpit Press "Real World Color Management"
5. Anon, 1998, Konica Minolta "Precise color communication"
6. Kang, H. R. Color Technology for electronic imaging devices (1997). *SPIE-The International Society for Optical Engineering.* Chapter 3:55-62
7. C. Li, M. R. Luo: "Effective correction modelling between colorimetric datasets". *Proc. 14th Color Imaging Conference - CIC* (Scottsdale, 2006), 14, 252-256 (2005)

Rotogravure spot color proofing for decorative laminates using SmartColour iVue software

Alexandra Pekarovicova[1], Veronika Chovancova-Lovell[2], Sangmeshwar. L. Sangmule[1], Paul D. Fleming[1], Yu Ju Wu[3], Bill Guillot[4]

[1] Center for Ink and Printability, Department of Paper Engineering
Chemical Engineering and Imaging Western Michigan University, Kalamazoo, MI, 4909-5462, USA
E-mail: a.pekarovicova@wmich.edu

[2] Sun Chemical Corporation, Daniel J. Carlick Center, Carlstadt, NJ 07072, USA
E-mail: veronika.lovell@sunchemical.com

[3] School of Technology, Eastern Illinois University, Charleston, IL, 61920, USA
E-mail: ywu@eiu.edu

[4] OMNOVA Solutions, Inc., 2011 Rocky River Rd., Monroe, NC 28110,USA
E-mail: bill.guillot@omnova.com

Abstract

Spot colors are widely used in commercial, product or packaging printing to obtain a colorful appearance. In this work, we focused on spot color matching and gravure printing of decorative paper laminates. For proofing of spot colors, SmartColour™ iVue software was used. The iVue software enabled us to predict how the press job that was run on a low basis weight substrate will look like on a different substrate, in this case solid bleached sulfate board, based on the previously measured and proofed ink systems that are saved in Sun Chemical's Global Shade Library. The library is accessed via the iVue software and gives the way of choosing and implementing various ink systems on diverse substrates printed at different press conditions.

Two different ink jet printers were evaluated for their ability to cover the color space of the proposed library. The extra inks that are being incorporated into the newer versions of the digital printers allow for better color control and larger coverage of a color space. One of the printers was then used to produce a proof of the design that would be printed on a specific substrate and will be able to match the original press print. The proof was also previewed in the iVue application and compared to the preview of the commercially available prepress design software. The overprint model and the ability to work with the real data and ink settings in iVue produce incomparable better results when previewing the final job just on a calibrated monitor display.

Keywords: rotogravure, spot color matching, SmartColour iVue, digital proofing

1. Introduction

Specialty colors are commonly utilized in many printing processes in order to obtain larger color coverage when the standard process ink set cannot satisfy customers' needs [Hrehorova, 2005; Wilson, 2005]. Product branding, companies logos, or package branding are the areas utilizing spot color inks. Spot colors can be produced by mixing pr ocess color inks or using specialty inks on separate print units. The wallpaper industry, decorative furniture laminates and laminated flooring printed with gravure process have to look for providing customers with designs representing accurately matching colors of the gravure printed job and at the same time customers demanding constantly shortening lead times [Geerinckx, 2003]. The elimination of cylinder engraving at a proofing stage reduces cost for sample production to half of what it was per square meter of traditionally produced sample [Geerinckx, 2003]. Furthermore, with elimination of gravure proofing presses goes also dramatic reduction of ink and paper consumption. According to Chiyoda, Belgian decorative laminates manufacturer, digital proofing and sample preparation reduced paper waste up to ten times compared to traditional technology [Geerinckx, 2003]. With their unique properties, inkjet proofing and printing provides significant time and cost savings compared to conventional procedures (preparing image carriers and printing proof samples) for potential product verification, matching, and short run production [Suchy, 2005; Wu, 2006; Wu, 2008].

Digital proofing with good spot color matching is extremely important also for packaging and product printing, since they require the creation of economical proofs for spot colors, too. With the combination of the right software, inks and media, an inkjet printer can be treated as a digital proofer for spot color printing, providing significant time and cost savings compared to conventional procedures for job approval of printing technologies with or without master image carriers. In addition, using digital printers, short run jobs can be printed instead of using an analog press. The advantage is that a costly process of image carrier preparation could be eliminated for certain extremely short run jobs.

The possibility of implementing digital proofing is closely related to the developments in color management workflows [Sharma, 2004]. To mimic actual properties of a gravure press, using a different printing process, different inks, materials, and possibly devices at different locations, is quite a complex problem. The key to matching proof to press is how accurately the digital color numbers can be manipulated in comparison to printing set up. With a properly color managed workflow, where correlations between different printing devices are established via device profiles, and characteristics of materials used are taken into account, the flexibility of digital data processing allows digital proofs to simulate printing presses with an ink jet printer [Stewart, 2007; Suchy et al., 2005; Lo, 2006]. Digital proofing solutions for packaging or product printing require separate channels for each of the spot colors, specify substrate stock and use specific software to drive digital printers [Hamilton, 2004].

Recently, the main ink jet printer/proofer manufacturers introduced new proofing devices that employ extra ink cartridges with specialty inks added to the regular CMYK set of colors. These can include Red, Green, Blue and Orange inks in addition to the standard set of colors and their lighter options. The main reason for adding the specialty colors is the ability to cover a larger color space in order to correctly simulate the spot color from the presses.

The aim of this work was spot color matching and gravure printing of decorative paper laminates, or matching existing gravure print digitally, to create new samples for customers, or create the same design on different substrate, with the least possible color shift. For proofing of spot colors, SmartColour™ iVue software was used [SmartColour, 2009]. SmartColour iVue is an innovative color management system, which allows viewing predicted spot color at every stage of the process of design workflow. It also allows for an accurate production of digital hard proofs and soft proofs on the monitor screen. The color information is provided for a real ink on real substrates using real print processes. The same color can be then obtained, whether it's on the screen, on a proof or on a final printed product.

2. Methods and results

2.1 Press run

Yellow, orange, brown and charcoal spot colors were used for gravure printing of a wood grain design (Figure 1). Solvent based proprietary inks had surface tension in the range 21 - 23 mN/m, about 20 mN/m lower than the surface energy of the substrate, thus good wetting properties were ensured. Particle size of inks was measured using Submicron Particle Sizer 370 NICOMP based on dynamic light scattering. Inks particle size was as follows: 98 ± 19.5 nm for yellow, 116 ± 23.6 nm for orange, 131 ± 22 nm for brown and 305 ± 58 nm for charcoal ink. Inks viscosity measured as efflux time on Shell #2 cup was 18 - 22 s.

An EMVECO stylus profilometer was used to determine roughness of the paper substrates. An Autopore IV 9500 mercury porosimeter, measuring the incremental increase of volume penetrated as the pressure rises, was employed for the porosity-related characteristics, such as of pore size, and total pore volume. A first Ten Angstrom FTA200 contact angle instrument was used to measure contact angle with water and hexadecane. Results from FTA200 were averaged from ten values of surface tension or contact angle for individual drops. The interactions between liquid and paper surfaces were demonstrated in terms of the dispersive and polar energy contributions according to the Owens and Wendt equation [Owens and Wendt, 1969; Barber et al., 2004; Pietak et al., 2007]. Total surface energy of low basis weight paper used for gravure press run was 42.2 mJ/m. Some of physical and optical parameters of both print substrates for press run and digital proofing are given in the Table I.



Figure 1: Wood grain design with spot color control patches

Table I: Selected properties of print substrates

Substrate	Low Basis Weight Paper (LBW)	Semi-matte Inkjet Paper
Emveco Roughness [μm]	1.88	1.06
Average pore diameter [nm]	396.9	47.4
Porosity [%]	36.7	28.9
Opacity [%]	55.6	96.7
Specular gloss at 75 deg [%]	22.5	47.5

The final print job, including tone step gradations for all four spot colors, and wood grain pattern (Figure 1), was done on a Cerutti (Cerutti Model 118, Italy) four color web fed gravure press using LBW paper. Cylinders were electromechanically engraved with 120-150 lpi resolution, creating cells with 40 - 60 deg compression angles. Press speed was 700 ft/min, electrostatic assist was on at all four stations. The order of colors was yellow-orange-brown-charcoal at all times.

2.2 Proofer test

Two different Epson ink jet proofers were evaluated in terms of gamut size and the ability to reproduce different spot colors. The printers differ in number of colors employed, Epson Stylus Pro 9800 uses C, c, M, m, Y, K, LK, and Llk (Cyan, light Cyan, Magenta, light Magenta, Yellow, Black, light Black and Light light black) inks, and Epson Stylus Pro 7900 uses the same set plus G and O (Green and Orange). The gamut projection in 3D and 2D were obtained in CHROMiX ColorThink Pro 3 from the calculated ICC profile. The profiles were created for both printers on semi-matte ink jet substrate, characterized in the Table I. Figure 2 shows the comparison of the two printers as a 3D and 2D projection of color space. Gamut volumes were calculated in the same application, the values are shown in Table II.

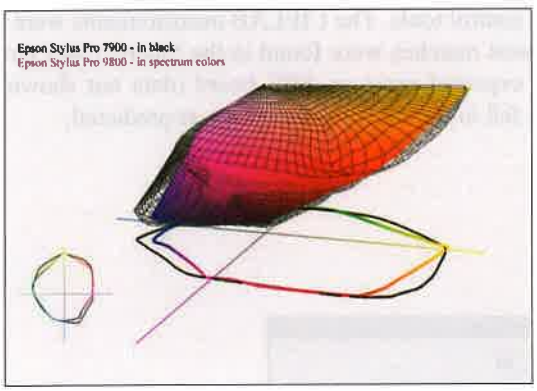

Figure 2:
3D and 2D projection of color space of two different Epson printers

Adobe® Photoshop has an option for a SmartColour iVue plug-in. The software is equipped with the SmartColour Color Picker (Figure 3), which enables using specific ink on a discrete substrate and predicts color appearance of an actual print. The color picker allows individual selection of colors for any spot element either from brand-specific libraries or general libraries. All libraries contain colors from common substrates and print parameters allowing selection among those colors that can be achieved on press.

Fifty different spot colors shown in Figure 4 were picked from a specific gravure library to create a target for testing the digital proofer ability to match the colors on an ink jet printed proof. These colors were picked to cover the largest portion of color space and differ in lightness and hue. Some of the colors are intentionally out of the printers' color gamuts to evaluate the matching process. The color accuracy of both printers was evaluated

in terms of color differences between the stored CIELAB data of the target and measured CIELAB data on the digital proofs.

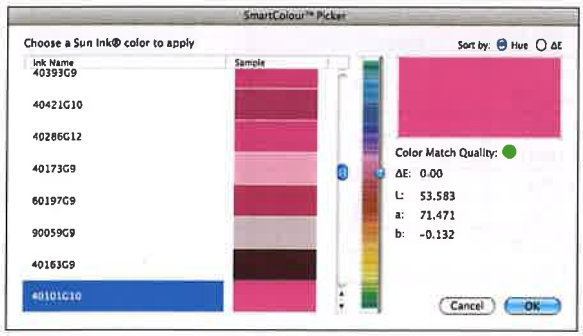

Figure 3: Example of SmartColour iVue Color Picker with the Gravure Library Shades

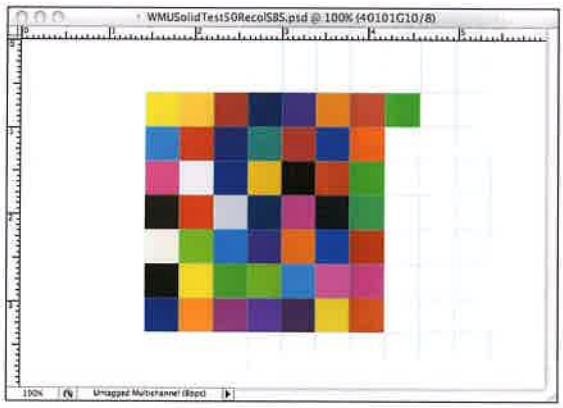

Figure 4: Fifty Test Colors from the Gravure Library Shades

A spectrophotometer i1-iO from X-Rite with 45°/0°degree geometry was used with no filter applied; the CIELAB data were calculated for D50/2° illuminant/observer combination. Color differences were expressed in Delta E_{ab} and Delta $E_{cmc\ (2:1)}$, which were specified by customer request.

Table II: Gamut volume and color accuracy of digital printers Epson Stylus

	ΔE_{ab}	ΔE_{ab}	$\Delta E_{cmc(2:1)}$	$\Delta E_{cmc(2:1)}$	Gamut Volume
	Mean	Max	Mean	Max	cCu
Pro 9800	3.83	14.84	1.63	4.33	741,513
Pro 7900	2.91	7.34	1.60	3.59	853,212

2.3 SmartColour iVue proofing

SmartColour iVue software was used to match four spot colors necessary to print wood grain pattern on the newly picked simulated SBS substrate (Figure 5), semi-matte ink jet and LBW paper. The wood grain design included solid and tone patches in order to provide color control tools. The CIELAB measurements were taken for the solid four spot colors on LBW paper and the closest matches were found in the SmartColour Gravure SBS library (Figure 6). Color differences between the expected press on SBS board (data not shown) and current press print and digital proof on semi-matte prints fell in the ΔE 2 - 4 unit range as predicted.

Spot 1 - Yellow ($L^* = 80.05$, $a^* = 9.93$, $b^* = 31.31$)
Spot 2 - Orange ($L^* = 70.69$, $a^* = 22.05$, $b^* = 45.24$)
Spot 3 - Brown ($L^* = 59.84$, $a^* = 23.48$, $b^* = 33.23$)
Spot 4 - Charcoal ($L^* = 23.80$, $a^* = 0.94$, $b^* = 1.41$)

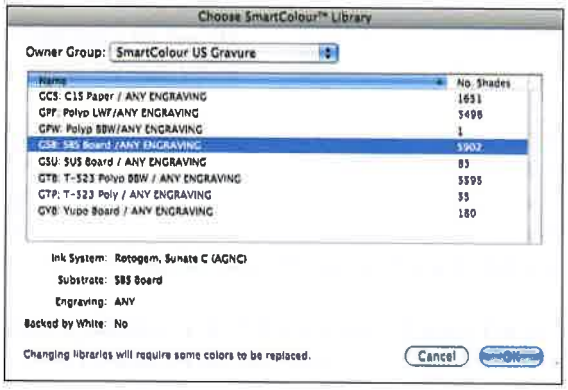

Figure 5: SmartColour gravure library for SBS board using rotogem sunate ink system

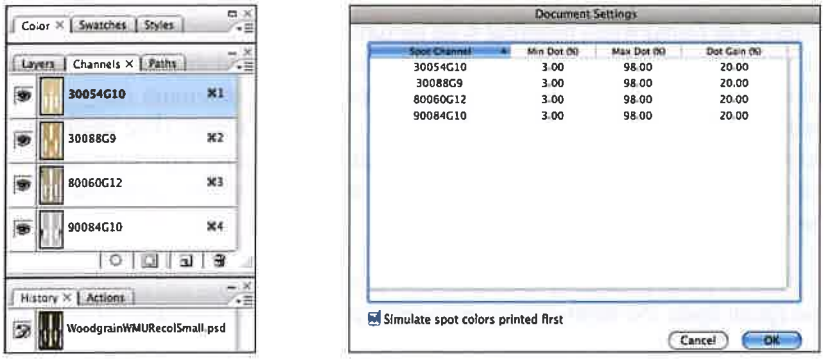

Figure 6: SmartColour re-colored spot channels and document settings

The design was rendered using the SmartColour iVue color management engine and displayed in the SmartColour Preview window on a calibrated monitor with an ICC profile assigned to it. Accurate previewing is a key feature of iVue and helps to prevent mismatches at press due to inaccurate spot color predictions throughout the workflow. In order to send the data to a digital printer or correctly preview the design on a monitor SmartColour iVue engine renders the image on pixel-by-pixel basis and calculates the color CIELAB values for single color or overprints of the spot colors.

The illustration of final job previewed on a calibrated monitor is shown in the Figure 7. It shows the difference between the Adobe Photoshop Preview window on the left and SmartColour Preview window on the right displayed on a calibrated Apple Cinema Display. The SmartColour rendered image applies the substrate characteristics and shows more true looking and accurate results.



Figure 7: Wood grain design displayed in Adobe® Photoshop (left) and SmartColour iVue (right)

The hard proof was printed on a digital ink jet printer on semi-matte digital paper using a specific ICC profile. Specific tone value increase at 50%, minimum dot and maximum dot values can be set for each spot channel in order to match specific press conditions or simulate the condition of the press that the job will be printed on. This option is also very valuable in predicting the result on a different substrate, such as SBS board in this case. Color differences between actual digital and press proofs are listed in Table II, which includes ΔE values for prints with no simulation of paper white. The same measurements were done with simulation of paper white, as listed in the Table III. Print without simulated paper white resulted in slightly lower overall ΔE_{ab} and $\Delta E_{cmc(2:1)}$ (data not shown), and the reason for it is probably because the yellow print separation gives almost 100% total area coverage to create basis for wood grain pattern, and thus paper white does not affect the color appearance of the printed job.

The next step was to digitally proof on the actual press substrate, LBW paper, which was done only on the Epson Stylus Pro 9800. It was decided that it is not necessary to deal with tone value increase on yellow printer, because it will print close to 100% coverage on all wood grain area anyway. Multiple tests were conducted to come up with best match for wood grain pattern. It should be noted that the digital printers are not designed to

use press production substrates, as these are not coated with ink jet ink receptive coatings. The best visual match of wood grain pattern was found when proofing with no tone value increase for yellow, orange, brown, and 25% TVI for charcoal. The color difference between original press proof and digital proof on LBW was $\Delta E_{cmc(2:1)}$ = 1.78 for solid yellow, maximum $\Delta E_{cmc(2:1)}$ was 10.60 for orange; and maximum $\Delta E_{cmc(2:1)}$ 10.95 for brown. The worst match was found for charcoal printer, with $\Delta E_{cmc(2:1)}$ 16.21. Software iVue treats the printer as an RGB device, and there is no control over dealing with the black printer, creating four color black with maximum a* of -8.22. Figure 8 shows running $\Delta E_{cmc(2:1)}$ values of between the digital proof and the press print on the low basis weight paper printed on Epson Stylus Pro 9800.

Table II: Delta E values of solid spot color between press sheet and digitally printed on Epson Stylus Pro 9800 on semi-matte inkjet paper without simulation of paper white

Color	ΔE_{ab}	$\Delta E_{cmc(2:1)}$
Yellow	5.83	3.05
Orange	2.69	1.47
Brown	3.38	2.51
Charcoal	3.72	3.76

Table III: Delta E values of solid spot color between press sheet and digitally printed on Epson Stylus Pro 9800 on semi-matte inkjet paper with simulated paper white

Color	ΔE_{ab}	$\Delta E_{cmc(2:1)}$
Yellow	3.71	3.24
Orange	4.13	2.38
Brown	6.81	5.07
Charcoal	2.74	3.41

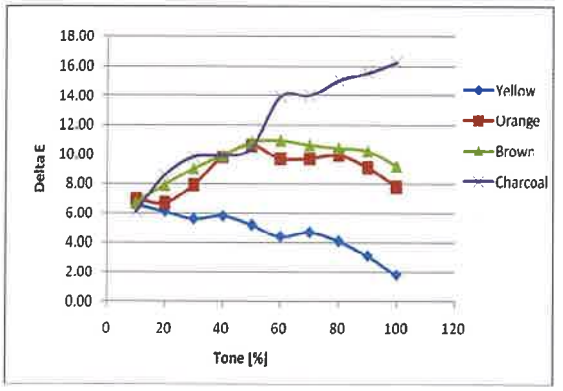

Figure 8: $\Delta E_{cmc(2:1)}$ of best wood grain digital match on LBW substrate

3. Discussion

The aim of this work was to confirm that depending on a specific substrate and a printing process and software application that enables selection of proper spot colors from a library of inks, previously matched on substrates with specified physical and optical properties, it is feasible to predict the results that will be achieved on a designated printing press. The software is also able to predict ΔE color tolerances to be expected on the press.

The print was achiev ed from a controlled gravure press run on a substrate that was designed for one type of application. This proof was then set to be a standard for matching the colors and design when printed on a different type of a substrate.

The same layout file was then brought to the SmartColour iVue application environment and the solid spot colors were matched to the ones measured for the press print. The specific library within the Global shade library was specified and the closest matches to all spot colors were found for a new substrate. The design was then rendered to the SmartColour iVue Preview window with specific settings set for the substrate, ink system and printing process.

The colors and the design of the print job were then checked on the screen, as SmartColour iVue offers the preview with all the possible press settings and overprint model available to the user. When the monitor display system is correctly calibrated and profiled, the iVue preview window shows the soft proof of the design when digitally proofed and printed on a press.

Two different ink jet printers were considered to be the devices for creation of digital hard proofs. The two proofers differed in the amount of the inks/colors used in them. One using the single CMYK set the other one in addition to CMYK set included Orange and Green inks. The digital proofers were submitted to the test of correctly proofing 50 different spot colors that were designed to cover the majority of the color hues. The colors were intentionally picked to be in and out of the proofers' achievable color gamut in order to see the rendering capabilities of both printers. Expectedly, the proofer with the extra ink set produces better results in achieving the correct colors on a digital media.

The digital proofs made for the SBS board were then printed in actual size on the digital printer using semi-matte inkjet substrate and compared to the press print made on the LBW paper. The capability to predict the real colors that will be achieved on the real press is available from iVue that is able to deliver the real press color data that were precisely measured, stored and maintained within the Global Shade Libraries.

We could see from this experiment that the accuracy of proof-press color matching is affected by the printer, software, and substrate involved in the digital proofing processes. There is also a significant dependence of color reproduction on the choice of substrate. This is manifested when attempting to proof spot colors on the same substrate as employed on the gravure production press. The gravure production substrate has a more open structure (with average pore size of 396.9 nm) than digital semi-matte paper (average pore size of 47.4 nm). It is likely that LBW is trapping the small ink pigment particles along with vehicle, which resulted in the smaller color gamut (111,997 cCu on LBW paper compare to 741,513 on semi-matte one), and larger ΔE values of solids compared to digital proofs made on semi-matte paper. The particle size of ink sets for both Epson Stylus Pro 7900 and 9800 were not measured at this point. Based on our past work on an Epson 2200, these digital inks should have particle size around 100 nm [Chovancova 2004, 2005], which is much smaller than the average pore size of the production LBW substrate, thus sinking of pigment into LBW porous network is inevitable.

Previously, authors were involved in several projects matching spot colors, but not their overprints [Wu et al., 2006; Wu et al., 2008]. The software SmartColour™ iVue is tailored for packaging printing. Therefore, in the library of inks and substrates are found substrates and inks for that purpose. If print on decorative laminates substrate, such as LBW paper, is to be color matched, we needed to test several different ink sets in iVue library to achieve the best match. Another issue in proofing of spot color inks is their overprint. The final appearance will definitely depend on particle size of pigments and other ink components, such as order of printing, among others.

4. Conclusions

In conclusion, with the well maintained calibrated and profiled system and a source of data that is available to any key user throughout the printing production process, starting with ideation, creation, prepress, proofing, and printing the real job, one is able to achieve reasonable good results from the start to the end of the workflow. With the help of Smart color iVue, it was possible to match gravure printed job on one substrate digitally to a different substrate, which can be helpful in creation of new applications for the same design. Also, it was possible to digitally print on production substrate with decent visual match. However, it was confirmed that Epson Stylus Pro 9800 was deficient in charcoal, especially in areas of 70 - 100% tone. Of course, ΔE values for production substrate printed on the digital press were much higher than those for manufacturer recommended digital paper, mainly due to its large porosity. For the best visual proof, it is necessary to match solids of first printer and achieve the best possible mid-tones for the charcoal.

References

1. Anon, (2009), SmartColour, http://www.sunchemical.com/products/services/services_catalog#, accessed June 27, 2009
2. Barber, A. H., Cohen, S. R. & Wagner, H. D., (2004), Static and Dynamic Wetting Measurements of Single Carbon Nanotubes, Physical Review Letters, 92, 18, 186103
3. Chovancova V., Howell, P., Fleming III, P. D. and Rasmusson, A., (2005), Color and Lightfastness of Different Epson Ink Jet Ink Sets, J. Imaging Sci. Technol., 49 (6), November/December, 652-659
4. Chovancova V., Howell, P., Fleming III, P. D. and Rasmusson, A., (2004), Printability of different Epson ink jet ink sets, Proc. IS&T's NIP20:International Conference on Digital Printing Technologies IS&T, Springfield, VA, pp. 457-463
5. Fenton, H. (2000), Digital is Faster, but not Always Better, Folio: The Magazine for Magazine Management, 29, 59
6. Geerinckx, J. (August 2003), A Teaming Technologies in the Gravure Decorative Printing Market, Gravure, 70-71
7. Hamilton, A., (2004), What is new in digital color proofing for package printing? Converting Magazine, 22, 6
8. Hrehorova E., Pekarovicova A. & Fleming P. D., (2005), Spot Color Consistency for Product Gravure, Proceedings of the 57th TAGA Annual Technical Conference, TAGA, Toronto, Ontario, 3-4
9. Hulsman, W. J. and Notermans, J. T. E. C., (2000), Color Management Requirements in Contract Proofing, IS&T's NIP 16: 2000 International Conference on Digital Printing Technologies, 796-800
10. Jouany, C., (1991), Surface Free Energy Components of Clay-Synthetic Humic Acid Complexes from Contact-Angle Measurements, Clays and Clay Materials, 39, 1, 433-439
11. Lo, M. C., Chen, C. L., Perng, R. K. and Hsieh, Z. X., (2006), The Characterization of Color Printing Devices via Physical, Numerical and LUT Models, CGIV 2006 Final Program and Proceedings, 95-99
12. Owens, D. K. & Wendt, R. C., (1969), Estimation of the Surface Free Energy of Polymers, Journal of Appl. Polymer. Sci. 13, 1741-1747
13. Pietak, A., Korte, S., Tan, E., Downard, A. & Staiger, M. P., (2007), Atomic Force Microscopy Characterization of the Surface Wettability of Natural Fibers, Applied Surface Science 253, 3627-3635
14. Stewart, R.: Choosing a Color Printer for in-house Proofing, Publish, http://www.findarticles.com/p/articles/mi_zd4149/is_200404/ai_n9475140, accessed August 8, 2008
15. Sharma, A., (2004), Understanding Color Management, Thomson Delmar Learning, 1st Ed., New York
16. Suchy, M., Fleming, III P. D. and Sharma, A., (2005), Spot Color Reproduction with Digital Printing, Proceedings of the IS&T NIP21: International Conference on Digital Printing Technologies, Baltimore, 93-97
17. Wilson, D. G., Signor, M. and Schmidt, K., (2005), Color Quality Assurance for Package Printing, Journal of Industrial Technology, 21, 1-3
18. Wu, Y. J., Fleming, III P. D. and Pekarovicova, A., (2008), Gravure Spot Color Reproduction with an Inkjet Printer, Journal of Imaging Science and Technology, 52, 6, 060501-1-060501-12
19. Wu, Y. J., Suchy M., Fleming, III P. D. and Pekarovicova, A., (2006), Quality Analysis of Spot Color Reproduction with an Inkjet Printer, Proceedings of the IS&T NIP22: International Conference on Digital Printing Technologies, Denver, September 17-22

Electric field assisted ink lifting in gravure

Soile Passoja, Jorma Koskinen, Robert Roozeman

Technical Research Centre of Finland
P. O. Box 1000, FIN-02044 VTT, Finland
E-mails: Soile.Passoja@vtt.fi, Jorma.T.Koskinen@vtt.fi, Robert.Roozeman@vtt.fi

Abstract

The influence of electric field on gravure ink lifting from engraved structures was studied. Ink transfer without electric field occurs only if the physical contact between ink and paper in the nip is achieved. The use of electric field in ink transfer promotes the ink lifting and enables the contact between ink and paper before the actual nip contact. In a nip a non-uniform electric field lifts the ink near the engraved edges over the cylinder surface. This phenomenon is explained by dielectrophoresis and supported by simulation. The electric field lifts the liquid on a microsecond timescale and it defines the ink transfer in gravure as the nip contact in the real press occurs on a millisecond timescale.

Keywords: gravure printing, electric field assistance, ink transfer

1. Introduction

In gravure printing efficient ink transfer defines print quality. However, quite often ink transfer related print quality problems can be seen as incomplete or totally missing dots. Normally electric field assistance (ESA) is used to promote ink transfer.

Gravure ink transfer has been studied widely and it has been shown that the use of ESA improves ink transfer. For example, Serafano et al. [1998] made a study of the optimal level of ESA to improve ink transfer. Sprycha et al. [2007] described the effect of ESA on ink - paper contact formation, and further, on dot formation. Experimental studies relating to liquid release from grooves and cells has been published by Yin et al. [2006]. In addition, modelling has been used to explain the liquid movements in electric field e.g. by Piette et al. [2002] and Powell et al. [2002].

The objective of this work was to study ink lifting in the nip when the ink is transferred with and without electric field. The efficiency of ink lifting from the cell was seen as the most important issue defining the contact formation between ink and paper. Two approaches were selected for studying the ink lifting: experimental studies in laboratory and numerical simulation with computer. Laboratory studies with simple engraved designs were used to illustrate the ink movements in the nip. The simulation was used to explain the experimental results and to look for deeper understanding of ink movements in the nip.

2. Methods

The influence of the electric field on ink movement was studied using a laboratory set-up with scaled-up engraved grooves and cells. V-shaped grooves of two different sizes were machined on a polished aluminum plate (Figure 1). In addition, a round cell, diameter ~ 200 µm, was drilled near the edge of the aluminum plate.

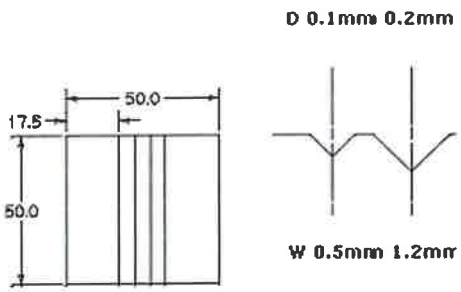

Figure 1:
Sketch of the aluminium plate with V-shaped grooves used for the study of ink lifting with and without electric field. Engraved aluminium plate (left) and the sizes of the engraved grooves (right)

An experimental set-up was arranged with an engraved aluminum plate and metal cylinder depicting the gravure printing cylinder and the impression roller, respectively. A paper sample was tightly wrapped around the cylinder (Figure 2).

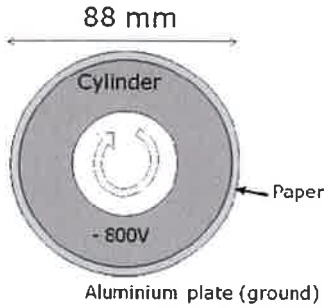

Figure 2:
Test arrangement for ink lifting studies

Ink transfer on paper was studied both with and without electric field. The experiments were carried out with the test device connected to an adjustable power source. The aluminum plate was set to ground potential and the voltage of the metal cylinder was set to - 800 V. This voltage level was chosen as it corresponds to the surface potential of real impression rollers. The nip pressure was kept constant during the tests.

The ink lifting tests were carried out by putting a droplet of ink into a groove or cell. The ink amount was constant as the excess of ink was doctored off with a razor blade before starting each experiment. After doctoring the paper-covered metal cylinder was rolled over the groove or cell at a speed of about 1 cm/s. The ink lifting was monitored from the side using a black and white camera taking 60 frames per second. This corresponds to a 16 ms time interval between images. A picture size of 512 x 480 pixels was used. The actual size of the image was 2.7 mm x 2.5 mm giving a resolution of 5.3 µm/pixel. Three light sources were used during imaging.

The ink lifting tests were carried out using commercial, cyan packaging ink, and coated paper. The viscosity of the ink was 27 s (measured with a DIN4 cup) and the average pigment size was 201 nm. The pigment size was measured using a Coulter N5 submicron particle size analyzer. The commercial coated paper had 58 gsm grammage, PPS10 roughness 0.98 µm and oil absorption 2.6 ml/m² (measured with the KCL nozzle applicator: transferred amount of mineral oil during 10 ms). The Heliotest result of this coated paper was 74 mm.

Numerical simulation was used to gain knowledge from the liquid movements in an electric field. The simulation is based on the notion that in a suitable geometry with abrupt changes, the electric field will be non-homogenous. For example, close to sharp edges the electric field is stronger. The explanation is dielectrophoresis: the movement of a liquid caused by a non-homogeneous electric field as explained by the Korteweg-Helmholtz equation (Eq. 1). It describes the force density in a dielectric fluid.

$$\vec{f} = \rho_f \vec{E} - \frac{1}{2}E^2\nabla\varepsilon + \nabla\left[\frac{1}{2}E^2\frac{\partial\varepsilon}{\partial\rho}\rho\right] \quad (1)$$

Here, f is the force density (force per unit volume), ρ_f the density of free electric charge within the liquid, E the electric field, ε the permittivity, and ρ the density of the material.

Starting from the Eq.1, a model was developed to simulate the impact of an electric field on a dielectric liquid. The liquid was assumed to be Newtonian and its movement was simulated using the Navier-Stokes equation. The physical properties of the simulated liquid were those of toluene since its properties are better known than the once of the ink. The simulation was carried out using standard gravure cell geometry in a slightly tilted (2°) plate geometry imitating the approaching impression roller in the nip.

3. Results

The side view monitoring of the ink movements in the nip shows the importance of the ink-paper contact in ink transfer. When transferring ink without electric field the ink surface in the groove does not move and the ink transfer occurs only if a physical contact between ink and paper is achieved (Figure 3, top). When the electric field is applied to the system (Figure 3, bottom) the ink is lifted from the groove even before the actual physical contact between the ink and the paper. This early lifting of ink surface enhances the ink transfer.

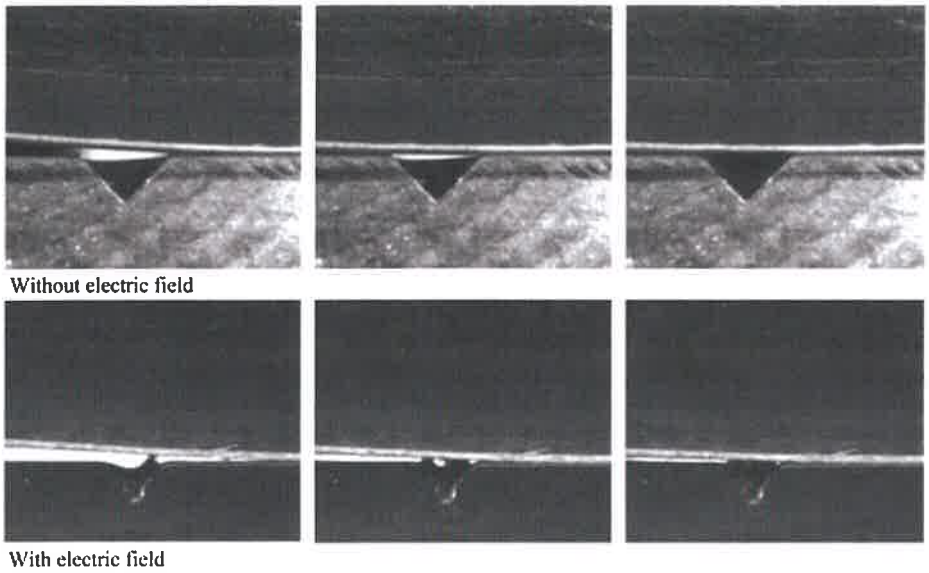

Figure 3: Gravure ink lifting from an engraved groove without (top) and with electric field (voltage - 800V, bottom) using a laboratory set-up

The image series at the bottom of Figure 3 shows how the electric field lifts the ink surface from both front and back edges of the groove. This increases the concavity of the ink surface in the groove resulting stronger contact between ink and paper mainly at the edges of the groove. We suggest that this phenomenon can explain the formation of the doughnut shaped printed dots.

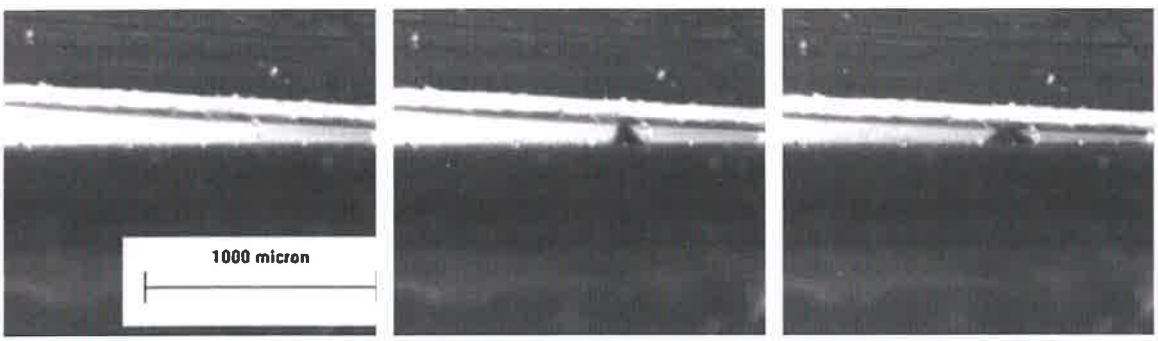

Figure 4: Gravure ink lifting from round cell to paper, diameter ~ 200 µm. Voltage - 800 V

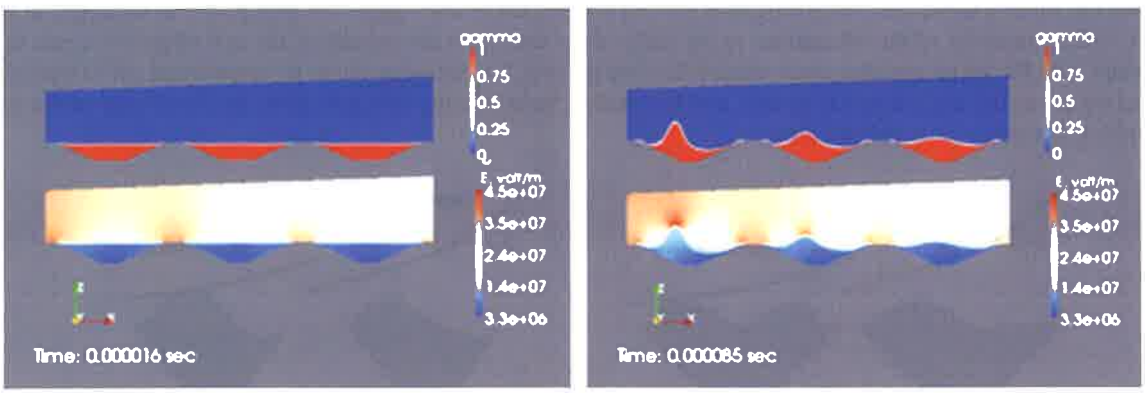

No electric field Strong electric field

Figure 5: Simulation of liquid behavior in cells under non-uniform electric field conditions. Upper graph: movement of liquid in an electric field. Lower graph: electric field strength distribution in engraved structure, higher field level in red

Ink lifting from a round cell with electric field is shown in Figure 4. In round cell design we are able to notice ink lifting as the impression cylinder with electric field is approaching the cell: the ink is raised before the actual physical nip contact resulting in easier ink transfer.

The simulation confirms the observations of the experimental work: the liquid moves first towards the "approaching" plane showing that the effect of the electric field is the strongest at the cell side which is the closest to the charged plate. Moreover, the liquid movement occurs inside the cell and the ink is lifted near the cell edges. Figure 5 shows the simulation of liquid behavior in a cell as the result of the non-uniform electric field.

The agreement between the experimental ink lifting studies and the simulation is excellent. This allows us to think that dielectrophoresis is a very credible explanation for the observed ink behaviour.

The ink lifting experiments were carried out at quite a low speed when comparing those to the actual printing speed at the press. The simulation, however, showed that the liquid movement in a non-uniform electric field occurs on a microsecond timescale whereas the printing nip contact time is on a millisecond timescale. Differences in timescale proves that this kind of ink lifting can take place in a real printing process and, further, the liquid movement in an electric field is so fast that the experimental studies of ink lifting at low speed do not restrict the validity of the experimental results.

The influence of the electric field on ink movement with several cells next to each other was simulated as well. This simulation showed that the electric field is the strongest in the non-image areas between big cells. The strong electric field at the narrow non-image areas promotes ink lifting providing easier ink release from the bigger cells. Smaller cells that are also situated quite far from each other do not experience this enhancement and the ink lifting force generated by the electric field is therefore lower. This might partly explain uneven ink release from the smaller cells that can lead to incomplete or missing dots.

4. Discussion

The laboratory arrangements in ink lifting studies may raise a question of how relevant these studies are in real gravure nip conditions. One could criticize the scale of the used experimental set-up: the engraved designs were bigger than the actual engraved cells of a printing cylinder. The groove set-up and the bigger dimensions of the engravings were selected mainly to visualize the effect of the electric field in ink lifting. Furthermore, the set-up provided a possibility to monitor the ink movements in nip conditions. Actually, the ink lifting studies with the engraved cell correspond well to the actual printing cylinder cell as the size of the studied cell was only slightly bigger than the size of the biggest cells (diameter up to 145 μm) in an engraved gravure cylinder. Also the simulation supported the experimental observations of the ink lifting studies.

When we consider the influence of the orientation of the mechanically engraved cell on ink lifting we can assume that the orientation of the cells has an influence on the efficiency of the electric field in ink lifting (Figure 6). In elongated cells (typically used for magenta) the nip contact between ink and paper is longer and the electric field has more time to act on both front and back edges of the cell. This two-sided ink lifting increases the concavity of the ink surface in the cell. Ink lifting near the cell edges induces ink - paper contact mainly at the edges of the cell. If the concavity of the ink surface in the cell is deep the ink in the middle of the cell might not come into contact with the paper and doughnut shaped dots are printed. On the other hand, in compressed cells (typically used for cyan) the nip contact is shorter and the electric field lifts the ink only from the front edge of the cell resulting in more evenly printed dots.

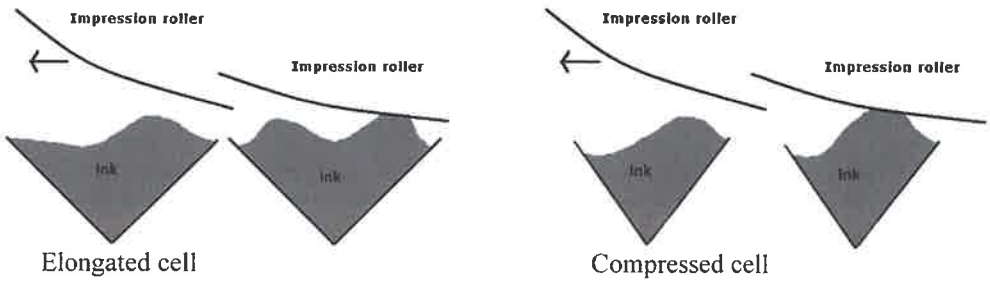

Figure 6: Influence of the cell orientation on ink lifting in an electric field

The simulation of liquid movements in a non-uniform electric field was carried out using the physical properties of toluene and using only an air gap between the charged plates instead of paper. This simplification of the nip phenomena showed clearly the ink movements in the nip. In the future, the simulation is planned to be expanded with the values of real printing ink and with the relevant values of paper, such as thickness, moisture content and electrical properties. With this extension of the model we expect to establish more precisely the critical parameters affecting ink lifting efficiency in gravure.

5. Conclusions

The study showed that the electric field lifts the gravure ink from the engraved structure even before nip contact thus promoting ink transfer. In the nip, the non-uniform electric field raises the ink inside the cell: the ink is lifted near the cell edges above the cylinder surface. This phenomenon can be explained by dielectrophoresis, which takes place on a microsecond timescale. This fast liquid movement determines the ink transfer as the nip contact occurs on a millisecond time on a real gravure press.

The developed simulation model provides excellent possibilities to study the underlying mechanisms affecting gravure ink lifting and ink transfer. The model will be used in further studies by adding the values of ink and paper properties to gain deeper understanding relating to formation of incomplete or missing dots. Furthermore, the model provides possibilities to find out the optimal shape of the engraved cell with respect to ink lifting and ink transfer efficiency. Also the optimal ink amount in the cell or the ink viscosity for ink lifting is expected to be solved for various printing conditions.

Acknowledgements

This work was done at KCL and the authors thank Asko Sneck, Yingfeng Shen and Katja Jokiaho for their essential input at all stages of the work. The financial support of Metsäliitto, Myllykoski, Stora Enso and UPM-Kymmene is gratefully acknowledged.

References

1. Sprycha, R., Durand, R. Jr., Pace, G., (2007), *Mechanism of abnormal dot deformation in gravure printing,* TAGA, pp. 42-45
2. Serafano, J., Triantafillopoulos, N., (1998), *Optimizing ESA To Improve Ink Transfer, Ink World,* 5, pp. 22-25, 67
3. Yin, X., Kumar, S., (2006), *Flow visualization of the liquid-emptying process in scaled-up gravure grooves and cells, Chemical Engineering Science,* 61, pp. 1146-1156
4. Piette, P., Trehoult, C., (2002), *Ink transfer theory in Rotogravure Printing, International Printing and Graphics Arts Conference, Bordeaux,* p. 5
5. Powell, C. A., Savage, M. D., Guthrie, J. T., (2002), *Computational simulation of the printing of the Newtonian liquid from trapezoidal cavity. Methods for Heat & Fluid Flow,* 12, 4, pp. 338-355
6. Jones, T., (2002), *On the Relationship of Dielectrophoresis and Electrowetting. Langmuir* 18, pp. 4437-4443



Spray inking unit for offset printing machines

Gert Schlegel[1], Arved Hübler[1], Robert Thieme[1],
Alexander Böddicker[1], Thomas Hädrich[2], Günter Wozniak[3]

[1] Chemnitz University of Technology, Institute für Print und Media Technology
Reichenhainer Straße 70, D-09126 Chemnitz, Germany
E-mails: gert.schlegel@mb.tu-chemnitz.de, arved.huebler@mb.tu-chemnitz.de,
robert.thieme@mb.tu-chemnitz.de, boale@hrz.tu-chemnitz.de

[2] SIVUS gGmbH
Schulstraße 38, D-09125 Chemnitz, Germany
E-mail: TH@innovent-jena.de

[3] Chemnitz University of Technology
Professorship of Fluids Mechanics
Straße der Nationen 62, D-09111 Chemnitz, Germany
E-mail: guenter.wozniak@mb.tu-chemnitz.de

Abstract

This paper has two objectives: First, it aims at defining theoretically and determining by means of experiments ink film formation of sprayed offset printing ink. This refers to the analytic description of the surface covering process in the inking system of an offset printing press. Influencing factors are the temperature-dependent, rheological properties of the printing ink and the resulting drop size spectrum of an offset printing ink sprayed with a two-component jet (external mixture). The main problem is to transfer standard, highly viscous, sticky offset inks into a sufficiently fine spray that guarantees a fine, homogeneous ink film on an ink carrying roller in the inking system of an offset printing press.

The second aim is to design a prototype of a functioning spray inking system and to determine optimum working parameters for the employment of this new inking system in an offset printing press. The analysis is focused on standard offset printing ink (heatset ink, black). Practical tests are done on a rotary offset press.

Keywords: offset printing, inking unit, atomization, spray, nozzle

1. Introduction

The Offset Printing Process is the most dominant printing process with the maximum fields of applications. For a defined circulation, the offset printing process stands for low manufacturing costs of the printing product and at the same time it has a capacity to produce high print quality.

During the printing process, the printing plate and the blanket transfer the printing ink in form of a thin film onto the substrate. The inking units carry out the functionality to transfer a defined amount of ink onto the printing plate. The requirements and specifications of an inking unit are defined in the Literature [Kipp00, Mau02, Riedl89, Tesch89, Wal91a, Wal91b] as follows:

- High Consistency of ink film thickness on the printed sheets in grain and cross direction;
- Fast Reaction to change in ink input value;
- Less Ink film thickness variation by change in the input value;
- Larger bandwidth of the variable amount of ink and water;
- Economical.

For different applications, different types of inking systems are installed and developed in an offset printing machine. These types are primarily listed in Fig. 1.

Roll inking units, also known as long inking units because of the ink train (a series of rollers used to split the amount of ink on the rollers) to produce the desired tone and print quality. An exact zonal colour control leads

to a complete product spectrum with significant variability in the colour reproduction out quality. The assembly is a hi-tech construction and finishing technique, similarly more energy is required to run the high number of rollers.

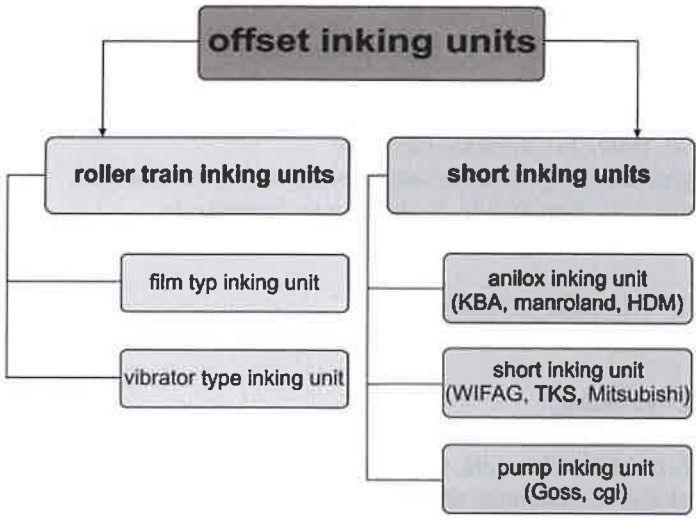

Figure 1: Types of offset inking units as defined by Maurer [Mau02] (source)

On the other hand, the short inking unit stands for lesser number of rollers and reduced wastage. Simple operation, constant speed which is not dependent on the ink input are some of the important factors in the short inking unit. The difficulty on the other side is to achieve a balanced ink-water combination and control the ink quantities during the running production.

In references [Mau00, Mau02, Mau05], a new concept for inking units is introduced, where the ink supply from an inking unit is independently and mechanically decoupled. The dosage and infeed/inlet of the printing ink is not carried out with intermediate rollers, but as a spray. The major advantages with a spray inking unit over both of the conventional inking unit principles, is a zonal colour control coupled together with the reduction in the number of rollers for the necessary ink film uniformization.

The experiments done on the principal feasibility of spray inking units are elaborated and discussed in references 6-8. The results achieved in these experiments have been taken up and developed further. In the following experiment, the spray properties of offset printing inks (heat set inks, Sun Chemical Hartmann, black ROO S 6809/Panorama), diluted with 6% Mineral Oil is introduced and discussed. A precise spray inking unit concept is demonstrated based on the construction implementations and the analysis of the spray properties. The experiments on an offset printing machine and a presentation of the results wind up the experimental work. At the end of the conclusions, the investigations and technical expertise, a vision for the future work is stated.

2. Viscosity of printing ink

The rheological properties, particle size of the printing ink and spraying properties have an influence on the printability of the ink [Bau77, Berg 98, Lef89, Mau00, Mau02, Mau05, Schi73]. Generally, it could be stated that with reduced viscosity, the spray properties related to smaller droplet formation are improved [Woz02]. A decrease in viscosity can be achieved with different methods. In the present experiment, three possibilities are investigated: shear rate, temperature and defined addition of mineral oil. In the first part, the pseudoplasticity of the printing ink was calculated. The shear rate was for three ink variations (0%, 3% and 6% mixing of mineral oil) at a test temperature of 80°C and was increased from 1/s up to 2500/s at 30 different speeds (time taken to measure every point was 5 sec). The results are summarized in Figure 2. It was identified that at a constant test temperature, the viscosity reduces due to an increase in shear rate. Both of the curves (80°C/0% and 80°C/3%) fall down to a certain shear rate of 100/s steeply and and flatten towards higher shear rates. The addition of 6% mineral oil leads to a lower shear rate. The ink feeding inner tube to the jets experience a much less shear than the predominant ink in the nozzle (approximately 1900 1/s). The flow of ink would be an advantage within the ink feeding inner tube. An inner-tube diameter of 6 mm leads to a shear stress of 0.26 1/s.

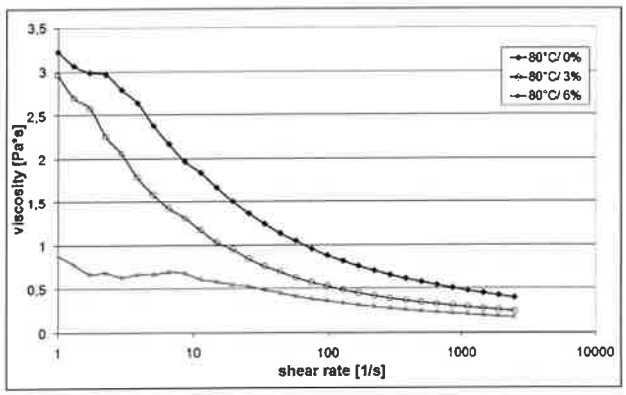

Figure 2:
Viscosity as function of shear rate and defined addition of mineral oil

Figure 2 clearly illustrates that the influence of the dilution degree decreases with increasing shear rate. As shown the distance between the three graphs decreases together with an increasing shear rate.

The most important influence on the viscosity of the ink is that of the temperature. To these assertions, the viscosity dependence of temperature is determined for two inks. The results are shown in Figure 3 and summarized below. Besides unchanged cans of fresh ink (0%), measurements were made for ink in which 6% mineral oil had been added.

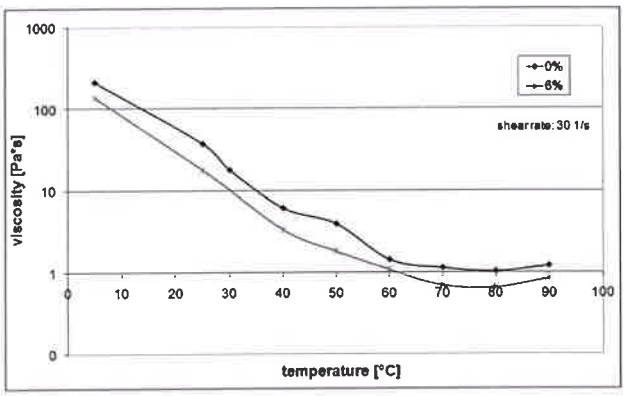

Figure 3:
Viscosity as function of temperature and defined addition of mineral oil

The determination of the viscosity was at a constant shear rate of 30 1/s. The temperature was determined at a minimum of three times with a waiting time of 5 s. Both inks were highly dependent on temperature and the viscosity decreased significantly with increasing temperature. A temperature increase from 5°C to 80°C lowers the viscosity by a factor of 200. As expected viscosity values for a 6% oil diluted ink are lower than those for fresh ink cans (0%), in average by a factor of 1.6. It should be noted that both inks behave qualitatively similar. It can be concluded that both inks exhibit the same temperature dependence.

In summary it is concluded that it is necessary to heat up the ink up to 80°C in the spraying of ink for realization of the small drops. This is because the influence of temperature on the viscosity and thus on the spectrum of the spraying droplet size is crucial. Reducing the viscosity by dilution with 6% mineral oil is an advantage at room temperature for an even flow of ink through the unheated ink feeding tube to the spraying nozzles. The influence of temperature on the ink droplet sizes are determined in the following chapter: The properties of ink spray are hence summarized.

3. Properties of ink sprays

For the spraying of the ink the so-called pneumatic sprayers, also known as two-component jets were developed. These nozzles can also be used for higher viscosity fluids such as inks. They usually use compressed air as source of energy. The used two component jets external mix nozzle has a diameter of 0.3 mm. The most important influence on the homogeneity of the ink film sprayed on a roller surface in a printing press is the

size spectrum in the spray, the more even and quicker printable ink film in the presses can be generated. As a measure of the quality of the spray the Sauter diameter is chosen. There was a minimum target size for the Sauter diameter of D3/2 = 20 microns, since an impurity of this size can be smoothed out by 3 to 4 ink splitting points [Mau02] in the inking unit. In order to determine the characteristic droplet sizes and the resulting drop size spectrum, a laser diffraction spectrometer type - Malvern Master-sizer is used. One can measure drop sizes in the range of 0.1 microns to 2000 microns. The instrument works with the principle of laser diffraction. In Figure 4, the Sauter D3/2, the D10 and D90 for a constant nozzle air pressure of 4 bar, depending on the ink temperature at the moment of spraying are displayed. As expected, from the decreasing viscosity with increasing temperature,droplet sizes decrease with increasing temperature.

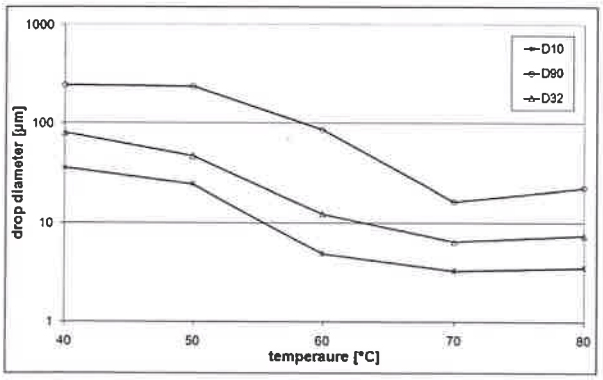

Figure 4: Characteristic droplet sizes as function of temperature

The Sauter diameter reached has a value of less than 10 microns at 80°C, which is 50% below the target size. The D90 has a value of 22.4 microns at this temperature. That means, that 90% of the existing spray droplets are smaller than 22.4 microns, which suggests the feasibility of a homogeneous ink film formation. The determination of the ink film thickness formation from sprayed ink in offset printing is discussed in the following chapter.

4. Determination of surface coverage and the process ink film thickness

The investigations regarding the sprayed ink film formation were performed on a dormant plan surface equipped with static testing equipment, which is shown in figure 5.

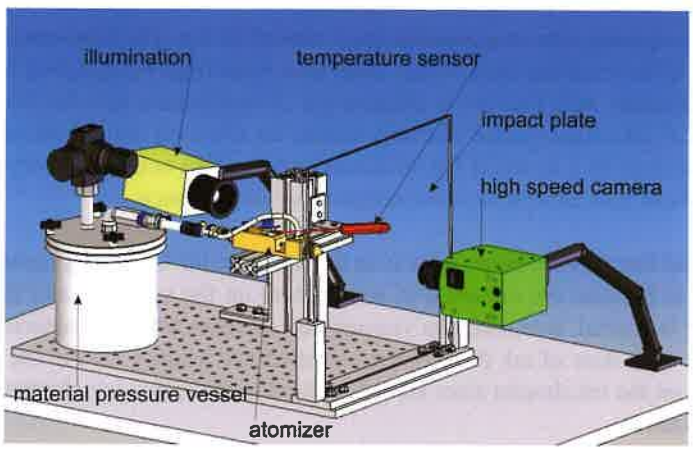

Figure 5: Static testing assembly

The test set-up consists of a spraying assembly, a high speed digital camera and a glass pane with suitable lighting. The formation of the ink film is determined as a function of the time frame by making single image sequences (grayscale tiff). For analysis of the ink film formation effect the images were transferred into a binary image (black/white) with the software IgorPro. The background image is defined as white and the surfaces covered with ink as black. This makes it possible to determine the areas covered with ink. The relationship of

the total image size to the sum of the surface elements of each image is provided. The time interval between two subsequent individual images is 2 ms. Thus, any percentage of area coverage of a specific picture could be specifically determined for a time slot. The trials took place with a stationery spray. This means that the determination of the covered area of the observed image was done only after complete development of the sprays. The aperture could be found in-between the spray assembly and the glass pane, in which after the start of the spraying action the printing ink was suspended. After 5 s of the spraying time the image capturing with the camera was started at the same time as the aperture was detached. The first time picture on which the aperture was no longer recognizable was fixed as the start-up picture (time 0 ms / 0% area coverage).

Table I: Test parameters for the static experiments

Image Aquisition Frequency	500 Hz
Picture Resolution	640 X 640 Pixel (= 3.5 X 3.5 mm)
Position of Image Aquisition	Centre of Spraying Cone (Nozzle Axis)
Ink Mass Flow Rate	0.8 g/min
Inter-spaced Nozzles – Glass Pane	100 mm
Ink Temperature	40°C - 80°C
Spraying Air Pressure	4 bar
Nozzle Aperture	0.3 mm

The experimental studies included the determination of the time-dependent area covering process, depending on the ink temperature at constant ink mass flow rate (0.8 g/min) and nozzle air pressure (4 bar). For each ink temperature there have been at least 10 separate experiments. The results of the experiments are shown in Figure 6 and are summarized below. As expected, the process of covering the surface completes much faster with increasing temperature. While at 40°C a 90% coverage requires 500 ms, this time decreases below 100 ms already at an ink temperature of 60°C. This is due to the significant improvement of the spray properties at temperatures above 50°C. Since the droplet size spectrum shift towards smaller drops with significantly increasing ink temperature and the relative width of the spectrumat higher temperature is constant, the ink flow rate drops more. The steeper rise of the curve taken at 60°C is therefore explainable by the effect, that smaller drops tend to hit an uncovered area with a higher probability than larger ones.

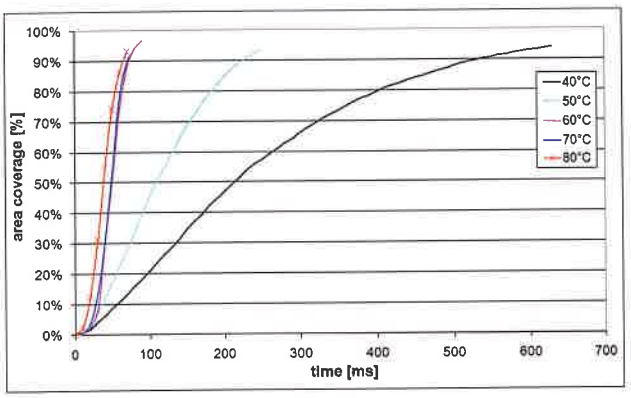

Figure 6:
Area coverage as function of time (4 bar, 0.8 g/min)

As a result of the previous static tests, statements on how a specific area is covered with ink over time. However, it is not possible to conclude on the resulting ink film thickness profile. In order to obtain a uniformly printed image, it is necessary to minimize the thickness variation. In order to explain the formation of ink film layer by sprayed ink including the applied ink film thickness a simulation was carried out. The simulation of the process of ink film formation is done with the help of the software IgorPro4 by the company Wave Metrics. Laser diffraction spectrometer drop size distributions depending on temperature served as the basis of the simulation. For the simulation, the most simple assumption is that the ink drops cover the area one by one. As termination criteria for the simulation coverage of 90% was selected. The results of the ink film thickness determination are shown in Figure 7. As expected, there is a decrease in the thickness of the ink with increasing temperature. While at 40°C an average ink film has a thickness of 63.73 microns (standard deviation 8.4%), at 80°C this value decreases to 5.36 microns (standard Deviation 0.54%) ,a factor 11.9 lower than before. At 80° C the ink film is also much more homogeneous compared to 40°C.

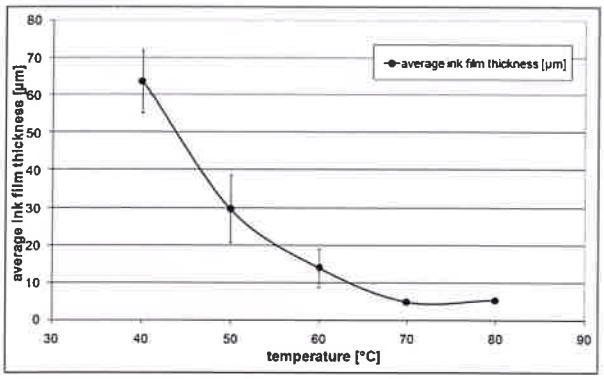

Figure 7:
Average ink film thickness as function of temperature (area coverage 90%)

The results are illustrated in terms of ink film thickness distribution and displayed together (40°C and 80°C) in Figure 8.

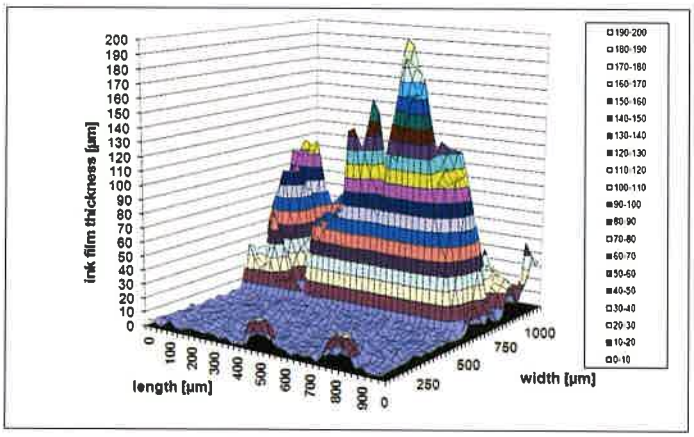

Figure 8: Ink film thickness for 40°C and 80°C (area coverage 90%)

The ink at 80°C has a much smoother course with few `ink elevations` (up to 20 microns). The ink at 40°C, however, shows large areas with elevations of more than 100 microns. The main result of these investigations was the determination of 80°C as a potentially optimum process temperature. In the further course of the work it was important to clarify whether an ink heated to 80°C could finally be good enough to typically offset print quality. This is discussed in detail within the following chapter.

5. Application in a web offset printing press

In order to check the operation and the print quality achievable with a developed spray inking system, certain printing tests were carried out. The tests were divided into two major areas. On the one hand, the ink on a conventional roll inking system was fed with an inking roller on the printing plate in form of a thin film while on the other hand the ink was applied using the spray inking system. This makes it possible, to achieve a direct print comparison between both the processes. The ink used was exclusively selected as black heat set ink and printed on glossy coated paper (135 g/m², type of NOPA Coat Stratos Fa INAPA Germany). The basic structure of the spray inking system is shown in Figure 9.

For the inking of the printing width of laboratory-type press Labor MAN with a web width of 140 mm, 8 inking nozzles were used. It was important to clarify which influence the dilution of the ink with a 6% mineral oil, the warming of the ink to 80°C and the atomizing of the ink have on the dot gain effect. The print run of a suitable test form was done on the conventional inking unit with cans of fresh, undiluted printing ink and for both types of inking units with diluted ink with the addition of 6% mineral oil. The amount of circulation was 1.000 copies. Halftone areas (squares with side = 1 cm) of 10% coverage until solid 100% in 10% stages were developed on the printing plate. For obtaining the characteristic curve of the print, by measuring the halftone, a densitometer was used. In Figure 10, the three identified characteristic curves are summarized.

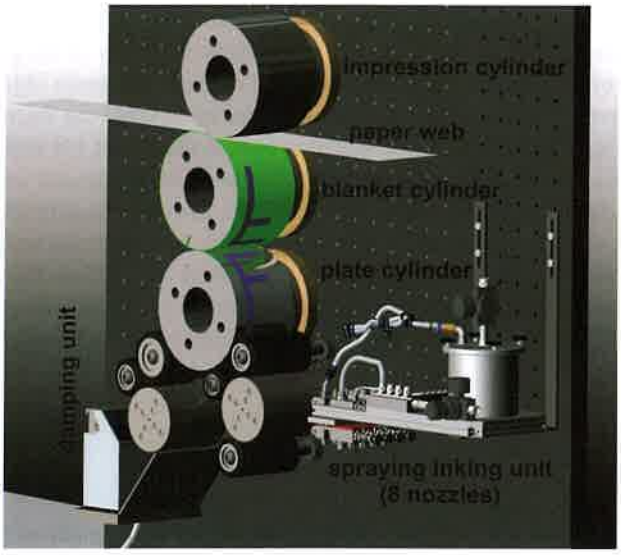

Figure 9: Printing test station with spraying inking unit

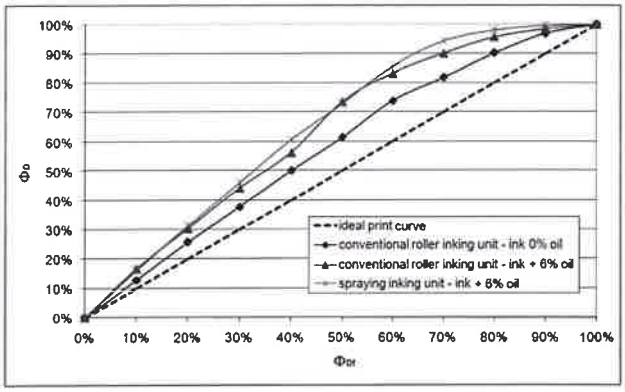

Figure 10:
Dot gain curve

The can fresh ink exhibits the typical dot gain curve obtained in the offset printing process. As expected, the dot gain for the diluted ink with oil was clearly measurable. The printing of the two inking unit variants for 6% diluted ink have an almost identical performance. This result states that the additive mixture with mineral oil has an increasing effect on the dot gain, but the atomizing of the ink is not influenced.

Another area of the print testing is the printing of full tone areas (1 cm x 1 cm), which have been stochastically distributed over the printing plate. Every printed copy was evaluated in each full tone area twice by optical density measurements and the average over all measurements per printed samples was taken. The results are summarized for both inking unit variants in Figure 11.

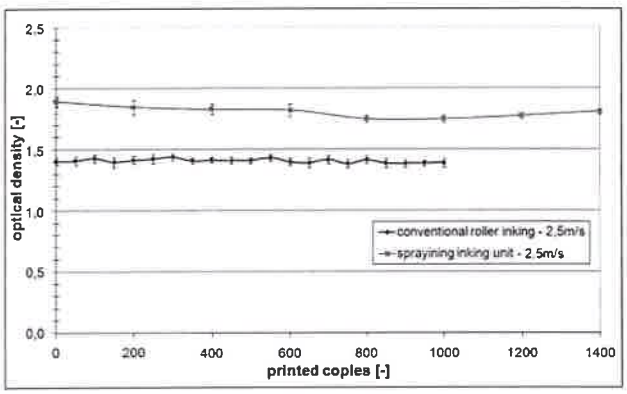

Figure 11:
Optical density during printing process

It can be noted that with the conventional roll inking system a smaller amount of ink was transferred, resulting in lower optical density. Since no inline measurement of the optical density in the printing process is possible, the only way of evaluation of printed samples was the offline method. The main objective of these experiments was to determine and understand the fluctuation of ink and thus understand the fluctuation of optical density in the production run. On the spray inking unit, the full tone optical density of 1.8 with very good stability in the print on paper was achieved at a printing speed of 2.5 m/s. For both the inking unit variants, a standard deviation of optical density achieved during the print run was less than 2%. In comparison to [BvDM03, Hel93] the results of stability conditions were very good within the investigated area for the conducted printing experiments. This means, that the results obtained with the inking system used were as good as the conventional roller inking system on the laboratory press. This statement is so far restricted to the laboratory in specifically examined parameters window. The further work on this area would concentrate on the production machines under actual production conditions.

6. Summary and Outlook

Table II, shows the images of three selected full tone print examples with the chronological development stages of the spray inking unit. It is important to understand that at the beginning of the work, sufficiently fine spray was developed which was used for the printing tests. As a result, this paper has succeeded in outlining the theoretical considerations and experimental studies for a spray inking system and constructively developed a way with which very good printing results could be produced. As a summary, a spray inking system has the potential to response more rapidly than other inking units. With further research in this scientific field, it seems possible that with a spray inking unit, a tow dimensional ink control [Mau02, Schl09] could be achieved, with the combined advantages over the classical roll inking systems and short inking systems.

Table II: Chronological development stages of the spray inking unit (full tone print examples)

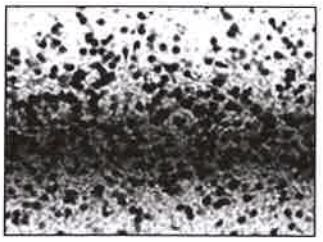

2002

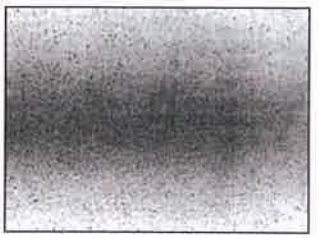

2005

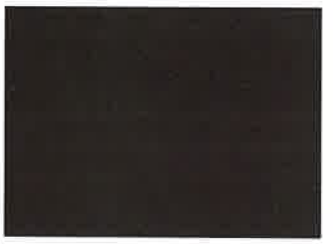

2007

The investigations carried out show not only the strengths but also the weaknesses of the spray inking unit. First of all, a sensible use of electrical energy is needed to enhance economical use of air for atomization and for heating of the ink. Secondly, the processes of spraying cone overlapping, for which modifications in the inks zones are necessary, are still largely unknown. The above findings and experiments have led to the need for further research and development. The In a first instance, these efforts should target the improvement of the spray inking system for offset printing, while further developments should explore and develop this technology as a new kind of inking units for other printing methods.

References

1. [Bau77] Bauer, M., Decker, P., Bosse, R.: Zusammenhang zwischen Viskosität und Zügigkeit von Druckfarben: Theoretische Analyse und Laboruntersuchungen an einer Offsetdruckmaschine. FOGRA Forschungsbericht 5.009, 1977
2. [Berg98] Berg, M.: Untersuchungen zur Erzeugung und Dosierung dünner Flüssigkeitsschichten auf Walzen. Dissertation, TU Chemnitz, 1998
3. [BvDM03] Bundesverband Druck und Medien e.V.: Prozess-Standard Offsetdruck - Wege zu konstanter Qualität von der Vorstufe bis zum Druckprodukt. Wiesbaden, 2003
4. [Hel93] Helbig, T.: Druckqualität - Grundlagen der Qualitätsbewertung im Offsetdruck. Polygraph Verlag Frankfurt am Main, 1993

5. [Kipp00] Kipphahn, H.: Handbuch der Printmedien. Axel Springer Verlag, 2000
6. [Lef89] Lefebvre, A. H.: Atomization und Sprays. Hemisphere Publishing Corporation, 1989
7. [Mau00] Maurer, A., Hübler, A.C., Wozniak, G.: Rheological Demands on Offset Printing Ink for New Inking Unit Concepts. In: Proceedings of the 2nd International Symposium on Printing and Coating Technology, Swansea, Wales, pp. P9-1-P9-12, 2000
8. [Mau02] Maurer, A.: Grundlagen und experimentelle Untersuchungen zum Zerstäuben von Druckfarben zur Farbdosierung bei Offsetfarbwerken. Dissertation, TU Chemnitz, 2002
9. [Mau05] Maurer, A., Wozniak, G., Hübler, A. C., Beier, W.: Über das Zerstäuben von Offset-Druckfarbe. Forschung im Ingenieurwesen. Volume 69/ Number 4/ S.223-S229, Springer Verlag Berlin/ Heidelberg, 2005
10. [Riedl89] Riedl, R., Neumann, D., Teubner, J.: Technologie des Offsetdrucks. VEB Fachbuchverlag Leipzig, 1989
11. [Schi73] Schirmer, K. H., Yoshijima, S.: Rheologische Eigenschaften von Druckfarben bei verschiedener Temperatur. FOGRA-Forschungsbericht, 5.008, 1973
12. [Schl09] Schlegel, G.: Experimentelle Untersuchungen zu Farbfilmbildungsprozessen von Sprühfarbwerken in Offsetdruckmaschinen. Dissertation, TU Chemnitz, 2009
13. [Tesch89] Teschner, H.: Informationsverarbeitung Offsetdrucktechnik Technologien und Werkstoffe in der Druckindustrie. Fachschriftenverlag GmbH Co KG, Fellbach, 1989
14. [Wal91a] Walenski, W.: Der Offsetdruck - Einführung in Theorie und Praxis, DuMont Buchverlag Köln, 1991
15. [Wal91b] Walenski, W.: Polygraph-Handbuch Offsetdruck, Polygraph Verlag Frankfurt am Main, 1991
16. [Woz02] Wozniak, G.: Zerstäubungstechnik - Prinzipien, Verfahren, Geräte. Springer Verlag Berlin, 2002

Investigation of the influence of the composition and rheological characteristics of photopolymerized systems (vehicles) on the rheological behavior of the UV-curing inks for screen printing

Tatiana Sretentseva and Julia Timchenko

Moscow State University of printing arts (MSUPA)
Pryanishnikova st., 2a, RU-127550, Moscow, Russia
E-mails: tsreten@rambler.ru, ytimchenko@inbox.ru

Abstract

This paper is devoted to the investigation of the influence of the composition, functionality, nature and rheological characteristics of the model vehicles on rheological properties (anomaly of viscosity, the yield stress P_k) of model UV curing inks for screen printing. Also we have studied the dependence of the rheological characteristics of model inks (viscosity, yield stress, structuring degree, structure strength, rate of destruction and reconstruction of the structure, rate of thixotropy) on concentration and functional features of a number of pigments added to the ink compositions.

Keywords: rheology, yield stress, anomaly of viscosity, thixotropy, screen printing inks

1. Introduction

In the screen printing as in no other printing method the role of rheological properties of inks is extremely great. The inks for screen printing must have a whole complex of certain rheological properties: explicit thixotropy, low yield stress (limit of fluid properties), relatively high rate of destruction and reconstruction of the ink dispersion structure.

The achievement of optimal rheological parameters provides the necessary technological properties of inks, to a greater extent their printing properties, stability in process of printing and finally the high quality of color imaging.

It is known that the rheological properties of inks are determined by a number of factors: nature and concentration of dispersed phase and dispersion medium (ink vehicle), dispersion degree, additives, temperature.

This paper presents the research results of the influence of the functionality and rheological characteristics of photopolimerized compositions (resin vehicles) and the influence of pigment nature on rheological properties of UV curing inks for screen printing, that, on our opinion, represents both theoretical and practical interest. Objects of the study are UV curing inks for screen printing and included in their composition UV-curing vehicles. Three model systems of vehicles and their inks were analyzed. In this research we used the model ink systems which are being developed at the Material Science Chair (MSUPA).

2. Methods and results

We have studied the rheological behavior of model vehicles, which have included oligomer E-220 (polyurethanediacrylate, molar mass = 1.000). We have chosen this oligomer, because it provides high curing speed, which allows to obtain excellent performance characteristics of films and strong adhesion to different substrates. Molecules of this oligomer are polyfunctional and have a tendency to dipole-dipole interaction, also they have "acid" hydrogen atoms, that are capable to generate hydrogen bonds, so it is obvious, that used oligomer may form quite strong structures as a result of interaction between oligomer and monomer molecules.

We used TPGDA (tripropyleneglycoldiacrylat) as a reactive monomer in pair with oligomer E-220. This monomer is polyfunctional, capable to generate hydrogen bonds with oligomer, and also comes into dipole-dipole interaction.

So based on the theoretical consideration it is obvious, that oligomer-monomer system should protect quite significant structuring in vehicle. We have used model vehicles in our investigation. The first model vehicle

consists of 40% of polyurethanediacrylate oligomer and 60% of monomer, the second model vehicle consists of 60% of oligomer and 40% of monomer.

The third model vehicle represents the composition of 40% TPGDA (monomer) and 60% bisphenylpolyepoxyacrylate (oligomer) with molar mass = 900, which also should generate strong structures. This oligomer, as it is known, significantly accelerates UV-curing of printing inks.

We also have studied rheological characteristics of monomers and oligomers, which form parts of model vehicles, and this information of course was very important for creating vehicles composition.

Rheological investigations were conducted on the rotary viscosimeter "Rotovisco" with measuring system cone-plate.

Deformation in all cases was realized with strict temperature conditions (25°C). For oligomer and monomer and all samples of model vehicles, we obtained viscosity curves $\eta = f(D)$ and yield curves $D = f(P)$.

The results of rheological research of monomer, oligomer and model vehicles presented in table I.

Table I: The results of rheological research of photopolimerized composition components

Monomer/Oligomer	anomaly of viscosity $\frac{\eta_{max}}{\eta_{min}}$	the yield stress P_k, N/m²
TPGDA	0,95/0,12=7,9	360
E-220	40,9/26,3=1,6	700
bisphenylpolyepoxyacrylate	24,4/10,8=2,2	1000

As one would expect, all the studied samples of oligomers and monomers represented a non-Newtonian fluids. Oligomers, according to the obtained values of viscosity anomaly, represented a system with a low degree of structuring, but with a relatively high structure strength. Observed structuring in monomer TPGDA is probably connected with the formation of volume associates of high molecular weight.

Study of the rheological curves of the model vehicles revealed that all the studied systems are structured liquids with a characteristic for these fluids form of the yield curves and viscosity curves, with parts of the highest (η_{max}) and of the lowest (η_{min}) Newtonian viscosity and the area between them with the effective structural viscosity (η_{eff}). The results of model vehicles rheological studies are represented in table II.

Table II: Rheological characteristics of model vehicles

Vehicles	anomaly of viscosity $\frac{\eta_{max}}{\eta_{min}}$	the yield stress P_k, N/m²
Vehicle №1	4,1/0,18=22,8	380
Vehicle №2	4,1/1,3=3,15	550
Vehicle №3	5,2/1,4=3,7	420

Viscosity of non-destroyed structure (η_{max}) was identical in the first two samples of model vehicles ($\eta_{max\ 1,2}$ = 40,6 Poise), but viscosity of destroyed structure (η_{min}) in case of model vehicle №2, as one would expect, was much higher ($\eta_{min\ 2}$ = 13 Poise), than in case of vehicle №1 ($\eta_{min\ 1}$ = 1,8 Poise).

Anomaly viscosity of the sample №1 is much higher (γ_1 = 22,6) than the viscosity anomaly of sample №2 (γ_1 = 3,4), which we believe is connected with the much higher viscosity of the oligomer destroyed structure (content of oligomer in the sample №2 is 20% more, than in the sample №1) and with low value of the monomer minimum viscosity (η_{min}). A significant decrease of viscosity in non-destroyed structures of model vehicles (η_{max}) compared with η_{max} of the oligomers and monomers is attributed apparently firstly to the decrease of intermolecular interaction of oligomer molecules, secondly to a specific degree of oligomer ball deploying with it dissolution in TPGDA monomer, which has a linear structure and thirdly to high dilution capacity of monomer.

This has led to a significant decrease of vehicle viscosity.

Structuring in the model vehicles, the presence of anomaly viscosity in them, that indicates on structure in model systems, driven by the characteristics of polyfunctional molecules of oligomer E-220, polyepoxydiacrylate and polar bifunctional monomer molecules, in case of high concentration of oligomer (concentration is 40% in the sample №1 and 60% in the sample №2).

Swollen molecules of oligomer are oriented in the direction of flow under the influence of an external deformation effect, also upsets an associated interaction of oligomer and monomer. As a result the structure is destroyed and resistance to external impact falls.

Thus, we obtained for all model vehicles typical for structured systems rheological curves $\eta = f(D)$ and $D = f(P)$. Obtained curves are fully consistent with reasoning above. The yield stress is 5.500 dyn/cm^2 in case of the sample №2, where concentration of oligomer is higher. Anomaly viscosity is γ_2 = 3,12 in this case. It was found that yield stress is slightly lower for the sample №1, where concentration of monomer is higher, so for the sample №1 P_k = 3.600 dyn/cm^2 and appropriate value of anomaly viscosity is much higher (nearly 7 times higher) than this value for model vehicle №2 (γ_2 = 22,5). This allowed us to make a conclusion about great contribution of monomer and oligomer molecules to the structuring and strength of intermolecular interaction. As one would expect the strength of the structure decreased and the degree of structuring increased with the increasing concentration of the monomer. The degree of structuring was significantly higher, and the strength of the structure was significantly lower in case of increasing concentration of the monomer by 20% in the sample №1 compared with the sample №2.

It should be noted that even at relatively small values of the velocity gradient D = 70 - 140 s^{-1} fast decrease in viscosity is happening in all cases. This shows the ease of destruction of all model vehicles, which is quite close to the requirements for the structuring of the vehicle systems for standard screen printing inks.

The sample №3 based on bisphenylpolyepoxydiacrylate was similar to the rheological properties of the sample №2 based on the oligomer E-220.

Further, we have prepared model UV-curing inks for screen printing, taking into account the rheological studies of the vehicles. As the vehicles we used model vehicle №2, that represented composition of oligomer E-220 + monomer TPGDA, and model vehicle №3, that represented composition of oligomer bisphenylpolyepoxydiacrylate + monomer TPGDA. These vehicles, as we have found, have similar rheological characteristics. We used number of organic pigments with different functionality and nature (magenta - ruby vanish "SK", cyan phthalocyanine β-form, yellow lightfast "23" and the most used for printing inks non organic black pigment - technical carbon). Pigments were introduced into the model inks in the number of 5%. Grit of the model inks was 10 micron.

Cyan phthalocyanine pigment presents an organometallic complex substance phthalocyanin of copper. Yellow lightfast pigment "23" is an azopigment, that was synthesized on the base of acetic acid anilide. Ruby vanish "SK" is a sample of the baric or calcic vanishes based on the **sulfonic acid** toluidine.

Technical carbon (we used for investigation brand K-354) is a gas non-oxidated channel black that consists of pure carbon, which represents a quite hydrophobic non-organic pigment without any functional group.

Rheological research of model inks were realized, as in the case of model vehicles, on the rotary viscosimeter "Rotovisco" with measuring system cone-plate and temperature 25°C.

Investigation of the dependence of model vehicles rheological characteristics (viscosity, yield stress, structuring degree, the structure strength, speed of distruction and restoration of the structure, thixotropy) on the functional characteristics of pigments and vehicles, which were included into ink compositions, were conducted by analysis of viscosity curves and $\eta = f(D)$ and yield curves $D = f(P)$ (direct and reverse). On this basis the anomaly viscosity $\gamma = \eta max / \eta min$, yield stress (limit stress of stepping) P_k were calculated, also structuring degree and the structure strength of model ink dispersion were assessed. By constructing rheological diagrams (hysteresis loop) we evaluated the thixotropy of studied model inks.

The obtained rheological characteristics of investigated model ink dispersions are adduced in table III.

Table III: Rheological characteristics of model UV-curing inks based on different pigments

Pigments	Vehicle: 60% E-220 + 40%TPGDA		Vehicle: bisphenylpolyepoxydiacrylate 60% + 40%TPGDA	
	anomaly of viscosity $\frac{\eta_{max}}{\eta_{min}}$	yield stress, N/m²	anomaly of viscosity $\frac{\eta_{max}}{\eta_{min}}$	yield stress, N/m²
Magenta vanish ("SK")	6,82/0,48 = 14,2	400	28,3/1,4 = 20,3	2800
Cyan phthalocyanine pigment (β-form)	6,23/0,46 = 13,5	450	8,1/1,3 = 6,3	1300
yellow lightfast "23"	5,21/0,52 = 10	500	10,83/1,2 = 9,0	1500
Black (K 354)	15/0,78 = 19,2	1800	16,24/1,12 = 14,5	1300

3. Discussions

On this basis of the data analysis we have determined, that in all cases of obtained filled systems we stated typical for structured pseudo plastic liquid compositions the nature of viscosity and yield curves.

We have found, that all investigated inks were quite structured, but at the same time inks based on oligomer E-220 have demonstrated close to requirement values of yield stress P_k = 18.000 dyn/cm² (the black ink is exception), what indicated the low structure strength of colour inks and quite strong structure of black inks.

In case of model inks based on polyepoxydiacrylate, we obtained significant increase of structure strength in colour inks compared with inks based on polyurethanediacrylate. It seems that, in case of acrylate system, that has phenylic group in every molecule, spatial factor plays very important role. As a result of this factor formation of strong adsorption-solvate layer (like in case of polyurethanediacrylate) on the surface of the pigment is complicated. Besides polyurethanediacrylate more actively than polyepoxydiacrylate interacted with the pigment molecules, because of functionality of it molecules. As a consequence more strong coagulation structure generate inks based on polyepoxydiacrylate. It is especially apparent in case of magenta pigment with ion structure.

Thus we obtained model ink systems, with rheological behavior close to the rheological requirement for screen printing inks in all cases, except black and magenta pigments.

All rheological characteristics are sensitive to nature and functionality of pigments, and also to oligomer functionality. The comparison of rheological characteristics of model inks based on polyurethanediacrylate and bisphenylpolyepoxydiacrylate showed, that anomaly of viscosity has a hicher value in case of model systems based on polyurethanediacrylate with all pigments except magenta, which showed the highest value of structuring in combination with bisphenylpolyepoxydiacrylate. The latter is attributed, probably, firstly to a weak adsorption interaction of the purple pigment, which molecules have, as we have shown, ion structure with functional groups of polyepoxydiacrylate oligomer molecules, and as a consequence, generation on the surface of this pigment of thin (poor) adsorption-solvate layers, that can not provide the desired stability of dispersion system and can not adequately protect this system in interaction of pigment particles. For the same reason, as one would expect from theoretical considerations, we have found the high degree of structuring in black ink samples for both vehicle systems, which were the basis for model systems. Completely hydrophobic surface of the particles of the technical carbon without any functional groups doesn't provide the required interaction with polar functional groups of oligomer molecules, that doesn't create the conditions for generating of strong adsorption-solvate layers, that could protect system against coagulation structuring.

In case of colour inks based on epoxydiacrylate we obtained significant increase in structure strength (more than 3 times). We observed the lowest structuring in case of cyan and yellow pigments with both oligomers and quite low structure strength in case of cyan, magenta and yellow pigment in composition with polyurethanediacrylate oligomer. The reason is the strong interaction (van der Waals forces, dipole-dipole interaction, hydrogen bonds) of polyfunctional UV-curing vehicle with surface of colour pigments particles in these compositions, that provides generating of adsorption-solvate layers on the surface of pigments particles. These layers allow to receive systems with lower structure strength and so more fluid ink compositions.

It should be noted, that all studied ink systems are characterized by a rapid restoration of the structure and extensive destruction in case of all model systems, except magenta pigment, have already been observed in the velocity gradient D = 80–150 s^{-1}, while the value of viscosity fell more than 2 times.

The studied model inks had high value of thixotropy. According to these data model systems can be arranged in the following series: a) inks based on polyurethanediacrylate: black > cyan > magenta > yellow; b) inks based on polyepoxydiacrylate: magenta > yellow > black > cyan. It means that thixotropy of UV-curing inks is the function of type and functionality of oligomer component and pigment nature, which are parts of ink dispersion.

4. Conclusions

Thus we conducted a study of rheological properties of vehicles for UV-curing screen printing inks and inks compositions based on them, with different type of pigments and this allows us to make the following conclusions:

1) Measurement of yield and viscosity in a wide range of speeds showed that the model UV-curing inks are liquid structured suspensions with variable effective viscosity, decreases from the highest value of the dispersion structure η_{max} to at least limit of the destruction η_{min}.

2) The value of the viscosity anomaly expressed by the ratio $\gamma = \frac{\eta_{max}}{\eta_{min}}$, and varies depending on the nature of pigment and the type of oligomer. The highest value of viscosity anomaly provides magenta pigment with ion nature and technical carbon that are extremely hydrophobic pigment without any functional groups. These pigments are strong structured in model systems and provide quite resistant structure.

3) It was found, that all even quite structured colour inks based on polyurethanediacrylate have a weak structure, which is destroyed even at low values of shear stress. The speed of restoration of the structure is quite similar to the requirements for screen printing inks. Inks based on polyepoxydiacrylate have a higher structure strength.

4) Our research showed, that, thixotropy of ink dispersions is different and very sensitive function depending on the nature of the pigment and functionality of oligomer. The thixotropy has the highest value in composition based on polyurethanediacrylate with black pigment and in composition based on bisphenylpolyepoxydiacrylate with magenta pigment.

5) It was found, that oligomer has a significant dependence of the stabilizing ability from the pigment nature. Also it was found, that in photopolymerized compositions selection of vehicle is problematic in the case of magenta pigment and technical carbon.

6) We obtained the character of changes in effective viscosity of UV-curing inks systems depending on pigments nature and vehicles type.

7) The flow of all pigment dispersions becomes almost close to the Newtonian even at low values of shear because of significant destruction of Coagulation.

8) The investigation of oligomers, monomers and vehicles based on them was conducted. It was found that model systems are non-Newtonian structured fluids, that have an influence on rheological characteristics of the inks.

9) It was found that tripropyleneglycoldiacrylat is an effective thinner for vehicle system.

10) On the basis of these results the optimal composition and rheological properties of the vehicles for UV-curing screen printing inks could be estimated.



Ink formulation with the new multi-phase ink model

Juha Saari[1], Roger Bollström[2], Ken Mueller[3], Martti Toivakka[2]

[1] VTT-Technical Research Centre of Finland
P. O. Box 1000, FIN-02044 VTT, Finland
E-mail: Juha.Saari@vtt.fi

[2] Åbo Akademi University, Laboratory of Paper Coating and Converting and Center for Functional Materials
Porthaninkatu 3, FIN-20500 Turku, Finland
E-mail: Roger.Bollstrom@abo.fi, Martti.Toivakka@abo.fi

[3] Specialty Minerals Inc.
35 Highland Avenue, Bethlehem, PA 18017-9482, USA
E-mails: Ken.Mueller@Mineralstech.com

Abstract

The multi phase ink setting mechanism gives new insight into lithographic sheet fed offset ink modifications. The ink setting in sheet fed offset is by absorption and oxidation and the inks have a relatively high tack. Because of the wide variations in sheet-fed offset ink formulations the ink to paper interactions are extreme.

The problems related to ink setting is mainly set-off (slow setting), mottling (ink setting variations), ink tack build up and surface strength problems (fast setting) and other print quality defects that can be caused by paper variations, print variations, slow/fast ink setting, dusting, base paper and coating structure, etc.

The trend for more porous coatings with better whiteness, printed colour gamut, and light scattering properties will require ink modification to control the ink setting phenomena. It is assumed that by changing the resins, solvents etc. of the printing ink, it is possible to adjust the ink setting in such way that the printing result is good for papers with different coating porosity volumes and porosity size distributions.

Keywords: ink setting, sheet-fed offset, multiple-phase mechanism, coated paper, porosity

1. Introduction

The objectives of the research were to demonstrate the possibility to formulate sheet fed offset inks with the multi-phase ink model [Donigian, 2006] and to provide tools to minimize the effects of the substrate in the final print quality. This means that the ink setting must be similar on porous and compact substrates, in our case coated papers, to produce high film gloss and have low enough tack to avoid disruption of the coated surface. Typical other properties such as optical density, colour gamut and fountain solution compatibility must be maintained.

Two main ink setting theories has been presented in literature and it is known that ink levelling [Keunings et. al, 1987, Ström et. al, 2000], solvent loss [Ström et. al, 2007, Rousu et. al, 2001], and ink film viscosity increase [Gane et. al, 2000, 2003] is affected by the coating porosity [Donigian et. al, 1996, Dalton et. al, 2002, Gane et. al, 2000, Xiang et. al, 1998, Saari et. al, 2008] and binder interactions [Van Gilder et. al, 1994, Foughet et. al, 2006, Rousu et. al, 2002]. These two previous ink setting theories, including homogenous resin solution with uniformly dispersed solid phase and a particulate suspension with a growing "filter cake" zone, have been analysed in the literature.

However, there are some inconsistencies, such as the prediction of excessive material flows to account for the gloss behaviours without the explanation of the effect of oil removal rate on the ink viscosity increase. Therefore a new novel perspective was taken in the ink formulation, adapting the multi-phase hypothesis, to produce a more universal ink for various substrates.

With the increasing use of narrow particle size distribution coating pigments to improve brightness, opacity,

in the coatings. This additional porosity has in some cases been shown to accelerate offset ink tack build and limit ink gloss. This means that the ink setting appears to be a well defined process with the first step being the solvent removal by the paper coating porosity. Therefore the ink setting depends largely on the mechanism by which the ink film surrenders the solvent. Diffusion, phase transition, deformation, and the effect of these on rheology seem to be the important issues.

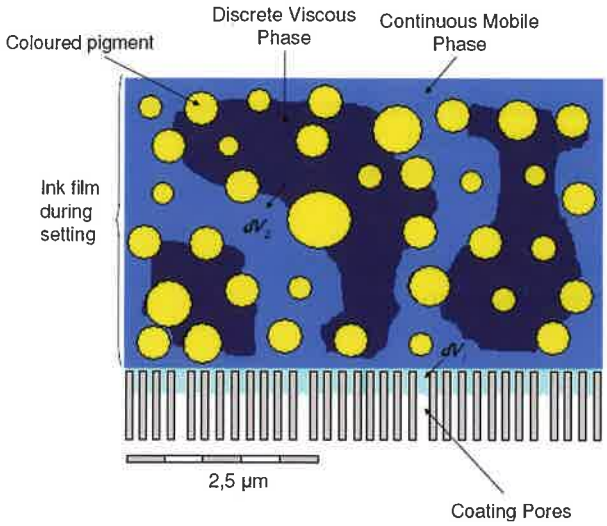

Figure 1: Principle of the multi-phase ink setting mechanism and the phases with different concentrations and viscosities where dV_1 = Oil Loss dV_2 = Oil Transfer (Bollström, 2007)

The ink setting speed depends on how the low and high viscosity phases give up the oil to the attraction force from the coating pores and how fast the high viscous phases lock together in the ink film.

$dV_1 >> dV_2$: The mobile phase is rapidly depleted, ink tack and viscosity increases really fast and levelling is stopped prematurely with low print gloss.

$dV_1 > dV_2$: The ideal case, oil leaves the dilute phase more rapidly than it is replenished. Ink viscosity grows fast enough to avoid set-off.

$dV_1 = dV_2$: The surface pulls out oil only at the slow concentrated phase diffusion rate. The ink film remains too mobile and ink marking and set-off can occur.

2. Research methods

The research method to regulate the multi-phase ink setting in our study was changing the ink formulation with available resins that differ in solubility, molecular weight, glass transition point, chemical composition, and compatibility. The ink properties depend on the interactions of resin blends, solvent, pigmentation and the ink making process. With the combination of different ratios of resin, alkyd, mineral/vegetable oil, while the pigmentation level was kept constant, the ink properties could be adjusted [Bollström, 2007].

Specialized tests were used to characterize the materials and inks. The viscosity, yield value, tackiness and stability were measured for both the ink varnish and final ink to secure the functioning on the printing press. The cloud point measurement is a standard measurement method for the printing industry and is a characteristic parameter for the solid and solvent systems. Therefore, cloud point determinations are used to test the compatibility of many systems and are very important for the stability of many formulations.

For the practical study of the ink setting and print quality a well characterized series of 16 pilot coated papers with different coating pigment and binder combinations was produced at The Centre International de Couchage CIC Inc. A great deal of rheology and runnabilty development work for these coatings with different porosities was performed to achieve an optimal set of substrates for the experimental testing of the inks [Teerimäki, 2008]. These 16 coated papers and a commercial reference were also printed at the KCL 4 colour sheet-fed offset

Table I: The coating formulations to achieve a wide range of coatings with different porosities

PRECOAT															
Medium ground calcium carbonate	100	100	100	100	100	100	100	100	100	100	100	100	100	100	100
Standard SB Latex A	7	7	7	7	7	7	7	7	7	7	7	7	7	7	7
Hydroxyethylated starch	4	4	4	4	4	4	4	4	4	4	4	4	4	4	4
Coating insolubilizer	0,25	0,25	0,25	0,25	0,25	0,25	0,25	0,25	0,25	0,25	0,25	0,25	0,25	0,25	0,25
TOPCOAT	601	602	603	604	605	606	607	608	609	610	611	612	613	614	615	616
Narrow PSD Aragonite PCC				100	100	70	100	100	70	100	100	100			100	70
Fine particle size clay	30	30	30			30							30	30		30
Fine ground calcium carbonate	70	70	70						30				70	70		
Standard SB Latex B	11	9	7							4			6	4	6	
Modified SB Latex C				9	7	7					4					
Modified SB Latex D							9	7	7			4				7
Partially Hydrolyzed PVOH	0,7	0,7	0,7										0,35	0,35		
Modified starch										2,5	2,5	2,5	2,5	2,5	2,5	
Coating insolubilizer										0,2	0,2	0,2	0,2	0,2	0,2	
Carboxymethylcellulose				0,6	0,6	0,6	0,6	0,6	0,6	0,5	0,5	0,5			0,5	0,6

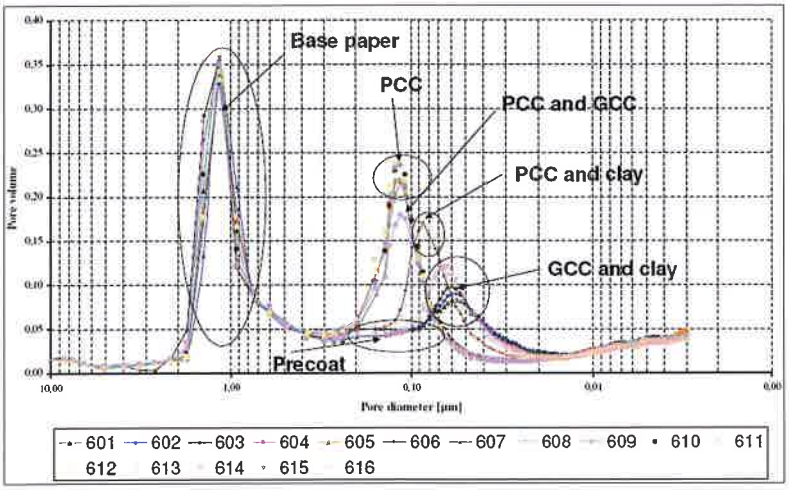

Figure 2: The porosity range of the coated papers with different pigment and binder combinations

Statgraphics regression analysis was used for the interpretation of the results, which means fitting linear or nonlinear models, for several variables. In a regression model, a response variable Y is expressed as a function of one or more predictor variable X, plus noise. A useful function in the programme is the Multiple Variable Analysis, with which it is possible to build a regression model out of several variables.

3. Results

The ink setting and print quality can be adjusted to a high standard for a wide range of coated papers with the right ink formulation. The optimization of the ink formulation can be initiated by adjusting the ink varnish multi-phase cloud points curve. Natural polymers behave similar to other polymers in polymer-solvent systems and produce spinodal curves and critical points. This means that in the varnish two (or more) phases can coexist at equilibrium with different oil to resin ratios. The cloud point measurements also give an indication that this is the case.

The ink setting was measured with the Ink Surface Interaction Tester (ISIT) that measures the tack versus time on a printed sheet. The tack rises when the ink sets or dries and then again decreases when the ink has dried or set into the paper. A new interpretation of the ISIT curve can also reveal more information about the ink setting when the ink and coating parameters are well known. From an ISIT curve it is possible to collect several variables that show different characteristics of both the ink and the paper properties. The variables used in this project is a linear regression line for the three first points for the rise of the tack. It shows the speed of the rise in tack. A higher value means a faster setting since zero would mean a horizontal line. For the slope of the decay two newton was chosen as the end point as after that the curve is almost horizontal. In this case the values of the slope are negative and a higher negative value means faster setting. The maximum force value and the time it takes to reach that value were also used as variables.

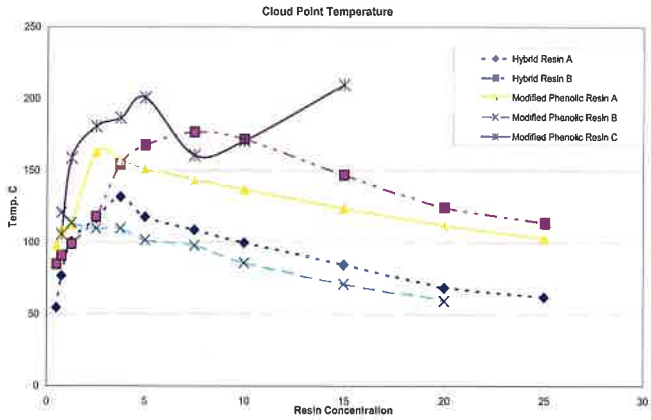

Figure 3:
The resin solubility and behaviour in solvent depends on the resin chemistry and processing steps. The cloud point measurements show different spinodal and critical point behaviour for the different resin - oil systems

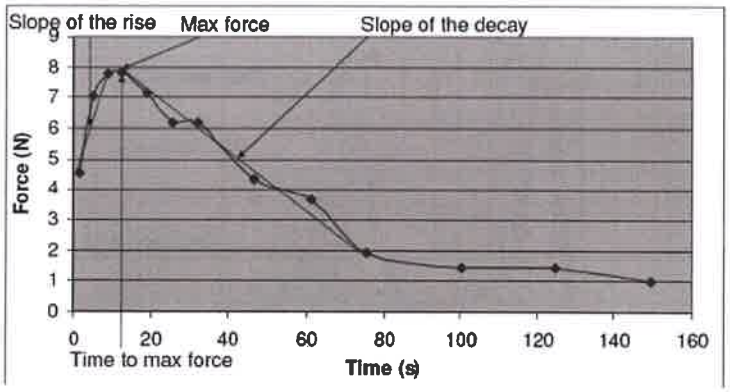

Figure 4; ISIT ink setting tack curve showing the variables used. The slopes are regression lines, for the rise calculated of the three first points and for the decay from max value down to a two Newton force

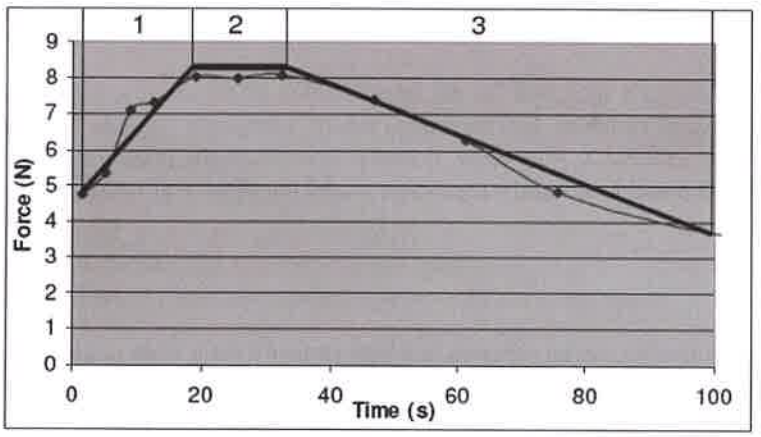

Figure 5: Ink setting, 1:Thin oils penetrate into the pores, dV_1, 2:Oil transfer from the viscous phase, dV_2, and final drying 3:Drying of the ink when oxidation begins

In Figure 5 the ISIT curve is divided into three steps represented by linear lines. The first step shows the first part of the ink setting where thin oils penetrate into the pores. The first part can be compared to dV_1 explained in Figure 1. In the second part where the maximum tack is achieved and the ISIT curve stays horizontal, oil from the viscous phase in the varnish transfers to the pores and high viscous phases lock together in the ink film. This part can be compared to dV_2 in Figure 1. The third part is affected by the drying of the ink due to oxidation.

For the measurements shown in Figure 6 a commercial ink with a relatively slow setting was used. The values introduced here were chosen to get more variables out of the curve. 7N was chosen as the limit because every curve reaches it but at varying times. The reason for choosing the B and C variables, or especially the time

between B and C, was that for almost all curves the maximum force lasts for a while. The time before B and the time between B and C may also explain the ink setting and the setting of the different phases in the multi-phase ink model. It shows the growth of tack and viscosity when oil loss appears.

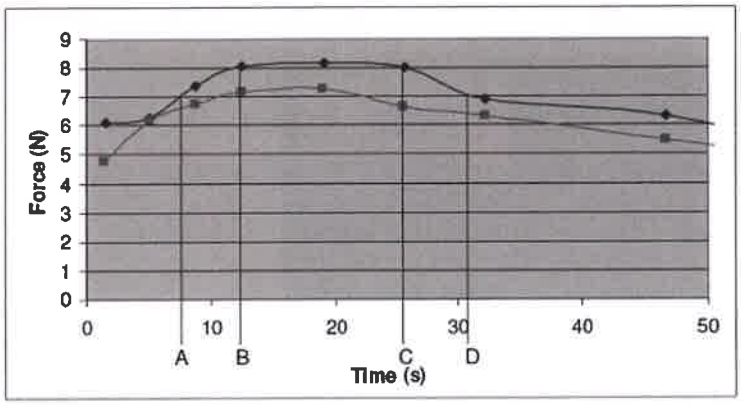

Figure 6: ISIT with a zoom on the first 50 s showing the time variables used. The units for the values are in seconds

- A = time to reach 7N force
- B = time to maximum tack
- C-B = the time when maximum tack appears
- D = time when force declines to 7N
- D - A value used as a parameter, correlates with porosity and pore diameter

The porosity of the coatings was analysed with mercury porosimetry and paper properties such as gloss, whiteness and roughness were taken into account when looking at the final print quality. The Statgraphics regression analysis shows that whiteness, brightness and opacity correlate linearly with the pore diameter when considering pore diameters in the range of 0,05 to 0,15 µm. In the pore size range a larger pore diameter and in most cases at the same time total pore volume results in an increase of these optical values. However, this pore size and volume increase also results in a faster ink setting.

The print quality, considering print gloss, density, and colour gamut, was analysed from the printed ECI 2002 target lay out, indicating that the coating porosity and whiteness have a clear positive effect on the print quality and with the right ink formulation this positive trend can be spread out to a wide range of coatings.

Several ink formulations were tested before the final ink formulations were chosen [Bollström, 2007]. The increase of vegetable oil in the inks results in a slower ink setting and therefore a standard ratio of 70/30 mineral/vegetable oil was set for the final varnishes for the ink formulations. The resin content in the varnish for the final inks was 40% and 2,5% of alkyd was used. The ink varnish was then adjusted to the same viscosity level. With the same viscosity levels the different resins in the varnish give the varnish different stability and tack behaviour. These varnishes where then used to produce the CMYK ink series with the alkyd resin, antidryer, pigments, wax, driers and mineral oil for viscosity adjustment. Four different resins were used to produce the varnish resulting in a series of 4 CMYK ink series.

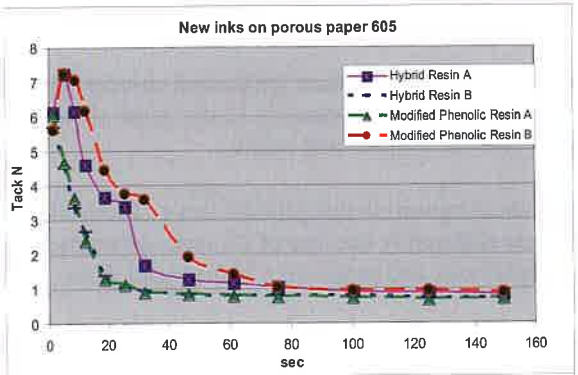

Figure 7:
Nk setting with the modified inks on the fast porous paper 605

In Figure 7 the ink setting is fast and with the proper resins, modified phenolic resin B, in the varnish the ink setting can be slowed down to a functional level so that the tack rises to a suitable level and the final drying starts after the printing units.

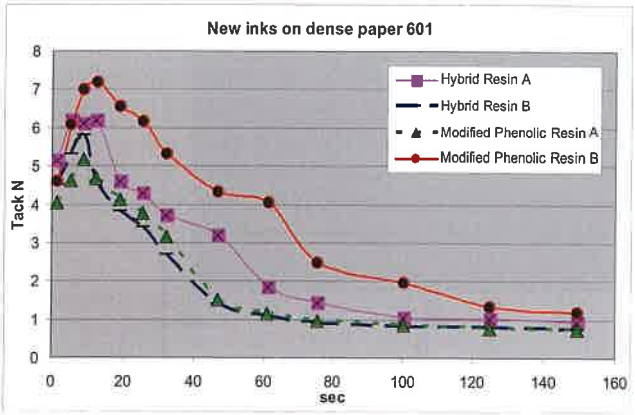

Figure 8:
Ink setting with the modified inks on the slow dense paper 601

Figure 9 illustrates the effect of the ink formulation varnish change in the final colour gamut shown, with the same ink pigmentation in the final ink and on the same coated paper. The same trend could be seen throughout the coating range, good ink formulation gave a bigger colour gamut for both porous and compact coated paper grades. The printed colour gamut is given as delta E volume and the colour space can be viewed from different hue angles, lightness levels and delta E steps.

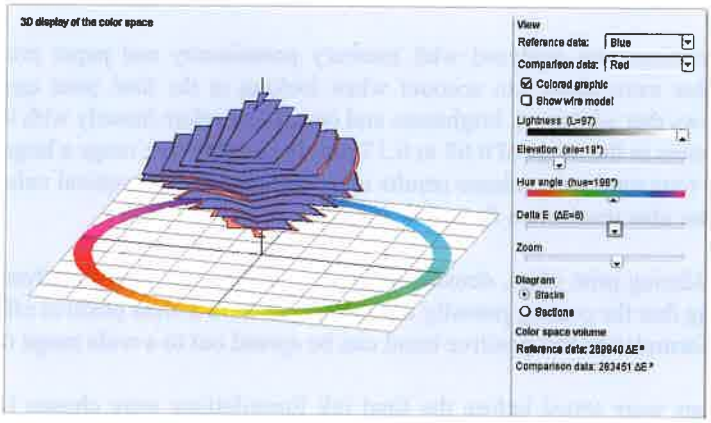

Figure 9: The printed colour gamut measured from the printed ECI 2002 target with the light colours on top and dark colours at the bottom

The modified ink formulations with a smooth spinodal cloud point curve for the varnish and good solubility in the oils used have a good ink setting for both porous and compact coatings. This means that with these formulations the low cloud point resins feed the oil from the dilute phase more rapidly than it is replenished from the concentrated phase and the effect of the coating porosity is reduced. Still the ink layer viscosity grows quickly enough to prevent set-off and slowly enough to prevent too rapid tack build up in printing.

The varnish for the inks can be adjusted with a combination of resins to produce the desired cloud point spinodal curve and it is important to measure the cloud points in several resin concentration levels in the oil vehicle, not just in the desired final concentration for the ink to know how the varnish will behave.

Two varnishes can have the same cloud point in one resin concentration but the spinodal curve can be different and therefore the inks produced with these varnishes can behave differently because of the multi-phase mechanism. In these test inks a lower cloud point correlated with a higher tack and produced a higher print gloss.

Figure 10 and Figure 11 show that the modified ink result in a better printed colour gamut on both fast and slow papers compared to the commercial ink.

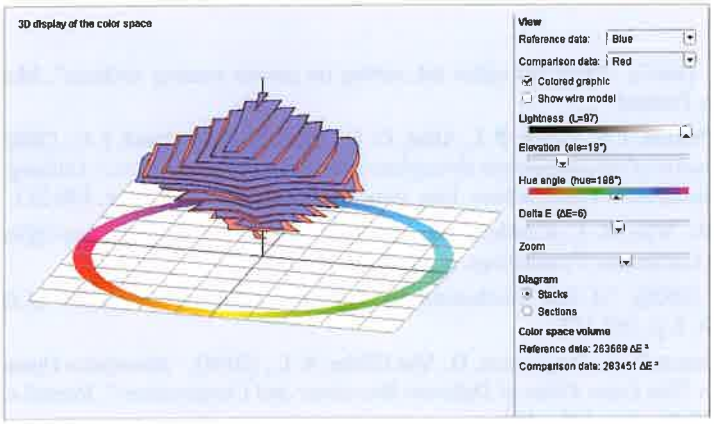

Figure 10: The commercial ink as reference and modified ink as the comparison data printed on the porous 605 coating

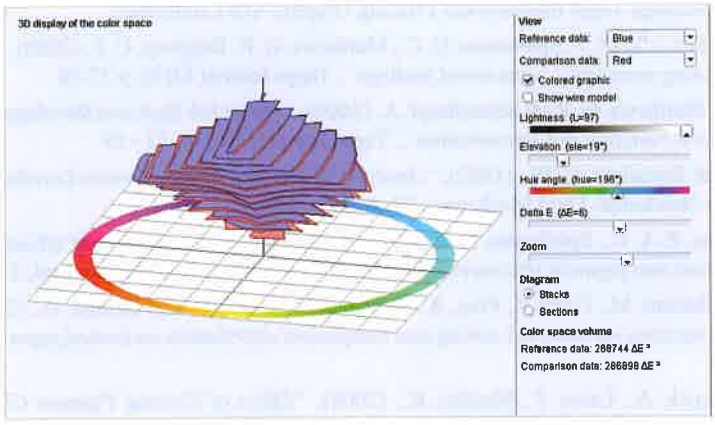

Figure 11: The commercial ink as reference and modified ink as the comparison data printed on the less porous 601 coating

The new modified inks also had a higher print density with the same amount of ink provided to the paper surface. This would mean a better ink milage in print due to the fact that less ink is needed to print the dark gray tones. The 3D colour space volume also indicates that the new inks have a better reproduction of the dark colour tones, in addition to the colours in general.

4. Conclusions

The results show that there is a multiphase behaviour in the ink varnish which can explain the fast ink setting mechanism. The effect of the ink varnish cloud point behaviour, combined with the final ink formulation, on the ink setting and final print quality on different substrates is a novel approach to explain the rate dependence of ink setting phenomena and provides routes for design of an ink that glosses without set off on both slow and fast papers.

This work was financed by Tekes, the Finnish Funding Agency for Technology and Innovation, and Specialty minerals Inc. with close co-operation with Åbo Akademi University, Siegwerk Finland Oy and Hexion Specialty Chemicals.

References

1. Bollström, R., (2007), "*Sheet fed offset ink setting on porous coating surfaces*", Masters thesis, Åbo Akademi, Åbo, Finland
2. Dalton, J. S., Preston, J. S., Heard, P. J., Allen, G. C., Elton, N. J., Husband, J. C., (2002), *"Investigation into the distribution of ink components throughout printed coated paper Part 2: Utilising XPS and SIMS"*, Colloids and Surfaces A: Physicochem. Eng. Aspects, Volume 205, No. 3, pp. 199-213
3. Donigian, D. W., Wise, K. J., & Ishley, J. N., (1996), *"Coated Pore Structure and Offset Printed Gloss"*, Tappi Coating Conference Proceedings, p. 39 - 45
4. Donigian, D., (2006), *"A New Mechanism for Setting and Gloss Development of Offset Ink"*, JPPS Volume 32, No. 3, p. 163-177
5. Foughet, B., Noirot, P.-A., Desjumaux, D., Van Gilder, R. L., (2006), *"Absorption Dynamics of Offset Ink Components in Thin Latex Films of Different Structures and Compositions*", Journal of Pulp and Paper Science: Vol. 32 No. 3, p. 123 - 130
6. Gane, P. A. C., Schoelkopf, J., Matthews, G. P., (2000), *"Coating imbibition rate studies of offset ink: A novel determination of ink-on-paper viscosity and solids concentration using the ink tack force-time integral"*, Proceedings Tappi International Printing Graphic Arts Conference
7. Gane, P. A. C., Schoelkopf, J., Spielmann, D. C., Matthews, G. P., Ridgway, C. J., (2000), *"Fluid transport into porous coating structures: some novel findings"*, Tappi Journal 83(5), p.77-78
8. Gane, P. A. C., Matthews, G. P., & Schoelkopf, J., (2003), *"Offset Ink Tack and Rheology Correlation - 1: Ink Rheology as a Function of Concentration"*, Tappi Journal, 2(6), p. 13 - 19
9. Keunings, R., & Bousfield, D. W., (1987), *"Analysis of Surface Tension Driven Leveling in Viscoelastic Films"*, J. Non-Newtonian Fluid Mechanics, 22, p. 219 - 233
10. Rousu, S., Gane, P. A. C., Spielmann, D. C., Eklund, D., (2001), *"Separation of off-set ink components during adsorption into pigment structures"*, Nordic Pulp and Paper Research Journal, 15(5), p. 527-535
11. Rousu, S., Lindström. M., Gane, P., Pfau, A., Schädler, V., Wirth, T., and Eklund, D., (2002), *"Influence of latex-oil interactions on offset ink setting and component distribution on coated paper"*, Graphic Tech. 1(2), pp. 45-46
12. Saari, J., Dimmick, A., Laine, J., Mueller, K., (2008), *"Effect of Coating Pigment Choice on Printed Color Gamut"*, Proceedings TAPPI/PIMA PaperCon '08 Conference
13. Ström, G., Gustafsson, J., & Sjölin, K., (2000), *"Separation of Ink Constituents During Ink Setting on Coated Substrates"*, 2000 Tappi International Printing and Graphic Arts Conference Proceedings, p. 89 - 99
14. Ström, G. R., Karathanasis, M., (2007), *"Relationship between Ink Film Topography and Print Gloss in Offset Prints on Coated Surfaces"*, Proceedings Tappi Coating and Graphics Arts Conference, p. 15
15. Teerimäki, J., (2008), *"The effect of the binder level on coating color rheology and paper properties"*, Masters thesis, Åbo Akademi, Åbo, F inland
16. Van Gilder, R. L., Purfeerst, R. D., (1994), *"Commercial Six-Color Press Runnability and the Rate of Ink Tack Build as Related to the Latex Polymer"*, Tappi Coating Conference Proceedings, p. 229 - 240
17. Xiang, Y., Bousfield, D. W., (1998), *"The influence of coating structure on ink tack development"*, TAPPI & Pan Pacific, Proceedings Printing & Graphic Arts Conference, p. 93

Nanopigments in offset printing inks

Verónica Marchante[1], Francisco Martínez-Verdú[1], Elena Marchante[1], Juan Antonio Maciá[1], Elisabeth Chorro[1], Esther Perales[1], Vicente de Garcia[2], Jesus Inarejos[2], Susana Otero[2]

[1] Departamento de Óptica, Farmacología y Anatomía
University of Alicante
Carretera de San Vicente del Raspeig, s/n, S-03690 San Vicente del Raspeig, Spain
E-mail: esther.perales@ua.es

[2] Technological Institute of Optics, Colour and Imaging (AIDO)
C/ Nicolás Copérnico, 7-13. Parque Tecnológico, S-46980 Paterna, Spain
E-mail: aagg@aido.es

Abstract

Nanopigments are a new type of pigment. They are hybrid materials consisting of organic dyes and layered silicate nanoparticles. Nanopigments are already applied to make polymeric coatings and they had shown improvement in mechanical, thermal and stability properties of the substrate and dyes [Batenburg and Fischer, 2001].

In this work, nanopigments had been synthesized to be applied in the manufacture of offset printing inks. Therefore, four different nanopigments are pursuit: cyan (C), magenta (M), yellow (Y), and black (K), in order to obtain primary colour for a four-colour-process system.

Keywords: colorimetry, nanopigments, offset printing inks

1. Introduction

Nanopigments or Planocolors® are a new kind of pigment developed by researchers of TNO-TPD Eindhoven (Netherland). Nanopigments are hybrid materials obtained through the combination of organic dye molecules and layered clay nanoparticles, in a special phyllosilicate from the smectite group (figure 1). Nanopigments gather advantages of dyes and pigments, such as brilliant colours, wide colour gamut, while avoiding their drawbacks, like bleeding, low lightfastness, low stability against oxygen, temperature, UV radiation, etc. [Batenburg and Fischer, 2001].

Although nanopigments can be applied in a wide variety of substrates [Batenburg and Fischer, 2001] to make coatings or to colour materials, they have been used and studied mainly in the field of polymers. In fact, for decades, organically modified clays have been studied and used as reinforcing additives to improve mechanical and thermal properties in polymers [Mai, Yu, 2006], [Batenburg and Fischer, 2001].

However, nanopigments combine two important tasks: they improve physical-chemical properties of the polymer while giving colour [Batenburg and Fischer, 2001].

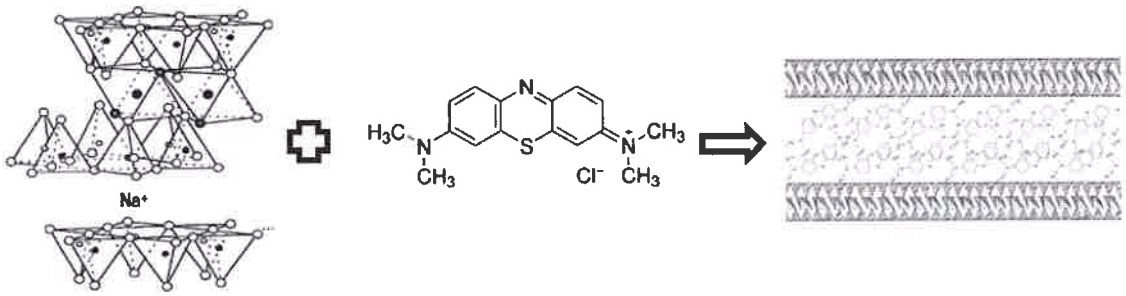

Figure 1: Schematic representation of clay sheet, dye molecule (methylene blue) and blue nanopigment

In this research collaboration between Colour and Vision Group from University of Alicante (CVG-UA) and Optics Colour Imaging Technological Institute (AIDO), nanopigments have been synthesized to be applied in the manufacture of offset printing inks. That is, CVG-UA has developed specific nanopigments and has supplied them to AIDO. Then, AIDO has been responsible for assessing their advantages and drawback as raw material for manufacturing offset printing inks.

2. Methods

2.1 Nanopigments synthesis

At a laboratory scale, nanopigments are obtained in a simple process with two main steps [Batenburg and Fischer, 2001]:

Firstly nanoclays have to be dispersed in a solvent, better in deionized water. This causes the nanoclay to swell. This increases the distance between clay sheets and, as a consequence, reduces the ionic bond force of the counterions of the clay.

After that, a dye solution is added to the dispersion. Then the ionic exchange takes place: Dye molecules replace counterions of the clay. This gives colour to clay nanoparticles and makes them compatible with the polymer.

At this moment, nanopigment is formed but dispersed in the deionized water. In order to isolate and purify the nanopigment we have to, firstly, wash and filter the dispersion, and then dry the cake. It can be done through several techniques: freeze drying, spray drying or in a muffle.

In figure 2 there is a schematic flowchart of laboratory synthesis process.

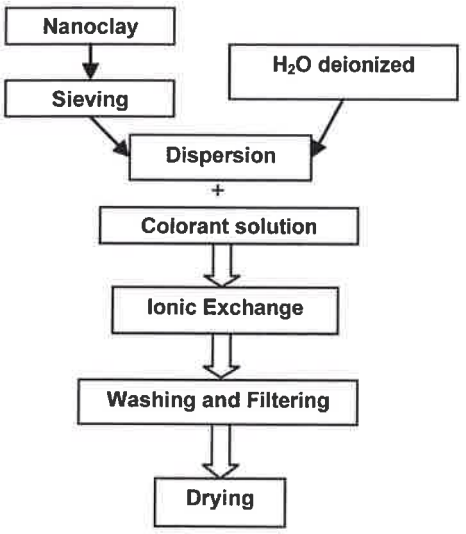

Figure 2:
Scheme of nanopigments' synthesis at laboratory

As a result, a light, dry powder is obtained that can be used such as a pigment, so it can be added directly to the material to colour, or to make coatings and cover a substrate.

2.2 Nanopigments for offset printing inks

The purpose of the research is to obtain primary colours for four-colour-process printing system for making offset inks. Therefore four different types of nanopigments, cyan (C), magenta (M), yellow (Y) and black (K) were obtained.

First step was selecting organic dyes. These dyes must be able to be attached to clay nanoparticles and, at the same time, match the primary colours requested (cyan, magenta, yellow or black). In table I there is a list of

selected dyes that in advance seem to be able to reach and develop the suitable colour shade. This list is the result of a deep search in the Colour Index database [http://www.colour-index.org/].

Table I: Dyes selected to obtain nanopigments for primary colours in four-colour-process offset printing system

Dye	CIE	Shade	Supplier
Methylene Blue	C.I. basic blue 9	Greenish blue	Sigma-Aldrich
Methyl Red	C.I. acid red 2	Red-Yellow	Sigma-Aldrich
Malaquite Green	C.I. basic green 4	Light bluish green	Sigma-Aldrich
Rodhamide 6G	C.I. basic red 1	Fluorescent bluish pink	Sigma-Aldrich
Thioflavine T	C.I. basic yellow 1	Light greenish yellow	Sigma-Aldrich
Acridine Yellow	C.I. 46025	Yellow	Sigma-Aldrich
Basic Blue 3	C.I. basic blue 3	Greenish blue	Sigma-Aldrich
Neutral Red 5	C.I. neutral red 5	Bluish red	Sigma-Aldrich
Maxilon Black		Black	Ciba
Fast Black K	C.I. Azoic disazo component 38	Black	Sigma-Aldrich

The nanoclay used to obtain nanopigmtens was montmorillonite Nanofil® 116 from Süd-Chemie. It is a phyllosilicate clay from smectite group, with a cationic exchange capacity of 120 meq/100 g_{clay}. Layers of montmorillonite particles have the shape of small flakes. The layers are 20-200 nm in diameter laterally and come in aggregates known as tactoids, which can be 1 nm or more thick [Ajayan, Schadler, Braun2003].

After synthesizing several nanopigments, which are listed in table II, they were sent to AIDO in order to assess their suitability as raw material to make offset printing inks.

Table II: Nanopigments synthesized for AIDO

Nanopigment		Dye	% dye
Nnp	blue 1	Methylene blue	27,5
Nnp	blue 2	Basic Blue 3	30,7
Nnp	magenta	Rodhamide 6G	41
Nnp	yellow 1	Thioflavine T	27,2
Nnp	black 1	Maxilon Black	30
Nnp	black 2	Fast Black K	35,7

2.3 Nanopigment ink fabrication

The nanopigment ink fabrication process, done in laboratory and can be explained in figure 3.

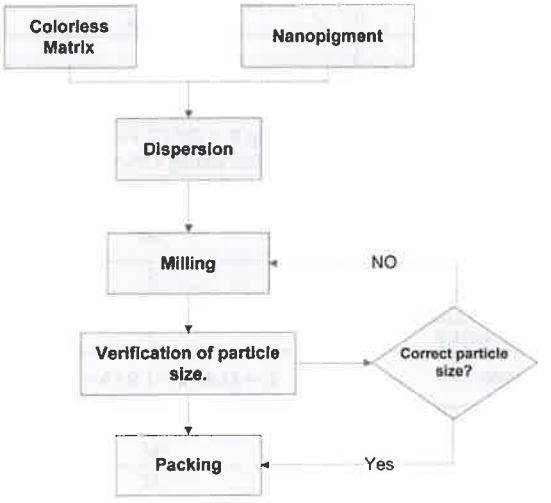

Figure 3: Nanopigment ink fabrication flowchart

In the first place nanopigments are pre-dispersed in an uncoloured matrix, then the pigments are ground in a three cylinder mill during a period of time. After this, the particle size is checked with a Grind-o-meter. If the particle size is under 5 μ the fabrication is finished; if the particle size is over 5 μ, ink is ground again in the three cylinder mill.

2.4 Physicochemical proprieties of the obtained nanopigment inks

Different proprieties of the nanopigmented inks obtained in laboratory have been studied to try to evaluate their behaviour as offset inks.

The more important physical proprieties for offset inks have been studied in this research.

These are:

- Particle size.
- Gloss at 60° degrees.
- Tack following the standard ISO 12634 "Determination of tack of paste inks and vehicles by a rotary tackmeter".
- Viscosity following the standard ISO 12644:1996 "Graphic technology Determination of rheological properties of paste inks and vehicles by the falling rod viscometer."
- Rigidity following the standard ISO 12644:1996 "Graphic technology Determination of rheological properties of paste inks and vehicles by the falling rod viscometer."
- Grinding time, Time in minutes needed to achieve 5μ of particle size with the three cylinder mill.
- CIELab Colour, L*,a*, b* values measured by the Standard ISO 13655:1996 "Graphic technology -- Spectral measurement and colorimetric computation for graphic arts images"
- Fluidity, measured in centimetres, is the space covered by a given quantity of ink in a space of time, being more fluid the ink which covers more space.

This includes applying standard procedures (ISO, UNE, ASTM, etc.) to evaluate physical properties (rheological, etc...) chemical and optical properties (colour, etc...) of the Nanopigmented inks.

3. Results

In "*Table III*" there is an example of the results obtained in the characterization tests of nanopigmented inks.

Table III: Studied product: Ink made from nanopigment synthesized from "methylene blue"

N°	Studied Property	Units	Test	Results
1	General characteristics	n.a.		Regular dispersion, some residue after the 1st pass through three roll mill but flowing well.
2	Scope	n.a.		Offset
3	Color Index	n.a.		n.a
4	Viscosity (0'8-0.4)	Poises	ISO 12644:1996.	Starting speed = 4584, Finish speed = 599 (alter adding 13% of solvent)
5	Stiffness (0'8-0.4)	Dyna/cm²	ISO 12644:1996.	Starting R = 20537, Finish R = 17918 (alter adding 13% of solvent)
6	Viscosity at 2.5 s-1	Pa*s	ISO 12644:1996.	n.a
7	Tack	30°C; 100m/min.	ISO 12634 Determination of tack of paste inks and vehicles by a rotary tackmeter.	80
8	Fineness	μm	Grindometer	5
9	Milling Time	minutes	Three roll mill	35
10	Hardness		N° of times grind is needed	2
11	CIELab Colour	n.a.	ISO 13655:1996	L = 51.4 / a = 1.9 / b = - 49.3
12	Colour strength	%	IGT tester	n.a
13	Brightness	%	Micro-gloss 60°	44
14	Fluidity	cm.	Inclined Plane 85°	27

4. Conclusions

After preparing several nanopigment inks, some ideas can be pointed out:

- Following the bibliographic database search, we have checked that a wide number of dyes can be used to synthesize nanopigments.
- From a physical point of view, nanopigments obtained with selected dyes have a good behaviour as raw material for making offset printing ink. However, they have a major drawback; their shade is not exactly the shade requested in the standard for printing inks.
- As well as the shade difference. Due to a dye concentration between 27% and 41%, colour saturation of the inks is very small, and the high amount of nanoclays in offset inks affect to their proprieties.
- Offset inks can be prepared from the synthesised nanopigments with similar physical proprieties than the standard inks.
- Despite nanopigments having a particle size from 20 to 200 nm in diameter, due to the aggregate formation during the dispersion process, particle size in offset inks is more than 5μ. This needs to be improved in futures studies by changing the dispersion process, adding surfactant additives, or improving the drying stage.

Therefore, as future perspective, new efforts have to be done to approach nanopigments' colour shade to the standards and improve the dispersion and grinding processes. These are the main new aims for the research during the year, probably by making hybrid inks from nanopigments and standard pigments and adding surfactant additives.

Acknowledgements

Thanks to TNO-TPD Eindhoven for allowing us to reproduce the synthesis of Planocolors® and for their technical and knowledge support.

This research was financed by the Generalitat Valenciana, through IMPIVA by means of the grant number IMIDIN 2008/17 and co-financed by the ERDF: European Regional Development Fund.

References

1. Batenburg, L. F., Fischer, H. R., "Planocolors® - a combination of organic dyes and layered silicates with nanometer dimensions". E-polymers (http://www.e-polymers.org), 2001
2. Fischer, H., "Polymer nanocomposites: from fundamental research to specific application". *Material Science and Engineering*, C 23, 763-772, 2003
3. Fischer, H., Batenburg, L. F., "Coloring Pigment", patent WO0104216, 2001
4. Zeng, Q. H., Yu, A. B., (Max) Lu, G. Q., Paul, D.R., "Clay-based polymer nanocomposites: research and commercial development". *Journal of Nanoscience and Nanotechnology*,Vol 5, pp. 1574- 1592, 2005
5. Ajayan, P. M., Schadler, L. S., Braun, P. V., *Nanocomposite Science and Technology*, Wiley-VCH, Weinheim, 2003
6. Mai, Y. W., Yu, Z. Z., *Polymer nanocomposites*, Woodhead Publishing Limited and CRC Press LLC, Cambridge, 2006





3

Printing and print quality

Pressroom draw variation and its impact on web breaks Part II: Commercial pressroom trials

Nina Deng, Frédéric Parent, Tony Manfred, Joe Aspler, Jean Hamel

FPInnovations - Paprican Division, 570 Blvd. St. Jean
Pointe-Claire, QC, Canada, H9R 3J9
E-mail: nina.deng@fpinnovations.ca

Abstract

In the first report of this series, we characterized the draw variation of newsprint webs in a number of North American newspaper pressrooms using the technique of laser Doppler velocimetry. We showed that there is a good correlation between web break rates and pressroom draw variation. In this report, we have extended the draw variation study to commercial pressrooms, including heatset offset, coldset directory offset, and gravure printing. A wide range of draw variations was seen, likely related to the wide range of press operating and maintenance conditions. Also, as is the case with daily newspaper pressrooms, the contribution of paper is small. For a given draw variation, the web break rate in a heatset offset pressroom is significantly higher than that in newsprint pressrooms. This may be due to the fact that heatset offset presses are more complex. Case studies demonstrated that the draw variation can be reduced through improved press maintenance and operation.

Keywords: runnability, web breaks, tension, offset printing, gravure printing

1. Introduction

As discussed in Part I of this series [1], web breaks have always been a major problem in pressrooms. Efforts from the paper industry to reduce web breaks include increasing the average tensile strength of paper, improving the uniformity of paper strength, reducing the number of physical flaws and foreign contaminants in the sheet, and improving roll quality in terms of winding, reduced out-of-roundness, and so on. However, the way in which press design and operation affect web breaks has been less well understood.

We previously [1] measured the draw variation of newsprint webs in a number of North American newspaper pressrooms using the technique of laser Doppler velocimetry. We showed that the greater the draw variation on the web, the greater the possibility of web breaks. The draw variation was found to be almost entirely a pressroom property, and only in exceptional circumstances did the properties of the paper web have an effect. In particular, in one pressroom, we showed that after press adjustments, both the web break record and the draw variations were improved [1].

In the current paper, we extend the work from Part I to commercial printing plants. The following grades of paper were examined:

- Supercalendered and lightweight coated paper, printed by heatset offset
- Supercalendered paper printed by rotogravure
- Lightweight directory paper, printed by coldset offset.

As shown in detail in this paper, commercial printing processes put their own additional demands on the paper. These can be summarized as follows:

1. Heatset offset printing: while the basic printing technology is the same in both coldset offset newspaper printing and commercial heatset offset printing, the difference between heatset and non-heatset is primarily dependent on the type of ink used and how it is dried. The heatset process usually puts extra demands on the paper as discussed below, in the section on Results and Discussion.

2. Directory printing: directories are printed by either heatset or coldset offset. The web paths through the folder in directory printing are simpler than in heatset offset printing. On the other hand, directory paper is

3. Gravure printing: gravure printing is distinguished by the use of very wide paper rolls, and by the use of a separate drying oven for each colour, rather than the much longer single drying oven used in heatset offset printing. A wide gravure or heatset offset web is also slit into many ribbons - up to 10 or more - each of which is susceptible to breakage.

2. Experimental

2.1 Draw variation measurements on printing presses using laser doppler velocimetry

The technique of laser Doppler velocimetry was used to measure the velocity of a moving web without contact by utilizing the Doppler frequency shift technique. It can measure the velocity at a very high frequency (every 2 ms or 500 Hz), which allows detection of high frequency speed variations. The accuracy of this device is 0.05% [2].

A detailed description of the technique is given in Part I [1]. To measure the draw variation on a printing press, two synchronized laser Doppler sensors are installed at different locations. On heatset offset presses, one sensor is usually installed at the infeed, while the other sensor is moved to different locations (Figure 1).

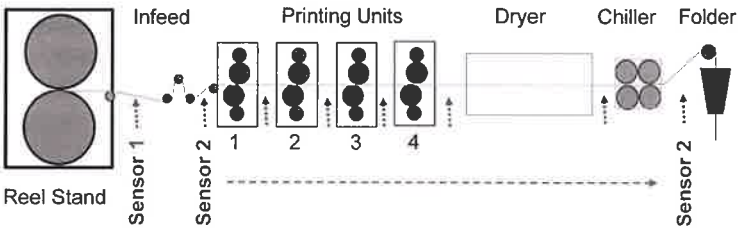

Figure 1: Heatset offset press schematic, showing the positioning of the laser sensors

Draw is the relative speed difference between the two sensors as calculated from the following equation:

$$Draw(t) = \frac{V_2(t) - V_1(t)}{V_1(t)} \quad (1)$$

The standard deviation of the draw is used as an indication of draw variation.

2.2 Information on printing presses and paper samples

Information on the presses and paper samples used for each pressroom trial is listed in Table I. As can be seen, a large number of presses were characterized and various paper grades including newsprint, directory, SCA, SCB and LWC were tested.

3. Results and discussion

3. 1 Draw variation of heatset offset presses

We measured the draw variation on several heatset offset presses, in different pressrooms. Figure 2 shows a typical set of draw variation measurements, with the sensors placed before the infeed and after the chill rolls, for three presses in the same pressroom (pressroom A). As can be seen, the draw variations vary significantly among these three presses. Press 1 had a very low draw variation (STD = 0.04), while Press 3 had a much higher draw variation (STD = 0.14). The papers printed on these three presses are from the same paper machine. This confirms that the draw variation is related mainly to press conditions. In addition, the range of the draw variation

Table I: Pressroom information

Pressroom	Press	Press Type	Paper Supplier & Grade
A	1	Heatset offset, Goss	Mill A, SCB
	2	Heatset offset, Harris	Mill A, SCB & Mill B, Newsprint
	3	Heatset offset, Harris	Mill A, SCB
B	4	Heatset offset, Man-Roland	Mill C, SCA
	5	Heatset offset, Man-Roland	Mill C, SCA
C	6	Heatset offset, BP G-14	Mill D, LWC
D	7	Heatset offset, Harris	Mill D, LWC
	8	Heatset offset, Harris	Mill D & E, LWC
E	9	Heatset offset, Lithoman	Mill E, coated paper
	10	Heatset offset, Harris	Mill F, coated paper
	11	Heatset offset, Harris	Mill G, coated paper
	12	Heatset offset, Heidelberg	Mill H, SCA
	13	Heatset offset, Heidelberg	Mill H, SCA
F	14	Heat set offset, Harris	Mill I, SCA
	15	Heatset offset, Heidelberg	Mill I, SCA
	16	Heatset offset, Heidelberg	Mill I, SCA
G	17	Heatset offset, Heidelberg	Mill J, White Paper
	19	Coldset offset, KBA	Mill K, Directory
	20	Coldset offset, KBA	Mill K, Directory
	21	Coldset offset, KBA	Mill K, Directory
F	22	Coldset offset	Mill L, Directory
	23	Coldset offset	Mill L, Directory
	24	Coldset offset	Mill L, Directory
G	25	Gravure, KBA	Mill M, SCA
	26	Gravure, KBA	Mill M, SCA
	27	Gravure, KBA	Mill M, SCA
	28	Gravure, KBA	Mill M, SCA

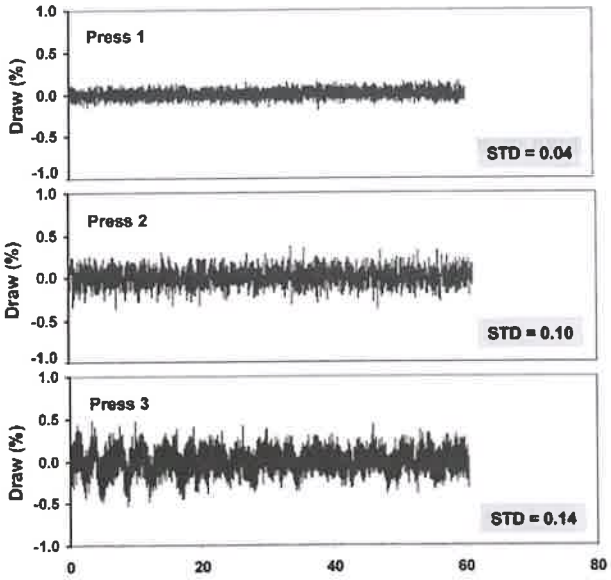

Figure 2:
Draw variation on different presses

Different papers (SCB vs. newsprint) were also tested on the same press in Pressroom A to see if paper grade has a significant effect on draw variation. As shown in Figure 3, no significant difference in the draw variation was found between the two papers. This again shows that the draw variation is controlled mainly by the press. The contribution of paper is small.

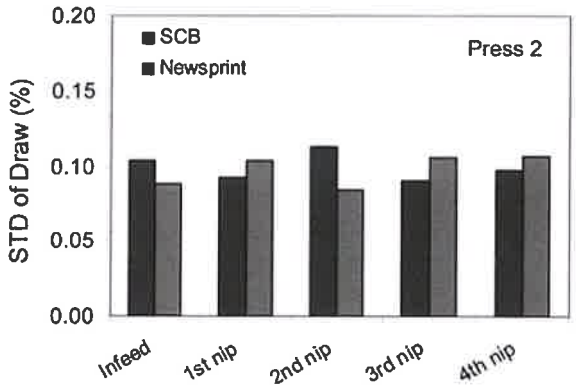

Figure 3:
Draw variation of different papers printed on the same press in Pressroom A

In the newspaper pressroom trials [1], draw variations were found to increase significantly on some presses during pasting cycles. Therefore, we also measured the draw variation during pasting on the heastset presses in Pressroom A. As shown, the draw variation increases significantly during pasting on Press 3, while as on Press 2, there is only a small increase (Figure 4). This indicates that the effect on pasting on draw variation is press-dependent. The pressroom confirmed that Press 3 had a high break rate during pasting.

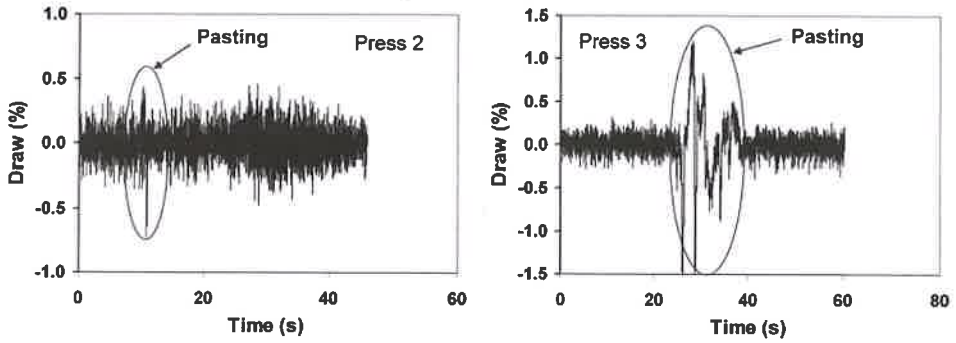

Figure 4: Draw variations during pasting - Press 2 (left) and Press 3 (right)

A high web break rate often occurred at press start-up in many pressrooms. To see if this is related to the draw variation, we also measured the draw variation during press start-up on several presses in different pressrooms. For some presses, very high draw variations were observed during press start up, similar to newsprint presses. Figure 5 shows an example of the draw variation during press start up of three gravure presses in the same pressroom. As can be see, draw variation is very high on Press 25, while as it is low on Press 27 which is the same type of press as Press 25 but a newer press (3 years old). The papers printed on the three presses are the same SCA paper from the same paper machine.

3.2 Comparison of draw variation on different presses

The draw variations of all the presses we have measured are plotted in Figure 6 and can be grouped into five categories: newsprint coldset, newsprint flexo, commercial heatset offset, directory coldset offset and gravure presses.

As can be seen, there is a wide range of draw variation even within the same category. This reflects many differences including the type and age of each press, the difference in the operating conditions, and the maintenance conditions. In particular, coldset newspaper presses and commercial heatset offset presses cover

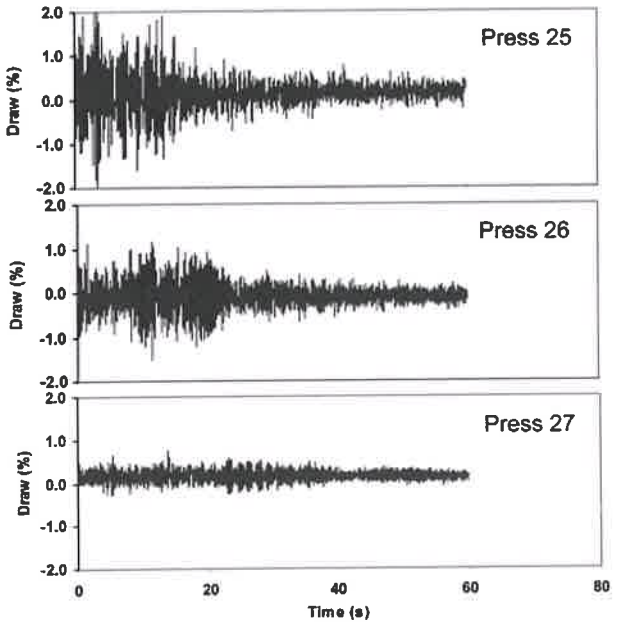

Figure 5: Example of draw variations during press start up

Flexo newsprint presses showed a draw variation similar to those of newsprint coldset offset presses. Coldset directory offset presses seem to have a low draw variation and this may explain why they can maintain reasonable web breaks records even with very low basis weight paper.

Only four gravure presses were studied, in a single pressroom. Low draw variations were observed on these presses. However, for safety reasons, the measurements were only taken between the last dryer and the slitter section. For the other presses, draw variation was measured between the infeed and the folder.

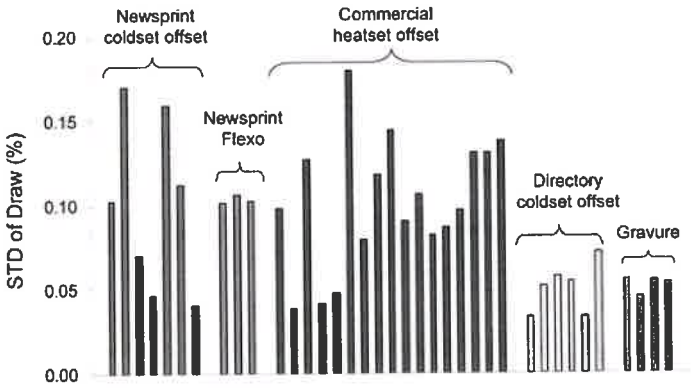

Figure 6: Comparison of draw variation of different presses

3.3 Correlation between break rate and draw variation

Unlike newsprint pressrooms, the paper used in the commercial pressrooms can vary considerably in terms of grades (e.g. coated and super-calendered papers) and basis weights. For most commercial pressrooms, web break statistics are not separated by paper grade. Therefore, it is difficult to establish any correlation between web break and draw variation for commercial presses.

Only pressroom A recorded web break statistics for different grades. We measured the draw variation on three different presses using the same SCB paper. Similar to the newsprint trial results, a good correlation between the draw variation and web break rate was found for these heatset offset presses (Figure 7). At given draw variation, the break rate is significantly higher for heatset offset presses compared to coldest offset newsprint presses.

- *Ink tack*: Heatset offset inks have higher tack values than coldset newspaper inks. These higher tack inks require a greater web tension to pull the paper through the multiple printing nips.
- *Drying oven*: The paper temperature reaches 125° - 130° in the heatset drying oven, reducing the moisture content to less than 1%, thereby embrittling the paper.
- *Web path*: The web path in the folder of a heatset offset press is much more complex than in a newspaper press. The web is slit into six or more ribbons to generate the printed signatures or booklets, with each ribbon becoming a potential source of web breaks.

4. Case studies

A number of case studies were carried out in pressrooms with poor web break records. The detailed analyses are described below.

4.1 Case study 1

Press 3 in Pressroom A (heatset offset) had a high draw variation. FFT analysis showed frequencies that corresponded to the diameter of the chill rolls. Upon investigation, the chill roll gear box was replaced. Additional measurements confirmed that the draw variation had decreased significantly (Figure 8) and that the frequency associated with chill roll diameter had disappeared (Figure 9).

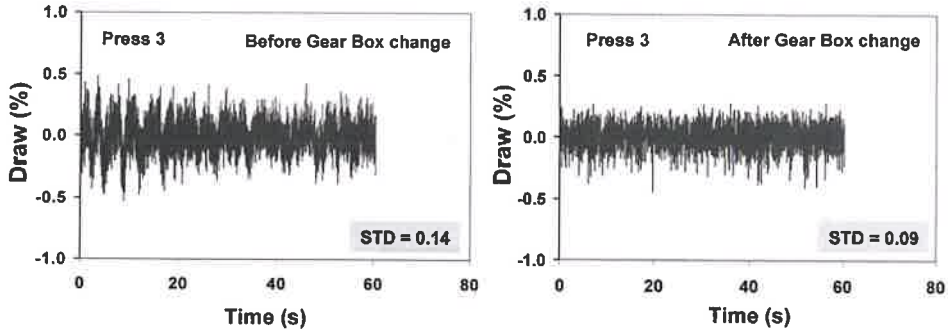

Figure 8: Draw variation before and after chill roll gear box change on Press 3

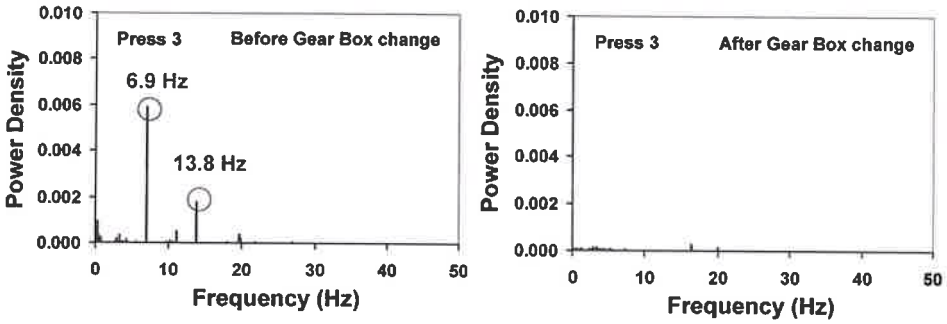

Figure 9: FFT analysis results before and after chill roll gear box change on Press 3

4.2 Case study 2

On Press 4 in pressroom B, the web tended to move towards the back side of the press after the dryer. A shift of more than 20 mm would cause a web break. As shown in Figure 10, a higher draw on the back side was observed, indicating a non-uniform draw across the web width. Examination of the dryer showed that some drying elements were not functioning, creating a non-uniform temperature profile (Figure 11). This led to the non-uniform draw. After repairs, the non-uniformity of temperature and draw were significantly reduced (Figures 10 and 11) and the web lateral movement problem was reduced.

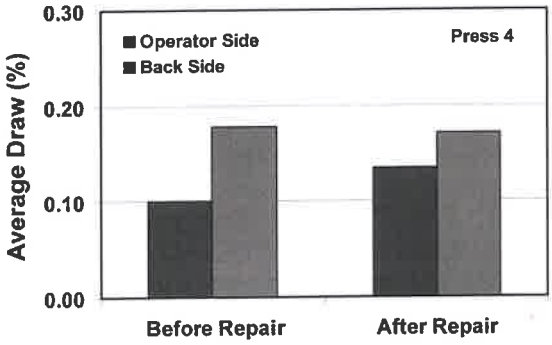

Figure 10:
Draw non-uniformity before and after repair of dryer

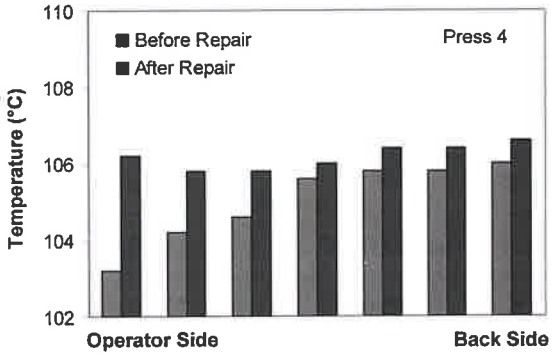

Figure 11:
Temperature profile before and after repair of dryer

4.3 Case study 3

Gravure printing uses very wide paper rolls that are slit into many ribbons which then follow a very complex path (Figure 12). Each of the ribbons is susceptible to breakage.

Press 25 (gravure) in pressroom G had a high web break at the slitter. We found that the draw variation at the slitter section was very high (> 2%) during press startup on this press (Figure 13). We also found that the speed variation before and after the slitter were not perfectly matched, causing the high draw variation at press start-up (Figure 13).



Figure 12: Slitter section of gravure press

Figure 13: Speed and draw variation during press start up Press 25, Pressroom G

A web break occurred while measuring draw variation on Press 25. A tension spike was found immediately before the web break, caused by a sudden speed increase at the folder (Figure 14). Previous study has shown that under normal pressroom tension (about 10 to 20% of the paper strength) the web should hardly ever break and web breaks are most likely caused by tension spikes [3, 4, and 5].

5. Conclusions

High frequency draw variations in commercial pressrooms (heatset offset, coldset directory offset, and gravure) were quantitatively characterized using laser Doppler velocimetry. The main conclusions from these trials are:

1. A wide range of draw variations was measured, similar to the range observed for daily newspaper pressrooms, and are likely related to the wide range of press operating and maintenance conditions.

3. For a given draw variation, the web break rate in a heatset offset pressroom is significantly higher than that in newsprint pressrooms. This may be due to the fact that heatset offset presses are more complex. However, this could be confirmed only in a single pressroom where roll break data were separated by paper grade.
4. Case studies demonstrated that the draw variation can be reduced through improved press maintenance and operation.

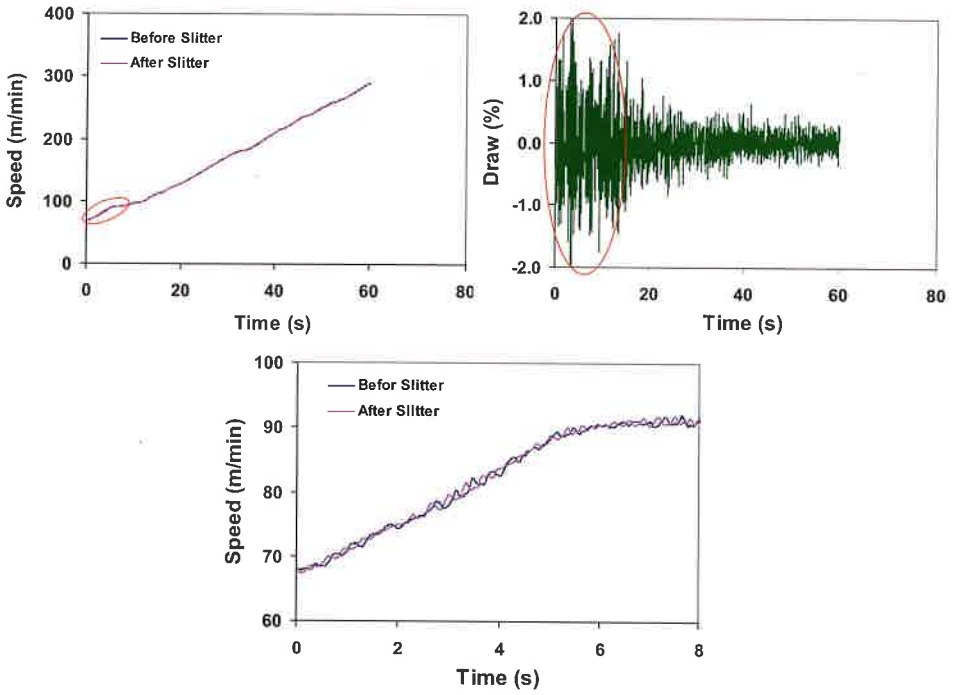

Figure 14: Speed and draw variation measurement during web break on Press 25 in Pressroom G

Acknowledgements

The authors would like to thank Paprican's Member Companies and the pressrooms that assisted us in carrying out the pressroom trials and provided information on printing press and web break data. We also wish to thank Pierre Lepoutre for reviewing this report.

References

1. Deng, N., Parent, F., Manfred, A., Aspler J. and Hamel J., "Pressroom Draw Variation and Its Impact on Web Breaks: Part I: Newspaper Pressroom Trials", Paprican, Adv. Printing Sci. Technol. 35:119 (2008)
2. TSI Incorporated, LaserSpeed 1100, Speed and Length Measurement System, Instruction Manual (2001)
3. Page, D. H. and Seth, R. S., "The Problem of Pressroom Runnability", *Tappi J.* 65:8, 92 (1982)
4. Uesaka, T. and Ferahi, M., "Principal Factors Controlling Pressroom Breaks", Proceedings of the 1999 TAPPI International Paper Physics Conference, TAPPI Press, Atlanta, 229-245
5. Uesaka, T., Ferahi, M., Hristopulos, D., Deng, N. and Moss, C., "Factors Controlling Pressroom Runnability of Paper", The Science of Papermaking, 12th Fundamental Research Symposium, Oxford, UK, 17-21, Sept. 2001, 2:1423

How to utilise improved newsprint - balancing image quality and set-off

Marianne Klaman, Per-Åke Johansson, Erik Blohm

Innventia
P. O. Box 5604, SE-114 86 Stockholm, Sweden
E-mails: marianne.klaman@innventia.com, perake.johansson@innventia.com, erik.blohm@innventia.com

Abstract

Contrary to standard newsprint, which is highly standardised when it comes to paper properties and the prepress and printing parameters, there is a lack of standards governing improved newsprint. If the prerequisites are not accurate, the quality can actually be worse than for standard newsprint, due, among other things, to set-off and smearing, which is the most evident problem with improved newsprint, related to print quality. One occurring problem is also that the images are too dark and, as a result, there is a loss of detail. In the investigation presented here, the necessary actions to ensure optimal print quality and the lowest possible level of set-off were considered. Paper samples were printed with different levels of print density and total ink coverage area (TIC). The printing trials were conducted at three newspaper printing houses. If certain measures are taken, it was shown that improved newsprint has the potential of resulting in improved image quality, due to a larger colour gamut and a higher relative contrast, when compared with standard newsprint. An ICC Profile, well adapted to the conditions in different printing presses and paper qualities and careful adaptation with regard to crucial parameters, such as the total ink coverage area and K value, is helpful for achieving a high quality image, together with a minimised risk for set-off.

Keywords: improved newsprint, adapted ICC profiles, set-off, print density, image quality

1. Introduction

Compared to standard newsprint, improved newsprint is brighter, while often having a lower surface roughness and a higher grammage and stiffness.

The term *improved* gives the expectation of always providing a better print quality in comparison to standard newsprint. Contrary to standard newsprint, which is highly standardised not only regarding the paper but also the parameters for prepress and printing, there is a lack of standards governing improved newsprint. In essence, this is the reason why printing houses are sometimes disappointed when using improved newsprint because they do not achieve the print quality they expect. If the prerequisites are not accurate, the quality can be even worse, due to set-off/smearing, for instance, which is the most obvious problem related to print quality on improved newsprint. A common problem is the images being too dark and, as a result, there is also a loss of detail. This paper presents the actions that should be taken to ensure a high print quality and to properly take advantage of the potential that improved newsprint offers. Theoretically, this paper grade ought to have a lower ink demand, a property that can be used to decrease the inking level and, thus, reduce the tendency for set-off. The following shows how such actions can have an impact on image quality.

The aims of the research presented in this paper are:

- The actions that have to be taken when printing on improved newsprint instead of standard newsprint, in order to ensure optimal print quality.
- How to balance image quality against set-off.

The current research was carried out jointly with a group consisting of companies from the entire value chain, viz. paper producers, ink suppliers and newspaper printing houses.

2. Research methods

Three samples of newsprint were chosen for the investigation.

- One standard newsprint, as a reference,

These papers were printed with different combinations of total ink coverage area (TIC) and print density. The print trials were conducted at three newspaper printing houses.

To find the best possible ICC profile for the improved newsprint grades, full scale print trials were carried out in several steps, in which the level of density, the total ink coverage area and the K value (GCR setting for black) GCR (= Grey component Replacement) [IFRA, 1996] were changed.

The starting point for the creation of the profiles was the ISO Standard [ISO, 2005] for printing on standard newsprint. Based on these values, the density was changed, as were the TIC and the K values in the initial trials. Finally, trials were carried out with fixed density levels, with the TIC value and the K value being based on the results from the initial trials.

In the first step, the ICC profiles were based on print from the printing house that produced the best quality printing, while, in the second step, the profiles were calculated from the mean values of the print from all the three printing houses. Moreover, the mean values were calculated for the papers and these were used in both steps.

In the final step, two profiles were calculated from profile data available from Fogra and used for comparison. These profiles were calculated with the same values for TIC and K, as for the other profiles.

The various prints were evaluated by measuring the grey balance, the level of set-off and perception of the image quality, together with certain other parameters.

The grey balance was calculated as the chroma difference ΔC^*, see *Equation 1*. It was calculated with reference values defined according to the procedure used at the IFRA International Newspaper Color Quality Club (INCQC) (www.ifra.com) and with the test form from the quality club, see *Figure 1*:

$$\Delta C^* = \sqrt{ ((a^*_{sample} - a^*_{ref})^2 + (b^*_{sample} - b^*_{ref})^2)} \quad (1)$$



Figure 1: The test sheet used for the evaluation of grey balance. Reference values for each tone value are calculated from the measurements of paper white and four colour black. These values, representing the darkest grey balance patch and paper white, are divided linearly for each tone value

Set-off was determined from five black test areas, with different values of TIC (total ink coverage = sum of CMYK%) and GCR. Samples of newspapers were taken straight from the presses and the test areas were exposed to a set-off experiment after 20 seconds or 5 minutes. In the experiment, the fresh print was laid out, in contact with a piece of the same paper grade and, after a chosen time lapse, a metal cylinder was rolled over the samples. The line pressure in the nip was approx. 200 N/m. The resulting set-off on the receiving paper was reported as print density. However, since the set-off was only in the range of 0.01 to 0.02, the readings from an ordinary densitometer were too imprecise and scattered. The average reflectance of the set-off stains was recorded, instead, by a calibrated desktop scanner and recalculated to a print density.

For the perception of image quality, two sets of images were used:

Set 1: The images are chosen from different sources, see the references in *Figure 2*. These three images were classified as an image with skin tones, an image with bright colours and a low-key image.

Set 2) These images are available from Bundesverband Druck und Medien e.V. (bvdm) on www.roman16.com, see *Figure 3*.



Figure 2: Test Set 1, used for perception evaluation. From left to right: a) An image with skin tones (Grafisk Assistans AB), b) Cyclists, an image with bright colours (IFRA Color Quality Club 2006, photo: Gero Breloer), c) A low-key image (OK Color, E. Enoksson)



Figure 3: Test Set 2, used for perception evaluation. (Bundesverband Druck und Medien)

The printed images were evaluated in the perception laboratory at Innventia. The panel consisted of twelve expert observers. For every set of the randomised printed images (on different papers, with different ICC profiles and the other parameters), the instructions to the panellists were as follows:

- Classify the samples into homogenous groups, when it comes to image quality.
- Give each group a number for the quality, as perceived.

3. Results and discussion

3.1 Standard newsprint compared to improved newsprint

Initial tests showed that the relative contrast was slightly higher for the improved grades, compared to the standard grade, see *Figure 4*. For the black ink, the contrast curve was more flattened out and the maximum was between 1.0 and 1.15, see *Figure 5*.

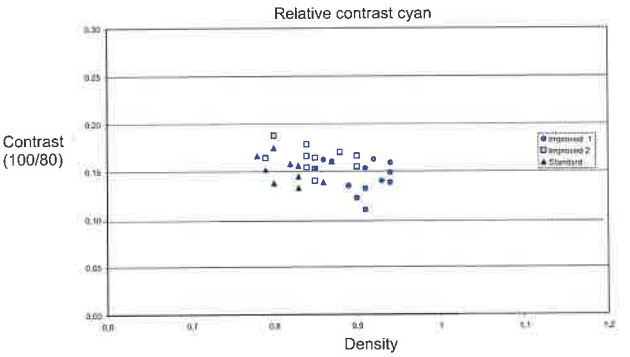

Figure 4: The relative contrast curve for cyan for the improved newsprint grades and the standard grade

Compared to the standard newsprint, the gamuts for the improved grades, as expected, were larger, due to higher brightness. In *Figure 6,* the gamuts can be seen for improved and standard newsprint and also for improved newsprint at different density levels. At a higher density level (D ≈ 1.0), the gamut for one of the improved grades was measured as being 105 000 L*a*b* volume units and, at a lower density level (D ≈ 0.85), it was 90 000 units, compared to 70 000 for standard newsprint. Lowering the density on improved newsprint still gives a much

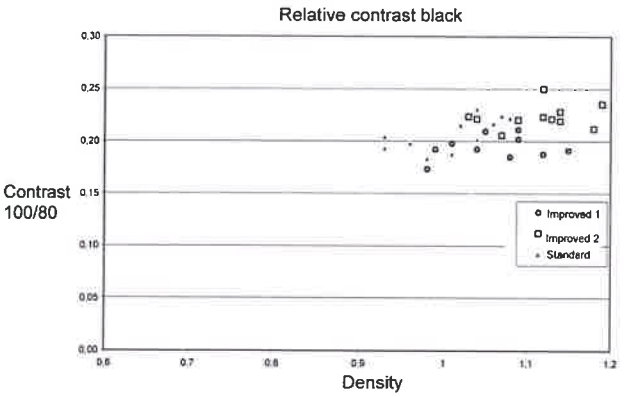

Figure 5: The relative contrast curve for black for the improved newsprint grades and the standard grade

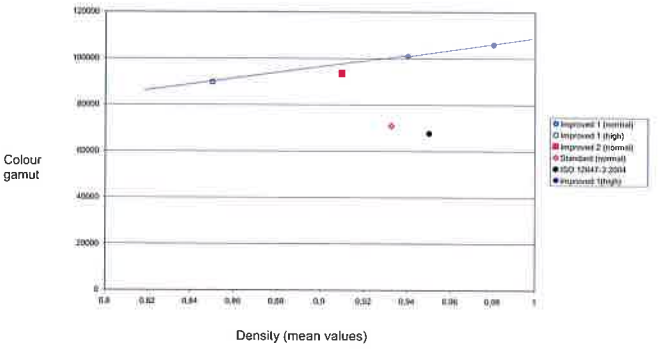

*Figure 6: The colour gamut (L*a*b* volume entities) for improved and standard newsprint at low, normal and high print densities*

3.2 Grey balance

When it comes to grey balance, the initial trials gave the lowest chroma differences for an ICC profile, with a TIC value of 195 and a K value of 93%. The following trials showed that a GCR, with a K value of 96%, gave a slightly better grey balance, which also corresponds well with what is expected theoretically. This was the K value that was chosen for the last trial. A mean value, calculated from the chroma differences ΔC^* for all tone steps in the evaluation chart for grey balance (as seen in Figure 1), showed that profile 3 (with a TIC value of 195 and a K value of 96) clearly gave the best, ie most neutral, grey balance, see *Figure 7*. Profiles 1 and 2 (synthetic profiles calculated from the available Fogra data (www.fogra.com) did not improve the image quality.

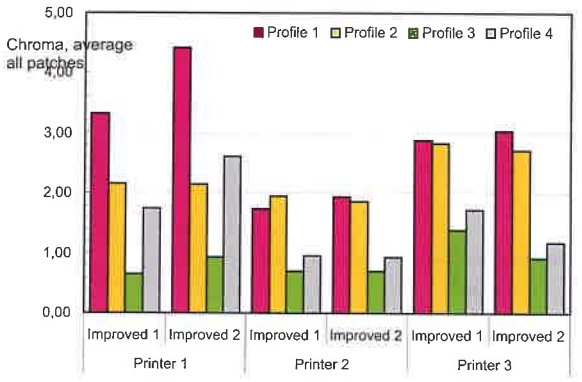

Figure 7:
Profile 3, based on a TIC value of 195 and a K value of 96, gave the most neutral grey balance

3.3 Set-off

Unwanted set-off will, of course, increase, the more ink there is on the paper, which is one of the reasons for the attempts to reduce the total ink coverage, using methods such as GCR. A complete removal of CMY in dark

image sections will, however, result in an unsatisfactory saturation and contrast. A compromise between print density and a tendency for set-off had to be looked for as a result. In the tests, the following combinations of TIC% and maximal K% were printed:

1) TIC = 200%, K = 70%
2) TIC = 200%, K = 100%
3) TIC = 230%, K = 85%
4) TIC = 260%, K = 100%
5) TIC = 290%, K = 70%

Figure 8 shows the resulting set-off (an average of three papers printed with two densities at three printing houses). It is evident that the set-off increases almost linearly with the TIC level.

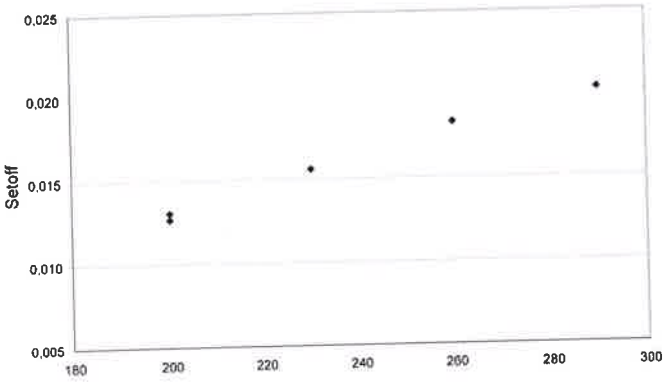

Figure 8:
Set-off has a nearly linear dependence of TIC% (Total Ink Coverage)

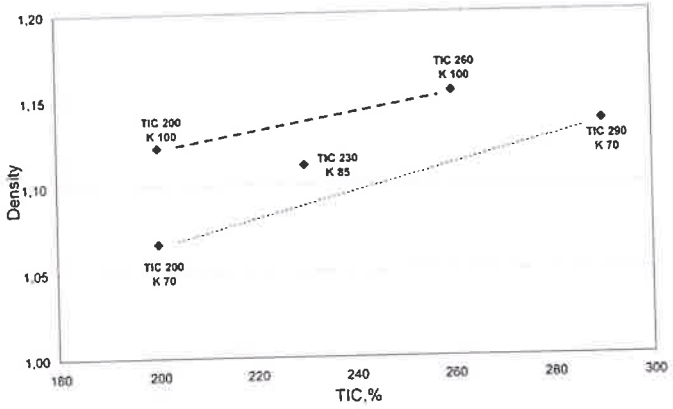

Figure 9:
Print density depends not only on TIC%, but also on amount of black (K %)

The aim of printing is to create contrast, but the print density does not follow the TIC level as linearly, which can be seen in *Figure 9*. At a certain TIC value, a higher amount of black ink, K%, will give higher density. Consequently, set-off will also depart from a linear dependence on print density, see *Figure 10*. Since we strive for a high density and a low set-off at the same time, the optimal section is the lower right part of this diagram. Of the combinations present in this study, the TIC = 200% / K = 100% point stands out as useful compromise. This point produces a lot of density per set-off or little set-off per density, so to say.

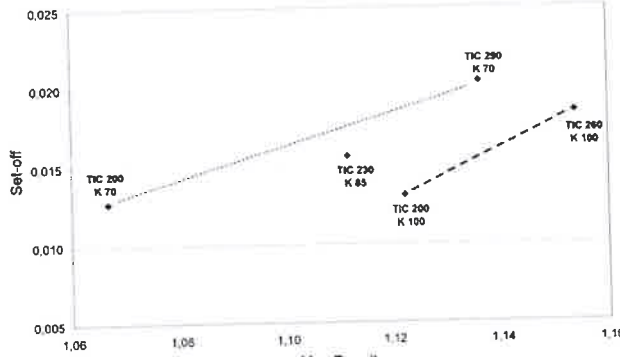

Figure 10:
Set-off increases with density. Set-off however gets lower at a given density level, if the maximal density is created with a high amount of black ink (K 100%)

3.4 Perception studies

The perception results showed that, for images with bright colours without any natural references, the panel judges more often preferred a higher TIC value, but for skin-tone and low-key images, lower TIC values were preferred.

Figures 11a, 11b and *11c* show how an adaptation to an ICC profile, based on mean values, calculated from the different printing houses, improved the performance of the profile. While in 8a, the result was very dependent on the printing house where the images are printed, for 8b and 8c, the results were dependent on the profile, not on the printing house.

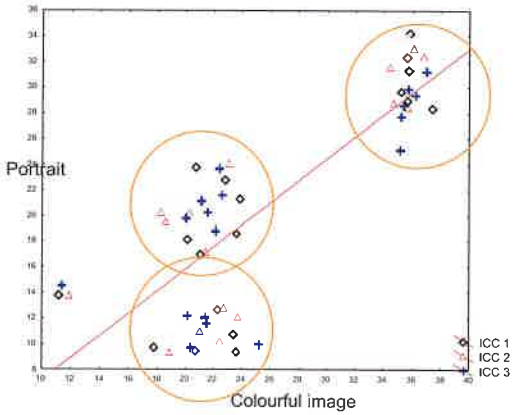

Figure 11a: The impact from the printer (three groups of samples) was dominating. Quality scores for two images of different characters: higher values indicate higher image quality, as perceived by the panel. The printers appear from the upper part of the diagram to the lower part: printer 2, printer 3 and printer 1

3.5 Density

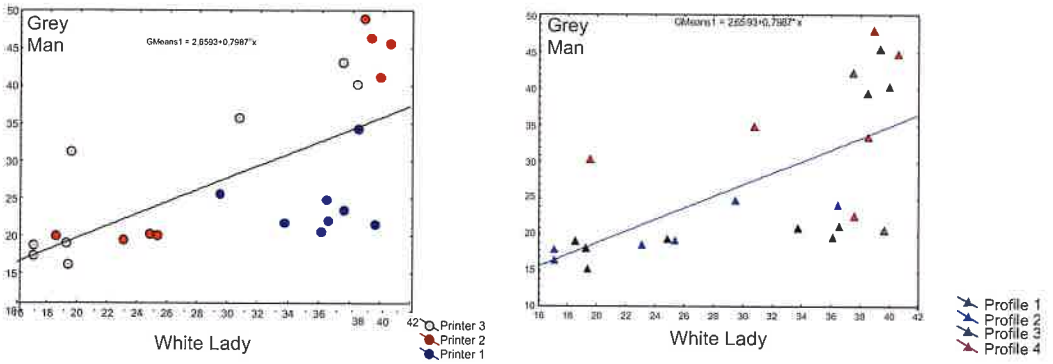

Figures 11b and 11c: The image quality depended more on the ICC profile than on the printing house, when compared to Figure 11a. A higher value indicates a higher image quality, as perceived by the panel

3.6 Density level

Trials with different density levels showed that it is possible to find a good compromise between the aim of reaching as large a colour gamut as possible while, at the same time, reducing the tendency for set-off to a minimum. The use of a lower density level for CMY, i.e. D = 0.85, compared to that which is recommended for standard newsprint, D = 0.90, is beneficial for the image quality (detail rendering in low-key images) and for reduced set-off. Nevertheless, it was decided to keep the level for black at D = 1.1, due to a better contrast for the text.

3.7 Total Ink Area coverage (TIC Value) and K Value

The print trials showed that an appropriate TIC level, lower than what is recommended for standard newsprint, is favourable for improved newsprint. A K value of 96 gave the best grey balance.

3.8 Grey balance

The TIC Value that gave the best grey balance, TIC of 195, was chosen to be used in the ICC profile. This value, together with the calculated mean values for all papers and printers, gave the best overall (measured) technical grey balance.

3.9 ICC profile

The final ICC profile, which gave the best image quality, also gave the best grey balance, together with the lowest set-off value.

4. Conclusions

It was shown that improved newsprint has a large potential for achieving high image quality, due to a greater colour gamut and a higher relative contrast, compared to standard newsprint if certain measures are taken.

An ICC Profile, well adapted to conditions in different printing presses and paper qualities and a careful adaptation, when it comes to crucial parameters, such as total ink coverage area (TIC) and K value (GCR settings), will be a helpful tool for achieving a high quality image, together with a minimised risk for set-off.

Perception studies showed that colourful images, without natural references, are not very sensitive, with regard to the different prepress and press parameters, while skin tone images, high-key images and low-key images are. Results from the perception studies also showed that it is important to create the ICC profile from mean values from printers, rather than values that come from only one printer, even though high quality print is being produced. Such a mean profile will perform well. It will perform equally well on different presses. For low-key images, a relevant ICC profile is crucial, since, detail rendering is otherwise seriously lost, which the perception studies clearly showed.

To minimise the risk of set-off, a lower inking level is favourable and, since the ink demand for improved newsprint is low, this will not affect the image quality in a negative way. The colour gamut for improved newsprint will still be greater than for standard newsprint. A low density level is favourable for low-key and skin tone images, which the perception study positively showed.

The best way to utilise improved newsprint and achieve the potentially high image quality and, at the same time, reduce the risk for set-off, is to be aware of and maintain the prepress and printing conditions at the crucial break-even point, where quality and potential disturbances are most balanced and will work together.

Acknowledgement

We would like to thank all participants in the carrying out of the project. These participants are paper producers, Holmen Paper and Stora Enso, ink suppliers, Sun Chemical and Flint Group Europe, newspaper printing companies, V-TAB Örebro, EKTAB and DNEX and the Swedish Newspaper Publishers' Association. We would especially like to thank Axel Irestedt at Sun Chemical, Niclas Noord at V-TAB Örebro, Samuel Starkenberg at EKTAB, Christer Hagman at Flint Group Europe, Lars Åkesson at Stora Enso, Jan Andersson at Holmen Paper and Per Carleson at DNEX for their valuable and wide-ranging contribution to the particular work presented in this paper.

We would also like to extend our thanks to Sofia Thorman, who measured and analysed the grey balance and other parameters as well as the Innventia perception laboratory for carrying out the perception study. Thanks also go to Jenny Hellenberg, who did her Master's thesis in the project and carried out part of the measurements and analyses

References

1. ISO, (2005), *12647-3:2005. Graphic technology - Process control for the production of half-tone colour separations, proofs and production prints - Part 3: Coldset offset lithography on newsprint*
2. IFRA, (1996), *Special Report 2.16, potential and Restrictions of Grey Component Replacement (GCR) in Newspaper Printing, 15 pages*

Links

International Newspaper Color Quality Club, www.ifra.com

Characterization data for offset, newspaper and screen printing. The Characterization data for offset, newspaper and screen printing provided in the Fogra characterisation tables provides colorimetric characterisation of various reference printing conditions that relate back to conditions specified in the parts 2 to 5 of the ISO 12647 series of international standards, www.fogra.org

Printing by the numbers on commercial paper grades

Petter Kolseth[1], Luc Lanat[2], Örjan Sävborg[3]

[1] Stora Enso
SE-79180 Falun, Sweden
E-mail: petter.i.kolseth@storaenso.com

[2] Stora Enso, Mönchengladbach Research Centre
Krefelder Strasse 560, DE-41066 Mönchengladbach, Germany
E-mail: luc.lanat@storaenso.com

[3] Stora Enso
Karlstad Research Centre, P. O. Box 9090, SE-65009 Karlstad, Sweden
E-mail: orjan.savborg@storaenso.com

Abstract

Printing standards have been around for many decades, but the detailed ISO standardisation evolved only a little more than ten years ago. The graphic standard series *ISO 12647 Graphic technology - Process control for the production of halftone colour separations, proof and production prints* is making an ever stronger impact on the graphic industry. This has, unfortunately, created unnecessary confusion. Especially there are some details in *Part 2: Offset lithographic processes* that sometimes result in a clash between supplier, printer and print buyer. The limitation to a few specific paper types with characteristics that hardly match commercial paper grades, and the not always realistic targets for printed colour and tonal transfer giving rise to sometimes endless debate. The present work describes some of the measures that have been taken by us as a paper supplier to alleviate the situation. As a general conclusion, we may state that a majority of commercially available papers could be confined in rather narrow groups with respect to shade, attainable printed colour and tone value increase, provided that the right parameters are chosen.

Keywords: color management; lithographic offset; paper characterisation; paper optics

1. Introduction

Standardised Print - or Printing by the Numbers - has evolved from a buzz to something that is demanded from many printers today. Standardised Print is not as straightforward as it may seem. What we today refer to as Standardised Print has a long background history. The German graphic research institute *FOGRA* and the German Printers and Media Association *bvdm* presented their first guidelines in the early 80's. The Swedish merchant Pappersgruppen (now Papyrus) were early adopters in Sweden with seminars for the printers. In 1993, Michael Haas at FOGRA invited representatives of mainly pre-press companies to a meeting in München. This was the starting point of the *ICC* - International Color Consortium. They agreed upon a specification of a standard file format for the description of colour, and how the conversion between different colour spaces should be handled using *ICC profiles*. It has however always been up to the different colour software suppliers to use these specifications in building their proprietary *colour management* systems.

Colour management is all about transforming colour information from one device to another, typically from an input such as a digital RGB-coded colour image to an offset press printing the four process colours Cyan-Magenta-Yellow-Black (CMYK). There are still many unresolved issue in how colour management should be best implemented, and the ICC colour management system is still evolving as understanding increases. We will not go into any details in the field of colour management in the present work; the interested reader can find pertinent information in the many *white papers* issued by the ICC [http://color.org].

From the German printers in particular, there has since some years now been a request for the papermakers to specify key properties of all papers related to colour management and print process control in a uniform way. One important issue is the colour appearance and tone rendering achieved when putting ink on paper in the

first parts of the graphic standard series *ISO 12647 Graphic technology - Process control for the production of halftone colour separations, proof and production prints* were released in 1996. The ISO 12647 standard covers not only lithographic offset (sheetfed and heatset), but also coldset offset, gravure, screen and flexography print. "Digital" printing is not included, but there is one part dealing with contract proofs. The common debate has been primarily focused on the offset lithography, partly because it was the first to appear, and maybe also because it is the most common process by number of practitioners. The newspaper associations have since long worked according to well-accepted *de facto* standards, so there has been rather limited debate. The work presented here deals only with offset lithography, but we will most certainly find reason to follow up on rotogravure, which today is being pushed by large print buyers such as IKEA.

The ISO 12647 parts 1 - 3 are presently under systematic revision, a progress report being presented by a working group at the recent TC130 meeting in Fort Worth 19 - 21 May. The aim is obviously to get out of the notion of "ISO compliant papers", and rather base paper categorization on achievable colours in solid and halftone print. The working group has not really abandoned paper categorization, presenting four categories: coated and uncoated, of high grammage and low grammage. Each of these four categories is still linked to paper shade, achievable ink coloration and specific TVI (Dot Gain) curves. This approach seems anyway constructive, but there are still many obstacles to overcome, including fluorescence effects. With the recent strong engagement from paper industry in the TC130 processes, there is good hope that graphic and paper industries may come to a mutual understanding on the content of these standards.

The objectives of our present work have been to clarify some of the more common issues in the current debate. Particularly, we have studied the effect of paper shade and paper fluorescence, achievable colour coordinates of the CMY-RGB hexagon, and the contribution of paper to the tone value increase (TVI/dot gain). Standardization and UV calibration of light sources, choice of proof to print papers, repeatability of equipments have also a major influence on printing quality control. We therefore studied and evaluated the importance of these elements on our road to "Printing by the numbers".

2. Results and discussion

2.1 Paper shade

The ISO 12647 standard did not evoke any significant discussion between printer and papermaker during its first years of existence. The paper shade issue was one of the first questions to reach our sales force, and that did not happen until the years 2004 - 05, more than eight years after the standard was published. The standardisation of paper shade is certainly not very clear though. The exact wording in the ISO standard is as follows:

> ***Print substrate colour:*** *The print substrate used for proofing should be identical to that of the production. If this is not possible, the properties of the print substrate should be a close match to that of the production in terms of colour, gloss, type of surface (coated, uncoated, super-calendered, etc.) and mass per area. Press proofing should be carried out on the closest match selected from five typical paper surface types whose attributes are listed in Table I. For off-press proofing the print substrate should be selected to conform as closely as possible to the attributes listed in Table 1 of the paper type representing the envisaged production paper. The type of paper shall be stated.*

Table I: CIELAB coordinates and gloss for typical paper types according to ISO 12647-2

Paper type	L*	a*	b*	gloss
1. Gloss-coated, woodfree	93(95)	0(0)	-3(-2)	65
2. Matte-coated, woodfree	92(94)	0(0)	-3(-2)	38
3. Gloss-coated, web	87(92)	-1(0)	3(5)	55
4. Uncoated, white	92(95)	0(0)	-3(-2)	6
5. Uncoated, slightly yellowish	88(90)	0(0)	6(9)	6
Tolerance	±3	±2	±2	±5

D50 illuminant, 2° observer, 0/45 or 45/0 geometry, black backing (values in brackets refer to white backing)

This is obviously related to the print substrates used for proofing? It is stated that both shade and gloss are normative, but is this for the proof substrate or the production paper? Clearly, the (mis-)interpretation so far is

printer only if you print on a production paper that fits into one of these categories. The real problem is now that the prescribed CIELAB coordinates do not comply with what is common for today's commercial paper grades. The discrepancy is mainly related to the b* coordinate, most paper having a stronger bluish shade making them look whiter. This whiteness is partly due to the addition of fluorescent whitening agents (FWA, also called OBA – optical brightening agents). The paper types chosen in writing the standard may have been "typical" then - long before 1996 – but are far from typical today.

In order to explain the situation to our sales force and our customers, we analysed a large set of gloss-coated (Paper Type 1) and silk/matt-coated (Paper Type 2) offset papers from the European market in 2005. *Figure 1* shows that all products except for one wood-containing product were out of range when colour was determined the paper industry way with D65/10° settings.

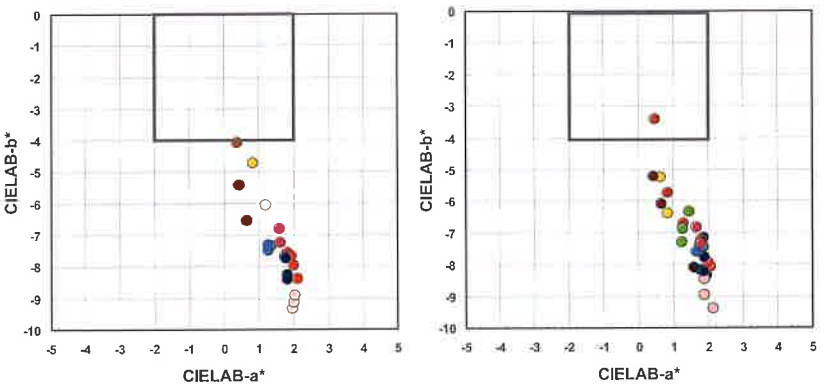

Figure 1: Paper shade in D65/10° for 51 coated papers of 90-250 g/m². Left: Paper Type 1; Right: Paper Type 2

Making the measurements in C/2° conditions move some papers, mainly wood-containing, into the prescribed tolerances, left part of *Figure 2*. Measurements with a graphic industry instrument (Spectrolino) in D50/2° allowed most glossy products to fit inside the tolerances, right part of Figure 2. It is however clear that the "natural" range of commercial products is wider than the given ISO standard tolerances.

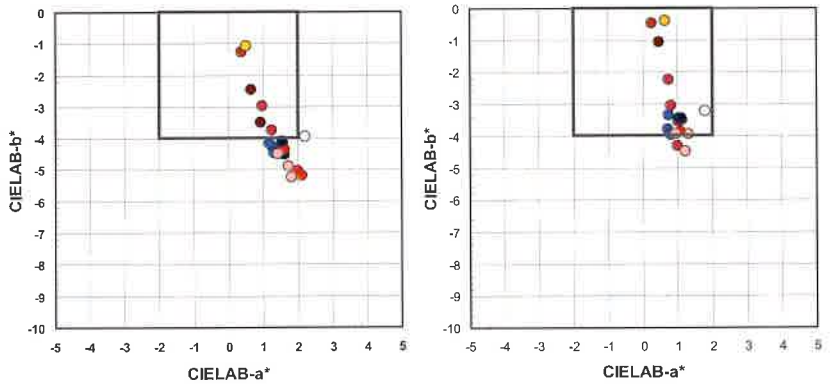

Figure 2: Paper shade in C/2° (Elrepho - Left) and D50/2° (Spectrolino - Right) for the gloss-coated papers (PT 1) in Figure 1

In June 2006, there was a joint ICC, ISO TC130 (graphic) and ISO TC6 (paper) meeting to address Paper Categorization, where representatives from both graphic industry and paper industry met for the first time to discuss these matters (ICC 2006). The meeting agreed to set up a working group with Uwe Bertholdt of FOGRA as coordinator, asking the group to come up with recommendations for changes to the existing standards and any new standards which are required. FOGRA measured about 500 papers from around the world, and the data definitely showed that papers intended for offset printing were significantly bluer than indicated in the ISO 12647-2. FOGRA came however to the conclusion that even though changing the prescribed paper shades in the standard would result in a more valid paper description of real papers, this would result in an increased visual mismatch between proof and print because most (all?) digital proof systems simulate the fluorescent blue shift of printing papers by using blue dye instead of fluorescent agents. The results were presented at the ISO TC130 meting in Bangkok in

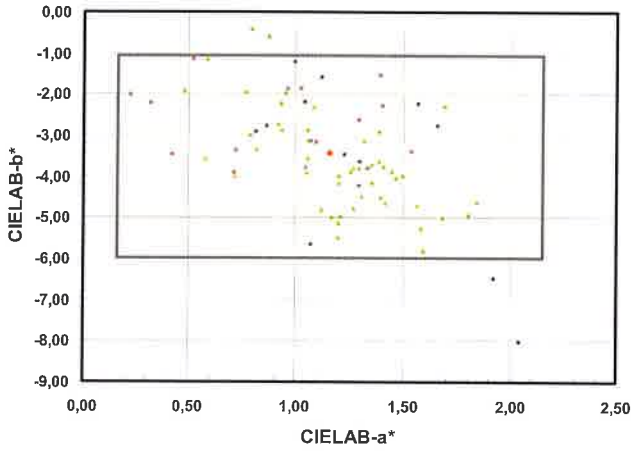

Figure 3: Shades of double-coated glossy papers determined by FOGRA for the ISO TC130 paper characterization working group. A relatively small change of the allowed a-b* range would allow more than 80% of the samples to fit inside these tolerances*

2.2 CIELAB coordinates of colours for four-colour printing

The ISO 12647-2 also specifies the CIELAB colour coordinates of the process colour solids (CMY) and the two-colour overprints (RGB).

Figure 4 shows the achieved colour on the same papers as shown in Figure 1. The press settings were the same for all papers, using the same target densities for process control. The resulting CMY and RGB colour coordinates were found in a rather narrow range for all 51 papers. The wider range of Yellow in the b* direction was due to silk-coated papers only, and was not related to bluish paper shade.

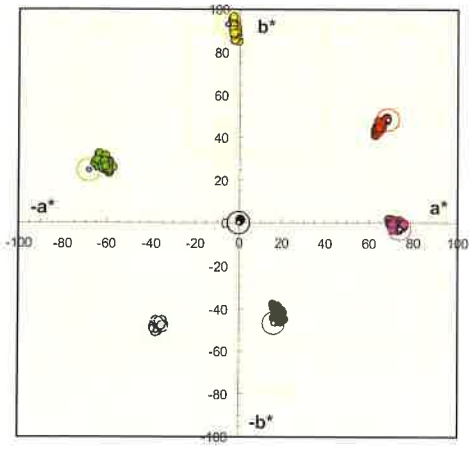

Figure 4: Colour gamuts (D50/2° Spectrolino) of 51 gloss and silk-coated papers and target values given in ISO 12647-2

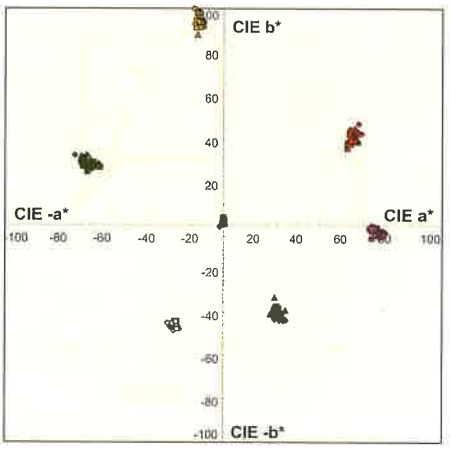

Figure 5: Colour gamuts (C/2° Elrepho) of ten different inks on gloss ◇, silk △ and matt □ coated fine paper

We have also tested ten different inks from six ink suppliers. One supplier was asked to select five different types of inks, which were combined with standard inks from the other five suppliers. *Figure 5* shows the achieved colour on three coated papers: gloss, silk and matt. The press settings were the same for all 30 combinations, using the same target densities for process control. The resulting CMY and RGB colour coordinates were again found in a rather narrow range. The main difference between the inks was a wide range of print gloss levels: print gloss in 100% black was in the range of 45 - 55% on matt, 58 - 72% on silk and 78 - 92% on gloss.

It is clear that most - if not all - papers of the same basic type are able to reach the same CMY-RGB colour targets.

the ISO 12647-2, these colours do not usually coincide with the targets of the standard. Surprisingly, the recent FOGRA characterization data fit these targets to the second decimal. The data have obviously been smoothed and shifted to comply with the ISO standard and may therefore, be of limited value to the press operator.

2.3 Fluorescence effects

The high Whiteness levels of paper are mainly achieved via fluorescence, *Figure 6*. A more bluish shade is perceived as more white according to research by the CIE that resulted in the CIE Whiteness equation. Therefore, we can expect that fluorescence continues to be a significant paper property also for many years to come, and it has to be accounted for in colour management.

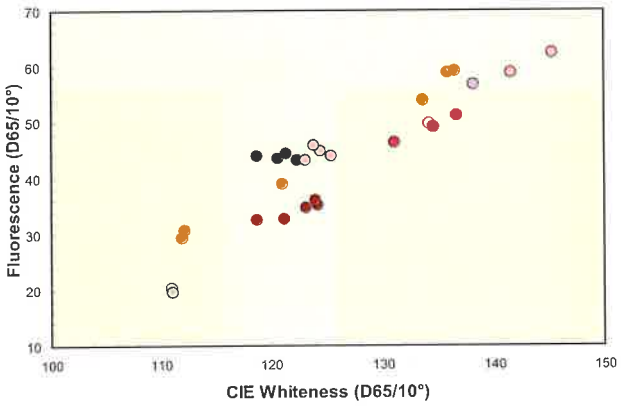

Figure 6: Fluorescent component of coated fine papers in a wide range of whiteness levels. Products in the range of 200-350 g/m² from Europe, USA and China

The colour coordinates of printed tonal steps in CMY-RGB were determined with different illuminant-observer combinations. *Figure 7* shows the D65/10° and D50/2° colour on a silk-coated fine paper. The upward shift at the origin reflects the lower relative UV content in D50. As a result of the more red D50 illuminant and the stronger colour vision of the 2° observer, this combination shows more colour saturation, especially in the red region.

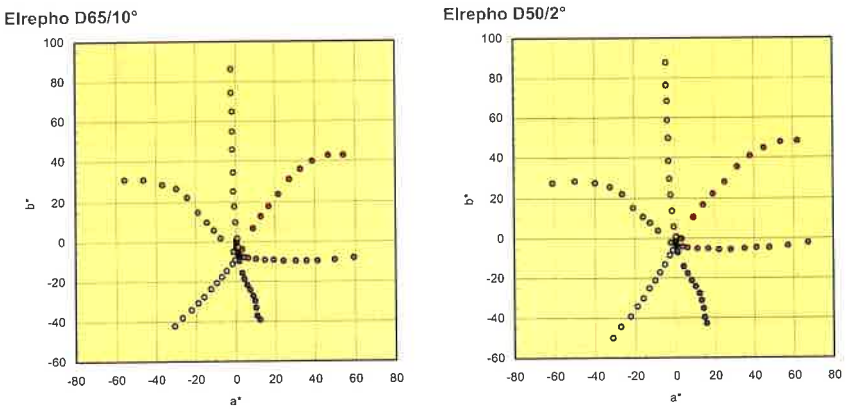

Figure 7: Colour coordinates in tonal steps of CMY-RGB on silk-coated fine paper

In order to see the effect of fluorescence, the D50 readings were made also with a UV-cut filter, *Figure 8*.

Paper fluorescence is seen through almost any ink coverage used in commercial printing. The CMY primaries were clearly shifted towards higher b* over the entire tonal range, with the UV-cut filter. The secondaries were less affected due to a higher UV screening power. The only point that did not show a shift on UV-cut was solid Green, all other data points moved slightly. Similar data were reported in a diploma work by Katharina Kehren [2008]. She also provided a mathematical model for predicting the effect of different fluorescence levels. The corresponding shifts on a highly fluorescent uncoated fine paper were of course larger, and consequently, there

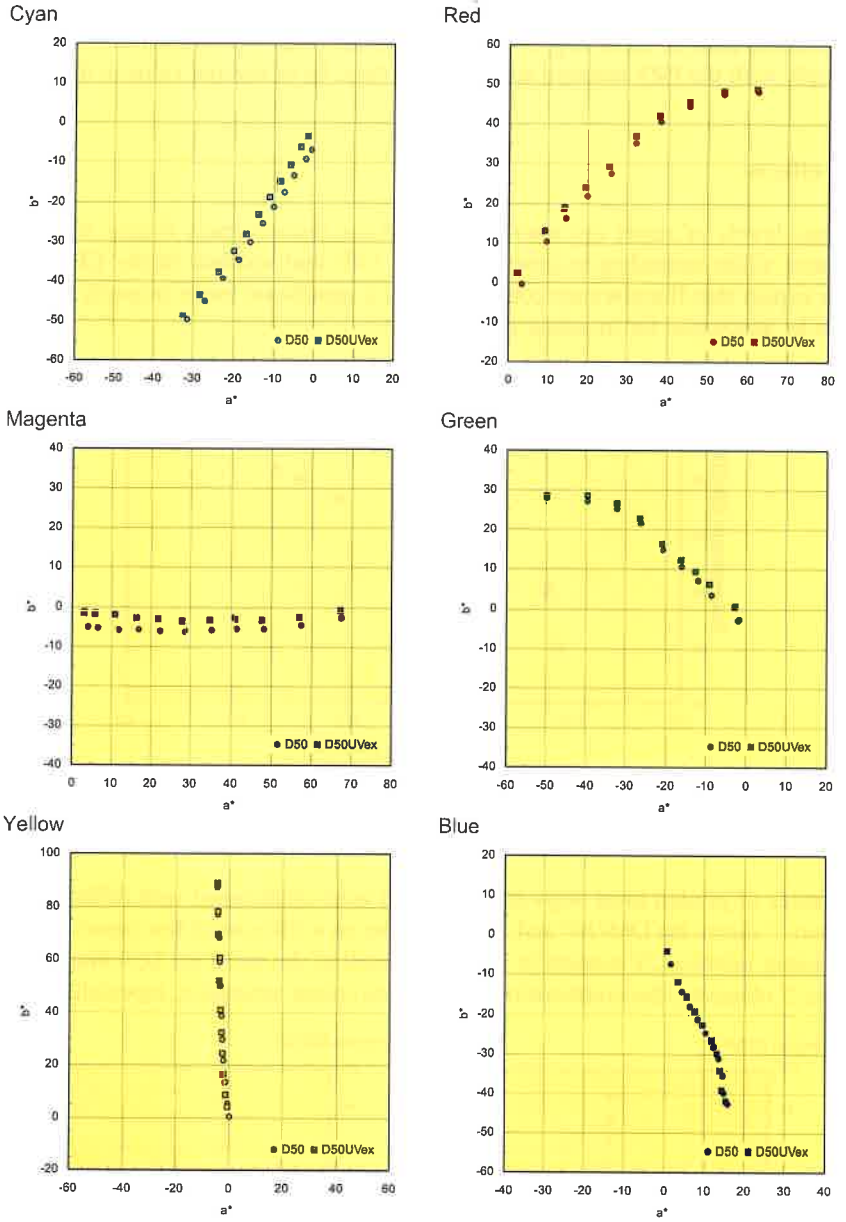

Figure 8: The effect of a UV-cut filter on printed colour coordinates on silk-coated fine paper

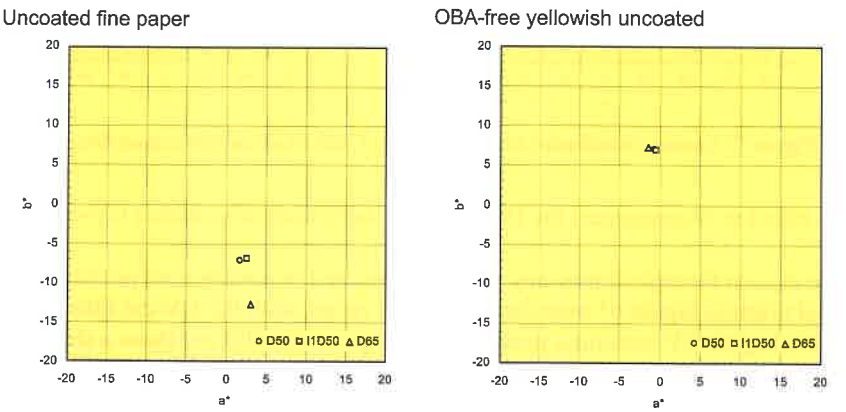

Figure 9: Paper white colour coordinates determined with Elrepho D65/10° and D50/2°

The contribution of fluorescence is of course dependent on the relative UV content in the measuring instrument. Paper industry and graphic industry standards differ in this respect. A draft revision of the ISO 13655 standard includes the measurement condition M1, which should give results close to a true Illuminant D50. The calibration of relative UV content is however still not clearly addressed, a fact that may lead to poor match between production paper and proofing substrates. Paper industry needed and therefore developed fully operational calibration procedures (and standards), valid for illuminants D65, C or D50 (at UV level of C illuminant).

The exact measurement conditions for spectral measurements in graphic and paper industry standards are under development and debate. The paper industry standard conditions for measurement of CIELAB coordinates of paper and print is described in ISO 5631, where detailed instructions are given for adjusting the relative UV content. Part 1 is for D65/10° and Part 2 for C/2° settings. A draft version of Part 3 describes D50/2° settings with the same UV adjustment as for the illuminant C. This choice may have seemed practical for the ISO working group, but unfortunately, the relative power of D50 is more than twice that of C between 340 and 380 nm. *Figure 10* shows the spectral power relative to 440 nm, which is the wavelength where we see the fluorescence peak of all our tested papers (coated and uncoated).

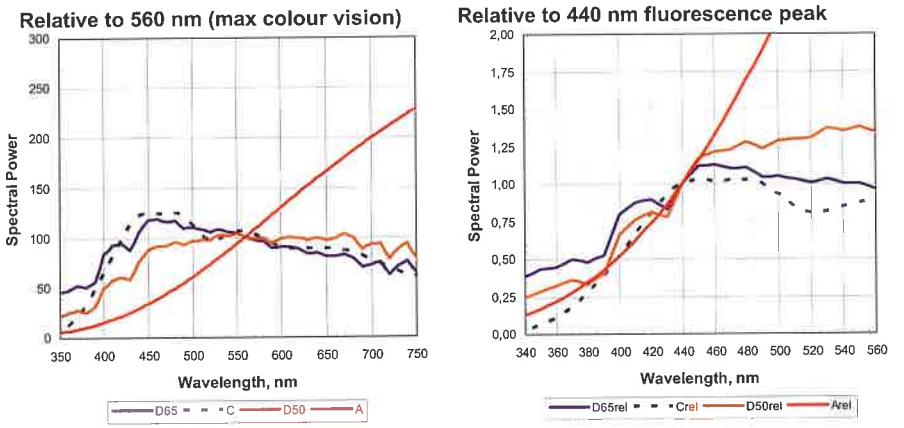

Figure 10: Absolute and Relative UV content of the four Illuminants D65, C, D50 and A

In the draft revision of ISO 13655, four measurement conditions are described: M0 (no filter = Illuminant A), M1 (true D50), M2 (UV-cut filter) and M3 (polarization filter). The M1 condition should be possible to achieve with a Tungsten lamp as used in standard graphic spectrometers by applying a filter working in the visual region that would increase the relative UV content to the D50 level.

The match between measurement conditions and the actual spectral power distribution in viewing booths remains to be addressed. Standard viewing booths as used at many printers are usually quite far from true D50 conditions, and the lighting conditions at the end user are totally unknown.

2.4 Tone Value Increase (Dot Gain)

The transformation of tone value from digital file to the final print on paper plays an important role in the control of the printing process. Earlier, this was often referred to as Dot Gain (Tone Value Increase), since the perceived tone in print was always higher than the tone value on the film that was used to make the printing plates. From the papermaker's point of view, the Tone Value Increase (TVI) from the imaged printing plate to the final print is the main interest; the paper can have no effect on the earlier pre-press stages. It is sometimes suggested that the TVI should be an inherent paper property, a misconception that fortunately is generally disputed by specialists within the field of printing and graphic arts.

The TVI behaviour of the same set of coated papers as in the sections on paper shade and printed colour was analysed in detail. The TVI curves obtained with standard densitometry are shown in *Figure 11*.

A subset of 40% black halftone (K40) prints over the TVI range was selected for a *detailed microscopy analysis*. The extremes are shown in *Figure 12*, where it is clear that the higher TVI was related to severe doubling or slur.

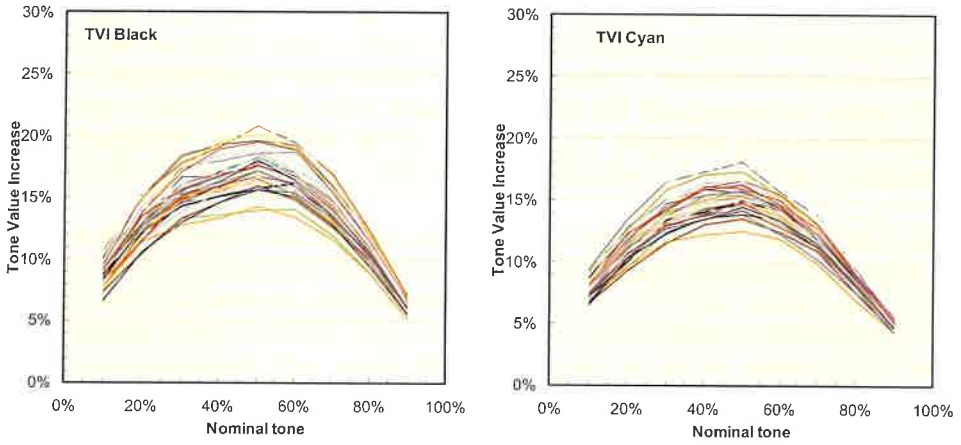

Figure 11: TVI curves for Black and Cyan of 51 gloss and silk-coated papers. Almost all curves fall inside the allowed range 14% ±4% TVI for the 50% control patch

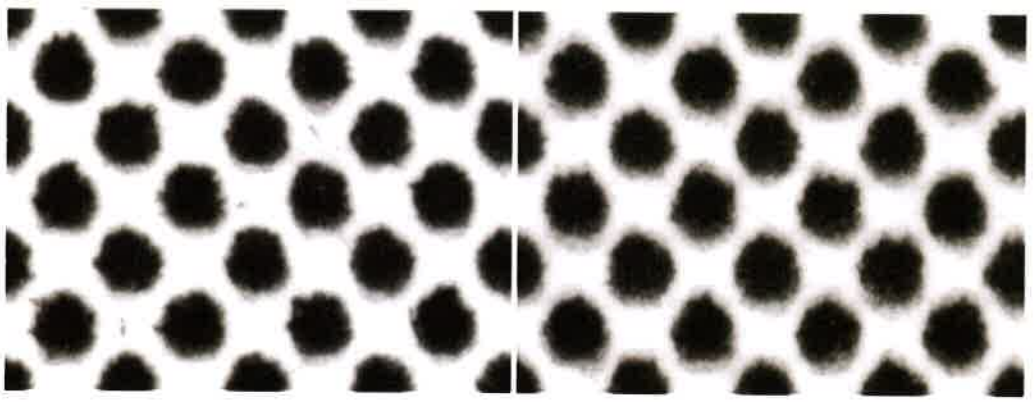

Figure 12: Nominal 40% Black halftone prints of 13,2% TVI (left) and 20,1% TVI (right)

Figure 13 shows histograms of the reflectance values of the two prints. Two characteristics can be seen in the diagrams: the white peak between-the-dots is both wider and darker in the high-TVI print. This is mainly related to the poor dot quality, but the also the paper white seems to be a bit darker. The darker paper between dots is commonly referred to as "optical dot gain" as described by Yule and Nielsen [1951]. The effect was recently reviewed in a conference paper by Smith *et al.* [2009].

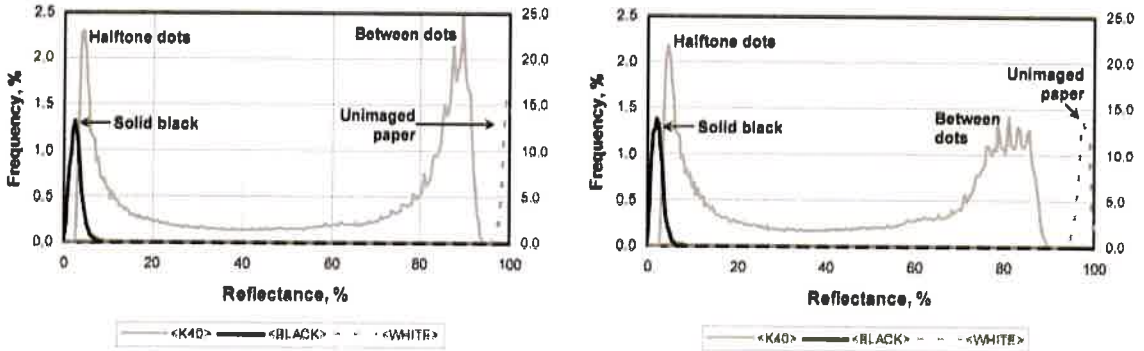

Figure 13: Reflectance histograms of the microscopy images in Figure 12 together with histograms of solid black and unimaged paper

A simple analysis was based on the reflectance histograms. The position of the four peaks (solid black, halftone dots, paper between dots, unimaged paper) and the average reflectance under the three curves were determined. The edge of the **physical dots** was defined by setting a threshold at the mean reflectance between the peak of

halftone dots and the peak of paper between dots in the K40 histograms. The corresponding tone values are denoted "Physical" in *Table II*.

The **K40 Tone Values** given in Table II were calculated from the average reflectance values of the Black halftone, solid Black and unimaged paper:

$$ToneValue_{K40} = 100 \times \frac{R_{K40}}{R_0 - R_{K100}} \quad (1)$$

The **Optical Tone Value Increase** was calculated as the difference by the Tone Value and the Physical Dot as seen in microscopy.

The "**brightest area between dots**" was estimated as the average reflectance of the 15% of the region between dots that was far away as possible from the dots.

Table II: Tone values of nominal 40% Black halftones as seen by densitometer and by microscopy

Paper	---- Densitometer ----		---------- Microscopy ----------		
	TVI-40	DensTone	Physical	ToneValue	Optical TVI
Multicoated silk 250	13,2	53,2	42,0	47,2	5,2
Multicoated silk 115	13,4	53,4	41,6	47,7	6,1
Multicoated silk 250	15,1	55,1	42,5	48,2	5,7
Single-coated matt 90	15,5	55,5	41,9	50,4	8,5
Multicoated gloss 115	16,3	56,3	42,7	48,6	5,9
Multicoated gloss 250	16,9	56,9	44,6	50,2	5,6
Single-coated matt 90	19,3	59,3	47,4	54,7	7,3
Multicoated gloss 250	20,1	60,1	44,0	51,4	7,4

Compared to the target of 40%, the physical dot sizes of 41,6 - 47,4 displayed in Table II, indicate a mechanical TVI in the range of 1-8%. The exact determination of printed dot size is fraught with error, mainly because of uncertainties in setting an exact threshold for the extension of the dots. The low-end of 1,5 - 2% mechanical TVI was found for the most perfect dots, but a minute change in thresholding would bring the mechanical TVI down to zero. The large mechanical TVI values were clearly related to less than perfect dots that displayed both doubling and slur. The analysis of the microscopy images gave a disappointing underestimation of the Tone Values by approximately 6%, *Figure 14*. The reason for this was not fully understood by the authors at the time of this report.

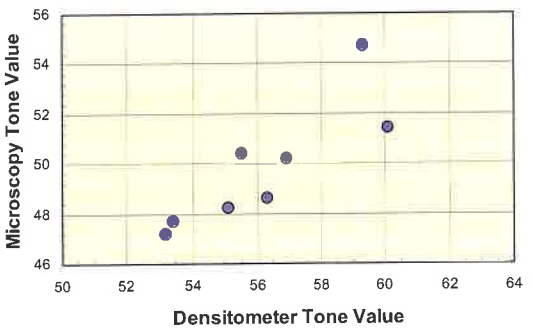

Figure 14: Comparison of Tone Values determined by microscopy and densitometer

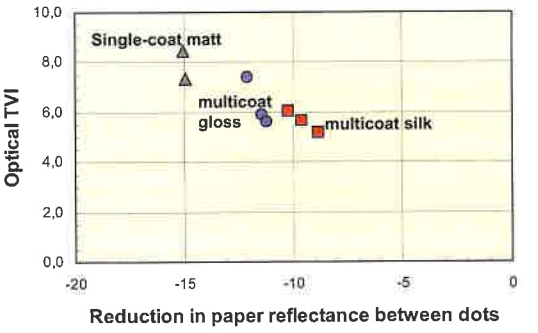

Figure 15: The optical TVI as a function of the shift in paper reflectance from "unimaged paper" to "brightest between dots"

Table II also shows that an optical TVI in the range of 5 - 9% was found in the analysis of microscope images. This optical TVI was closely related to the reduction in paper reflectance between the dots as compared to the unimaged paper, *Figure 15*. Please note that the reduction in paper reflectance is highest for single-coated matt and lowest for multicoated silk, with multicoated gloss in between. This follows the expected visibility of the

be an inherent paper property, with a contribution to the total TVI seen by densitometry that is at least in the range of 5-10% TVI for the paper Types 1 and 2.

3. Conclusions

The paper shade, especially if it is affected by blue fluorescence, may introduce problems in matching to proofs, but such problems should be possible to handle by a well-working colour management system. There seem to be two main reasons for the sometimes poor match between proof and print regarding paper shade.

First, the proofing substrates generally have less fluorescence than the corresponding commercial paper. Some colour management software seems to compensate for this by printing a light blue shade on the white substrate, which of course, does not provide fluorescence. The opposite may also be true, with highly fluorescent proof substrates, *Figure 16*. An (obviously) ideal solution would be to choose a proof substrate approaching the fluorescence level of the production paper. A *New Working Item* (NWI) will be proposed to ISO TC130 to this end. The shade of commercially available paper grades fall in general within a rather tight range. This range is offset mainly in the negative b*-direction from the ISO 12647-2 standard paper types, but the limits could quite easily be adjusted to comply with real papers. This was concluded in an investigation by FOGRA already two years ago, but for some reason it was decided not to make this rather obvious change.

Secondly, the offset inks provide a stronger blocking of UV rays than the inkjet inks used for proof prints. The fluorescence contribution should therefore be treated differently in proof printing and production printing. In a diploma work initiated by our company, it has been shown that the fluorescence effect in real prints can be described by a quite straightforward model over the whole CMY-RGB tonal range.

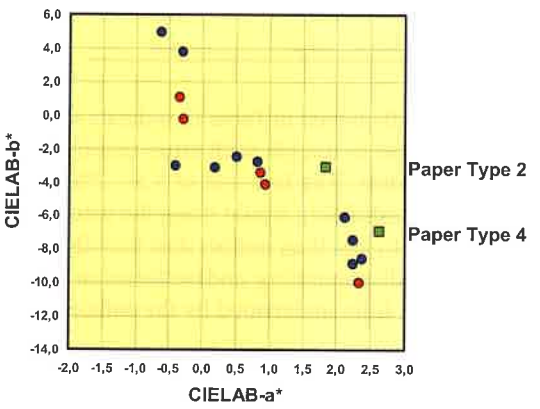

Figure 16:
CIELAB shades of proof substrates (circles) and production paper (squares). The red symbols denote FOGRA certified proof substrates

The intrinsic Tone Value Increase (TVI or "dot gain") of the paper is clearly related to the Yule-Nielsen effect – the optical TVI. On a "perfect" print, the physical dot coverage was found to be very small or almost zero, coinciding with the values on the printing plate, so mechanical TVI may not explain the high tone values measured with a densitometer. The grey shadow between dots may fully explain what the densitometer "sees" as higher dot coverage. This basic level seems rather to coincide with the norms presented by for example FOGRA and bvdm. Excess "dot gain" would have to be attributed to pre-press settings from digital file to plate, or to non-ideal printing conditions with doubling or slur.

The debate is presently about calibration procedures, where paper industry is promoting the advanced calibration systems used for their spectrophotometers, and the possible mismatch between relative UV content in D50 as defined by paper industry and graphic industry. Paper industry representatives also encourage the addition of D65 as a fifth measurement condition in the ISO 13655, hence called M4. ISO 13655 version 2 is still judged to be misleading, until proper calibration procedures, in particular in the UV level of the light source, have been added. As an example of the wide variety of instruments in use, the reader is referred to the PIA/GATF report by Radencic *et al.* [2008].

The situation has improved considerably over the last years, since paper industry is now engaged in the development of printing standardization. This contributes to the success of printed media obviously. This is the common goal of all of us, printers, papermakers, suppliers to the graphic indust[illegible]

As an example, this work was widely reviewed and discussed within the "Paperdam" technical working group, gathering experts from Burgo, Norske, UPM, Myllykoski, Stora Enso and Sappi/M-real, on Colour Management and Standardization issues.

Printed Media is highly needed for human communication and Quality Print Media will support its development. Print Media Quality - "We know it when we see it".

4. Measurement methods

We have used a wide arsenal of techniques, from full-scale printing trials in sheetfed offset and heatset web offset, to detailed optical analyses of paper and print. The prints were analysed both with standard instruments from the graphic industry and with the special equipment used in the paper industry.

Optical properties: All paper optical properties were obtained with an L&W Elrepho 3000 instrument, calibrated using ISO Level 3 reference papers from STFI (now Innventia). The CIELAB coordinates of paper and print were determined both with D65/10° and C/2° settings according to ISO 5631. L*a*b*-coordinates were also evaluated with D50/2° settings according to a draft version of ISO 5631.

Spectrodensitometry: Two instruments were used: a Gretag Spectrolino and an X-Rite iOne, both with "No filter" option and thus in essence an Illuminant A. The CIELAB coordinates were calculated with the D50/2° arithmetic, but the relative UV content was still corresponding to illuminant A, which is slightly higher than true D50.

Densitometry: Print density was determined using a Tobias scanning densitometer without polarizing filters, calibrated according to DIN Status E(47B). The output from the instrument is about 0,1 density unit lower than normal European densitometer readings (*e.g.* Gretag) in the CMY process colours, and 0,3 units lower in Black.

Microscopy: Images (micrographs) were recorded by a digital camera NIKON DXM1200 mounted on a LEICA MZ12 stereomicroscope. The images were saved as "BW". Illumination was from two light sources mounted at about 45° on either side of the sample.

When the images were inspected with Adobe Photoshop CS3 it was discovered that the "BW" tiff format was of the type "Indexed color" and to remove this they were saved as "grey".

The **physical size of the halftone dots** was measured using a simple Visual Basic program. The two maxima in the histogram corresponding to ink and unprinted paper were determined and the image thresholded at the midpoint between these maxima. All dark objects that are not in contact with the image border and that have an area greater than 200 pixels were measured.

The "**brightest area between dots**" was evaluated from the segmented images of dots and background (between dots) as described above. A distance transform was calculated where each pixel in the background was given the value of its shortest distance to the foreground (dot). The maximum in the distance transform is simply the pixel furthest away from its surrounding dots. The distance transform was thresholded at 75%, 80%, 85% and 90% of the maximum in order to get small regions as far away as possible from the surrounding dots, and the average brightness of these pixels was determined. The average showed a slight increase with the threshold (less than 1 unit between the highest and lowest threshold) and the value at 85%, rounded to a whole number was chosen as "brightest between dots".

The 255 grey levels were transformed into reflectance by matching the paper white peak level with the Y-value of the papers.

Printing plates Kodak Electra Excel positive thermal plates were imaged on a Creo Lotem 400 Quantum CTP plate setter, using SQUAREspot exposure technology. The screening used was Euclidean dot (round dot shape at 40% tone), 175 lpi. The plate setter was calibrated to give a linear tonal transfer curve (zero dot gain).

Printing trials Printing trials were performed on a Heidelberg Speed-Master 6-colour sheet-fed offset press.

made with a vegetable oil based ink from Akzo Nobel Inks, using an 8% IPA fount system. The ink transfer to the paper was optimised using compressive blankets with a microground surface and a relatively high blanket-to-paper impression at 0,18 mm. The printed papers were gloss- and matt/silk-coated papers for sheetfed offset, covering a grammage range of 90 - 250 g/m^2.

Acknowledgements

We want to acknowledge valuable contributions by many colleagues, among those we want to especially mention Anna Nicander, Sofia Thorman (ex Norstedt), Stefan Eriksson and Olle Henningsson.

References

1. Kehren, K. (2008), Einfluß optischer Aufheller auf die Druckbildwiedergabe, Diplomarbeit TU Darmstadt
2. Radencic, G.; Neumann, E.; Bohan, M. (2008), Spectrophotometer Inter-Instrument Agreement on Standard Reference Materials and Printed Samples, PIA/GATF Catalog No. 1646
3. Smith, D. A.; Williams, D. M.; Salminen, P. J.; Welsch, G. W.; Heeschen, W. A.; Nicholas, N. R.; Arney, J. S. (2009), Definition and Model for Primary Grey Scale Mottle as a Variation in the Yule-Nielsen Effect in Offset Printed Coated Paper, TAPPI PaperCon '09, St. Louis, USA
4. Yule, J. A. C.; Nielsen, W. J (1951), The penetration of light into paper and its effect on halftone reproduction, TAGA Proceedings 3:65-76
5. Print Media Production Forum 2007 (bvdm/ECI): http://www.print-media-production-forum.de/eng/index.php
6. FOGRA Characterization data: http://www.color.org/FOGRA.xalter
7. ICC (2006), ICC / ISO TC130 Meeting on Paper Classification, http://www.color.org/papermeeting2006.xalter

Drying in heatset web offset printing

Kaisa Koivumäki and Erkki K. O. Hellén

VTT
P. O. Box PL 1000, FIN-02044 VTT, Finland
E-mails: kaisa.koivumaki@vtt.fi, erkki.hellen@vtt.fi

Abstract

Drying dynamics was studied by extensive measurements on a full-scale heatset web offset press. The most important parameters influencing on drying are dryer air temperature, temperature profile and ink amount. For coated papers also the coat weight has a significant effect. Unexpectedly, considerable amount of solvent evaporates simultaneously with moisture at the early stages of drying. For normal drying conditions, some solvent and moisture remain in paper structure. Physical modeling was used to help in interpreting the experimental observations and in seeking for deeper understanding of the underlying drying mechanisms.

Keywords: heatset printing, drying, solvent evaporation, moisture evaporation, residual solvent, modeling

1. The objectives of the research

The main mechanism of ink drying inside a heatset dryer is ink solvent evaporation but also dryer construction and paper structure play an essential role from the energy point of view. It is believed that the drying process in heatset web offset printing is not fully optimized and that printers typically dry paper too much to avoid certain quality problems like smearing. Improper drying conditions may also generate blistering or fluting. It is fair to ask: Are there ways to increase the drying efficiency, to reduce energy consumption, improve runnability, or reduce printing costs without decreasing print quality? Answering these questions requires fundamental understanding on drying mechanisms.

The focus of studies concentrating on drying during heatset web offset printing has been mainly on the effects that drying has on print quality. The current understanding is based on trials and not much attention has been paid to the drying mechanisms. However, a deeper understanding of the actual drying process and the drying mechanisms is required to improve cost efficiency in press houses and help to improve products and processes without decreasing print quality. The development of inks and dryers may provide new means for improve the drying efficiency, offer possibilities to lower production costs or set new demands for paper.

The objective of this study was to determine the critical parameters describing heatset drying and find out their relative importance on drying dynamics. Evaporating components were analyzed at a full-scale heatset web offset press using four GASMET™ gas analyzers. Modeling was used to help in interpreting experimental results and seeking for a deeper understanding of the underlying drying mechanisms.

2. Research methods

The drying dynamics was studied by full scale heatset trials combined with detailed physical modeling [1]. The printing trials were run at KCL's Albert-Frankenthal A 101 S press at a speed of 5m/s. The press is equipped with a modified M.E.G. Sigma dryer, which consists of four independently controllable dryer modules giving a total dryer length of 8 m.

Two drying profiles were used: "a flat profile" with the same air temperature in all the four dryer modules, and "a normal profile" with the drying air temperature being the highest in the 1st drying module. For the normal profile, the temperature differences between the consequent modules were kept fixed to +60°C, +30°C, and 0°C. The out coming web temperature in the reference drying conditions was fixed to 136°C for both profiles.

The layout consisted of a 200% full tone area on both sides, simple enough for the model verification. A

SC grade, LWC/MWC gloss grades 65 g/m², 70 g/m² and 80 g/m². Target density for LWC/MWC papers was 1.5 and for SC paper 1.3. The fountain solution with a fount additive level of 3.5% and with 4% IPA was kept constant.

During the trials DX 4000 GASMET™ gas analyzers (see Figure 1) were used in every dryer module to measure the gaseous compounds inside the dryer [2,3]. The devices were connected to the dryer modules via sampling lines. The measured concentration data was analyzed with GASMET's Calcmet™ software. All calculated and reported concentration values were based on beforehand made calibrations with known gas standards. The on-line process data from the trials were collected with the WEDGE process analysis system. The measurement results were converted to the evaporated amounts of solvent and moisture in units of g/m². The residual solvent content of the printed sheets was determined using a hexane extraction method [4].

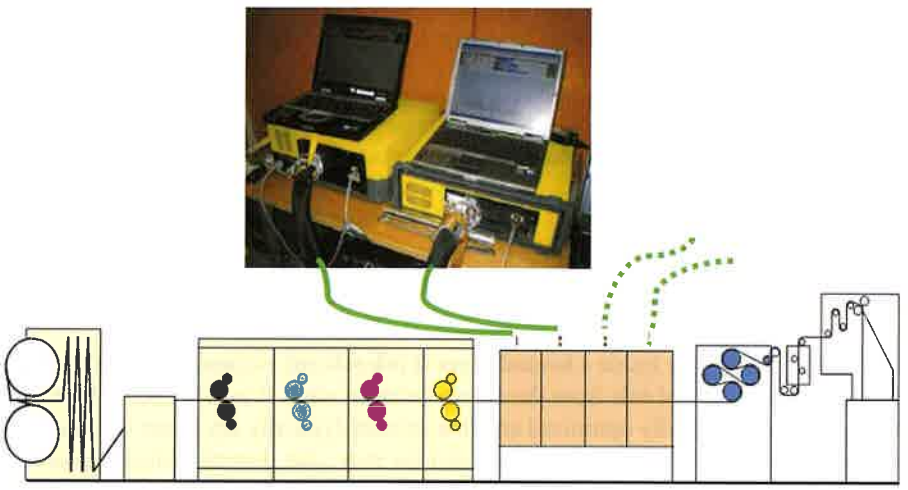

Figure 1: GASMET™ gas analyzers were installed in every dryer module to measure gaseous compounds inside the dryer

3. A summary of results

The sensitivity of drying efficiency for a few process and material parameters is illustrated in Figure 2. The figure shows the changes in residual solvent and moisture content when the parameters were increased 10% from the reference conditions. At the reference conditions the air temperature in the dryer was 175°C and a flat drying profile was used, resulting in an out coming web temperature of 136°C. Ink amount was 200% on both sides, the amount of fountain solution in ink was 1.1 g/m² and the grammage of paper was 65 g/m².

Of all the studied variables, dryer air temperature had the biggest influence on drying, both for SC and LWC papers. Increase in drying air temperature decreased the residual solvent and moisture content the most. The temperature profile had a clear effect on the residual solvent content of paper. A high ink amount resulted in a clearly higher residual solvent content. For coated paper also the coat weight was important: the increase of coat weight increased the residual solvent and moisture contents significantly. This implies that thicker coating retains solvent more effectively. The amount of fountain solution emulsified in the ink and the initial paper moisture content did not a have clear effect on the residual solvent of the dried paper web.

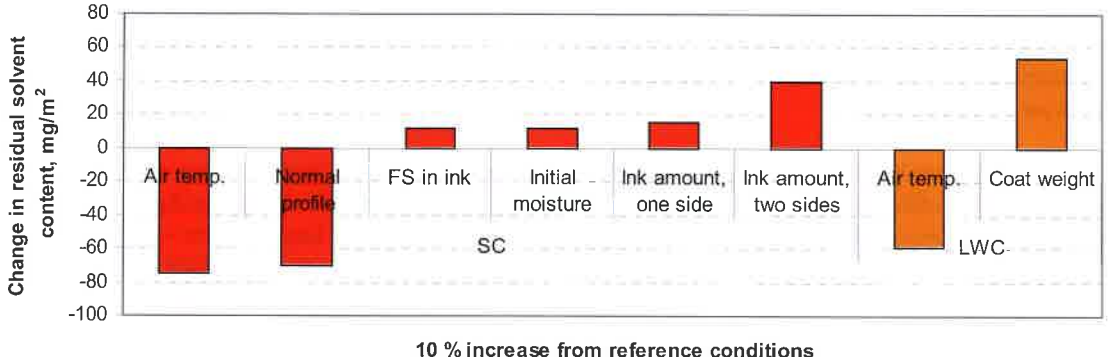

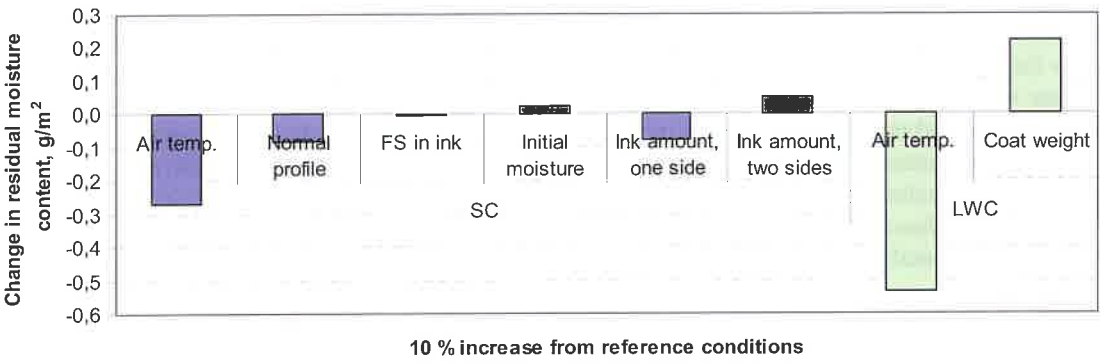

Figure 2: Residual solvent (above) and moisture content (below) of printed SC and LWC papers after 10% increase from reference conditions. At the reference conditions the air temperature of 175°C and a flat drying profile was used (out coming web temperature 136°C). Ink amount was 200% on both sides, the amount of fountain solution in ink was 1.1 g/m² and the grammage of paper was 65 g/m². The dryer air temperature had the biggest influence on drying

The residual solvent and moisture contents depend strongly on the drying temperature and profile as depicted in Figure 3. The effect of drying profile was most pronounced at low drying temperatures. For temperatures well above the reference temperature, 136°C, all ink solvent evaporated whereas some of the moisture still remained. This suggests that while some of the water molecules are tightly bound to fibers, the solvent molecules are more loosely bound to the other structural components.

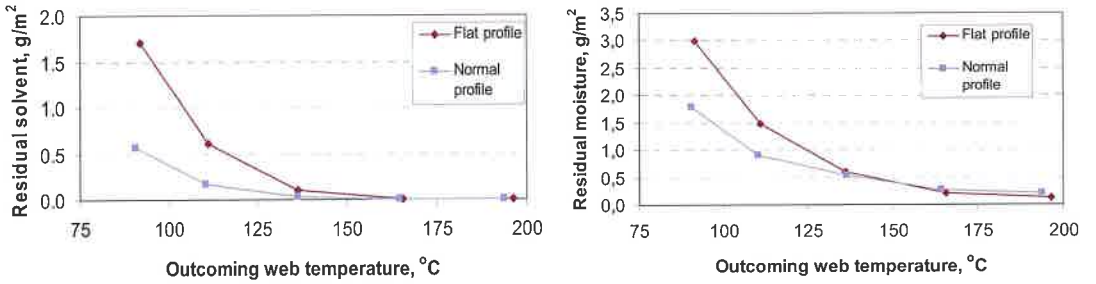

Figure 3: Residual solvent (left) and moisture (right) content of printed SC paper as a function of out coming web temperature for flat and normal drying profiles. Drying profile influences residual solvent and moisture especially at temperatures below reference conditions (136°C)

The dynamical drying behavior is exemplified in Figure 4, which shows the amounts of solvent and moisture evaporated in different drying modules when SC paper was dried with the normal drying profile. Moisture evaporated mainly at the early stages of drying. Interestingly, also most of the solvent evaporated simultaneously with moisture in the first two drying modules. This is against the common belief the solvent starts to evaporate significantly only after most of the moisture has been evaporated. Within this study, no indication of moisture evaporating before the solvent was seen. Instead, for high enough drying temperatures solvent evaporation was highest already in the first drying module (see Figure 4).

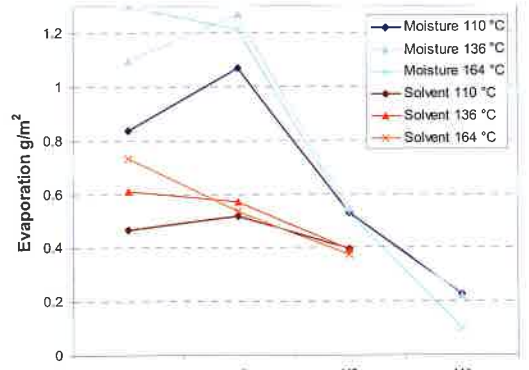

Figure 4:
Moisture and solvent evaporation profiles at different drying temperatures for SC paper dried using a normal drying profile. U1 to U4 denote the dryer modules and the out coming web temperatures are indicated in the legend. Considerable amount of solvent evaporated simultaneously with moisture. The shape of the evaporation profile depends on drying conditions

A physical model was developed to better understand the drying dynamics [1]. The model was verified using the extensive on-line and off-line measurements done during the trials. Figure 5 shows how well the model captures the moisture evaporation dynamics for various drying conditions for the LWC paper. The drying conditions were varied well outside what is normally used in print houses. Even so, the model was able to predict the measured moisture evaporation profiles. As the model includes detailed description of the material and process parameters, it offers a cost effective way of checking how changes in these affect on issues of interest. Within simulations, one can control each parameter or interaction independently of the others to find out the sensitivity these on the drying efficiency. The model can also be used to reveal issues which cannot be measured experimentally, for example the vapor pressures inside paper, which are relevant for blistering.

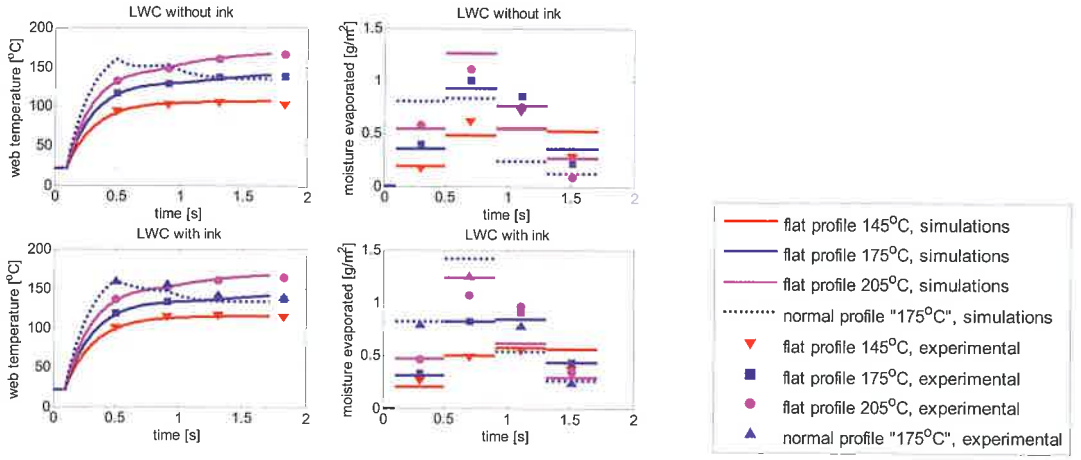

Figure 5: The simulated temperature and moisture evaporation profiles agree with the measured ones. The experimentally measured out coming web temperatures were 103°C, 138°C and 167°C when no ink was applied and in 115°C, 137°C and 163°C with ink. For the normal temperature profile the out coming web temperature was 138°C, respectively. No trial point was run for normal profile without ink

4. Conclusions

Extensive measurements and physical modeling were used to characterize the dynamics of drying in heatset web offset printing. Both solvent and moisture evaporation were addressed, the latter being essential from the energy efficiency point of view. Contrary to a common belief, the measurements showed that for normal drying conditions most of the solvent and moisture evaporate simultaneously at the early stages of drying. The residual solvent content is sensitive to the drying profile at low temperatures. For high enough drying temperatures the sensitivity decreases as almost all of the ink solvent evaporates. However, even at extreme drying temperatures some moisture will remain in the paper structure. Overall, solvent and moisture evaporation are most sensitive to the dryer air temperature, coat weight and ink amount. This implies that when optimizing drying, none of the three components - dryer, paper or ink - can be neglected.

Increasing drying efficiency requires optimization of the dryer air temperature and the drying profile such that interactions between paper and ink component are taken into account. Within this context and especially in product development, the drying model offers a cost effective way of checking how changes in materials or process parameters affect the drying dynamics. With modeling one can also obtain information which is not experimentally measurable. When simulations can be further related to print quality, the real optimization of heatset drying will become possible.

Acknowledgements

This work was done at KCL and the authors thank Virpi Jaakkola, Kari Juvonen, Jukka Ketoja, John Kettle, Raimo Kokkonen, and Martin Thüring for their essential input at all stages of the work. The financial support of M-real, Myllykoski, Sun Chemical, Stora Enso and UPM-Kymmene is gratefully acknowledged.

References

1. Hellén, E. K. O., Ketoja, J., Koivumäki, K., Jaakkola, V., Juvonen, K. and Kokkonen, R., (2008), *Drying Mechanisms in Heatset Printing, Proceedings of the Progress in Paper Physics Seminar,* June 2-5, Otaniemi, Finland, 83-86
2. GASMET Technologies Oy. *Application sheet. GASMET™ in industrial air-quality-applications.* Measurement of Solvent in Print Factories. 2 p
3. GASMET Technologies Oy, (2005), *GASMET calibration components*
4. Aurela, B. and Räisänen, T., (1993), *Residual Solvent Content in Heatset Offset Print, Journal of High Resolution Chromatography,* Vol. 16, 422-424

Rubber blanket surface energy modification using oxygen plasma treatment

Gorazd Golob[1], Miran Mozetič[2], Kristina Eleršič[2], Ita Junkar[2], Dejana Đorđević[1], Mladen Lovreček[3]

[1] University of Ljubljana, Faculty of Natural Sciences and Engineering
Snežniška 5, SI-1000 Ljubljana, Slovenia
E-mails: gorazd.golob@ntf.uni-lj.si, dejana.djordjevic@ntf.uni-lj.si

[2] Jožef Stefan Institute - Ljubljana, Department of Surface Engineering and Optoelectronics
Jamova cesta 39, SI-1000 Ljubljana, Slovenia
E-mails: miran.mozetic@ijs.si, kristina.elersic@ijs.si, ita.junkar@ijs.si

[3] University of Zagreb, Faculty of Graphic Arts
Getaldićeva 2, HR-10000 Zagreb, Croatia
E-mail: lovrecek@grf.hr

Abstract

The goal of investigation was to determine surface free energy, roughness and other properties of NBR and EPDM rubber blankets, modification of the surface properties using oxygen plasma treatment and defunctionalization of the surface. Characterization of the surface free energy by contact angle measurements using different disperse and polar liquids, SEM and roughness analysis of the investigated untreated and plasma treated elastomers gives a quantitative description of achieved surface modifications. Plasma treated rubber blankets achieved higher surface free energy and have become more hydrophilic but a superhydrophilic stage with contact angle with water near 0° was not achieved during the investigation. Contact angle with water remained almost unchanged after 24 hours. Roughness of treated surface has arisen. There were no significant differences between NBR and EPDM rubber blankets.

Keywords: EPDM rubber blanket, NBR rubber blanket, oxygen plasma, surface free energy

1. Introduction

Rubber blanket is a well-known ink transfer media in lithographic offset and other conventional or digital printing techniques. Mechanical properties, composition of surface layer, its roughness and other surface properties should give a good ink transfer factor as a necessary condition for high print quality. The surface energy of the blanket should be higher than surface energy of the ink and print areas of the printing plate and lower than the surface energy of the print substrate - usually paper. By modification of blanket surface energy we open a possibility to use a wide pallet of different printing inks, not only those based on synthetic or vegetable oil vehicle but also water-based and other types of inks.

Contact angle based measurements of surface energy are widely used in research and industry. By using different polar and non-polar liquids and proper calculation methods we should get information about polar and disperse part of surface energy of the material and indirectly we can conclude about its hydrophilic/oleophilic or hydrophobic/oleophobic properties.

By plasma (or corona) treatment of plastic film or other print substrates by the material producer or on the press we can raise its surface energy, usually over 40 mN/m. There is no other known wide use of plasma treatment in printing industry, except some experiments with treatment of printing plates for flexo printing.

During our investigation we tried to modify the surface energy of different rubber blankets to raise their surface energy and achieve nearly perfect hydrophilic surface. We also studied the stability of achieved modifications, methods for a reverse process and changes on the blanket surface at different stages during the experiments.

2. Research methods

In the experimental phase, four different blanket samples were used:

1. EPDM rubber for UV printing, non-polar, silica filler (RED),
2. EPDM rubber for UV printing, non-polar, soot/carbon conductive filler (BLACK),
3. NBR/TM (90/10) blend rubber for conventional printing, polar, silica filler (BLUE),
4. NBR blend rubber for conventional printing, polar, silica filler (LIGHT BLUE).

For oxygen plasma treatment of the samples we use lab plasma reactor with a vacuum pump and an inductively coupled RF generator at the power of approximately 200 W. Each sample was exposed to oxygen plasma with the neutral atom density of 5 x 10^{21} m^{-3}, the electron density of 8 x 10^{15} m^{-3} and the electron temperature of 35000 K for 0, 3, 9, 27, 81, 243 and 729 s. The samples were kept at floating potential that was -15V [Cvelbar, Mozetič].

For the first set of contact angle measurements we used 3 µl drops of distilled water and a CCD camera connected to a computer to get contact angle. Contact angle measurements were performed immediately after treatment and repeated after 3 and 24 hours. At the end we used the test-pen method, too.

For the second set of measurements we used the same samples, treated for 27 s by oxygen plasma under same conditions. We measured contact angles after approximately 24 hours on Krüss DSA 100 apparatus with three liquids: water (1 µl), diiodomethane (0.5 µl) and formamide (1 µl). For calculation of surface free energy we used Wu (Wu), Owens Wendt (OW) and AcidBase theory (AB) methods, supported by Krüss software [Brady, Erbil]. Surface free energy data of test liquids were obtained from Krüss database. For each measurement set we performed at least 6 measurements and excluded results with extreme deviation to mean value.

SEM images at 1000 x and 8000 x magnification show the changes of the surface on untreated and samples treated for 243 s.

Measurement of roughness using Perthometer gave us information about modification of surface morphology after plasma treatment.

3. Results

Results of the first set of contact angle measurements to find out ageing resistant after plasma treatment are presented in Table I. Because of thermal degradation at the edges of samples exposed for long time to oxygen plasma we did not use very long time of plasma treatment for LIGT BLUE samples. We repeated the measurements for RED, BLACK and BLUE samples several times and got very similar results that are not published in this report. Test-pen for surface energy testing indicated over 44 mN/m on all untreated and treated samples.

Table I: Contact angles of RED, BLACK, BLUE and LIGHT BLUE rubber blankets

Plasma treatment time (s)	RED			BLACK			BLUE			LIGHT BLUE		
	Contact angle (°) for water after											
	0 h	3 h	24 h	0 h	3 h	24 h	0 h	3 h	24 h	0 h	3 h	24 h
0	130.0	130.0	130.0	121.0	121.0	121.0	125.1	125.1	125.1	135.4	135.4	135.4
3	83.0	82.3	81.7	75.2	74.1	76.5	75.9	78.6	75.0	70.2	78.7	78.6
9	72.4	74.3	73.5	65.2	71.5	73.0	68.0	65.2	69.7	67.6	71.0	74.2
27	71.5	73.0	71.6	61.5	68.5	69.6	62.5	62.9	68.3	61.5	60.5	68.5
81	63.6	62.6	63.8	52.6	61.5	61.0	60.2	58.9	60.0	53.7	54.6	51.1
243	39.9	51.0	49.3	46.8	57.6	56.7	58.0	51.0	49.0	-	-	-
729	36.7	44.2	44.7	53.7	64.5	66.7	51.4	50.4	47.4	-	-	-

Results of second set of measurements of contact angles of treated and untreated samples using different liquids are presented in Table II.

Results of calculations using Owens Wendt, Wu and AcidBase theory methods, presented in Tables III and IV

Results of surface free energy (total, disperse and polar part) of untreated and treated samples using Owens Wendt method are presented in Figure 1.

Table II: Contact angles for different liquids (water - W, diiodomethane - D, formamide - F) of untreated and plasma treated samples

Sample	Contact angle (°) untreated			Contact angle (°) plasma 27 s		
	W	D	F	W	D	F
RED	132.4	75.3	104.2	66.7	48.3	62.9
BLACK	108.9	65.4	98.3	57.3	34	51.7
BLUE	100.2	49.9	76.9	52.8	39.5	38.7
LIGHT BLUE	111.0	65.9	99.8	50.3	41.7	44.8

Table III: Surface free energy of untreated samples (total - T, disperse - D, polar - P, acidbase - AB, acid - A, base - B)

Sample	Surface free energy (mN/m) untreated										
	Owens-Wendt			Wu			AcidBase theory				
	T	D	P	T	D	P	T	D	AB	A	B
RED	21.28	19.70	1.58	19.83	23.41	-3.58	21.48	19.96	1.51	0.48	1.19
BLACK	21.40	21.36	0.04	25.12	27.19	-2.07	20.55	25.47	-4.93	2.16	2.81
BLUE	32.73	32.59	0.14	35.01	34.75	0.27	33.66	34.33	-0.67	0.14	0.79
LIGHT BLUE	21.16	21.16	0.00	24.63	27.06	-2.44	20.62	25.19	-4.57	2.31	2.26

Table IV: Surface free energy of plasma treated samples (total - T, disperse - D, polar - P, acidbase - AB, acid - A, base - B)

Sample	Surface free energy (mN/m) plasma 27 s										
	Owens-Wendt			Wu			AcidBase theory				
	T	D	P	T	D	P	T	D	AB	A	B
RED	40.15	29.34	10.81	43.25	32.12	11.13	31.52	35.22	-3.70	0.14	24.46
BLACK	49.00	35.70	13.29	51.70	37.57	14.13	39.27	42.49	-0.32	0.09	28.89
BLUE	50.32	33.46	16.86	52.86	35.42	17.26	39.46	39.86	-0.40	0.01	33.22
LIGHT BLUE	51.98	33.22	18.76	54.29	34.95	19.34	42.39	38.74	3.65	0.10	32.94

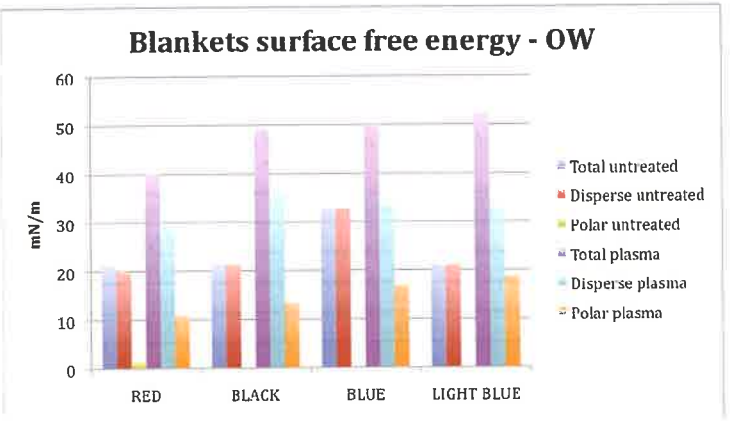

Figure 1: Surface free energy of untreated and treated samples, calculated using Owens Wendt method

SEM images at 8000 x magnification of RED, BLACK and BLUE samples are presented in Figure 2, 3 and 4 where each image pair of untreated and plasma treated (243 s) samples gives us the basic visual information about surface changes.

Changes in roughness after treatment in oxygen plasma (729 s) for RED, BLACK and BLUE sample are

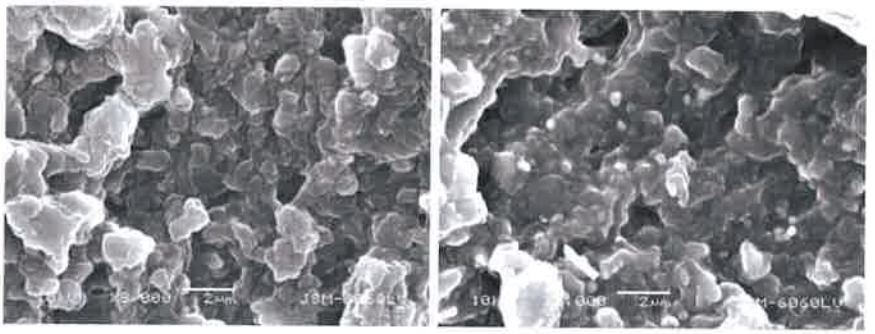

Figure 2: RED rubber blanket untreated (left) and treated (right)

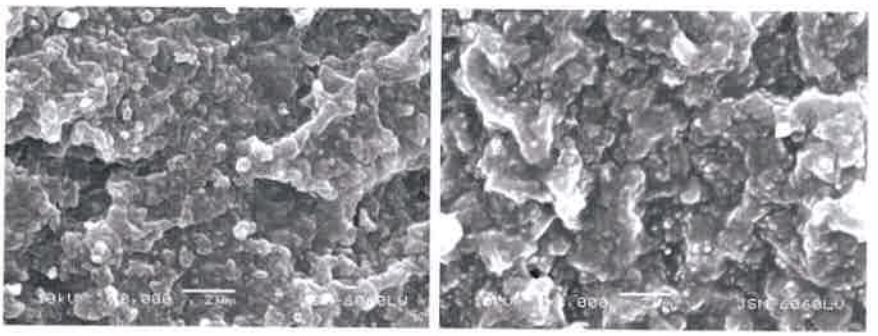

Figure 3: BLACK rubber blanket untreated (left) and treated (right)

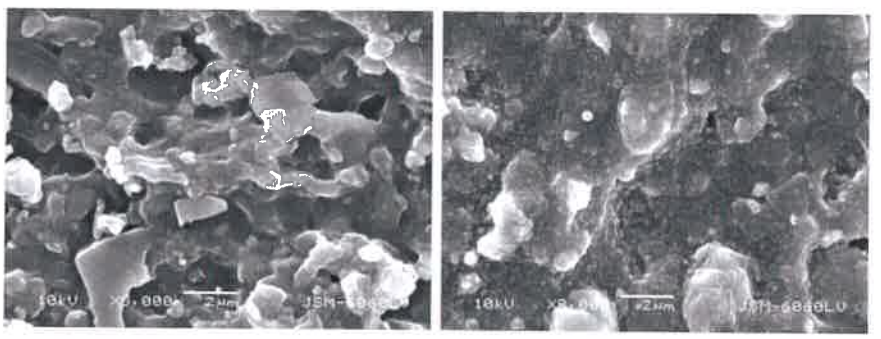

Figure 4: BLUE rubber blanket untreated (left) and treated (right)

Table V: Average roughness (Ra) of untreated and treated of RED, BLACK and BLUE samples

	Untreated samples	Plasma treated samples
Sample	Ra (μm)	Ra (μm)
RED	1.040	1.160
BLACK	0.708	1.100
BLUE	0.736	0.797

Results of reversible process or defunctionalisation of the surface properties using hot air dryer or laser show only limited success. Results of achieved contact angles for RED, BLACK and LIGHT BLUE samples, treated after 9 days for 10 min at 100 °C in hot air dryer are presented in Table VI.

Table VI: Contact angles for RED, BLACK and CYAN samples after hot air treatment

	Contact angle (°)		
	Water	Diiodomethane	Formamide
RED	100.9	60.1	71.2
BLACK	96.1	58.9	78.6
LIGHT BLUE	71.6	50.8	60.4

4. Discussion

Different types of rubber blankets give us similar results after treatment with oxygen plasma. For the first 25 s of treatment the colour of the plasma was red, typical for oxygen. After that the colour changed to white. The colour of the samples remained the same at short treatment time, BLACK and BLUE changed their colour at 243 s and RED at 729 s because of thermal degradation. For LIGHT BLUE sample we observed some traces of burning at the edges and therefore we used only short time for treatment up to 81 s. With all samples we saw traces of burning at the edges after treatment for 729 s.

Untreated samples were very hydrophobic, after short treatment of 3 s they became slightly hydrophilic and by increasing the treatment time the hydrophilicity increased [Gojo, Lovreček, Mozetič]. The hydrophilic condition remained very stable during 24 h. During our investigation we used equipment at different locations. Stability of the samples hydrophilicity gave us opportunity for contact angle measurements using different liquids after 24 h at another location. After oxygen plasma treatment surface free energy has arisen in all samples.

Results of contact angle measurements and surface energy calculations are not reliable and we have to repeat this part of investigation. Reasons could be in inappropriate handling with equipment, test liquids with characteristics that are not the same as in database, unhomogenity and roughness of rubber blanket surface, differences in air temperature and humidity or some other reason. It is well known from references that different methods for surface free energy give us different results and that some methods are not appropriate for all solid materials. At this stage of investigation we got enough information about influence of oxygen plasma on different types of rubber to continue with measurements of surface free energy using other types of rubber blankets and raw materials like basic polymers and fillers for rubber production.

It is interesting that so called polar NBR rubber shows us almost no polar part of surface free energy before treatment and non-polar EPDM rubber has higher amount of polar part compare to NBR rubber. After treatment with oxygen plasma we have achieved higher level of total surface free energy and polarity with NBR rubber, but defunctionalisation seems better using EPDM rubber. Reason for such deviation could be impurities at the rubber surface. The untreated samples were wiped with ethanol five minutes before measurements and plasma treatment but obviously this treatment was not efficient and for now chemical structure of untreated and plasma treated samples remains unknown.

During the investigation we did not achieve very hydrophilic stage with contact angle near 0° on our rubber blanket samples. On many other metal and organic materials we achieved super hydrophilic surface in very short time during oxygen plasma treatment. We observe some unusual phenomena like raised water drop on wet surface of the rubber and wicking of the water drop on the surface.

Surface roughness is slightly higher after treatment for RED and BLUE rubbers filled with silica, for BLACK sample it raised for 55 %. Roughness measurements are confirmed by SEM images where we see some changes in surface structure, caused by plasma etching of rubber components in the surface layer. Rubber consists of ten or more components like one or more polymers, fillers, additives for cross-linking of basic monomer, additives for hardness and elasticity control, pigments and dyes (Salamone). According to manufacturer's specifications of silica fillers we expected conglomerates of silica in dimensions up to 80 nm but at SEM images we can observe round shapes with bigger diameter. The shape of surface layer structure was typical for ground finished surface layer, it remained almost unchanged after plasma treatment and obviously there was no significant etching of polymer on surface layer.

5. Conclusions

To get more reliable results the analysis of pure basic materials before and after plasma treatment is necessary. We should continue our investigation using typical EPDM, NBR and other types of crude rubber and different fillers to get surface free energy of untreated and plasma treated basic rubber components. After that new set of rubber samples should be prepared for further investigations.

XPS analysis should give us chemical fingerprint of the sample surface. Surface free energy measurements are

and after treatment. Impact of impurities at the rubber surface layer is still unknown and with repeated series of plasma treatments and defunctionalisation we should get pure surface to perform measurements of surface free energy and chemical analysis.

In this paper the first results of oxygen plasma treatment of rubber blanket surface are presented. It can be concluded that such a treatment gives us a rubber blanket with new characteristics that open new opportunities for improvements of their characteristics and new functionality of blankets in different printing processes.

Acknowledgements

We would like to thank coleagues from Savatech, Kranj; Faculty of Pharmacy, University of Ljubljana and from Department of Graphic Arts and Photophysics, University of Pardubice for technical support and cooperation.

References

1. Brady, R.: *Comprehensive Desk Reference of Polymer Characterization and Analysis*, Oxford University Press, 2003, ISBN 0 8412 3665 8
2. Cvelbar U., Mozetič M.: *Method for improving of electrical connection properties of a surface of a product made from a polymer matrix composite*, international patent WO 2006/029642
3. Erbil, H. Yildrim: *Surface Chemistry of Solid and Liquid Interfaces*, Blackwell Publishing, 2006, ISBN 1 4051 1968 3.
4. Gojo, M., Lovreček, M.: *Characterisation of Surfaces on the Offset Printing Plate*, Proceedings of Lectures and Posters, 1st International Symposium of Novelties in Graphics, Ljubljana: Faculty of Natural Sciences and Engineering, 1998. 253-260
5. Lovreček, M., Gojo, M., Dragčević, K.: *Interfacial Characteristics of the Rubber Blanket - Dampening Solution System*, Bristow, J., Anthony (ur.). Leatherhead, Surrey, UK : Pira International, 1999. Str. 370
6. Mozetič M., Alenka Vesel, Cvelbar U.: *Method and device for local functionalization of polymer materials*, international patent WO 2006/130122
7. Mozetič, M.: *Controlled oxidation of organic compounds in oxygen plasma.* Vacuum. [Print ed.], 2003, vol. 71, p. 237-240
8. Salamone, J.: *Polymeric Materials Encyclopedia*, CRC Press, Taylor & Francis LLC, 1996, ISBN 9780849324703

Ink ribbing in printing nips

Tim C. Claypole, Georgios Vlachopoulos, David C. Bould

Welsh Centre for Printing and Coating
Swansea University, Singleton Park, Swansea, SA2 8PP, UK
Email: t.c.claypole@swansea.ac.uk

Abstract

Ink film splitting in flooded nips of non Newtonian fluids is core process physics of the inking train of the offset litho press. Understanding the interactions of the ink and the dynamics of the fluid flow to the printing plate is key to improving press design and also eliminating problems such as inconsistency, ghosting and misting. The splitting mechanism gives rise to local variations in the ink film thickness. In coating, where there is no oscillation of the rolls across the direction of print, this can lead to the development of discrete ribs of ink across the width of the roller.

A printability tester was used to recreate the conditions in a rolling nip contact and operated in such a manner as to enable the study of film splitting instabilities. The method of operation and measurement techniques use to study the ribbing phenomenon are described as well as preliminary measurements undertaken to evaluate the technique.

Ribbing was found to be primarily generated due to elongation mechanism at the nip exit, where ink is deformed in filaments and splits. The rotation rates do not allow ink to recover its elasticity or redistribute itself before the next time it is split. The film thickness, viscosity and speed were found to have the most effect on ribbing both the frequency and width of the ribs.

Keywords: offset, ink transfer, film splitting, instabilities

1. Introduction

Printing nips, where the surfaces of two rollers covered with a film of ink are forced into intimate contact, occur throughout the offset lithography roller train. As the rolls separate, the ink film is splits between the two rolling surfaces in a region of negative pressure. The continuous film splits into a series of discrete filaments which extend and rupture. This can give rise to an uneven distribution of the ink on the roller which is carried through to the image and also to misting (detachment of small droplets and ligands of ink). In the absence of lateral oscillation of one of the rolls, this instability can give rise to ribbing, a variation in fluid thickness in the lateral direction with discrete circumferential concentrations of ink (ribs). There is a strong interaction between the cavitation and the ribbing in the exit of the nip. The physics of this situation is similar to that of printing solids by flexography and roller coating.

Instabilities associated with ink film splitting are key to understanding the process physics of ink transfer. Previous researchers had studied the phenomena both experimentally and analytically. Banks and Mill [1954] investigated the ribbing pattern created by fluid during rotation and found that ribbing was a function of the ratio of the gap to the roller radius. They suggested cavitation patterns were affected by ribbing phenomena and those patterns were randomised by the oscillator roller mechanisms. MacPhee [1998] refers ribbing as the onset of hydraulic instability in accordance with the work of Pitts and Greiller in 1961. Many authors have concluded that ribbing instability strictly depends on the capillary number $Ca = \mu V / \sigma$, where: μ is the liquid viscosity, σ its surface tension, and V is the mean roll speed. [Savage 1984, Coyle et al., 1990, Carvalho and Scriven 1996, MacPhee 1998, Lopez et al., 2002]. The capillary number was used to explain the onset of the meniscus at the free surface of the nip exit. Newtonian liquids produced unstable flow at higher Capillary numbers than with Non-Newtonian fluids. Savage [1977] and Coyle [1984] studied the perturbation of the ink splitting mechanism using two-dimensional approximations of the Navier-Stokes equation to analyse ribbing phenomena of Newtonian fluids between rigid rollers. However, their theoretical results were not in good agreement with the experimental instabilities. Carvalho et al. [1994] described ribbing as three-dimensional periodic flow variation in forward roll coating film splitting. They used the capillary number to predict the onset of ribbing due to deformation of the soft rubber roller at the nip. A forward roller coating system was used to generate ribbing.

used to measure the ribbing wavelength. When both rollers are rigid, the flow was stable at values of capillary number up to about 0.1, but was unstable at higher values. They found higher capillary numbers for the onset of ribbing than Savage and Coyle. However, their capturing technique focused at a narrow scale across the rollers length and they also used a high coating film thickness. Lopez et al [2002] used a convective Maxwell model to keep track of deformation along the nip. They used a Runge-Kutta boundary value algorithm to solve the ribbing profile. Pressure was found to increase everywhere along the nip especially at higher shear zones. However, their calculation did not follow the Newtonian case and with viscoelastic properties the ribbing threshold was reduced. They also found that the periodic steady variation of ink film thickness became unsteady when speed was increased. Zevallos et al. [2004, 2005] analysed the two-dimensional flow of viscoelastic liquids in a forward roll coating gap, by solving the continuity and momentum equations coupled with two differential constitutive equations, the Oldroyd-B and FENE-P models. They found the stress field changed with rising liquid elasticity. They concluded a critical Weissenberg number makes the fluid meniscus unstable. The elastic forces change the flow characteristics near the free surface. At a fixed capillary number, the stresses at the free surface raised because of the strong extensional character of the flow at the nip exit region.

In general, poor correlation has been achieved between theory and experiment. The experiments and results focused on the formation of the meniscus at the nip exit and not at the ribbing profile. The perturbation theory tends to average the phenomenon and denigrate the effect on transfer mechanism. Also, all of these studies were on Newtonian liquids, generally of low viscosity and thick films, unlike offset printing where the inks are non Newtonian, highly viscous and there is only a thin film of ink on the roller train.

The objective of this research was to create an experimental method that allowed a parametric study of the ribbing due to ink film splitting in roller trains under conditions approximating to a litho offset printing nip. This paper presents the development of the method and initial results of an experimental investigation. The aim was to establish the relationship between ink film thickness and ribbing patterns. Unlike previous studies which have used photographic techniques to capture a short area along the nip and focused only profile variation, the aim was to measure the ribbing profile across the width and the length of the rollers.

2. Experimental method

An IGT Tack tester 450 was used to simulate a high speed distribution system with a short roller train with characteristics similar to a printing press. It has a three rollers train configuration in order to distribute the ink and measure its "tack" in gm meters units (Fig 1). The driven metallic roller generates rotation in the two elastic rollers. The one elastic roller is supported by load sensors to measure the friction applied via the ink film (tack). The other is an oscillator roller to equalise the ink film thickness across the rollers length. The ribbing phenomena was reproduced by running the tack tester without oscillation. Ribbing patterns develop on the rollers as they rotate against each other.

The repeatability of the experiment was highly dependent on the pre-distribution of a uniform ink film thickness. The ink was applied into the system by a pipette. The volume of the ink for the exact ink film thickness is calculated by the IGT manual. This assumes an even distribution of ink and is based on the surface volume of the roller train. The ink was applied on the rollers in fine ink lines across the length. The system speed was then

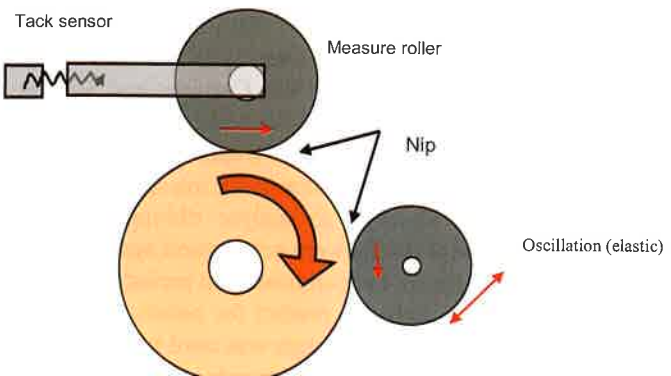

Figure 1:
Schematic of the IGT Tack tester 450

adjusted to the lowest level of 50m/min in order to avoid ink loss due to misting. The ink volume was distributed for 2 minutes using the full system geometry with the measure roller (rider) and oscillator. After the distribution process was stopped, the ink was allowed a relaxation time of 10 minutes. The relaxation time was determined from ink shear rheology tests. Care was essential with the cleaning process between experiments to ensure the solvent which is deposited into rubber rollers surface was completely evaporated.

Ribbing was induced by running the Tack tester for a predetermined time (Fig. 2) with only two rolls in contact (either the measurement or oscillation roll was in contact with the driven metallic roll). Ribbing is an outcome of the ink transfer process. Therefore, parameters that affect ink transfer were selected to evaluate their effect on ribbing mechanism. These were roller ratio, viscosity, speed, time and volume of ink on the rolls.

The roller ratio was varied by using either the oscillator or measurement roller with the motor roller. The oscillator is smaller compared to the measurement roller. This gives peripheral ratios 1.48 and 1.85, with corresponding angles separation of 18° and 22°, for the oscillator - motor and measurement-motor rollers combinations respectively.

Viscosity was varied by diluting a lithographic coldset cyan ink with different concentrations of Butyl-Diglycol, which can be used to modify the rheology especially with respect to the inks levelling characteristics. The dilution decreased the inks viscoelastic properties, tack and surface tension of ink.

Speeds used were 50 m/min, 200 m/min and 400 m/min, run times were 3 minutes and 6 minutes and ink film thickness 3.9 μm and 7.8 μm.

Ribbing forms lines parallel to the rotating direction. To capture the ribbing pattern, a paper was placed between the two rollers after the end of the run while system was stopped. The paper was folded in half to simultaneously capture the ribbing image of each roller on the single side of the substrate. Rollers were rotated drawing the paper through the nip creating a ribbing imprint. Two ribbing images of the metallic and rubber rollers were on the unfolded substrate.

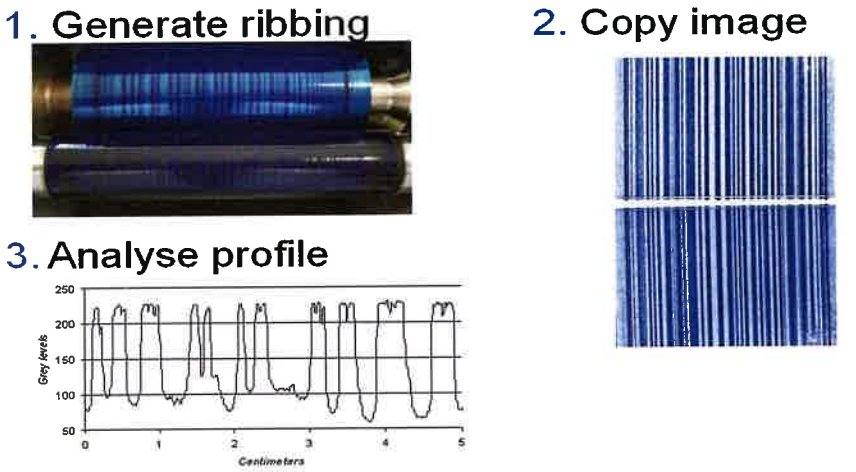

Figure 2: Ribbing generation on Tack tester (1) The pattern is captured on paper (2). The ribbing sample is scanned and transformed into grey levels (3)

The ribbing images were scanned with a flat bed scanner and the grey density along the length of the ribbing pattern was averaged. The ink volume can be estimated from the grey levels of the captured image. High grey values indicate a decreased ink volume because grey scale tends to higher power till 255 when the image is white. The grey troughs indicate the number and width of the ribs. The number of troughs indicates how many lines are generated per area but does not provide a detailed description for the actual ribbing pattern. The ribs were converted into a binary signal based on whether the rib grey scale value was above or below the moving average of the grey scale (Fig. 3). This gave both the number of ribs and their width. The separation of the ribs can be related to the fluid instabilities as the ink film splits i.e. the initial film failure. The width of the ribbing is related to the ink film thickness across the width of the roller. The ribbing can be characterised by the averaged

thickness on rollers. Variations on ribbing lines width across the roller surface indicate variations of the ink film thickness. Uniform distributed ink film thickness determines low variability. Variability increases with increased instability. Fourier analysis was also used to extract the power spectrum from the grey scale data. This gives a measure of whether the ribbing phenomenon is consistent across the width of the roller.

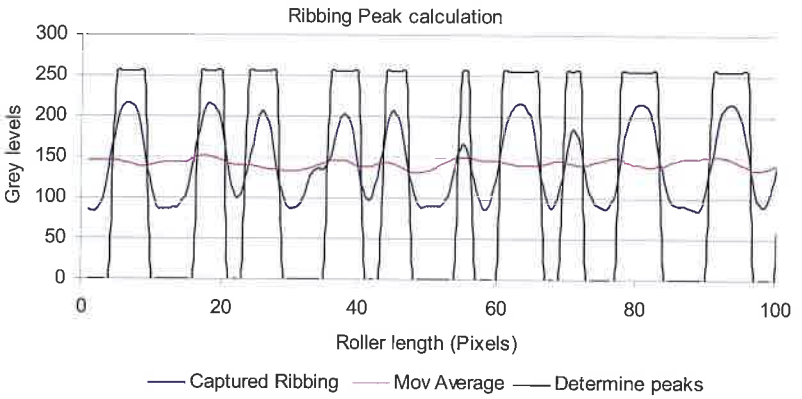

Figure 3: The number and width of the peaks is determined by where the moving average axis cross to the captured ribbing profile according to grey levels of the digital image

Additional studies were used to identify motion and further phenomena during splitting mechanism (Fig. 4). A high speed camera was used to capture images from the rollers rotation and the ink splitting mechanism. The video capturing process focused at the nip exit of the rollers where cavitations were formed. Variation in magnification was used to locate and capture the ink splitting process between the two rollers.



Figure 4: Nip exit video

3. Results and discussion

While the ribbing occurs as a regular pattern across the majority of the roller, there is an end effect particularly with thicker films (Fig 5). This thick edge was evaluated using the scanner and the grey scale technique to measure the shaded area on the image. It is symmetrical on both sides with the peak appearing 0.2 cm from the end. The ribbing becomes established after 0.6 cm with a higher frequency. As the higher grey levels correspond to an absence of ink, in the end region there is a local build up of ink, but not the creation of areas without ink as are seen between the ribs once they have become established.

The ribbing profile on the roller was measured white light interferometer (Figure 6). The profile was measured at the edge (points 1 and 5), in the centre (point 3) and at the quarter points (points 2 and 4). They represent the average of three discrete measurements. The heights of the ribs of the thinnest film (3.8 μm) were only slightly higher (10%) than the initial applied ink film. This can be attributed to the fine gap between the ribs. However, the thicker films resulted in taller ribs at the ends, 30% higher than the initial ink film thickness, with lower ribs in the middle. This could be attributed to the oscillator mechanism used to ensure an even spread of ink before the start

of the experiment. A tendency for lateral flow due to the oscillator mechanism has been previously observed in offset presses by Chou [1977]. The ribbing patterns would therefore appear to be generated according to the initial ink film thickness. This affects the thickness and the width of the actual pattern.

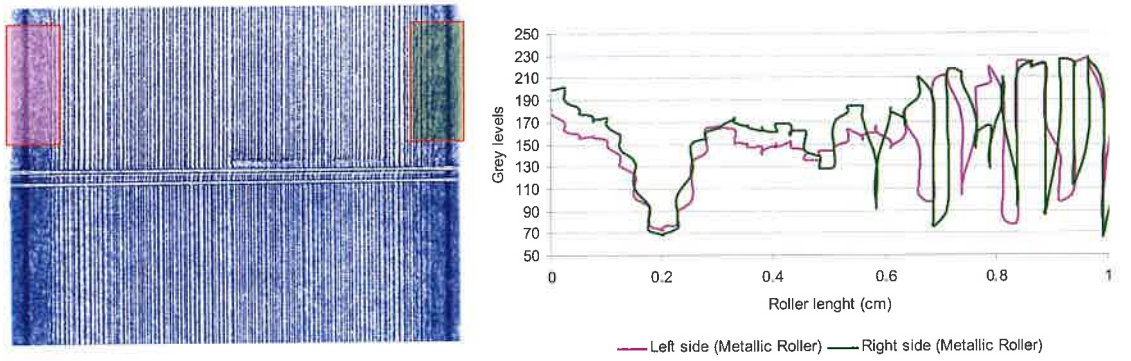

Figure 5: Side to side variation in ribbing

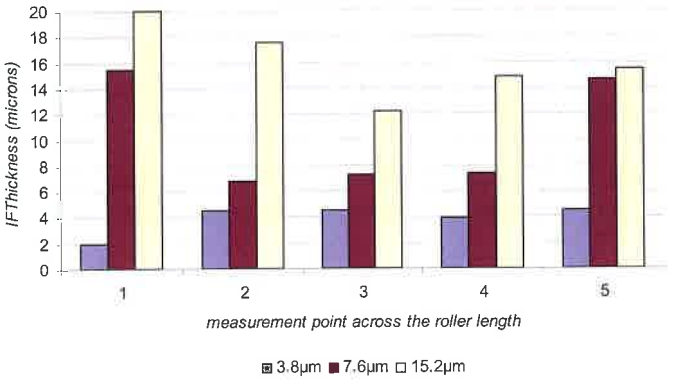

Figure 6: White light measurements across the roller width

The consistency of the ink film splitting is also influenced by the initial ink film thickness. The thicker films tend to produce an uneven splitting across the width of the roller, which lead to a spreading of the power spectrum obtained by Fourier analysis (Figure 7). By comparison, the thinner film has a predominant single peak. This could be a consequence of the variation in initial film thickness across the width of the roller changing the frequency of splitting but is more likely to be due to an instability in the splitting process in the exit nip.

The ribbing is not uniform in the direction of rotation reflecting the discrete random nature of the filamentation to failure (Figure 8).

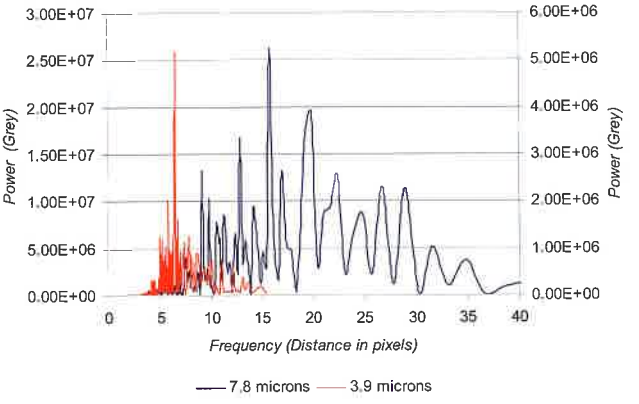

Figure 7: FFT analysis of ribbing patterns

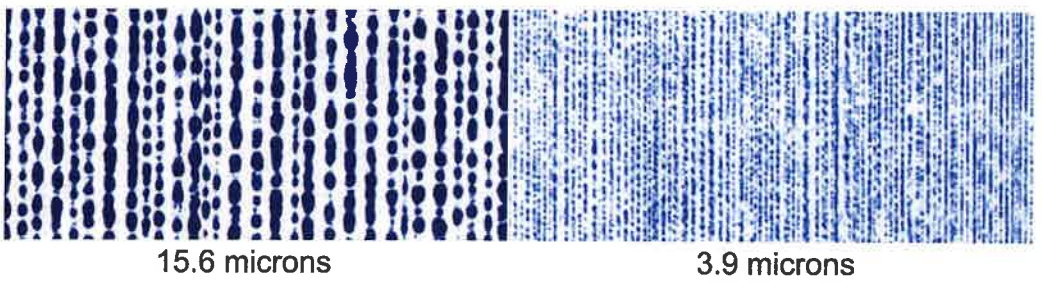

Figure 8: Ribbing presents variations across both in the width and the direction of rotation

Ribbing patterns are strongly influenced by speed, ink film thickness and viscosity (Figure 9). Number of ribs/ cm profile increases with viscosity but decreases with increasing speed and ink film thickness.

Ribbing is affected by viscoelastic properties of the ink. The filament split faster when viscosity is decreased. When the viscosity increases there is more elastic extension of the ligament before failure. More ink is transferred to a filament which follows the rotating direction of the rollers.

Ink film thickness also shows a significant effect on ribbing formation. The contact angle area increases with ink film thickness and so ribbing with increased width is formed. The increase in ink film thickness generates less filaments and ribbing follow that decrease in lines and width.

Ribbing is formed faster with increase in distribution speed where increases cavitations across the nip length. High speed with lower viscosity is possible to generate similar ribbing with low speed but higher viscosity.

Rollers ratio and time have insignificant effect on ribbing formation (less than 1 rib/cm). It was anticipated the separation angle (roller ratio) would effect the ribbing formation as it governs the extension of filaments by changing the elongation speed. It is likely a wider range of separation angles would have produce a more significant change.

The lack of effect of run time suggests the ribbing pattern forms and becomes fully developed within a few revolutions. This infers ribbing is dominated by the filament failure process.

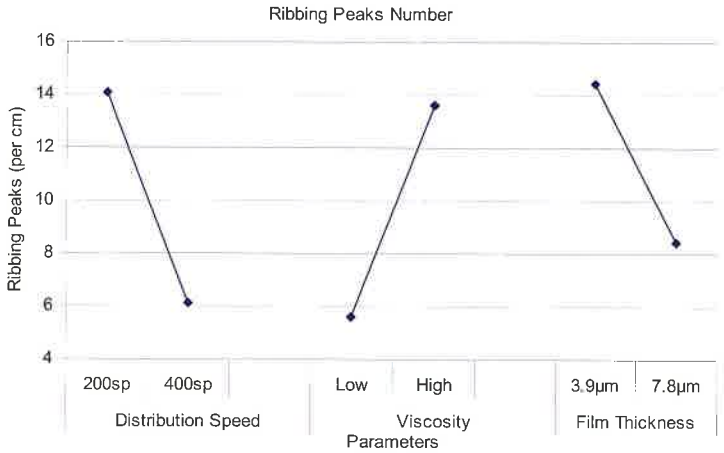

Figure 9: Effect of ink film thickness, viscosity and speed on number of ribbing peaks

While number of ribs indicates the general pattern, it does not provide detailed information about ribbing width instabilities. Roller ratio and time have a minimal effect on rib width (approximately 0.1 mm) or variability (less than 0.1 mm). Speed has a major effect on ribbing width and variations (Figure 10). Ribbing width increases with increase in speed but there is also an increase in width variation. The decreased viscosity increases ribbing width and generates more width instability.

The ribbing peaks significant decrease with increase in ink film thickness where slight wider ribbing is formed with no significant effect on width variations. The increase of ink volume at the nip exit decreases capillarity and negative pressures. The contact area of the ink on the rollers increases with the volume of the ink at the nip exit and wider ribbing is formed. The increase instabilities occur as the flooded nip where rollers rotate under micro slip mechanism. The effect can be compared with the roller ratio effect where decreased negative pressures are generated at the nip exit. The ribbing width increases with roller ratio or ink film thickness where nip flood is determined.

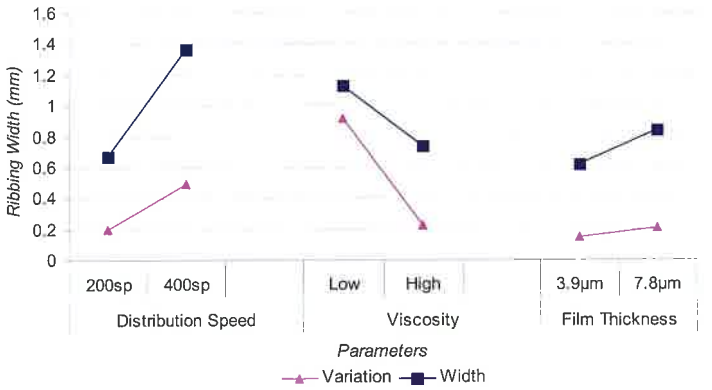

Figure 10: Ribbing width and variations for changing speed, ink film thickness and viscosity

In rolling nips, the ink arrives on the surface of the rollers, is squeezed in the nip and is pulled apart at the exit. A separation meniscus forms at the nip exit as the free surface of the ink is pulled by the visco-elastic forces generated by the separating roller surfaces and the ink which remains in the nip. Cavity is generated by meniscus failure when the forces due to the ink volume increase at the two rollers exceed the pull back strength at the nip exit. The ink draws into a film between the rollers in the direction of rolling, i.e. it forms a rib between the two rollers. The continuing separation, leads this film to break up into filaments between the rollers which are extended until failure occurs (Figure 12). The filaments lay back after splitting causing the ink to increase in the direction of rolling. The ink falls back onto the roller as the point of attachment is accelerated towards the centre of the roll by the centripetal forces. However, if there is a large amount of ink in the point of attachment, then the inertial forces will cause this to fly outwards and for it to become a misting droplet.

This process creates an uneven distribution of ink across the width of the roller when it re-enters the nip. On exit this could lead to areas where there is a larger amount of ink so the ink film where the ink film will preferentially extend and regions of lower volume where the ink film with preferentially split. The frequency between these areas of high and low thickness will be related to the natural filamentation frequency determined by the original thickness of the film. Thus, providing feedback to the splitting process and creating ribs within a few revolutions. This will be particularly prevalent with thinner initial ink films (such as the 3.8µm) where there could be localised starvation in the nip. Also, the height of the ribs with the thin film are only slightly higher than the initial ink film thickness, therefore the ink mechanism would remain approximately the same. With the thicker films the squeeze in the nip would be sufficient to reduce the variation in film thickness and therefore reduce the interaction between the splitting process on successive revolutions. Analysis of distribution rollers illustrates how ribbing evolves with time (Fig 12). There is evidence of the onset of ribbing from the out set although it is not visible to the naked eye.

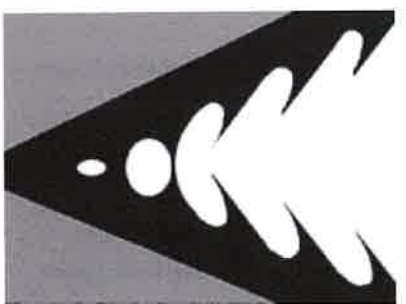

Figure 11:

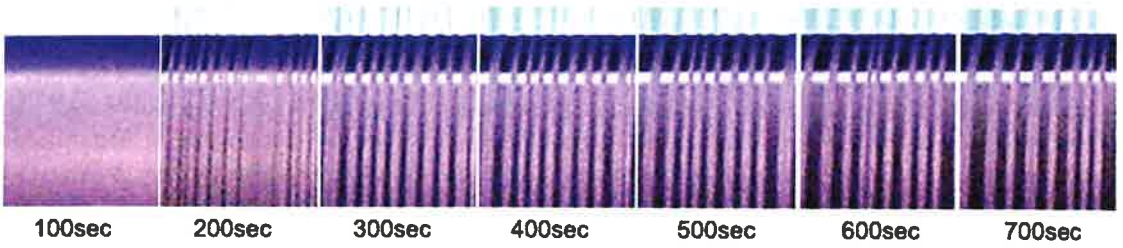

Figure 12: Evolution of ribbing with time

4. Conclusions

A method has been developed to enable the investigation of the process physics of ink film splitting a roller train similar to an offset litho press. The splitting of thin films of non Newtonian inks has been investigated. Ribbing is primarily generated due to elongation mechanism at the nip exit, where ink is deformed in filaments and splits. The rotation rates do not allow ink to recover its elasticity or redistribute itself before the next time it is split. The film thickness, viscosity and speed were found to have the most effect on ribbing both the frequency and width of the ribs.

In offset presses the inking trains are more complex, with multiple nips on a single roll, have larger diameter rolls and include oscillating rolls to distribute the ink. While these will prevent the build up of ribbing, the interaction of variations in the ink film thickness caused by the splitting process will feed through the press. Understanding the fundamental physics of the splitting process and its interaction with subsequent nips will contribute to the design of roller trains. It will also lead to a better understanding of the printing of solids in processes such as flexography.

Acknowledgements

Georgios Vlahopoulos would like to acknowledge the financial support of IKY State Scholarship Fundation.

References

1. Banks, W. H., Mill, C. C., 1954.: Some Observations on the Behavior of Liquids Between Rotating Rollers, Proceedings of the Royal Society, Ser. A, Vol. 223, No. 1154, pp 414-419
2. Carvalho, M. S., Anderson, T. J., Scriven, L. E., 1994.: Ribbing Instability in Forward Deformable Roll Coating, Proceedings of the 1994 TAPPI Coating Conference, pp 99-107
3. Carvalho, M. S., Scriven, L. E., 1996.: Capillary and viscoelastic effects on elastohydrodynamic lubrication in roller nips, J. Trib. Trans. ASME, Vol. 118.4, pp 872-879
4. Coyle, D. J., 1984.: The Fluid Mechanics of Roll Coating: Steady Flows, Stability, and Rheology, PhD Dissertation, University of Minnesota at Minneapolis
5. Coyle, D. J., Macosko, C. W., Scriven, L. E., 1990.: A Simple Model of Reverse Roll Coating, Ind. Eng. Chem. Res. 1990.29, pp 1416-1419
6. Lopez, F. V., Rosen, M., 2002.: Rheological effects in roll coating of paints, Latin American Applied Research, Vol. 32.3, pp 247-252
7. MacPhee, J., 1998.: Fundamentals of Lithographic Printing, GATF Press
8. Pitts, E., Greiller, J., 1961.: The flow of Thin Liquid Films Between Rollers, J. Fluid Mechanics, Camb. Uni. Press, Vol. 11, p 33
9. Savage, M. D., 1977.: Cavitation In Lubrication, J.Fluid Mech., Vol. 80, pp 743-757
10. Savage, M. D., 1984.: Mathematical Model for the Onset of Ribbing, AIChE Journal, Vol. 30, No. 6, pp 999-1002
11. Zevallos, G. A., Carvalho, M. S., Pasquali, M., 2004.: Forward roll coating flows of viscoelastic liquids, Moving Boundaries VII: Computational Modelling of Free and Moving Boundary Problems, Vol. 10, pp 235-244
12. Zevallos, G. A., Carvalho, M. S., Pasquali, M., 2005.: Forward roll coating flows of viscoelastic liquids, J. Non-Newtonian Fluid Mech. Vol. 130, pp96-109

Dynamic evaluation of lint build-up during newspaper production

Miroslav Hoc

Innventia AB
P. O. Box 5604, SE-114 86 Stockholm, Sweden
E-mail: miroslav.hoc@innventia.com

Abstract

In newspaper production dusting or linting is one of the most troublesome problems associated with the surface of paper. During offset printing dust and fibre particles leave the paper surface and adhere to the printing blanket. These lint particles will eventually cause deterioration in the printed image, and the printing cylinder must be cleaned. This cleaning process takes time, costs money and will create health hazards, so printers are keen on reducing lint build-up. Linting is a phenomenon caused by the interaction between printing press and paper. The mechanism of linting is generally described as a combined effect of the ink film splitting forces and the inter-fibre bonding energy in the paper surface.

A dynamic On-Line Linting Measurement System (OLM) has been developed. The build-up of lint on the blanket is measured dynamically during the ongoing printing. The OLM test printing emulates a commercial printing, this although it is carried out in the laboratory. The OLM-technology is a way of carrying out dynamic linting studies even with a small amount of test material, while at the same time retaining the effect of the variables of the printing process on the lint transport. Measurement of lint circulation by the OLM-technology makes it possible to judge whether the build-up of lint on the rubber blanket is caused by the paper or is due to the printing conditions. Both the paper-maker and the printer have obtained an extraordinary tool for studying the reasons for the build-up of lint.

Keywords: linting, newsprint, offset printing, paper properties, test methods

1. Introduction

In papermaking, the paper produced has a given potential to cause linting, i.e. it has a tendency to release particles from the surface depending on the forces in the printing nip. All the fibres, fibre fragments and other particles which together form the paper surface can be regarded as candidates for linting. Particles which are poorly bound in the surface will come loose in the printing and can cause linting problems. If particles are sufficiently bound or anchored in the surface, they will withstand the stresses in the printing nip without coming loose. Such a surface will then be regarded as "lint-free".

Several dozens of different methods are used to characterize the "linting propensity" of a paper [Elphick, 1976; Gratton, 2006; Heintze, 1992; Mangin, 1989; Moller et al., 1995; Parker, 1970; Sudarno et al., 2005; Trollsås, 1995]. These include both laboratory tests and small-scale test printings. The different laboratory tests sometimes give a fairly good correlation with the behaviour of the paper in commercial printing and sometimes no correlation at all [Hoc, 2005; Möller, 1992]. This uncertainty in the results is presumably the chief reason why none of these methods has yet been standardized or universally accepted. In order to measure the linting propensity, an offset paper must be test printed. Small-scale test printings, which best imitate the complicated process of the full-scale press, of course give the best correlation with a commercial printing. The more extensive the test printing, the better the correlation. The disadvantage is that this type of evaluation is time-consuming and expensive, and it is not certain that the amount of paper test printed will be sufficient to ensure a valid prognosis.

The principal reason for the uncertainty in the prediction of "linting propensity" by a laboratory test, regardless of whether it uses a printing nip or measures the linting tendency indirectly, is that linting is a statistical phenomenon. This means that the measurement of a large area is required for the results to be reasonably relevant. An investigation of a small surface area can thus only give a partial indication of whether a surface particle or a part of the surface can resist the stresses to which it is subjected in its passage through the printing nip.

The second reason why laboratory tests give uncertain results is the fact that they do not analyse what happens to the particles which come loose from the surface. The particles which cannot resist the stresses in the printing

nip and come loose from the surface can either be deposited on the printing cylinder (the rubber blanket) or be transported away from there during the printing. This transport can take place either to other parts of the printing machine or back to the paper, see Figure 1. Process variables, such as the press geometry and component materials such as the rubber blanket, printing ink, fountain solution and printing plates, no doubt have an influence on the occurrence of linting and they must therefore be carefully documented in each study [Hoc, 2000]. When particles are transported via the printing plate to the dampening unit (not a brush or spray construction), they change the quality of the fountain solution but do not otherwise disturb the printing. On the other hand, when particles are transported to the inking unit, they change the rheology of the ink and thus render the transport of the printing ink to the printing cylinder more difficult, with a deterioration in print quality as a result. Both these causes are however, less troublesome from a print quality point of view and are not dealt with in this study. The most interesting and presumably also the greatest transport takes place from the rubber blanket directly back to the paper. These particles are not visible in the print and can therefore be regarded as completely harmless from a linting viewpoint, although they came loose from the paper surface in the passage through the printing nip. The main purpose of the present work was to investigate how large a proportion of the particles have been transported in this way, and in particular the effect of different printing parameters on this transport.

Linting problems do not arise when the particles come loose from the paper surface but when a large proportion of these dislodged particles get stuck on the rubber blanket. The magnitude of this transport is determined by the materials used in the printing process such as the rubber blanket, printing ink, fountain solution and by the settings of the printing process such as the nip pressure, the impression or, under certain circumstances, differences in speed between plate and rubber blanket cylinders.

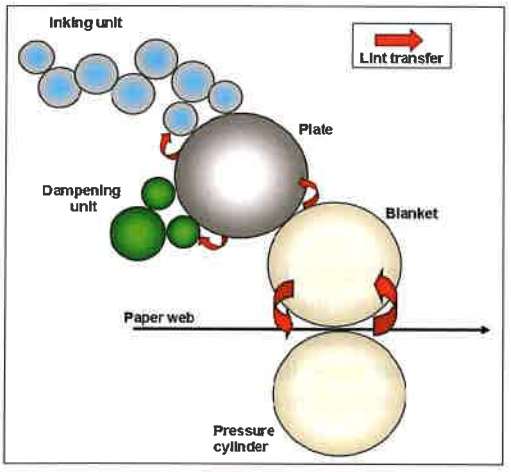

Figure 1:
In printing, some of the particles which have come loose from the paper surface in the printing nip are transported back to the paper and some to the dampening and inking units. The amount of particles transported back to the paper is several times larger than the amount transported via the plate to the remaining parts of the printing machine

To be able to study the effect of different printing parameters on this removal of particles from the rubber blanket, one must have access to a technology with the help of which particle transport to and from the rubber blanket can be studied. The objective of the research was to develop a dynamic on-line test method to be able to separate the effects of paper and printing press on build-up of lint on the blanket during offset printing.

2. Method development

2.1 On-line linting measurement (OLM)

To be able to study the mechanisms which influence the transport of lint, an on-line system for recording the lint particles on the rubber blanket has been developed. The system consists of a camera, microscope optics, a stroboscope and software for recording and measuring particles on the rubber blanket. This makes it possible to photograph the rubber blanket after each cylinder revolution during the printing. The images of the lint are analysed after the completed printing with the help of an image-analysis program developed especially for this application. The amount of lint on the rubber blanket is determined as the number of particles or the lint coverage (the proportion of the surface area of the rubber blanket which is covered by lint particles). In addition to these parameters, the size distribution and the lint circulation (the amount which comes loose from the paper plus the amount which is transported away) are also measured.

2.2 Printing

2.2.1 Sheet-fed offset

The OLM-system has been developed and tested in the laboratory on a two-colour commercial sheet-fed offset printing machine, Fuji Sheet Offset 52 II, see Figure 2, right. In this press, sheets with dimensions 52 x 40 cm can be printed. The speed in the machine can be varied from 2.000 to 12.000 revolutions per hour, which corresponds to a peripheral speed of 0.5 to 2.0 m/s. The press is furnished with a separate dampening unit, including two dampening rollers, and an inking unit with four ink rollers.

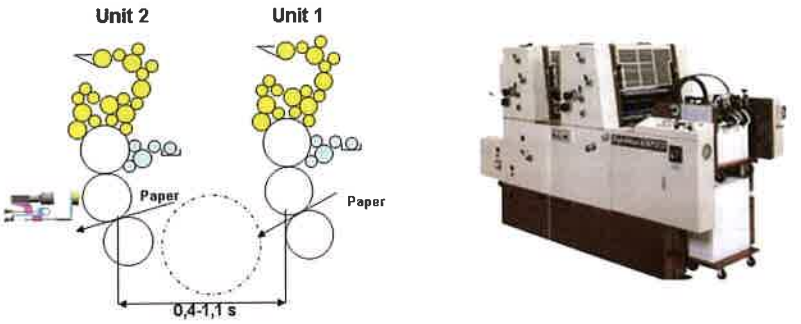

Figure 2: The commercial two-colour sheet-fed offset machine, Fuji Sheet Offset 52 IIP, used for dynamic measurement of the build-up of lint. To the left is a sketch of the printing units with dampening and inking systems

The printing cylinder to which the rubber blanket is fastened has a diameter of 180 mm. The impression cylinder is of steel. The printing nip thus resembles a satellite printing unit in a commercial press. All the cylinders are equipped with bearings, and make-ready of different thicknesses is used for the impression. The nip length with standard make-ready is about 5 mm.

Figure 2, left shows a schematic picture of the printing machine as it is used in standard test printings, that is single-colour printing (SCP). The first printing unit is disconnected, so that the sheet passes through without coming into contact with the rubber blanket. That is more practical for space reasons to photograph the rubber blanket in the second printing unit in this press.

2.2.2 Web offset

The OLM-system has as well been used on LINDA, the Innventia pilot scale dynamic paper web testing machine, see Figure 3. LINDA is well equipped for systematically studying paper web behaviour and paper/ink/fount interactions under conditions similar to those in an industrial printing press. The equipment has a driving roll nip through which a 400 mm wide paper web can be run and the peripheral speed of 2 to 5 m/s. LINDA is equipped with an offset printing nip, which is used to study the effects of different paper qualities, chemical additives, founts, printing inks, rubber blankets and settings of the printing press.

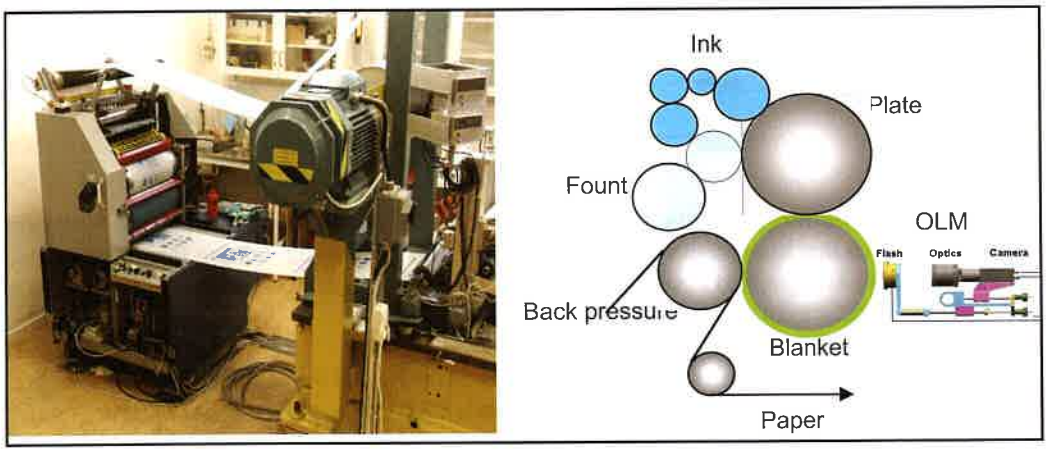

Figure 3: LINDA, the Innventia pilot scale test site for web offset printing, used for dynamic measurement of the build-up of lint. To the right is a sketch of the printing unit

2.2.3 Printing routine

The test printing is carried out according to a well-defined routine. This includes control of the print density, the moisture level and the temperature of the press. A "standard" test printing consists of 2.000 and 12.000 - 25.000 cylinder revolutions on Fuji Sheet Offset and LINDA, respectively. In more accurate investigations and when the amount of test material permits, an investigation with more cylinder revolutions is carried out.

The design of the printing form is very important for the build-up of lint on the rubber blanket. The different regions from non-ink areas to full-tone areas have different effects both on the removal of lint from the paper and on the further transport of lint from the rubber blanket. The layout of the printing plate therefore includes 0%, 30%, 50%, 80% and 100% tone areas, Figure 4.

The amount of ink in the printing nip influences the amount of lint which is removed from the paper, and also the lint transport to the rubber blanket. It is thus important that the amount of ink on the rubber blanket is kept constant throughout the test printing. However, in practice, there is always a variation in the ink flow, even if the settings on the press are unchanged, and this leads to a variation in print density. According to the ISO Standard (SS-ISO 2004), the variation in print density shall not be greater than ± 0.05.

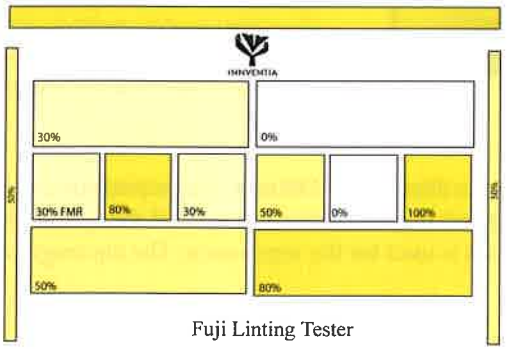

Figure 4:
A layout in single-colour printing. There are image areas with different tone values for OLM photographing (0%, 30%, 50%, 80%, 100% and FM) and large image areas (0%, 30%, 50% and 80%) for tape pull-off

2.3 Image capture and analysis

To be able to study the build-up of lint during printing, a camera, microscope optics, a lighting and software for the recording and measurement of particles has been fitted onto the printing press. A detailed sketch of the OLM system is shown in Figure 5.

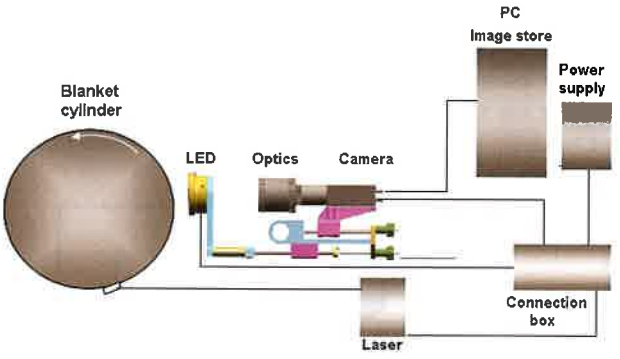

Figure 5:
The fitting of the "On-Line Linting Measurement System" (OLM) in a printing press

To obtain a sufficiently good image quality, the system must fulfil a number of requirements. The exposure must be extremely short so that blurredness due to the movement is minimised. During this short exposure, it is important that the area photographed is strongly and uniformly illuminated. An annular illumination with a flash of light emitting diode is used in this assembly.

Since the rubber blanket with lint particles is moving rapidly past the lens of the camera, the exposure time must be very short. At the highest printing speed (12.000 sheets/hour), a particle on the rubber blanket is moving at 2 m/s , which means that it moves circa 2 µm in 1 µs. For the picture to be sufficiently sharp, a flash of light emitting diode unit is therefore used. A CCD-camera of the Merlin type with a resolution of 16 µm/pixel has been fitted on a device which makes it possible to move the camera across the rubber blanket.

The OLM takes one picture at exactly the same position on each revolution of the cylinder, so that the number of images captured corresponds to the number of printed copies. This technique requires however that the revolution be monitored with a sensor, and it makes high demands on the exactness of the triggering. To ensure accurate triggering in OLM, the cylinder has been equipped with a reflectance ribbon. The difference in reflectance between the rubber blanket and the ribbon is recorded by a laser detector and this impulse starts the flash unit.

The analysis of the image comprises three stages. First, a filter is applied to correct for the uneven illumination and the background. Thereafter, a threshold is applied and the image is transformed to a binary image. Finally, the lint particles are identified.

The average size of newsprint lint particles is about 30 µm. To be able to record and identify these small lint particles with an acceptable resolution, zoom optics and intermediate lenses in front of the camera are used.

The region photographed with this installation has an area of 29 mm^2 (6,5 x 4,5 mm^2), Figure 6. The size of the smallest particle recorded in the analysis is determined by setting a size threshold after the grey-scale image has been transformed to a binary image. The setting of this threshold is a key stage in the identification of lint particles. In this appraisal, the threshold criterion is adjusted manually, i.e. a subjective decision is made as to which objects shall be identified or not. The new threshold value is used for the each image in the measurement series.

All the particles identified in accordance with this criterion are counted and measured with the help of an image analysis program developed for this purpose. In addition to the number and the size distribution, the total area of the rubber blanket covered by the lint particles can also be calculated.

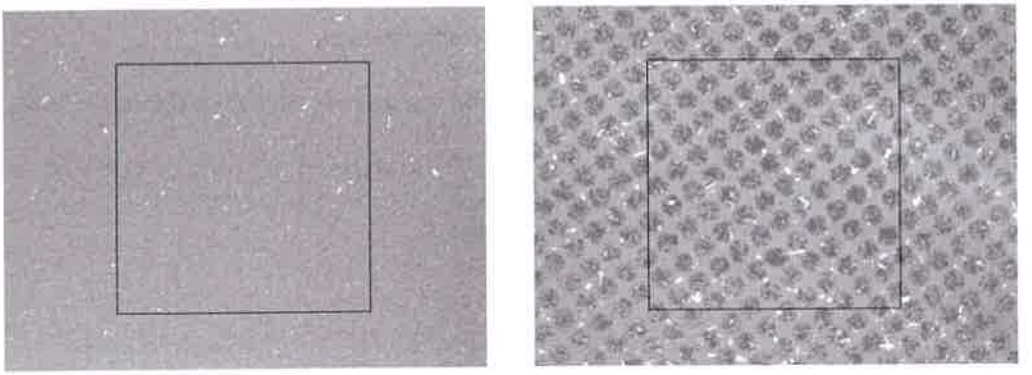

Figure 6: To the left, a picture of lint particles on the rubber blanket on 0% screen and to the right, a picture of lint particles on rubber blanket on 50% screen. The frames in the middle mark the area to analyse (3 x 3 mm^2)

3. The dynamics of the build-up of lint

The transport of lint pulp during printing can be described schematically as in Figure 7.

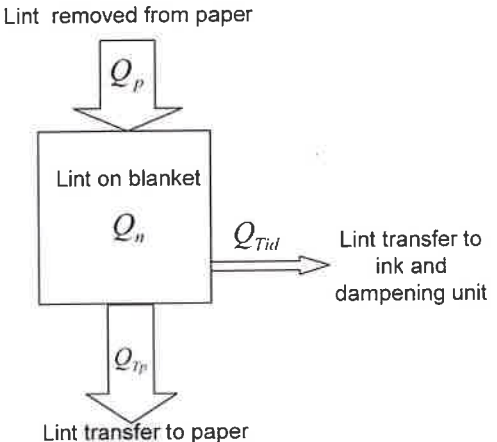

Figure 7:
Schematic model for the transport of lint during printing in a printing press

The amount of lint remaining on the rubber blanket Q_n is given by the material balance of added and removed lint:

$$\frac{dQ_n}{dn} = Q_P - Q_T = Q_P - Q_{Tp} - Q_{Tid} \quad (1)$$

where

Q_n = The amount of lint on the rubber blanket after n cylinder revolutions,
$Q_{P=}$ Lint removed from the paper to the rubber blanket,
Q_T= Lint transported away from the rubber blanket,
$Q_{Tp=}$ Lint transported back to the paper,
$Q_{Tid=}$ Lint transported to the printing plate (and further to the dampening and inking unit).

The fact that the number of particles on the printing plate is very small compared with the amount of particles on the rubber blanket indicates that the proportion of the particles transported back to the paper is much greater than the proportion transported via the printing plate to the inking and dampening units, that is: $Q_T \approx Q_{Tp}$

It is possible to calculate both Q_P and Q_T by the differential equation which describes the build up of particles on the rubber blanket.

$$\frac{dQ_n}{dn} = Q_P - \lambda Q_n \quad (2)$$

Where

Q_n = number of particles on blanket after n rotations,
λ = probability of a particle to be transported away from the blanket.

Even Wiik used the equation (2) (Wiik, 2006) which solution was given by Lindqvist (Lindqvist 1980).

$$Q_n = Q_\infty (1 - e^{-\lambda n}) \quad (3)$$

Where Q_∞ is the saturation level of particles after a long run.
In the initial stage with $n = 0$ and $Q_n = 0$ is

$$\frac{dQ_n}{dn} = Q_P \quad (4)$$

At the saturation level Q_∞ is $\frac{dQ_n}{d_n} = 0$ so that according to (2)

$$\frac{dQ_n}{dn} = Q_p - \lambda Q_n = 0 \quad (5)$$

and thus =

$$Q_P = \lambda Q_\infty \quad (6)$$

4. Results and discussion

The OLM-system has been developed and tested on a two-colour commercial sheet-fed offset printing machine and on LINDA, the Innventia pilot scale dynamic paper web testing machine. The Fuji Sheet Offset printing machine is preferably used when the amount of paper sample is limited. LINDA is preferably used when a higher speed is demanded. Standard as well as improved newsprint papers have been tested. The tested commercial paper samples were collected from different mills.

4.1 Lint build-up and screen

The different regions from non-ink areas to full-tone areas have different effects both on the removal of lint from the paper and on the further transport of lint from the rubber blanket [Hoc and Trollsås, 1977]. The build-up of

lint on the rubber blanket at different tone values during offset printing of newsprint paper is shown in Figure 8. The amount of lint particles on the blanket reached a maximum already at about 100 revolutions for the non-ink area. For the halftone area the amount of lint increased with the number of copies printed up to 1.000 copies, as shown in Figure 8. For the full-tone area a fast build-up was observed for the first hundred revolutions, thereafter a slow increase occurred. The maximum number of lint particles on the blanket was observed for the 50% screen. This is in agreement with an earlier report where it was observed that the 50% tone area usually releases the largest amount of lint to the rubber blanket [Hoc and Trollsås, 1977].

The OLM takes one picture at exactly the same position on each revolution of the cylinder. A movie can be made from the captured images. In a movie from printing a 50% screen on newsprint paper it was observed that particles were sliding on the rubber blanket. When some particles reached a halftone dot they were further transported from the rubber blanket. Earlier is has been reported that lint accumulates on areas outside the halftone dot area whereas the dot area has almost no lint [Hoc and Trollsås, 1977].

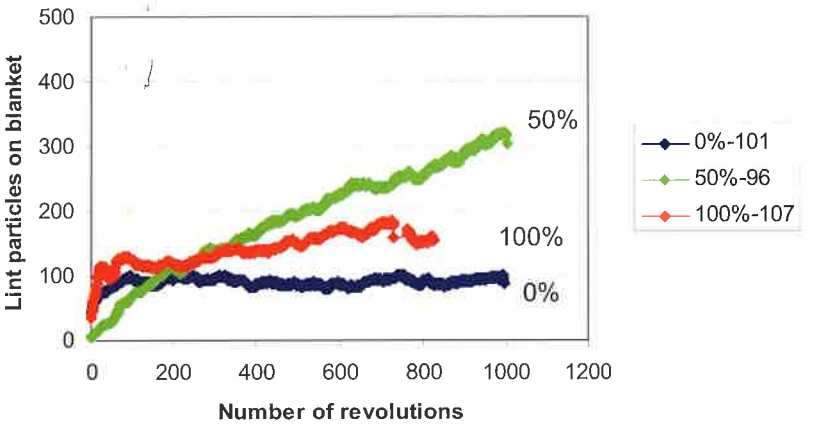

Figure 8: Lint build-up on the rubber blanket during printing for 0%, 50% and 100% tone values

4.2 Lint build-up for different sides of newsprint

The result of fitting equation (3) to the experimental data is shown in Figure 9. The same newsprint paper has been printed at identical print conditions on the top side and on the reverse side of the paper. The bottom side has a higher propensity to shed lint particles than the top side. Most probably the bottom side will cause problems in the print house. This is an example of two-sidedness of a newsprint paper.

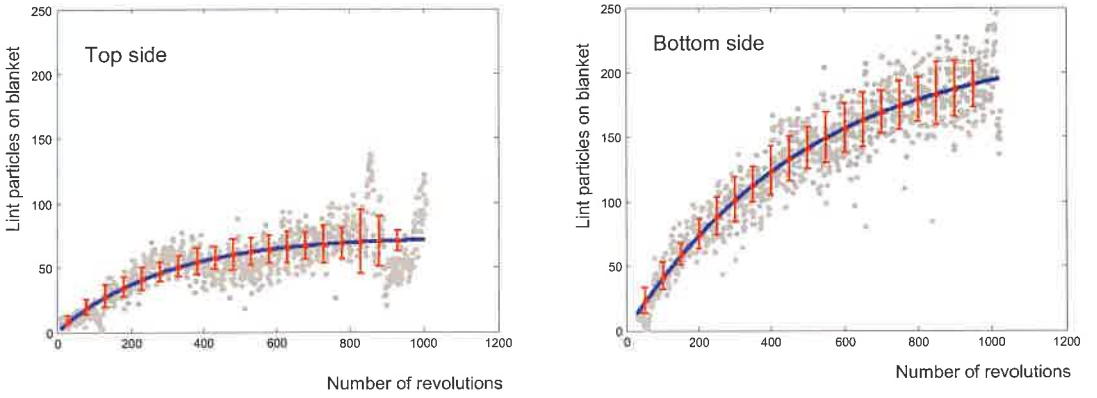

Figure 9: Examples of observed data and the fitted lint model (solid line with error bars). The number of lint particles on the blanket plotted against the number of images captured by the CCD-camera during two test printings. The Figure shows the build-up of lint from different sides of the same newsprint paper. To the left, top side ofthe paper and to the right, the reverse side of the paper

5. Conclusions

A dynamic On-Line Linting Measurement System (OLM) has been developed. The OLM-technology is a way of carrying out dynamic linting studies even with a small amount of test material, while at the same time retaining the effect of the variables of the printing process on the lint transport.

The OLM-technology makes it possible to on-line follow the build-up of lint on the blanket during offset printing. Images of lint particles on the blanket are captured for each cylinder revolution. The OLM-method has been tested in different test printings in a sheet-fed offset press. The technique functions well and gives sufficiently good images for a further analysis of the amount of particles.

The dynamics of the process can be followed by making a movie from the captured images. Depending on printing conditions and paper lint particles might accumulate on the blanket, leave the blanket or slide on the blanket.

Measurement of lint circulation by the OLM-technology makes it possible to judge whether the build-up of lint on the rubber blanket is caused by the paper or is due to the printing conditions. Both the paper-maker and the printer have obtained an extraordinary tool for studying the reasons for the build-up of lint.

Acknowledgements

The author thanks Holmen, Norske Skog, Stora Enso and Voith for financial support and PFI for cooperation with image analysis of lint particles and Per-Åke Turesson for the assistance during the printing trials.

References

1. Elphick, J., (1976), *Measuring the Linting Performance of Offset Newsprint, TAPPI/CPPA Graphic Arts Conf.: Toronto, Ontario*
2. Gratton, M. F., (2006), *Predicting lint propensity of paper at the mill: A test that works, PAPTAC's Annual Meeting*
3. Heintze, H. U., (1992), *The measurement of linting technology in mechanical printing papers, Int. Printing and Graphic Arts Conference: Pittsburgh, USA*
4. Hoc, M., Trollsås, P-O., *(1977), Inverkan av tryckningsparametrarna på tidningspappers damning i offset, SCAN-forskrapport 146*
5. Hoc, M., (2000), *The phenomenon of linting in newsprint printing*, IFRA special report 1.19
6. Hoc, M., (2005), *Dynamic characterisation of fibre rising on paper surface after dampening and* drying, *Paper IV, Licentiate Thesis, Royal Institute of Technology*
7. Lindqvist, U., Meinander, S., (1980), *A pilot test for linting propensity of papers, Printing and Reprography Conference: Chicago, USA,* 59-63
8. Mangin, P. J., (1989), *Can laboratory tests predict offset linting propensity of paper 75th Annual Meeting, Technical Section: Montreal, Canada,* B386
9. Moller, K., Thomassen, B., Weidemmuller, J., Menzel, P., Walther, K., Falter, K., Sporing, G., Meissner, M., Azxell, O., (1995), *Factors Influencing linting in offset printing of newsprint, 49th APPITA Annual General Conference: Hobart, Australia,* 115-121
10. Möller, K., (1992), *Using a modern commercial pressroom as a print quality laboratory, Appita Journal* 45(1992):6, 408-412
11. Parker, J. R., (1970), *The measurement and Control of Linting From Web Offset Newsprint, Printing Technology* 14:1, 31-37
12. SS-ISO, (2004), *Graphic technology - Process control for the production of half-tone colour separations, proof and production prints*
13. Sudarno, A., Gujjari, C., Rand, S., Janko, P., Batchelor, W., Banham, P., (2005), *Comparison of size distributions of lint particles from different printing operations, 59th Appita annual conference and exhibition: Auckland, New Zealand, vol. 1,* Paper 3B33, 279-284
14. Trollsås, P. O., (1995), *Linting tendency in newsprint of different manufacture, TFL*
15. Wiik, K., (2006), *Dynamics of linting, 60th Appita annual conference and exhibition: Melbourne, Australia,* 2006, 33-35

Methodology for identification of papers causing critical lint issues on printing presses

Christine Canet, Michel Martineau, Valériane Vigne

Quebec Institute of Graphic Communications (QIGC)
999 Emile Journault East, Montreal, QC, H2M 2E2, Canada
E-mail: ccanet@icqg.gc.ca

Abstract

Lint is a secular and critical problem for printers. Even if numerous methods exist to predict paper tendency to create lint, none of them permits to define its impact on print quality. Even if all papers tend to create lint, not all forms of lint are equally problematic for offset printers. This paper describes main results of an applied project conducted at the Institute aiming to develop a methodology predicting the lint impact on print quality and its severity for printers.

Keywords: printing, offset, lithography, quality control, paper, lint, image analysis

1. Introduction

Meanwhile energy and paper costs increase in percentage from year to year, selling prices of prints decrease. This difficult economic situation has forced printers to improve their productivity, while maintaining their print quality. That is the reason why they severely control their paper, which represents about 50% of the total print cost depending on applications. Printers are not only paying attention to the price per tonnage, they also try to avoid running papers creating problematic lint on their printing presses and thus creating a production variance.

Lint is without any doubt the oldest and the most severe press problem against which every printer struggles daily in North America. This issue stands today for more than half of the claims emitted worldwide and not less than 75% of those in Quebec.

In order to help printers and paper makers, an applied research project from the Quebec Institute of Graphic Communication (QIGC) was carried out to develop a methodology that will help paper manufacturers to detect problematic papers in terms of linting issues before sending it in pressrooms. This could help both printers and paper producers to save precious and expensive production time on press.

Lint - Definition

In this paper as in the printing industry, «lin» designates commonly all built-up types appearing on blankets including: piling phenomena or other chemical reactions occurring between press consumables (ex. «downstream piling»).
«Lint» is typically composed of paper components (fibers, fillers) mixed with ink components (such as pigments, waxes and resins). While printing, «lint» may cause a growing deterioration of the print quality: loss of details, color variations and even printing of undesirable information. When the image deterioration is no longer acceptable, the printing production has to be stopped to wash blankets.

Even if all papers tend to produce «lint» from a low to a greater extent, lint is not always problematic for printers. In fact, higher lint amount does not systematically induce a worse problem for printer than a light lint deposit increasing along the print run. Thus a large lint amount quickly formed (ex. within the first 5.000 copies) and rapidly stabilized will not disturb the printer, whereas small increasing lint quantity along the print run will disrupt the printing production a lot. In the same way, a small lint quantity - which is quickly formed, but falling off the blanket from times to times will considerably affect print quality (cf. Figure 1). And to complicate matters a little more, for a given press environment, severity of the «lint» issue varies from one paper to an



Figure 1: Example of lint on blankets after printing a newspaper

2. Objectives

Numerous methods exist to predict the paper tendency to lint. However although all these measuring methods perform adequately and correlate well between each other, none is able to determine the lint impact on print quality before printing the substrate.

Objectives of this applied research project were then:

- To develop a methodology predicting the lint impact on print quality;
- And to establish for paper makers a test method evaluating lint severity before going on printing press.

3. Research methodology

Due to the vast area of investigation, it was decided in a first step to restrict the project to super-calendered (SC) paper grade, which corresponds to the widest type of paper used today.

The methodology used to conduct this project was divided into three successive steps:

- Development of a method for characterization of the lint impact on print quality,
- Development of a measurement of unprinted paper to predict lint severity in term of print quality,
- And establishment of specifications for a paper quality control.

QIGC selected four different SC papers produced by the same North American paper manufacturer (cf. Figure 2) and generating various lint forms. So in order to ensure choosing representative papers to carry out this project, specific linting profiles of SC paper were established via feedbacks collected from the field and confirmed by preliminary printability tests conducted on the QIGC heatset web press set up with a controlled heatset ink series and run with a K\C\M\Y sequence.

- **Reference #1:** This paper produced a *small lint amount increasing while printing*. Deposit was mainly visible in *printing areas* on the first *two units*,
- **Reference #2:** This paper produced *a larger lint amount than Ref. #1*, also *increasing while printing.* Deposit was on the *whole blanket surface, and thus mainly on the first two units.* In that specific case, *lint was essentially made of paper dust**.

**Paper dust is typically made of unbounded fibers, fines or paper particles (fillers, fiber fragments), which are not strongly embedded on the paper surface. They are easily removed and tend to build up on printing blankets (generally in the first printing unit).*

- **Reference #3:** After few thousands copies, this paper produced a **s***imilar lint amount than Ref. #2***.** After few thousand copies (i.e.: at the beginning of run), *this lint quantity remained stable.* Deposit was *on the whole blanket surface, and thus mainly on the two first units.*
- **Reference #4:** This paper produced *a larger lint amount than Ref. #3. Lint quantity remained stable* after few thousand copies (i.e.: at the beginning of run). *Deposit was on the whole blanket surface, and thus mainly on the two first units.*

In order to conduct the present applied research project, printing tests were run with each of the selected papers on the Harris M110 press available at QIGC. Papers were printed with the same heatset ink series and with the

same ink sequence than the ones used for the preliminary tests. All press parameters remained unchanged during the whole printing trials: same ink series, same fountain solution, same press speed, same press adjustments, same plates and blankets, same target solid ink densities, etc…

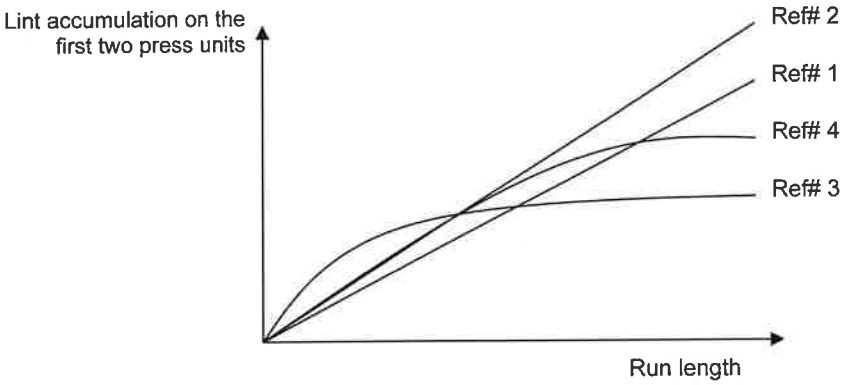

Figure 2: Four selected papers - Profile of lint formation

4. Summary of experimental results

4.1 Development of a method for characterization the lint impact on print quality

On print samples, numerous controls were carried out, among which some are listed hereafter.

- ***Visual assessment to identify potential print defects***
  No matter the paper reference, print defects became noticeably visible after about 40 000 printing copies only and corresponded to a loss of details (see Figures 3 & 3bis – printed images obtained when printing the paper Ref. #4).



Figure 3: Printed image after 5 000 copies (Ref.#4)

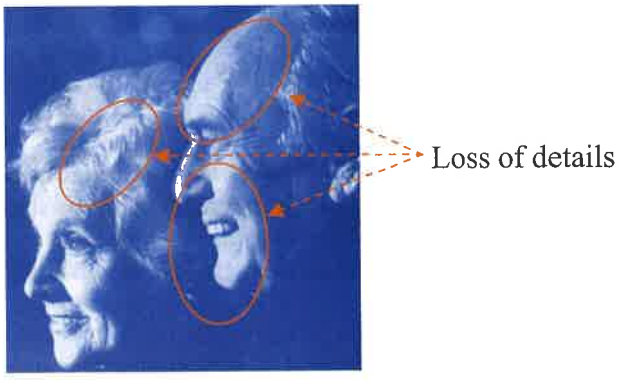

Figure 3bis: Printed image after 40 000 copies (Ref.#4)

- ***Densitometric measurements***
  These measurements (dot gains, contrasts and trappings) happened *to be not significant to evaluate print quality deterioration.* Whereas quality deterioration was visually detected, densitometric measurements remained unchanged as readings remained within narrow tolerances.

- ***Mottle measurements***
  Compared with visual assessments, *mottle measurements then appeared to be the most appropriate characterization method to be used to quantify print quality deterioration.* Such measurements take indeed into account changes in luminance values of given areas, which correlate well with visual observations.

That is the reason why QIGC decided to focus its efforts to develop a mottle measurement methodology, based on image analysis technology. Measurements were carried out first on monochrome tone scales printed areas (same areas than the ones used to collect lint on blankets) on samples (see Table I). Visual mottle is easily distinguishable as it corresponds to a non-uniformity luminance signal either in transmission or in reflection modes.

Table I: Mottle values measured on cyan screened area

Run length	5.000 copies	15.000	25.000	35.000	40.000
Paper Ref # 1	700	549	434	533	531
Paper Ref # 2	609	526	494	500	454
Paper Ref # 3	524	518	546	447	476
Paper Ref # 4	539	506	471	439	397

Whatever the paper, mottle index decreases as the run length increases.
Also on all paper conditions, printed dots in lightest areas (3, 5 and 10% coverage) tended to disappear (cf. Figures 4 & 4 bis), and mainly for cyan and black colors. The intensity of this defect followed lint gravity for the four paper conditions.

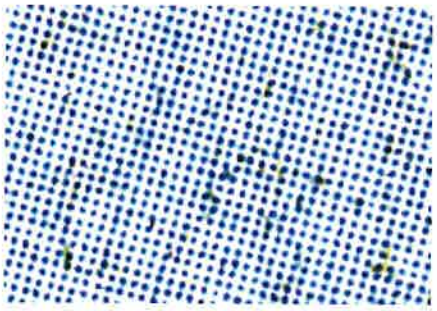

Figure 4: Cyan - Printed dots in 10% coverage Rref #4) - After 5.000 copies

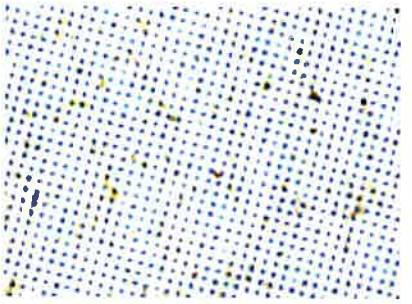

Figure 4 bis: Cyan - Printed dots in 10% coverage (Ref #4) - After 40.000 copies

Even if mottle appeared to be an interesting tool to quantify print quality deterioration, it also appears as being not accurate enough to correlate accurately with visual assessment. That is the reason why other types of measurement are still being investigated; the idea being that an index combining mottle measurement with other potential data will provide an assessment as close as possible from visual evaluation.

4.3 Development of a measurement of unprinted paper to predict lint gravity in term of print quality

Knowing that all existing methods of characterization lint tendency of unprinted paper correlate well between each other (it was established in a preliminary project), QIGC chose to use one methodology only. QIGC then selected the fibrometer (i.e.: a lint collector coupled with an image analyzer), which was developed by the CRIQ, a Canadian Research center. This equipment was installed in line on the QIGC printing web press, right before the first printing unit (cf. Figure 5). It permits to collect, to analyze and to quantify lint in real-time, on both sides of the paper web.

Measurements carried out were successfully used to predict the speed of lint formation on blankets via usage of mathematical model integrating data collected by the fibrometer. Those measurements were then combined with visual assessment of prints in term of print quality to build a second mathematical model able to predict lint severity of a specific paper.



Figure 5: Fibrometer equipment in-line with the web offset press used at QIGC

5. Conclusions

With its partner, QIGC was in a position to develop a mathematical model allowing paper maker to identify a problematic paper for lint issues, and thus before printing it. Right now, the validation of the robustness of the established model is still going on.

Therefore the severity of the lint impact on print quality is still assessed visually, as mottle measurements are not accurate enough to quantify print quality deterioration. QIGC is right now investigating other potential measurements, the idea being that an index combining these data with mottle measurement will provide an assessment as close as possible from visual evaluation.



Characterization and modelling of the effect of calendering on coated polyester film

Erik Bohlin[1], Ludovic Coppel[2], Caisa Andersson[1], Per Edström[3]

[1] Karlstad University
Dept. of Chemical Engineering, SE-651 88 Karlstad, Sweden
E-mails: erik.bohlin@kau.se, caisa.andersson@kau.se

[2] Innventia AB
Drottning Kristinas väg 61, P. O. Box 5604, SE-114 86 Stockholm, Sweden
E-mail: ludovic.coppel@innventia.com

[3] Mid Sweden University
NAT, Universitetsbacken 1, SE-871 88 Härnösand, Sweden
E-mail: per.edstrom@miun.se

Abstract

Polyester films were coated with a coating colour based on a ground calcium carbonate with narrow particle size distribution. Four different coat weights were produced. The coated sheets were calendered and the samples were exposed to up to twenty nips in the calender at a line load of 300 kN/m at 50°C. The brightness and the thickness were measured after each calendering nip. Reflectometry was used to measure the refractive index and the microroughness of the samples. Calendering lead to a decrease of the Kubelka-Munk scattering coefficient and an increase of the absorption coefficient of the coated transparent films. Taking into account non-uniform surface reflection at the boundaries between media of different refractive indices, a large part of the reflectance decrease due to calendering could be attributed to an increase of the effective refractive index at the coating surface and a decrease of the surface microroughness.

Keywords: coating, calendering, gloss, brightness, refractive index

1. Introduction

Absorption of printing ink into the pores of a coating layer is an important process. The appearance of the finished product is very much dependent on the complicated physical and chemical phenomena that occur in ink setting and drying. Due to separation of ink components caused by chromatographic effects, the optical properties of a printed area can differ if the porosity of the substrate changes [Rousu et al., 2005]. Increased surface roughness, or decreased coating density, increases the ink penetration depth [Eriksen et al., 2007] which also affects the appearance of the print. The structure and optical properties of the paper and the coating layer is therefore important to consider when a printed product is planned.

To be able to study the coating layer separately, the coatings can be applied onto plastic films as non-absorbing model substrates. This technique is often used to reduce the influence from a non-uniform paper substrate. The smooth surface of a plastic film is of course different compared to the relatively rough surface of a fiber-based substrate, but trials have shown that the difference in final coating layer porosity is only about 10% [Larsson and Engström, 2007], and that coated plastic films are good predictors of the performance of papers.

Calendering is widely used to decrease the surface roughness and thereby improve the optical properties, such as gloss, of coated paper. However, calendering also decreases the opacity and the paper strength and it is therefore crucial to understand how different calendering conditions such as line load, temperature and speed, affect the substrate properties. The speed of the laboratory calender that was used in this study is much lower compared to full scale calenderers, and the samples are thereby held in the nip for a longer time. This prolonged exposure to compressional forces will affect the coating structure differently than a conventional calendering nip with shorter dwell time. The large number of nips used in this study was performed to exaggerate any

Changes in optical properties caused by calendering have been discussed in numerous articles. They are often explained by changes in the coating structure, but the mechanisms are complex due to the wide range of particles, and interaction between particles, in coating colours of different recipes. Coating layers that contain ground calcium carbonates (GCC) as pigment tend to remain more unaffected than those containing kaolin clays. This is due to the pigment shape. Clay consists of plate-like particles which build a structure that is easily destroyed during calendering, while GCC particles are more sphere-like and harder to rearrange. An evidence for this is that the pore volume is reduced almost twice as much for a clay coating than for a GCC coating after calendering [Larsson and Engström, 2007]. GCC was used in this study because of the surface properties that were investigated.

Other chemical components also influence the structure and the optical properties of the coating layer. Different types of thickener added to the coating colour for adjustment of the viscosity of the mixture has been shown to affect properties such as brightness and gloss [El-Sherbiny and Xiao, 2005]. The nature of the latex binder also influences the final appearance of the surface. Increased latex content reduces the pore volume, and the effect is even magnified by calendering [Larsson and Engström, 2007].

Thanks to its simplicity and the fact that it is invertible (enabling material constants to be directly determined from a pair of reflectance measurements), the Kubelka-Munk (KM) model [Kubelka, 1931] is still extensively used to describe the optical properties of paper and coatings. The reported decrease of the apparent KM scattering parameter with calendering has been attributed to an increase of gloss and a reduction of pore size down to the scattering limit. However, the KM model assumes a diffuse reflection from the sample and standard reflectance factor measurements are made with a gloss trap removing specular reflection from the surface. The surface reflection from glossy samples is thus not taken into account, whereas more diffusely reflected light from matte surfaces are captured by the instrument detector [Makarenko, 2000]. Since calendering makes the surface smoother, part of the reflectance decrease can be attributed to a change of the surface roughness. Another aspect neglected by the KM theory is internal reflections at the boundary between media of different refractive index, which in some cases is approximated with the Sauderson correction [Saunderson, 1942]. A change of the refractive index at the coating surface would hence also affect the reflectance factor.

In order to differentiate these different contributions to the decrease of the reflectance factor due to calendering, a model taking the angular-resolved reflection from rough surfaces and refractive index changes is required. DORT2002 [Edström, 2005a and Edström, 2005b] is an angular-resolved light scattering model that handles refractive index discontinuities at the top surface, but it is restrained to perfectly flat surfaces, therefore a Monte-Carlo method is employed here [Coppel et al., 2009]. By modelling the change of surface roughness and effective refractive index, the aim of this work is to get a better understanding of how the optical properties of coating layers are affected by calendering.

2. Methods

In order to minimise the effect of the substrate and to determine the optical properties of the coating colour alone, a non-absorbing plastic film (Lumirror 54.41, Toray Plastics Europe SA, Miribel Cedex, France), with a thickness of 75 µm, was used as substrate. A well-defined coating colour was applied onto the plastic film sheets, and the samples were exposed to various numbers of calendering nips.

The coatings were applied by means of a bench coater, K202 Control Coater (RK Print LTD., Royston, UK) using a series of wire-wound rods. For the calendering a soft-nip laboratory calender (Oy Gradek AB, Kauniainen, Finland) was used. The calendar was fitted with a heated steel roll and a soft polymer roll. The coating recipe contained 100 pph calcium carbonate, a narrow particle size distribution pigment (Covercarb 75, Omya AB, Malmö, Sweden), 12 pph SB latex with a particle size of 120 µm, and a T_g of 24°C (Eka Polymer Latex Oy, Oulu, Finland), and 0.5 pph carboxymethyl cellulose (Finnfix 10, CP Kelco Oy, Äänekoski, Finland). The coated polyester films were dried at 105°C for two minutes in a laboratory oven to ensure good film formation of the latex.

Four different coating coat weights were used for the trials, 16, 26, 43 and 71 g/m^2, all created with single coating layers using rods 3, 4, 6 and 8 with increasing diameter of the wire. All the samples were exposed to 20 nips at a line load of 300 kN/m. Before calendering, and after each one of the first ten nips and after the fifteenth and the twentieth nip, the optical properties were investigated. All the trials were performed at a calender speed of 34 m/min, and a

calendering temperature of 50°C. Some of the samples were also calendered at 6 x 50 and 3 x 100 kN/m to be able to compare the result for exposure to several nips with low line load to exposure for one nip at 300 kN/m. Uncoated plastic film was also exposed to calendering to detect any compression of the substrate.

Gloss measurements were performed by means of a gloss meter (Zehntner glossmeter, 20° - 75°, Shropshire, UK) at 75° according to ISO 8254-1. For the brightness (R_{457}) measurements, a Minolta 3630 Brightness tester (Basildon Essex, UK) was used. The reflectance factors were measured using a black background (R_0), a plastic plate that is a part of the equipment, and a white background (R_w) constructed of a pile of coated samples. A STFI Thickness tester (M201, Stockholm, Sweden) was used for the thickness measurements. Reflectometry was used to measure the refractive index, the macro- and microroughness of the samples with coat weights 16, 43, and 71 g/m^2, after 0, 8 and 20 calendering nips. The instrument and measurement method are described by Elton and Preston [2006] and Elton and Day [2009].

Open PaperOpt [Coppel et al., 2009] was used to model the optical properties of the coating layers and compute their spectral reflectance factor in a d/0° geometry. The model allows taking the surface roughness and the refractive indices of the coating layer and the plastic film into account. The effect of calendering on the measured optical properties of the coating layer could then be studied separately in terms of surface roughness induced measurement differences, internal structure modifications, and refractive index changes at the coating surface. Surface scattering is treated as a combination of two effects. The long-range topographic structure, called the surface waviness, is the part that deflects incident wave packets according to Snell's law and the Fresnel equations. In addition, the short-range topographic structure, called the microroughness, scatters the light diffusely. The scattering by the microroughness is introduced by letting a fraction of the reflected and refracted light be distributed in a Lambertian manner [Coppel et al., 2009]. Within a layer, the scattering process is controlled by the scattering (s) and absorption (k) coefficients. The process is schematically given in Figure 1.

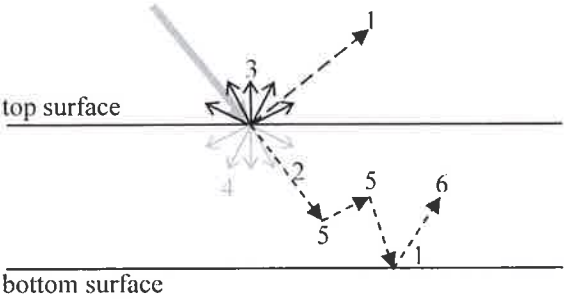

Figure 1: Schematic representation of the light processes for one layer. Incident light can be specularly reflected (1) or refracted (2) at the top surface. If the surface is rough, parts of the light will be diffusely reflected (3) or refracted (4). The process is governed by the refractive index ratio of the media at the surface boundary, the wavelength and the microroughness of the surface. The same process occurs at every surface boundary. Within a layer, light is scattered isotropically (5) or absorbed (6) depending on the scattering and absorption coefficient of the layer. In the Monte Carlo implementation, light is represented by indivisible wave packets, whose direction is changed statistically according to the physical probability distributions in each step. By recording the average final direction of a large number of wave packets, the mean reflectance or transmittance in a given detector geometry can be computed

3. Results

3.1 Thickness measurement

No significant change in thickness could be detected for any of the samples after twenty nips (Figure 2), and the results from measurements of the uncoated plastic film showed no signs of compression after calendering.

3.2 Optical measurements

As expected, the gloss increased with increased number of nips (Figure 3). The same trend can be seen for all the coat weights, although they are slightly parted. This is due to the uncalendered gloss value that varied approximately one unit between the samples. The gloss was always higher when calendering in several nips at

low line load, compared to when exposing the coated substrate to the same total line load with one single nip at high line load (Figure 4). The same trend was also observed in the 2 x 50 trial compared with the 1 x 100 kN/m.

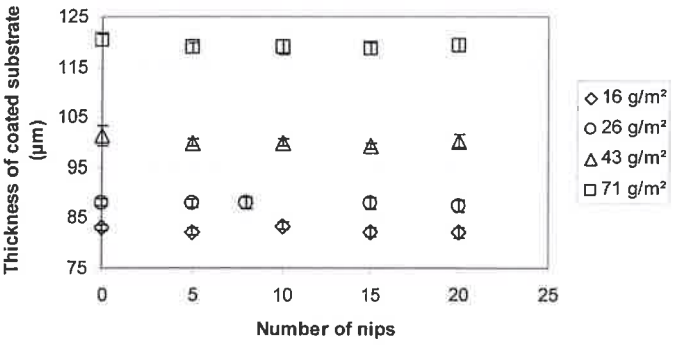

Figure 2:
Result of thickness measurements. Error bars show the standard deviations for five measurements. No significant change could be detected for any of the coat weights even after twenty nips

Figure 3:
Result of gloss measurements. As expected the gloss increased with increased number of nips. All the samples follow the same trend but the gloss values differ slightly between the coat weights

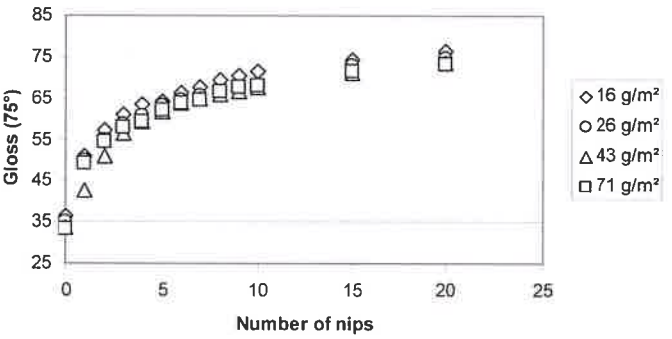

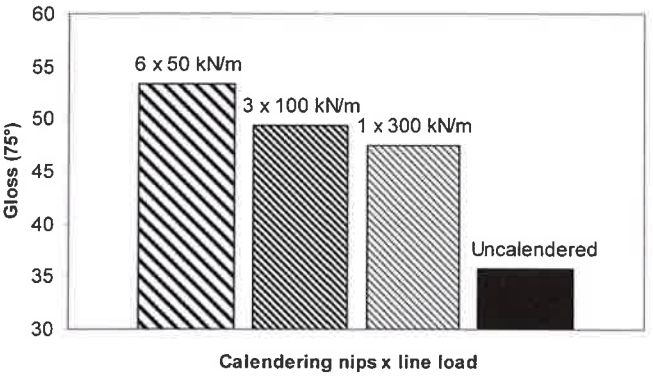

Figure 4:
Gloss results from different combinations of nips and line loads. A coating layer of 26 g/m² were used for this example. A higher gloss were reached when several nips were used compared to a single nip at the same total line load

The reflectance factors, R_0 and R_w, decreased with increased number of nips and increased with increased coat weight (Figure 5).

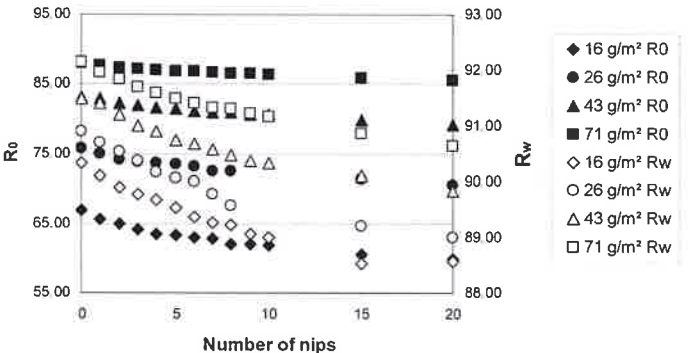

Figure 5:
Reflectance factor of coated films over black background (R_0) and over a white background (R_w). Reflectance values decreased with increased number of nips

The microroughness and refractive index obtained from reflectometry measurements are shown in Figure 6. Calendering causes the surface to become smoother on the micro scale and the measured microroughness decreased with increasing number of nips. The surface macroroughness was so low that it could not be measured, presumably due to the very smooth surface of the substrate. Hence the surface of the coating layer was modeled as a flat surface with a microroughness. The effective refractive index increased with the number of calendering nips (Figure 6).

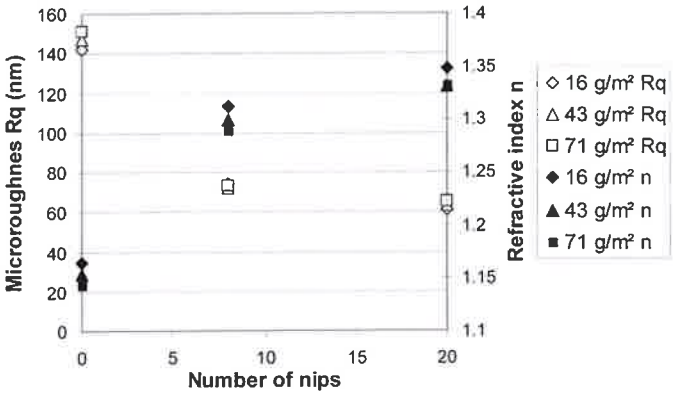

Figure 6:
Measured microroughness (Rq) and refractive index (n) for the samples with different coat weight plotted versus the number of calendering nips

3.3 Kubelka-Munk analysis

The Kubelka-Munk scattering, S, and absorption, K, coefficients were calculated from the reflectance factor of one coated film on a black background ($R = 0$), R_0, and the reflectance factor of the same coated film on the white background, R_w over R_{back}, according to Equations 1-4 (Pauler, 1999).

$$a = \frac{1}{2}\frac{R_{back}\left(1 + R_w R_0\right) - \left(R_w - R_0\right)}{R_0 R_{back}}, \tag{1}$$

$$R_\infty = a - \sqrt{a^2 - 1}, \tag{2}$$

$$S = \frac{1}{w\left(\frac{1}{R_\infty} - R_\infty\right)} \ln \frac{\left(1 - R_0 R_\infty\right) R_\infty}{R_\infty - R_0}, \tag{3}$$

$$K = \frac{S \cdot \left(1 - R_\infty\right)^2}{2 \cdot R_\infty}, \tag{4}$$

where w is the coat weight. With increasing number of nips, the light scattering decreases whereas the light absorption increases. The latter effect was most pronounced with the lowest coat weights (Figure 7).

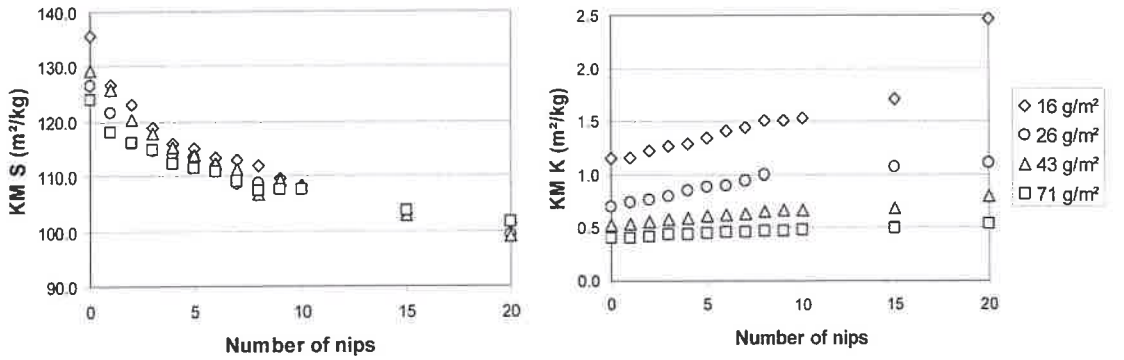

Figure 7: Kubelka-Munk scattering (left) and absorption (right) coefficients derived from the reflectance factor of one

3.4 Influence of the microroughness and refractive index at the top surface

The samples with coat weights 16, 43 and 71 g/m², after 0, 8 and 20 calendering nips, were selected for reflectometry measurements and further analysis with the *Open PaperOpt* Monte Carlo simulation tool. The coated films were modelled as two continuous layers with a scattering (s) and absorption (k) coefficients, a refractive index (n), and a grammage (w), as shown in Figure 8. The film was assumed to be perfectly flat with no scattering or absorption. The grammage of the film had thus no impact on the simulations and was set to 100 g/m². The refractive index of the film was 1.6. A Lambertian illumination was used with no light incident at incident angles lower than 15.5°. The light reflected at angles between 0 and 4° from the normal was detected. The illumination and detector geometry simulated the geometry of the brightness tester. The coating layers were assumed to have no macroroughness (and hence constant thickness), but a microroughness (Rq_{coat}) as obtained from the reflectometry measurements. The white background, made of a pile of the coated film with 71 g/m² coat weight, was modelled as an opaque layer of the same top surface refractive index as the 71 g/m² sample.

As opposed to the Kubelka-Munk model for which the model parameters can be determined from a pair of reflectance measurements, Monte Carlo simulations can only compute the reflectance from a set of scattering parameters. Therefore, the parameter estimation requires an optimisation algorithm, optimising the input parameters to fit simulated reflectance values to measured ones. The background scattering and absorption coefficients were optimised to fit the background reflectance factor (91.8%). The scattering and absorption coefficients of the uncalendered coating layer were then optimised to fit the measured reflectance factor of the coated film on the black and white backgrounds, for each coat weight.

The reflectance factor of the coated films over a black background was then simulated with different coating surface microroughness and refractive indices, corresponding to the measured ones after 8 and 20 calendering nips. The scattering and absorption coefficients were kept constant. The simulated reflectance factors are compared to the measured reflectance factors in Figure 9. The simulated reflectance factors of the uncalendered coated films were optimised and differ from the measured reflectance factors only due to the noise inherent to the Monte Carlo simulations. A decrease of the microroughness and an increase of the refractive index lead to lower simulated reflectance factors.

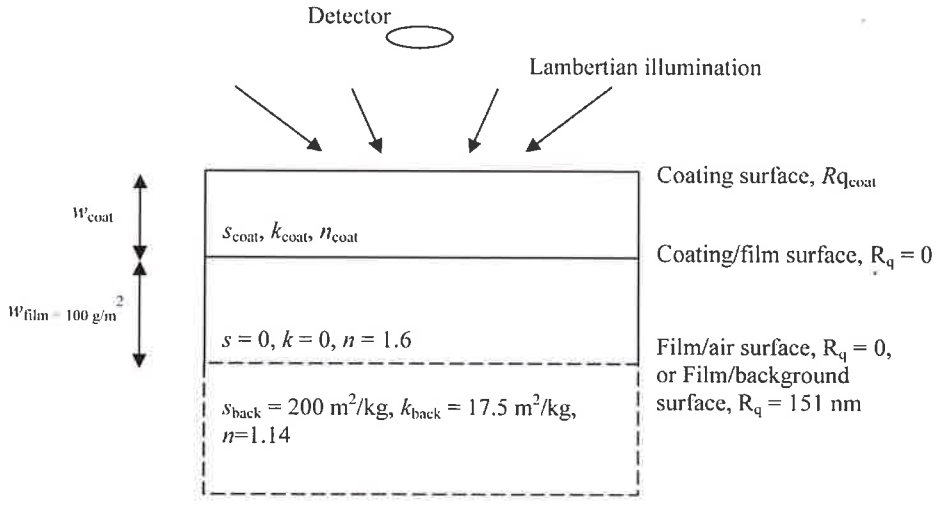

Figure 8: Model for the Monte Carlo light scattering simulations. The coated film is illuminated with a Lambertian illumination, with no light at incident angles lower than 15.5°. The coating on top of the transparent film has a constant thickness but its microroughness controls the amount of surface reflection that is diffusely reflected, and hence recorded by the detector

The simulated reflectance factors of the 43 g/m² samples agreed well with the measured reflectance factors after 8 and 20 calendering nips. Since the scattering and absorption coefficients were kept constant, it means that a reduction of the microroughness combined with an increase of the refractive index at the top coating surface can account for the reflectance decrease, which is interpreted as decrease of the effective Kubelka-Munk scattering coefficient. However, the model underestimates the reflectance factor decrease at a coat weight of 16 g/m², and

The effects are separated in Figure 9 for the 16 g/m² samples. The microroughness reduction (and hence gloss increase) due to calendering leads to more specular surface reflection. Because of the gloss trap of the instrument, the measured reflectance is then lower. The refractive index had a stronger impact on the reflectance factor than the microroughness. A larger refractive index leads to more internal reflection at the coating top surface, which leads to a decrease of the reflectance factor.

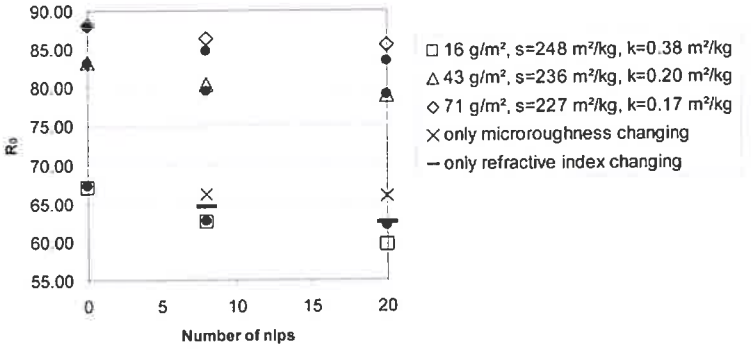

Figure 9: Measured (open symbols) and simulated (dots) reflectance factor of the coated films over a black background. The scattering and absorption coefficients of the coating were kept constant with calendering but the microroughness and refractive index were modified according to the measured ones For the 16 g/m² samples, the effect of refractive index increase and microroughness decrease are separated

4. Discussion

The initial gloss values differed between the samples (Figure 3). This can be explained by the fact that a thin coating layer follows the very smooth plastic surface to a greater extent than a thick one, and thereby gains a higher gloss value. On the other hand, the scattering and absorption coefficients were varying with coat weight. The Kubelka-Munk (KM) coefficients (S and K in Figure 7) should not be compared to the physical coefficients (s and k in Figure 9) in the Monte Carlo (MC) model, especially with the introduction of refractive index changes in the structure. Nevertheless, the decrease of the scattering coefficient with increasing coat weigh was lower (8%) with the MC model than with the KM model (30%). A change of the scattering coefficient with coat weight could be attributed to a structural change, but the observed rather large decrease of the absorption coefficient with coat weight increase cannot be explained by a potential change of the pore structure. Because of the large coat weights, the reflectance factors with white background were close to those on black background. This made the optimization of the scattering and absorption parameters very sensitive to small changes of the measured reflectance factors. Therefore, the results presented here should be completed by measurements in different geometries, including the transmittance of the coated films.

The effective refractive index at the upper coating layer surface had a strong impact on the reflectance factor. Its increase with calendering can be explained by a tighter and less porous structure at the surface. The simulations indicate that a large part of the reflectance decrease due to calendering can be attributed to an increase of the effective refractive index at the coating surface, resulting into larger internal reflections and a decrease of the microroughness, resulting into a reduction of the light diffusely reflected at the coating back to the detector of the brightness tester. This suggests that the internal scattering and absorption properties are not significantly affected by calendering. This is supported by the fact that the thickness of the calendered coating layers did not change. Further work should involve porosity measurements to potentially validate these findings.

5. Conclusions

Calendering lead to a decrease of the Kubelka-Munk scattering coefficient and an increase of the absorption coefficient of coated transparent films. This could be attributed to a change of the coating structure and porosity, which was not supported by the fact that the thickness remained constant after calendering. Taking into account non-uniform surface reflection at the boundaries between media of different refractive indices, the decrease of the reflectance factors could instead be attributed to a change of the refractive index and microroughness at the

Acknowledgements

The Swedish Governmental Agency for Innovation Systems (VINNOVA), and the industry participants in the PaperOpt project are gratefully acknowledged for their financial support. Janet Preston and her colleagues at Imerys are thanked for the measurements of microroughness and refractive index.

References

1. Coppel, L. G., Edström, P., Lindquister, M., (2009), *Open source Monte Carlo simulation platform for particle level simulation of light scattering from generated structures*, In Proc. Papermaking Research Symposium, Kuopio, Finland
2. Edström, P., (2005a), *Fast and stable solution method for angle-resolved light scattering simulation III - Handling refractive index discontinuities*, FSCN Report R-05-62, Mid-Sweden University
3. Edström, P., (2005b), *A fast and stable solution method for the radiative transfer problem*, SIAM Review, 47:447-468
4. El-Sherbiny, S., Xiao, H., (2005), *Characteristics of clay and GCC pigment coatings containing synthetic polymeric thickeners, Appita, 2005 Mar.;*58(2):116-121
5. Elton, N. J., Day, J. C. C., (2009), *A reflectometer for the combined measurement of refractive index, microroughness, macroroughness and gloss of low-extinction surfaces*, Meas. Sci. Technol., 20:1-11
6. Elton, N. J., Preston, J. S., (2006*), Polarized light reflectometry for studies of paper coating structure. Part 1. Method and instrumentation*, Tappi Journal, 5(7):8-16
7. Eriksen, O., Johannesen, E., Gregersen, O. W., (2007), *The influence of paper surface roughness on ink pigment distribution, Appita, 2007 Sept.;* 60(5):384-389
8. Kubelka, P., Munk, F., (1931), *Ein beitrag zur optic der farbanstriche*, Z. Tech. Phys., 11, p. 593-601
9. Larsson, M., Engström, G., Vidal, D., Zou, X., (2007), *Impact of calendering on coating structures, Nord. Pulp Pap.Res.J., 2007;* 22(2):267-274
10. Makarenko, A. V., Shaykevich, I. A., (2000), *Dependence of the whiteness of paper on surface roughness and illumination conditions*. Color Research & Application, 25(3), p. 170-175
11. Pauler, N., (1998), *PaperOptics*, Lorentzen & Wettre, Kista, Sweden
12. Rousu, S., Gane, P., Eklund, D., (2005), *Print quality and the distribution of offset ink constituents in paper coatings, Tappi J., 2005 July;* 4(7):9-15
13. Saunderson, J. L, (1942), *Calculation of the color of pigmented plastics*, JOSA, 32(12), p. 727-729

Estimation of rubber ink transfer effectivity in flexography on the basis of laboratory studies

Marie Kaplanova, Jiri Hejduk, Ondrej Panak

University of Pardubice, Department of Graphic Arts and Photophysics, Pardubice, Czech Republic
E-mails: marie.kaplanova@upce.cz, jiri.hejduk@upce.cz, ondropanak@gmail.com

Abstract

The goal of this work was to understand how the surface properties of rubber sleeves (particularly the surface tension) affect ink spreading, ink splitting and ink transfer in flexography printing processes. A set of EPDM (ethylene-propylene-diene terpolymer) rubber sleeves, differing in composition and surface treatment, was used for the study. Its focus was to demonstrate the influence of the surface properties of rubber solids and ink composition (solvent- and water-based flexograhpy inks) on the ink transfer efficiency on different printing materials (polyethylene and paper). The results of laboratory nonimpact ink transfer experiments were compared with laboratory printing results.

Keywords: flexography, rubber sleeves, ink transfer, surface tension, EPDM

1. Introduction

During the several recent decades, flexography was becoming increasingly more prevalent, especially in the packaging industry, for printing on the most varied materials. Flexography uses low viscosity inks and resilient or soft, flexible printing plates and the pressure applied between the plate cylinder and the substrate is low ("kiss printing"). The print quality that can be achieved in flexography is lower compared to offset printing, but the use of new types of printing plates with adapted inks and the technical printing press developments have tremendously improved the printing quality offered by flexography. The use of sleeves as a printing master is making a strong contribution to good printing results. The digitally produced seamless sleeves that are now in common use are comparable to gravure cylinders. They produce prints of an entire circumference. The best quality of rubber and elastomer plates is achieved when the print image relief is applied by laser engraving to plate cylinders that have been fully coated with elastomer and then precision-ground.

The rubber sleeves are produced of composite materials, mainly on the basis of natural rubber, styrene-butadiene rubber, ethylene-propylene, silicone, acrylonitrile-butadiene-styrene or butadiene rubbers. The materials usable for the majority of flexography sleeve applications are products on the basis EPDM (ethylene-propylene-diene terpolymer). The copolymer EPDM has an outstanding resistance to ageing, weathering, to ozone, oxygen and many chemicals. EPDM is polymerized from 60 parts of ethylene, 40 parts of propylene, and a small amount of non-conjugated diene. The non-conjugated diene permits sulfur vulcanization of the polymer instead of using peroxide. EPDM is a non-polar material. The structure of the polymer can be altered to give a fairly wide range of properties and uses. EPDM sleeves may be used for direct laser engraving of printing forms and for all types of flexography inks (mainly solvent-based and UV printing inks).

Flexography inks are very similar to gravure inks in their viscosity; they are in the viscosity range of 0.05 - 0.5 Pas. As in gravure printing, the type of solvent also plays a critical role in flexography printing. After the transfer to the substrate, through the application of heat, the solvent is evaporated and a dry film remains. The following solvents are predominantly used in flexography printing: ethyl acetate, alcohol and water. The correct choice of sleeve material, optimized to meet exactly the customer's needs, is the main requirement to achieve top-quality printing.

The transfer of ink from the rubber printing form onto the printing material is conditioned by the adhesion and cohesion powers, and is very closely connected with the surface free energy of both solid surfaces and the transferred liquid ink. The surface free energy, or the surface tension of materials, is determined not only by the composition of the respective material, but also by its surface smoothness or roughness.

This study aims to understand how the surface properties of EPDM rubber sleeves affect the ink transfer in the flexography printing process by means of model studies in laboratory conditions. The paper presented is a part of a wider project which includes not only EPDM, but also other materials used as a printing master in flexography [Kaplanová and Hejduk, 2006].

2. Methods

Many structural characteristics can be varied in the EPDM copolymer to accommodate the varying requirements of the flexography printing industry [Pluhar, 2004]. The solid samples used for this surface tension and ink transfer study were prepared from 25 samples of EPDM sleeves produced from different blends and additives (Ligum Ltd., Jablonec n/N, Czech Republic). The samples differ in hardness, compressibility and elasticity, but exhibit very similar surface roughness characteristics. The surface roughness was measured by the portable surface roughness tester Surftest SJ-301 and the average roughness of all tested samples was very similar (R_a = 0.49 ± 0.13 μm and R_z = 2.00 ± 0.60 μm).

Red printing flexography inks, both solvent-based (RSI) and water-based (RWI)), polyethylene and supercalendered printing paper (basis weight 73 g/m^2) were used for the ink transfer tests. The rheological properties of inks were estimated by means of flow curves measurement (rheometer Haake RotoVisco 1) using Casson model and Casson yield point τ_C and viscosity η_C were 0.780 Pa and 17.18 mPa.s for RSI and 0.378 Pa and 78.18 mPa.s for RWI.

The research study could be divided into three steps:

1. Determination of the surface properties of the materials

At the liquid to solid interfaces there are interfacial tensions. Due to the existing interactions their values are generally lower than those of surface tensions of the individual products taken separately. This characteristic is expressed in terms of the contact angle, or wetting angle. The measurement of the contact angle of liquids is important in characterizing the surface of solids. The contact angle θ is a quantitative measure of the wetting of a solid by a liquid. It is defined geometrically as the angle formed by a liquid drop at the three-phase boundary where a liquid, a gas and a solid intersect. The contact angle is dependent upon the equilibrium between the surface tension and the interfacial tension of the material in question.

The surface energy (surface tension) of a solid or a liquid is made up additively of the components that correspond to the intermolecular interactions. Common simplification is to consider only two components: the component resultant from the London dispersions forces (γ^d) and the so-called polar component (γ^p) that incorporates all the other interactions. One of the common approaches to the evaluation of surface tension of solids involves testing the solid against a series of well characterized wetting liquids. The used liquids must be characterized, so as the polar and the dispersive components of their surface tensions should be known. The polar and the dispersive components of the solid surface tension are then evaluated using the Owens-Wendt equation [Owens and Wendt, 1969]

$$(1+\cos\theta)\gamma_l = 2\left(\sqrt{\gamma_s^d \gamma_l^d} + \sqrt{\gamma_s^p \gamma_l^p}\right) \quad (1)$$

where θ is the equilibrium contact angle, γ_l is the liquid surface tension and γ_s is the solid surface tension. The addition of *d* and *p* in the superscripts refer to the dispersive and the polar components of each. The form of the equation is of the type $y = mx + b$. You can graph $(\gamma_l^p)^{1/2}/(\gamma_l^d)^{1/2}$ vs $\gamma_l(1+\cos\theta)/(\gamma_l^d)^{1/2}$. The slope will be $(\gamma_s^p)^{1/2}$ and the y-intercept will be $(\gamma_s^d)^{1/2}$. The total surface tension is the sum of its two component forces. On the same assumption of the liquid/solid interactions it is possible to calculate the adhesion energy, using the polar and the dispersive parts of the free surface energy σ

$$W_a = 2\left(\sqrt{\sigma_s^d \sigma_l^d} + \sqrt{\sigma_s^p \sigma_l^p}\right) \quad (2)$$

where σ_i^j are the surface free energies of the solid and the liquid numerically equal to the surface tensions of these materials. The cohesion energy of the liquid can be calculated as $W_c = 2\,\sigma_l$.

For the measurement of the contact angles, a PC-controlled KSV CAM 100 USB video camera at resolution of 640 x 480 pixels was used. The image of "sessile" liquid drops was captured immediately after a droplet of a liquid (volume ~ 0.01 ml) was placed on the sample surface and followed further every second during an interval of 20 seconds. Three independent measurements were made for every sample and standard liquid and the equilibrium contact angle was evaluated by the method described in detail in our last paper [Kaplanova, M., Otahalova, L., Muck, T., 2008].

The contact angle measurements of solids were made at room temperature 22 °C ± 2 °C , using standard liquids: formamide (γ_l = 58.2 mN/m, γ_l^d = 39.5 mN/m), diiodomethane (γ_l = 50.8 mN/m, γ_l^d = 50.8 mN/m), ethylene glycol (γ_l = 48.3 mN/m , γ_l^d = 29.3 mN/m), and water (γ_l = 72.8 mN/m, γ_l^d = 21.8 mN/m). The surface tension of inks was measured on the K6 Krüss tensiometer (Du Noüy Ring tensiometer) and the polar and the disperse parts were evaluated by means of contact angle measurement of ink drops on a polytetrafluorethylene calibration solid plate with surface tension of 18.74 mN/m (no polar part of surface tension).

2. Nonimpact ink transfer tests

The tests were carried out with the use of laboratory equipment specially constructed for the study of ink setting, ink splitting and ink transfer from a rubber surface onto a paper (or polymer foil) in the process of drawing both the surfaces very slowly apart (approximately at 1 mm/min.) as is illustrated in Fig.1. The major elements of this testing device were a micrometer (digital reading) and an optical projection system. The amount of ink on the rubber and on the printing material was established by weighing and the ink transfer efficiency (ITE) was established as a percentage of the ink amount on the printing material and the total weight of the ink droplet. The initial ink droplet volume on the rubber surface was approximately 0.15 ml.

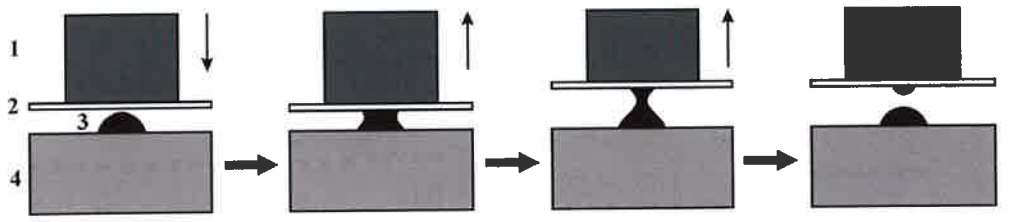

Figure 1: Laboratory apparatus for nonimpact ink transfer tests and illustration of the ink transfer process (1-micrometer, 2-paper, 3-ink, 4-rubber)

3. Laboratory printing tests

To evaluate the effect of EPDM materials on ink transfer at printing conditions, printing runs on the laboratory flexography press with an anilox roller 100 lines/cm and EPDM as a transfer roller were carried out. The ink transfer efficiency was evaluated by means of optical density (OD) measurement using the spectrophotometer Gretag SPM 50 and the wavelength of absorption maximum of ink.

3. Results and discussion

3.1 Surface tension measurements of materials

Rubber materials are composite materials with a nonhomogeneous surface microstructure, as illustrates the SEM image of a rubber sample surface in Fig. 2. The spreading of low viscosity liquids on these surfaces was relatively rapid and the equilibrium contact angle was reached in 1 or 2 seconds, as is illustrated by the time course for water and diiodomethane, respectively, for one of the EPDM samples (Fig. 3a). The ink spreading on a rubber surface was much more complicated and the rate of spreading much slower. The equilibrium contact angle evaluation was carried out with the use of the mathematical model described in [Kaplanova, M., Otahalova, L., Muck, T., 2008].

The results of the surface tension evaluation using the Owens-Wendt equation (1) for all tested EPDM samples and the adhesion energy of inks on rubber materials are summarized in Table I. The surface tension of inks and printed materials are presented in Table II. The cohesion energy of ink was estimated on the basis of the surface energy - for RSI 54 mJ/m^2 and for RWI 77 mJ/m^2; the adhesion energy of RSI and paper was 62.6 mJ/m^2, RSI and PE 62.3 mJ/m^2, the adhesion energy of RWI and paper was 74.8 mJ/m^2 and of RWI and PE 74.4 mJ/m^2.

The estimation of the contact angles of small ink drops (~ 0.02 ml) on EPDM solid samples was performed by the method described in [Kaplanova, M., Otahalova, L., Muck, T., 2008]. Figure 4 shows the dependence of ink contact angle on the surface tension of EPDM solids for a solvent based ink (RSI) and for a water-based ink (RWI).

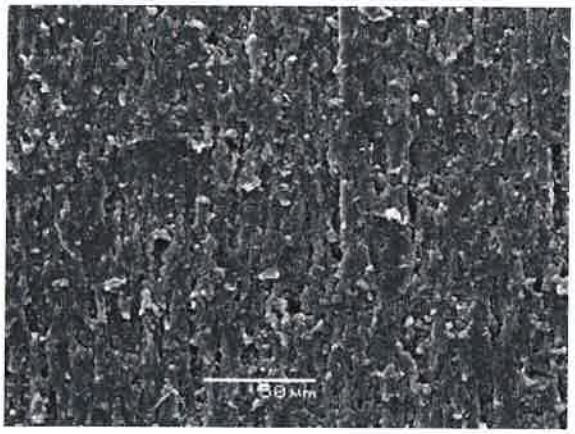

Figure 2:
SEM image of EPDM 2-8 sample surface

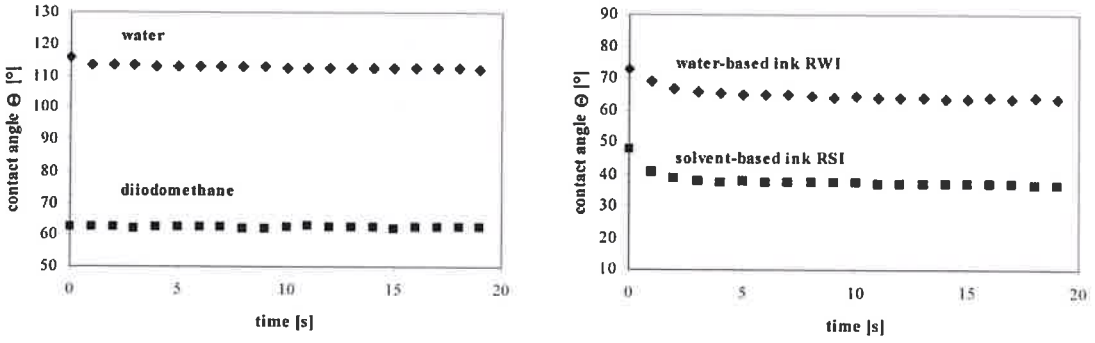

a) b)

Figure 3: Time dependence of the contact angle of drops of water and diiodomethane (a) and inks (b) on EPDM 2-8 surface

Table I: Surface tension, the dispersive and the polar components of the surface tension of EPDM sleeves and the adhesion energy of inks and EPDM

Sample		Surface tension [mN/m]			Adhesion energy of inks [mJ/m²]	
No.	colour	γ_s	γ_s^p	γ_s^d	RSI	RWI
2-1	dark green	25.30	1.48	23.82	51.03	59.33
2-2	orange	23.16	1.19	21.97	48.65	56.65
2-3	light green	19.99	2.59	17.40	46.26	53.10
2-4	green-black	19.80	0.03	19.77	42.16	50.11
2-5	dark green	27.33	2.74	24.59	53.79	62.04
2-6	black	21.32	4.05	20.27	51.20	58.47
2-7	light green	19.10	3.59	15.51	45.41	51.72
2-8	black	30.29	1.47	28.82	55.55	64.73
2-9	yellow	20.36	1.32	19.04	45.91	53.30
2-10	dark green	23.79	3.29	20.50	50.52	57.92
2-11	dark green	26.93	1.03	25.90	52.04	60.79
2-12	orange	19.33	0.58	18.75	43.80	51.30
2-14	grey	22.18	0.47	21.71	46.51	54.63
2-15	black	23.04	1.92	21.12	49.17	56.87
2-16	orange	18.89	0.21	18.68	42.32	49.93
2-17	dark turquois	23.48	6.65	16.83	50.11	56.42
2-18	black	31.80	2.19	29.61	57.47	66.66
2-19	black	27.61	0.31	27.30	51.18	60.37
2-20	dark grey	28.89	0.32	28.57	52.33	61.74
2-21	light green	13.38	1.08	12.30	37.44	43.33
2-26	green	34.11	9.85	24.26	60.36	67.91
2-27	brick	40.98	11.39	29.59	66.24	74.62
2-28	green	27.55	9.96	17.59	53.64	59.86
2-29	orange	23.81	4.65	19.16	50.71	57.69
2-30	blue-green	14.90	1.55	13.35	39.75	45.82

Table II: Surface tension and the dispersive and the polar components of the surface tension of inks and printed materials

Sample	Surface tension [mN/m]		
	γ_s	γ_s^p	γ_s^d
RSI	27.00	5.37	21.63
RWI	38.50	7.66	30.84
white polyethylene	39.54	0.96	38.58
printing paper	36.76	4.43	32.33

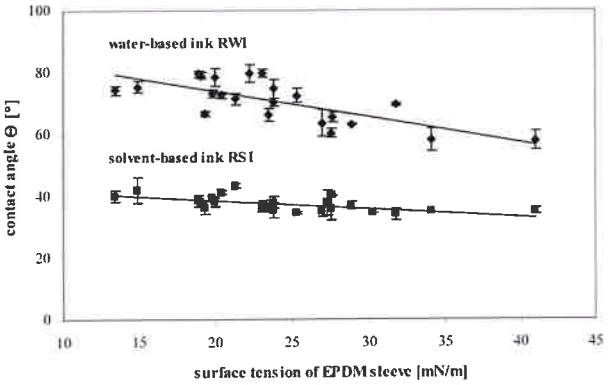

Figure 4:
Contact angle of an ink drop on an EPDM surface in dependence on the surface tension of solid samples

3.2 Nonimpact ink transfer tests

By means of static ink transfer tests, the ink transfer efficiency (ITE) was established as a percentage of the ink amount on paper (or on polymer foil) and the total weight of the ink droplet [Kaplanová and Hejduk, 2006]. No significant changes in the "ink length", defined as the distance from the start position (the point of touch of the paper or PE with the top of the ink drop) to the position of the rupture of the ink fibre formed between the rubber and the paper, were observed for all series of the EPDM samples. The measured values of "ink length" were 1.13 ± 0.11 mm for solvent-based red inks (RSI) and 1.07 ± 0.10 mm for water-based ones (RWI). The results of the ink transfer tests clearly demonstrated the dependence of the ink transfer efficiency on the surface tension of the tested EPDM samples, or on the adhesion energy between the inks and the EPDM surfaces, as is illustrated in Figure 5 for rubber/paper tests. The ink composition, cohesion and surface tension has prime importance in the transfer phenomena, as the ITE of the solvent-based ink extended from 19% to 26% whereas the ITE of the water-based ink ranged from 8% to 10%. The ITE value depends on the surface tension of the EPDM samples in either event.

3.3 Laboratory printing tests

To evaluate the effect of EPDM materials on optical density in printing conditions, printing runs on a laboratory flexo press with an anilox roller 100 lines/cm were carried out. Good correlation was observed between the ink amount on prints (the optical density) and the surface tension of EPDM sleeves and the effectivity of static ink

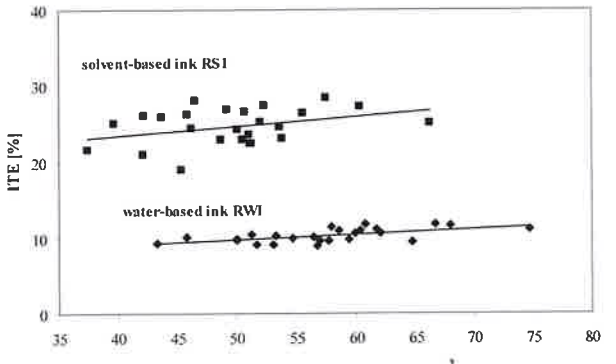

Figure 5:
The ink transfer efficiency (ITE) from rubber onto paper in dependence on the adhesion energy between inks and EPDM rubber surfaces

transfer (ITE). The typical optical densities and the ITE correlation is demonstrated in Fig. 6 for RSI prints on white polyethylene and similar properties were observed for printed papers.

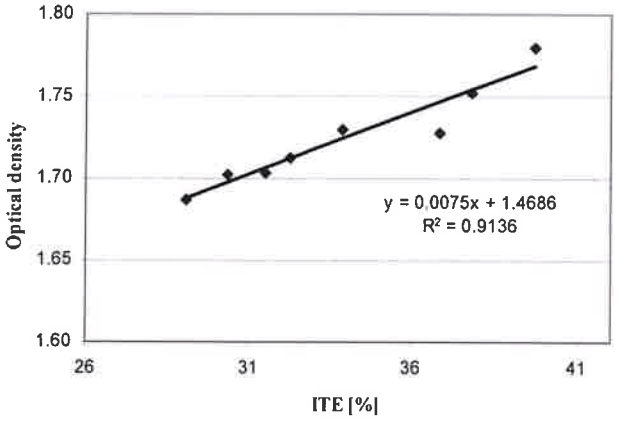

Figure 6:
Optical density of RSI solid prints on white polyethylene in relation to ITE tests for the same EPDM samples

4. Conclusions

The results obtained from this research study indicate the influence of the transfer properties of flexography inks from EPDM sleeves on the ink composition and surface tension of rubber solids. In recent literature, interesting studies dealing with the influence of surface energy on ink transfer in flexo printing were reported [Fouché and Blayo 2002, Lagerstedt and Kolseth 1995]. Their authors mostly agreed that the surface energy of the printing form would have little or no influence on the transfer of ink. Our study shows that in the case of EPDM sleeves, usually used for direct laser engraving, the surface tension of the printing form could be a significant factor. Knowledge of the surface properties and rheology could help to choose the best sleeve material for the actual printing conditions, thus allowing to predict the outcome of the flexography printing process.

The methodology presented in this study could be also used in the investigation of the ageing process of rubber sleeves and its influence on the final print. The measurement of the surface tension of ageing rubber is less resource-consuming than the evaluation of the final prints produced with the use of this rubber.

The ongoing research focuses on a wider range of rubber sleeves, such as natural rubber, styrene-butadiene rubber and silicone rubber sleeves. Moreover, the next research aims to investigate rubber sleeves with a surface physically modified by a corona discharge or a high-powered laser. For more comprehensive understanding of the transfer properties of flexo inks, other properties of rubber sleeves (roughness, elasticity) will have to be considered in further research.

Acknowledgements

This work was supported by the Ministry of Education, Youth and Sports of the Czech Republic; research project No. MSM 0021627 501.

References

1. Fouché, L., Blayo, A., (2002), *Transfer Characterization of UV Flexo Inks, Ink Maker,* May 28
2. Kaplanova, M., Hejduk, J., (2006), *Influence of Rubber Surface Tension on Ink Transfer In Flexography, Conference Proceedings of Printing Technology SPb'06,* 26-30 June 2006, St. Petersburg, Russia, 59
3. Kaplanova, M., Otahalova, L., Muck, T., (2008), *Insight into IJ-ink/paper Interaction using Drop Spreading Model, Advances in Printing and Media Technology,* V35, 213
4. Lagerstedt, P., Kolseth, P., (1995), *Influence of Surface Energetics on Ink Transfer in Flexo Printing, Advances in Printing Science and Technology* V23, 269
5. Owens, D. K. and Wendt, R. C. (1969), *Estimation of surface free energy of polymers, J. Appl. Polym.* Sci, V13, 1741
6. Pluhar, J., (2004), *Die Suche dem Universellen Material, Flexo+Tief Druck,* Nr 5, 102

Research of interaction on the border polymer film - ink

Evgeny Bablyuk and Konstantin Farenbrukh

Moscow State University of Printing Art
2a Pryanisnikova St., RU-127550 Moscow, Russia
E-mails: kachestvo@mgup.ru; babliukevgen@mtu-net.ru

Abstract

The article demonstrates the experimental results on feasibility study of the normal fracture method for a quantitative evaluation of adhesive strength on the interface "polymer film-ink". Evaluation of the adhesive strength level has been made for water-based and solvent-based inks spread on PP, PE and PET films surface.

Keywords: adhesive strength, polymer films, printing inks

1. Introduction

The supposition for performance of the present work was the fact, that large volume of graphic product are packaging materials during production of which film printing is performed. In this regard, high claims are made on different steps of packaging production concerning adhesive strength of inks and other coated layers on polymer film surface.

In connection with this, the work is extremely of current interest because its results can find practical application when creating quantitative methods of adhesive strength evaluation. Presence of quantitative methods of adhesive strength evaluation allows more effectually to develop compositions of various primers as well as to work out activation modes of polymer film surface by different methods.

The normal fracture method [Bablyuk, E. B., 2007] successfully used in different fields of science and engineering, was chosen as a basis of procedure for evaluation of adhesive strength on the border polymer film - ink.

2. Methods

Subjects of research were films from PP, PE, PET with thickness 25 - 100 μm. There were used inks both water-dispersed and inks containing organic vehicles (ethanol, ethyl acetate), in particular, water-dispersed ink FlintGroup AquaFlex 007 and ink containing organic vehicles FlintGroup Flexoplastol APF.

Adhesion can be measured with help of direct (effort at violation of adhesive contact), nondestructive (through change of parameters of ultrasonic and electromagnetic waves owing to absorption, reflection or refraction) and indirect (characterizing adhesion in comparable conditions, only concerning for example with films lift-off after cut, with inclination of surface for powders and other) methods.

The procedure essence of adhesion evaluation by normal fracture method is in definition of quantitative index of ink adhesion to polymer materials on imposed load at right angle to contact surface on the border ink – polymer film (that is, on normal). Earlier [Farenbrukh, K., 2008] we tested this method in researches of microgeometry surface influence on ink adhesion to polymer films surface.

During developing design of measuring cell it was foreseen:

- high level of adhesive strength of fitted glue to "mushroom" metal;
- verticality of strength distribution on all parts of measuring cell together with fastened specimen in it for testing;
- reduction to the minimum of specimen deformation (polymer film with coated ink layer on it) during testing;
- picking up evaluation methods of real area of contact destroyed in the process of testing on the border ink

When choosing glue, the following requirements were formulated:

- diffusion rate of glue composition should be lower than process rate of its consolidation;
- glue cohesive strength should be higher than measured adhesive strengths;
- used glue should not changed physical and mechanical properties of inks;
- glue should be easily removed from "mushroom" surface after testing.

First requirement practically means that glue should "seize" in a moment, not penetrating deep into ink layer. That is why search of glue was carried out from the line of cyanoacrylate compositions. The best indexes of glues, as it can be seen from the results represented in Table I, demonstrated cyanoacrylate glue №3. Glues are differed with concentration of cyanogen-containing groups. As it can be seen from represented results, glue №1 changes ink properties in the process of agglutination. It penetrates into ink layer and as a result cohesion ink strength is decreased greatly.

The distinctiveness of chosen glue is high setting rate and as well as lack of influence on ink layer properties. These qualities allow to use it during researches and to a high accuracy to evaluate adhesive strength.

Table I: Evaluation results of adhesive strength values on model combination at choice of glue type (ink FlintGroup Flexoplastol APF and polymer film PET were used)

№	Glue type	Duration of agglutination, sec.	Type of destruction	Adhesive strength, N/cm²
1.	cyanoacrylate №1	5	Mixed on border metal-glue	2,8
2.	cyanoacrylate №1	8	Mixed on border metal-glue	3,1
3.	cyanoacrylate №1	30	Cohesive on ink	5,7
4.	cyanoacrylate №2	5	Mixed on border metal-glue	3,2
5.	cyanoacrylate №2	8	Mixed on border metal-glue	3,5
6.	cyanoacrylate №2	30	Mixed on border glue-ink	6,7
7.	cyanoacrylate №3	5	Adhesive on border ink-film	7,6
8.	cyanoacrylate №3	8	Adhesive on border ink-film	7,6
9.	cyanoacrylate №3	30	Adhesive on border ink-film	7,6

In Figure 1 construction of measuring cell is represented. Its parts were gi ven prove as a result of fulfilled researches. For providing hold-down of specimen to lower metal plate, it is foreseen in the construction of a cell a pressure plate with opening for "mushroom" (pos. 8, Figure 1).

Application of flexible joint (pos. 9, Figure 1) between "mushroom" and upper immovable clamp of fracture machine allows to make fastening of upper end of joint in a clamp, not allowing untimely rupture of adhesive bond and also to the maximum provides verticality of load distribution when evaluating adhesive strength.

Elastic deckle (pos. 5, Figure 1) is used for providing with uniform hold-down of film specimen to metal plate. Diameter of "mushroom" was chosen in 11,29 mm because in this regard sectional area will be 1 cm^2, that it is convenient to carry out calculations of adhesive strength.

Special emphasis during researches was given to picking up material for producing "mushroom".
As a result two types of "mushrooms" were produced:

1. Metallic (steel) - for determination of higher indexes of adhesion. The advantage is high glue adhesion to metal "mushroom", metal durability and steadiness during grinding. Minus - large weight of "mushroom" that sometimes tearing off took place during cell assembling in case of low adhesive strength of ink to

2. Polymer - is produced from firm and lightweight plastic (polycarbonate). Advantage - small weight. Minus - higher deterioration during grinding for reuse.

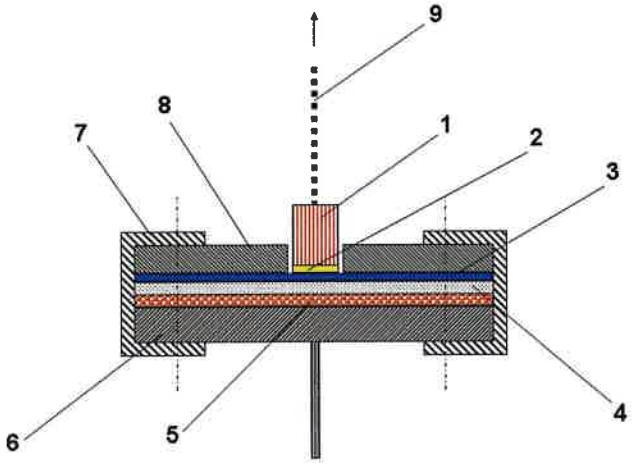

Figure 1: Construction of a cell for quantitative evaluation of adhesive strength by normal fracture method, where: 1 - metal 'mushroom', 2 - glue layer, 3 - printing ink, 4 - polymer film, 5 - deckle, 6 - lower metal plate, 7 - clamp, 8 - pressure plate, 9 - flexible joint

For carrying out experiments on evaluation of adhesive strength, large meaning besides construction of measuring cell and fracture machine has assembling process of measuring cell and its fastening in the clamps of testing machine. Preparation and fastening of specimen into measuring cell is realized in the following way: From each sheet of selected sample it is cut out film specimens of the size 15 x 50 mm.

"Mushroom" surface is cleaned with help of grinder. The surface should be to the maximum flat and then it is deprived of fat with ethyl alcohol.

The optimal quantity of cyanoacrylate adhesive is uniformly applied on the "mushroom" (pos.1, Figure 2). Given "mushroom" is fastened in clamps of a compression unit. A specimen with testing side upwards is placed on a sample stage. Then pressing up to full contact with specimen is carried out. This pressure is being held till the absolute dry out of adhesive (approximately 5 - 7 s). Remains of run out glue are removed. For uniform gluing of "mushroom" in a compression unit, tympan material is used as a substrate (pos. 4, Figure 2).

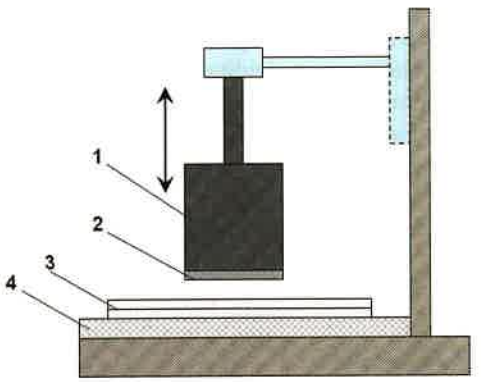

Figure 2: A compression unit: 1 - metal "mushroom"; 2 - glue; 3 - polymer film with coated ink layer; 4 - tympan material

The "mushroom" together with glued specimen are taken away from compression unit and are laid on the lower plate of the cell for definition of adhesion (pos. 6, Figure 1). A pressure plate is laid over. Then it is necessary to carry out centering of "mushroom" relative to the upper pressure plate (pos. 8, Figure 1). After that, lower and pressure plates are fixed hard by clamps. Assembled in such a way, add-on device is fastened in fracture testing machine by fixing of upper end of flexible joint (pos. 9, Figure 1) in upper clamp of fracture testing machine. It is necessary to pay special attention to the strict observance of verticality of testing in the

Then "mushroom" tearing off from tested specimen is fulfilled in fracture testing machine. The traverse speed of a movable clamp was 100 mm/min. Testing results of specimens which were not fastened upright, slipped out from a clamp or broken, are not taken into consideration.

2.1 Express - method

Suggested above methods adhesive strength evaluation can be used at developing technological printing processes on polymer films, and also at picking up receipt of inks, adhesive compositions with preliminary activation of printed surface. First of all, it is connected with the fact that for using normal fracture method, time is needed for preparation of specimens and measuring cell to tests. That is, these methods can be recommended for adhesive strength evaluation when carrying out tests and researches at laboratories.

Nowadays most of printing enterprises face the challenge of quick and quantitative definition of adhesion, but in this regard, not having funds on laboratory equipment and also on maintenance quality control department. For determination of adhesion by normal fracture method described in this work, it is necessary to have fracture machine PM-50 or its construction analogues. However for evaluation of adhesion at works such approach is inapplicable. For solving this problem, the following compact assembly is offered (Figure 3).

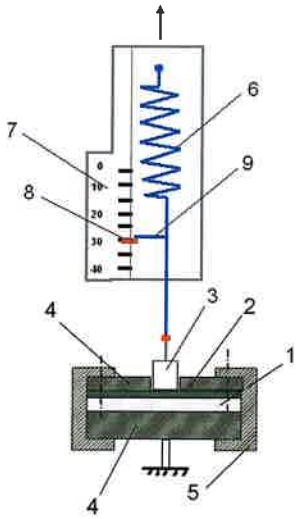

Figure 3:
Express- assembly for definition of adhesion by normal fracture method: where
1 - substrate
2 - adhesive
3 - "mushroom"
4 - metal plates
5 - clamps
6 - hard spring
7 - measuring scale
8 - scrollable passive index
9 - scrollable active index

Express-assembly for definition of adhesion consists of measuring cell, the lower part of which is fastened motionlessly. "Mushroom" (pos.3, Figure 3) is connected by flexible joint with hard spring (pos.6, Figure 3) which is fastened on the body. There are divided scale (pos.7, Figure 3) depending upon rigidity of spring, and also active (pos.9, Figure 3) and passive (pos.8, Figure 3) indexes. During uniform vertical shifting of this measuring device, the spring starts to lengthen out shifting active index which in its turn shifts passive one. When definite effort comes, "mushroom" tearing off takes place, passive index fixes maximum value of applied effort.

Table II: Results of comparative tests of adhesive strength by normal fracture method

№	Polymer film	Printing ink	Adhesive strength, N/cm²	
			Using universal machine PM-50	Using express- assembly
1.	PET	Aquaflex 007	2,6	2,7
2.	PET	Flexoplastol APF	3,3	2,9
3.	PET, activated	Aquaflex 007	14,3	16
4.	PET, activated	Flexoplastol APF	15,1	16
5.	PP	Flexoplastol APF	6,6	7,3
6.	PP, activated	Flexoplastol APF	23,1	24
7.	PE	Aquaflex 007	1,5	1,7
8.	PE, activated	Aquaflex 007	18,0	17,6

Advantages of this method and assembly is in simplicity of construction, rate of definition, relatively high accuracy (± 0,9 N) of adhesion definition (results of comparative tests are represented in Table II).

Disadvantage of this method is lack of shift with constant rate and also certain difficulties in maintenance of verticality depending upon investigator experience.

3. Results

Experimental results processing has exceptional place in the procedure of carrying out tests with use of measuring cell. For this, it is important to determine area of contact on the border ink - polymer film after its destruction. In case of destruction having adhesive character, there are no difficulties in this regard - contact area will be equal to the "mushroom" sectional area that is 1 cm^2. In this case, received effort value at destruction of adhesive bond should be referred to contact area that is 1 cm^2.

However, in many cases destruction picture of adhesive bond has mixed character. It is clearly seen from photomicrographys of surfaces after destruction of adhesive bond. For such results it is necessary to determine correctly contact area after destruction of adhesive bond. This task can be decided by processing of perplexing image (photographs, micrographs) of destruction surface in corresponding programs (Pinnacle Studio v9 and in universal program "VideoTest"), in which it is possible to calculate areas of perplexing images. In this case it is necessary to refer received effort value of adhesive bond destruction to the area, the size of which is determined in indicated above programs.

Developed methods of adhesive strength evaluation allow to appreciate the level of adhesion and character of adhesive bond destruction, that is to determine the weakest point in the system metal - glue - printing ink - polymer film. However, in this regard we will not have information about reasons of one or another level of adhesive strength. That is why it is necessary to study adhesive interaction on the border polymer film - printing ink.

Using method of ATR FT-IR spectra -spectroscopy, IR-spectra of polymer films (PP, PE, PET) with coated ink layer were received, as well as after destruction of adhesive bond. It was detected that after destruction of adhesive bond between polymer film and ink, IR-spectra had greater concentration of functional groups belonging to polymer. To the most, it was expressed with PET (Figure 4 and 5), then PP (Figure 8 and 9) and least of all with PE (Figure 6 and 7).

Concentrations of functional groups were differed for the same polymer film with different types of inks. For example, it was observed some intensity increase of absorption bands as for ink FlintGroup Flexoplastol APF containing organic vehicles in comparison with water-dispersed ink FlintGroup AquaFlex 007. This testifies to the fact that at adhesive destruction, tearing off of polymer thin layer takes place on nano-level, in that way concentration of functional groups is increased. In other words, the surface is as though being renovated.

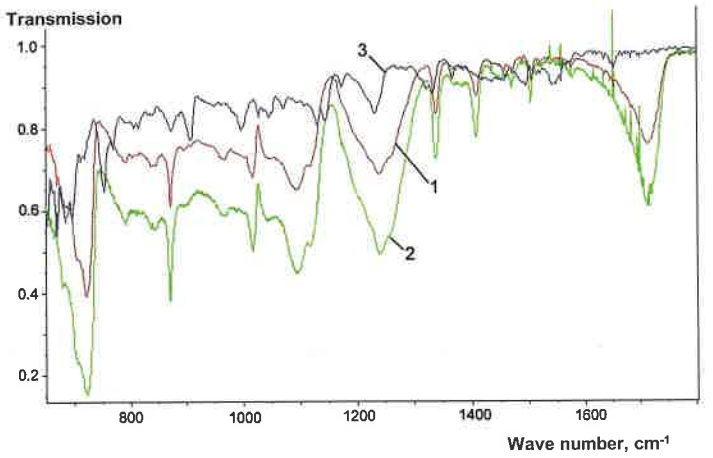

Figure 4: ATR FT-IR spectra: 1 - film from PET, 2 - PET after destruction of adhesive bond with

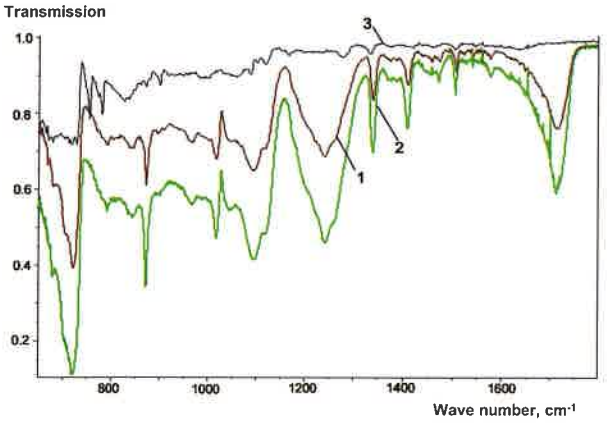

Figure 5:
ATR FT-IR - spectra: 1 - film from PET, 2 - PET after destruction of adhesive bond with ink FlintGroup Flexoplastol APF containing organic vehicles, 3 - ink FlintGroup Flexoplastol APF

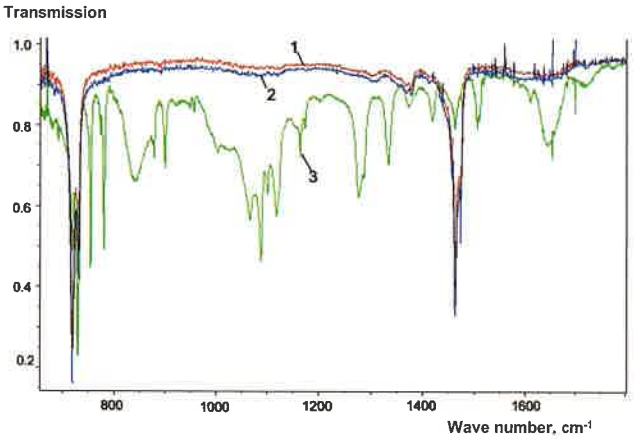

Figure 6:
ATR FT-IR -spectra: 1 - film from PE, 2 - PE after destruction of adhesive bond with ink FlintGroup Flexoplastol APF containing organic vehicles, 3 - ink FlintGroup Flexoplastol APF containing organic vehicles

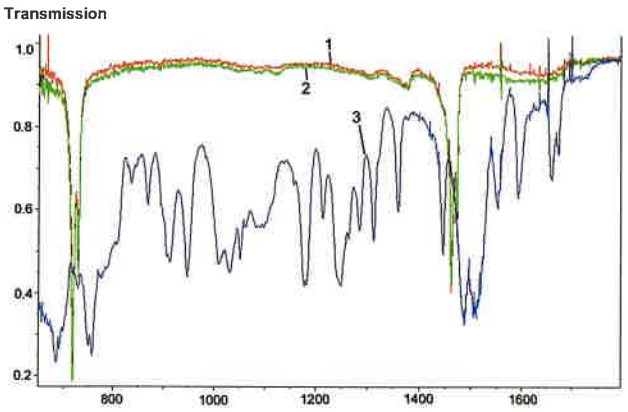

Figure 7:
ATR FT-IR -spectra: 1 - film from PE, 2 - PE after destruction of adhesive bond with water-dispersed ink FlintGroup AquaFlex 007, 3 - ink FlintGroup AquaFlex 007

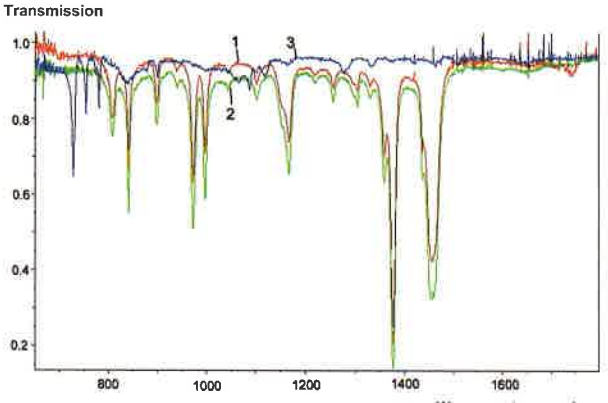

Figure 8:
ATR FT-IR -spectra: 1 - film from PP, 2 - PP after destruction of adhesive bond with ink FlintGroup Flexoplastol APF containing organic vehicles, 3 - ink FlintGroup Flexoplastol APF containing organic vehicles

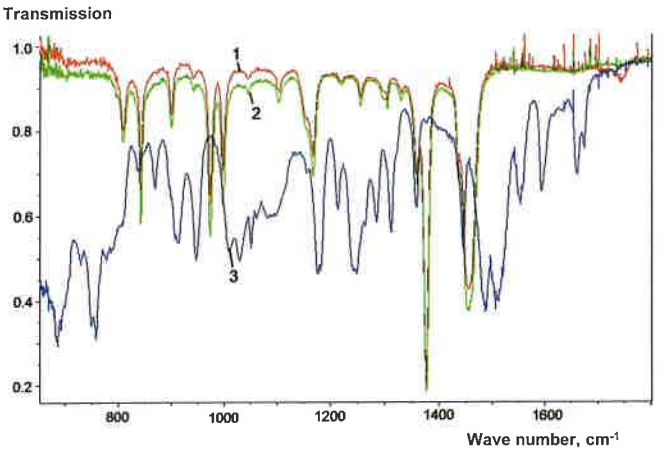

Figure 9:
ATR FT-IR -spectra: 1 - film from PP, 2 - PP after destruction of adhesive bond with water-dispersed ink FlintGroup AquaFlex 007, 3 - ink FlintGroup AquaFlex 007

It is possible to substantiate increase of absorption band intensity at inks containing organic vehicles relatively water-dispersed inks by the fact that adhesion of the first is greatly higher, all other things being equal, that results to stronger cohesive destruction of polymer thin layer (Figure 4, 5).

Analyzing data represented on IR-spectra (Figure 4, 5), in what connection comparing them with values of adhesive strength represented in Table III, it is evident that the higher adhesive strength is the higher intensity of polymer bands testifying to adhesive character of destruction. However, increasing bands intensity at frequencies 722, 872, 1097 and 1242 cm^{-1} testifies that concentration of groups at these frequencies increases.

Table III: Definition of ink adhesive strength to polymer films by normal fracture method

Polymer	Ink	Adhesive strength, N/cm²	
		before activation	after activation
PET, 25 μm	on organic vehicles	3,36	15,1
	water dispersed	2,61	14,3
PET, 40 μm	on organic vehicles	3,5	15,35
	water dispersed	2,83	15,04
PET, 100 μm	on organic vehicles	4,17	15,2
	water dispersed	2,37	14,65
PP, 20 μm	on organic vehicles	6,62	23,1
	water dispersed	3,41	16,52
PE, 20 μm	on organic vehicles	2,93	17,74
	water dispersed	1,5	18,0

In other words, it is possible to say that new surface is being organized and this testifies already to cohesive character of destruction not on ink but on film. In this case, it is possible to state that adhesive strength is higher on border polymer film - ink than cohesive strength of thin polymer layer.

On the results (Table IV) it is possible to draw a conclusion that in IR-spectra of films from PET on which printing inks were applied, ratio of bands at 1725/1410 cm^{-1} is changed. Less noticeably it is expressed with PP and is not expressed with PE totally. Results of this experiment testifies that intensity of band, responsible for oscillation of group CO = in PET, is increased. In such a way, it is possible to assume that new surface is formed. It is different from the one, spectrum of which was received before applying ink but after processing it by corona discharge.

Table IV

Polymer film	Brands in sIR-spectra	Ratio of brands intensity at different level of adhesive strength N/cm²				
		3,5	7,0	10,2	16,5	23,2
PE	1370/1460	0,13	0,13	0,13	0,13	0,13
PP	1300/1160	0,28	0,30	0,32	0,32	0,36
PET	1725/1410	1,92	2,1	2,4	2,6	2,7

It can be explained by the fact, that polymer materials, which we compare (PET, PP, PE) are possessed of different deformation characteristics and according to deformation properties they may be ranged in the following order (according to decreasing deformation):

PE < PP < PET

In such a way, quantitatively evaluating adhesive strength on border ink – polymer film, it is important to determine what strength characteristics of this composition are. At the same time it is not important entirely, from the practical point of view, where destruction took place, but it is only in the case when strength of composition is high. In the case of low values of composition strength, it is necessary to know what border needs to be increased. It may be ink cohesive strength, ink interaction strength with polymer surface or cohesive strength in thin polymer layer. Developed guidance approaches allow determining the weakest border in the system polymer film - ink and evaluating the level of "adhesive" strength.

At the same time, by using this technical approach, it is also possible to work out more complicated multilayer systems. For example, it may be used when developing formulas of various primers, as well as working out modes of polymer films activation by different methods.

4. Conclusions

On the basis of carried out theoretical and experimental researches, means of identification of adhesive interaction character on border polymer film - ink have been proposed.

On the basis of researching surface properties after destruction of adhesive bond, means of identification of adhesive interaction character on the border polymer film-printing ink have been proposed.

For the first time, it has been experimentally proved by ATR FT-IR - spectroscopy methods that seeming "adhesive" destruction at high strength values received by normal fracture method has cohesive character. At the same time, the level of polymer films destruction in thin layer in many respects is determined by polymer deformation-strength properties.

It has been determined experimentally that normal fracture method can be used for evaluation of ink adhesive strength on surface of polymer films in the range of destructing efforts from 0,7 to 55 N/cm^2

It has been grounded structure of measuring cell, selection of glue and preparation succession of specimens and cell itself to tests for quantitative evaluation of ink adhesive strength on polymer films surface.

Express - assembly structure for quantitative express-evaluation of adhesive strength has been developed for graphic enterprises. Given method had passed through practical tests at a graphic plant.

References

1. Bablyuk, E. B., Bakanov, V. A., Farenbrukh, K. V. (2007) Evaluation of adhesive strength in printing on polymer films // News of Higher Educational Establishments. Problems of graphic arts and publishing, № 5, P. 31-39
2. Farenbrukh, K. (2008) Features of Printing Quality Control on Polymer Films // Conference abstracts, 40th Conference of the international circle. Warsaw. P. 21-22

Penetration of microscopic drops into paper structures

Martin Dube[1], Francois Drolet[2], Claude Daneault[1], Patrice Mangin[1]

[1] Centre Intégré en Pâtes et Papiers, Université du Québec à Trois-Rivières
3351 Boul. Des Forges, C.P. 500 Trois-Rivières, Québec, G9A 5H7 Canada
E-mails: Martin.Dube@uqtr.ca, Claude.Daneault@uqtr.ca, Patrice.Mangin@uqtr.ca

[2] FPInnovations-Paprican
570 Boul. St-Jean, Pointe-Claire, Québec, H3R 3J9 Canada
E-mail: Francois.Drolet@fpinnovations.ca

Abstract

We develop a model describing the penetration of small fluid droplets inside the three-dimensional structure of paper. We numerically solve the Navier-Stokes equations governing fluid motion and discuss how paper structure influences the penetration and distribution of fluid inside the sheet. We consider small droplets and discuss our results in light of ink-jet printing applications. Our results show that paper density influences greatly ink coverage but that ink penetration is mostly dependent on the available fiber surface, a quantity not directly related to density.

Keywords: capillary pressure, paper structure, inkjet printing

1. Introduction

The penetration of small liquid drops (with volume ranging between 1 and 20 pl) into paper is at the core of modern inkjet printing. It is a notoriously difficult problem to tackle due to a number of reasons. For example, droplets are not simply deposited on paper but are rather projected on the paper surface at a given velocity [Alam et al., 2007]. Once the droplet has impacted the paper surface, the underlying fibrous structure causes both surface spreading and bulk penetration [Modaressi and Garnier, 2002]. In addition, for water-based inks, penetration within the fibres is possible. These processes are further influenced by ink viscosity, surface tension and evaporation as well as by the presence of pigments in the ink or that of filler particles or sizing agents at the paper surface.

The impact of droplets on model porous structures has been examined previously as well as the penetration of large droplets in a fibrous structure [Alam et al., 2007, Hyväluoma et al., 2006]. In this paper, we develop a model describing the penetration of small fluid droplets inside the three-dimensional structure of paper. We numerically solve the Navier-Stokes equations governing fluid motion and discuss how the paper structure influences the penetration and distribution of fluid inside the sheet. The paper structures are obtained numerically through a fibre deposition process followed by consolidation to a fixed caliper [Drolet and Uesaka, 2005]. The structures are described in terms of their transverse porosity profile, pore size distribution, specific surface and by their surface characteristics (roughness and power spectrum). Drops deposited on the surface of the paper penetrate the structure under the influence of capillary forces. We characterize the dynamical penetration of the drop and the fluid distribution inside the pores. Print quality is quantified from the final ink distribution inside the structure (drop roundness, spreading and optical density).

2. Fibre structures

The fibre structures used in this study are generated with a numerical algorithm that consists in first depositing fibres sequentially at random on a flat surface. The fibre mat thus created is then consolidated to a fixed caliper. Although fines, fillers and sizing agents can be included in the model, we concentrate here on networks composed of fibres only. The three-dimensional structures are defined by the density field $\rho(x,y,z)$ such that $\rho = 1$ if the volume element located at (x,y,z) is occupied by a fibre and $\rho = 0$ otherwise. The width and thickness of the fibres are fixed to 20 and 8 microns, respectively and the length to 400 microns. The fibres have an elliptical

Table I: Bulk and surface descriptors of the fibre networks

Caliper (μm)	ρ_b (kg/m³)	φ_b	R_{xy} (um)	R_z (um)	S_z (10^4 um²)	S_{xy} (10^4 um²)	S_q (um)
60	1000	0.2	9.1	4.3	10.8	10.0	4.8
80	750	0.3	12.5	5.5	11.5	11.5	7.1
100	600	0.4	16.5	6.8	10.7	10.7	9.6
120	500	0.55	21.1	7.8	9.2	9.2	11.9
140	430	0.6	25.7	8.3	7.8	7.8	13.5

For this study, we consider structures with a basis weight of 60 g/m² (assuming a coarseness ω = 0.1 mg/m) consolidated to five different calipers of 60, 80, 100, 120 and 140 μm. For each caliper, five statistically equivalent networks were simulated and used for averaging. Fluid simulations were performed on a subset of the structure with an area of 150 x 150 μm² and a depth of 55 μm. These structures are first characterized by their bulk density ρ_b and porosity φ_b, as listed in Table 1. The density is simply obtained by dividing the basis weight by the caliper. The porosity is obtained from the porosity profiles φ(z), defined as

$$\varphi(z) = 1 - \langle \rho(x,y,z) \rangle_{x,y}, \tag{1}$$

and corresponding to the porosity of the structure at a fixed position z along the thickness direction. The brackets in Eq. (1) correspond to an average over *x* and *y*. Figure 1 shows the porosity profiles for the calipers under consideration. The plane z = 0 is fixed at the point where φ(z) becomes unity and represents the "highest" point of the paper surface. At large negative values of z, φ(z) reaches a constant value taken as the bulk porosity φ_b listed in Table I. The surface of the paper corresponds to the transition zone between φ(z) = 1 and φ(z) = φ_b. It is clear that the surface is more clearly defined and presents less variation as the caliper of the paper is reduced.

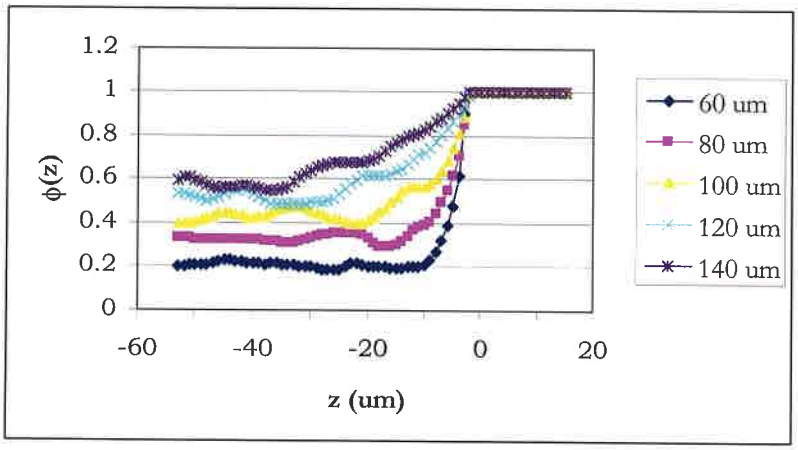

Figure 1: Average porosity profiles for the different fibre networks

Also calculated and shown in Table I are R_{xy}, the average pore size in the XY-plane and R_z, the average pore size along the Z-direction. The table also lists the total fibre surface area in the sample. That quantity depends on the number of fibres in the volume considered, the surface area of each fibre and the area of contact between fibres in the network. In the table, it is separated in S_{xy}, the total surface in an XY-plane and S_z, the total area in the XZ- and YZ-plane. It is interesting to note that the surface available for droplet spreading is smaller at a caliper of 60 μm than at 80 μm, due to an increase in the total area of contact between fibres in the network. To examine this effect more closely, the sample is decomposed into slices of area 150 μm x 150 μm and 1 um thickness. The solid area within each slice is then calculated. The result of this procedure, analogous to the calculation of the porosity profiles, is shown in Figure 2. The peak that appears for the denser structures (60 and 80 μm) indicates that there are a large number of exposed fibres at the paper surface. It is also interesting to note that the total area for each slice in the bulk of the paper is actually smaller for samples with a caliper of 60 μm compared to samples at 80 μm. This again reflects the fact that the area of contact between fibres in the network increases at caliper of 60 μm

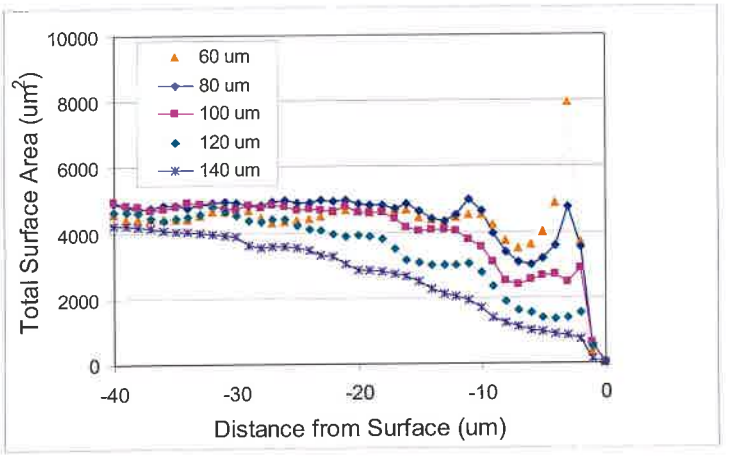

Figure 2:
Average surface area as a function of depth for the different paper structures

Finally, we explore the surface properties of the structures in more detail. The surface S is defined as the largest value of z, for a given r = (x,y), occupied by a fibre, i.e., S® = zmax. There exist several descriptors for the surface. We concentrated on the global width,

$$S_q^2 = \left\langle \left(S(\mathbf{r}) - \bar{S}\right)^2 \right\rangle, \tag{2}$$

where $\bar{S}$ is the average surface height and ⟨...⟩ indicates a statistical average. This quantity, which is also listed in Table 1, corresponds well with roughness measurements using air flow, although it only gives information on the global roughness of the surface.

3. Fluid flow and droplet descriptors

The flow of a fluid in contact with the fibrous structure is determined from a numerical solution of the Navier-Stokes equations. Capillary forces, arising from the liquid surface tension and the fibre surface energy are explicitly included in the simulations through the use of a diffuse-interface technique. This technique, described previously [Dubé, Drolet et al., 2008], considers a concentration field c(**x**,t) which takes value c = 1 in the liquid and c = 0 in the air. This field has a thermodynamic origin and there exists an interface, with a finite width ζ between fluid and air regions. This interface also gives rise to a surface tension σ at the liquid/air and liquid/solid interfaces and hence to an equilibrium contact given by Young's law:

$$\sigma_{sa} - \sigma_{sl} = \sigma\cos\theta, \tag{3}$$

where σ_{sl} and σ_{sa} are the surface tensions of the fibres in contact with the fluid and air respectively. Numerically, we solve simultaneously the dynamics of the field c(**x**,t), together with the velocity field v(**x**,t) as given by the Navier-Stokes equations. The existence of a dynamical contact angle, together with hysteresis phenomena, is thus naturally included in the model. The numerical simulations are performed with a simple finite volume and time explicit technique on a staggered grid. The resolution of the computational grid is 1 micron, which is the same as the resolution used to create the fibre network.

We set the interfacial width ζ = 1 μm. This is an approximation that neglects physics below the micron scale. It is however consistent with the resolution of the fibre network. The time scale τ_s of the simulations is then fixed by the capillary number

$$C_a = \frac{\sigma\tau_s}{\zeta\eta}. \tag{4}$$

We consider a model fluid with surface tension σ = 25 mN/m. The simulations are performed with C_a = 100. For a typical inkjet ink with viscosity η = 5 Pa-sec, τ_s = 20 μsec, with an evaporation time scale of the of a few milliseconds [Lim et al., 2009]. Drops, with initial volume of 10 pl are initially placed in contact with

with the following set of descriptors. Except when explicitly mentioned, all simulations are performed for an equilibrium contact angle of 30° between the fluid drop and the fibre surface.

3.1 Center of mass $\mathbf{R}_{cm}$ and second moment of the distribution I

Information on the fluid distribution can first be obtained from a calculation of the center of mass of the drop as well as the dynamical evolution of the second moment of the fluid distribution c(x, y, z, t). The coordinates of the center of mass $\mathbf{R}_{cm} = (X_{cm}, Y_{cm}, Z_{cm})$ are defined by the relation

$$\int_{V_d} dV(\mathbf{r} - \mathbf{R}_{cm})c(\mathbf{r}, t) = 0 . \tag{5}$$

Here we focus mostly on the displacementof the center of mass $\Delta\mathbf{R}_m = \mathbf{R}_m(t) - \mathbf{R}_m(t = 0)$. The matrix **I** of the second moment of the distribution is

$$\mathbf{I} = \int_{V_d} dV(\mathbf{r} - \mathbf{R}_{cm}) \otimes (\mathbf{r} - \mathbf{R}_{cm})c(\mathbf{r}, t) , \tag{6}$$

where tensorial product is implied. For simplicity, we concentrate on the diagonal elements of the matrix I_{xx}, I_{yy} and I_{zz}. Of particular interest is the ratio

$$I_p(t) = \frac{I_{xx}(t) + I_{yy}(t)}{2I_{zz}(t)} , \tag{7}$$

which equals 1 for a perfect sphere while a value $I_p > 1$ indicates a greater extension in the XY-plane than in the Z-direction.

3.2 Fraction of penetrated fluid F_p

Another indicator useful for printing applications is the fraction of fluid that has penetrated inside the fibrous structure. In order to avoid any reference to the paper surface reference level, a concept which cannot be properly defined at the micron scale, we define the fraction of fluid that has penetrated the fibre structure as the fraction that is covered by at least one fibre element.

3.3 Coverage A_s

The descriptors defined in Section 3.1 and 3.2 make abstraction of the fibre network. It is clear that fibres must be taken into account if optical properties are considered. While it is not our goal to describe in details the optical properties of the drop in the fibre network (e.g., reflectance and dot gain), it is interesting to measure the coverage of the drop, ie., the area of the drop A_s that covers the surface of paper. This quantity is of course related to the spreading factor (ratio of the effective drop radius at time t to the drop radius at time t = 0).

4. Results

We first show in Figure 3 the dynamical z-displacement of the center of mass of the drop for the various calipers.

It is interesting to note that the displacement is similar in all cases, indicating the same tendency to penetrate the paper structure. The repartition of the fluid is of course different. Figure 4 shows the evolution of $I_p(t)$ (c.f., Equation 7). It is clear that more lateral spreading occurs compared to bulk penetration of the drops, a trend observed at all five sheet densities. The dynamics of I_p presents some interesting features. The ratio increases rapidly for about 200 μsec after which it tends to level off to a constant value. The value of I_p tends to increases more rapidly with decreasing caliper (or increasing density). This is clearly the case for calipers of 140 μm, 120 μm and 100 μm. This trend is also confirmed at early times for calipers of 80 μm and 60 μm. The late time behavior is however different, with the structure at 80μm showing more relative spreading than the structure at 60 μm. This behavior has to be related to the total surface available to spreading as a function of the sample's depth, shown in Figure 2. The closed surface structure of the samples with 60 μm promotes a very fast initial spreading on the paper surface

This spreading is however eventually stopped and fluid penetration in the bulk then becomes predominant. In the final stages of penetration, lateral expansion dominates again. For a fixed caliper, Figure 5 clearly shows that increasing fibre wetting leads to an increase in lateral spreading relative to bulk penetration.

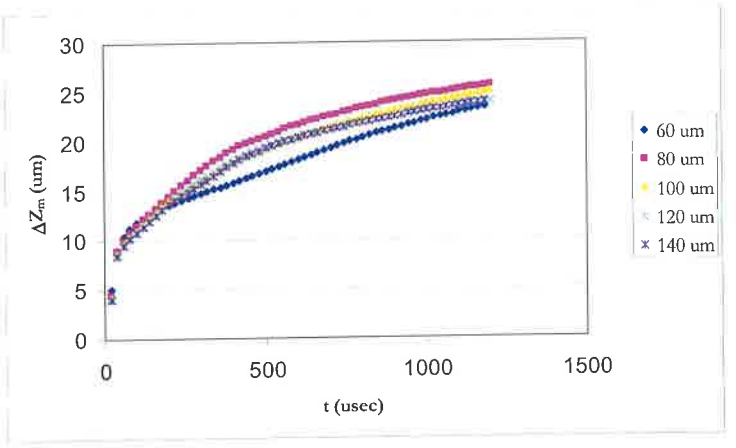

Figure 3:
Z-displacement of the center of mass for the different fibre structures

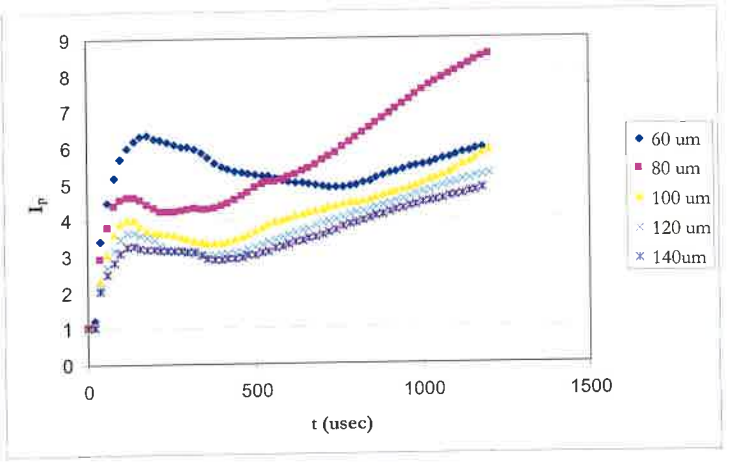

Figure 4:
Dynamical evolution of the ratio I_p, showing that more lateral displacement than bulk penetration occurs at all sheet densities

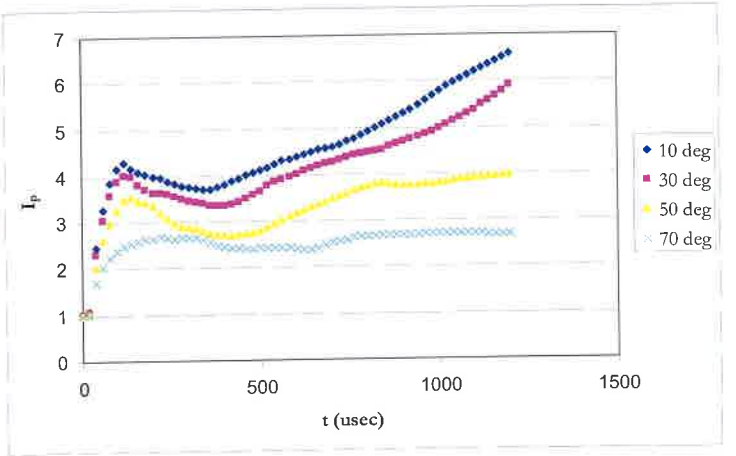

Figure 5:
Dynamical evolution of the ratio I_p for different wetting properties of the fibres. The labels represent the equilibrium contact angle of a droplet placed upon a flat fibre surface

We now briefly comment on the descriptors used specifically to quantify the amount of fluid remaining on surface of the paper. Figure 6 shows the fraction of penetrated fluid inside the fibrous structure. As for the center of mass (Figure 3), it shows limited dependence on sheet density. However, the results of ink penetration for sheets with 60 μm caliper are systematically lower than for sheets with other caliper, in particular for caliper of 80 μm. This tendency is also present in the dynamics of the center of mass (c.f., Figure 3) and again can be related to the closed surface and smaller available surface of the 60 μm samples as shown on Figure 2. Nevertheless, the increased tendency towards lateral spreading with decreasing caliper is still present and confirmed from a study of the

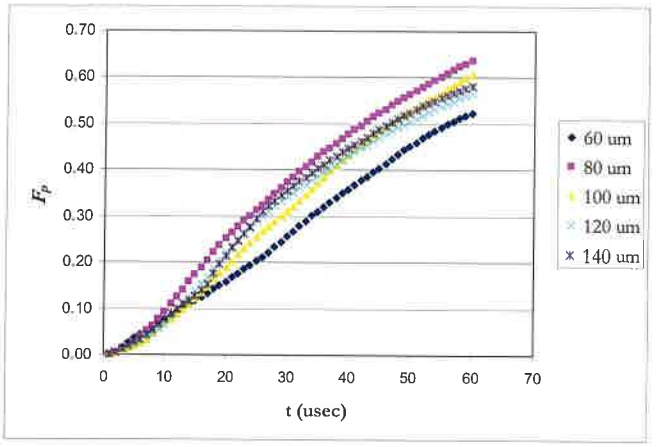

Figure 6:
Dynamical evolution of the fraction of fluid penetrated inside the fibrous structure

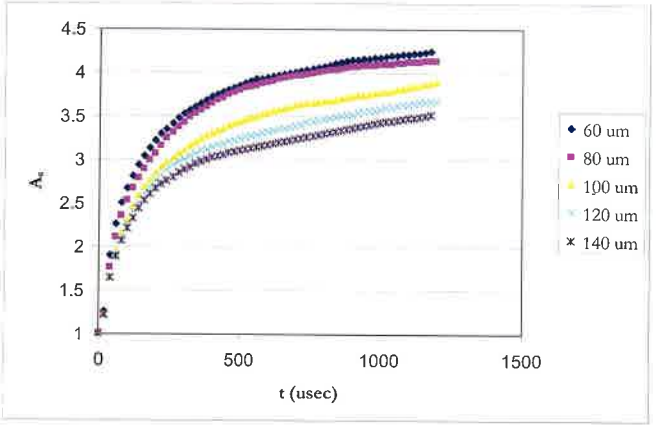

Figure 7:
Dynamical evolution of the coverage for the calipers under consideration

5. Conclusions

We have shown that the density of the fibrous network can have a large influence on the spreading and penetration of a small droplet placed upon it. Increased density leads to increased spreading relative to bulk penetration. However, some quantities, such as drop circularity or the vertical displacement of the center of mass are relatively independent of density. In this paper, we have concentrated solely on average properties. Future work will focus on the distribution of the drop measurements and the link between those measurements and structure variations in the samples.

References

1. Alam, P., Toivakka, M., Backfolk, K., Sirvio, P., (2007), *Impact spreading and absorption of Newtonian droplets on topographically irregular porous materials. Chemical Engineering Science,* ***62****, 3142-3158*
2. Modaressi, H., Garnier, G., (2002), *Mechanism of wetting and absorption of water droplets on sized paper: effect of chemical and physical heterogeneity. Langmuir,* ***18****(3), 642-649*
3. Hyväluoma, J., Raiskinmäki, P., Jäsberg, A., Koponen, A., Kataja, M., Timonen, J., (2006), *Simulation of liquid penetration in paper. Physical Review E, 73, 036705*
4. Drolet, F., Uesaka, T., (2005), *A stochastic structure model for predicting sheet consolidation and print uniformity, Advances in paper science and technology. S.J. l'Anson ed, vol 2, 1139-1154*
5. Dubé, M., Drolet, F., Daneault, C., Mangin, P. J., (2008), *Hydrodynamics of fluid transfer. Journal of Pulp and Paper Science,* ***34****(3):171-181*
6. Lim, T., Han, S., Chung, J., Chung, J. T., Ko, S., Grigotopoulos, C. P., (2009), *Experimental study on spreading and evaporation of inkjet printed pico-liter droplet on a heated substrate. International Journal of Heat and Mass Transfer,* ***52****: 431-441*

Printed interference effect colours - process control and quality assurance

Katharina Kehren, Edgar Dörsam, Heike Hupp

Technische Universität Darmstadt, Institute of Printing Science and Technology
Magdalenenstraße 2, D-64289 Darmstadt, Germany
E-mails: kehren@idd.tu-darmstadt.de, doersam@idd.tu-darmstadt.de, heike.hupp@boschrexroth.de

Abstract

Strategies for process control and quality assurance are well-established in printing with absorption inks. In the case of interference effect colours, usual optical parameters and common measuring geometries are not appropriate. A new optical parameter for process control and two necessary but sufficient measuring geometries for quality assurance were found.

Special properties of printed interference effect inks are outlined compared to conventional printing inks with absorption pigments. The comparison accounts for the necessity of adjusted concepts for process control and quality assurance. First examinations showed that the appearance of printed interference effect colours in fact depends on the thickness of the ink layer.

For interference effect colours, the difference between the lightness of the unprinted paper and of the printed result linearly correlates with the ink layer thickness. Therefore, the lightness difference is a suitable parameter to control the printing process by means of the ink supply.

Analyzing colour distances, two measuring geometries were found to be necessary but sufficient to represent aspect line and interference line in the a*b*-plane of the CIELAB-color space. Measurements of colour coordinates in the common geometry 45°/0°(+45°) far from gloss and the additional geometry 45°/-30°(+15°) near gloss guarantee the quality in printing.

Keywords: interference effect colours, process control, quality assurance, lightness difference, measuring geometry

1. Introduction

In case of printing using conventional inks that contain absorption pigments, optical density measured instrumentally serves for process control. In quality assurance, colour coordinates of a sample are determined in common 45°/0°-geometry. In contrast to absorption colours, several measuring geometries are necessary to guarantee the quality of printed interference effect inks. The machine operator runs the printing process of interference effect colours by visual inspections. At the "Institute of Printing Science and Technology" of "Technische Universität Darmstadt", printing with interference effect inks was investigated by Heike Hupp [Hupp, 2006; Hupp, 2007; Hupp, 2008]. An optical parameter for process control and two essential but adequate measuring geometries for quality assurance were found.

First, the presumption was proven that the visual perception of interference effect inks depends on the ink film thickness. An optical parameter that correlates with the thickness of the ink layer is required for process control. This parameter was found to be the lightness difference. The large number of standardised measuring geometries should be reduced to a sufficient minimum for quality assurance. Two geometries, 45°/0° (+45°) and 45°/-30° (+15°), were identified to be sufficient.

In the following, some information on interference effect colours in comparison to absorption colours is given. The methods of printing samples and measuring optical parameters are described. Finally, the obtained results about the optical parameter for process control and the measuring geometries for quality assurance in printing using interference effect inks are presented.

2. Principles

Interference effect pigments differ from absorption pigments that are contained in common black, cyan, magenta and yellow printing inks in terms of optical properties. Therefore, the usual methods for process control and

quality assurance are inapplicable. Subsequent to a description of the specific optical characteristics, the current methods adapted on printed interference effect inks are presented.

2.1 Properties of interference effect colours

Printing inks consist of solvents, binders, colorants and additives. Colorants are pigments or dyes. Pigments are dispersed in the solvent and binder before used on the printing press. In the course of application, solvent and binder partly penetrate the printing substrate. The solvent volatilizes while drying. The pigments are embedded in the binder as a layer on the printing substrate. Figure 1a visualizes a paper printed with a conventional ink that contains absorption pigments. A paper printed with a special ink containing interference effect pigments is shown in figure 1b.

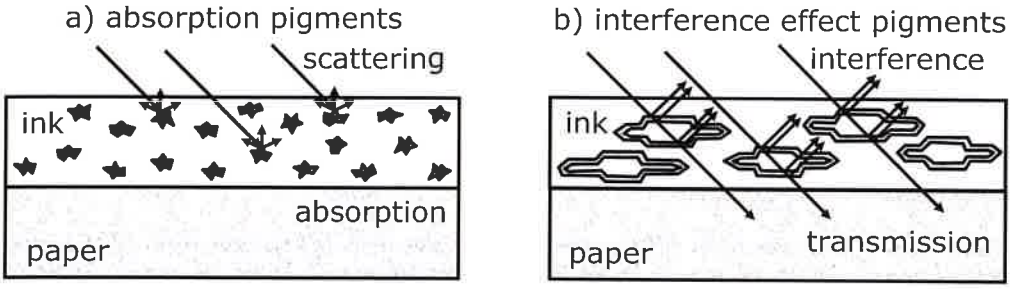

Figure 1: Optical phenomena in printed inks containing a) absorption pigments and b) interference effect pigments on paper as printing substrate

Absorption pigments are included in conventional black, cyan, magenta and yellow inks for four-color printing. Carbon black pigments measure between 0,02 µm and 0,08 µm in diameter. The particle size of coloured pigments varies from 0,2 µm to 0,7 µm. These small, spherical pigments absorb the incident light in specific spectral regions and scatter the remaining part in all directions.

With diameters up to 300 µm and thicknesses from 0,3 µm to 0,6 µm, the flaky interference effect pigments are bigger than absorption pigments. Most interference effect pigments are composed of a coated substrate with a 40 nm to 160 nm thin film of an intensely refracting medium. The phenomenon affecting the colour of these otherwise transparent pigments is the interference of thin layers.

The reflected component and the transmitted component of the incident light are coloured complementary. The appearing colour depends on the thickness of the thin layer and the geometric conditions of illumination and observation. The dependence of lightness and chromaticity on the directions of incident light and reflected light causes problems in description of optical properties.

2.2 Optical density as control variable

The printing process is usually controlled by means of the ink supply, which predefines the thickness of the ink layer. In the range typical for printing absorption inks, the ink film thickness linearly correlates with the optical density shown in figure 2a [Kipphan, 2001]. The optical density is measured with common densitometers in 45°/0°-geometry. As shown in figure 2b, the reflected radiation is detected normal to the sample at 0° which is illuminated from 45° to the perpendicular.

It is not possible to control a printing process by measurements of optical density in case of interference effect inks. For this reason, the machine operator visually matches printed samples in different configurations generated as shown in figure 2c [Cramer, 2001a; Cramer, 2001b; Cramer, 2006]. The aspect angle, i.e. the angular difference from the direction of specular reflection, is varied by tilting the sample. In consequence of a vertical motion, different angles of illumination counted to the perpendicular on the sample are obtained. Aspect angle as well as illumination angle is marked in figure 2d.

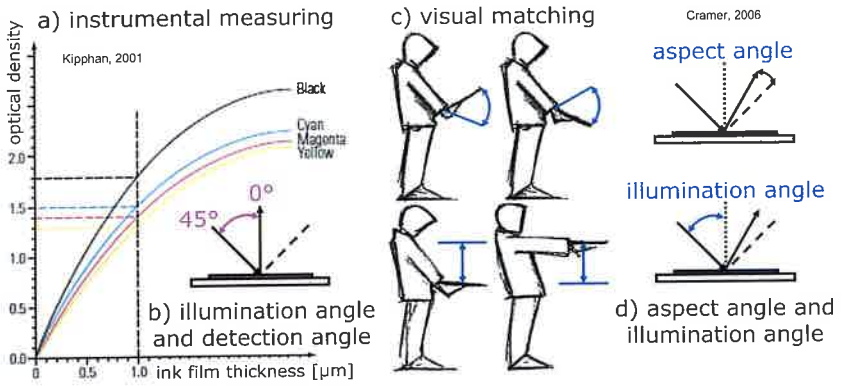

Figure 2: a) Instrumental measuring of optical density of absorption colour [Kipphan, 2001] in b) 45°/0°-geometry and c) visual matching of optical appearance of interference effect colours [Cramer, 2006] in d) multiple geometries

2.3 Colour distance as quality criterion

To guarantee a product of high quality, the colour coordinates L*, a* and b* of the print are usually evaluated in only one measuring configuration. This configuration is the common 45°/0°-geometry shown in figure 3a. The colour distance of the sample to a reference serves as criterion to accept the print. Figure 3b visualizes the colour distance between two colour coordinates in the CIELAB-colour space.

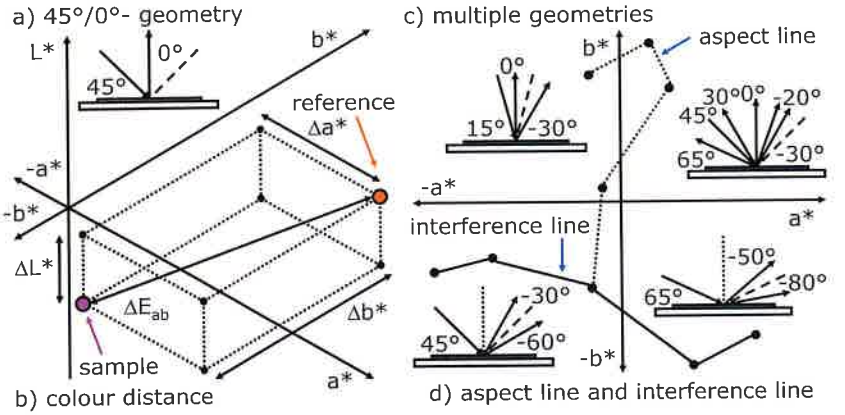

Figure 3: a) 45°/0°-geometry for measurements of b) colour distance between sample and reference of an absorption colour and c) multiple geometries for measurements of d) aspect line and interference line of an interference effect colour

In contrast to absorption inks, the apparent colour of interference effect inks depends on the angles of illumination and observation. For research purposes, colour coordinates are determined on large samples using various measuring geometries listed in figure 3c. The measured colour coordinates are visualized as aspect line and interference line in a*b*-plane of the CIELAB-colour space as shown in figure 3d [Glausch, 1996; Maisch, 1991; Pfaff, 2007]. This type of measurements is too costly in terms of measuring time, printed material and labour instrumentation for quality assurance of printed interference effect inks.

3. Methods

Samples were printed and measured in order to generate optical data for evaluations. Materials and instruments for laboratory printing and optical measurements were selected. Different materials, printing inks and printing substrates, were combined with each other.

Blue, red and white interference effect inks as well as magenta and black absorption inks were chosen for printing on several papers. The papers differ from each other in surface properties and brightness. In the main, a glossy coated paper with a yellowish tint was printed and measured. The surface quality of this paper is

representative for papers usually printed with interference effect inks. Fluorescence could be neglected since the paper contains no optical brightener.

The "inking unit AE" and the "printability tester AC2" of "IGT" were used to apply ink layers of a defined thickness on the paper (Hupp, 2007). The "IGT inking unit AE" for dosing and distributing the printing ink on the application roll is shown in figure 4a. Figure 4b visualizes the "IGT printability tester AC2" to transfer the printing ink from the application roll on the printing substrate.

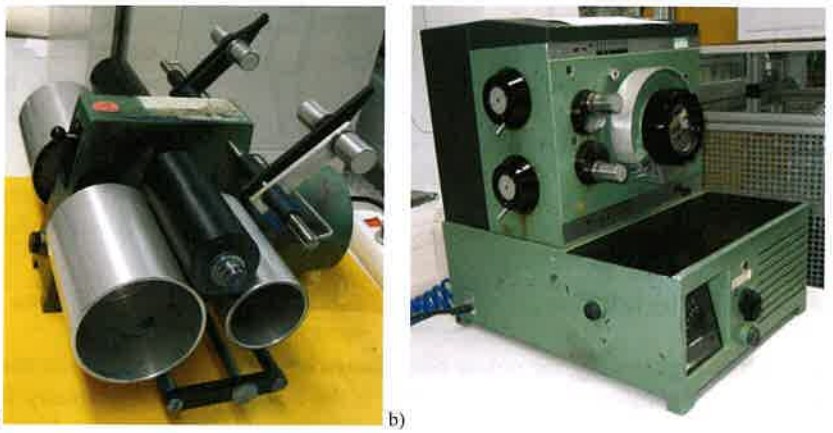

Figure 4: a) "Inking unit AE" for dosing and distributing printing ink on application roll and b) "printability tester AC2" of "IGT" for transferring printing ink from application roll to paper

The transferred amount of printing ink was determined by weighting the application roll before and after printing. Volatilisation of solvents while drying can be neglected in the case of offset printing inks used in this study. The ink film thickness is calculated under consideration of the area covered with printing ink and the density of the printing ink.

The printed samples were measured with different optical instruments in common 45°/0°-geometry typified in figure 3a. All other combinations of illumination angle and detection angle listed in figure 3c are realized with the multi-angle spectrophotometer "Multi FX10" from "Datacolor" shown in figure 5 [Hupp, 2006; Hupp, 2007].

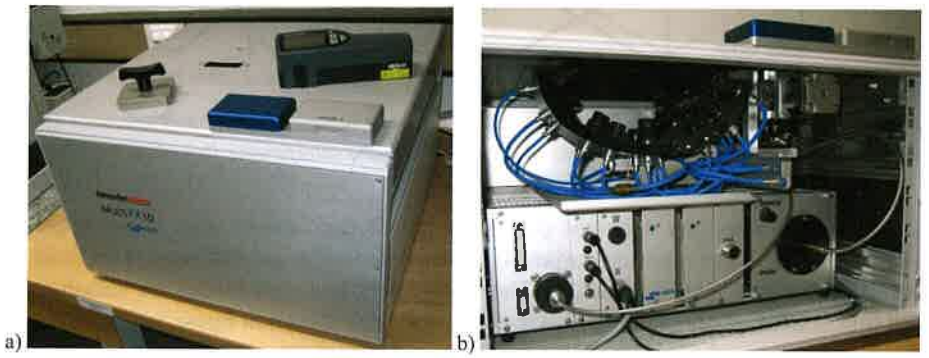

Figure 5: Multi-angle spectrophotometer "Multi FX10" of "Datacolor" in a) exterior view with sample port and white calibration standard as well as in b) interior view with illumination optics and detection optics on movable half pipe and fibre-optical light guides

The dimensions of "Datacolor Multi FX10" compared to a common portable spectrophotometer can be guessed of figure 5a. The multi-angle spectrophotometer is 530 mm wide, 470 mm deep and 320 mm high. The sample port on the top of the instrument measures 22 mm times 69 mm. Before measurements, the "Datacolor Multi FX10" is calibrated using a white standard tile.

As visible in figure 5b, ten pairs of an illumination and detection optic are arranged on a movable half pipe. Fibre-optic light guides connect the illumination optics and the detection optics with the tungsten halogen lamp and the spectral detection system respectively.

4. Results

The colour coordinates determined in all measuring geometries were first tested for a dependency on ink film thickness. As described in the following, further examinations regarding an optical parameter for process control and necessary measuring configurations for quality assurance were performed.

4.1 Influence of ink layer thickness

The influence of ink layer thickness on the optical appearance was investigated using colour coordinates in the CIELAB-colour space. Some results of the dependency of lightness and chromaticity on the thickness of the ink layer are presented in figure 6.

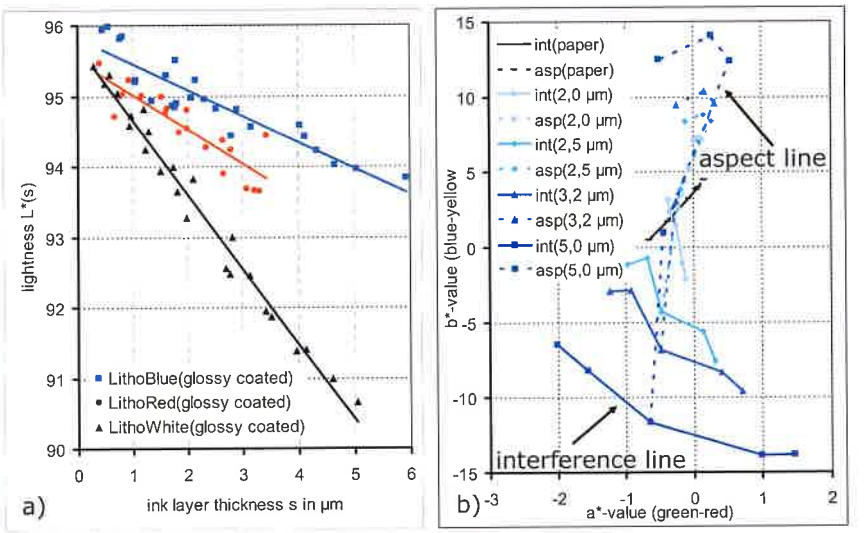

*Figure 6: Influence of ink layer thickness on the optical appearance quantified by a) lightness as function of ink layer thickness for different interference inks as well as by b) aspect lines and interference lines in a*b*-plane for different ink film thicknesses*

Figure 6a shows the correlation of lightness and ink film thickness for three different interference effect inks on glossy coated paper measured at the widespread geometry 45°/0°. The decrease of lightness for an increasing ink film thickness is approximately linear far from gloss. This is an interesting fact that might be used for a method to control the printing process.

The aspect lines and interference lines of a blue interference effect ink printed on a glossy coated paper are shown in figure 6b. The connected lines have similar shapes but different extensions for different ink film thicknesses. The representation of aspect line and interference line in a*b*-plane is a proper tool for multi-angle evaluations and needs to be taken into account in quality assurance.

4.2 Optical parameter for process control

Based on the results of the preliminary evaluations, it seems to be reasonable to control the printing process by an optical parameter that correlates with the thickness of the printed ink layer. The lightness as function of the ink film thickness linearly decreases for different interference effect inks as already shown in figure 6a.

Level and gradient of the curve also depend on the lightness of the unprinted paper as visualized in figure 7 for three different papers. The curves shown in Figure 7a are presented in Figure 7b after a linear displacement along the vertical axis.

The shift results from subtracting the lightness $L^*(s = 0)$ of the unprinted paper from the lightness $L^*(s)$ of a sample printed with an ink layer of a known thickness s. According to that, the lightness difference $L_H(s)$ is

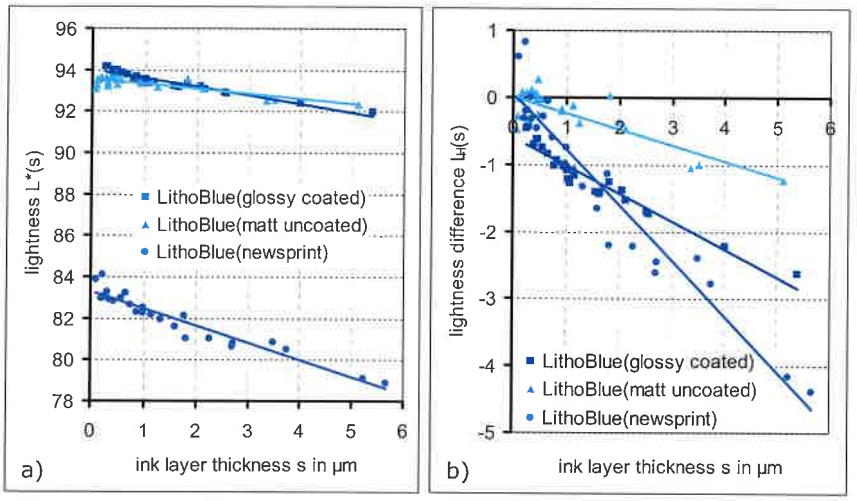

Figure 7: a) Lightness and b) lightness difference as function of ink layer thickness for different papers printed with blue interference effect ink

$$L_H(s) = L^*(s) - L^*(s = 0) \tag{1}$$

For process control of interference effect inks, the lightness difference $L_H(s)$ is a convenient parameter because it linearly depends on the ink film thickness s. In equation 2, the linearity is indicated by the constant $C_{\text{int.ink}}$

$$L_H(s) = C_{\text{int.ink}} \times s \tag{2}$$

Figure 8a shows this linear correlation for three blue, red and white interference effect inks printed on glossy coated paper. The linear equation is not valid for absorption inks as shown in figure 8b for conventional magenta and black absorption inks on glossy coated paper.

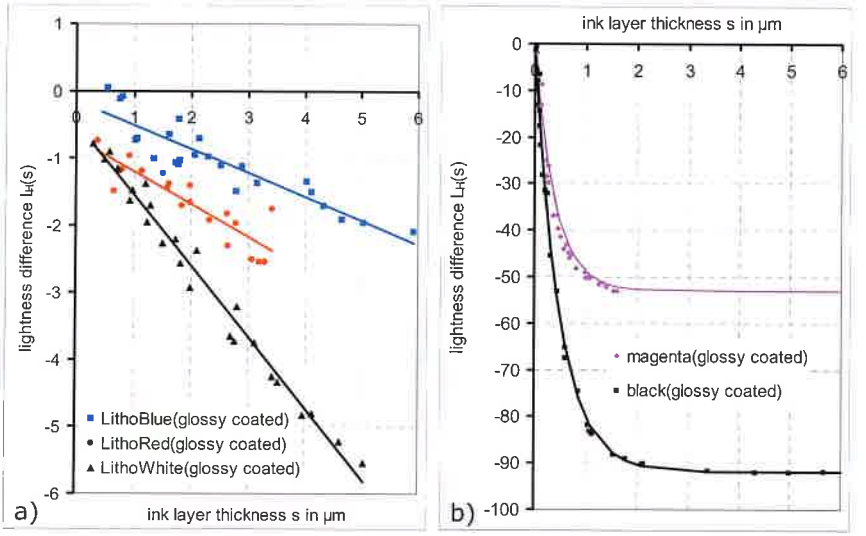

Figure 8: Lightness difference as function of ink layer thickness for a) different interference effect ink and b) different absorption inks printed on glossy paper

For absorption inks, the curve of lightness difference $L_H(s)$ decreases exponentially and reaches a constant level, called lightness difference $L_H(s \rightarrow \infty)$ of an infinitely thick ink layer. The constant $C_{abs.ink}$ in equation 3 decides about the bending of the curve.

$$L_H(s) = L_H(s \rightarrow \infty)(1 - \exp(- C_{\text{abs.ink}} \times s)) \tag{3}$$

Because of the explicit linear dependency or exponential dependency on the thickness of the printed ink layer containing interference effect pigments and absorption pigments respectively, each printing process can be controlled by the lightness difference as actuating variable.

4.3 Measuring geometries for quality assurance

As already mentioned, one single measurement in 45°/0°- geometry is insufficient for quality assurance in the case of interference effect colours. Multi-angle spectrophotometers like the "Datacolor Multi FX10" provide reflectance data for a multiplicity of angle combinations. This is reasonable for research but consumes too much measuring time, printing material and labour instrumentation to be acceptable for quality assurance. Therefore, measuring geometries have to be identified that represent the aspect line and the interference line in figure 6b best.

The identification was realized by comparing colour distances between two colour coordinates on the aspect line and between two colour coordinates on the interference line. Figure 9a shows colour distances for the aspect line with respect to the common geometry 45°/0°(+45°). The angle of +45° in parentheses represents the aspect angle. The aspect angle is the angular distance of the detection angle to the gloss angle. The colour distances with respect to an aspect angle of +15°, i.e. to the geometry 45°/-30°(+15°), are shown in figure 9b.

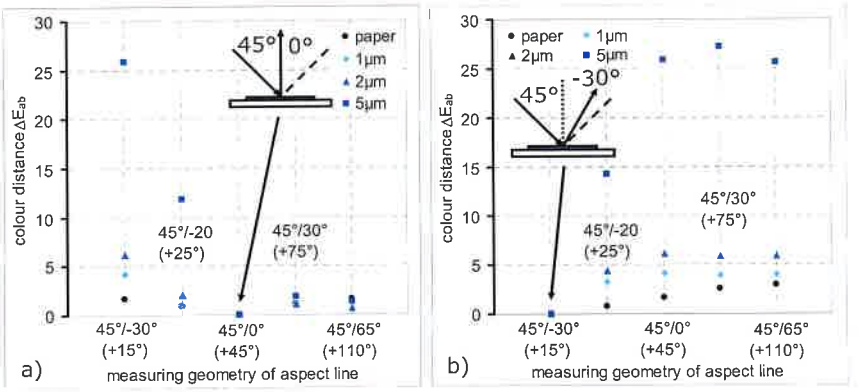

Figure 9: Colour distance along the aspect line with respect to a) 45°/0°(+45°)-geometry and b) 45°/-30°(+15°)-geometry for different ink film thicknesses

The colour distances between two colour coordinates of different geometries along the aspect line are high. Considered alone, the 45°/0°(+45°) - configuration far from gloss is not representative. A second reference point on the aspect line is required. The 45°/-30°(+15°) - geometry near gloss has been chosen. For this measuring geometry, common instruments have to be enhanced by an additional sensor. This sensor would be located at -30° from the normal on the opposite of the light source.

In addition to an end point of the aspect line, the measurement in the 45°/-30°(+15°) - geometry produces a point in the middle of the interference line. The point of the 45°/0°(+45°) - measurement is located near the other end of the aspect line. The location of both points in a*b*-plane is shown in figure 10a for the blue interference effect ink printed on glossy coated paper.

Figure 10b presents the colour distances to the central point of the interference line belonging to the measurement in 45°/-30°(+15°) - geometry. The small colour distances justify the measuring geometry 45°/-30°(+15°) as a sufficient reference for the interference line.

Location and extension of aspect line and interference line are adequately represented by measurements in the geometries 45°/0°(+45°) and 45°/-30°(+15°). The measured data contains information on the colour perception far from gloss and near gloss, which is likewise necessary and sufficient for quality assurance.

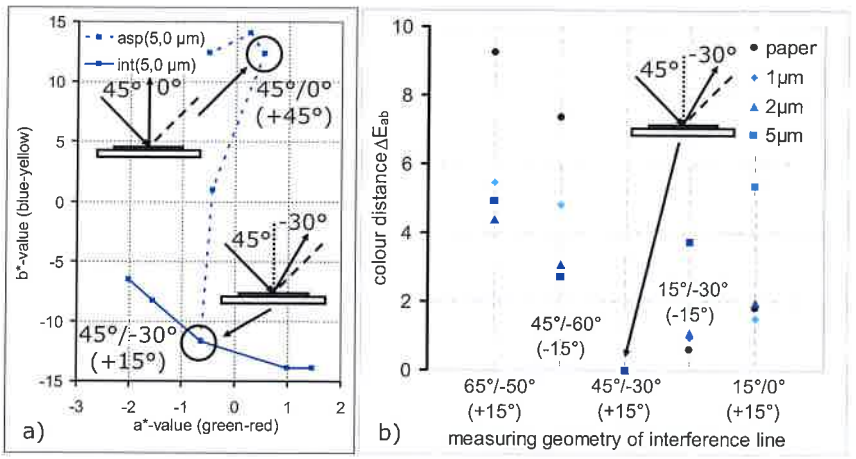

*Figure 10: a) Location of a*b*-coordinates for 45°/0°(+45°)-geometry on aspect line and for 45°/-30°(+15°) - geometry on aspect line and interference line and b) colour distances along the interference line with respect to 45°/-30°(+15°)-geometry for different ink film thicknesses*

5. Conclusion

The lightness difference as parameter for process control and two adequate measuring geometries for quality assurance are based on a fundamental determination. In addition to the direction of illumination and observation, the optical appearance of interference effect inks depends on the ink layer thickness.

The printing process can be controlled by the lightness difference instrumentally measured at the geometry 45°/0°. In the examined range, the lightness difference linearly correlates with the ink layer thickness for interference effect inks and exponentially for absorption inks. The correlation allows the machine operator to control the ink supply by optical measurements.

For quality assurance, an instrument with the common geometry 45°/0°(+45°) far from gloss and the additional geometry 45°/-30°(+15°) near gloss is proposed. The colour coordinates obtained in measurements in these geometries adequately represent location and extension of aspect line and interference line.

References

1. Cramer, (2006), Der richtige Blickwinkel * Visuelle und instrumentelle Abmusterung von Interferenzeffektpigmenten im Vergleich, Farbe und Lack, 112, 9, 26-30
2. Cramer, Gabel, (2001a), Effektvolles messen, Farbe und Lack, 107, 1, 42-49
3. Cramer, Gabel, (2001b), Measuring Special Effects – A Comparison of Various Spectrophotometers, Print and Coating Industry, 29, 39-46
4. Glausch, Kieser, Maisch, Pfaff, Weitzel, (1996), Perlglanzpigmente, Hannover, VincHupp, Dörsam, (2006), Measuring printed special-effect colours * First Experiences with the Multi FX10 spectrophotometer, 33rd International Research Conference of iarigai, Leipzig
5. Hupp, Dörsam, (2007), Quality control for printed interference colours * Investigation for a basic measuring geometry, 34th International Research Conference of iarigai, Grenoble
6. Hupp, (2008), Qualitäts - und Prozesskontrolle gedruckter Interferenzeffektfarben erster Generation, Darmstadt, Technische Universität, Fachbereich Maschinenbau, Institut für Druckmaschinen und Druckverfahren, Dissertation, Download: http://tuprints.ulb.tu-darmstadt.de/1016/
7. Kipphan, (2001), Handbook of Print Media - Technologies and Production Methods, Berlin, Heidelberg, New York, Springer
8. Maisch, Weigand, (1991), Perlglanzpigmente - Physikalische Grundlagen, Eigenschaften, Anwendungen, Landsberg am Lech, Verlag moderne Industrie
9. Pfaff, Gabel, Kieser, Maile, Weitzel, (2007), Spezielle Effektpigmente - Grundlagen und Anwendungen, Hannover, Vincentz

Physical and optical dot gain: separation and relation to print resolution

Daniel Nyström[1] and Li Yang[2]

[1] Dept. of Science and Technology (ITN), Linköping University
SE-60174 Norrköping, Sweden
E-mail: daniel.nystrom@itn.liu.se

[2] Holmen Paper Development Center, Holmen Paper AB
SE-60188 Norrköping, Sweden
E-mail: li.yang@holmenpaper.com

Abstract

Accurate determination of physical dot gain is essential for correct tone reproduction and for quantitatively evaluating the effect of optical dot gain. Due to the fact that, in reflectance measurements, physical and optical dot gains always co-exist, it is a difficult task to separate one type of dot gain from another. In this study we investigate three different methods to determine the physical dot gain, using spectral reflectance measurements, transmission scans and microscopic images of halftone prints. The different methods produce similar results and the good correspondence to experimental data confirms the validity of the methods. Further, the relation between the physical dot gain and the halftone dot size is investigated, by using FM halftones of various print resolutions. The physical dot gain demonstrates a clear correlation with the halftone dot size, with the increase in dot gain proportional to the increase in halftone resolution. The experimental observations are illustrated by theoretical analysis, showing that the physical dot gain is proportional to the nominal dot area, the side-length extension of the halftone dots, and the print resolution.

Keywords: physical dot gain, optical dot gain, Yule-Nielsen effect, halftone printing, print resolution

1. Introduction

The tone value increase in halftone printing commonly referred to as "dot gain" actually encompasses two fundamentally different phenomena. *Physical dot gain* (also known as mechanical dot gain) refers to the fact that the size of the printed halftone dots differs from their nominal size. Physical dot gain is closely related to the printing process, including the operation settings on the press such as nip pressure in offset, the ink-transfer and ink-setting processes. *Optical dot gain* (also known to as the Yule-Nielsen effect) originates from light scattering inside the substrate, causing light exchanges between different chromatic areas, and making the dot appear bigger than its physical size when it is perceived/measured. The effect of optical dot gain depends on the ratio of the length of the lateral light scattering within the substrate to the size of the printed halftone dots. In the case of big dot size, the light exchange only occurs in the vicinity of bounders between different chromatic areas and the optical dot gain is relatively small compared to the physical size of the dot. When the dot size is small in relation to the lateral scattering length, the optical dot gain increases. The lateral scattering length in paper is typically in the order of 0.1 mm [Arney, et al., 1996; Rogers, 1998].

Due to their different intrinsic nature, physical and optical dot gains need to be treated separately in order to accurately model the outcome of halftone prints. However, in reflection measurements of halftone prints the physical and optical dot gains always co-exist, making the separation of one type from another a difficult task. In this study different methods to determine the physical dot gain in halftone prints, thus separating it from the optical dot gain, are investigated. Physical dot gain is computed in three different ways: from spectral reflectance measurements, from transmission scans using a flat-bed scanner, and from microscopic images of the prints, respectively. Further, the relation between the physical dot gain and the size of the halftone dots is investigated by using frequency modulated halftones of various print resolutions and thus different dot sizes. The validity of the complete-light-scattering approximation is also evaluated, by using print resolutions where the printed dot size is no longer small in relation to the lateral scattering of the light.

2. Methodology

2.1 Physical dot gain from spectral reflectance

When the size of the printed halftone dots is small enough in relation to the lateral scattering length, complete light scattering within the substrate is considered, also known as complete photon diffusion (Rogers, 2000). In such cases, the reflectance of a halftone print can be described by the Clapper-Yule model, modeling optical dot gain by taking into account the bulk reflection as well as multiple internal reflections (Clapper & Yule, 1953):

$$R(a) = Kr_s + (1-r_s)(1-r_i)\frac{R_0(1-a+at)^2}{1-r_iR_0(1-a+at^2)} \quad (1)$$

In the equation, a is the physical dot area coverage, t is the spectral transmittance of the ink, R_0 is the bulk reflectance of the paper substrate, r_s and r_i are the Fresnel reflectance values of external and internal reflections. Both the external reflection, r_s, and the internal reflection, r_i, depend on the refraction indices of the air ($n = 1$) and the paper. In the current study the general assumption that the paper and ink share the common refraction index $n = 1.53$ is adopted, giving $r_s = 0.054$ and $r_i = 0.641$, for light at an incident angle of 45° [Hersch, et al., 2005]. The factor K, ranging from 0 to 1, gives the fraction of the specular surface reflection that reaches the detector and depends on the measurement geometry. Ideally, measurements should be performed using an integrated sphere, i.e. using the d/0°geometry where there is no specular reflection. However, it has been shown that for spectrophotometers using the 45°/0° measurement geometry, the specular component can be discarded in measurements on paper with refraction index $n = 1.53$ [Hersch, et al., 2005]. In the current study, all reflectance measurements are performed using the 45°/0° measurement geometry and the specular reflection component has been discarded, i.e. being set as $K = 0$.

With the measured spectrum of a test patch, one may obtain the physical dot area coverage, a_{phy}, by fitting the computed spectrum to the measurement, using a as the single fitting-parameter in Eq. 1. The physical dot gain, Δa_{phy}, is then simply given by the difference between the physical dot area, a_{phy}, and the nominal one, a_0, as:

$$\Delta a_{phy} = a_{phy} - a_0 \quad (2)$$

2.2 Physical dot gain from transmission scans

An alternative method to compute the physical dot gain is to use transmission images of the printed halftones where no optical dot gain is present. The relationship between the physical dot area and the transmission intensity has been derived in previous work, taking into account the light scattering within the substrate and the internal and external surface reflections [Yang & Lundström, 2007]:

$$\frac{(1-a+at)}{1-r_1R_0(1-a+at^2)} = \frac{I_t(a)}{I_t(0)}\frac{1}{1-r_1R_0} \quad (3)$$

In the equation, $I_t(a)$ is the intensity from the light transmitting through the printed patch, and $I_t(0)$ is the corresponding value for the plain paper. After deriving the paper bulk reflection, R_0, and the ink transmittance, t, the physical dot percentage can be computed from transmission images of the prints according to Eq. 3, and the corresponding physical dot gain is then given by Eq. 2.

2.3 Physical dot gain from microscopic images

Another possibility to estimate the physical dot area coverage is to use microscopic images, where the resolution is high in relation to the resolution of the halftone, and the individual halftone dots are easily detectable. From reflectance histograms computed from the microscopic images, the physical dot area can be computed by integrating the histogram up to a threshold, R_t. The reflectance threshold value, R_t, representing the boundary between the printed dot and the paper, is computed from the microscopic reflectance images, using image analysis methods [Nyström & Yang, 2008; Nyström, 2008b].

3. Experimental setup

The test prints used in this study consisted of offset prints on coated and uncoated paper grades. To study the dependency of the dot size, test patches of varying print resolutions, 150, 300, 600 and 1200 dpi, were generated using frequency modulated (FM) halftoning. The halftone algorithm employed uses an iterative method for optimal dot placement [Gooran, 2001]. The nominal dot area coverage of the patches are 2, 5, 10, 15,..., 90, 95, 98 and 100% respectively, and all the patches were printed using the same plate. The test charts were printed with a commercial 4-color offset press on both coated and uncoated substrates.

The spectral reflectance values of the printed test charts were measured using a Gretag Machbeth Spectrolino spectrophotometer. The scanner used is a FujiFilm FineScan 7250 flatbed scanner. The printed test charts were scanned in the resolution of 300 ppi in transmission mode, and stored as 16-bit tiff images. The transmission intensities were then computed as the mean value over the area for each color patch, from the transmission images. Since the color channel in the image that is complementary to the printed color (e.g. the green channel for a magenta print) is most sensitive to variations, it has been used when computing the transmittance intensities, $I_t(a)$.

The micro-scale images were acquired using an experimental image acquisition system, specially designed for microscopic images of prints and substrates. Images of the printed test charts have been captured using the 45°/0° measurement geometry, using a highly linear CCD camera equipped with macro optics. The field of view was 2.7 × 2 mm, giving a resolution corresponding to 2 µm/pixel and the illumination was provided using a tungsten halogen lamp through optical fibers. Color images were captured sequentially, using filters mounted in a filter wheel in front of the light source, and the color channel that is complementary to the printed color has been used in the computations, to maximize the dynamic range. All images are first calibrated against a white reference and corrected for dark current and CCD gain. [Nyström, 2008b]

4. Results and discussions

4.1 Estimations of physical dot gain

Figure 1 displays examples of computed physical dot gain for magenta prints of different print resolutions on coated paper. The solid lines correspond to the physical dot gain computed from spectral reflectance measurements, the dashed lines from the transmission scans, and the dotted lines from micro-scale images. The corresponding results for uncoated paper are displayed in Fig. 2.

Clearly, the physical dot gain computed using the three different methods agree fairly well (Figs. 1 and 2). It is obvious that the method using micro-scale images fails to predict the physical dot gain for the dark tones in the 1200 dpi prints. The reason is that with such small dots, it is difficult to distinguish the inked from the non-inked areas when ink coverage is high. The combination of physical and optical dot gain in the prints result in images where the paper between the dots is no longer visible and the threshold, R_t, cannot be accurately computed from the images [Nyström, 2008a].

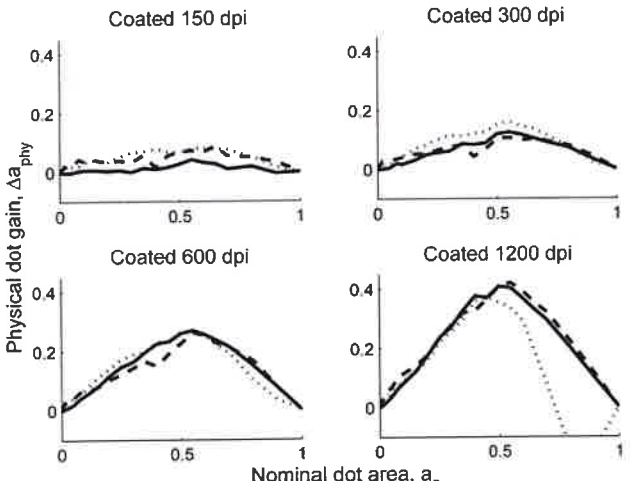

Figure 1:
Physical dot gain of magenta prints on coated paper. Solid lines: estimated from reflectance spectra. Dashed lines: estimated from transmission scans. Dotted lines: estimated from microscopic images of the prints

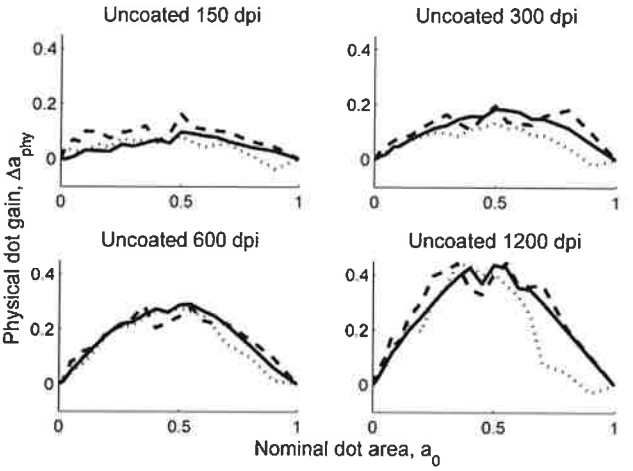

Figure 2:
Physical dot gain of magenta prints on uncoated paper. Solid lines: estimated from reflectance spectra. Dashed lines: estimated from transmission scans. Dotted lines: estimated from microscopic images of the prints

The method using transmission scans gives a somewhat better result for the coated paper grade compared to the uncoated paper, where the paper fibers are more clearly visible. In previous work [Nyström, 2008a], attempts were made to use microscopic transmission images. However, in such high magnification, paper fibers become clearly visible, while the imaged area is too small to be statistically significant. Consequently, the computed intensity values become unstable and depend strongly on the local structure of the fibers captured in the image, which varies over the substrate area. Using transmission scans from a flatbed scanner averaging the intensity over a larger area clearly produces more stable and reliable results.

4.2 Spectral estimations

Figure 3 displays the computed spectra for coated paper using Eq. 1 with the estimated physical dot percentage, a_{phy}, compared to the experimentally measured spectra, for 20, 40 and 60% nominal dot percentage, a_0. Clearly, the estimated spectra are in very good agreement with the corresponding measurements. The middle tones are selected for the comparison because they are far from the constraints, 0 and 100%, and are thus most difficult to predict. The mean and maximum spectral RMS difference between the measured and predicted spectra for all color patches are presented in Tab. I together with the corresponding CIE1976 color differences.

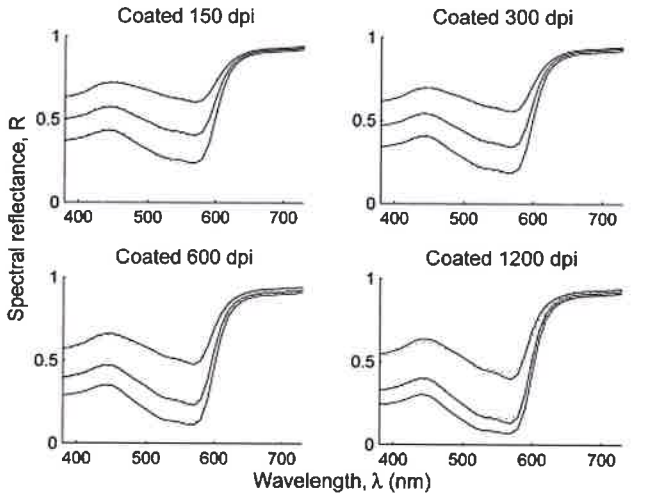

Figure 3:
Computed (dots) and measured (solid line) reflectance spectra for magenta prints on coated paper, with 20, 40 and 60% nominal dot percentages

The good agreement of the spectral predictions even for the lower print resolutions further shows that the assumption of complete light scattering holds surprisingly well, even for a resolution as low as 150 dpi. Recall that the basic assumption in the Clapper Yule model is that the lateral light propagation inside the paper bulk is large compared to the size of the halftone dots, and thus that the probability of light exiting a specific colorant is equal to the colorant coverage [Hersch, et al., 2005]. A 150 dpi halftone gives a dot size of about 0.17 mm, i.e. halftone dots that are no longer small in relation to the length of the lateral scattering of light (typically about 0.1 mm). Nevertheless, the results when employing the Clapper Yule formula according Eq. 1 are still reasonably good.

Table I: Spectral RMS difference and CIE 1976 color difference between predicted and measured spectra

Paper	Resolution	RMS $\times 10^{-4}$		ΔE_{ab}	
		Max	*Mean*	*Max*	*Mean*
Coated	150 dpi	4.51	1.41	5.66	3.17
	300dpi	1.46	0.69	4.16	2.28
	600dpi	0.57	0.22	1.57	2.16
	1200dpi	1.03	0.35	2.16	0.90
Uncoated	150 dpi	2.51	0.47	3.17	1.45
	300dpi	0.52	0.16	1.26	0.65
	600dpi	0.86	0.34	2.34	1.18
	1200dpi	2.44	0.78	4.11	1.68

4.3 Dot gain and print resolution

From the experimental results, it is also obvious that the physical dot gain demonstrates a clear correlation with the print resolution, namely the higher the print resolution (and the smaller the dot), the greater the physical dot gain. When studying the physical dot gain with respect to the print resolutions, it becomes clear that the increase in physical dot gain is proportional to the increase in resolution. For example, the ratio of the physical dot gains is about 1:2:4, for halftones of 150, 300 and 600 dpi, respectively. In additional to the resolution, there is another factor (modulate factor) that affects the physical dot gain, as explained below, which explains why the physical dot gain of the print with 1200dpi is only 50-60% percent bigger than that of the 600 dpi. A comparison of the physical dot gain for the different print resolutions on coated paper is displayed in Fig. 4.

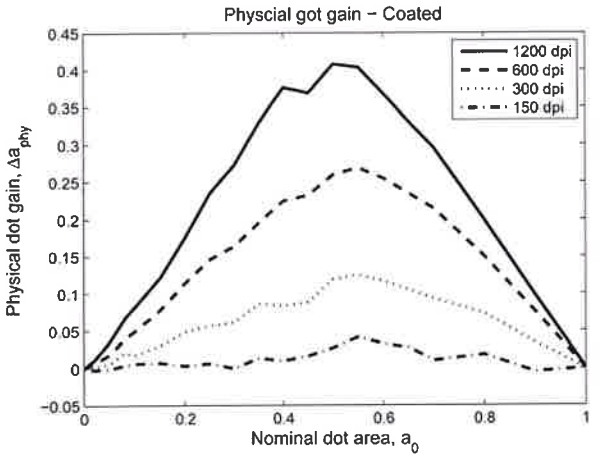

Figure 4: Physical dot gain of magenta prints on coated paper estimated from reflectance spectra, for 150, 300, 600 and 1200 dpi

For simplicity, we explain the observation with FM screening and square halftone dots, which have been used in the test prints employed in this study. It is easy to prove mathematically that the argument also holds for round dots. With FM screening, all the dots are identical and different tone values are achieved by applying different numbers of dots. For a nominal tone value, a_0, the dot area coverage can be expressed as:

$$a_0 = Nd_0^2 \tag{4}$$

where d_0 is the nominal side-length of a single halftone dot and N is the number of dots. According to the definition, the print resolution, l, is inversely proportional to the side length, i.e.

$$l = \frac{1}{d_0} \tag{5}$$

In the case of a physical dot gain with a side-length extension, Δd, the real tone value, a, becomes:

$$\begin{aligned} a &= N(d_0 + \Delta d)^2 \\ &\approx Nd_0^2 + 2Nd_0\Delta d \\ &= a_0 + \Delta a_{phy} \end{aligned} \tag{6}$$

where the physical dot gain, Δa_{phy}, corresponds to:

$$\begin{aligned}\Delta a_{phy} &= 2Nd_0\Delta d \\ &= 2a_0 l \Delta d\end{aligned} \tag{7}$$

Equation 7 indicates that the physical dot gain, Δa_{phy}, is proportional to the nominal tone value, a_0, the print resolution, l, and the side length extension, Δd. The relation of the physical dot gains for two halftone prints of resolutions l_1 and l_2, printed with the same nominal dot area, a_0, will be:

$$\begin{aligned}\frac{\Delta a_{phy,1}}{\Delta a_{phy,2}} &= \frac{2a_0 l_1 \Delta d_1}{2a_0 l_2 \Delta d_2} \\ &= \frac{l_1 \Delta d_1}{l_2 \Delta d_2}\end{aligned} \tag{8}$$

Equation 8 indicates that the ratio of the physical dot gains is proportional to that of the print resolutions, as demonstrated in Fig. 4. The relative side-length extensions, $\Delta d_1/\Delta d_2$, serves as a modulate factor.

4.4 Physical and optical dot gain

Figure 5 depicts the physical dot gain, Δa_{phy}, plotted together with the optical dot gain, Δa_{opt}, and the resulting total dot gain, Δa_{tot}, for coated paper using the various print resolutions. The effective dot area, a_{eff}, has first been computed employing the Murray-Davies formula [Murray, 1936]:

$$a_{eff} = \frac{R_{meas} - R_p}{R_i - R_p} \tag{9}$$

where R_{meas} is the measured spectral reflectance, R_p is the reflectance of the bare paper and R_i the reflectance of the full tone ink. Because of the spectral dependence of optical dot gain, the effective dot area, a_{eff}, was computed as the best fit to spectral reflectance data. The total dot gain, Δa_{tot}, and the optical dot gain, Δa_{opt}, are then given by:

$$\Delta a_{tot} = a_{eff} - a_0 \tag{10}$$

$$\Delta a_{opt} = a_{eff} - a_{phy} \tag{11}$$

From Fig. 5 it is clear that, with the exception of the 150 dpi print where the physical dot gain is almost negligible, the optical dot gain curves are asymmetric with respect to the nominal dot area, a_0. For the higher print resolutions, 600 and 1200 dpi, the optical dot gain curves reach their maxima already at nominal dot areas

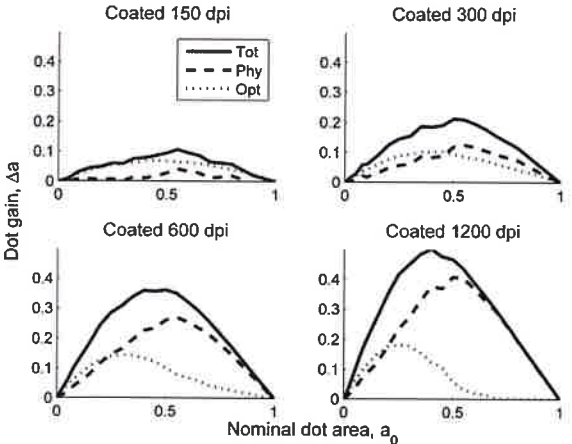

Figure 5:
Total (solid line), physical (dashed line) and optical (dotted line) dot gain for magenta prints on coated paper, using the resolutions 150, 300, 600 and 1200 dpi

about 20 - 25%. The simple reason is that the optical dot gain responds to the physical dot area, including the physical dot gain, rather than the nominal dot area, a_0. In Fig. 6, where the optical dot gain is plotted against the estimated physical dot area, a_{phy}, the curves are clearly symmetric around the maxima at the mid tone a_{phy}= 50%.

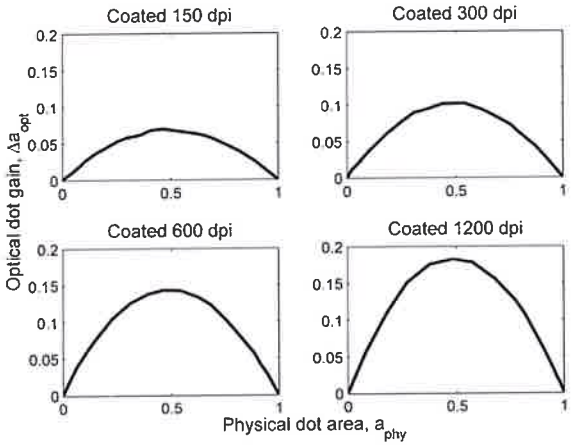

Figure 6:
Optical dot gain, Δaopt, in relation to the physical dot area, aphy, for magenta prints on coated paper, using the resolutions 150, 300, 600 and 1200 dpi

The symmetric form of the optical dot gain vs. the physical dot area around its maximum at a_{phy}= 50% (Fig. 6) is a further indication to the applicability of complete-light-scattering assumption, even for print resolution of 150 dpi. As earlier reported [Yang et al., 2001a], in the case of complete light scattering, the optical dot gain can be expressed as:

$$\Delta R_{opt} = P(1-t)^2 a_{phy}(1-a_{phy}) \tag{12}$$

where P is the quantity describing the probability of light exchanges between the imaged and non-imaged areas and t is the transmittance of the ink. From Fig. 6, one clearly observes that the light-exchange probability, P, intensifies with increasing print resolution, or decreasing dot sizes. When the ratio of the length of the lateral scattering of light compared to the size of the printed halftone dots becomes larger, the probability for light exchange between the inked and non-inked areas increases, and so does the effect of the optical dot gain. The light-exchange probability, P, can be computed if the point spread function (PSF) of the paper substrate is known [Yang et al., 2001a]. This was demonstrated [Yang et al., 2001b] for multicolor prints by employing Gaussian type of PSFs.

The results from Figs. 5 and 6 clearly illustrate the importance of using the correct physical dot area, a_{phy}, instead of the nominal one, a_0, in all attempts of describing or modeling optical dot gain. Thus, accurate methods for separating the physical dot gain from the optical dot gain are essential in all models coping with halftone printing.

5. Summary and further discussions

In this study, three different approaches to determining the physical dot gain in halftone prints, thus separating it from the optical dot gain, have been evaluated. These methods use different inputs: spectral reflectance measurements, transmission scans and microscopic images of halftone prints, respectively, yet produce similar physical-dot-gain estimations. Their good correspondence to the experimental data in terms of spectral estimations confirms the accuracy of the methodologies. However, it should be pointed out that the methods based on reflectance measurements (Eq.1) and on transmission scans (Eq. 3), both assume that the ink transmittance is constant and independent of the dot area coverage, an assumption which may not always hold in practice.

Using line-scans in microscopic images of the prints to estimate the physical dot gain suffered from some problems for the darker tone values in the highest print resolution, when it is no longer possible to accurately determine the edges between dot and paper. Estimating physical dot gain using transmission scans gives a somewhat better result for the coated paper grade compared to uncoated, where the visible paper fibers caused a minor instability. However, compared to spectral measurements using spectrophotometers and microscopic images (where special equipment is required), using a flatbed scanner is a fast and inexpensive alternative to

The fundamental assumption of the Clapper-Yule model is complete light scattering within the substrate, i.e. halftone dots which are small in relation to the lateral scattering length (typically about 0.1 mm). Otherwise, the probability of light exiting from a specific colorant is no longer equal to the colorant area coverage [Hersch, et al., 2005]. Nevertheless, the spectral estimations when applying the model were reasonably accurate even for a FM halftone print with a print resolution as low as 150 dpi, giving a dot size of about 0.17 mm.

To investigate the relation between physical dot gain and halftone dot size, offset prints of FM halftones with different print resolutions were examined. The experimental results revealed a clear correlation between physical dot gain and halftone dot size, with increases in the physical dot gain proportionally to the increase in print resolution. The experimental findings were discussed and explained theoretically; showing that the physical dot gain is proportional to the nominal dot area, the side-length extension and the print resolution. For a more in-depth analysis and discussion on the causes and the physics behind physical dot gain in offset prints, we refer to Yang & Lundström [2007] and Yang [2008].

The optical dot gain responds to the physical dot area (including the physical dot gain) not to the nominal dot area. This was shown by the optical dot gain curves which were highly asymmetric when plotted against the nominal dot area, a_0. When plotted against the estimated physical dot area, a_{phy}, the optical dot gain curves were symmetric around the mid tone a_{phy} = 50%, with increasing optical dot gain for increasing print resolutions (or decreasing halftone dot size) This clearly illustrates the importance of using the correct physical dot area, a_{phy}, instead of the nominal one when describing or modeling optical dot gain. Hence, accurate methods to first estimate the physical dot area, thus separating the physical dot gain from the optical, are essential in all models coping with halftone color prints.

References

1. Arney, J. S., Engeldrum, P. G., Arney, C. D., Katsube, M. (1996), *An MTF analysis of Paper, J. Imaging Sci. Technol. 40(1),* pp19-25
2. Clapper, F. R. & Yule, J. A. C (1953), *Effect of Multiple Internal Reflections on the Densities of Half-Tone Prints on Paper. Journal of the Optical Society of America, vol. 43, no. 7,* pp 600-603
3. Gooran, S., (2001); *High Quality Frequency Modulated Halftoning. Ph.D. Thesis. Dissertation No. 668, Linköping University, Sweden,* 2001
4. Hersch, R. D., Emmel, P., Collaud, F., Créte, F., (2005), *Spectral Reflection and Dot Surface Prediction Models for Color Halftone Prints, J. Electronic Imaging,* 14(3), pp. 33001-330012
5. Murray, A., (1936), *Monochrome reproduction in photoengraving, J Franklin Institute,* 221, 721
6. Nyström, D., (2008a), *A Close-Up Investigation of Halftone Color Prints. Proc. TAGA - Technical Association of the Graphic Arts,* pp 347-363
7. Nyström, D., (2008b), *High Resolution Analysis of Halftone Prints - A Colorimetric and Multispectral Study, Ph.D. thesis, Dissertations No. 1229, Linköping University,* 2008
8. Nyström, D. and Yang, L., (2008), *Dot Gain and Screen Resolution". Proc. IMQA 2008 - The Third International Workshop on Image Media Quality and its Applications,* pp 45-50
9. Rogers, G. L. (1998), *Effect of Light Scatter on Halftone Color. Journal of the Optical Society of America A, vol.* 15, No. 7, pp 1813-1821
10. Rogers, G. L. (2000), *Spectral Model of a Fluorescent Ink Halftone. J. Opt. Soc. Am. A, 17(11),* pp 1975-1981
11. Yang, L., Lenz, R. and Kruse, B., (2001a), *Light Scattering and Ink Penetration Effects on Tone Reproduction. Journal of the Optical Society of America A, vol. 18, No.* 2, pp 360-366
12. Yang, L., Gooran, S. and Kruse, B., (2001b), *Simulation of Optical Dot Gain in Multi-chromatic Tone Reproduction, Journal of Imaging Science and Technology, Vol.* 45, pp 198-204
13. Yang, L. and Lundström, N., (2007), *Physical Dot Gain of Offset: Understanding and Determination. Nordic Pulp and Paper Research Journal, vol. 22, No* 3, pp 388-393
14. Yang, L. (2008), *Estimating Physical Dot Gain in Offset Using a Scanner. Proc. TAGA - Technical Association of the Graphic Arts*
15. Yule J.A.C. Nielsen W.J. (1951), *The Penetration of Light Into Paper and Its Effect on Halftone Reproductions. TAGA Proc.,* 3, pp. 65-76

The effect of tone measure spatial dispersion on the fine detail accuracy at the anew image encoding in the process of screening

Andrey Schadenko and Yuri Kuznetsov

North-West Institute of Printing of the St. Petersburg State University of Technology and Design
13, Jambula Lane, RU-191180, Saint Petersburg, Russia
E-mail: yurivk@mail.ru

Abstract

Fine detail distortion by the halftone dots is investigated with taking into account the quantization errors accompanying the image tone measure spatial dispersion in screening process. The number of these errors correction methods is discussed with illustration of models of test images reproduction.

Keywords: halftone, screening, quantization, sampling, error

1. Introduction and background

To make a hardcopy of continuous tone original the image data are, at least, twice subjected to the encoding procedure in modern graphic data processing environment. Each time it involves the operations of an image spatial sampling and of its tone scale quantization. The first of these encodings takes place at the stage of an input image digital file formation. The scanner or camera resolution defines here the image spatial sampling frequency while the "bit depth" of the device being responsible for the "color depth" of an input file. The image code comprising a "byte map" of multilevel tone values is replaced in further halftoning by the another code to produce the bit map as result of once again spatial sampling the image data, for example, at screen ruling frequency, and of anew quantization the tone value by the discrete alphabet of dispersed or clustered halftone dots, each of the latter being formed by the whole number of tiny microdots.

1.1 Quantizing the tone value in halftone printing

Any spatial sampling is accompanied by the low pass filtration resulting in the loss of an image fine detail within the limits defined by the common propositions of the sampling theory. Fine detail destroying by halftone dots comprises the other, specific kind of image deterioration inherent in screening [1]. The interference of the number of sampling frequencies and their interaction with periodic patterns or textures of an image adds to the latter an unwanted data of different kind of moiré and aliasing.

In continuous tone imaging, such as TV, the quantization scale is positioned in the third dimension, which is orthogonal to an image (x, y) plane (Figure 1a). It has no direct effect on fine detail accuracy or image structure but mostly defines the tone/color rendition of an image stationary area.

The halftone imaging, to the contrary and according to its earlier suggested [2] more or less universal definition, comprises the transformation of an image structure by means of "spatial dispersion of image tone measure among the output pixels to print them bi-level as result of comparison of dispersed value with an input tone one".

As illustrated by figure 1(b, c), the quantization scale of this measure is located in the same plane where the image is spatially sampled thus involving the eternal conflict of autotypie printing in providing both the desired number of reproduced grey levels and appropriate spatial resolution.

Relying on over the hundred years of autotypie practice the ISO 12 647 (2) resolves this trade off on behalf of the first of these requirements by specifying the tone value range of about 4 to 96% for the most kinds of print jobs. With taking into account said priority of an image contrast the screen frequency, which is generally

on the spatial resolution of printing as on an ability of the latter to provide the necessary number of quantization steps within the above mentioned spatially dispersed scale.

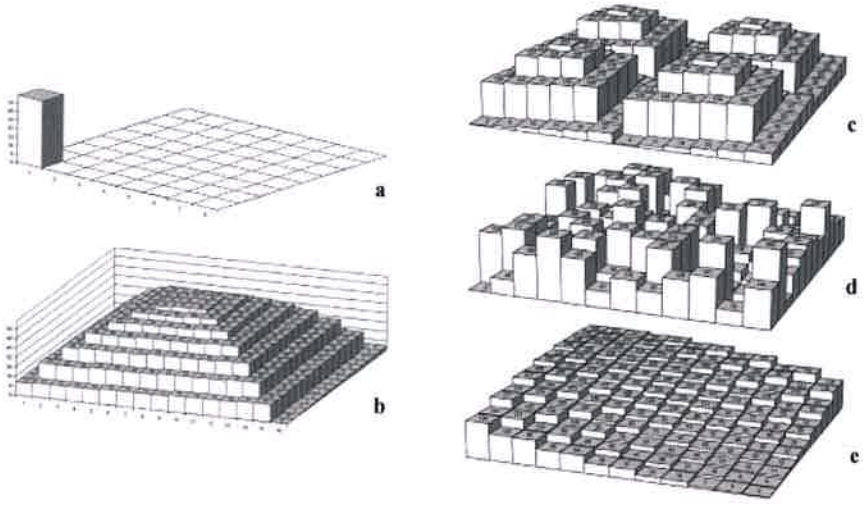

Figure 1: The quantization scale positioned orthogonally to the image plane (a) and variants of its dispersion in the plane of an image (b - e)

1.2 Tone measure spatial dispersion

As shown in table I, the parameters of dispersion such as margins of its spatial bounds, regularity, linearity, discreteness and direction (geometry) strongly correlate to corresponding properties of a halftone image itself or of its structure.

Bounds of dispersion define the print screen period (ruling) finally affecting an image sharpness and definition. The illustrative examples of figure 1 (b - e) relate to the case of beforehand defining the dispersion by the use of corresponding weight or spot functions. However, in locally adaptive and error diffusion screening techniques, which provide the dispersion "on-fly", such spatial period does, nevertheless, exist. It's defined there by the code length of an input pixel. Eight bit input pixel requires, for example, the margins of, at least, 16x16 microdots for adequate presentation of one of its 2^8 quantization levels on a copy.

The comparison of models of figure 1 (a) and (b) shows that about ten fold excess of the output device resolution over the resolution of an input image file is generally required to provide the corresponding print definition. Moreover, the ability of printer to operate by an ink increments corresponding to the size of a microdot in the idealistic bit-map presentation of raster processor should be also taken into account.

Within said physical margins of dispersion bounds the tone measure distribution can be periodic (Figure 1 b, c) or non-periodic (Figure 1 d) resulting correspondingly in regular (AM) or irregular (FM, stochastic) placement of print elements on the picture.

Table I: The parameters of tone scale spatial dispersion and parameters of the screen pattern thereby produced

Dispersion parameter	***Halftone image parameter***
spatial bounds	screen period (definition)
regularity	AM, FM (stochastic
linearity	tone response curve
discreteness	number of grey levels
direction	form of print element, screen geometry

The input image file metric relates to visually uniform optical densities or CIE Lab values which are in logarithmic or cubic degree relationship to the absorbance's (tone values) on a print. So, the dispersed quantization scale should be in the rather strong non-linear connection to that of the input file, requiring, in its turn, the certain excess of dispersion discreteness and, once again, the greater resolution of an output

At last, the symmetry or direction (geography) of dispersion directly defines the form of print element and screen geometry as demonstrated by quantization scale distribution on figure 1 (e) providing the predominantly triangular shape of a halftone dot.

2. Tone value quantization and spatial phase relationships

The basic error, as the metrological characteristic inherent in any quantization process, doesn't directly affect the fine detail quality and mostly results in the so called banding which is visible at the vast image areas of continuously varied tone value. It appears for given input value quantized by the whole quantization scale and takes place in the both of the above mentioned quantization processes. The probability of banding is redoubled here by the earlier discussed non-linear connection of the input and output image data metrics. At scanner/camera encoding it is prevented by the excess of binary digits in analog-to-digital converter (ADC) in relation to eight bit of more or less visually uniform output signal sent to computer. The 16 digits or about 64000 quantization levels per channel are, for example, used in ADC to definitely encode the light intensities transmitted by a slide with its maximal optical densities of about 3.5 - 4.0.

The reverse transformation from 256 visually uniform levels to light intensities (halftone values) on a print undermines the use of 256 x 256 microdot matrix for an each input pixel in the process of screening. However, this formal requirement appears practically easier with taking into account the specific of viewing an image on reflection media, its maximal density lower than 2.0, etc. Nevertheless, from the very beginning of digital electronic screening in 1970ies the spatial margins of tone measure dispersion for high quality halftone printing were bounded in matrixes of up to 30 x 30 microdots requiring as high imagesetter resolution as 5000 dpi.

As far as the quantization scale of digital screening is dispersed in the same image plane where the image signal is two-dimensionally sampled, this quantization introduces its own specific share of error in the reproduction of an image high frequency data. The area or period of this scale distribution doesn't, in general, coincide with that of the input pixel for their mutual position depends not only on the kind of screening but also on such obligatory factors as the input/output media resolutions relationship or on the so called screening (sampling) factor – SF. The latter is varied from a unit (coarse scan/fine print mode) up to over 10 (fine scan/fine print mode). This relationship also depends on the ruling of a screen, its geometry, angle, and other factors.

The investigation of such specific errors and the possible ways of their correction with the use of a computer model of spatially dispersed quantization scales comprise the objective of this research.

Firstly the additional errors which are monotonously changed over the spatial interval occupied by the quantization scale were examined. They arise because this scale is complete just in its full two-dimensional spatial interval. So, just the part thereof may cover the given area of an input tone signal and it also may happen that for the certain input pixels combination all their values are lower of spatially corresponding them quantization levels.

Such examples are modeled on figure 2. The test image (Figure 2a) of these models contains two characters, simulating the line work (LW) original, and a couple of CT textures with each their element being comprised of bell-shape grey level distribution shown by the lower columns on figure 2 (c). The average grey level of an each texture element corresponds to 35% tone value on a print. The screen period or the matrix of quantization scale dispersion is comprised of 12 x12 printer microdots. So, each of them is supplied by the individual multilevel value in an input image file at the SF = 12, i.e. six times higher of that used in common pre-press practice and corresponding to the above mentioned fine scan/fine print reproduction conditions. The textures 1 and 2 are shifted in relation to each other on a half of said period in vertical and horizontal directions.

Figure 2 (b) shows that the texture 2 isn't reproduced on a halftone copy because the all of its input values happen to be lower than corresponding spatially dispersed quantization levels (Figure 2 c). It's clear from this example that the texture of intermediate spatial phase will be somehow reproduced but with distortions due to covering the input texture element signal by just the part of quantization scale and resulting in its non-complete, abrupt presentation of tone signal range. This depends on the relationship of spatial position of tone signal and interval occupied by the scale.

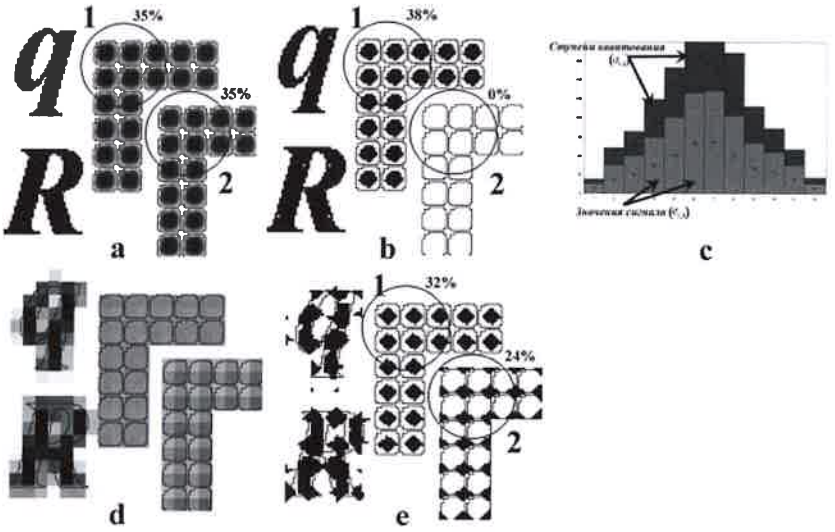

Figure 2: The texture distortion of the continuous tone (CT) original because of the phase shift between the spatially dispersed quantization scale and input image signal in fine scan/fine print mode:

a) test with the textures (1 and 2) both orthogonally shifted on half period at the CT original and corresponding to 35% tone value of halftone copy;
b) halftone copy at SF = 12;
c) the relationship of spatially dispersed quantization levels and input signal values for texture (b);
d) the same 36 times downsampled test at screening factor SF =2;
e) halftone copy produced at SF =2.

One of the possible ways to guarantee the both of these textures reproduction is, for example, to 36 times down sample the input data, i.e. to use the SF of 2 instead of 12. The model of such way down sampled test and its halftone copy are illustrated on figures 2 (d) and 2 (e). The both of textures are reproduced with still recognizable characters. So, this example vividly shows the usefulness of an input data extra redundancy in the commonly used periodic halftoning.

There is the theoretically possible other way to somehow improve the situation, i.e. to make the greater use of the input data excess. It comprises the low pass filtration the input image file with providing the higher, than at SF = 2, number of samples, but with geometry each of the latter matching a certain part of quantization scale. This part is coarser but, however, is complete in its range. The form of such averaged in value input samples may comprise the triangular sectors which are indicated by color on figure 3 (a) on the background of these samples resulting values for one of the texture elements.

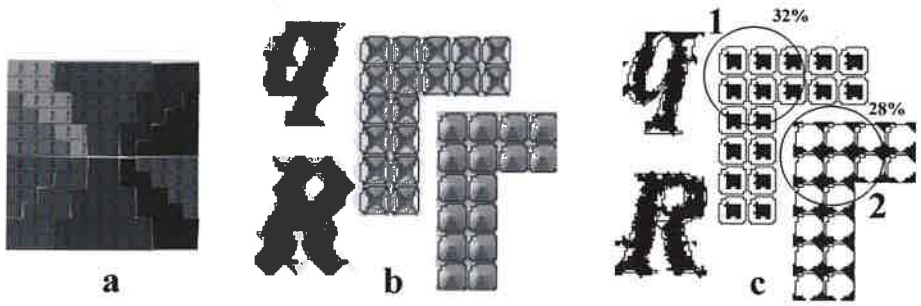

Figure 3: Screening with the use of optimal filtration of high resolution input data: (a) - geometry of spatial filter and segmentation of the whole period of dispersed quantization scale on the background of sampling values of the texture element after filtration; (b) - the signal of the whole test sampled this way; (c) - the halftone copy

With reducing the number of samples by 14.4 times the SF comprises here about 3.3. This way sampled test image is illustrated by Figure 3 (b) and its halftone copy by figure 3 (c). The result of screening shows in this

3. Locally adaptive halftoning

The locally adaptive quantization scale dispersion is used to improve the fine detail reproduction quality. There is, for example, the ready made set of scale distributions of various geometry but about four times shorter length is used in the High Definition Halftone Printing - HDHP technology to provide twice higher halftone print definition and facsimile thin line rendition at the commonly used SF of 2 [3].

The greater SF value or input data redundancy (fine scan/fine print) is theoretically more effectively used in error diffusion screening. However, for over 30 years of its exploring this approach couldn't find wide practical implementation because of providing the non-periodic screen pattern for the stationary image area and thus ignoring physical specific of printing channel [3].

This specific is taken into account by preserving the regular and, so, printable halftone structure for such an area in one of the other of our screening approaches [4]. The method is also intended for the fine scan/fine print reproduction. However, it uses the quantization scale dispersion which is adaptive or variable not to the tone value *itself*, as it takes place in error diffusion screening, but just to the tone value *gradient*. At the same time, it uses, to the contrary to HDHP technology, the dispersion which is adaptive to the arbitrary contour of an image and allows for the complete use of an excessive input resolution in the process of printing as illustrated by the models on figure 4.

The input test comprises here the dark grey character and its lighter background the both to be screened to provide a halftone copy. The 3D presentation of multilevel, for example, 8 bit tone value of this test is given on figure 4 (a), while the figure 4 (c) shows its halftone copy produced with the commonly used periodically dispersed scale of figure 4 (b).

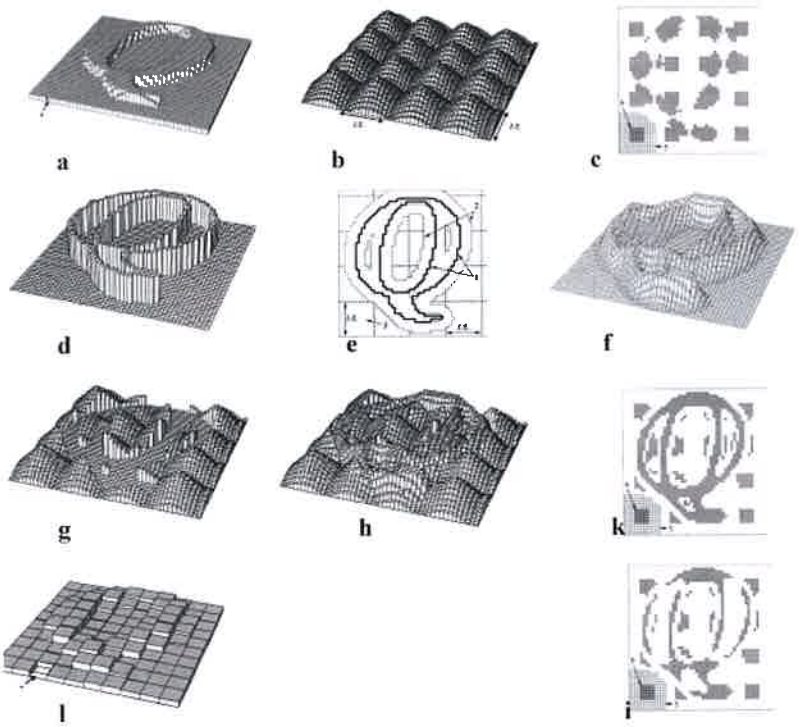

Figure 4: Screening with scale dispersion adaptively to arbitrary image contour.
Variants of: traditional (b) and adaptive (f, g, h) scale distributions; halftone copies (c, k, i); multilevel signals of test (a, l).
The bi-level contour trace signal - (d). Positioning of contour trace signal 1 and bounds 2 of scale dispersion - (e)

To improve an image quality the auxiliary one bit signal of a contour trace or path (Figure 4 d) is generated by marking, for example, the peaks of first spatial derivative of an input tone values in their local neighborhood. The quantization scale dispersion is then provided outward this trace 1 (Figure 4 e) within the bounds 2

the lower ability of human visual system (HVS) to discern grey steps for smaller image details the margins of this dispersion may be much narrower of the period of basic dispersed scale of figure 4 (b) thus providing the coarser quantization. However, such coarser but, nevertheless complete scale is still necessary because the fine detail of the CT original may have the different contrast and tone value the both of these parameters have to be faithfully reproduced on a halftone copy.

With replacing the corresponding part (Figure 4 g) of initial periodic scale of figure 4 (b) by the adaptive one the final scale is provided as shown on figure 4 (h). This combined scale allows for the input image reproduction (Figure 4 k) which is much more accurate than on figure 4 (c) due to the complete use of printing process resolution.

After the presentation of high spatial frequency image data by trace of a contour the input signal can be down sampled by about 100 times (Figure 4 l), i.e. to the volume which is commonly used in coarse scan/fine print way of reproduction. The screening of such file by the adaptively dispersed scale of figure 4 (h) still provide the good rendering of detail as is shown on figure 4 (i). So, there may be recommended the specific two-component compact file format for pre-press image processing which, at the same time, provides the high definition on a halftone print. This file may comprise the down sampled multi-level input data of a whole image in combination with the previously made bit map of counter trace signal.

4. Topologic approach to tone value transformation in screening

Reproduction in graphic industry results in creating the physical image by placing the ink on printing substrate. All the pre-press operations are guided by this final stage and can be brought to it through the common variable of physical volume V of conditional ink placed on ideal substrate. For an each two-dimensional unit image area S_u (Figure 5 a) this volume can be expressed by the ordinate $0 < V < V_{max}$ to consider such presentation as the secondary one which completely matches the original within the limits of its sampling and quantization at the digital encoding stage. According to autotypie principle the same ink volume can be expressed by the area S with a unit ordinate V_{max} (Figure 5 b) which comprises the image signal in form of Boolean numbers plurality (0; 1) instead of multilevel sampling values. However, such form of an input signal can't be directly repeated in real printing process due to its limited resolution.

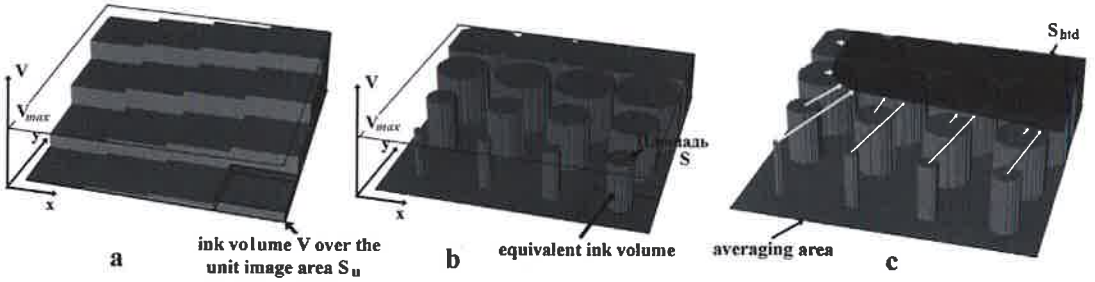

Figure 5: The principles of an image data presentation within its halftone symbol by the amount of conditional ink V:
a) - by ordinate $0 < V < V_{max}$ over unit area S_u of a symbol;
b) - by area S of a unit ordinate V_{max} ;
c) - by grouping the volumes of conditional ink within symbol margins into halftone dot area S_{htd}

There are two operators used in topologic approach for optimal ink distribution over the halftone symbol area [5]. Both of them operate the form of halftone dot as the dependant variable. However, the first of these operators is based on the principle of a halftone dot perimeter minimization for all values of its area thus taking into account the physical specific of real printing channel and thereby to continuously render the image stationary areas. This is performed in conventional way of applying the threshold screen weighting function of the kind illustrated on figure 1 (b) or figure 2 (b). The second, topologic operator provides the sorting of an input image data within the halftone symbol margins to create the, so called, spot function providing the form of a dot precisely matching the image fine detail geometry within a halftone symbol as is schematically shown on figure 5 (c).

The models of test image and its reproduction by the traditional way and with the use of topological approach are given on figure while the results of screening the watermark kind of an image are illustrated on figure 7 in

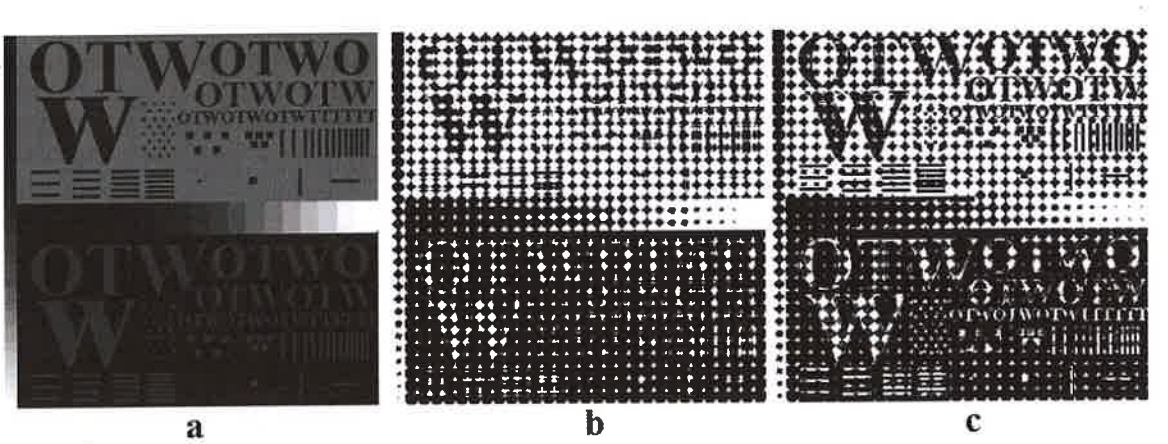

Figure 6: Halftone transformation of test (a) by traditional (b) and topological (c) methods

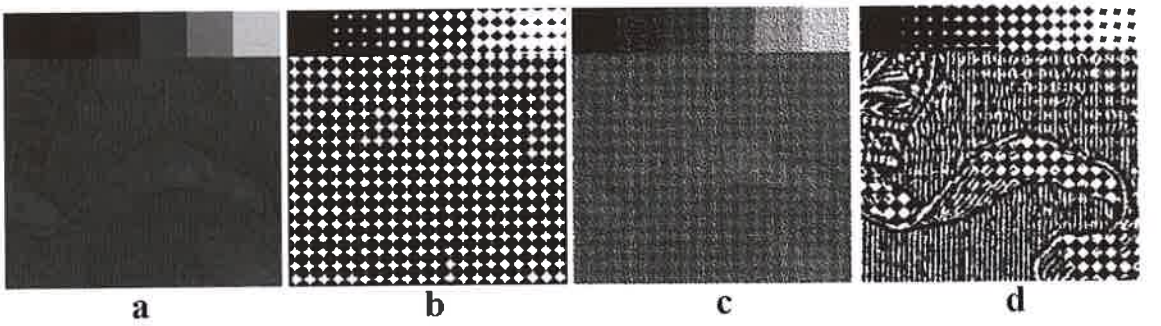

Figure 7: The reproduction example of watermark and engraved area (a) of a banknote by topological screening algorithm (d) as compared to traditional (b) and error diffusion (c) halftoning

As can be seen from figures 6 and 7, this approach provides the greatest accuracy as compared to the other above discussed methods. However, it undermines the use of iterative sorting procedures and that's why is computationally more busy.

5. Conclusions

The parameters of spatial dispersion providing the tone measure quantization scale strongly correlate to corresponding properties of a halftone image and its structure.

Along with the basic metrological error inherent in quantization process there are the specific ones lowering the fine detail reproduction accuracy in screening.

At the fine scan/fine print resolutions relationship these errors can be corrected by the reducing of an input image signal redundancy or by this signal optimal filtration.

The complete use of said redundancy and output resolution can be provided by the tone measure spatial dispersion adaptive to arbitrary contour of an image.

The greater effect can be achieved in topologic approach of sorting the amount of ink within the margins of a halftone symbol.

References

1. Kuznetsov, Y., Zheludev, D., (2008), *Method of objective evaluation the fine detail distortion in process of screening. Proc. of IARIGAI conf., Valencia,* vol. 35, pp. 347-353, 2008
2. Kuznetsov, Y., Schadenko, A., Kostuk, I., Wolneykien, P., (2004), *Combining the advantages of alternative screening modes with image decomposition on continuous tone and line matter constituent parts. IS&T NIP20 Conf. proc., Salt Lake City, Oct.-Nov. 2005,* pp. 632-637
3. Kuznetsov, Y., (2008), *High Definition Halftone Printing - HDHP: Background, Current Status and Challenges of the Adaptive Screening Developments. Proc. of 35 Int. Conf. of IARIGAI, Valencia(Spain), 2008,* pp. 323-331
4. Kuznetsov, Y., Schadenko, A., (2007), *Method for adaptively screening a halftone original and device for carrying out said method. Int. pat. publ.* WO 2007/018448 A1, 2007
5. Schadenko, A., (2009), *Aadaptive screening of an image in autotypie graphic technology. Trans. of Higher Education Institutions, Printing and Publishing Industry, №1, 2009,* pp. 59-68 (Russ.)

Water induced irregularity of halftone dots and its impact on print mottle

Göran Ström[1] and Sandra Madstedt[2]

[1] Innventia AB, Box 5604, SE-11486 Stockholm, Sweden
E-mail: goran.strom@innventia.com

[2] Strålfors Svenska AB, Terminalvägen 14, SE-17300 Solna, Sweden
E-mail: sandra.madstedt@stralfors.se

Abstract

Print mottle is one of the most severe print quality d efects in offset lithography. There are several types of this phenomenon, with back-trap mottle and water interference mottle being the two most important ones.

The dot shape from halftone areas of full scale offset prints that showed water interference print mottle was characterized by image analysis. Measured quantities were areas within the dot area without ink (referred to as white spots), areas outside the dot area that carried ink (black spots) and the increase in dot perimeter (PI) relative to the theoretical value. Good correlations were found between print mottle and PI as well as with the sum of white and black spots. Poor correlation was found when only white spot area or black spot area was considered. A point-wise variation in dot shape, characterized by the coefficient of variation showed no correlation to print mottle.

The content of white spots (but not black spots) decreased with printing impression. Calendering reduced the content of white spots but increased that of black spots. A more open coating structure generated by the use of less latex binder resulted in lower content of black spots and lower content of white spots when the impression was low. Dot non-uniformity expressed as white and black spots is discussed in terms of forced and capillary absorption of fountain solution by the coating, local variations in pressure and excess water acting as weak boundary layer and lubrication layer.

Keywords: print quality, print mottle, offset printing, image analysis

1. Introduction

Unevenness in print density, also referred to as print mottle, is one of the most troublesome print quality defects of offset prints on coated substrates. This problem was more severe two decades ago when starch was widely used as binder. Quite often it was explained by binder migration, and the drying strategy was identified as crucial to obtain a coating surface that showed low tendency to print mottle [Engström et al., 1987; Norrdahl, 1991]. The drying strategy is important also in coatings with latex binder [Kim et al., 1998], and binder migration of latex particles has been identified in coatings with large voids between the mineral particles [Bitla et al. 2003]. The increasing demand for print quality has led to extensive research within this area and a large number of scientific and technical articles are available. Concurrently, with an increased knowledge in the area and use of latex binder the problem has been mitigated but not solved. However, today when the use of starch is increasing due to cost and environmental factors, research in this area is becoming increasingly urgent.

Several types of print mottle have been suggested [Plowman, 1994] due to the many causes of this print defect. The most common ones are back-trap mottle (BTM) and water interference mottle (WIM). The former has been studied extensively, and the most accepted theory today is based on uneven ink setting which results in uneven ink transfer. One of the most convincing pieces of evidence of the relation between uneven ink setting and BTM has been reported by Xiang et al. [1999]. Using especially designed equipment able to measure ink tack on a small spot, the study was able to show that the local variations in tack force correlated with BTM.

The reasons suggested for the uneven ink setting is an uneven pore structure and/or an uneven distribution of latex binder. Evidence of the importance of uniform coating structure for uniform print density has been reported by Preston et al. [2008] and Shen et al. [2005]. Preston et al. [2008] used a new technique [Elton and Preston, 2006a; Elton and Day, 2009] to characterize variation in coating pore structure from variation in refractive index [Elton and Preston, 2006b]. The data on variation in coating porosity showed a very good

correlation with BTM. Shen et al. [2005] showed correlations between BTM and the coating local permeability coefficient, as well as local variations in liquid absorption. A work by Chinga and Helle [2003] showed that coating surface variations in closed areas affected BTM. The correlation between the closed area and BTM increased with increasing size of the closed areas.

Coating thickness variation, which often is a consequence of poor base sheet formation, is frequently considered to be one main reason for uneven pore structure. However, we cannot rule out other causes, such as the aggregation of pigment and latex in the coating layer. A correlation between coating thickness variation and BTM has been reported by Kolseth [2004]. Beside uneven pore structure, BTM is also explained by a high degree of surface roughness. Lares [2003] reported from a pilot coating and printing trial that Bendtsen roughness and topography on the 0.5 to 8 mm length scale strongly correlated with print mottle in a 20% cyan area printed in the second unit out of four.

Water interference print mottle has received much less attention. Identified causes are excessive water feed and unfavourable interaction between the fountain solution and the coating. On the microscopic scale, BTM shows up as areas with more or less ink, whilst areas with WIM show spots where ink is missing completely [Plowman, 1994]. The non-inked spots may be due to poor ink transfer [Shen et al., 2004] or poor ink adhesion, meaning that the ink has been transferred to the paper but lifted off in a subsequent printing unit. The latter phenomenon is currently the subject of research at this laboratory in collaboration with Omya Development. In a recent publication [Kamal et al., 2008] it was shown that a coating with high amount of dispersant (sodium polyacrylate) became more hydrophilic than one containing a low amount, and this coating showed a stronger interaction with water. The ink adhesion to this coating became very low when it had been pre-damped. One reason for this may be the change in the hygroscopic properties of the coating due to the high amount of dispersant.

The unfavourable interaction between the coating and the fountain solution may stem from two origins. Firstly, too slow absorption by the coating of water from the previous printing units, and secondly the chemistry of the surface. It has been shown by Lafaye et al. [1987] that an addition of an anionic surfactant to the coating colour lowered the water contact angle from 90 degrees to about 50 degrees. This resulted in severe WIM in the second unit, while no print mottle was observed in the first unit where no dampening had taken place. Thus, a hydrophilic coating, whether this is induced by the dispersant or a surfactant possibly originating from the latex binder can produce severe WIM problems.

Lie and Kolseth [2007] reported that WIM increased due to pre-dampening but that the mottling could to some extent be reduced by back-trap smoothing, which took place in the subsequent units. Both Lafaye et al. [1987] and Lie and Kolseth [2007] found that WIM increased with printing speed, which is logical since there is then less time for the water to disappear from the surface prior to printing, either through absorption or evaporation.

The data presented in this paper is extracted from a more comprehensive pilot coating and full-scale printing trial. The data is basically an image analysis study of water-induced mottled areas to determine the extent to which dot shape may cause print mottle effects. It was concluded that the observed print mottle was strongly affected by the irregularity of the print dots themselves, rather than by a non-uniform transfer of ink point-wise over a larger scale. Report of the results of the full study will be published elsewhere.

2. Experimental

2.1 Coating formulation

The papers were pilot-coated with a coat weight of 12 g/m^2 and side. This report includes calendered and uncalendered papers with three different coating colour formulations. The only difference between the formulations was the content of latex binder, which was 9 (paper marked 1), 11 (paper marked 2) and 13 (paper marked 3) parts per hundred parts pigment (pph). The binder was a styrene butadiene latex (DL 920) supplied by Dow Europe. It had a particle diameter of 0.14 μm and a glass transition temperature of +13 °C according to the supplier. The pigment was ground calcium carbonate (Carbital 90 supplied by Imerys International) with a broad particle size distribution, where 90% of the pigment mass had a particle size of less than 2 μm as determined by Sedigraph. Carboxymethyl cellulose (FinFix 5 from Metsä Speciality Chemicals, Finland) was used as thickener. The dosage was 0.5 pph.

The base paper (grammage 60 g/m^2) was based on a mixture of chemical and mechanical pulp and was supplied by Husum Mill, M-real Sweden. Blade coating and calendering was done at Vestra in cooperation with Imerys International. The solid contents of the colours were 69.7 - 70.5 wt.-% and coating speed was 1000 m/min. Calendering was done in an 11-nip supercalender at a speed of 300 m/min and a line load of 260 N/m. The sheet gloss values (Tappi gloss at 75° measured by Zehntner, ZLR 1050 M according to ISO 8254-1) after calendering were 51, 52 and 54% for papers 1, 2 and 3 respectively. The gloss values of the uncalendered papers were 17% for all three papers.

2.2 Printing conditions, paper and print quality evaluation

Printing was done on a commercial 6-colour sheet-fed offset printing press, a Heidelberg Speedmaster 74 at a printing speed of 7000 sheets/h and at three impressions, 0.1 mm, 0.18 mm and 0.25 mm. The printing ink was LithoFlora FTX (Akzo Nobel Inks, Sweden, now Flint Group Sweden AB). The dampening water contained 2% Aqualith (Akzo Nobel Inks, Sweden) and 8% isopropyl alcohol. One test point was run at a 15% reduced water feed.

The halftone dot area of the second print unit (cyan) and that of the fifth unit (also cyan) were analysed with respect to print mottle. Print mottle (STFI mottle [Johansson, 1993]) is defined as an average coefficient of variation in the 1 - 8 mm frequency band. The coefficient of variation is the standard deviation of reflectance relative to the mean reflectance level of the print.

2.3 Image analysis of dot shape

Halftone areas printed in the fifth nip at a print impression of 0.1 mm and 0.25 mm were subjected to a microscope and image analysis study to characterize the dot uniformity.

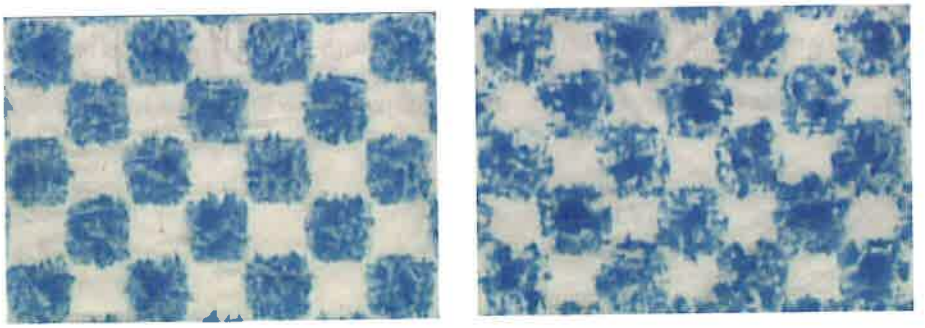

Figure 1: Microscopic images of 50% raster taken with a magnification of 50 times

Figure 1 shows examples of halftone dots from the study. The left picture shows dots with uniform shape. This print had a low print mottle value (1.2%). The dots in the right picture are much more non-uniform, and the print had a high print mottle value (2.7%).

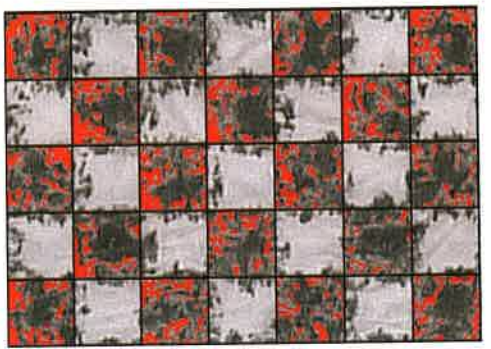

Figure 2:
Illustration of the image analysis procedure to quantify white and black spot areas. The squared grids are 42 x 42 pixels (130 x 130 µm). The white spot areas are marked with red. Black spots are the ink outside the grids. The content of white spot area was 20% while that of black spot area was 21%

A squared grid was fitted to the microscope images prior to the image analysis. An example is shown in *Figure 2*. This is the same image as the right one in Figure 1. Areas within the squared dot area that did not carry ink were identified. These areas are referred to as "white spots". Areas of ink outside the squared dot area were also determined and are referred to as "black spots" even though the process colour was cyan. Four sub-areas on five different sheets i.e. twenty areas having a size of 7 x 5 raster dots (as illustrated in Figure 2) were counted for each print. Mean values of areas of white spots and black spots, as well as the coefficient of variation (CoV) of the mean values of the 20 sub-areas, were calculated.

Characterization of dot perimeter is illustrated in *Figure 3*. Fifty raster dots on five different sub-areas (i.e. 250 dots) were counted for each print. A value of the percentage increase in perimeter (PI, short of perimeter increase) is given. This is defined as follows:

$$PI = 100\ (A_p/T_p - 1),$$

where A_p is the number of actually measured pixels and T_p is the theoretical number of pixels, which was 168 (i.e. 4x42). Mean values and coefficient of variations were calculated. The CoV was calculated on A_p, not *PI*. It is given for all 250 measured dots as well as for the mean values of the sub-areas.

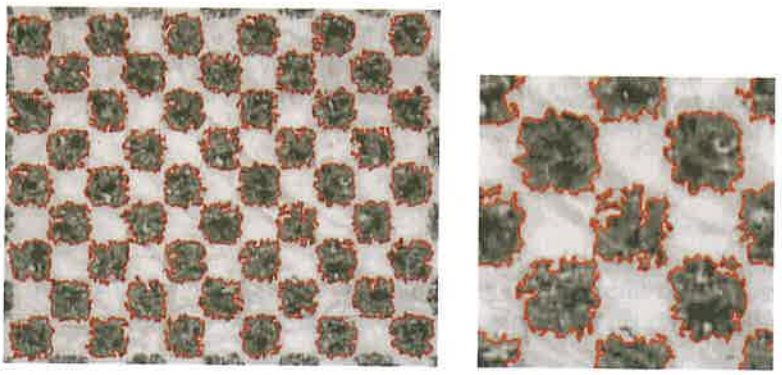

Figure 3: Illustration of the image analysis procedure to quantify dot perimeter. The left image shows the 50 dots characterized on each sub-area (1.43 x 1.17 mm). Five sub-areas were measured for each print. The enlargement in the right image shows quite a large difference in perimeter for dots close to each other

3. Results and discussion

3.1 Print mottle in the second and fifth units

Figure 4 shows print mottle in the second and fifth print units for the six different papers, and at three different impressions. It is clear that the highest print mottle was obtained in the fifth unit and at a low printing impression with the paper that contained the highest amount of latex. A number of observations led to the conclusion that the print mottle could be classified as water interference mottle. These were:

- The appearance of white spots, which is characteristic for WIM [Plowman 1994].
- Print mottle in the fifth print unit cannot be BTM since this was the last unit.
- When ink is transferred in the fifth unit, the surface had been exposed to dampening five times before printing. Thus, a high amount of water had been transferred to the surface.
- When the water feed was reduced by 15%, the print mottle in the fifth unit disappeared.
- The print mottle in the second unit was very low. However, it could have been higher directly after this unit but reduced by back-trap smoothing as was found by Lie and Kolseth [2007].

3.2 White and black spots in relation to printing impression and coating properties

The effect of printing impressions and paper properties on the content of spots was quite different for white spots as compared to black spots. *Figure 5* shows that print impression had a strong effect on the content of white spots but only a slight effect on that of black spots. It is interesting to note that calendering reduced the content of white spots but increased the content of black spots.

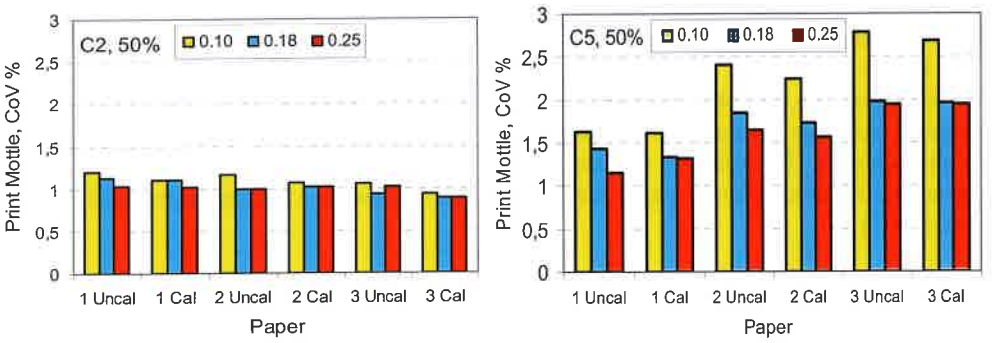

Figure 4: Print mottle of prints from the second unit (left) and fifth unit (right) at three impressions. The latex content of the coatings was 9 pph, 11 pph and 13 pph for papers 1, 2 and 3, respectively

The effect of latex, which influences coating porosity can be evaluated by comparing paper 1 (low latex content and high porosity) with paper 3 (higher latex content and lower porosity). The latex content had no effect on white spots at high printing impressions. In all other cases, lower porosity due to higher latex content had a detrimental effect, since there were higher numbers of both black and white spots for prints on the less porous coatings. Low coating porosity generated by low amount of latex appears to be an advantage in reducing WIM, but unfortunately, decreasing coating porosity results in faster ink setting [Ström and Karathanasis, 2008] which may cause problems with back-trap mottle and ink piling.

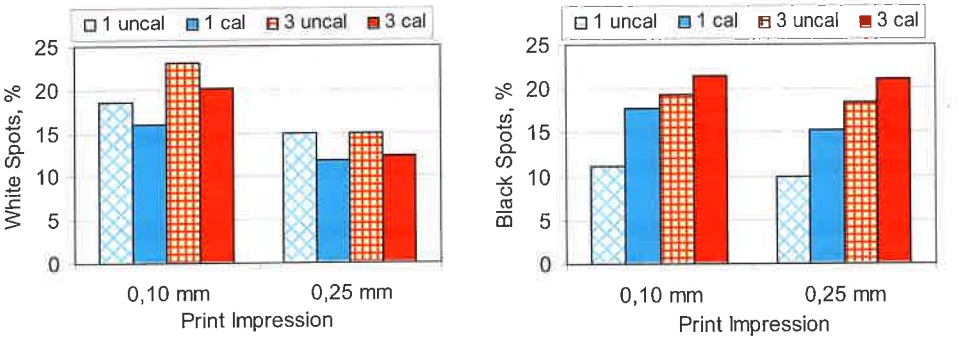

Figure 5: White (left) and black (right) spot areas within the prints of the different papers printed at two different print impressions

An indication of the porosity of the coatings due to increased latex content can be obtained from laboratory coatings laid on a polymer film, dried at 95°C and subjected to mercury porosimetry [Ström and Karathanasis, 2008]. This work suggests a difference in porosity of 4 absolute percentage units between the two coatings (i.e. a coating with 9 pph latex obtained a porosity of 27% while one with 13 pph latex obtained a porosity of 23%).

Coating porosity is also affected by calendaring. According to Johnson et al. [1999], the porosity of a coating increases in the following order: calendered coating laid on base paper < coating laid on plastic film < uncalendered coating laid on a base paper. The coating may have lost 15 - 20% of its porosity due to calendering [Johnsson et al., 1999; Larsson et al., 2007] which indicates the same order of magnitude as the loss of porosity due to an increase of latex content from 9 to 13 pph. The effect of calendaring will be discussed below in terms of variation in water film thickness and local pressure.

Shen et al. [2004] stresses the importance of a weak boundary layer of water for ink transfer in offset printing. A thin layer of water will cause ink refusal. It is reasonable to assume that the content of white spots depends on how efficiently the dampening water is removed (disappears) from the surface prior to contact with the ink. A high coating porosity will promote capillary absorption of the surface water, and a high printing impression will push the surface water into the coating so the ink comes into contact with a water-free surface. The effect of the printing impression on white spots was clearly demonstrated (left diagram in Figure 5). Thus, pushing the water away from the surface, either by pushing it into the coating or laterally away from the area to be printed,

The effect of porosity is not seen for the high impression which might mean that forced absorption dominates over spontaneous absorption, a conclusion that was also demonstrated by Sandås and Salminen [1987]. Forced absorption is largely determined by coating permeability. Both capillary absorption and permeability are promoted by high porosity, but show different degrees of impact on pore size. Small pores result in higher capillary pressure, and thus favour capillary absorption, while large pores result in lower flow resistance and thus favour permeability. The relative importance of coating capillarity and permeability, and base paper absorption potential for absorption of a thin film of fountain solution on a coating has resently been discussed by Gane et al. [2007].

A reversed effect of porosity at high impressions was observed; the content of white spots was lower on the calendered papers which should have had a lower porosity due to the calendering.

The lower content of white spots on calendered papers may instead be a result of a smoother paper. High macro roughness will result in strong variations of local pressure (i.e. the actual point-to-point pressure over the surface) [Endres and Tietz, 2007], and this pressure is indeed important for the content of white spots. When pressure was low (print impression 0.1 mm), we observed a strong impact of coating porosity, increasing the significance of capillary absorption.

To summarize, the forced removal of dampening water is important, and if the paper is very rough, the local pressure may be too low for efficient removal. The areas that are exposed to low pressure will show shallow depressions and thicker water films. The work of Shen et al. [2004] has shown that water film thickness determines ink transfer to a moist surface. A thick water film will form a weak boundary layer that prevents ink from being transferred. At low pressure (overall or locally) capillary absorption therefore becomes important.

Print impression showed no impact on black spot area, but calendering and porosity due to latex content did. The presence of black spots means that ink is pushed out from the raster dot area (i.e. the ink slides out from its pre-determined area). Such behaviour would be more pronounced on the inlet side of the printing nip. To some extent, this is indicated in Figure 2 and other figures not shown here. We observed a tendency that black spots, to a greater extent, were located on one side of the dot, the right side in Figure 2.

This observation would support the suggestion that ink slides out from the dot. Such sliding would be increased by the presence of surface water, which makes the surface more slippery. The thickness of the water film and its local variations must have a significant influence. Due to the macro roughness of the coating and non-uniformity in absorption, the thickness of the water film is most likely non-uniform. Uncalendered papers showed lower area of black spots compared to calendered papers. An uncalendered paper, due to its higher roughness, would have features that protrude from the water film and may act as ink adhering spots. (A smooth layer of ice is more slippery than one containing small protruding stones).

3.3 Print mottle and dot shape uniformity

Non-uniformity of raster dots was quantified as the content of white spots, black spots, sum of white and black spots as well as the dot perimeter. These measures were then compared to print mottle, measured on the halftone area of the fifth unit. There was little correlation between print mottle and areas of white or black spots. The curves in *Figure 6* show a correlation coefficient slightly higher than 0.5. However, when print mottle was plotted against the sum of white spot and black spot areas, the correlation was very high, $R^2 = 0.96$ as shown in *Figure 7*. No correlation was found for print mottle and the difference between black and white spot areas, which would represent ink coverage.

The coefficients of variation for white spot area were typically between 9% and 12%, while that of black spot area were between 7% and 12%. One point had an extraordinary high coefficient of variation, 20% for white spot area and 15% for black spot area. This was the point that falls below the line in Figure 7.

The irregularity of the halftone dots was also characterized by the increase in dot perimeters. The value is given as the percentage increase from the theoretical value. This measure does not consider white spots in the interior of the dot. Only white spots on the circumference of the dot, together with black spots, will be included in the value. The diagrams in *Figure 8* show that the perimeter increase (PI) correlated poorly with black or white spot area, although there was a somewhat higher correlations with black spot area.

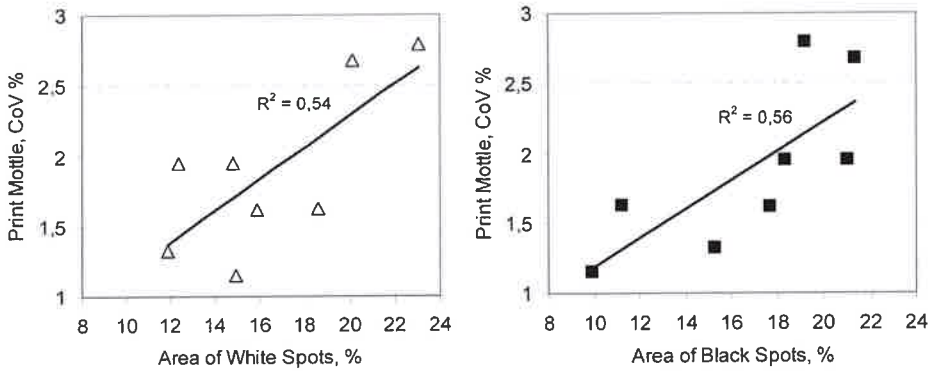

Figure 6: Print mottle of halftone area printed in the fifth unit vs. the area of white (left) or black (right) spots. The correlation is low

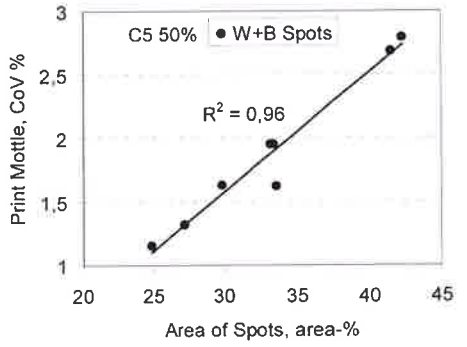

Figure 7: Print mottle of halftone area printed in the fifth unit shows strong correlation with non-uniformity of raster dots, expressed as white and black spot areas

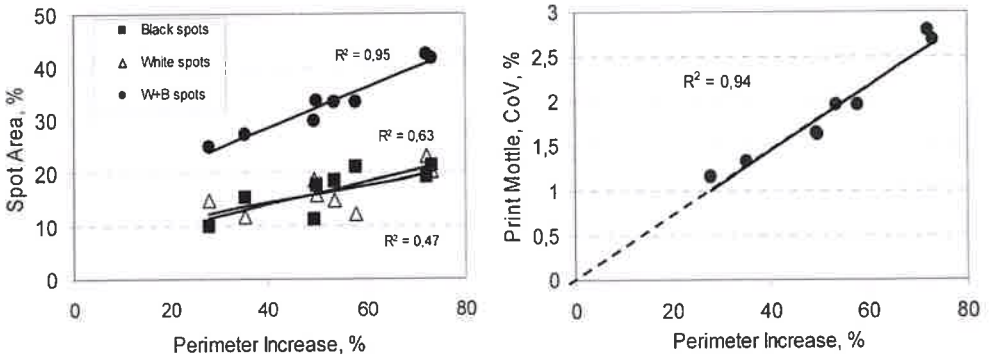

Figure 8: Correlation between areas of spot and perimeter increase (left) and the correlation between print mottle and perimeter increase of halftone dots (right)

However, PI showed strong correlation to the sum of white and black areas, as well as to print mottle. It is interesting to note that an extrapolation to zero increase in the perimeter goes through the origin, meaning that a perfect dot shape results in no print mottle even though there can be some white spots in the dot. These observations suggest that white spots in the interior of the raster dots have less influence on print mottle than the ones located on the circumference and/or that they represents a smaller area.

3.4 Effect of local print dot non-uniformity on print mottle

We have shown a good correlation between print mottle and non-uniformity in dot shape when the non-uniformity was expressed either as the sum of white and black spot areas or as the increase in dot perimeter. Since it is believed that print mottle is due to non-uniformity in ink amount over the print on a mm scale it is reasonable to believe that the non-uniformity in dot shape also changes over the surface (i.e. a point-wise difference), and that this would be the primary reason for the measured print mottle. In order to cover this

aspect, this investigation included measurement of 20 sub-areas where white and black spots were determined, and five sub-areas where the perimeter was determined. The sizes of the sub-areas were 0.13 x 0.13 mm for the spot area characterization and 1.43 x 1.17 mm for the perimeter characterization. The point-wise difference in these values was quantified by the coefficient of variation, i.e. the standard deviation divided by the mean value.

The CoV of white spots for 20 different sub-areas of the six prints were 9.3, 11.3, 11.4, 11.5, 10, 7, 12.2, 14.0 and 20.7%. The values for black spots were 6.6, 7.3, 9.6, 10.1, 10.4, 12.1, 12.1 and 15.0%. These values as well as the sum of the value of white and black spots were plotted against the corresponding print mottle value. The result is given in the left diagram of *Figure 9,* with no correlation being found. Thus, the point-wise variation in print dot uniformity expressed as white and black spot areas had no impact on the measured print mottle.

A corresponding plot, but now with dot uniformity expressed as dot perimeter, is shown in the right diagram. Again, no correlation was found. The low CoV for the mean values of the dot perimeters of the different sub-areas show that the point-wise dot uniformity did not change much. Thus, the mean value of 50 dots taken at different positions over the print had roughly the same value.

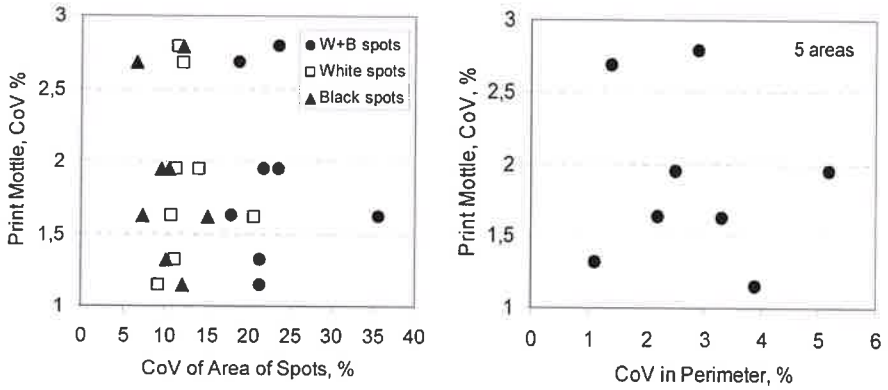

Figure 9: Print mottle showed no correlation to a point-wise variation in dot uniformity. Left diagram shows the effect of CoV of mean values of 20 sub-areas, while the right diagram shows that of 5 sub-areas

However, a correlation between print mottle and CoV in perimeter was found when all 250 dots were included in the calculation, as can be seen in *Figure 10.* This is not a point-wise variation. It is rather a variation in dot shape, meaning that for one print, the dot uniformity varied a great deal from dot to dot. This variation increased with greater dot shape non-uniformity expressed as PI as shown in the right diagram of Figure 10. Expressed somewhat differently, when the dots became more irregular, the variation in irregularity among the dots increased.

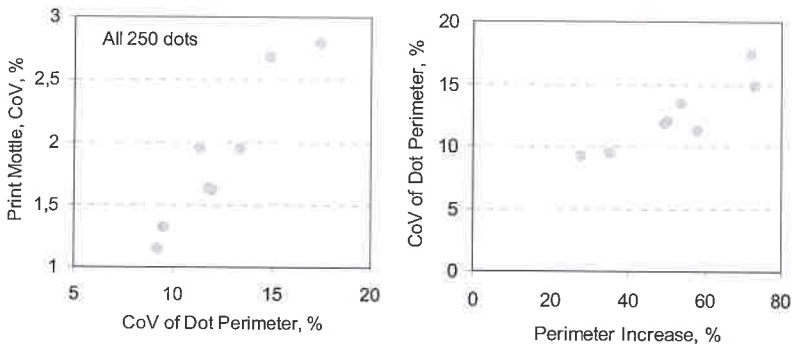

Figure 10: Print mottle showed good correlation to coefficient of variation in dot perimeter (left diagram). The uniformity between dots expressed as CoV of dot perimeter increased with the average PI of the 250 dots analyzed by print (right diagram)

4. Conclusions

This work has shown that an increased amount of latex binder in the coating and a decreased impression during full scale sheet-fed offset printing induced water interference print mottle (WIM) in the fifth printing unit. WIM

was strongly influenced by the amount of fountain solution. Print mottle was low for prints in the second nip where the paper had been damped by the fountain solution only once, while it was high in prints produced in the fifth nip where the paper had been damped four times. Furthermore, a reduction of the water feed strongly reduced the print mottle in the fifth nip.

The dot shape of halftone prints from the fifth unit was analyzed with respect to dot uniformity using microscopy and image analysis. The dot shape was quantified in terms of perimeter increase, white spot area (i.e. area within the dot area without ink) and black spot area (area outside the dot area with ink). WIM strongly correlated with the non-uniformity of the dot shape when the dot shape was quantified either as the sum of white and black spot areas or as perimeter increase. The point-wise variation of the mean value of dot shape for a small sub-area showed no correlation to print mottle.

Print mottle not only correlated with the perimeter increase, but also with the variation in single dot perimeter when this was quantified as the coefficient of variation. It was not possible to decouple the average non-uniformity in dot shape from the variation in dot shape since a print with dots of higher irregularity also showed greater dot shape variation from dot to dot.

The occurrence of black and white spots depended on print impression, coating roughness and coating absorption potential. It is suggested that surface water (non-absorbed water) may act as a weak boundary layer and prevent ink from being transferred, which would result in white spots, and as a lubricating layer that promotes the sliding of ink out of the dot area, thus causing black spots. Both effects are strongly influenced by water film thickness, a property that varies over the surface. The local variation in thickness will depend on coating roughness and uniformity in porosity.

Acknowledgement

The authors acknowledge the assistance of Imerys Minerals in financing the coating trial, and of Janet Preston (Imerys) and Michael Karathanasis (Innventia) for their cooperation during the coating and printing trial. We also thank Stora Enso, M-real, Norske Skog, Arctic Paper, Korsnäs, Frövi, Kemira and Voith for financial support of the printing trial, and Vinnova, for financing the microscopy and image analysis of dot non-uniformity.

References

1. Bitla, S., Tripp, C. P. and Bousfield, D. W., (2003): *A Raman spectroscopic study of migration in paper coatings. JPPS 29(11),* pp. 382-385
2. Chinga, G. and Helle (2003): *T. Relationship between the coating surface structural variation and print quality.* JPPS 29(6):179-184
3. Elton, N. J. and Day, J. C. C., (2009): *A reflectometer for the combined measurement of refractive index, microroughness, macroroughness and gloss of low-extinction surfaces. Meas. Sci. Techn.* 20, 025309, (11pp)
4. Elton, N. J. and Preston, J. S., (2006a): *Polarized light refractometry for studies of paper coating structure, Part I. Method and instrumentation.* Tappi J 5(7), pp. 8-15
5. Elton, N. J. and Preston, J. S., (2006b): *Polarized light refractometry for studies of paper coating structure, Part II. Application to coating structure, gloss and porosity.* Tappi J 5(8), pp. 10-15
6. Endres, I. and Tietz, M., (2007): *Blade, film and curtain coating techniques and their influences on paper surface characteristics.* Tappi J, 6(11) pp. 24-32
7. Engström, G., Ström, G. and Norrdahl, P., (1987): *Studies of the drying process and its effect on binder migration and offset mottle.* Tappi J, 70:12, pp. 45-49
8. Gane, P. A. C., Ridgway, C. J., Burry, P., Arnold, M., Kagerer, K.-H., Madden, B., Ristolainen, M. and Purontaus, J., (2007): *Aquapiling: Coated substrate-related influences on reverse piling from a one-side single colour image in multicolour offset printing. In Advances in printing and media technology, Ed. N Edlund and M Lovrecek, Acta Graphica Publishers* ISBN 978-953-7292-04-1, Zagreb, pp 31-48
9. Johansson, P.-Å. (1993): *Print mottle evaluation by band-pass image analysis, In Advances in Printing Science and Technology,* pp. 403-413, W. H. Banks Ed., Pentech Press.
10. Johnson, R. W., Abrams, L., Maynard, R. B. and Amick, T. J. (1999): *Use of mercury porosimetry to characterize pore structure and model end-use properties of coated papers-Part i: Optical and strength properties.* Tappi J 82:1, pp. 239-251

11. Kim, L. H., Pollock, M. J., Wittbrodt, E. L., Roper III, J. A., Smith, D. A., Stolarz, J. W., Rolf, M. J., Green, T. J. and Langolf, B. J., (1998): *Reduction of back-trap mottle through optimization of the drying process for paper coatings, part I.* Tappi J, 81:8, pp. 153-163
12. Kamal, H., Ström, G., Schoelkopf, J. and. Gane, P. A. C., (2008): *Characterization of ink adhesion failure; effect of pre-dampening of carbonate containing coatings.* In: proc. from *10th Advanced Coating Fundamentals Symposium,* P 228-241 Montreal, Canada, June 11-13
13. Kolseth, P., (2004): *Coating structure and print quality.* Paper presented at *New Concepts in Paper Surface Treatment, Stockholm, October 19-20, 2004.* (Data also given in Ström G: *Interaction between offset ink and coated paper - a review of the present understanding. In: Proceedings from the 13th Fundamental Research Symposium, Cambridge, UK, September 2005*
14. Lafaye, J. F., Maume, J. P., Gervason, G. and Piette, P., (1987): *Some aspects of coating with surfactant upon quality and offset printability. In proc. from Tappi 1987 Coating Conference,* pp107-115
15. Lares, M., (2003): *Basestock influences on coated board surface and print quality. In proc. Tappi 2003 Spring Technical Conference & Trade Fair*
16. Larsson, M., Vidal, D., Engström, G. and Zou, X. (2007): *Paper coating properties as affected by pigment blending and calendering.* Tappi J 6:8 pp. 16-22
17. Lie, C. and Kolseth, P. (2007): *Aspects of water-induced mottle when printing on coated paper in sheet-fed lithographic offset. In Advances in printing and media technology, Ed. N Edlund and M Lovrecek, Acta Graphica Publishers* ISBN 978-953-7292-04-1, Zagreb, pp 59-67
18. Norrdahl, P. C., (1991): *Effect of drying conditions on the quality of wood-containing lightweight coated paper.* Tappi J, May pp 73-78
19. Plowman Sandreuter, N., (1994): *Predicting print mottle: A method of differentiating between three distinctively different types of mottle: Back-trap mottle, water sensitivity mottle and wet ink trappimg mottle. In proc. from Tappi 1994 Coating Conference San Diego,* USA May 1-5
20. Preston, J. S., Hiorns, A. G., Elton, N., Ström, G., (2008): *Application of Imaging Reflectometry to Studies of Print Mottle on Commercially Printed Coated Papers. Tappi J, vol.7 No. 1,* Jan 08 pp 11-18
21. Sandås, P. E. and Salminen, P. J. (1987): *Water penetration in coated papers. In proc. 1987 Tappi Coating Conference, Houston, USA, May 17-21,* pp. 97-101
22. Shen, W., Hutton, B. and Liu, F., (2004): *A new understanding on the mechanism of fountain solution in prevention of ink transfer to the non-image area in conventional offset lithography, J. Adhesion Sci. Technol. 18(15-16),* pp. 1861-1887
23. Shen, Y., Bousfield, D. W., van Heiningen, A. and Donigian, D. (2005): *Linkage between coating absorption uniformity and print mottle.* JPPS 31(3), 105
24. Ström, G. and Karathanasis, M., (2008): *Ink setting on coated media-Importance of pore structure and latex content, In proc. 2nd Intern. Papermaking & Environmental Conf., Tianjin,* P. R. China pp. 894-900, 2008
25. Xiang, Y., Bousfield, D. W., Hassler, J., Coleman, P. and Osgood, A., (1999): *Measurement of local variation of ink tack dynamics. JPPS 25:9,* pp 326-330

Quality prediction of printed photographs using computational and instrumental methods

Raisa Halonen[1], Tuomas Leisti[2], Pirkko Oittinen[1]

[1] Department of Media Technology, Helsinki University of Technology
P. O. Box 5500, FIN-02015 TKK, Finland
E-mails: raisa.halonen@tkk.fi, pirkko.oittinen@tkk.fi

[2] Department of Psychology, University of Helsinki
P. O. Box 9, FIN-00014 University of Helsinki, Finland
E-mail: tuomas.leisti@helsinki.fi

Abstract

The growth of on-demand and home printing has created new needs for paper producers to specify the quality potential of paper using metrics which are relevant to end-users. This study is a part of research which aims at developing a quality model and index for the visual quality of digitally printed photographs. In the study, the subjective quality of printed photographs is predicted using regression analysis with instrumental measurements from prints and computational quality attribute values separately as predictors. As the quality attributes are computed without a reference, both positive (contrast, colourfulness) and negative (blur, noise) attributes can be used for the prediction of subjective print quality. This creates a preferential model as opposed to the typical distortion models of image quality. To meet the objective, the sample set used in the study includes ink-jet and electrophotographic prints made on a wide range of papers. The results of the study suggest that the subjective quality of printed photographs can be predicted to a reasonable extent using quality attributes computed from digitized prints or instrumental measurements from objective test fields. The models given by the regression analysis clearly depended on the analyzed image content. This was seen in the set of included variables as well as the goodness-of-fit of the models.

Keywords: electrophotography, ink-jet, print quality, paper grade, image quality model

1. Introduction

This study is a part of research which focuses on printed image quality with applications in quality measurement and use of quality data in the development of coated and uncoated papers and printing in different digital methods. This is for the purpose of developing a quality model and index for the visual quality of digitally printed photographs in a collaborative project [Oittinen et al. 2008; Pulla et al. 2008; Eerola et al. 2008a, 2008b]. The standpoint is that of paper. The work has analogy with efforts ongoing in the printer systems [Zeise et al. 2008] and mobile camera (I3A 2007) communities from the respective perspectives.

The study approaches the concept of subjective print quality with a five-layer hierarchy shown in Table I. The final quality model will consist of the four highest layers, thereby excluding paper properties. The role of paper properties in predicting the subjective quality of printed photographs has been studied separately in the project. This study evaluates the feasibility of instrumental measurements from prints (Layer 2) and respective computational quality metrics (Layer 3) for the overall print quality prediction.

Table I: Quality hierarchy (from left to right) considered in this study

Layer 1	Layer 2	Layer 3	Layer 4	Layer 5
Instrumental measurements from papers	Instrumental measurements from prints	Computational quality attributes	Subjective quality attributes	Subjective print quality
Factors				
Brightness, whiteness, roughness, gloss etc.	Edge sharpness, RMS noise, K100 density, colour gamut etc.	Blur, noise, contrast, colourfulness etc.	Sharpness, graininess, contrast, colourfulness etc.	MOS

The literature on computational image quality metrics developed for digital images is abundant, but such metrics have not been used in the context of printed images. Computational quality metrics can be used to either predict the overall quality of the image or to represent human perception of a specific quality attribute in the image. Examples of image quality metrics for specific attributes can be found for blur in Marziliano et al. [2002], Ferzli and Garam [2007], and Crete et al. [2007], for noise in Olsen [1993], Immerkær [1996], and Tai and Yang [2008], for contrast in Peli [1990], Bex and Makoux [2002], and Frazor and Geisler [2005], and for colourfulness in Fedorovskaya et al. [1997], Yendrikhovskij et al. [1998], and Hasler and Süsstrunk [2003].

Computational image quality metrics can be classified based on the availability of a reference, i.e. an original image considered to be of perfect quality or distortion-free [Wang & Bovik 2006]. Image quality metrics can be full-reference, no-reference or reduced-reference metrics. In reduced-reference metrics, certain features can be extracted from the reference image and employed as side information to help the quality assessment. The studied metrics operate without a reference. No-reference metrics are of interest as it is desired that the developed quality model would be applicable to any given image content printed on any paper by any digital method.

In the study, the subjective quality of printed photographs is predicted using regression analysis with the computational quality metrics and instrumental measurements from prints separately as predictors. As the quality attributes are computed without a reference, both positive (contrast, colourfulness) and negative (blur, noise) attributes can be used for the prediction of subjective print quality. This creates a preferential model as opposed to the typical distortion models of image quality. To meet the objective the sample set used in the study includes ink-jet and electrophotographic prints made on a wide range of papers.

2. Methods

A series of samples was prepared for the study. The test layout covering two A4 sheets included three photographs (Figure 1) and test fields. The chosen image contents included typical content types such as objects with details (*cactus*), a human portrait (*man*) and a landscape (*lake*). The test fields consisted of full-tone CMYK patches, a large 50% gray patch, RGB and CMYK wedges with 10% increments from 10% to full tone, and vertical and horizontal lines with a width of 1 - 10 pixels (one pixel increments).



Figure 1: The different contents of the photographs used in the study

The photographs were captured by a semi-professional photographer using a professional digital camera. Several content-related requirements were considered in photographing the images [Salmi et al. 2009]. In the images, versatile memory colors, e.g. skin, sky and foliage, as well as memory shapes, e.g. a human face and a cactus, were included. Different types of surface materials from smooth and shiny, e.g. fabric and porcelain, to detailed and textured, e.g. a zipper and rock, were also considered. All photographs had a considerable amount of detail, e.g. cactus spikes, human hair and tree leaves. Moreover, perceptual and aesthetical aspects were considered.

Desired variation in paper properties was achieved by selecting 36 different papers for the study: 15 electrophotographic (EPG), 6 multipurpose (MP) and 15 ink-jet (IJ) papers. Electrophotographic and ink-jet papers were printed using their respective printing methods and multipurpose papers with both. Table II presents

Table II: The variation in paper and print characteristics in the test series [Halonen et al. 2008]

Paper		Grammage (g/m²)	Whiteness (%)	Brightness (%)	Opacity (%)	Fluorescence (%-units)	Permeability Bendtsen (ml/min)
EPG		91-274	107-161	90-101	92-100	24-73	0-213
MP		77-84	79-157	89-100	86-94	0-68	392-706
IJ		98-280	91-150	86-98	89-99	7-59	0-193
Paper / Print		Roughness PPS (µm)	Roughness Bendtsen (ml/min)	Paper Gloss (GU)	Print Gloss (Black, GU)	Print Density (Black, D)	Color Gamut (a*b*)
EPG		0.7-4.1	0-122	8.2-87	13-53	1.55-1.80	7700-9000
MP	EPG	4.5-7.2	91-247	4.0-7.4	9.0-20	1.59-1.65	7500-8500
	IJ				0.6-0.9	1.09-1.18	5600-6300
IJ		0.6-5.7	0-270	2.2-96	0.1-88	1.32-2.11	8700-13800

Each sample was printed and digitized according to a distinct process. The electrophotographic samples were printed with a Xerox DocuColor 6060 Digital Color Press (CMYK) and the ink-jet samples with an Epson Stylus Pro 3800 desktop printer (CMY, light CMK, light light K and photo/matte K). Paper-specific ICC profiles and print settings were determined for both devices. DC6060 enabled also paper-specific calibrations. The photographs had a print size of 10 cm x 15 cm. For more details on the printing process, see Halonen et al. [2008].

The printed images were digitized with a calibrated camera. The digitization plane was illuminated by a filtered halogen lamp. The illuminance level on the plane was 2000 lx and the color temperature was 4800 K. The samples were captured with three exposures (1/10 s, 1/5 s and 2/5 s). From these exposures a single 16 bits linear high dynamic RGB raw image was combined. The high dynamic RGB image was transformed first to the absolute XYZ space and then to the LAB space. In addition the photometric distortion of the camera was compensated by the uniform test field of the integrating sphere. [Nuutinen et al. 2010]

The following algorithms were used for the computation of quality in the study: Crete et al. [2007] for blur, Tai and Yang [2008] for noise, rms [e.g. in Peli 1990] for contrast, and Hasler and Süsstrunk [2003] for colourfulness. The algorithms were chosen as they are well-documented, widely used and perform well in the context of digital images. Blur, noise and contrast were computed from the lightness channel L* of the CIELAB color space. For blur and contrast computation, L* was scaled to [0, 1] and for noise to [0, 255]. Contrast was computed as the standard deviation of the luminance values (rms). Colorfulness was computed from chroma components a* and b* with the equation

$$M^{(1)} = \sigma_{ab} + 0.37 \times \mu_{ab} \tag{1}$$

where σ_{ab} is the trigonometric length of the standard deviation in a*b* space, andm μ_{ab} is the distance of the centre of gravity in a*b* space to the neutral axis [Hasler & Süsstrunk 2003].

The blur metric by Crete et al. [2007] is based on the discrimination between different levels of blur perceptible on the same image. The original image is blurred with a strong low-pass filter to get a comparison image with more blur. From both images, the variation in the neighbouring pixels is analyzed. A large difference between the original and the blurred image indicates a sharp original image, whereas a small difference indicates a blurry original. The algorithm by Marziliano et al. [2002] was previously used in the project for the computation of blur. It was, however, found that the edge detection based metric was sensitive to the threshold used to classify the edge and was also mislead by the presence of noise. This had also been pointed out by e.g. Crete et al. [2007], but was found to be particularly challenging in the context of printed photographs.

The noise metric by Tai and Yang [2008] is based on a method for estimating additive zero-mean Gaussian noise by Immerkær [1996]. Immerkær's algorithm filters off the real structure of the image by using the difference between two masks approximating the Laplacian of the image. The metric by Immerkær [1996] was previously used in the project, but was found to have difficulties with the different types of noise produced by electrophotography and ink-jet as well as in distinguishing the image structure from the noise. Tai and Yang [2008] criticized the metric of Immerkær [1996] for failing with certain image types with low noise levels and

Laplacian convolution to improve the metric. The metric defines the edge map with a threshold parameter that is adaptive to image content. After the edge detection, the metric of Tai and Yang [2008] follows the procedure of Immerkaer[1996].

A series of instrumental measurements was also carried out from the samples. The instrumental measures respective to the computational quality metrics were edge sharpness, rms noise, density of full-tone black and colour gamut. Edge sharpness values for the vertical lines of the printed samples were computed in the following manner. The edge profiles of the vertical lines were first estimated with a function

$$f(x) = \frac{b_1}{1 + e^{-b_2 x}} + b_3 \qquad (2)$$

Edge sharpness was considered as the maximum value of the function's derivative and was then defined as the average value over the whole edge (a minimum of 15 data points). RMS noise of a 50% gray field in the test layout was measured by digitizing a 30 mm x 30 mm area of the K50 field and then computing the pixel-based standard deviation in the lightness component of the digitized area. The absolute density of full-tone black was measured with a Macbeth RD918 densitometer. From both sheets of each sample three measurements were made and the average of the six measurements was calculated. Color gamut was determined by first measuring LAB values of the full-tone RGBCMY patches with the i1 Pro spectrophotometer. From both sheets of each sample three measurements were made and the average of the six measurements was calculated. Finally, the color gamut was defined as the a*b* area of the hexagon formed when the LAB values were plotted in an a*b* chart. The lightness component was ignored as the colorfulness computation used only the a* and b* color components.

Overall quality along with sharpness, graininess, colourfulness and contrast were evaluated from the samples in subjective tests. Observers (n = 59) were university students and naïve as regards to print and image quality. The EPG samples were evaluated separately from the IJ samples: 29 of the subjects evaluated the EPG samples and 30 the IJ samples. Both tests followed the same procedure for the results to be comparable. The overall quality of the samples was evaluated on a 5-point category scale (i.e. 1: bad, 2: poor, 3: fair, 4: good, 5: excellent). Sharpness, graininess, colourfulness and contrast were evaluated as semantic differentials (e.g. blurry–sharp) also on a 5 - point category scale (e.g. 1: clearly blurrier than sample set average, 2: slightly blurrier, 3: about the average, 4: slightly sharper, 5: clearly sharper). The scale of graininess was of opposite direction compared to the other scales, i.e. grainy - non-grainy. The subjects were asked to reach their ratings to both ends of the scale.

All subjects rated first the overall quality of each sample in order to avoid any bias from evaluating the quality attributes. The samples of one image content at a time were placed on the table in a random order. The evaluation order of the contents was also randomized. After evaluating the overall quality of all the samples the subjects were asked to rate the sharpness, graininess, colourfulness and contrast of the samples. The samples were again presented one image content at a time; the subjects rated the content on all scales before moving on to the next content. Again the order of the contents was randomized along with the order of the evaluated quality attributes.

Stepwise (backward) multiple linear regression analysis was used for creating the quality models relating instrumental measurements from prints (Layer 2) and computational quality attributes (Layer 3) to MOS values (Layer 5). Two sets of models predicting the subjective print quality were created. In the first set, the instrumental measurement values were the independent variables used as the predictors. The other set of models was created with the computational quality attribute values as the predictors. The goodness-of-fit of the produced models was evaluated with the coefficient of determination, R^2. SPSS 17.0 was used for the creation of the regression models and the assessment of their goodness. Each image content and printing method was analyzed separately.

3. Results

Table III presents the regression models predicting MOS by instrumental measurements (Layer 2) for the printing methods separately and combined. All models explained the variation in the overall quality well with coefficients of determination of over 75%. The models for the EPG and IJ samples separately had a better fit than the models for the printing methods combined. Of the attributes, edge sharpness and rms noise were of great importance in the models as they were included in six of the nine models, i.e. in all models for the EPG samples and for the samples of EPG and IJ combined. The models for the IJ samples contained only one predictor, colour gamut. This

single variable explained over 94% of the variation in the overall quality for all three image contents. Overall, colour gamut appeared in five of the nine models, but had no contribution to the quality prediction of the EPG samples. The density of full-tone black appeared only in two models, both for image content *lake*. In all nine models, the coefficients of the variables had a logical sign, i.e. the coefficients were negative only for the rms noise. The variables included in the models seemed to depend both on the printing method and the image content. The image content with the models of the weakest explanatory power was *lake*.

Table III: The regression models predicting MOS by instrumental measurements (Layer 2) for the EPG and IJ samples separately and combined

	All samples		EPG samples		IJ samples	
	Model	R^2	Model	R^2	Model	R^2
Cactus	1.53 +0.41·Edge Sharpness -0.48·RMS Noise +0.36·Colour Gamut	76.2%	0.17 +1.47·Edge Sharpness -0.91·RMS Noise	89.2 %	-1.11 +1.17·Colour Gamut	97.2%
Lake	1.36 +0.36·Edge Sharpness -0.47·RMS Noise +0.43·K100 Density	77.3%	-2.58 +1.06·Edge Sharpness -0.90·RMS Noise +0.98·K100 Density	81.6 %	-0.83 +1.08·Colour Gamut	94.6%
Man	1.45 +0.41·Edge Sharpness -0.49·RMS Noise +0.38·Colour Gamut	79.7%	0.76 +1.41·Edge Sharpness -1.00·RMS Noise	91.1 %	-1.23 +1.19·Colour Gamut	96.7%

Table IV presents the regression models predicting MOS by computational attribute values (Layer 3) for the printing methods separately and combined. While the variation in the IJ print quality was explained well by the computational attribute values (coefficients of determination again over 94%), the models for the EPG samples were significantly weaker with only 29 - 59% of the variation explained. The models for the combined EPG and IJ samples had a reasonable explanatory power with coefficients of determination of over 70%. Of the attributes, contrast was the most significant as it appeared in eight of the nine models. Noise was included in five of the nine models and blur in four, whereas colourfulness did not contribute to the quality prediction in any of the cases. In three of the nine models, there were coefficients with an unexpected sign. Similarly to the case of instrumental measurements as predictors, the variables of the quality models depended both on the printing method and the studied image content. With computational attribute values as predictors, image content *lake* had the models of the best explanatory power.

Table IV: The regression models predicting MOS by computational attribute values (Layer 3) for the EPG and IJ samples separately and combined [Halonen et al. 2009]

	All samples		EPG samples		IJ samples	
	Model	R^2	Model	R^2	Model	R^2
Cactus	0.43 -11.51·Blur -2.84·Noise +17.22·Contrast	70.2%	-96.92 +84.10·Blur +21.65·Noise	48.9%	-11.07 +15.64·Contrast	94.3%
Lake	-6.61 -2.35·Noise +12.83·Contrast	80.8%	-13.30 +17.55·Contrast	58.8%	-21.36 +17.86·Blur +1.41·Noise +7.10·Contrast	97.6%
Man	-2.87 -3.02·Noise +8.96·Contrast	70.3%	-8.74 +12.57·Contrast	28.8%	-10.82 +5.66·Blur +9.96·Contrast	95.9%

For comparison, Table V presents the regression models predicting MOS by respective subjective attribute values (Layer 4) for the printing methods separately and combined. The models predicting MOS by instrumental

subjective attributes as predictors. E.g. in the models for all samples, the only difference was the missing equivalent for contrast in the model by instrumental measurements for *cactus*. The connection between the variables in the models predicted by computational and subjective attributes was less clear.

Table V: The regression models predicting MOS by subjective quality attribute values (Layer 4) for the EPG and IJ samples separately and combined [Halonen et al. 2009]

	All samples		EPG samples		IJ samples	
	Model	R^2	Model	R^2	Model	R^2
Cactus	-0.44 +0.25·Graininess +0.37·Sharpness +0.28·Contrast +0.26·Colourfulness	96.1%	-0.52 +0.84·Sharpness +0.34·Colourfulness	91.2%	-0.30 +0.29·Graininess +0.81·Colourfulness	98.2%
Lake	-0.18 +0.38·Graininess +0.42·Sharpness +0.27·Contrast	95.9%	-0.02 +0.38·Graininess +0.62·Sharpness	93.1%	-0.05 +0.47·Graininess +0.56·Colourfulness	98.4%
Man	-0.28 +0.23·Graininess +0.66·Sharpness +0.21·Colourfulness	97.2%	0.02 +0.96·Graininess	96.2%	-0.27 +0.50·Sharpness +0.59·Colourfulness	98.6%

4. Conclusions

The purpose of the study was to evaluate the feasibility of instrumental measurements from prints (Layer 2) and respective computational quality metrics (Layer 3) for the overall print quality prediction. The results suggest that the subjective quality of printed photographs can be predicted to a reasonable extent using quality attributes computed from digitized prints or instrumental measurements from objective test fields. Both the models with computational quality attribute values and the models with instrumental measurements as predictors explained up to 97% of the variation in the overall quality for the ink-jet samples. The models had a similar fit also for the electrophotographic and ink-jet samples combined, with coefficients of determination of approximately 70 - 80%. The largest difference in terms of explanatory power was found between the models for the electrophotographic samples. While the models predicting MOS by instrumental measurements explained up to 91% of the variation in the overall print quality, the models with computational quality attributes as predictors explained up to 59% of the variation at best. The model with the weakest fit accounted just for 29% of the quality variation.

Included variables and the goodness-of-fit of the models seemed to depend on the image content, the quality of which was predicted. Of the four studied computational quality metrics, blur and contrast made the most significant contribution to the quality prediction of the samples. The instrumental measurements that contributed the most to the models were edge sharpness and rms noise. Altogether, computational quality metrics and instrumental measurements from prints were found to be suitable for the quality prediction of printed photographs. A set of instrumental measurements from prints predicted the subjective quality of prints more precisely than a respective set of computational quality metrics, even though they do not take image content into account. This indicates that further development on the computational metrics is needed.

Acknowledgements

The authors would like to thank the Finnish Funding Agency for Technology and Innovation (TEKES) and partners of the DigiQ project for support.

References

1. Bex, P. J. & Makous, W., (2002), *Spatial frequency, phase, and the contrast of natural images, Journal of the Optical Society of America A 19, 6,* pg. 1096-1106
2. Caviedes, J. & Oberti, F., (2004), *A new sharpness metric based on local kurtosis, edge and energy information. Signal Processing: Image Communication* 19, 2, pg. 147-161
3. Crete, F., Dolmiere, T., Ladret, P. et al., (2007), *The blur effect: perception and estimation with a new no-reference perceptual blur metric.* Proc. SPIE 6492, pg. 64920I-1-64920I-11
4. Eerola, T., Kämäräinen, J.-K., Leisti, T. et al., (2008a), *Is there Hope for Predicting Human Visual Quality Experience? Proc. IEEE SMC,* pg. 725-732
5. Eerola, T., Kämäräinen, J.-K., Leisti, T.et al., (2008b), *Finding Best Measurable Quantities for Predicting Human Visual Quality Experience. Proc. IEEE SMC,* pg. 733-738
6. Fedorovskaya, E. A., de Ridder, H. & Blommaert, F. J. J., (1997), *Chroma Variations and Perceived Quality of Color Images of Natural Scenes. COLOR research and application 22, 2,* pg. 96-110
7. Ferzli, R. & Karam, L. J., (2007), *A no-reference objective image sharpness metric based on just-noticeable blur and probability summation, Proc* . ICIP, pg.445-448
8. Frazor, R. A. & Geisler, W. S., *(2005), Local luminance and contrast in natural images, Vision Research 46, 10,* pg. 1585-1598
9. Halonen, R., Leisti T. & Oittinen, P., (2008), *The Influence of Image Content and Paper Grade on Image Quality Attributes computed from Printed Natural Images, Proc. IS&T NIP24,* pg. 459-462
10. Halonen, R., Leisti T. & Oittinen, P., (2009), *The Challenges in Modeling Image Quality in Digital Printing. Proc. IS&T NIP25,* to be published
11. Hasler, D. & Süsstrunk, S., (2003), *Measuring colourfulness in natural images, Proc. SPIE 5007,* pg.87-95
12. I3A, (2007), *CPIQ Initiative Phase 1 White Paper, http://www.i3a.org/wp-content/uploads/2008/03/cpiq_white_paper.pdf*
13. Immerkaer, J., (1996), *Fast noise variance estimation, Computer Vision and Understanding, 64, 2,* pg. 300-302
14. Marziliano, P., Dufaux, F., Winkler, S. et al., (2002), *A no-reference blur metric, Proc. ICIP,* pg. 57-60
15. Nuutinen, M., Halonen, R., Leisti T. & Oittinenm P., (2010), *Reduced-reference quality metrics for measuring the image quality of digitally printed natural images, to be published*
16. Oittinen, P., Halonen, R., Kokkonen, A. et al., (2008), *Framework for modeling visual printed image quality from the paper perspective, Proc. SPIE 6808,* pg. 68080L-1-68080L-11
17. Olsen, S. I., (1993), *Estimation of Noise in Images: An Evaluation, CVGIP: Graphical Models and Image Processing 55, 4,* pg. 319-323
18. Peli, E., (1990), *Contrast in complex images, Jour. Optical Society of America, 7, 10,* pg. 2032-2040
19. Pulla, J., Mettänen, M., Konkarikoski, K. et al., (2008), *Bayesian Network Model as an Overall Image Quality Measurement System, Proc. IMEKO TC1-TC7,* pg. 67-73
20. Salmi, H., Halonen, R., Leisti, T. et al., (2009), *Development of a balanced test image for visual print quality evaluation, Proc. SPIE 7242,* pg. 72420B-1-72420B-11
21. Tai, S.-C. & Yang, S.-M., (2008). *Fast Method For Image Noise Estimation Using Laplacian Operator and Adaptive Edge Detection, Proc. ISCCSP,* pg. 1077-1081
22. Wang, Z. & Bovik, A. C., (2006), *Modern Image Quality Assessment (Morgan & Claypool Publishers, USA).* 146 p
23. Yendrikhovskij, S. N., Blommaert, F. J. J. & de Ridder, H., (1998), *Optimizing color reproduction of natural images, Proc. IS&T/SID CIC 6.* pg. 140-145
24. Zeise, E. K., Rasmussen, D. R., Ng, Y.S. et al., (2008), *INCITS W1.1 development update: Appearance-based image quality standards for printers, Proc. SPIE 6808,* pg. 680802-1-680802-10





4

Digital and special printing

Mechanisms involved in the optical interaction between ink and substrate for Home&Office inkjet printing

Nils Pauler[1], Ole Norberg[2], Per Edström[3]

[1] M-Real
Saravägen 11, SE-894 31 Själevad, Sweden
E-mail: Nils.pauler@m-real.com

[2] Voxvil AB
Båtsmansgatan 31, SE-892 43 Domsjö, Sweden
E-mail: Ole.norberg@voxvill.se

[3] Mid Sweden University
SE-871 88 Härnösand, Sweden
E-mail: Per.edstrom@miun.se

Abstract

It is known that colour reproduction of inkjet comprises a range of mechanisms. It was possible to understand and explain some of these mechanisms by evaluating print tests with standard optical measurement and by calculations using algorithms of the Kubelka Munk and Murray Davies theories. The combined interaction of the substrate, the ink penetration, the optical properties of the inks and the dot size were clarified. Large colour gamut is governed by low ink penetration, low light scattering of the substrate and small dot size. The non-ideal property of process inks and the continuous tone character of colour reproduction of the studied desktop inkjets explained the observed convex shape of the colour gamut. For plain paper, dye-based and pigment-based inks were shown to follow different mechanisms, with lower penetration of the pigment-based ink. Colour gamut could be increased by a surface treatment that further reduced the penetration, but this treatment worked only for the pigment-based inks. Internal sizing of plain paper had only a very small influence on colour gamut for dye-based ink, even though the ink penetration was reduced.

Keywords: paper, inkjet, colour gamut, simulation, Kubelka Munk, Murray Davies

1. Introduction

Traditional printing technologies like offset usually use CMYK as process colours. Standardised methods are established to control the print process and evaluate the influence of the substrate. The reproduction is often made with well known halftone algorithms where the ink level is constant for each halftone dot and the tone values are controlled by varying the size of the dots. Print quality is normally evaluated by carrying out test printing in print shops where trained staff runs the machines. The practical and theoretical knowledge to evaluate traditional print is well established.

The test printing and evaluation of small digital print units such as home & office inkjet or xerographical printers is often made by paper manufacturers themselves. A thorough print quality evaluation requires extensive, partly new, knowledge in graphic technology topics. The home&office inkjet printers prefer RGB as colour input data, which must be considered when creating test charts. Inkjet evaluation such as line raggedness, line bleeding, mottling and print density in full tone and halftone are all dependent on how the coloured test patches are printed. A colour correction is normally active to give appealing print results. This colour correction must be turned off to obtain pure process colours but then the colour images may not be well reproduced. Printing the test charts and images must therefore be performed with different settings making it difficult to compare print quality to the values of the test charts.

In inkjet printing there is a possibility to vary both the ink level and the dot size. There is also the freedom to place the ink on the substrate independently of any screen pattern [Wan, 2003]. This makes reproduction very flexible. Users can select between a large number of settings for both photo printing and plain paper printing.

quality photo prints to ordinary printouts on plain paper. Moreover, vendors use different types of water based inks. Two main groups denoted the pigmented and the dye-based inks have been established. Lately a new technology for surface treatment of paper has entered the market. This technique fixates the colorants closer to the surface, resulting in an increase in colour gamut for plain paper printing.

For a papermaker there is a need for easy to use methods for evaluating and simulating colour reproduction in order to understand the optical interaction between ink and paper. The aim of this report is:

(i) To show how standard optical measurements can be used to evaluate colour reproduction on inkjet printers.
(ii) To indicate how optical simulations (using basic theories) together with test printing and measurements are a help in understanding the optical interaction between ink and paper.
(iii) To clarify different aspects of ink penetration by comparing two approaches for the enhancement of colour gamut for inkjet printing on plain paper: a) internal sizing for dye based inks and b) surface treatment for pigmented inks.

2. Previous work

Theories concerning the impact of ink penetration on optical properties have been a subject of research for many years [Lar, 1976]. A mathematical framework of print-through and ink penetration was presented at Iarigai 1987 [Bri, 1987]. Measurements using this theory have given valuable information about the optical interaction between ink and paper for offset prints on plain paper [Pau, 1986]. It has also been possible to simulate the effect of ink penetration by using Kubelka Munk theory [Pau, 1987 and Yan 2005]. The Kubelka Munk theory gives fairly good correlation with measured data when simulating the colours of inkjet prints [Eng, 1986 and Kan, 1991]. By applying the simulation of ink penetration for all wavelength it has been possible to simulate how colour gamut is influenced by different ink penetrations [Pau, 2002a and Pau, 2002b].

Halftoning is described by the Murray Davies equation saying that the reflectance is directly related to the surface area covered by ink [Mur, 1936]. The Neugebauer equations are the extension to four colour reproduction [Neu, 1937]. The optical dot gain was introduced by Yule Nelson [Yul, 1951] and it has been thoroughly investigated by introducing a point spread function of the light [Gus, 1997]. Gustafsson showed that a large dot gain can increase colour gamut. Attempts to include more and more detail in the simulation of colour reproduction have been accomplished over the last 50 years. The Clapper Yule equation [Cla, 1955] is an algorithm that simulates halftoning, taking into account optical dot gain and surface reflection. Hersch and Emmel have also introduced ink spreading and fluorescence in their models [Eme, 2002 and Eme, 2003]. The new models are more accurate but the disadvantage is the complexity and the need for many unknown constants that must be established. This is a drawback when simulating digital print units since new inks and new colour reproduction methods are introduced which results in a range of new constants to be determined.

It is well known that photo-gloss papers give extremely high colour gamut and very appealing print. The main drawback with plain paper is the low colour strength. It has been shown however, that also moderate increases in colour gamut are important for the perception of print quality [Nor, 2006].

3. Methods

3.1 Simulation

In this work the effect of ink penetration is simulated by using the Kubelka Munk theory. Light scattering and light absorption of the paper and the ink are the bases for the simulation. It is assumed that the ink penetrates into the paper in a linear fashion with increasing ink weight. The ink is further assumed to be homogenously distributed in the ink/paper layer. A barrier is simulated by constraining the penetration to a certain maximum penetration. The light scattering and light absorption of the ink/paper layer is calculated using the additively blending rule [Pau, 1986].

The simulation is extended to colour by including the process inks: cyan, magenta and yellow (CMY). The basis for calculation is then the spectral light scattering and light absorption of the process inks CMY ($s_{ink}(\lambda)$

spectral s and k of the two primary colours added together assuming additivity. It is then also assumed that ink weight and ink penetration are doubled. The colours between primary and secondary colours are calculated assuming linear additivity in light absorption of the inks. By adding the one or two remaining process inks the dark colours (lower part of colour gamut) are simulated ending with 300% ink coverage i.e. equal parts of the process inks cyan, magenta and yellow [Pau, 2002].

The denotation Simulated Halftoning is in this work, a combination of the Kubelka Munk theory and Murray Davies equation. The Kubelka Munk theory is used to calculate the full tones for different hues taking into account the ink penetration. The Murray Davies equation is thereafter used to simulate halftoning from 0 to 100% in 25 steps, see figure 1 and 2.

Light absorption of the ink was determined by the variable Rg method [Pau, 1995]. Full tones were printed on overhead film and the ink weight was determined by balancing before and after printing. The reflectance was measured for black and white background. Light scattering of the substrate was however assumed not to be influenced by the ink in the simulations presented in this work. Cyan and magenta of the process inks had typical unwanted absorption for the shorter wavelengths [Kan, 1999]. To study the effect of this unwanted absorption (the non ideal property) a set of ideal ink with very low light absorption in two third of spectrum and high absorption of the rest of spectrum was included in the simulations.

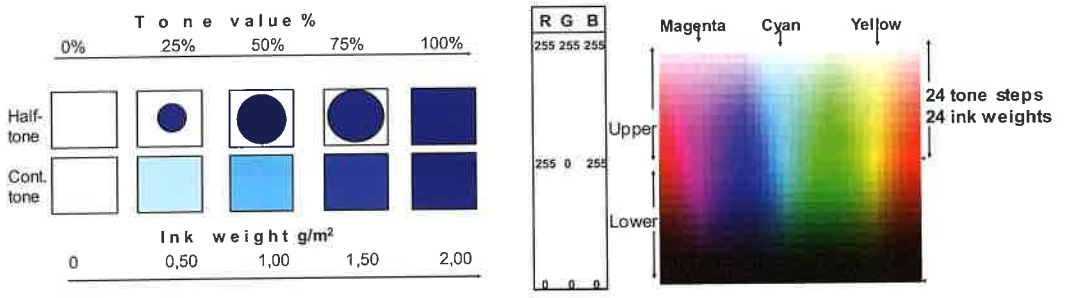

Figure 1 and 2: Schematic figure of halftone and continuous tone reproduction (left). The ink weight of the dots are 2,0 g/m². Schematic figure indicating how colours of the gamut are simulated by either continuous tone (ink weight) or half tone (tone steps) reproduction. The RGB shows how magenta was described in the RGB test chart

3.2 Measurements

The ink penetration was established by using the method described by Bristow [Bri, 1987]. The ink penetration depth is the ratio of the grammage in which the ink has penetrated to the total grammage of the substrate. The ink penetration (normally expressed in percent) can be calculated based on the reflectance values of equation 1:

$$W/W_p = \frac{Ln\left[\frac{(1-R_0R_\infty)(1-R_pR_\infty)(1-R_Q/R_\infty)}{(1-R_{0)}/R_\infty)(1-R_p/R_\infty)(1-R_QR_\infty)}\right]}{Ln\left[\frac{(1-R_0R_\infty)}{(1-R_0/R_\infty)}\right]} \quad (1)$$

where

R_o = Reflectance factor of one sheet over black background,
R_{oo} = Reflectance factor of an opaque pad,
R_P = Reflectance factor of printed paper backed with Roo,
R_Q = Reflectance factor of back side of printed paper backed with Roo.

Print density was calculated as D = log10 (Roo/Rprint). A spectrophotometer, DataColour 450 was used for these measurements. The calculation of ink penetration was made at the wavelength that had lowest reflectance factor.

The colour gamut was established by measuring a colour map comprising 925 colour patches, figure 2.
The measurements was made by a spectrophotometer attached to an x y table (Spechtrolino).

The spectral values were measured and CIE Lab coordinates D50/2° were calculated according to standard. The colour volume was calculated with a convex hull algorithm. A Convex/Concave number was calculated as a ratio of the volume of colour gamut to the body of the dodecahedron W, B, Y, R, M, C, G i.e L*a*b* of process colours, secondary colours and black and white. This gamut volume was calculated by adding volumes of tetrahedra [Ryd, 1995]. The tone value (TV) was calculated as TV = 100*(Roo-Rhalftone)/(Roo-Rfulltone). The colour area was calculated using Green Theorem for a closed polygon of the six colours of a*, b* values of process and secondary colours.

3.3 Test printing

The test chart for colour gamut, see figure 2, was printed in the normal way with printer settings for the respectively substrate i.e. plain paper quality or photo quality but with colour correction turned off. The halftone patches of the process inks were controlled to be pure i.e. without any ink dots of the other process inks included in the patches. One test printing was performed with colour correction activated.

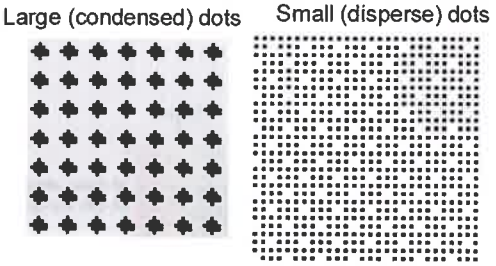

Figure 3:
Condensed and dispersed dots

Test charts for colour gamut and ink penetration studies were printed with different ink levels (one to five drops per pixel) and small (dispersed) and large dots (condensed). Weighting before and after printing of full tones gave the ink weight for the five ink levels, table I.

Table I: Number of printed dots and estimated ink weight

Number of drops	1	2	3	4	5
Ink weight g/m²	0,79	1,63	2,57	3,43	4,35

The dispersed and condensed ink dots were placed in 133 lpi halftone screen: The condensed dot was created by focusing the dots to the centre of the raster cell and the dispersed by placing the dots evenly distributed in the cell, figure 3.

4. Results

4.1 The influence of ink weight and dot size on colour gamut

Different relationships were observed from the test printing with increasing ink weight (by ejecting 1 to 5 drops per pixel) and the two dot sizes, figure 4.

- Total colour gamut (Tot) increased with ink weight and reached a plateau at 2 g/m².
- Tetrahedra colour gamut (Tet) showed a maximum value at 2 g/m² and decreased with higher ink levels.
- Dot gain or tone value increase (TVI) increased continuously with ink weight.
- For smaller dot size, higher levels of total gamut and dot gain were achieved. The tetrahedra colour gamut (Tet.S) reached the same value as for the larger dot (Tet.L) since full tones are not affected by dot size.

The influence of the smaller dots was recorded as a more convex colour gamut, with higher lightness in the upper part of the gamut, figure 5. As inkjet can both change ink weight and dot size the total colour volume must always be measured.

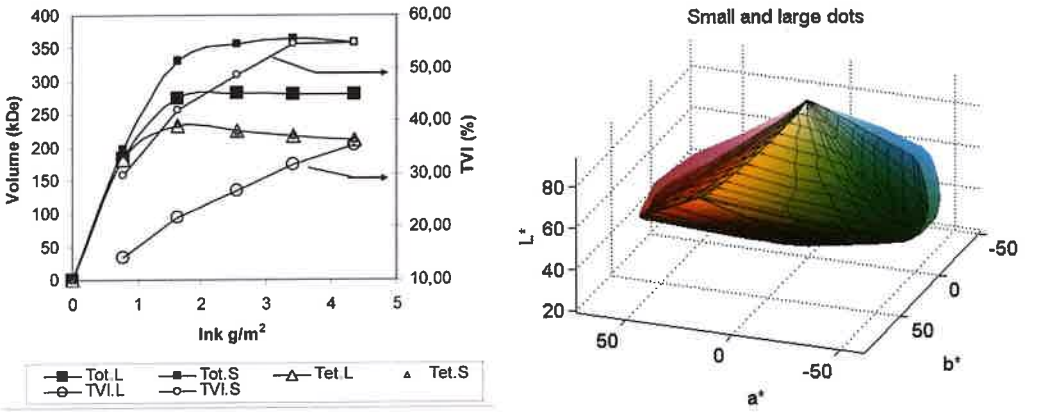

Figure 4 and 5: Total Gamut, Tetrahedra gamut and TVI (circles) vs. ink weights for prints with small and large dots (left). 3- D Colour gamut for prints made with highest ink weight with small (no grid) and large dots (grid marked), (right). Test printing with dye based ink on a photo-matt paper

4.2 The continuous tone character of inkjet

Calculating the upper colour gamut by increasing the ink weights means that a continuous tone algorithm is used in the simulation. Using properties of the ideal ink showed that colour strength then increased at almost constant lightness level in the upper part of the gamut. On the other hand the process inks generated a reduction in lightness and a colour change, figure 6. It is interesting to observe that measurements of printed inkjet showed the same shape of gamut as the simulated continuous tone colour reproduction, compare figure 7 with figure 6.

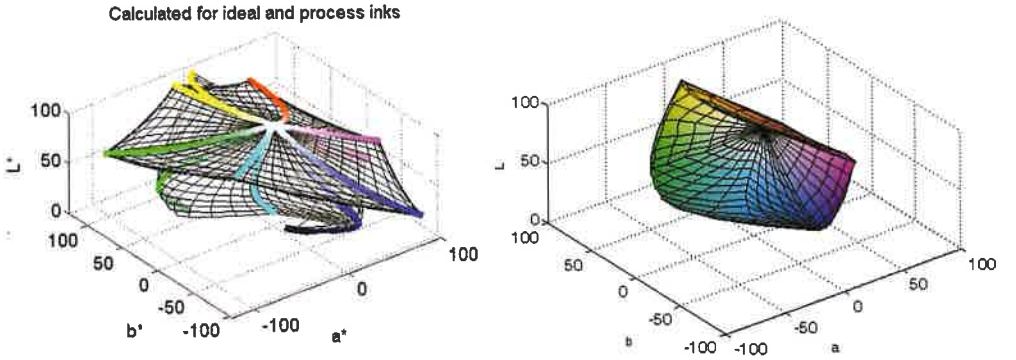

Figure 6 and 7: Calculated (using continuous tone algoritm) upper part of colour gamut with light absorption of ideal inks and process inks (left). Measured upper part of colour gamut of dye-based ink printed on photo-gloss paper (right)

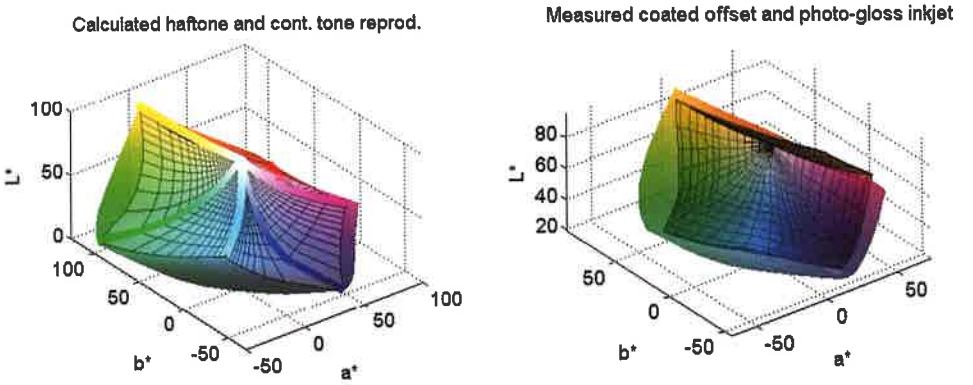

Figures 8 and 9: Colour gamut calculated with halftone tone algorithm (grid marked) and continuous tone algorithm (no grid) (left). Colour gamut measured for offset (grid marked) printed on glossy coated paper and for inkjet (no grid)

When colour reproduction was simulated with a halftoning algorithm a concave colour gamut was obtained, figure 8. Measurements of colour gamut, clarified that offset has halftone whereas inkjet has more continuous tone characteristics of colour reproduction, compare figures 8 and 9.

4.3 The influence of ink penetration and light scattering

4.3.1 Photo quality

The high colour gamut of prints made on photo-gloss paper is explained by low light scattering of the ink receiving layer at the top of the construction of this substrate, figures 10 and 11. The figures show simulated continuous tone reproduction and measured colour gamut of prints. It is of course a challenge to find ways for improving the colour gamut of plain paper printing.

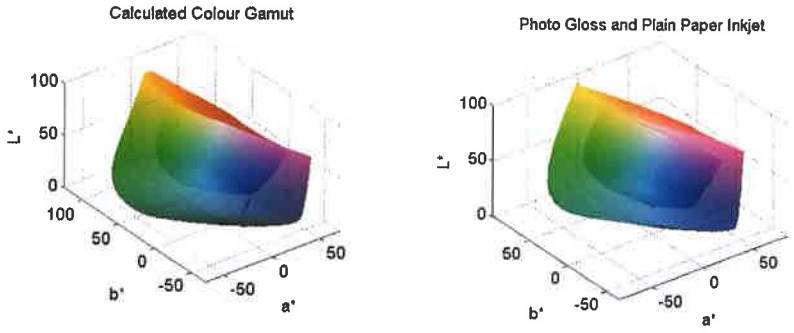

Figure 10 and 11: Calculated colour gamut using the continuous tone algorithm. The ink penetration was limited to 5% respectively 40% and the light scattering in the ink/substrate layer was 6 m^2/kg respectively 60 m^2/kg to simulate photo-gloss substrate and paper substrate (left). Measured colour gamut for inkjet printed on photo-gloss paper and plain paper (right)

4.3.2 Plain paper

The penetration of ink increased in an almost linear fashion with ink weight in plain paper, figure 12. Internal sizing of the paper reduced the penetration which was expected since hydrophobic treatment reduces the water uptake. Internal sizing also gave increased print density, figure 12. The print density was however reduced by adding the filler which is in line with the fact that increased light scattering reduces the colour strength. The normal option for a paper maker is to include filler in copy products, due to a desire to obtain low print through, but also for economic reason.

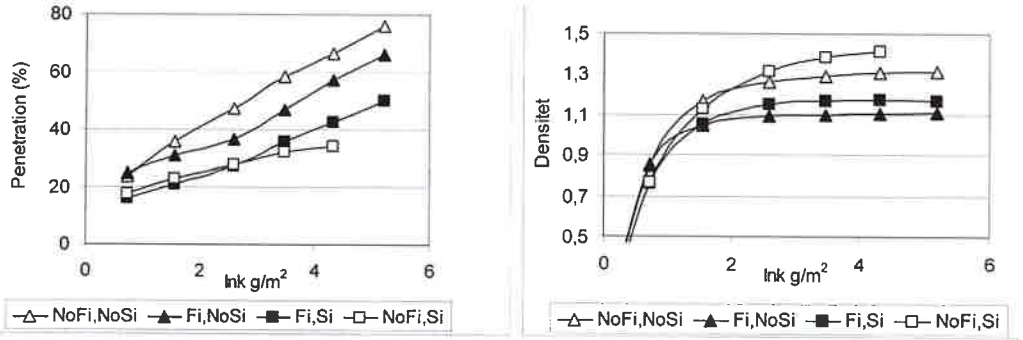

Figure 12 and 13: Ink penetration and print density vs. ink weights. Test printing with dye-based inks on paper with and without internal sizing (Si, NoSi) and with and without fillers (Fi,NoFi)

4.4 Internal sizing and surface treatment, the effect on colour gamut for plain paper printing

Internal sizing gave only a slight increase in colour area and tetraeder colour gamut, whereas total colour gamut did not show any change for printing with dye-based inks. The surface treatment aiming at fixing the pigmented-based inks to surface significantly increased colour strength. The surface treatment increased total

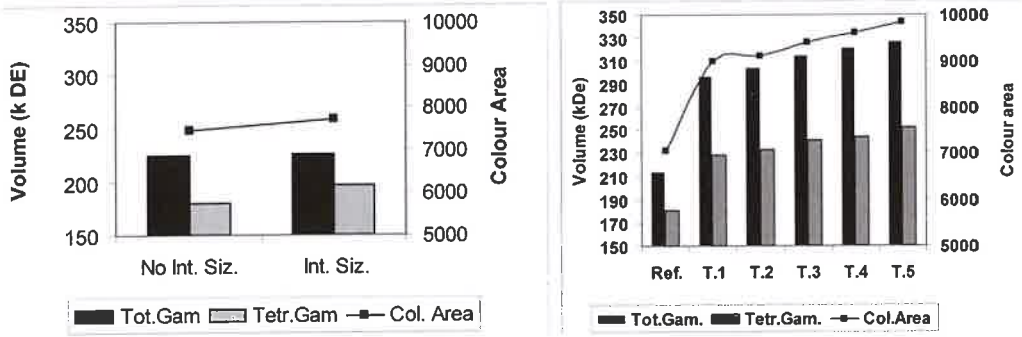

Figure 14 and 15: Colour gamut (total, tetraeder and colour area) of prints with dye-based inks on paper with and without internal sizing (left). Colour gamut of prints with pigmented inks on paper with five levels of surface treatment (right)

The surface treatment of pigmented inks not only gives higher colour strength in full tones but also increases colour gamut in the lower part of gamut, whereas the internal sizing showed a tendency to reduce colour strength in the upper part of gamut, figures 16 and 17.

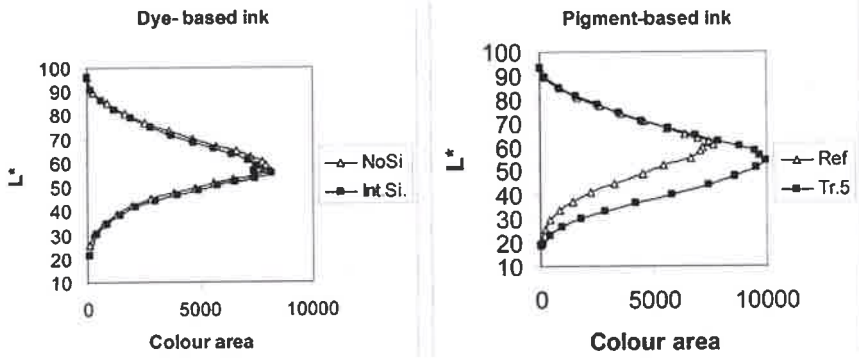

Figure 16 and 17: L vs. colour area of tones of the upper and lower part of colour gamut. Measurements of prints with dye- based inks of papers with and without internal sizing(left) and of prints with pigmented inks of papers with and without surface treatment (right)*

Even though the internal sizing had no or only slightly increasing effect on colour strength it did reduce the penetration of the dye-based ink. The surface treatment reduced the ink penetration of the pigmented inks to very low levels, figures 18 and 19.

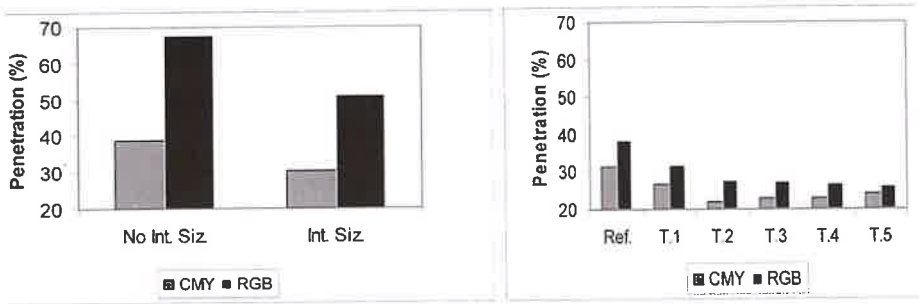

Figure 18 and 19: Penetration of dye-based inks in paper with and without internal sizing (left). Penetration of pigmented-based inks in papers with four levels of surface treatments (right). The penetration was established for process colours (CMY) and secondary colours (RGB)

4.5 The colour correction

The colour correction of inkjet printers are often based on sRGB that has low colour strength for cyan and blue colours, figure 20. Although colour gamut is reduced in the colour correction our experience so far is that gamut enhancement is largely retained even after colour correction. The result is a more colour full print, with correct

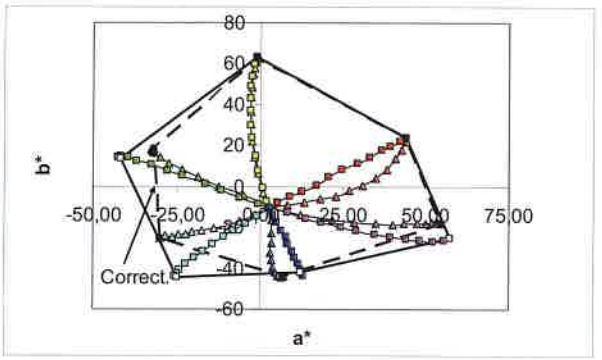

Figure 20: Colour area for inkjet printed on plain paper without and with colour correction

5. Conclusion

A range of mechanisms have been explained. Reduced ink penetration and low light scattering in the ink substrate layer promotes high colour strength. The non ideal characteristics of the process inks limits colour gamut at high ink levels. Inkjet has the character of continuous tone colour reproduction. The convex shape of colour gamut is probably a combined consequence of small dots and the non ideal properties of the process inks. Offset prints and simulated halftone colour reproduction have a concave colour gamut shape. A special surface treatment of plain paper increased the colour gamut for tested inkjet printers using pigmented inks. The ink penetration was reduced to very low levels. This treatment enhanced the colour gamut by increasing the colour strength of the full tones and of the dark colours. The internal sizing had no influence on the colour gamut, even though ink penetration was reduced. The ink penetration was however not reduced to very low levels. It should be investigated if the surface treatments actually make the ink stay above the surface. An interesting observation was that internal sizing did reduce the dot gain twice as much as the surface treatment did. As lower dot gain gives lower colour strength this may be another explanation why internal sizing did not give any colour gamut increase.

The observed higher colour gamut for the test-print with the smaller dots (dispersed dots) is probably related to the non ideal properties of the process inks. Dispersed dot printing means to distribute the ink over more dots i.e. the ink thickness of each dot decreases. Lower ink weight reduces the negative influence of the non ideal process inks. This reasoning can also be applied for optical dot gain. The light spreading gives rise to a coloured corona around the dot. In this area the light passes only in an upward direction whereas inside the dot light passes the colour twice i.e. optical dot gain can be seen as the ink weight is reduced. These explanations are supported by calculation were ideal inks gave the same colour gamut for continuous tone and halftone colour reproduction.

This work has shown that optical measurements combined with simulations can give a better understanding of the complex optical interactions of inkjet prints.

Acknowledgment

This work was financially supported by KK foundation. M-real supported with samples. MoRe Research supported with optical measurements. Ronnie Powell, M-real, made the linguistic revision.

References

1. Bristow, J. A., (1987), *Print-Through and Ink Penetration- a Mathematical Treatment*, Adv. Printing Sci. Technol, Vol 19 Pentech Press, London, 137-145
2. Clapper, F. R. and Yule, J. A. C., (1953), *The effect of multiple internal reflections on the densities of half-tone prints on paper*, J. Opt. Soc. Am, 600-603
3. Emmel, P., (2003) *Physical models for colour prediction in Digital Color* Imaging Hanbook, G Sherma

4. Emmel, P. and Hersch, R. D., (2002) Modelling *ink spreading for colour prediction,* J Imaging Sci. Technol. 45, 236-246
5. Engeldrum, P. G., (1986) *Computing color gamuts of inkjet printing systems.* Proceedings of the S.I.D, 2781, 25-30
6. Gustavson, S., (1997) *Dot Gain in Colour halftones Dissertation* No. 492, Linköping University
7. Kang, H. R., (1991) *Kubelka Munk modelling of ink jet ink mixing,* J. Imaging Technol., 17 (2), 76-83
8. Kang, H. R., (1999) *Digital Color Halftoning,* IEEE PRESS, 86-90
9. Larsson, L. O. and Trollsås, P. O., (1976) *Print- through as an ink/paper interaction effect in newsprint,* In The fundamentals of Paper related to its uses BPBIF 1976, 600-612
10. Norberg, O., Andersson, M., *Colour Gamut - Is Size The Only Thing That Matters?,* TAGA 2006 Conference, 2006, Vancouver, Canada
11. Murray, (1936) *A Monochrome Reproduction in Photoengravin,g* Technical Report of the J. Frankline Institute 221, 721
12. Pauler, N. and Bristow J. A., (1986) *Opacity is not the only direct guide to print-through,* Adv. Printing Sci. Technol., Vol 17 Pentech Press, London, 333-346 and 432-437
13. Pauler, N, (1987) *A Model for the Interaction between Ink and paper*, Adv. Printing. Sci.Technol. Vol 19 Pentech Pres,, London, 116-136
14. Pauler, N., (2002) *Ink penetration and its influence on print density and colour gamut.* TAGA Image processing and Graphical Art Conference
15. Rydefalk, S. and Wedin, M., (1997) *Literature review on the Colour Gamut in the printing process*, PFT nr 32 STFI
16. Yang, L., et al (2005) A *Novel method for studying ink penetration of printing.* Nordic Pulp Pap. Res J 20, 399-405
17. Yule, J. A. C. and Nielsen, W. J. (1951) *The penetration of light into paper and its effect on halftone reproduction,* TAGA Proceedings 3, 65-76.
18. Wandel, B. A. and Silverstein L. D., (2003) *Digital Colour Reproduction http://www.google.se/search?hl=sv&q=Wandel%2C+B+A+and+Silverstein+L+D%2C+%282003%29%2C+Digital+Colour+Reproduction&btnG=Google-s%C3%B6kning&meta=&rlz=1R2RNTN_svSE328&aq=f&oq=*

Methodology for evaluation of digital production printing

Abhay Sharma and Martin Habekost

Ryerson University, School of Graphic Communications Management
350 Victoria Street, Toronto, Ontario, M5B 2K3, Canada
E-mails: sharma@ryerson.ca, mhabekos@ryerson.ca

Abstract

Digital production printing technology is gaining a strong foothold in the print industry, complementing and often rivaling offset printing. There has been rapid growth in this new printing technology with suppliers adding faster and better machines every year. It is now appropriate to begin to develop a series of test protocols and quality metrics for benchmarking of digital production color printing. This research describes a series of tests and then shows and compares results from commercial digital print systems.

This paper summarizes the efforts being made in the area of digital print certification by ISO, FOGRA, IPA and IDEAlliance. This paper reviews the applicability of ISO 12647 standards to digital printing. Test protocols exist for offset printing and single sheet inkjet color proofing, this study examines how those tolerances may be adapted for digital production printing.

Tests were conducted in regards to color and color management, sheet-to-sheet variability, and physical properties such as rub resistance, cracking, fading, and deinking properties. Digital printing is often criticized as tending to drift, unable to color manage, unable to match Pantone colors, and many fear digital output cracks during folding in areas of high coverage. The results from this series of test demonstrates that these accusations are largely unjustified and that digital printing matches, and in some cases surpasses, offset in terms of color, print quality and durability.

Keywords: Digital printing, digital print certification, color matching, GRACoL, SWOP, ISO 12647

1. Introduction

Until fairly recently, digital presses were changing so rapidly that it was difficult to determine any baseline metrics. Now improvements have slowed down just enough for us to take a snapshot and state-of-the-art review. It is appropriate to begin to develop a series of test protocols and quality metrics for benchmarking of digital production color printing. In any certification process, it is important to measure parameters that matter to everyday printers, from color matching, to uptime free from jams. It is also necessary to establish realistic tolerances, these tolerances should be both meaningful to the end-user and achievable by the production press.

Every industry has a number of standards or specifications that provide a common benchmark and help both the supplier and the consumer. The car industry has crash ratings, highway mpg, etc. At the moment most printed-related certification procedures are aimed at inkjet contract color proofing. Inkjet proofing is one sheet from a carefully controlled inkjet printer on specialized media. For digital production printing we need different but realistic tolerances.

Global technical committees are working on an international standard called ISO 12647-7.2 [ISO, 2008] that was aimed primarily at offset printing and is now being adapted and expanded to include digital production printing. TC130 - WG3 - ISO 12647 is Technical Committee 130, with Working Group 3 that is looking at process control, proofing tolerances, print tolerances, and aim points for production printing. There have been two recent meetings of TC130, WG3 - 17-18 April, 2008, Paris and 23-24 September, 2008, Amsterdam. The minutes of the Amsterdam meeting suggest that there will be a division of ISO 12647 as follows:

ISO 12647-7 will deal specifically with a "Contract Proof" - existing standard,
ISO 12647-8 will deal specifically with a "Validation Print" - new standard.

There is further discussion between the so-called "one copy standard" and production printing, thus the ISO Working Group agrees that a separate standard on digital production printing might be needed. In the United

SWOP certification process to encompass digital printing. In Europe, the Fogra organization offers "FograCert" digital print certification and has confirmed Canon, Konica-Minolta/Océ and Xerox certified systems. It is encouraging that all current and proposed certification procedures are using very similar criterion and tolerances, based primarily on the evolving ISO 12647 standard. If a user is considering purchasing a digital press, it is always useful to consider any certification that the device has been awarded, this demonstrates the technical ability of the system and the global responsibility of the manufacturer.

The Association of Graphic Solutions Providers (IPA) has conducted two studies of digital production presses called the 2008 and 2009 IPA Digital Print Forums [IPA, 2008] *The purpose of this research is to summarize results of the 2009 IPA Digital Print Forum in order to determine useful metrics and tolerances for certification programs.* An example of a tolerance is the average Delta E color difference between a press sheet and a reference printing condition, this may be set at 4.0 or less. Another metric under discussion is the use of Delta H as a measure of gray balance, which some experts suggest should be replaced with a different metric called, Delta F. The procedures and data gathered from the IPA Digital Print Forum seeks to confirm and validate the metrics and tolerances being developed in the ISO technical working groups.

2. IPA Digital Print Forum

The results presented here cover 10 press systems - 8 digital toner based devices and 2 offset DI type technologies. The systems studied are Canon imagePRESS C7000VP, HP Indigo 7000, Kodak NexPress S3000, Océ CS665 Pro, Presstek 52DI, Screen Truepress 344, Toshiba e-STUDIO6530c, Xeikon 3300, Xeikon 8000, Xerox iGen4.

The study covered all aspects of digital print production including color management and Pantone spot colors and physical properties of the printed sheets. The study considered the ability to match GRACoL and SWOP on a digital press, and evaluated the deinking and recyclability of the submitted printed samples. The 2009 IPA Digital Print Forum results were published in a booklet at the IPA's Annual Technical Conference, Chicago, June 8-10, 2009.

The tests can be divided into three distinct categories relating to Managing Color, Properties of the Printed Sheet, and Production and Productivity. Where a relevant ISO tolerance exists, that tolerance is used to qualify the press output.

Managing Color: There were a number of tests in this category, described as follows. The supplier attempted to match 3 reference printing conditions - GRACoL, SWOP #3, SWOP #5, Delta E between the printed IT8.7/4 target and each data set was computed. Each supplier was provided a PANTONE GoeGuide swatch book and was required to match 10 spot colors using CMYK simulation. In a separate test, the number of Pantone colors that could be reproduced by each system was computed. For each system the "blackest black" was determined in CIELAB and the CMYK values at which this occurs was noted.

Properties of the Printed Sheet: Tests in this category included studying the variation in a near-neutral uniform tint at 9 equally spaced points to determine the variation across the sheet. A proprietary test page called the Resometer™ was printed by each supplier. This test page was used to determine the optical resolution of the digital press. An area of heavy coverage (100% K) was folded in grain direction and against grain direction, the amount of white paper revealed at the crease was measured. CMYK blocks were subjected to abrasion and rubbing using the Taber rub tester. The loss of density due to abrasion of the surface of the print was measured. Suppliers printed a page with known ink coverage and sent the samples to Fogra where they were deinked to reveal a universal deinkability score that enables us to assess their suitability for recycling. Print samples were placed in a Q-Lab test chamber and subjected to accelerated light and heat fading tests.

Production and Productivity: In this category test samples from a 1000 sheet press run were measured to determine the variation in density over this run length. In an ISO standard test, a control bar was measured from a print produced on day 1 and compared to a print prepared on day 2, at least 24 hours later. In a supplier suggested test, both sides of a duplex print were measured to determine the Delta E between both sides of the sheet. A unique process was initiated where end-users where surveyed and uptime measured as a function of total elapsed job time.

The tests provide a comprehensive assessment of technical parameters that are useful to different parts of the digital print market. Most suppliers conducted all tests as specified, there were however some exceptions. Some were unable to use the recommended paper in all tests due to runability issues and one system (HP Indigo 7000) did not enter the INGEDE Method 11 de-inking test.

3. Results

The test were conducted on a common substrate to eliminate a major variable, paper, from the test. The paper used for this study was NewPage Futura Laser Gloss 100 lb text (148 g/m²) and came from a single mill roll. The paper was made available in sheeted and roll format depending on the digital press.

The tolerances used in this research are derived, where appropriate, from ISO 12647-7. Throughout these results, traditional Delta E^*_{ab} is used. Delta E^*_{ab}, is also known as Delta E (76), after the year in which it was adopted. While many researchers are now using newer Delta E equations, Delta E^*_{ab} is the metric that is used in all current specifications/standards and is thus used in this work. It should be noted that newer metrics have been computed and are available for all the data presented here.

Due to space limitations, all results from all tests are not presented here, only a representative sample of test results are discussed in detail. The interested reader is directed to a separate publication that contains the print samples and full results and graphs [IPA, 2009].

3.1 Matching GRACoL

The digital press industry is beginning to develop systems to match color characterization data. It is useful to know if a process is in place to achieve a colorimetric match to a given reference printing condition. It is not essential that a digital press matches an offset press, however there are many situations where digital print may be placed alongside offset printing in a publication. The digital press industry is beginning to develop systems to match reference printing condition data and it is interesting to know if suppliers have a process to achieve a colorimetric match to a given reference printing condition data set.

This test is based on a colorimetric (CIELAB Delta E) correlation of the vendor's print to each of the three main North American offset reference printing conditions. The results shown here relate to GRACoL 2006 Coated #1, that represents commercial offset lithography, sheet-fed printing. Figure 1 shows that digital systems have an average Delta E that varies from around 2 to 6. For reference, most inkjet proofing systems would have a Delta E of 1.0 - 1.5. The figure also shows the error at the 95th percentile, this is interpreted as a measure of the maximum error, an indication of the value of the patches with the worst Delta E.

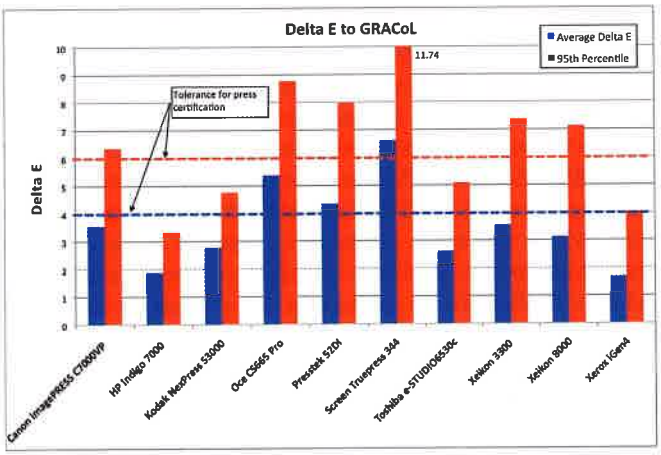

Figure 1: The graph shows the Delta E between each press and the GRACoL reference dataset, measured from targets submitted by each supplier

Inter-instrument differences will make a significant contribution to the results shown here. The supplier will have measured the prints using their instrument and minimized Delta E to the lowest practical value. The data shown in Figure 1 however is based on the X-Rite iSis XL instrument at Ryerson University in Toronto. The Delta E achieved by each supplier will depend primarily on the software process used to create the match. Generally an iterative process is likely to converge to give a better match. Operator expertise and color management software

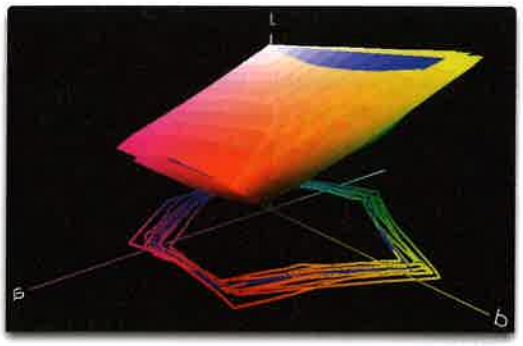

Figure 2:
The gamut of 10 digital presses are compared to the GRACoL gamut in blue, thus suggesting that the gamut of a digital press generally encompasses the offset-based reference data

The ISO 12647-7 standard requires an average Delta E ≤ 4.0, and at the 95th percentile, Delta E ≤ 6.0. The graphs shown here suggest that most digital press systems would pass certification. Thus this data suggests that the ISO tolerances are useful as they are achievable by most systems, yet they are not too lax. In addition to digital *press* certification, there is also digital *proof* certification. Based on the data shown here it is suggested that the HP Indigo 7000, Toshiba e-STUDIO6530c, and the Xerox iGen4 could also be certified as digital proofers, as they show an average Delta E ≈ 2.0, and indeed some are already certified [HP, 2009].

It is relevant to note that Presstek and Toshiba were unable to use the supplied stock in this test, for technical reasons and used different media as follows. Presstek used NewPage Sterling Ultra Digital 100 lb Gloss Text (148 g/m^2), and Toshiba used Toshiba Water Resistant Paper Simplex 230 g/m^2.

There are, in general, a few sources of error to consider. The gamut of the two processes may be different, thus there is the inherent, unavoidable errors due to gamut differences between the reference printing condition data and digital presses. The 3-D color gamut of a digital press generally encompasses the offset-based reference data, Figure 2, thus most of the error is likely to originate in color management and color control. The need to match other printing conditions is likely to become more and more important, it is therefore suggested that suppliers incorporate more mainstream functionality in their software DFE to facilitate cross-media color matching. It is not always necessary to match GRACoL or SWOP per se, but it is important for the digital press manufacturers to know how well their systems can match these printing conditions.

3.2 Matching the Pantone GoeGuide

Special colors are a necessary part of many print jobs today. The Pantone system may be used to specify special colors in a design or page. In this test it is useful to confirm that the RIP in a digital print system is able to detect spot color objects and produce a good match to the Pantone GoeGuide. The vendor was free to use any method to reproduce the color. A digital file was made available containing ten in-gamut Pantone Goe colors. The colors were labeled in the PDF file according to the new Pantone GoeGuide naming convention, Figure 3. Each press supplier was asked to print these colors using CMYK simulation. All suppliers were asked to use the Pantone GoeGuide Coated First Printing, which was made available by Pantone to the participating vendors. Delta E was computed between the press sheet and the GoeGuide for all 10 patches of each supplier submission. Figure 4 shows the average and maximum Delta E for 10 patches. In many cases the Delta E is larger than would be expected for a match to a special color.



Figure 3: Suppliers were provided a PDF file as shown here, and were required to print these 10 Pantone colors to match the PANTONE GoeGuide™ swatch book

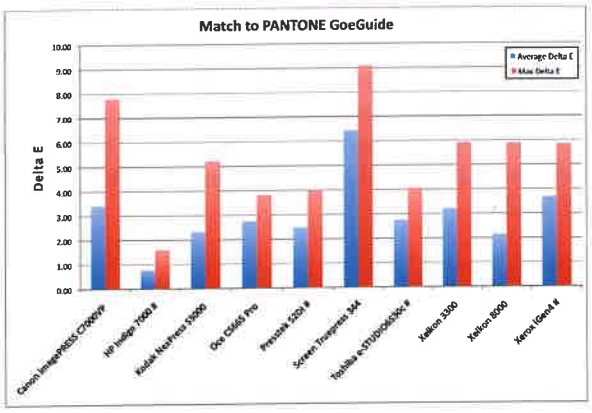

Figure 4:
Delta E between the press sample and the Pantone GoeGuide swatch book is shown. Data is based on matching 10 chosen patches

3.3 Variation in a tint

This test seeks to quantify a well-known issue in digital printing. Can a digital press reproduce a tint evenly across a page and does the press sheet show a pattern or color variation in some areas? In order to quantify the amount of variation in a near-neutral tint each supplier was required to provide a printed sheet, 12 x 18" or similar, with a nominal pixel value of (40, 30, 30, 30). The variation of color across the print was measured at 9 positions. Figure 5 shows the maximum standard deviation between the 9 points for L*, a* or b*. Also shown in the figure is the maximum Delta E between any point and the average L*a*b* of the 9 measurements. The ISO 12647-7 suggested tolerances for this test are 1.5 and 2 respectively; these are shown in the figure as dotted lines.

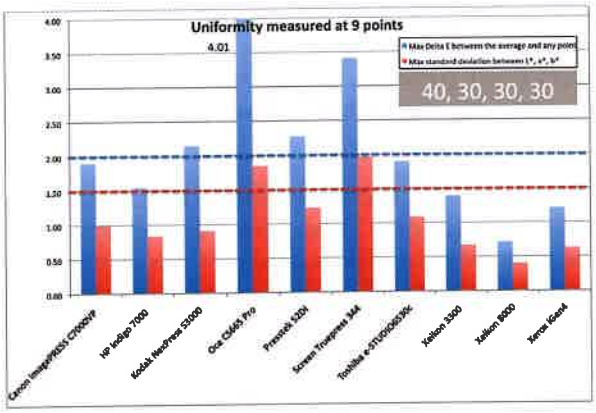

Figure 5:
Large near-neutral areas were evaluated at 9 positions; these graphs show the variation in those measurements. The same y-axis is used for two different parameters. The dashed horizontal lines represent ISO tolerances

The test was done at different density levels, the full results are not shown here, but it was found that the measured variation depends on density level and that most systems exhibit higher variation at higher densities. The actual printed density or L* value is not stipulated in the ISO specification, and due to the differences in setup there can be a difference in the printed density level, this ISO test should therefore have some procedure to ensure the printed density level is specified.

3.4 Resolution of the system

The Resometer™ test page [Freedman, 2009] is a very useful tool that can be used to reveal the effective resolution of the combined print engine and digital front end (DFE). Suppliers were required to print the EPS file of the test page. A number of parameters can be evaluated from the printed version of the target including horizontal and vertical resolution, font size, ink limits, and image contrast.

The page contains many test objects, we choose to describe here the results from the Contrast-Resolution target. In this test human observers viewed the test target and determined the resolution of the print system. Resolution is related to parameters such as addressability of the engine, paper, ink/toner, all these factors contribute to the appearance of the test target and the measure of optical resolution. Resolution is also a function of contrast. The resolution was measured at four contrast levels - 100%, 59.90%, 35.90% and 21.50%.

The blue column in Figure 6 represents the resolution at 100% contrast, this column can be used to predict the resolution of the system when dealing with thin black lines and solid black text. In this graph a higher number is better. When studying the results the reader may note the highest resolution of the offset technologies (Presstek 52DI and Screen Truepress 344) compared to toner based systems. Actually the two DI technologies are "off the scale" as a glance at Figure 6 will reveal that 6.25 is the highest resolution on this target. The DI presses may have even higher resolution than could be measured here. In general a higher column is better and it is best if this value stays high at the four measured contrast levels.

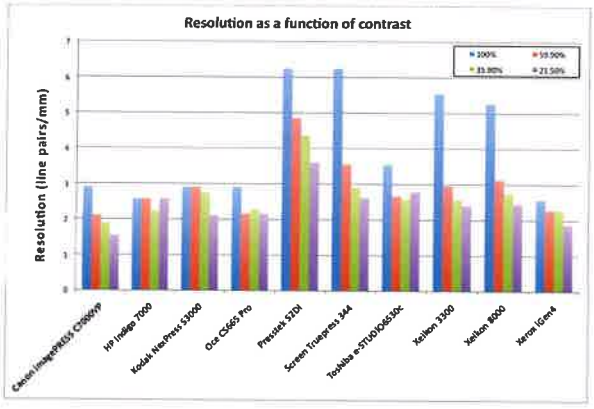

Figure 6:
The resolution for each system is shown at 4 different contrast levels. The column for 100% contrast (blue) can be used to predict the resolvability of fine lines and solid black text

3.5 Fold and crease resistance

Output from digital presses can create problems during finishing. Since toner sits on top of the paper and does not penetrate the paper like printing ink the sheet can crack when folded. This is especially evident in cases of heavy coverage and/or folding across the grain direction [DiSantis, 2007]. Traditional folding and creasing machines were not designed for digitally printed media thus there are many new products on the market for digital print scoring and folding.

This test was conducted at the Printing Applications Laboratory, Rochester Institute of Technology according to the ASTM F 1531 method. An image of a 100% K, "black cross", was printed on each system. The sheet was folded in the grain direction and at 90° to the grain direction. The cracked area was digitally analyzed to compute the visible white paper using image-processing techniques.The white area of the paper that is exposed after folding was measured using a microscope and image analysis techniques for edge detection, thresholding and area calculation based on prior "pixel to area" calibration techniques. The total exposed white paper area in mm^2 was computed for each system.

The results in figure 7 show that two digital printing devices have a better fold and crease resistance than the prints from the two offset devices, while the other digitally printed products have a lower fold and crease resistance manifesting itself in a higher area of white paper visible in the printed black cross.

3.6 Deinking and recyclability

Green printing and sustainability are becoming important considerations in the marketplace today. Good recyclability of printed products is highly desirable. Processes that improve print quality need to be balanced with the removal of these same particles during the recycling and deinking process. An established standard in Europe is the INGEDE test method, Method 11, and deinkability score [INGEDE, 2007]. The test is based on a test form of known CMYK coverage. Each vendor printed 200 pages of this form on their press and sent the samples to FOGRA in Germany for testing.

The deinking process consists of three main steps. The process begins with pulping where the dry printed press sheets are torn and disintegrated in a Hobart pulper with chemicals, this helps the detachment of the toner from the paper fibers or paper coating. After pulping, the chemical solution and paper fibres are transferred to a floatation tank where air bubbles are injected to remove toner particles via foam, which is skimmed off. Toner particles below 10 μm, in general are too small to be collected by floatation and particles bigger than 100 - 250 μm are too bulky to be successfully carried to the surface.

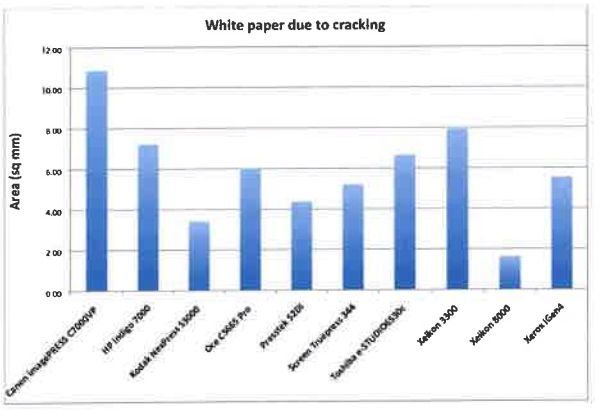

Figure 7:
The white paper area visible after folding is shown in this graph. In this graph, a lower number is better

In the Method 11 process, the froth is skimmed off and after 12 minutes of air bubbling a sample of pulp is removed and pressed onto a mesh filter, to remove water and form a handsheet. A set of filter pads /handsheets are made using before flotation, i.e. undeinked pulp, and a second set is made after flotation, i.e. deinked pulp. The assessment of deinkability of a print process is based on a single number called the deinkability score that can range from -100 to +100.

The score itself is based on six measurements that are made during and after the deinking process. All the sub-tests contribute to the overall deinkability score. The sub-tests include measurement of the Y (luminosity) and the CIE a* value of the deinked pulp. Other tests consider the toner or dirt in the samples, and the handsheet is analyzed for total area covered, size and particle count of the dirt specks. In the sub-tests, the amount of dirt particles between 50 and 250 µm diameter, and above 250 µm, remaining in the deinked pulp is measured. Finally ink elimination (IE) and a filtrate darkening parameter (ΔY) is calculated. Based on a threshold and target values these sub-test measurements are converted into an overall deinkability score, this final single number helps to assess the deinkability of a print product.

The eight systems measured here all have deinkability scores that are very good and range from 96 - 100 (maximum score is 100). From the results shown in Figure 8, we conclude that traditional offset ink and dry toner do not give any problem for deinking and paper recycling. While there may be small variation in the underlying sub-tests the overall deinkability score is similar in all cases. These findings are in agreement with the general consensus and with findings published by INGEDE [Fisher, 2008]. We may conclude that liquid toner has some challenges, while dry toner shows no problems for deinking. We note that HP Indigo 7000, that uses a type of liquid toner, declined the offer to participate in this test. These tests are difficult and expensive to conduct; yet they are of great interest and value to many in the wider print community.

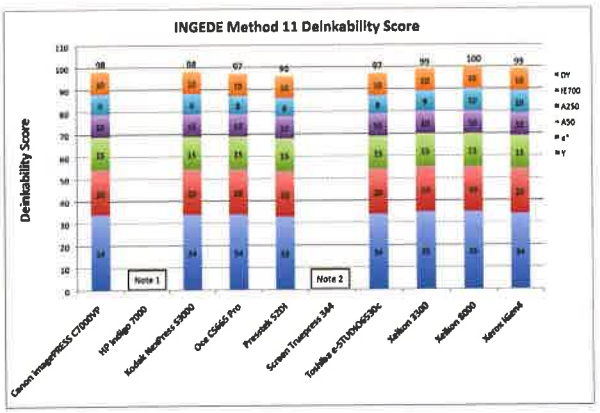

Figure 8:
The overall deinkability indicates excellent removal of toner or offset ink from the printed samples. Note 1: HP declined the offer to participate in this test. Note 2: Screen did not provide a sample due to time constraints

4. Conclusions

The reader is urged to recall the saying, "no free lunch". That concept is very applicable to digital presses. There is always a balance between, for example, paper weight and press speed; the heavier stocks often slow down a

machine. In other areas the supplier may seek to optimize and extend their color gamut, and the price to pay may be in light fastness. Toner research to improve print quality, for example, needs to be balanced with the removal of these same particles during the recycling and deinking process. R&D efforts are a continuous balancing act where we seek to extend the device in one area with minimum impact on other variables.

It is important to note that the *absolute* values of the data shown in this report will depend on the equipment being used, however the same instruments were used on all supplier systems so it is a level playing field when comparing the systems *relative* to each other. The reader is also urged to consider not just the height of the columns in each graph, but to also consider the scale on the vertical axis. Often there may be a difference of 0.1 density units, or 0.3 Delta E, we know that such small differences are not significant in everyday printing.

While most digital presses will be primarily used for production, there are a number of situations in which the same device can be used for digital color proofing. The digital press industry is beginning to develop systems to match color characterization data. Producing contract color proofs on a digital press provides a very economical and versatile proofing platform and a new opportunity for digital presses.

This type of independent technical study benefits the whole digital print community, from standards organizations to end-users, and enables digital printing to continue to increase its market share. The study seeks to further the development of standards and protocols in digital print production. The study shows that there exist some tolerances for digital printing and in tests where there are tolerances, they appear to be realistic and achievable in practice.

Acknowledgements

Abhay Sharma is supported by a Canadian NSERC Discovery Grant (341606-2008). The authors wish to thank the participating suppliers for their cooperation in submitting print samples for evaluation. We thank Steve Bonoff, President, IPA for supporting this research and allowing publication of the results.

References

1. DiSantis, N., 2007, Rub, fold, and abrasion resistance testing of digitally printed documents, MS Thesis, RIT
2. Fisher, A., 2008, Investigations on Deinkability and Ink-Paper Interactions, IS&T NIP24 Conference Proceedings, September 6-11, 2008, Pittsburgh
3. Freedman, H., 2009, Resometer™, Technology Watch, http://www.myresometer.com
4. HP, 2009, "HP Announces First-ever GRACoL Certification for Digital Production Presses at Dscoop Conference", Press Release, ORLANDO, Fla., Feb. 19, 2009
5. INGEDE, 2007, Assessment of Print Product Recyclables - Deinkability Test, Method 11, http://www.ingede.com
6. IPA, 2008, Digital Print Forum, An independent technical evaluation of digital printing technologies
7. IPA, 2009, Digital Print Forum, An independent technical evaluation of digital printing technologies
8. ISO, 2008, ISO/CD 12647-7.2 Graphic technology - Process control for the production of half-tone color separations, proof and production prints - Part 7: Off-press proofing processes working directly from digital data, Date of document 2008-05-23

Fusing of electrophotographic toner on thermally engineered coated paper

Philip Gerstner[1] and Patrick A.C. Gane[2]

[1] Helsinki University of Technology
Faculty of Chemistry and Materials Science, Department of Forest Products Technology
Vuorimiehentie 1A, P. O. Box 6300, FI-02150 Espoo, Finland
E-mail: firstname.lastname@tkk.fi

[2] Gane is also Head of Research and Development
Omya Development AG
CH-4665 Oftringen, Switzerland

Abstract

Rapid toner fusing and adhesion to coated paper is critical for energy efficiency and runnability in electrophotographic printing. The thermal transfer from the fusing roll to the toner layer competes with heat loss into the substrate. Whilst it is essential that the surface of the coated substrate displays a continuity of thermal conductivity to ensure uniformity at the coating-toner interface, the authors have previously shown by simulation that providing an insulating coating layer may provide advantages in terms of lower temperature fusing. To develop the concept further, two insulating constructions were formed using pre-coating layers consisting of either mica or a highly porous modified calcium carbonate (MCC). Thin top-coatings consisting of a fine narrow particle size GCC were applied to each to provide the predicted necessary surface continuity. A reference paper adopted a single coating layer having a similar coating formulation to that of the top-coatings, being predominantly carbonate-based. Adopting a method of controlling fusing roll temperature (KCL "DUPLO" apparatus), it could be shown that the onset of toner fusing and final adhesion could be developed at lower temperature for the case of the insulating pre-coat, the effect being most marked for mica. The MCC was compromised in this study due to poor binding strength of the coating layer, such that the porous MCC had to be diluted by blending with a standard broad particle size GCC, thus increasing coating density. Important differences were observed between the behaviour of full tone and half tone areas. The full tone response matched that of a tri-layer, consisting of the adhesive tape used to test the toner adhesion, the toner layer itself and the coating/base paper, in which the competition of internal cohesive development and toner-coating interface adhesion led to abrupt adhesion failure following the build of internal cohesion prior to complete establishment of fully fused adhesion. The half tone areas, by contrast, due to the absence of the thin film effect of continuous toner in the full tone case, displayed a smooth transition from adhesion failure to fully fused adhesion. Print gloss of the full tone area correlated with the transitional response, and could be used in this case to monitor toner fusing.

Keywords: electrophotography, thermal properties, properties of coatings, toner adhesion, heat transfer in porous materials, printability

1. Introduction

The use of heat in many conversion and printing processes of coated papers, together with the increasing cost of energy creates a need to, both understand better the mechanisms of heat transfer in coated papers, and further study the role of the thermal energy in such processes with regards to quality parameters. In electrophotographic printing, heat is used to permanently fuse the individual toner particles together and fix them on the printing substrate. Important quality parameters in such a thermal fusing process are toner adhesion and print gloss, both of which depend on the thermal conditions during fusing. Furthermore, surface roughness is regarded as a critical parameter for toner adhesion [Sipi, 2001; Hartus, 2001]. However, the works on the effect of surface roughness have not linked surface continuity to thermal conductivity.

The thermal response on the surface of a coated paper depends on the thermal conductivity of the coating. Gerstner and Gane [2008] showed recently by simulation of the thermal conditions in an electrophotography fusing nip, that a more insulating coating layer leads to faster and higher temperature responses at the interface of toner layer and paper coating. However, they also showed that, especially for good half tone toner adhesion, high surface-continuity is prerequisite. It was therefore suggested to complement the thermally insulating coating with a thin top-layer of a more conductive coating to provide surface continuity.

This study develops further the concept of modifying the thermal properties of paper coatings for electrophotography printability by introducing two different concepts of multilayer coatings: a thermally insulating mica pigment pre-coating and a porous Modified Calcium Carbonate (MCC) pre-coating, both having a similar top-coating layer. They are compared to a reference coating and discussed in terms of their thermal properties and print quality parameters.

2. Materials and methods

2.1 Materials

In this study, two thermally designed coating concepts are studied and compared to a reference. The first concept, henceforth simply referred to as "Mica", uses a mica[1] pigment pre-coating together with a fine, narrow particle size distribution ground calcium carbonate top-coating[2] (nfGCC). Compared to other minerals, mica has a very low inherent thermal conductivity of ca. 0.4 $Wm^{-1}K^{-1}$ [Landolt-Börnstein, 1980]. This is about a sixth of the inherent thermal conductivity of calcium carbonate. Mica is also a very platy pigment, having an aspect ratio of 20:1 to 40:1. Both factors make it an ideal choice to be used in a thermal barrier coating. The second coating concept, henceforth referred to as "MCC", consists of a porous Modified Calcium Carbonate pre-coating[3] (MCC). A coating using the porous modified calcium carbonate pigment alone showed greater thermal insulating behaviour compared to standard calcium carbonate pigments [Gerstner and Gane, 2008]. However, it was found that a coating consisting of MCC pigment only delaminates easily, for example in the tape test which is used to study toner adhesion (see Evaluation of the Toner Fusing). This was observed even at a binder concentration of 15 w/w %. In such toner adhesion measurements, it was often the MCC coating layer that showed to be the weakest link, exhibiting low cohesion. Therefore, to develop better internal cohesion of the MCC coating layer, it was used in blend combination with a broad particle size distribution ground calcium carbonate[4] (bfGCC). The MCC coating concept had a comparable top-coating formulation applied as was used in the mica concept.

Table I: Coating formulations and methods used in the pilot scale coating trial

Pre-coat	***Reference***	***Mica***	***MCC***
Method	Blade	Blade	Film
Pigment(s)	80 nfGCC	100 Mica	80 bfGCC
	20 Clay		20 MCC
Binder	11 w/w%, SA	9 w/w%, SA-R	12 w/w%, SA
Top-coat	*	***Top I***	***Top II***
Method		Film	Blade
Pigment(s)		100 nfGCC	100 nfGCC
Binder		6 w/w%, SA	10 w/w%, SA
		4 w/w%, Starch	

*single coating layer

Both the mica and MCC coating concepts are compared to a reference coating which is a monolayer of a calcium carbonate and clay[5] blend. The binders used were a standard medium T_g SA[6] latex and a self-thickening rotogravure latex (SA-R[7]) to promote the barrier properties in the mica formulation. Table I provides a summary of the coating formulations and the corresponding coating method used. All the coatings had a similar target coat weight of ca. 12 gm^{-2} per side and were coated on an industrial scale pilot coating machine[8] using both the blade coating and film press coating methods. After coating, the web was calendered to target gloss of 33 - 35% and cut to A4 sheets for printing.

1 Mica SFG 70 (Mica), Aspanger
2 Covercarb 75 (nfGCC), Omya AG
3 MCC564, 5 µm, 64 m^2g^{-1} (MCC), Omya AG
4 Hydrocarb 90 (bfGCC), Omya AG
5 Hydragloss 90, Huber Engineered Materials
6 Latexia 203, Ciba
7 Latexia 211, Ciba
8 FPC - Forest Pilot Center Oy, Raisio, Finland

2.2 Measurement of thermal conductivity

For the measurement of thermal diffusivity of the coating formulations, pigment-binder tablets of the coating colour formulations were formed. A constantly applied pressure of $p = 20$ bar was used to dewater the suspension mix (coating colour) through a membrane. After forming and decanting any remaining slurry, the tablets were removed and oven dried at 60°C, following the method of Ridgway et al. [2004].

The thermal diffusivity measurement is based on a technique introduced by Gane et al. [2006] and further developed by Gerstner et al. [2008]. The pigment tablets are subjected to a temperature step on one side while the temperature response on the other side is recorded. The measured temperature response, along with initial and boundary conditions, allows calculation of the tablet's thermal diffusivity by matching the numerical solution of the one dimensional heat diffusion equation to the measured topside temperature response. This is done by a self adaptive iteration of the parameters thermal diffusivity and heat loss. The numerical solution matching the experimental curve delivers the experimental value for thermal diffusivity D_{exp}. The effective thermal conductivity k_e is then calculated using the measured tablet density ρ_t and the heat capacity c_t:

$$k_e = D_{exp} \cdot \rho_t \cdot c_t \tag{1}$$

where c_t is calculated additively for the mass share of the two phases, pigment (c_{s1}) and binder (c_{s2}) for the given binder dosage β:

$$c_t = \frac{c_{s1} + c_{s2}}{1 + \beta} \tag{2}$$

2.3 Printing of the sample sheets

The printing trials were performed on the KCL electrophotography printing system "DUPLO" (Figure 1). This system allows individual adjustment of the process parameters, such as printing speed, toner transfer voltage and fusing temperatures. Because of its open structure it is also possible to sample in between process steps such as toner transfer and fusing.

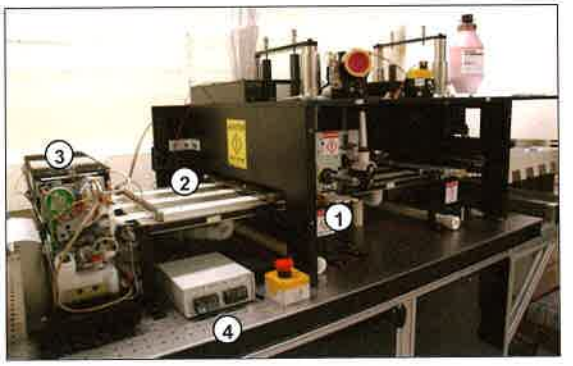

Figure 1: KCL electrophotography printing system "DUPLO". 1) Toner transfer unit, 2) Transfer belt, 3) Fusing unit, 4) Fusing temperature control

The sheets were printed with a 1 bit bitmap test pattern (Figure 2). The test pattern consisted of areas to measure toner adhesion on full-tone black (100% black) printed surfaces and on half tone (40% black) surfaces which were arranged in a matrix of three columns (1 - 3) and three rows (A - C). This allowed evaluation of the evenness of the fusing both lengthwise and crosswise. Because of the diameter of the fusing roll, the fields in row C were fused on the second turn of the fusing roll and therefore the fusing temperature might have been lower than on the first turn due to thermal loss to the toner and paper. For this reason only rows A and B were used for the quantitative evaluation of the fusing process.

For all prints the toner transfer adopted a voltage of 3.8 kV at a speed of 10 cms^{-1}. The toner[9] was a traditional melt grinded polyester based toner (T_g = 78°C, Hakola, 2007). Sampling of sheets after toner transfer confirmed

a complete and even toner transfer. The temperature of the fuser roll was set to temperatures ranging from 130°C up to 160°C. The KCL "DUPLO" test printing system also allows adjustment of the temperature of the backing roll. This was set constant to the lowest controllable temperature of ca. 90°C. However, the sample sheets were fixed onto a thick (240 µm), insulating carrier board, in order to minimise temperature fluctuation influences from the backing roll.

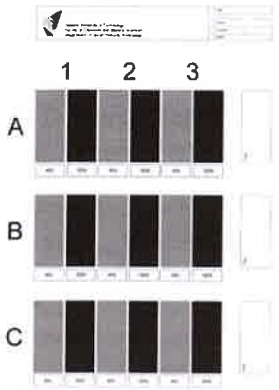

Figure 2:
Test pattern used to print the sample sheets. Each test cell consists of a full tone and half tone area. Rows A and B were used for calculation of the toner area fraction. Row C was used for visual evaluation during the printing trial

2.3 Evaluation of the toner fusing

In the previous study of the authors [2008], the relative loss in optical print density after removal of an adhesive tape was used as a quantification of toner adhesion. However, print density was found to be a rather imprecise measure when it comes to the area of very low toner adhesion as encountered in this study. Toner adhesion is therefore here expressed as the area fraction ξ of toner that remained on the test field after tape removal of the adhesive tape.

For the evaluation, the test pattern was scanned after performing the tape test in double the resolution as that of the printing (Nyquist sampling theorem). The scanned image was analysed using a custom made image analysis program that calculated the number of black (toner) pixels N_{Black} based on the total pixel number:

$$\xi = \frac{N_{\text{Black}}}{N_{\text{Black}} + N_{\text{White}}} \cdot 100\,\% \tag{3}$$

Because of the 1 bit printing and scanning, no thresholding was required. Figure 3 shows an example each of a scanned half tone area, full tone area and a full tone area after the tape test.

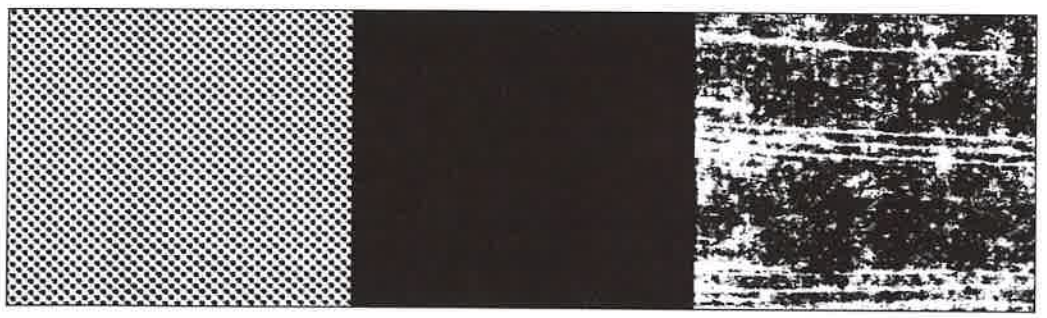

Figure 3: Left to right: magnified scan of a half tone area (40% black), scan of a full tone area and scan of a full tone area after the tape test

The total cohesion of the multilayer composite consists of the cohesions of the individual components γ_i as well as the adhesions between the layers γ_{ij}. Figure 4 lists the possible adhesion and cohesion energies for the case when the tape is fully covering the toner layer (full tone; Figure 4, left) or when the tape is also in direct contact with the coating (half tone; Figure 4, right). The nomenclature given in Figure 4 will be used in the subsequent discussions. Peeling off the adhesive tape will delaminate the structure at the weakest link [Thouless and Jensen, 1995]; i.e. at

the point of lowest cohesion or adhesion. As such, the tape test does not necessarily measure "toner adhesion" (γ_{23}) only. Delamination might occur because of adhesion failure at any of the material interfaces or because of cohesive failure within a material. Since the toner area fraction measurement evaluates the number of black toner pixels per area, the toner area fraction might deviate from recording purely toner adhesion because of cohesive failure of the toner layer (black remains black after the tape test) or because of cohesion or adhesion failures in the lower layers (black turns to white after the tape test even though there was full toner to coating adhesion), i.e. one needs to take into account whether toner is removed by the tape or whether a delamination of coating or base paper takes place. By definition, the maximum toner area fraction is 40% and 100% for the half tone and full tone area respectively. For future discussions, unless pointed out otherwise, any result of a lower toner area fraction will be regarded as low toner adhesion.

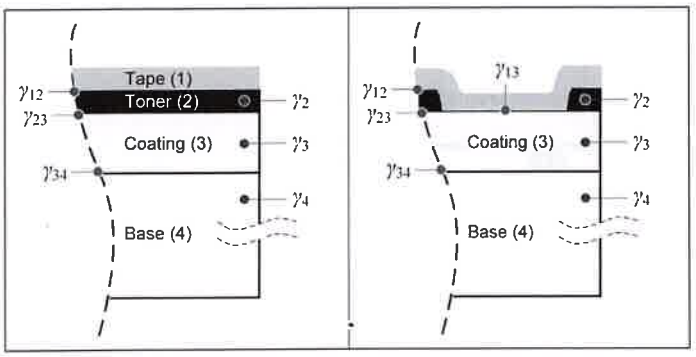

Figure 4:
Cohesion (γ_i) and adhesion (γ_{ij}) of the multilayer laminate consisting of tape (1), toner layer (2), coating layer (3) and base paper (4). Left: full tone laminate. Right: half tone laminate with the additional interface of tape to coating layer

3. Results and discussion

3.1 Thermal conductivity

Figure 5 shows the measured thermal conductivities of the coating formulations for both the pre-coatings and the top-coatings. The formulation "Top I" refers to the nfGCC top-coat formulation applied on the mica pre-coat, whereas "Top II" is the formulation used on top of the MCC base-coating. It can be seen that the conductivities of the reference coating, the MCC formulation as well as the top-coating formulations are very similar. While it was desired to achieve comparable thermal conductivities for the top-coatings and the reference coating, the thermal conductivity of the MCC formulation is higher than initially expected. When using only MCC pigment and a binder amount of 15 w/w%, the thermal conductivity was measured to be 0.12 $Wm^{-1}K^{-1}$ (Gerstner and Gane, 2008). However, in the case of the blend of 80 parts bfGCC and 20 parts MCC (used because of coating strength considerations - see materials discussion above), the thermal conductivity is raised to ca. 0.54 $Wm^{-1}K^{-1}$, due to the increased tablet density (1 666 kgm^{-3} for bfGCC/MCC compared to 825 kgm^{-3} for MCC pigment only) and due to increased solid phase connectivity because the bfGCC fills the MCC structure to some extent.

Despite the rather high thermal conductivity of the MCC formulation, Figure 5 shows that the mica formulation exhibits the desired distinctly lower thermal conductivity. Since the binder amount of 9 w/w% is close to the amount used in, say, the top II formulation, it suggests that the difference in thermal conductivity is in fact largely due to the inherently lower thermal conductivity of the mica pigment.

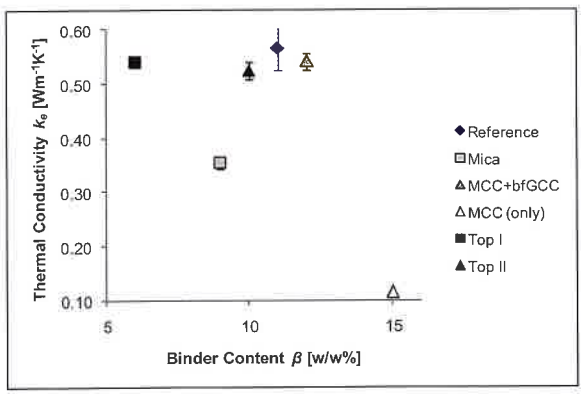

Figure 5:
Thermal conductivities of the coating formulations involved

3.2 Toner area fraction

Surface roughness is generally referred to as being a critical parameter for toner adhesion. Although Sipi [2001] showed that roughness for calendered grades is not the most critical factor, and also Gerstner and Gane [2008] could relate neither macro nor micro roughness directly to toner adhesion, PPS roughness shall be included in this discussion to point out the similar surface properties of the coatings. Table II shows the PPS roughness, measured on unprinted areas of printed sheets, together with the calendered gloss level. The roughness is slightly less for the mica coating concept, because of the platy particles providing excellent pre-coat coverage of the base paper. The MCC is slightly smoother than the reference, given the compressibility of the structured MCC, but generally all surfaces are at a similar level. In addition to roughness, surface chemistry of the calcium carbonate top-coatings can be regarded as similar. The subsequent discussion will therefore focus on thermal considerations during fusing.

Table II: PPS roughness measured on unprinted area after print and gloss level (TAPPI 75°)

	PPS *[µm]*	***Gloss level*** *[%]*
Reference	1.94	34.5
Mica	1.58	33.2
MCC	1.86	34.4

Figure 6 shows the measured toner area fraction after the tape test on the half tone area (left) as well as on the full tone area (right) as a function of the fusing roll temperature. First of all, one can see that there is a rather large standard deviation in both half tone and full tone areas at the onset of toner adhesion. On the one hand, this refers to the unstable nature of adhesion in the temperature range where toner begins to adhere. However, on the other hand it was observed that part of this deviation comes from slightly different adhesion levels in the test fields of the print pattern (see Figure 2). The fields in row B generally showed a lower toner adhesion than the fields of row A. The fusing roll temperatures given in Figure 6 are the temperatures of the fusing roll right before the fusing of the entire sheet. The lower adhesion on fields of row B could therefore be as a result of an effective local decrease in the roll temperature during the fusing process.

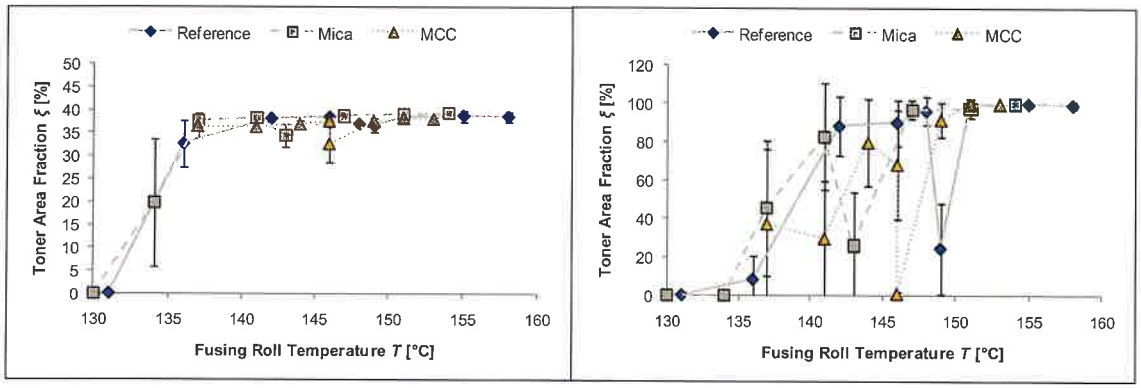

Figure 6: Toner area fraction as a function of the upper fusing roll temperature for half tone areas (left) and full tone areas (right)

While the half tone toner area fraction (Figure 6, left) is quite stable for all substrates when the fusing roll temperature is higher than 137°C, the toner area fraction in full tone areas shows a more complex behaviour (Figure 6, right). One can see that the temperature of ca. 134°C is the onset of the measured toner area fraction for the reference and the mica coating. The same holds for the MCC coating even though there is a larger standard deviation. Furthermore, all three coating concepts show the common trend that with increasing fusing temperature the toner area fraction increases as well. However, just before the full toner adhesion is achieved there is a significant drop in the toner area fraction. The toner area fraction subsequently reaches the constant maximum at fusing roll temperatures, respectively, of 147°C (Mica), 149°C (MCC) and 151°C (Reference) on full tone area. This trend correlates with the measured thermal conductivities (Figure 7). The lowest thermal conductivity of the coating provides the fastest temperature response in the thin more conductive top-coat, and

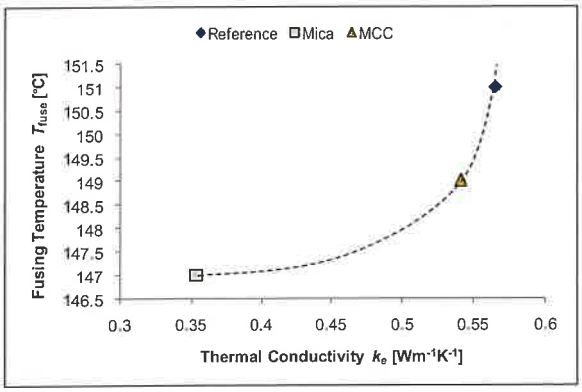

Figure 7:
Threshold fusing temperature where full toner adhesion is reached as a function of effective thermal conductivity of the thermally engineered pre-coat layer

The behaviour that all the coatings showed in the range of different fusing temperatures for full tone fusing is worth examining in further detail. For the mica data, which is exemplary for the MCC and reference data as well, Figure 8 shows the trend split into four temperature ranges:

In *range I* no toner adhesion can be observed by the tape test at all. This means that the entire toner layer must have been taken up by the tape removal. To achieve that, the tape to toner adhesion must be higher than the toner to coating adhesion ($\gamma_{12} > \gamma_{23}$), but also the toner cohesion must be higher than the toner to coating adhesion ($\gamma_2 > \gamma_{23}$). Hartus [2001] showed that the initial softening of toner occurs at temperatures above the glass transition temperature of the toner T_g = 78°C [Hakola, 2007] which is well below the threshold temperature of 134°C as given in Figure 8. During this initial softening, the temperature is high enough for toner particles to begin to coalesce and therefore build up cohesion forces. For that reason, the tape test can remove the toner quite effectively in range I.

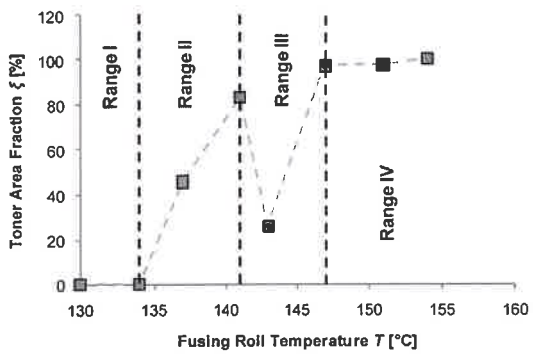

Figure 8:
Full tone toner area fraction on the mica coated paper to illustrate the four temperature ranges of the development of a fully cohesive laminate. This behaviour is exemplary for the Reference and MCC coating as well

In *range II*, the adhesion between toner and coating begins to build up in addition to the continuing increase of toner cohesion. The tape test cannot exactly quantify the magnitude of toner cohesion versus toner adhesion. However, the fact that this temperature range is characterised by a high variance in the measurement results suggests that there is a competition in delamination between the increase of internal toner cohesion and adhesion to the coating layer and that those forces are in the same order of magnitude ($\gamma_2 \approx \gamma_{23}$). This means that only part of the delamination force is transferred to the toner coating interface. The measurement becomes very susceptible to local variations caused by either the process (cooling of the fusing roll during fusing) or variations within the substrate such as interface flaws or residual stresses [Thouless and Jensen, 1995].

The temperature *range III* signifies a critical area for which the cohesion of the toner reaches its maximum while the adhesion to the coating layer is not fully established. The toner to coating adhesion is therefore the weakest link in the delamination process of the tape test. Such a response to delamination has been observed for the adhesion of offset ink on coatings as well, where the build up of cohesion (internal tack) reaches a point where the full delamination force is transmitted to the interface of coating and ink [Ridgway *et al.*, 2002].

For the higher fusing temperatures in *range IV*, both the toner cohesion and adhesion to the coating are complete. The high toner adhesion is observed as the tape test does not show a loss in the toner area fraction. At the same time, the high toner cohesion could be observed by attaching the tape used for testing to a blank sheet of paper. On the white background, no or very little toner on the tape could be identified visually. However, it should be

noted that also delamination of the base paper was observed (γ_4 becoming the weakest link). This occurred for all the coating concepts which is a testimony to the high internal coating strength (γ_3), including that of the MCC concept having the bfGCC blended in.

The discussion above about the four temperature ranges of adhesion/cohesion development focused on the tape test performed on a full tone printed area. The toner area fraction development on a half tone printed surface shows a different behaviour (see Figure 6, left). There is a more distinct "jump" to full toner cohesion/adhesion. Furthermore, the full adhesion level for all substrates is reached already at a fusing roll temperature of 137°C compared to the fusing roll temperatures of 147°C (Mica), 149°C (MCC) and 151°C (Reference) on full tone area. The sudden jump to full adhesion can be traced back to the fact that there is the additional tape to coating layer interface (see γ_{13} in Figure 4). The delamination force is almost exclusively transmitted through this interface before there is full toner adhesion: $\gamma_{13} > \gamma_{23}$. That means the tape picks up the half tone dots not because the toner particles fail to coalesce but because the toner to coating adhesion is smaller than the tape to coating adhesion the toner is removed completely by the tape. This effect is similar to the difference between separating a thin liquid film versus a single droplet, i.e. the surface energy associated with the continuous film dominates the transmission of forces, and is very difficult to break, whereas a droplet is a discrete system with minimised surface energy at the droplet-surface-air interface. Compared to the toner area fraction development on full tone areas this means that essentially the temperature ranges II and III (the toner cohesion build up) are "skipped" because of the additional interface, such that the tape test cannot observe the "competitive build-up" (see discussion in range II above) of toner cohesion and adhesion as applicable to thin films.

Two reasons come to mind why the half toner adhesion is formed at a distinctly lower temperature compared to the full tone. On the one hand, the thickness of a half tone dot might be lower than that of the full tone layer which would lead to a higher temperature at the interface of toner and coating and also to a faster temperature rise. On the other hand, direct contact of the fusing roll with the coating layer leads to faster temperature rise of the coating layer due to in-plane heat transfer in the continuous top-coat and thus it promotes the melting of the toner on its surface. Since all the coatings had comparable top-coating formulation to provide for surface continuity, the latter reason supports the previously stated hypothesis of the authors [2008] that surface continuity is vital for good half tone toner adhesion.

3.3 Print gloss

No coating would be designed regarding the thermal fusing properties only. Also other print quality parameters should reach desired targets and must therefore be taken into account. Print gloss is considered to be an important print quality parameter in electrophotography. Figure 9 shows the print gloss (TAPPI 75°) on full tone area as a function of the fusing roll temperature (left) and as a function of the toner area fraction (right). While it can be seen that a higher fusing roll temperature clearly improves print gloss, it is also visible that at the critical points where full adhesion failure would occur (range III, Figure 8) the gloss is reduced to almost the gloss level of the paper (horizontal lines in Figure 9, left).

The graph of print gloss versus toner area fraction (Figure 9, right) shows that there is a very linear correlation of measured full tone gloss (before the tape test) and the result in toner area fraction after tape test. However, this linear correlation holds solely for temperature ranges I to III, before the full adhesion is established. When the maximum toner area fraction is reached, print gloss continues to increase with fusing temperature. This can be seen in Figure 9, left, but also at the 100% toner area fraction in Figure 9, right. Nonetheless, the linear correlation of print gloss and toner area fraction during the build-up of toner adhesion means that the relatively simple measurement of print gloss could be used to anticipate toner adhesion.

Both parts of Figure 9 show that the printed gloss on the mica substrate is slightly higher than that of the MCC or reference coating, while the latter two coatings show very similar print gloss. Although it cannot be stated with absolute certainty that the higher print gloss observed for the mica coating is a direct result of its thermally insulating behaviour (compare Figure 5) and its beneficial fusing temperature development, it is clear that the print quality properties (low surface roughness, high gloss and good toner fusing) are not mutually exclusive and the combination of those is a clear advantage of the mica pre-coat formulation.

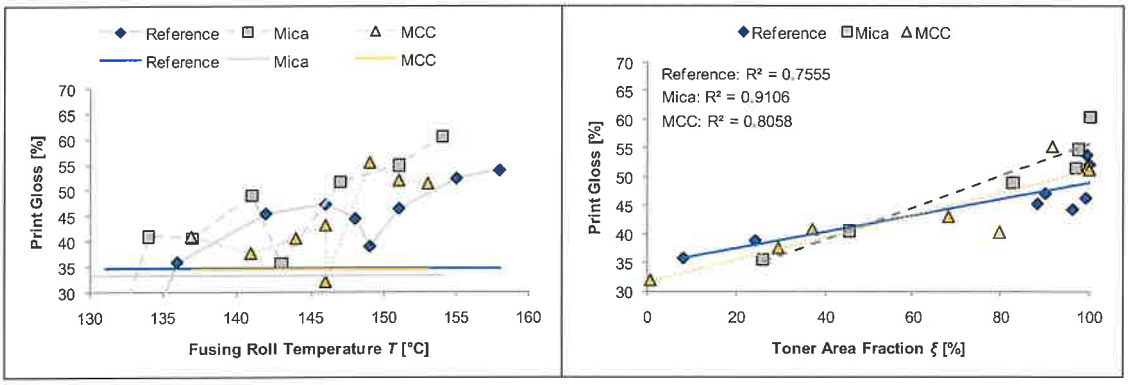

Figure 9: Left: print gloss as a function of the upper fusing roll temperature. The horizontal lines indicate the paper gloss levels. Right: printed gloss as a function of full tone area fraction after tape test, including linear trend lines for each substrate

4. Conclusions

Electrophotography toner fusing was studied for different fusing roll temperatures in the range of 130°C and 160°C for three different coating concepts: a reference coating, a thermally insulating mica pigment pre-coating as well as a porous Modified Calcium Carbonate (MCC) based pre-coating. The latter two pre-coatings had a thin top-coating applied for the surface continuity, which was comparable to the single coated reference. Toner fusing on those substrates was evaluated by means of a tape test to peel off non-cohesive and non-adhesive toner, in combination with subsequent analysis of the adhering toner area fraction for both full tone and half tone printed areas.

Four temperature ranges were identified for the fusing of full tone printed areas. At temperatures lower than 134°C there is no measurable toner adhesion (I). In the subsequent temperature range (II) there is a competitive build-up of toner cohesion and adhesion until at a critical temperature range (III) the cohesion of toner clearly exceeds the adhesion to the coating before the full fusing of the toner occurs (IV). It was shown that the mica thermal barrier pre-coating, provides complete fusing at the lowest temperature in comparison with the other concepts. The insulation behaviour of the porous MCC could not be fully utilised because of coating strength considerations, such that a blend a blend of MCC and standard GCC was used, but which in turn reduced the thermal insulating advantage of the MCC.

Half tone fusing was measured to be completed at significantly lower temperatures than full tone fusing. This was in accord with the high surface continuity of the coatings. Because of the additional interface of tape to coating, the tape test could not measure the build-up of toner cohesion and adhesion as on the full tone printed area. Therefore only two temperature ranges for the half tone fusing process could be identified: no toner adhesion or full toner adhesion.

The measurement of print gloss on full tone as another print quality parameter showed an increasing print gloss with increasing fusing temperature. However, it was also seen that at the critical point where toner adhesion failure would occur also the print gloss was lower. In the temperature range where adhesion builds up and the fusing process takes place, the print gloss correlates very well with assessed adhesion, and could therefore be used to anticipate toner adhesion.

Acknowledgements

The authors would like to thank Andrew Berry of University of Victoria, Canada for his assistance in recording the measurement data. Thanks to Teemu Grönblom of the FPC, Raisio, Finland for his assistance in the pilot coating and calendering. Thanks to Jorma Koskinen and Minna Hakkarinen of KCL, Espoo, Finland for their help in electrophotographic printing of the sample sheets. The financial support of TEKES, the Finnish funding agency for technology and innovation, is gratefully acknowledged. This work was done as part of the project THEOS, for "Thermal Effects and Online Sensing".

References

1. Sipi, K. M. (2001): *"Toner Layer Structure and Toner Adhesion on Coated Paper, NIP17: international conference on digital printing technologies"*, Fort Lauderdale, FL, USA, 30 Sept.-5 Oct. 2001, pp. 145-150
2. Hartus, T. (2001): *"Adhesion of Electrophotographic Toner on Paper"*, Graphic Arts in Finland, 30(3):14-19
3. Gerstner, P. and Gane, P. A. C. (2008): *"Considerations for Thermally Engineered Coated Printing Papers: focus on electrophotography"*, Advances in Printing and Media Technology, vol. 35, pp. 249-261
4. Landolt-Börnstein (1980): Zahlen werte und Funktionen, Band IV Technik, 4. Wärmetechnik a, 6. Auflage, Heidelberg
5. Ridgway, C. J., Gane, P. A. C. and Schoelkopf, J. (2004): *"Modified Calcium Carbonate Coatings With Rapid Absorption and Extensive Liquid Uptake Capacity"*, Colloids and Surfaces A, 236(1-3):91-102
6. Gane, P. A. C., Ridgway, C. J., Schölkopf, J., Bousfield, D. W. (2006): *"Heat Transfer through Calcium Carbonate-based Coating Structures: Observation and Model for a Thermal Fusing Process"*, Paper presented at the International Printing and Graphic Arts Conference, Cincinnati, Tappi Press
7. Gerstner, P., Paltakari, J. and Gane, P. A. C. (2008): *"A Method for the Measurement of Thermal Contact Diffusivity of Paper Coating Structures"*, Nord Pulp Paper Res. J, 23(4):354-362
8. Hakola, E. (2007): *"Toner Dynamics in Fixing"*, Licentiate's Thesis, Helsinki University of Technology, Espoo, Finland
9. Thouless, M. D. and Jensen, H. M. (1995): *"The effect of residual stresses on adhesion measurements"*, Adhesion Measurement of Films and Coatings, Mittal, K. L. (Ed.), Utrecht, The Netherlands, pp. 95-102
10. Ridgway, C. J., Kalela, E. and Gane, P. A. C. (2002), *"Ink-coating adhesion: Factors affecting deposits on the CIC in "satellite" type CSWO (cold-set web offset press) using VAC papers"*, Journal of Graphic Technology, 1(1):49-58

Printing of inorganic conductive layers

Ulrike Herzau-Gerhardt, Frank Hilscher, Henning Nagel

Hochschule für Technik, Wirtschaft und Kultur Leipzig (FH) / Fakultät Medien
(University of Applied Sciences, Department of Media)
Gutenbergplatz 2-4, D-04103 Leipzig, Germany
E-mails: uherzau@fbm.htwk-leipzig.de, hilscher@fbm.htwk-leipzig.de, henning.nagel@fbm.htwk-leipzig.de

Abstract

The research is focused on testing the possibilities of conventional flexographic printing process to transfer special conductive inorganic systems (nanoscaled Indium-Tin-Oxide / ITO) to plane glass and polymeric surfaces. Determinate parameters of the homogeneity of the transferred layers and the mean area resistance as well as the printing of defined structures had to be reached for the practical application (like OLED). Using a special developed proofing machine and the flexoprinting proofer (Type F1 by IGT) printing tests are organized with a range of coating materials which had different fluid properties depending on the ingredients in the dispersions. To compare the results constant viscosity of the tested fluids and constant printing conditions have been realized. The scaling procedure of the investigated coating fluids enabled to choose an optimal dispersion based on ITO for printing of functional layers in flexographic printing unit with conventional photopolymeric plates.

Keywords: flexographic printing, functional layers, inorganic conductive layers, nanoparticles

1. Introduction

Investigations of using printing processes for coating of very thin functional layers on the surfaces of different substrates are carried out with the aim to introduce a more effective production technology with lower costs. Different functions could be realized like conductivity, magnetic effects, surface effects based on roughness differences or various optical phenomena. Especially the application of conductive layers is of an increasing interest for the printing industry to extend the possibilities of traditional printing in the future [Rost, 2005], [Hübler, 2002].

The coating of thin conductive layers will be influenced by the real application (e. g. LED, OLED, RFID). For the different substrates are used different coating solutions: organic or inorganic dispersions with very different rheological properties. Printing technologies could be able to transfer those thin ink film layers with defined structures. The choice of the printing process will depend on the demands of the functionality of the application which have to be manufactured. So the limits of the coating like homogeneity of the transferred layer and/or the sharpness of the structure determine the transfer process in the printing unit.

The coating of conductive, transparent and structured dispersions based on nanoscaled Indium-Tin-Oxide (ITO) is one of the possibilities to manufacture functional surfaces on different materials for applications like OLED and others. Different printing processes seem to be able to meet the demands of the customers. These are screen printing, inkjet and flexographic printing.

Based on first investigations with flexographic printing machines [Nagel, 2007] the influence of different representative selected ingredients combined with ITO-dispersions are tested. The experiments have to be planned with the following aims:

- Printing of conductive layers in order to reach homogenous thicknesses less than one micrometer.
- Manufacturing structures with a resolution less than 150 µm for negative lines and 200 µm for positive lines.
- Realization of a mean area resistance of about 200 Ω.

The industrial application of functional layers based on inorganic dipersions like ITO is variable and is related with different substrates. Especially glass and polymeric foils could be of interest. Because of the different surface properties of those two materials it was expected that the wettability will be different and influence the

2. Research methods

The necessary testing program is carried out with a special printing proofer (fig. 1a) which is developed for the simulation of the flexographic printing process on plane sheets of glass materials.



Figure 1a: Printing proofer



Figure 1b: Printing unit

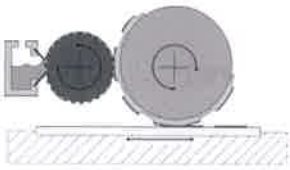

Figure1c:Printing principle [Nagel, 2007]

The printing unit is working as a closed chambered system with ceramic anilox rollers which could be moved on a plane surface in contrary to real flexographic printing on webs (fig. 1b, c). The printing tests are realized on plane glass plates with sizes of 100 x 100 mm and thicknesses up to 2 mm. Based on a continuous transport of the materials a twice-print-option is organized. The first print is stabilizing the transfer conditions. The second print has to transfer a homogeneous layer. The photopolymeric plates have a plate thickness of 1,14 mm and are mounted with a compressible tape of a thickness of 0,57 mm on the surface of the plate cylinder.

The photopolymeric plates were exposed with a special test image are used in all tests (Fig. 2). The positive and negative lines have thicknesses from 30 to 200 µm along, across and in 45° angle to the moving direction as well as full tone areas. The different directions of the lines allow an evaluation of the influence of the properties of the coating dispersions as well as the influence of the printing direction of the printing unit.

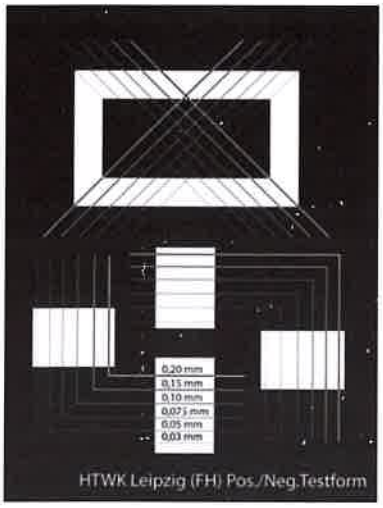

Figure 2:
Testing image

Figure 3:
Print proofer (Type F1 IGT)



For printing on plane polymeric materials is used a flexoprinting proofer (Fig. 3), where it is possible to realize repeatable printing conditions with defined ceramic anilox rollers, defined photopolymeric plates with test images comparable to that written above.

In a first part of the testing programme different ITO-dispersions and solvents have been investigated to find an optimal range for the possible printed ink film layer and the mean area resistance.

In a second part different additives have been compared to optimize the wettability and homogeneity of the printed layers. Especially pin holes should be avoided in order to guarantee the functionality of the transferred layer. The used testing procedure for both printing systems includes in all experiments the following steps:

(1) Manufacturing of the basic coating dispersion;
(2) Adjustment of the viscosity of the coating dispersion;
(3) Testing of different chemical additives to influence the homogeneity and the conductivity of the coating dispersion;
(4) Visual evaluation of the coated surfaces;
(5) Measuring of the surface profiles and the mean area resistance.

The manufacturing of the basic coating dispersion (step 1) is realized with special mixing techniques to guarantee an even distribution of the ITO-particles in the liquid. Only a homogenous distribution of the nanoparticles will enable to reach the demanded mean area resistance of the technical application.

The hydrodynamical conditions for liquid transfer inside of the flexographic printing unit should be comparable with standard waterbased printing inks. So the forming of printable ITO-dispersions (step 2) lead to a viscosity of about 100 mPas. This parameter is continuously controlled by measuring with a rotational viscosimeter (Fig. 4).



Figure 4:
Rotational viscosimeter (Type Physica)

To find out the optimal chemical ingredients for the transfer of the inorganic conductive coating dispersion in the flexographic printing unit a scaling off twelve different additives with two special solvents was made (step 3 to 5). The measuring of the surface profiles is made by a konfocal microscope.

3. Results

The results of the basic printing tests with pure ITO-dispersions and the different solvents showed a different influence on the forming of the transferred layers in the printing unit.

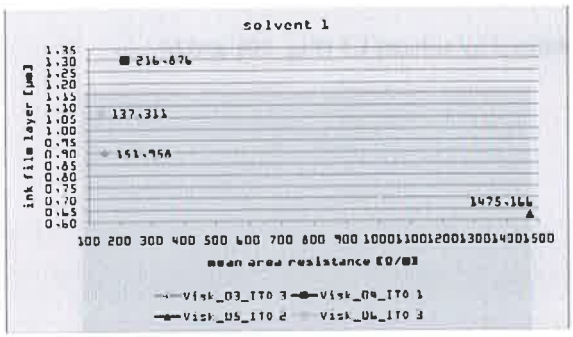

Figure 5: Testing of different ITO-dispersions

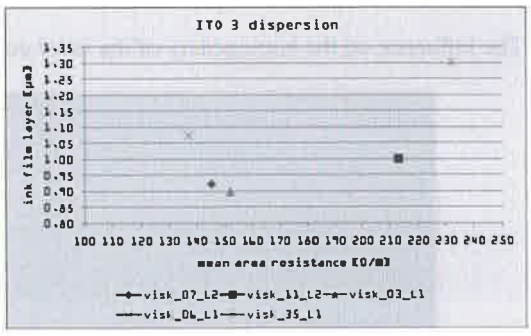

Figure 6: Testing of different solvents

It was concluded that the limited values for the transferred ink film layers should be less than 1 micrometer. The limited value for the mean area resistance should be less than 200 Ω/□.

So the ITO-dispersions of type 1 and 2 are rejected (Fig. 5). The tested solvents showed no real different behaviour in their influence on the both defined parameters (Fig. 6).

To improve the homogeneity and to reduce the mean area resistance different additives are tested in combination with the chosen ITO and different solvents. Almost all combinations with additives to increase the wettability showed no special phenomena like foaming or fast drying. About 10 special additives could be printed with ink film thicknesses less than 1 µm. But all tested ingredients had to high values of mean area resistance (Fig. 7).

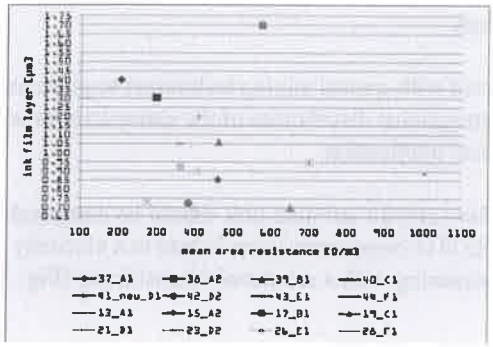

Figure 7: Testing of different additives to improve the wetting

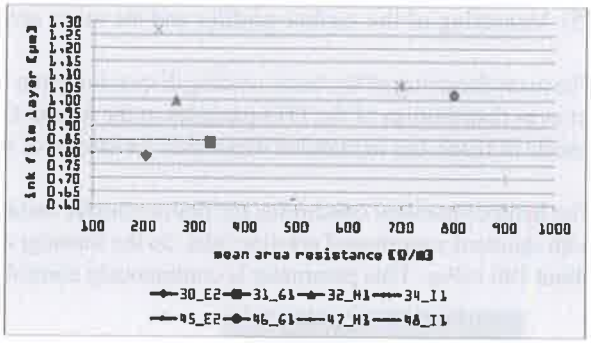

Figure 8: Testing of different additives to improve conductivity

To improve the conductivity of the ITO-dispersions 16 different combinations of additives and solvents were tested. No remarkable phenomena could be observed. Almost all combinations are in the ink film thickness in the range of less than 1 µm. But the realized mean area resistance was for all samples to high (Fig. 8).

To improve the forming of the layer on the surface of the substrate special tests with two new solvents (L1, L2) were organized and indicate different changes in the mean area resistance (Fig. 9).

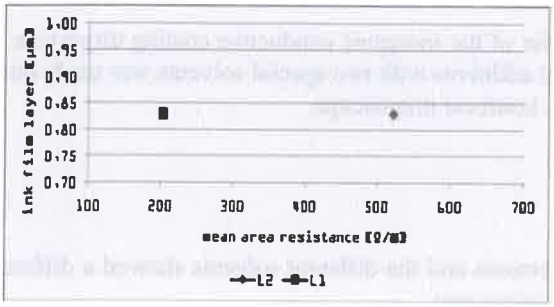

Figure 9: Testing of new solvents L1 and L2

The influence on the homogenety of the layer could be stabilized by solvent L1 (Fig. 10a and b).



Figure10a: Solvent L1



Figure 10b: Solvent L2

Testing the possibilities of printing structured layers with the testing image offered successful first results (Fig. 11a and b).



Figure 11a: Negative line (about 50 µm)

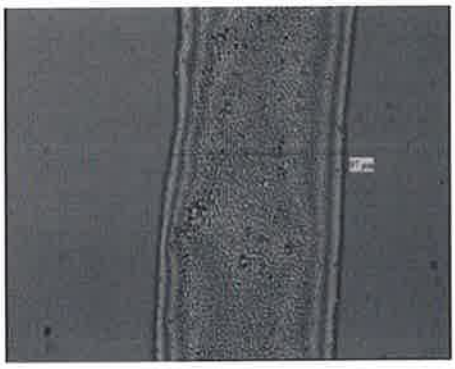

Figure 11b: Posive line (about 100 µm)

4. Conclusions

In general the printing results showed that the transfer of an inorganic conductive coating based on ITO-nanoparticles on plane glasses with a flexographic printing unit is possible. The realized liquid film layers of about 0.8 to 1.0 µm meet the demands for transferring the special functional dispersions. The fineness of the printed positive and negative lines is complying with the requirements. The scaling of the different additives shows a positive change of the homogeneity of the coated layers on plane glass surfaces.

Present problems with the mean area resistance should be improved in further investigations as well as the testing of printing on polymeric foils.

Acknowledgements

This work was funded by the German Organisation AiF represented by the research centre PTKA (Karlsruhe). The authors would like to thank the evonik AG as partner in the project for their support in measuring the surface properties of the investigated samples.

References

1. Rost, Henning, (2005): Vom Polymertransistor zur gedruckten Elektronik, Kunststoffe 10(2005), 209 214, Carl Hanser Verlag München
2. Hübler, A., (2002); Hahn, U.; Beier, W.; Lasch, N.; Fischer, T.: High Volume Printing Technologies for the Production of Polymer Electronic Structures, Proceedings of POLYTRONIC 2002 - 2nd Int. IEEE Conference on Polymers and Adhesives in Microelectronics and Photonics, Zalaegerszeg, Hungary, 2002
3. Nagel, H., (2007); Herzau-Gerhardt, U.: Printing of functional layers using flexography, Proc. of the 34th International Research Conference of iarigai, Grenoble, 2007

Inkjet printing of electrically conducting carbon nanotubes/conductive polymer composite inks

Aurore Denneulin[1, 2], Anne Blayo[2], Julien Bras[2], Charles Neuman[1]

[1] Polypore Europe
27, bld Louise Michel, F-92230, Gennevilliers, France
E-mails: Aurore@polypore.fr, Aurore.denneulin@pagora.grenoble-inp.fr

[2] Laboratory of Pulp and Paper Science and Graphic Arts (LGP2), Grenoble Institute of Technology
461 Rue de la papeterie, BP 65, F-38402 St Martin d'Hères Cedex, France

Abstract

In this work, formulation of inkjet printing inks combining the processability of the conductive polymer poly(3,4-ethylenedioxythiophene) (PEDOT) to the high conductivity of carbon nanotubes (CNTs) were developed. Patterns were printed on polymer films by using a piezoelectric inkjet printer. Then, morphological observations and sheet resistance measurements were made.

Electrical performances of several CNTs were evaluated (Single-walled, Di-walled, Multi-Walled, and Functionalized CNTs). Functionalized CNTs appeared to be the best candidates for printed electronics. The best configuration allows to obtain a sheet resistance of 225 Ω/sq which is very promising for many applications in printed electronics. This work also discusses the pros and cons of the different dispersion strategies developed here. The results obtained here represents an important step for the integration of CNTs in printed electronics applications and offers new opportunities to produce cost-effective electronics.

Keywords: conductive polymers, carbon nanotubes, inkjet printing, sheet resistance

1. Introduction

In the electronic industry, fabrication of conductive patterns is essential. Photolithography technology is traditionally used to produce circuit boards. Nevertheless, this latest method includes many complicated steps (etching, electroplating ... etc.) which are expensive, time consuming and waste producing [Lee, 2005]. For these reasons, the development of a cost-effective and convenient process to produce conductive patterns has attracted more attention. Inkjet printing is considered as one of the most promising technology. Indeed, it is a direct writing method that can be inserted in a relatively quick converting process. And this contactless technique allows the use of a large variety of substrates [Jung, 2007].

Most relevant recent studies have focused on metallic inks such as silver or gold ink because of their high conductivity [Magdassi, 2003; Lee, 2008]. However, these metals are loaded in the inks at a relatively high ratio, which increases ink cost. Carbon nanotubes (CNTs) can be a good alternative. Indeed, CNTs are well-known for their electrical properties and thanks to their high aspect ratio, enhancement of the electrical performances can be expected at very low loadings. This makes CNTs promising fillers for polymers.

In this study, we focused on the preparation of new inkjet inks that would combine the processability of conductive polymers with the high electrical properties of CNTs. Functionalized CNTs were identified as an appropriate solution because they allow to obtain highly stable suspensions without using any additional surfactant [Denneulin, 2008]. Two kinds of functionalized CNTs were selected: SWCNT-COOH (Single Walled CNTs grafted with carboxylic acid functions) and SWCNT-PEG (Single Walled CNTs grafted with polyethylene glycol functions). Trial with multi-walled CNTs (MWCNT) were also performed as reference. Influence of the number of walls forming the CNTs (single walled (SW), di-walled (DW) and multi walled (MW)) on the sheet resistance was also studied.

2. Materials and methods

2.1 CNTS/Conductive polymer composite inks

Firstly, highly homogeneous and stable CNTs suspensions were developed. Size, dispersion and stability of CNTs in the suspension are crucial parameters for the conductive ink, because aggregation of particles can lead to nozzle clogging. This step was quite difficult because CNTs tend to agglomerate into bundles, resulting in bad effects on electrical properties. Efficient techniques for dispersing CNTs such as sonication and centrifugation were performed. Sonication processes were carried out with a Branson 250 Sonifier (10 mm end cap diameter tip) which the output power was fixed at 35 W. Three centrifugation cycles of ten minutes were also performed at 3.500 rpm and each time, the supernatant was collected. For the grafted CNTs, the chemical function enables to obtain high stable CNTs suspension. In the case of MWCNT, sodium dodecylbenzene sulfonate (*NaDDBS*) was added as surfactant to the dispersions in order to optimize the quality of the dispersion. Table I summarized the physical properties and the dispersion process parameters for the different kinds of CNTs and figure 1 emphasizes the different strategies used to disperse each kind of CNTs with an evaluation of insulator elements (surfactant, chemical functions) added on the surface of CNTs.

Table I: Physical properties and dispersion process parameters for the different kinds of CNTs

CNTs origin	Arkema	Sigma-Aldrich	Sigma-Aldrich	Nanocyl	Nanocyl
CNTs nature	MWCNT	SWCNT-PEG	SWCNT-COOH	DWCNT-COOH	MWCNT-COOH
Purity (% by wt.)	> 90	80 - 90	80 - 90	> 90	> 90
Functionalization (% by wt.)	-	PEG: 30%	COOH: 3-6%	COOH	COOH
Solvent	Water	Water	Water	Water	Water
Addition of surfactant NaDDBS	1% by wt.	-	-	-	-
CNTs content (before centrifugation)	1 mg/mL	5 mg/mL	0.5 mg/mL	2 mg/mL	2 mg/mL
Sonication (minutes)	20	20	20	20	20
Centrifugation (minutes) + removal of the supernatant	3000 rpm 3 x 10 min	3000 rpm 3 x 10 min	3000 rpm 3 x 10 min	3000 rpm 3 x 10 min	3000 rpm 3 x 10 min
Solid Content (after centrifugation)	1.1% by wt	1.5% by wt.	0.2% by wt.	1.1% by wt.	1.0% by wt.

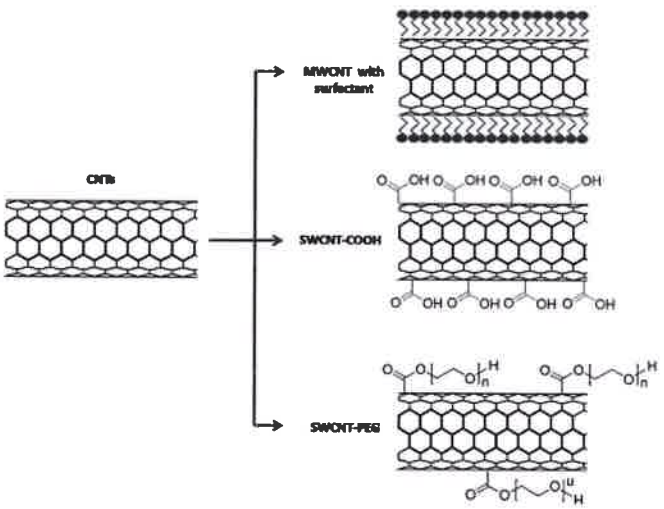

Figure 1: Summary of the different strategies used for disperse each kind of CNTs with a schematic representation of insulator elements (surfactant, chemical functions) added on the surface of CNTs

For monitoring the exfoliation steps, a technique based on UV-vis spectroscopy was used as reported by [Grossiord, 2007] for each kind of CNTs. The maximum degree of exfoliation is achieved when the time of sonication is sufficient to obtain a plateau of UV-vis absorption (Cf. Figure 2(a) and 2(b)). Samples were taken regularly during the sonication process and diluted by a factor of 30 to perform the UV-vis analysis (Cf Figure 1(c)). For each kind of CNTs, the maximum achievable dispersion of CNTs was obtained for a time inferior to 20 minutes.

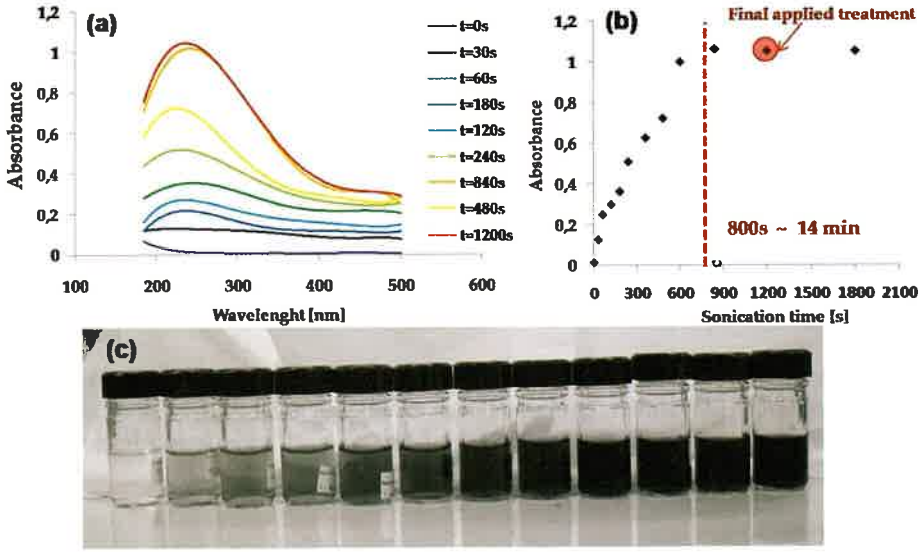

Figure 2: (a) Evolution of the UV- spectra of SWCNT-COOH suspension as a function of the sonication time
(b) Evolution of the height of the peak located around 240 nm for a SWCNT-COOH suspension
(c) Evolution of the SWCNT-COOH colour suspension as a function of increasing sonication time

Unfortunately, it was not possible to work with the same solid content for the different CNTs suspensions (Cf. Table I). Indeed, different functionalizations for grafted CNTs lead to different optimal CNTs concentrations. Concerning the non grafted CNTs, it was necessary to use surfactant and it leads again to a different final solid content. In this study, the chosen strategy was to work with suspensions having the highest ratio of CNTs in suspension.

On the other hand, a commercially available dispersion of PEDOT:PSS from H.C. Starck (CLEVIOS® P JET) has been used. It consists in a dark blue solution which presents a Newtonian behaviour with a viscosity of 7 mPa.s and a surface tension of 29 $mN.m^{-1}$ at 25°C. In order to optimize the conductivity and the stability of the CLEVIOS® P JET films, a secondary doping agent (ethylene glycol) was added. In a previous work, the optimal concentration was found to be 7% in volume [Denneulin, 2008].

The different inks were obtained by mixing the dispersed CNTs suspensions and PEDOT-PSS suspensions by vigorous stirring. The different functional inks developed here present viscosity and surface tension in accordance with the inkjet printing requirements. Indeed, the average viscosity is around 6 mPa.s. at 25°C and the average surface tension is between 30 and 40 mN/m. In order to find the optimal CNTs content in the printed film and so the percolation threshold of the CNTs, inks with different ratios between the two kinds of suspension were examined.

2.2 Inkjet printing of the CNTs/Conductive polymer ink

The composite inks were then printed using a laboratory piezoelectric inkjet printer (Fujifilm - Dimatix DMP 2831). Printed patterns were solid areas and lines. The printing conditions such as drop spacing, substrate and nozzles temperature, nozzle diameter and voltage of ejection were first optimized in order to achieve precise, smooth and continuous patterns. A flexible polymer film of polyethylene terephtalate (PET) was selected as substrate for its very smooth and closed surface, which does not affect the homogeneity of the conductive

2.3 Characterization of the printed samples

Morphology and thickness of the conductive patterns were characterized by optical and by environmental scanning electron microscopy (ESEM). Observation of CNTs random networks in the polymer matrix were also performed using a Field Emission Gun-scanning Electron Microscope (SEM-FEG).

The electrical properties were characterized by measuring the sheet resistance of the printed films by using a four-probes device. In this configuration, the two external probes impose a known current intensity and the two internal probes measure the corresponding voltage. The expression of the sheet resistance in this particular configuration is:

$$R_{square} = K \times \frac{U}{I} \text{ [Ohm/square]}$$

where: K is a constant depending on the geometry
U is the measured voltage, in Volt
I is the set intensity, in Ampere

To obtain an optimal contact between the four probes and the conductive pattern, silver plugs corresponding to the probes were printed using the Dimatix printer on each samples. The plugs were then cured at 90°C during 15 minutes. To minimise errors, five measurements were taken on each sample and linearity of measurement was checked for positive and negative current intensities.

3. Results and discussion

3.1 Morphology characterization of the printed samples

As shown on figure 3, the microscopy analysis demonstrates that the print quality was achieved with a high uniformity for most of the samples. Defaults such as ring-shaped marks, discontinuity of the deposit or edge irregularities were avoided thanks to the printing parameter optimization step. The average thickness of a unique printed layers is around 1µm with a slight variation depending on the final solid content of the ink.

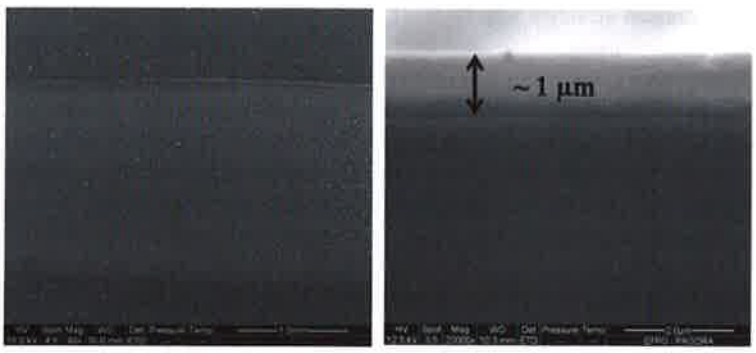

Figure 3: Example of surface (a) and cross-section (b) SEM views for a unique printed layer of MWCNT/Conductive polymer ink

3.2 Percolation threshold and CNTs network analysis

SEM-FEG observations made on surface and on cross section views of the printed samples reveal that the three-dimensional CNT network is formed with the presence of plausible conducting pathways (Cf Figure 4). The pictures confirm that CNTs networks are well beyond the percolation threshold. The number of CNTs forming the network is a crucial parameter for the prediction of the level of conductivity because both too high and too low CNTs loading in the printed film will lead to a limitation in conductivity. This trend was confirmed by the study of the sheet resistance variation over increasing loading of CNTs in the final dried printed film (between 0,1% to 15% $w_{CNTs}/w_{PEDOT:PSS}$), illustrated in figure 5. It emphasizes that the electrical performance depends strongly on the suspension ratio. Lowest resistances were obtained for low loading (≤ 2%) of CNTs

in the printed film. An increase in resistance was observed when the content of CNTs became higher. This phenomenon is certainly due to the high rate of contacts between CNTs: indeed, electrical conductivity between two CNTs is ensured by electron hopping. In this mechanism, the electron circulation performance is limited. If we have too high quantity of contacts between CNTs, conductivity decreases. Thanks to the high aspect ratio of CNTs, enhancement of the electrical performances is obtained at very low loadings, which can be cost effective.

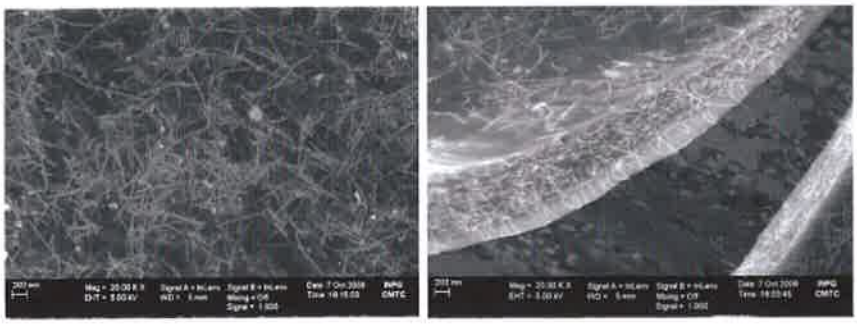

Figure 4: SEMFEG surface (a) and cross section (b) views of a printed sample with SWCNT-PEG/PEDOT PSS ink

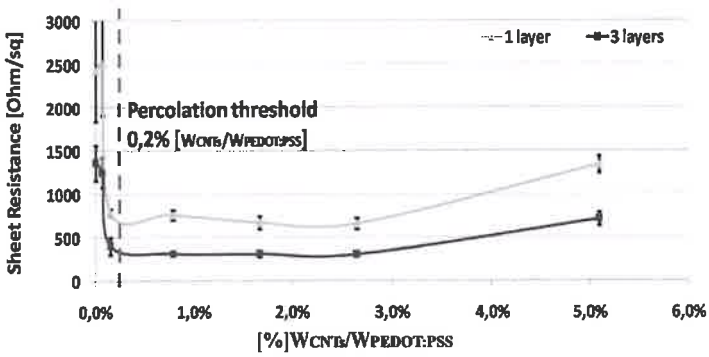

Figure 5: Evolution of sheet resistance over increasing CNTs loading in the final printed film for a SWCNT-PEG/PEDOT-PSS ink

3.3 Electrical performances

Whatever the ink used, the superimposition of conductive layers has a significant positive effect on sheet resistance as already proved for coatings [Denneulin, 2008]. Indeed, as the number of printed layers increases, the sheet resistance decreases. The same trend was found whatever the ink developed. The conductive film thickness has a considerable impact on the conductivity.

Unexpected result is the fact that the addition of CNTs leads to a positive or a negative effect on the sheet resistance depending on the kind of CNTs used (Cf. Figure 6). Indeed, the addition of MWCNTs involved an increase of sheet resistance whereas the addition of functionalized CNTs implied a decrease of sheet resistance, which means a higher conductivity. This phenomenon can be explained by comparing the impact of the insulating elements present on the CNTs surface (Cf. Figure 1). Chemical functionalization consists in introducing defects (covalent bonds) to CNTs surface. These defects acts as a disturbance for the electric performances because they are insulating elements. However the functionalization allows to obtain adequate colloidal stability. For the non grafted CNTs, it was necessary to use surfactant to obtain a good quality suspension. In this case, the surfactant remaining on the CNTs surface can significantly degrade the sheet conductivity, because of its high insulating nature.

The comparison of the two strategies reveals that the insulated element are in lower quantity for grafted CNTs than for non grafted CNTs. Indeed, on the grafted CNTs, the insulated elements are punctually located whereas on the non grafted CNTs, the insulated elements cover the totality of the CNTs surface. The surfactant acts as an insulated envelope. The insulating effect is so totally different for the two strategies of dispersion. A compromise had to be tuned between the dispersing and the insulating effect induced by the dispersing strategy.

The comparison between the two different kinds of functionalization reveals that the best candidate for conductive performance is the SWCNT-PEG. Indeed, the ink based on SWCNT-PEG provides lower sheet resistance than the ink based on SWCNT-COOH. The lowest resistance of 225 Ω/sq was obtained with an ink containing SWCNT-PEG and for the superimposition of 5 printed layers. This value corresponds to a conductivity of 37 S/m. Another important outlook is that SWCNT-COOH remains also a good candidate for printed electronics because less material is required to achieve a sheet resistance in the same range of value, which may be cost effective. Indeed, the optimal number of CNTs dispersed in the suspension, therefore the solid content depends strongly on the chemical nature of the grafted functions. In this study, the optimal solid content of the suspension containing SWCNT-COOH is seven times lower than for the suspension containing SWCNT-PEG (Cf. Table I).

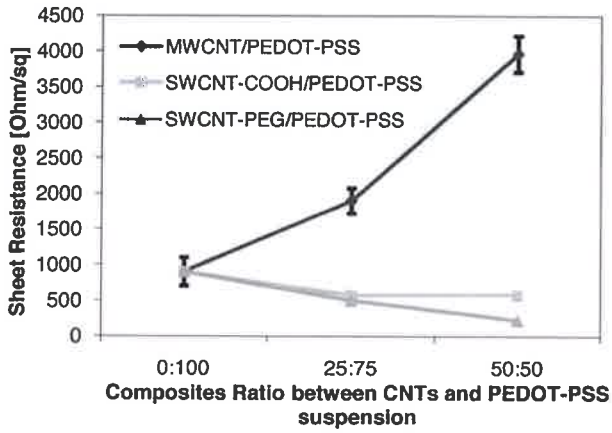

Figure 6:
Evolution of sheet resistance over increasing CNTs for three different kind of CNTs/PEDOT-PSS ink

To complete the comparison of CNTs materials, the influence of the number of walls on the CNTs was examined. The trial was focused only on the carboxylic acid functionalized CNTs. Results show a slight upgrade of conductivity with the use of both MWCNT-COOH and DWCNT-COOH in comparison with the use of SWCNT-COOH (CF. Figure 7). Indeed, sheet resistance decreases of approximately 20% with MWCNT-COOH and 35% with DWCNT-COOH for the printing of 3 conductive layers. For the application of a unique layer, the results were almost equivalent. These fluctuations may probably be explained by the fact that the electrical properties of CNTS depends strongly on their atomic structure.

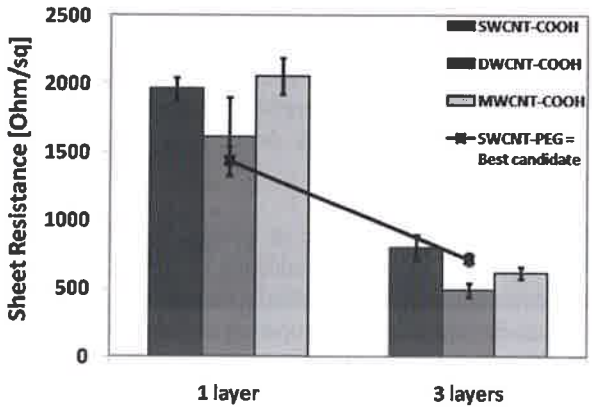

Figure 7:
Evolution of sheet resistance over increasing number of CNTS walls for -COOH grafted CNTs

4. Conclusion

Inkjet printing of stable CNTs/PEDOT-PSS inks was first demonstrated. After an optimization step of the printing parameters, a high print quality was achieved. This process to form conductive patterns allows to use flexible substrates which enables new opportunities (flexible devices). This study allows also to learn more about CNTs, which are still a recent material (Iijima, 1991). Indeed, a major difficulty concerning the CNTs is that the intrinsic properties of this material can significantly differ depending on the CNTs nature or structure. Most studies focused only on one kind of CNTs and do not take these considerations into account.

The results obtained here begin to overcome this lack of knowledge. The comparison between the different kinds of CNTs materials reveals that functionalized CNTs are good candidates for printed electronics. Indeed, functionalized CNTs offer a good compromise between the gain in suspension quality and the degradation of intrinsic nanotubes properties caused by the functionalization step. On the other hand, non grafted CNTs seems to be a wrong candidates for the formulation of conductive ink because it is necessary to introduce an insulating surfactant in the suspension, resulting in higher resistance. Finally, our approach provides an efficient way of making conductive patterns with improved performances. The best configuration allows to obtain a sheet resistance of 225 Ω/sq which is very promising for many applications in printed electronics.

References

1. Denneulin, A., Blayo, A., Bras, J. and Neuman, C., (2008) *PEDOT:PSS coating on specialty papers: Process optimization and effects of surface properties on electrical performances.* Progress in Organic Coatings 63(1) 87-91
2. Denneulin, A., Dhar, A., Bras, J., Bonnassieux, Y., Blayo, A., Cjocaru Sorin, C., Pribat, D. and Neuman, C., (2008) *Inkjet printing of conductive patterns using multi-walled carbon nanotubes and PEDOT:PSS suspension.* in Ninth Int. Conf. on the Science and Application of Nanotubes *M*ontpellier, France C71 p.248
3. Grossiord, N., Loos, J., Meuldijk, J., Regev, O., Miltner, H. E., Van Mele, B. and Koning, C. E., (2007) *Conductive carbon-nanotube/polymer composites: Spectroscopic monitoring of the exfoliation process in water,* Composites Science and Technology 67(5) 778-782
4. Iijima, S., (1991) *Helical microtubules of graphitic carbon,* Letters to nature 354, 56-58
5. Jung, H., Cho, S. H., Joung, J. and Oh, Y. S., (2007) S*tudies on Inkjet-Printed Conducting Lines for Electronic Devices,* Journal of Electronic Materials 36(9) 1211-1218
6. Lee, H. H., Kan-Sen, C. and Kuo-Cheng, H. L., (2005) *Inkjet printing of nanosized silver colloids* Nanotechnology (10)2436
7. Magdassi, S., Bassa, A., Vinetsky, Y. and Kamyshny, A., (2003) *Silver Nanoparticles as Pigments for Water-Based Ink-Jet Inks,* Chem. Mater. 15(11) 2208-2217
8. Lee, S. H., Shin, K. Y., Hwang, J. Y., Kang, K. T. and Kang, H. S., (2008) *Silver inkjet printing with control of surface energy and substrate temperature,* Journal of Micromechanics and Microengineering (7) 075014



An investigation into the performance of biodegradable plastic electronics by flexography

David Bould, Tim Claypole, David Gethin

Welsh Centre for Printing and Coating, Swansea University
Singleton Park, Swansea, SA2 8PP, United Kingdom
E-mail: d.c.bould@swansea.ac.uk

Abstract

An investigation has been performed to consider the performance of a flexographic carbon-based conductive ink, printed onto a biodegradable substrate. Although conductive carbon inks are widely used in screen printing, where controlled resistance of features is required, their use in flexographic printing represents a novel approach for producing functionality on the print. This, coupled with the use of a biodegradable substrate allows the possibilities for the production of low cost, fully disposable printed electronics. The aim of this study was to assess the performance of the carbon ink for varying anilox to plate and plate to substrate engagements. Two carbon inks were selected with different carbon to resin ratios.

The amount of carbon present in the ink was shown to affect the resistance per unit length of thinner lines. However, thicker lines, which had greater bulk, exhibited no difference between the two inks used. Anilox to plate engagement had negligible effect on the resistance of a printed line.

Keywords: flexography, electronics, biodegradable

1. Introduction

There is currently considerable research into the creation of electrical components and devices on flexible substrates, produced using reel to reel printing presses. However, one aspect which has not been considered in sufficient detail concerns product life cycle and the costs associated with disposing of the device. Much of the research into printed electronics is focused on devices which require high electron mobility [BERR, 2008]. These devices therefore need engineered substrates with planarising layers and barrier coatings, as well as inks, such as silver, which have the lowest resistivity possible. These substrates and inks have costs associated with reclaiming the product at the end of its life, to prevent it going to landfill. There are however, many applications for printed electronics, which do not require high mobilities and whose ink and substrate requirements are not as stringent.

In 2007, the Department for Environmental Food and Rural Affairs (DEFRA), produced a document [DEFRA, 2007], written with reference to a EU Council Directive [EU, 1999]. This directive stated that by the year 2016, member states are 'obliged to reduce the amount of biodegradable waste that goes to landfill to 35%.' The DEFRA report seeks to outline alternatives to landfill for Biodegradable Municipal Waste, with home composting of such waste being considered as a preferable option. A significant contribution of methane gas comes from landfill sites, due to the mass decomposition of paper and other similar materials [Fosbery et al, 1999]. However, home composting in soil, other than sending materials to landfill sites, would reduce methane emissions as the small amount of methane produced by the compost is taken up by the soil, which is a natural sink of methane. Home composting is therefore seen as a balanced way of degrading materials.

Films made from cellulose are vastly growing in popularity as a use for biodegradable packaging. Until recently cellulose films have used non-biodegradable coatings in order to produce a moisture barrier for films. However 'Natureflex™', produced by Innovia Films Ltd has biodegradable coatings, which comply with the international standards for composting.

Natureflex™ films are made from woodpulp, and have heatseal resins on each side. They are static free and have good gas barrier properties. Its coatings can be manipulated to provide varying degrees of moisture resistance.

A further issue concerning the composting of printed products has traditionally concerned the inks, which contained inorganic pigments and resins, which do not degrade in soil and are left the substrate composts in

the soil. However, use of a carbon ink, which is entirely organic allows the ink to fully break down during the composting process, resulting in no lasting environmental damage.

A previous investigation using carbon inks was performed by Jewell et al. [1999]. Using a screen press, an investigation was performed to correlate the rheological performance of inks of varying carbon content with printability and electrical performance. The investigation was unable to draw any correlations, although it was shown that the carbon content of the ink did have an effect on geometry of the printed features as well as affecting the electrical conductivity. This research highlighted the possibility for using carbon inks to produce biodegradable electronics and it was recommended that the use of flexography be explored, to combine low cost electronics onto biodegradable film to create environmentally friendly smart packaging.

The objective of the study was to assess the suitability of a cheaper carbon ink (in comparison with alternative silver inks) in terms of the printability onto a non-planarised biodegradable substrate and to quantify the resultant conductivity produced by the fine lines reproduced as part of the test image.

2. Methodology

The trial was performed on a Timsons T-Flex 508 flexographic printing press, using two solvent-based carbon inks, supplied by Gwent Electronic Materials Ltd. Each ink contained a different carbon to resin ratio, classified as Low and High. Different carbon inks were used in order to establish the optimum particle loading of the ink, in terms of printability and electrical conductivity. The substrate was a NatureFlex™, 45NVL biodegradable cellulose film which has a high dimension stability, sufficient thickness for efficient dispensing, biodegradable print and adhesive recpetive coatings.

Prior to printing the inks on the press, their rheological properties were established using a Bohlin Gemini HR Nano rheometer. The viscosity was recorded for increasing and decreasing shear rates, up to 100 s^{-1}. The results for the carbon ink with the 'Low' carbon:resin loading, Figure 1, show that the viscosity of the ink lies in the range suitable for flexographic printing. Furthermore, no thixotropic behaviour was observed.

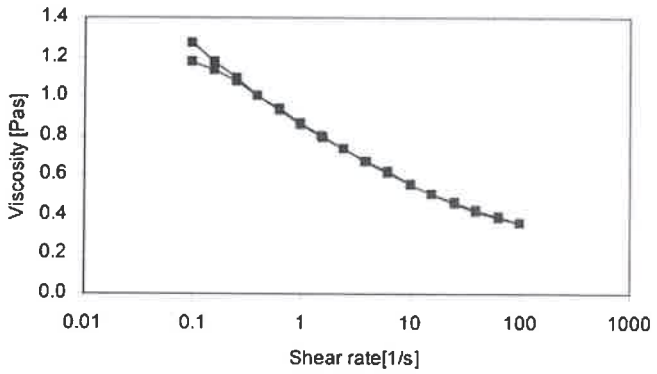

Figure 1:
Graph of viscosity vs shear rate for low carbon: resin carbon ink

An enclosed ink chamber was used to supply the ink to the anilox roll, segregated into discrete bands. The screen ruling and the cell volume of each of the bands is summarised in Table I.

Table I: Specifications for banded anilox rol

Band No.	1	2	3	4	5
Cell Volume (cm^3m^{-2})	36.5	31.01	24.22	21.69	17.92
Screen ruling (lpi)	120	140	180	200	250

Table II summarises the engagements used between the anilox and plate and between the plate and the substrate for each ink considered during the printing trials. Anilox to plate engagement was quantified using a dial test indicator (dti) gauge, mounted to the side-frame of the press to reduced vibration. Plate to substrate engagement was quantified using the calibrated indicator on the print unit (Figure 2).

Table II: Nip engagement settings for carbon ink trials

	Anilox to plate engagement (μm)	Plate to substrate engagement (μm)
Setting 1	15	50
Setting 2	40	75
Setting 3	65	100



Figure 2: Engagement control on printing press

The image on the printing plate consisted of a series of fine lines of varying thickness, at varying angles to the direction of print, as this has previously been shown to have an effect on the quality of line reproduction. The image had been designed such that it was segmented into five discrete bands, to correspond with the five bands on the anilox roll. The image used for the experimental trials is shown in Figure 3.

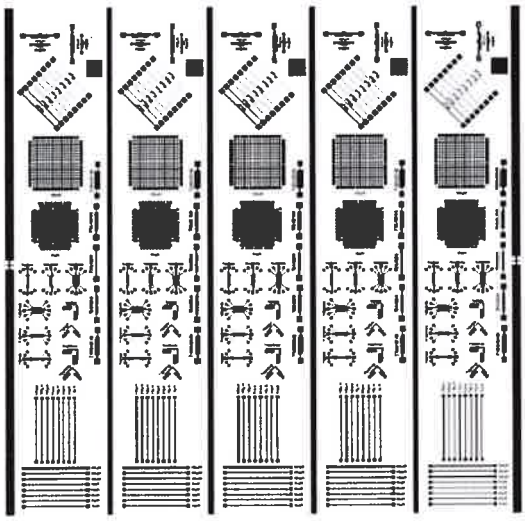

Figure 3: Test forme for carbon ink print trials

3. Results

The graph of anilox cell volume vs. line resistance, per unit length, for the low carbon to resin ratio ink, is shown in Figure 4. The data was obtained from the 35 μm anilox to plate engagement and for the 50 μm plate to substrate engagement. There is a large decrease in the line resistance as both anilox volume and line thickness increase, with the lowest resistances observed for the 300 μm line for the 36.5 cm^3m^{-2} anilox cell volume. A comparison of the data from Figure 4 with the data for the high carbon to resin ratio ink (Figure 5) shows that for the thinner lines, the resistances of the high Carbon: resin ink are lower than those for the low ratio ink. However, for the 200 μm and 300 μm lines, there was little difference in the data. The results suggest that where there is little bulk to the line (thinner lines) the high ratio ink provides better conductivity, due to the higher carbon content. However, for the thicker lines, which have greater bulk, the high ratio ink does not appear to have any effect.

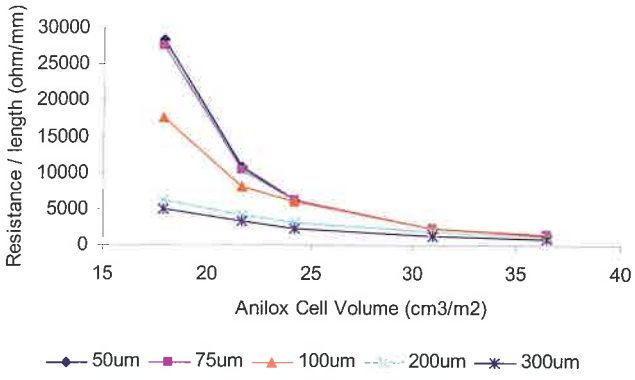

Figure 4:
Anilox volume vs Resistance per unit length for low carbon: resin ink

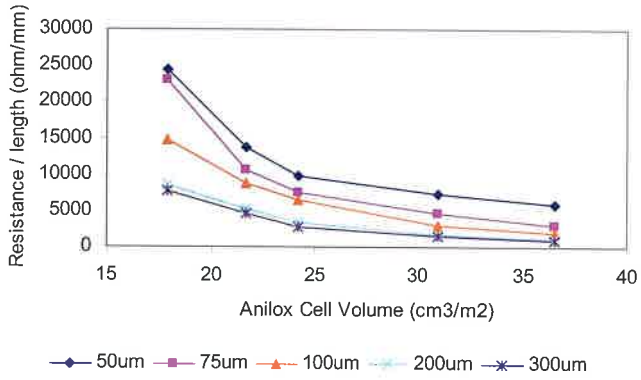

Figure 5:
Anilox volume vs Resistance per unit length for high carbon: resin ink

The effect of the anilox cell volume on printed line width is shown in Figure 6 for a 50 μm line for the high carbon to resin ratio ink. The results show large gain in the line width, due to the high anilox volumes considered as part of the investigation. However, the difference in line gain from the lowest anilox volume to the highest anilox volume is relatively low, in comparison with the decrease in conductivity observed in Figure 5. Therefore, as anilox cell volume increases, height of the printed line gains at a greater rate than the line width.

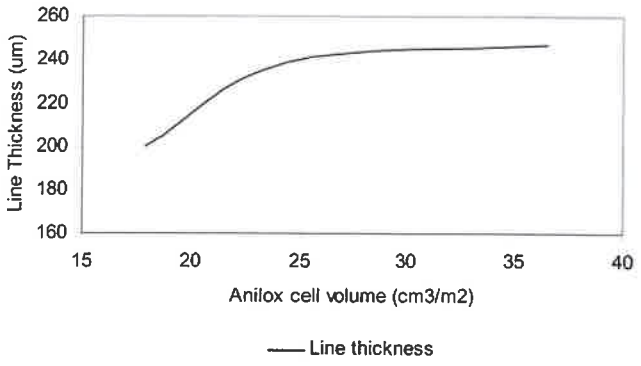

Figure 6:
Effect of anilox cell volume on printed line thickness for 50 μm line (high carbon: resin ink)

The effect of line direction on resistance is shown in Figure 7. The data shows that the lowest resistances were reported for the horizontal lines, with the greatest resistances for the vertical lines. This is due to the deformation mechanism of the plate as it passes through the printing nip. For the vertical line, the deformation of the line is symmetric about the line axis. However, due to the rolling nature of the contact, as the horizontal lines on the plate deform, there is a lateral force on the line and the line deforms unevenly. This results in the shoulder of the feature on the plate barrelling up, to form part of the printing surface, transferring a greater quantity of ink than occurs for the vertical line.

The results for the effect of anilox to plate pressure (Figure 8) show little effect on resistance per unit length, as the anilox cell volume increases. Therefore, any increase in ink transfer due to the increased pressure between the anilox roll and the printing plate does not result in the growth of the printed lines.

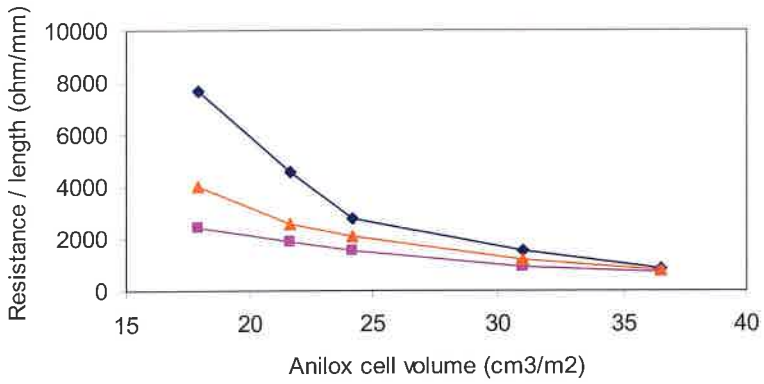

Figure 7: Effect of line direction on resistance per unit length (300 μm line)

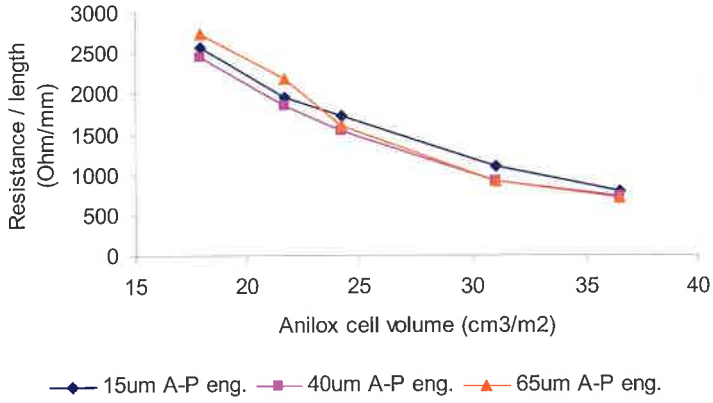

Figure 8: Effect of Anilox to plate engagement on resistance per unit length (300 μm horizontal line)

4. Conclusions

As a result of the investigation, it has been concluded that it is possible to print fully disposable electronic devices, using conductive carbon inks on a bio-degradable substrate. Although very high resistances were observed for fine lines, thicker lines allowed sufficient current to flow, which would enable low cost devices to be manufactured using flexography, where fine features and high registration are not required.

As anilox cell volume increases, the height of a printed line increases at a greater rate than printed line width.

The investigation has shown that line resistance varies with print direction, due to the differing deformation mechanisms of the plate for horizontal, diagonal and vertical lines. This will have an impact on the design of printed circuitry, as lines printed in the vertical direction, where the resistance is greatest, may need to be intentionally thickened, to compensate for the lower conductivity.

Acknowledgements

This research has been performed as part of the Technology Strategy Board funded project, Accuflex, whose partners include: Timsons Ltd, Tectonic International, Gwent Electronic Materials Ltd, Millennium Laser Systems, Innovia Films Ltd, Asahi Photoproducts (UK) Ltd, The Holst Centre, Swansea University.

References

1. BERR, 2008, "Plastic Electronics in the UK - A guide to UK capability 2008/9", Department for Business Enterprise & Regulatory Reform report
2. DEFRA, 2007, "Introductory Guide to Options for the Diversion of Biodegradable Municipal Waste from Landfill", Department for Environment Food and Rural Affairs Report
3. EU Report, 1999, Council Directive 99/31/EC Official Journal L 182
4. Fosbery, R., Gregory, J., Stevens, I., 1999, "OCR Revise A2 Biology 2001", Heinemann
5. Jewell, E. H., Claypole, T. C., Roberts, S. R. and Bould, D. C., 2008, "The impact of conductive carbon properties on print performance", Advances in Printing and Media Technology, pp 299-306

Electrical resistivity of screen printed conductive lines

Maša Žveglič[1], Valerija Demšar[2], Raša Urbas[3], Nina Hauptman[1], Marijan Maček[4], Marta Klanjšek Gunde[1]

[1] National Institute of Chemistry
Hajdrihova 19, SI-1000 Ljubljana, Slovenia
E-mail: masa.zveglic@ki.si, nina.hauptman@ki.si, marta.k.gunde@ki.si

[2] Etiketa, d.d.
Industrijska ulica 6, SI-4226 Žiri, Slovenia
E-mail: valerija.demsar@etiketa.si

[3] University of Ljubljana, Faculty of Natural Sciences and Engineering
Snežniška 5, SI-1000 Ljubljana, Slovenia
E-mail: rasa.urbas@ntf.uni-lj.si

[4] University of Ljubljana, Faculty of Electrical Engineering
Tržaška 25, SI-1000 Ljubljana, Slovenia
E-mail: marijan.macek@fe.uni-lj.si

Abstract

We have analysed thicknesses and shapes of narrow lines, which were screen-printed using commercially available silver-based conductive ink. The influence of wet-to-wet overprinted layers and the influence of the used substrate on the topology of the lines were evaluated by profilometer measurements, optical- and scanning electron micrographs. Finally, the specific resistivity of these lines was measured by the help of the four-terminal method, which enables elimination of the effects of contact resistance. The results show that overprinting of layers does not considerable influence on the shape of the lines but gives rise to smaller resistivity. Printed lines with larger resistivity where obtained on the porous substrate with poor adhesion, whereas on the smooth paper smaller resistivity was obtained. Some influence of the curing time was also measured. When using larger curing dose, lines with a somewhat smaller resistivity were obtained.

Keywords: Printed electronics, electrical resistivity, printing ink, screen printing

1. Introduction

Printed electronics, i.e. fabricating of an entire electronic device by printing, is expected to provide low-cost electronic systems on common surfaces such as paper, plastic and textile. Standard and digital printing processes are applied for this purpose and electronically functional inks are used instead of graphic art printing inks. It is expected that simplified structures of electronic devices printed by minimal number of different printing inks may provide the lowest possible target price, which was estimated to be below 0.2 € per piece [Berggren et al., 2007].

One of the most important applications of printed electronics is currently a RFID tag. It consists of an antenna for receiving and transmitting the signal and a silicon chip for signal processing. The quality factor of the antenna depends on the resistance of the coil, which is defined by the design of the antenna as well as by the resistivity of the conducting layer applied for it.

All printed electronic devices require some printed conductor which replaces pure metal applied in conventional electronics. Polymer inks containing electrically conductive particles are most common choice for this purpose in the field of printed electronics. They consist of suitable polymer resin with metal particles which are in most cases silver, gold, copper, nickel, platinum or carbon [Li et al., 2006; Strümpler et al., 1999; Park et al., 2007; Hauptman et al., 2009]. These conductive inks have various resistivities; the lowest could be obtained by silver particles. The producers provide resistivity data for a layer with specified thickness and recommend suitable preparation conditions. However, several printing parameters might influence the electrical properties of the printed conductive paths what could seriously influence the final application [Pudas et al., 2005]. Therefore, the objective of our research was to analyse the resistivity of lines prepared by screen printing. Commercially

available silver-based conductive ink was applied in our research. The results obtained here will be applied further to design the printed antenna for a RFID tag on common paper and foil surfaces.

2. Methods

Electrodag PM-470 conductive screen printable ink (Acheson Colloiden B.V., Netherlands) was used. This ink was designed for printing RFID antenna onto paper and polyester film. It contains finely divided silver particles in a thermoplastic resin and has approximate density of 2140 kg/m^3. The solid content is 58 - 62%. The manufacturer specifies the Broofield viscosity of the ink at 11000 - 140000 mPa×s (30°C, 20 rpm) and sheet resistance of 25 μm thick layers at 0.008 - 0.015 Ω/sq. This corresponds to the specific resistivity in the range of 2.0 - 3.75 × 10^{-5} Ωcm.

The ink was screen printed applying the SEFAR® high-modulus monofilament polyester plain weave mesh 43/80 Y and squeegee with hardness 75°Sh. Two substrates were applied, clear matt film (thermally and antistatic ally treated for transfer printing) and gloss-coated paper. Single and double layer prints (wet-on-wet) were made. The off-prints were cured at 120°C for 4, 9 or 13 minutes. In all cases dry prints were obtained.

Several shapes were printed on both substrates. The print form is shown on Figure 1. It contains two structures for resistivity measurements (R1, R2), and several lines with different target thickness for shape and profile analysis (L1 - L14). The dimensions of shapes are given in Table I.

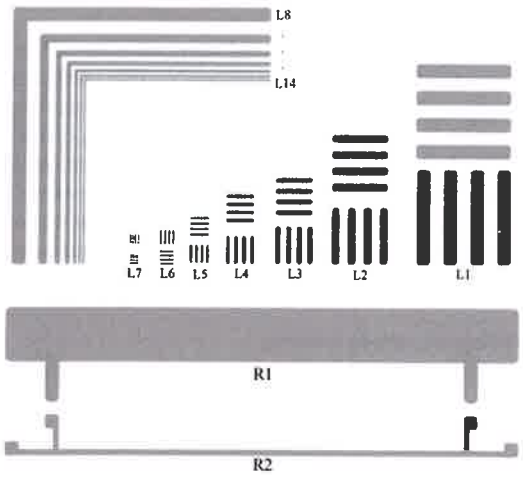

Figure 1: The print form

Table I: Description of shapes on the print form

Shape	Description				
R1	Four-terminal structure for resistivity measurements, W = 20 mm, L = 150 mm				
R2	Four-terminal structure for resistivity measurements, W = 2 mm, L = 150 mm				
Line	Width	Line	Width	Line	Width
L1	5 mm	L6	0.75 mm	L11	1.5 mm
L2	3 mm	L7	0.5 mm	L12	1 mm
L3	2 mm	L8	5 mm	L13	0.75 mm
L4	1.5 mm	L9	3 mm	L14	0.5 mm
L5	1 mm	L10	2 mm		

The thickness and profile of lines were measured by profilometer Talysurf (Rank Taylor Hobson Series 2). It scans the surface mechanically with diamond tip and transforms the data into a measured height profile of the surface.

The microtexture of printed shapes and profile of narrow lines were monitored by scanning electron microscope SEM - 6060 LV (JEOL, Japan). The shape of edges, the degree of wicking and the width of narrowest line were evaluated additionally applying the optical microscope Nanometrics (Olympus).

The adhesion of printed layers was determined by the cross-cut test applying the Byko-cut universal inspection gage (Byk-Gardner Instruments, Germany). The test method evaluates resistance of a coating to separation from substrate when a right-angle lattice pattern is cut well into the coating, penetrating into the substrate. First, the cross-cut pattern with appropriate depth was cut, and then badly adhered pieces were removed by a brush pen. The micrographs of so obtained samples were rated in classes in accordance to the scale with values 0-5 as given in ISO 2409:1997.

The electrical resistivity of samples was measured on printed strips R1 and R2 (Figure 1) applying four-terminal measurement method [Hauptman et al., 2009]. Electrical contacts were prepared by high-purity aluminium bonding wires (Heraeus, Germany) applying silver electro-conductive adhesive (Bison, Holland). A constant DC-current source was used to force the current of ~ 1 μA through the outer contacts of the structure. Voltage drop was measured by an electronic voltmeter (FLUKE 289) on the inner contacts. On this way the contact resistance was completely eliminated and the results represent the pure resistance of the layer between inner contacts. The specific electrical resistivity ρ of the printed layer with thickness d was calculated using measured voltage drop V_x and known current I according to the equation:

$$\rho = \frac{V_x}{I} \cdot \frac{W}{L} \cdot d \tag{1}$$

where W and L denote the width and length of the measured strip between inner contacts, respectively.

3. Results and discussion

3.1 Layer thickness and line profiles

The profile of four parallel L7 narrow lines was measured by profilometer on all prepared samples. A typical measurement of lines printed on gloss-coated paper and clear matt film are shown in Figure 2. Both samples were cured for 9 minutes. The mean height and width of each line was calculated according to the marked lines. All lines are well separated. Their large surface roughness is a consequence of silver flakes that are not fully covered by the resin. Such flakes can stick the diamond tip of the profilometer when scanning the surface. Thus, unreliably high surface irregularities could be obtained. The profiles also show large roughness of the clear matt film and smaller of the gloss-coated paper. The mean height and width of each line were determined by averaging the top of the line and the substrate surface. This way the mean height (layer thickness) and mean width of lines were obtained.

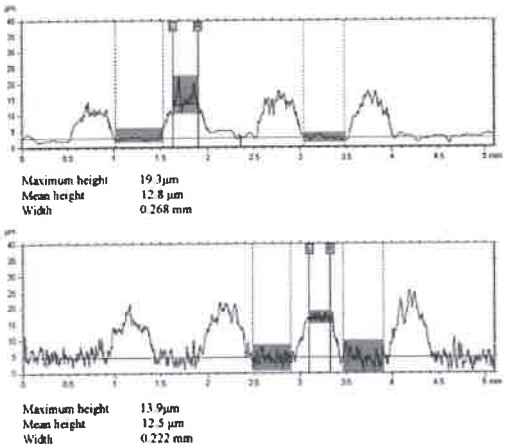

Figure 2:
The profile of the four parallel L7 lines printed by two wet-to-wet overprinted layers on the gloss-coated paper (top) and on the clear matt film (bottom)

The average thickness d and the average width W of the L7 line were calculated from the four line profiles, which were scanned on five different positions on the same sample. No systematic dependence of these values on curing time was obtained. The results are given in Table II. The overprinting (wet-to-wet) practically do not enlarge the thickness of the final layer. Single printing on the gloss-coated paper gives only slightly thinner layers than double printing. On the clear matt film substrate even a slightly reverse effect was measured, where the double layer is thinner than single ones. Single printed lines are on both substrates slightly broader than

The width of the L7 lines was also followed by the help of optical microscope. Good contrast was achieved in transmittance mode (Figure 3). The sample was printed as single layer on gloss-coated paper and cured for 4 minutes. These micrographs show narrower L7 lines that were also obtained by profilometer measurements. Moreover, broader vertical lines and narrower horizontal were obtained. The lines are broader on gloss-coated paper and narrower on clear matt film. The optical micrographs were also used to evaluate the wicking ΔW of L7 lines. It is larger for double printed lines and smaller for single printed ones. There were no appreciable differences for ΔW of L7 lines on both substrates. The results of an analysis of optical micrographs are collected in Table II.

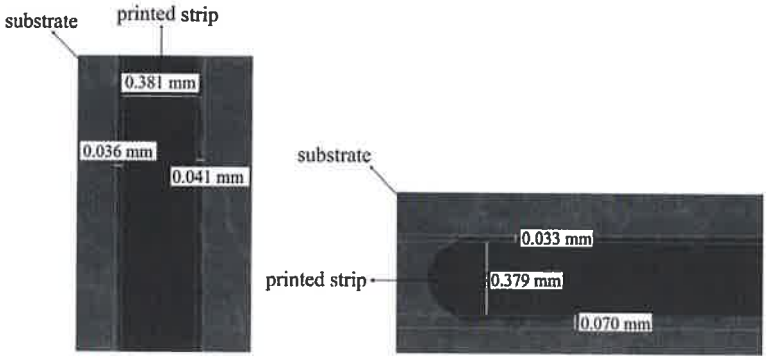

Figure 3: Line shape analysis applying optical micrograph: the L7 line printed vertically (381 μm) and horizontally ($W_{h(om)}$ = 379 μm)

Table II: Analysis of L7 line

Substrate	No. of layers	$d_{(p)}$ (μm)	$W_{(p)}$ (μm)	$W_{h(om)}$ (μm)	$W_{v(om)}$ (μm)	$\Delta W_{h(om)}$ (μm)	$\Delta W_{v(om)}$ (μm)
A	1 x	9.1 ± 7%	285.7 ± 3%	376.0 ± 2%	385.0 ± 1%	49.3 ± 21%	38.0 ± 20%
A	2 x	11.5 ± 8%	277.7 ± 14%	383.7 ± 4%	395.0 ± 3%	65.3 ± 17%	53.3 ± 8%
B	1 x	14.8 ± 6%	255.0 ± 11%	322.5 ± 4%	359.5 ± 3%	34.3 ± 20%	53.5 ± 17%
B	2 x	13.1 ± 5%	247.3 ± 7%	351.7 ± 3%	389.0 ± 2%	50.0 ± 15%	59.5 ± 27%

Thickness $d_{(p)}$ and width $W_{(p)}$ were obtained by profilometer measurements (Figure 2). $W_{h(om)}$ and $W_{v(om)}$ are width of the same line printed horizontally and vertically, measured on the optical micrographs. The wicking of these lines is given by $\Delta W_{h(om)}$ and $\Delta W_{v(om)}$ for horizontal and vertical lines, respectively (Figure 3). All layers were printed in one (1x) or two overprints (2x) onto gloss-coated paper (substrate A) and clear matt film (substrate B).

The profile of L7 lines was also analysed by SEM micrographs. They show that the surfaces of applied substrates are completely different: the gloss-coated paper gives uniform surface whereas the surface of the clear matt film is highly porous so that the edges of lines could be hardly observed (Figure 4). The samples were cured for 9 minutes. The micrographs also show that some wicking ΔW (determined on the optical micrographs) do not contain conductive particles but only a resin (Figure 5). The sample was single printed on gloss-coated paper and cured for 4 minutes. The surface feature is without silver particles. The wicking ΔW of electrically functional layer is smaller; therefore smaller width of lines should be taken into account accordingly.

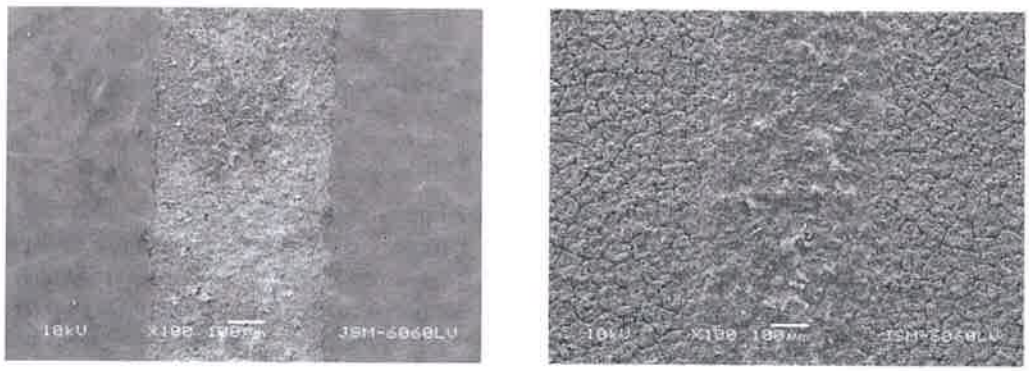

Figure 4: SEM micrographs of single printed layers on gloss-coated paper (left) and clear matt film (right) of L7 line

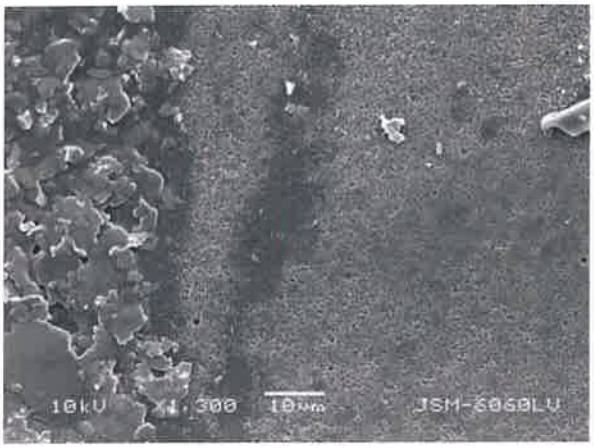

Figure 5:
SEM micrograph of the edge on L7 line

SEM micrographs were also used to monitor the cross-cuts of printed lines. All layers printed on the clear matt film show considerable cracks on the boundary between the layer and the substrate. The effect seems to be absent on the gloss-coated layers (Figure 6). Single printed layers shown on the Figure 6 were cured for 9 minutes. Both samples were tilted for 45°.

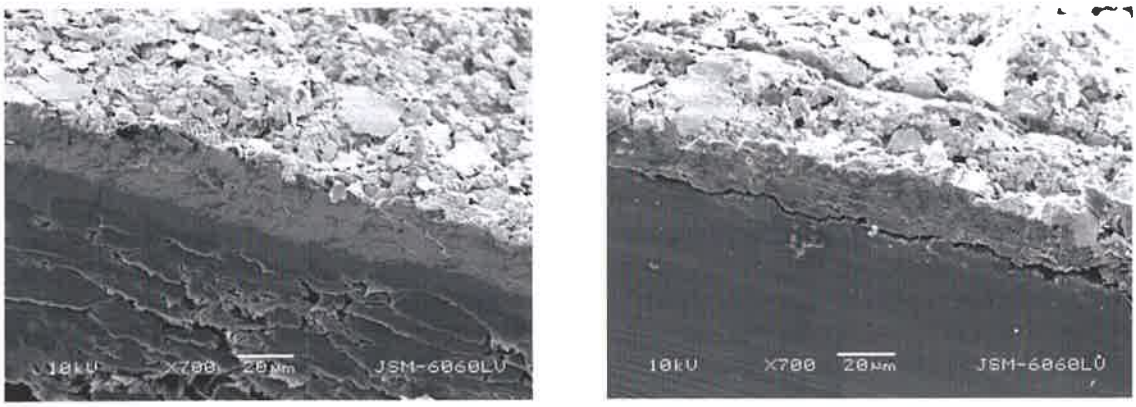

Figure 6: SEM micrographs of cross-cuts of samples printed on gloss-coated paper (left) and clear matt film (right) of L7 line

3.2 Adhesion

The quality of prints was evaluated by the cross-cut test. The results show that the adhesion is much better when layers were printed on the gloss-coated paper than on the clear matt film. In general, the second layer which is wet-to-wet overprinted on the same substrate might gives rise to smaller adhesion. The corresponding micrographs are shown in Figures 7 and 8. It is also possible to see that the second layer enlarges the coverage of the printed line (compare micrographs of single and double printed layer on the clear matt film).

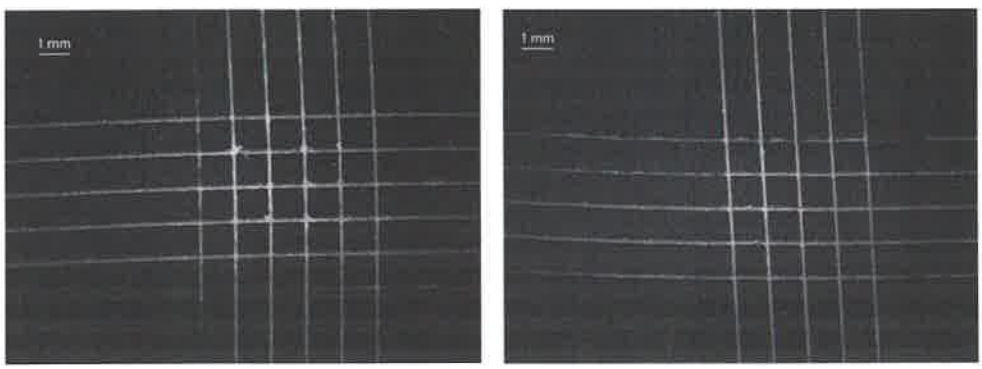

Figure 7: The cross-cut test of single (left) and double layer (right) which were printed on the gloss-coated paper

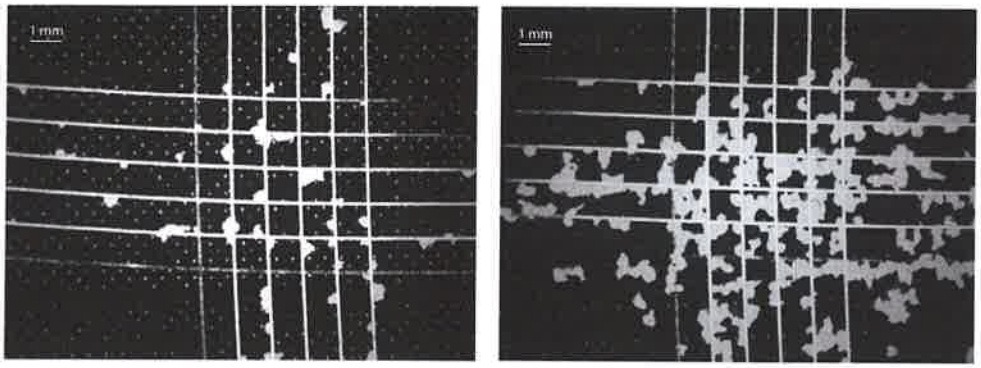

Figure 8: The cross-cut test of single (left) and double layer (right) which were printed on the clear matt film

Samples were cured for 4 min. The left sample on the Figure 7 corresponds to ISO Class 1 and the right one to the ISO Class 0. The left sample on the Figure 8 corresponds to ISO Class 3 and the right one to the ISO Class 5.

3.3 Specific resistivity

The specific resistivity ρ was measured by four-terminal method applying equation (1). The corresponding data for *W, L* and *d* given in Table II were taken into account in this calculation. This way the error of resistivity ρ was evaluated. The results are shown in Figure 9. Higher ρ was obtained when sample was printed on clear matt film and smaller if a gloss-coated paper was applied. In general, higher values of ρ were measured for single printed layers and smaller for double printed layers. Specific resistivity depends also on curing time: longer curing may give smaller resistivity. The effect was observed on samples cured for up to 9 minutes, whereas longer curing does not have larger influence.

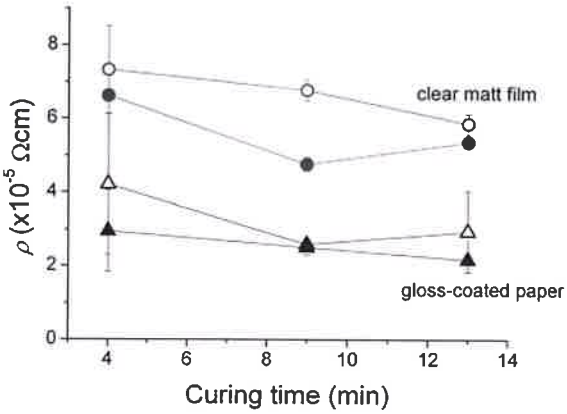

Figure 9: Specific resistivity ρ of single (open signs) and double layers (solid signs) printed on gloss-coated paper (triangles) and clear-matt film (circles) in dependence on curing time

The specific resistivity is an intrinsic property of material that forms printed lines: it reveals the ability of the material to conduct electric current. This property depends on the microstructure of lines. It appears that this microstructure is influenced by number of wet-to-wet overprinted layers, by the curing time and by the substrate used.

4. Conclusions

Detailed analysis of printed conductive lines is of crucial importance for several applications of printed electronics. Our research was done to analyse the resistivity of narrow screen-printed lines. The influence of the substrate, curing time and number of wet-to-wet overprinted layers were considered. The four-terminal resistivity measurement was applied to evaluate the resistivity in all samples.

Two substrates were applied, the gloss-coated paper and the clear-matt film. The thickness and the width of the line with target width of 500 μm were analysed by the help of mechanical profilometer, optical microscope and scanning electron microscope. These methods do not provide the same results. Thus, the data needed to calculate specific resistivity and to determine the functional properties of printed shapes have to be examined very carefully.

The gloss-coated paper has a smooth surface and the clear-matt film a very porous one. As a consequence, the smooth substrate provides good adhesion with no cracks between the layer and the substrate, whereas the porous substrate gives rise to poor adhesion and considerable cracks on the layer-substrate interface. Thinner and wider lines were printed on the smooth surface of the gloss-coated paper and thicker and narrower on the porous surface of the clear matt film. Printed lines show some wicking, which are clearly observable on the optical micrographs in the transmittance mode. Nevertheless, the corresponding SEM micrographs show that some of these features might be without functional particles, therefore cannot contribute to the functional width of the printed line. Such effects could hardly be observed on SEM micrographs of lines which were printed on a porous clear-matt film due to poor contrast between the layer and the substrate. The second wet-to-wet overprinted layer do not doubles the thickness of the final layer. Instead, its influences on the width of the printed lines were observed, in diverse meaning from profilometer results and from optical microscope. No systematic influence of curing time on thickness and width of printed lines were observed.

The resistivity is a property of material itself. It depends on the microstructure of printed line, where the microstructure of conductive inclusions inside the layer represents the most important contribution. Our results show that the resistivity of layers printed on gloss-coated layer is smaller than that printed on the clear matt film. The wet-to-wet overprinting gives rise to some diminish of the resistivity. Similar effect was obtained when the curing time was enlarged from 4 to 9 minutes whereas no appreciable influence was observed with further increasing time.

Our research shows that care should be taken when geometrical properties of printed lines such as thickness and wideness have to be determined. The parameters that practically do not influence on these results (such as curing time in our experiments), might influence on the intrinsic properties of the material inside printed lines and therefore also affects resistivity.

Acknowledgements

This research is supported by Slovenian Research Agency (Project No. L02-1097-0104-08). Maša Žveglič and Nina Hauptman acknowledge the Slovenian Research Agency for young researchers support.

References

1. Berggren, M., Nilsson, D., Robinson, N. D., (2007), *Organic materials for printed electronics, Nature Materials, 3, 3-5*
2. Hauptman, N., Žveglič, M., Maček, M., Gunde, M. K., (2009), *Carbon based photoresist, Journal of Material Science, (accepted for publication)*
3. Li, Y., Wong, C. P., (2006), *Recent advances of conductive adhesives as a lead-free alternative in electronic packaging: materials, processing, reliability and applications, Material Science and Engineering, 51, 1-35*
4. Park, B. K., Kim, D., Jeong, S., Moon, J., Kim, J. S., (2007), *Direct writing of copper conductive patterns by ink-jet writing, Thin Solid Films, 515, 7706-7711*
5. Pudas, M., Halonen, N., Granat, P., Vähäkangas, J., (2005), *Gravure printing of conductive polymer inks on flexible substrates, Progress in Organic Coatings, 54, 310-316*
6. Strümpler, R., Glatz-Reichenbach, J., (1999), *Conducting polymer composites, Journal of Electroceramics, 3(4), 329-346*



Colour changes of UV-curable thermochromic inks

Rahela Kulčar[1], Mojca Friškovec[2], Nina Knešaurek[1], Barbara Sušin[2], Marta Klanjšek Gunde[3]

[1] University of Zagreb, Faculty of Graphic Arts, Getaldićeva 2, HR-10000 Zagreb, Croatia
E-mails: rkulcar@grf.hr; nknesaurek@grf.hr

[2] Cetis, Graphic and Documentation Services, d.d., Čopova 24, SI-3000 Celje, Slovenia
E-mails: mojca.friskovec@cetis.si; barbara.susin@cetis.si

[3] National Institute of Chemistry, Hajdrihova 19, SI-1000 Ljubljana, Slovenia
E-mail: marta.k.gunde@ki.si

Abstract

UV-curable leucodye-based thermochromic inks with activation temperature of 31°C in blue, red and black shades were analysed. The colour of samples does not depend only on their temperature but also on thermal history - they show colour hysteresis. Similar hysteresis loops were obtained for the red and blue samples and narrower for the black sample, as measured by cycling in 14 - 40 - 14°C region. The blue and black samples have approximately closed loops but a small colour difference was obtained even after one cycle for the red one thus the loop remains slightly opened. The colour of all samples also depends on the UV dose applied at curing. This difference was followed over the whole hysteresis loop. The largest values were measured for the red sample where the CIEDE2000 total colour difference rises above 4 and remains well observable all over the temperature region applied for cycling. One of the possible reasons for this effect might be different degree of polymerisation of the polymer matrix achieved by different UV curing.

Keywords: thermochromic inks, UV curing, screen printing, colorimetry, dynamic colour, hysteresis

1. Introduction

Colour-changing inks become increasingly important for various applications in graphic art such as smart packaging, security printing and marketing. To achieve precise appearance and reasonable durability of prints, much knowledge about the dynamic properties is required. Extended research of dynamic appearance of the final product is presently covered only very approximately or not at all.

Liquid crystals and leuco dyes are thermochromic material types which are currently the most frequently used in printing inks. We have studied here leucodye-based printing inks. They consist of two-phases: a thermochromic phase is dispersed in a non-thermochromic polymer matrix, a resin. A thermochromic phase is realised in microcapsules which are mostly named simply as pigments. Both components build separate phases and it is supposed that they don't influence the other component. Leucodye pigments consist of a mixture of leuco dye, developer and solvent, which are microencapsulated in a protective polymer coating. Each microcapsule contains the entire system required to reproduce the dynamic colour. They are more than 10-times larger than pigment particles in conventional printing inks. They are not completely inert and insoluble and show practically negligible scattering effect. The activation temperature is determined by the temperature where the solvent changes from solid to liquid state. This phase change inhibits the colour-forming reaction between dye and developer below the transition temperature and protects it well above this temperature. The colouration/ discolouration process requires phase changes of the entire solvent in each microcapsule[1]. Therefore, a rather broad temperature range is needed for the process to be completed in all microcapsules. The colouration/ discolouration process is regarded to be reversible and it is believed that it can be repeated a few thousand times[2]. Leucodye-based thermochromic inks with various activation temperatures are available, from -15°C up to 65°C. Nevertheless, most applications are limited to three standard temperature ranges, cold (~10°C), human-touch (31°C) and warm (43°C)[3]. All major ink types such as water-based and photocuring for paper, plastics and textile are available.

Only few scientific studies applying leucodye thermochromic inks were reported until now. The most important is the work of Linda Johansson from University of Linköping, Sweden[4-8]. She investigated printed dynamic

images with completely different images in different temperature ranges. For this purpose, the leucodye thermochromic inks were combined with conventional process ink layers to obtain multicoloured printing dynamic images. Knowledge about the properties of leucodye-based thermochromic ink has to be enhanced for several areas of commercial applications[1]. The most important are the temperature-dependent properties of this complex system, the degree of its reversibility and the possible factors that may influence on it.

We have studied dynamic colorimetric properties of leucodye-based thermochromic inks. UV-curable thermochromic inks with activation temperature of 31°C in three hues were applied. Special attention was devoted to characterize the colour hysteresis and the meaning of the activation temperature. The influence of UV curing parameters was also analysed.

2. Experimental

UV-curable thermochromic screen printing inks UV TCX (Coates Screen Inks GmbH, Germany) in red (UV TCX R-31), blue (UV TCX B-31) and black (UV TCX N-31) shades were applied. They consist of acrylate UV-curable vehicle and leucodye thermochromic pigments with activation temperature (T_A) of approximately 31°C. The inks were screen printed applying SEFAR® PET 1500 high-modulus monofilament polyester mesh 120/34Y on gloss-coated paper (120 g/m^2). The off-prints were cured applying UV dryer Aktiprint L by UV energy of approximately 0,83 W/cm^2 at two different speed of conveyor belt, 22 and 8 m/min. At these speeds the maximum curing energy falling on the sample are approximately 150 and 400 mJ/cm^2, respectively. The UV integrator (Technigraf, Germany) was applied for these measurements.

Spectral reflectance of all prepared samples were measured by UV-VIS-NIR spectrophotometer Lambda 950 (Perkin-Elmer) with 150 mm integrating sphere applying (8°:di) measuring geometry (diffuse geometry, specular component included)[9]. The temperature of the sample was varied by the help of copper plate, which was heated/cooled by circulation of thermostatically controlled water in tubes inside the plate (Figure 1). The reflectance spectra were measured every 2°C at heating from 14°C up to 40°C and then at cooling down to 14°C. Colorimetric calculations were done in CIELAB space applying D50 illuminant and 2° standard observer. The total colour differences were calculated according to the CIEDE2000 colour difference equation.

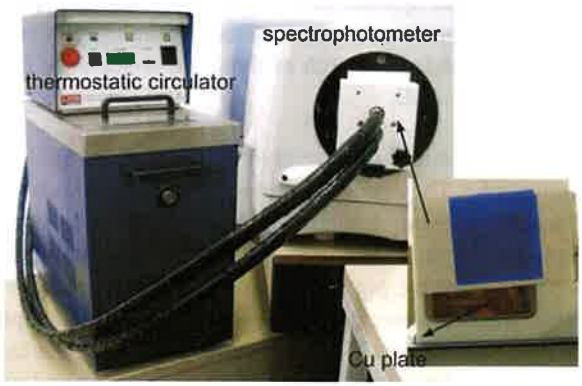

Figure 1:
Thermostatic circulator and the front view of the copper plate with sample

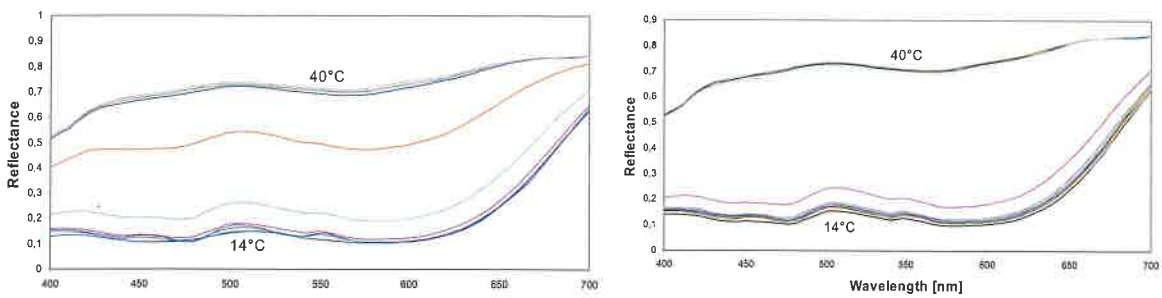

Figure 2: Spectral reflectance curves for the black sample measured at heating (top) and cooling (bottom). The spectra were measured in 2°C interval

The degree of polymerization of the acrylic vehicle was analysed applying infrared spectroscopy. For this reason a thin layer of thermochromic ink was applied on a ZnSe (Irtran-4) optical window. The as-deposited layer and layers cured by UV doses of 150 and 400 mJ/cm^2 were measured in the transmittance mode. The degree of polymerisation was followed by the intensity reduction of the C = C bond of the unsaturated acrylate group located at 1409 cm^{-1}. When the vehicle is fully polymerised, these bonds dissappear[10,11].

3. Results ad discussion

3.1 Changes of colour in dependence on temperature

The CIELAB values L^*, a^* and b^* in dependence on temperature of printed samples are shown in Figures 3 and 4. These figures show that the colour of samples does not depend only on temperature, but also on the thermal history, i.e. whether this temperature was reached during heating or during cooling. This phenomenon is known as hysteresis. Our samples become discoloured during heating and coloured again during cooling. The process is illustrated by change of lightness L^* as a function of temperature (Figure 3). When a sample is heated, L^* becomes higher. At T_A it rises above 80 whereas at somewhat larger temperatures the sample seems to be completely discoloured and L^* values remain approximately the same with further increasing of temperature. When the same sample is cooled, the reverse process (i.e. colouration) occurs at much lower temperatures. The entire $L^*(T)$ curve has a form of a loop, known as hysteresis loop. Similar loops were obtained also for $C^*(T)$ but in opposite direction. During heating the C^* diminishes and rises again at cooling. The samples studied here do not show equal colour hysteresis: they differ in the temperatures where the loop starts and finishes, in its steepness and area.

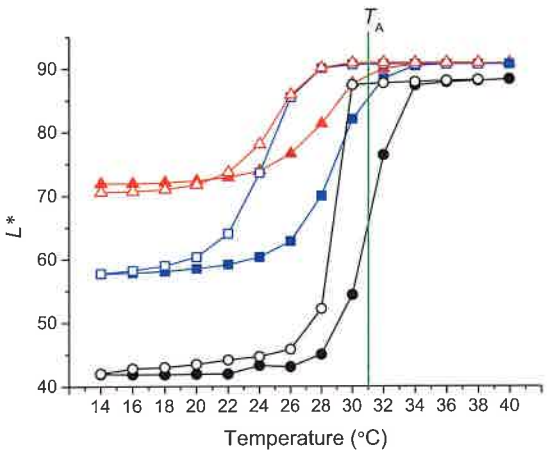

Figure 3:
CIELAB lightness L of red (triangles), blue (squares) and black (circles) thermochromic samples in dependence on temperature at heating (solid signs) and cooling (open signs). The samples were cured applying UV dose of 400 mJ/cm^2. The activation temperature is denoted by T_A*

If a completely reversible process is assumed, a thermochromic sample should return to the same colour after the whole heating/cooling cycle. Hysteresis loop of such a sample is closed. We have obtained approximately closed loops for black and blue samples. The loop of the red sample remains opened, where the final L^* is somewhat lower than the initial.

During heating/cooling cycle the a^*, b^*, L^* and C^* values of a thermochromic sample describe a path on the (a^*, b^*) and (L^*, C^*) planes (Figure 4). These paths are in general not the same at heating and cooling, but differences are small. It can also easily be recognized that the discoloration is not complete - all systems shown here retain similar yellow shade even at the highest temperature applied here (40°C).

The obtained hysteresis has to be shown for all three values of the colour space simultaneously, thus by a 4-dymensional graph. This was simplified by the colour gradient, i.e. the rate of colour change (expressed by CIEDE2000 colour difference) between the two adjacent measurements. It was evaluated in dependence on temperature. Such a graph represents the first derivative of the corresponding three-dimensional hysteresis. These graphs are shown in Figure 5. The largest colour gradient vas obtained for black samples, where it is smaller at heating and larger at cooling. The corresponding colour gradients for red and blue samples are smaller and approximately similar for heating and cooling. This figure may help in explaining the meaning of T_A at heating. For the black sample the T_A corresponds to the temperature where the colour gradient is maximal but for the red and blue samples it is located at the nearest neighbour measuring point after the peak of colour

gradient. In the reverse direction (when the sample is cooled) the colour gradient peaks much more apart form the T_A, at smaller temperatures.

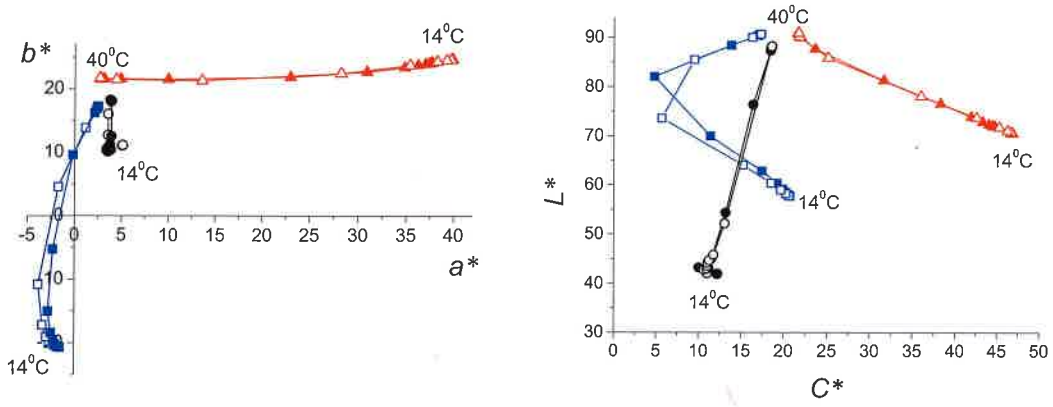

Figure 4: Changing of CIELAB values of red (triangles), blue (squares) and black (circles) thermochromic samples in (a, b*) plane (top) and (C*, L*) plane (bottom) at heating (solid signs) and cooling (open signs). All samples shown here were cured applying UV dose of 400 mJ/cm²*

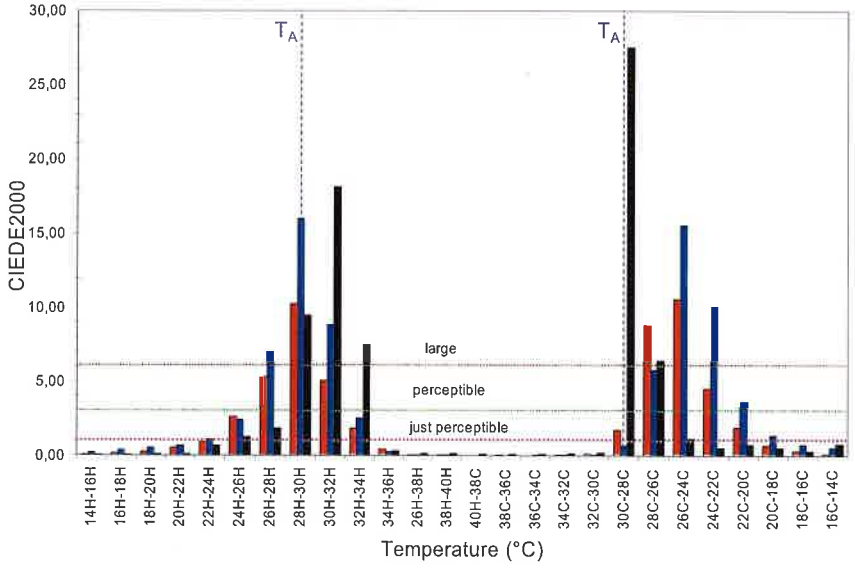

Figure 5: The total colour change (CIEDE2000) of the red, blue and black samples as obtained between two adjacent temperatures at heating (H) and cooling (C) (e.g. 26H-28H denotes the total colour difference measured on the same sample when it is heated from 26 to 28°C). All samples were cured applying UV dose of 400 mJ/cm²

The samples that were cured at different UV doses have somewhat different colour. The effect has to be analysed by the help of colour hysteresis. The colour differences between samples shown above and that cured at UV dose of 150 mJ/cm² in dependence on temperature are shown in Figure 6. This difference is the largest in temperature regions where big colour changes occur. The largest differences were obtained for the red ink where it is above the observable limit all over the entire measurement region and rises above 4,0 at the largest rate of colour change.

3.2 Degree of polymerisation

The samples cured at different UV dose do not exhibit the same colour. The CIEDE2000 colour difference between weakly (150 mJ/cm²) and hardly (400 mJ/cm²) cured samples with the same printed ink is shown on Figure 6. The possible reason for the effect was analysed by infrared spectroscopy.

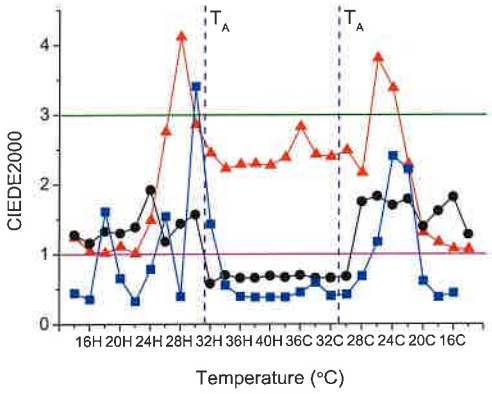

Figure 6: CIEDE2000 colour difference between red (triangles), blue (squares) and black (circles) thermochromic samples that were cured with UV dose of 400 and 150 mJ/cm² in dependence on temperature at heating and cooling. The temperature at heating is denoted by H and at cooling by C (e.g. 28C denotes 28°C on cooling)

Infrared spectra of the thermochromic inks depend on chemical structure of the ink. Absorption of UV light applied at curing process causes crosslinking of monomers and oligomers in the liquid resin whereby a solid polymer is formed. Therefore in the infrared spectra some peaks diminish and some new may appear. The effect on our samples is shown in Figure 7. The peak at 1409 cm^{-1} due to double-bond vibrations (C = C) of the acrylic group was applied here to measure α, the degree to which the unpolymerized sample was conversed to the polymerized state:[9]

$$\alpha = 1 - A_E / A_0$$

where A_E and A_0 are the infrared absorbance of the exposed and unexposed samples at the representative peak, respectively. This gives α = 0,87 for the lower UV dose and α = 0,91 for the higher UV dose.

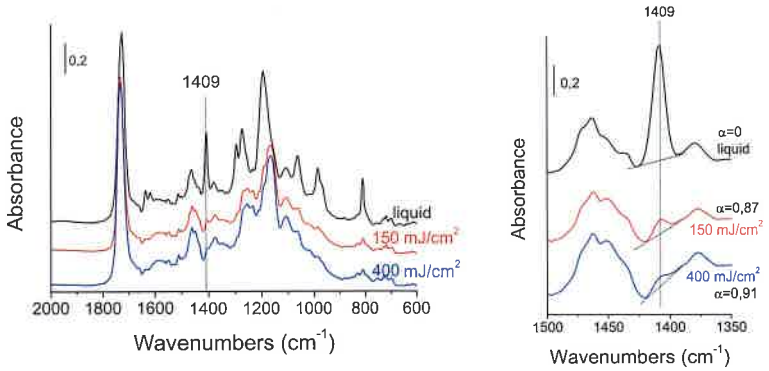

Figure 7: Infrared spectra of differently cured samples. After UV curing the peak at 1409 cm^{-1} diminishes. The effect is larger for higher UV dose, representing higher degree of polymerisation of the acrylic vehicle

4. Conclusions

The screen-printed UV-curable leucodye thermochromic inks with activation temperature of 31°C were investigated. The variation of colour as a function of temperature was measured and analysed.

No complete discoloration was obtained well above the activation temperature. This is not necessarily a consequence of imperfect discoloration, but could also be a combined effect of the vehicle, the properties of the thermochromic system in microcapsules and of the resin applied for microencapsulation. Similar yellow colour was obtained for all samples.

All the analysed samples show colour hysteresis: their colour does not depend only on temperature but also on the way this temperature was reached. A system with hysteresis has memory, i.e. it exhibits a path-dependence. The colour of samples prepared by a thermochromic ink is different when the same temperature is reached by heating or by cooling. Different colour hystereses were obtained. The steepest changes and the largest colour gradient were measured for the black sample and similar for the blue and red samples.

The activation temperature describes the temperature where a heated sample undergoes the largest colour change. This is well obeyed for black sample and more loosely for red and blue ones. When a sample is cooled, the activation temperature fails any meaning – the colouration process occurs at considerably lower temperatures. More-or-less closed loops were obtained in the measured temperature cycle, with observable opening for the red sample only. This shows that a small colour shift may retain after the entire temperature cycle.

When the layers are prepared by the same ink and cured by different UV dose they may have different colour. The effect is the largest for the red samples. A possible reason was investigated by infrared spectroscopy. The infrared spectra of thermochromic ink depend on the amount of UV energy applied to a sample at curing. Our results show that the degree of polymerization of the polymer matrix increases in samples cured with higher UV dose. This could be one among possible reasons for the colour difference obtained in differently cured samples.

Further research of the complex two-phase system is needed. It is very likely that the properties of colour hysteresis characterize the details of the microstructure inside thermochromic layers and is therefore the most important property of such samples. Special attention should be devoted to the span of temperatures applied for cycling and to durability of the colouration/discolouration processes. The influence of the UV energy applied for curing on the microstructure has to be analysed carefully. It is very likely that the change in crosslinking of the host polymer is only one among several reasons for the observed effect.

Acknowledgements

Mojca Friškovec acknowledges the Slovenian Technology Agency for young researcher support, operation part financed by the European Union, European Social Fund. Operation implemented in the framework of the Operational Programme for Human Resources Development for the period 2007-2013, priority axis 1: promoting entrepreneurship and adaptability, Main type activity 1.1.: Experts and researchers for competitive enterprises.

References

1. Seeboth, A. and Lötzsch, D.: "Thermochromic Phenomena in Polymers", Smithers Rapra technology Limited, Shawbury, UK, 2008
2. Homola, J.: "Color-changing inks", Color Change Corporation, 2003; http://www.screenweb.com/index.php/channel/6/id/1425/, http://www.mhest.com/supparticles/Color-changing-inks.pdf
3. "Thermochromatic effects", Printcolor high performance inks, http://www.apcis.fr/ft/printcolor/documents/

   Thermochromatic_Effects.pdf
4. Johansson, L.: "Chromatic properties of thermochromic inks", Proceedings of TAGA Conference, San Antonio, 2004
5. Johansson, L., Kruse, B.: "Colour separation with dynamically changeable inks", Proceedings of the TAGA Conference, Toronto, 2005
6. Johansson, L., Kruse, B.: "The influence of paper properties on colour reproduction with dynamics inks", Proceedings of the CSIST/IS&T 2005 International Conference on Imaging: Technology & Applications for the 21st Century, Beijing, 2005
7. Johansson, L., Kruse, B.: "A colour separation strategy for reproduction of printed dynamic image for paper substrate", Proceedings of the 32nd International iarigai Research Conference, Porvoo, 2005
8. Johansson, L.: "Creation of printed dynamic images", Linköping Studies in Science and Technology, Thesis No. 1234, Norköpping 2006
9. "Colorimetry", 3rd edition, CIE 15:2004. Vienna (2004)
10. Landry, V., Riedl, B., Blanchet, P.: „Nanoclay dispersion effects on UV curing coatings", Prog. Org. Coat. 62 (2008) 400-408
11. Colthup, N. B., Daly, L. H., Wiberley, S. E.: Introduction to Infrared and Raman Spectroscopy, Academic Press, Boston, San Diego, New York (1990)

Colour changes due to UV-varnishing at the production of the paper-based cards

Erzsébet Novotny[1] and Ildikó Endrédy[2]

[1] Állami Nyomda Nyrt/State Printing Company
H-1102 Budapest, Halom utca 5., Hungary
E-mail: novotny@any.hu

[2] Budapest Tech Politechnical Institution
H-1034 Budapest, Doberdó út 6., Hungary
E-mail: endredy.ildiko@rkk.bmf.hu

Abstract

Surface refining procedures have an increasing significance in satisfying quality and other special demands (uniqueness, appearance) made on printing house products. Besides the effects intended to be achieved (gloss, mechanical protection) surface refining technologies occasionally can go together with other changes of the optical appearance of the prints.

Within surface refining procedures our tests focused on the effect of varnishing on print appearance. The purpose was to determine the extent and direction of colour changes occurring when paper based cards are produced using different print carrier and varnish combinations.

We examined the change of metric chroma as a function of sample lightness, the change of lightness as a function of the chroma of the samples, hue differences as a function of hue angles of the samples. We established that the Sericol type varnish on matt paper samples showed the biggest, and Wessco type varnish on glossy paper samples the smallest change. Based on our test results we propose some improvement of technological processes.

Keywords: card printing, UV-varnishing, gloss measurement, abrasion test, colour measurement

1. Introduction

Besides plastic cards the market continues to demand considerable quantities of cards using paper as base material, such as prepaid phone cards, certain ID cards, loyalty cards, club membership cards and cards associated with certain bank cards, containing the PIN-code. These paper based cards represent a value both for the issuer and the card holder. Security elements providing protection against forgery, long-term usage and representation of brand names are important for them. Value in use, durability, and aesthetic value can be increased by surface refining– in the case of cards by varnishing - after printing.

Varnishing is applied to change and improve the aesthetic, physical, optical, mechanical, chemical, usage, application technical and environment resistant features of the face, to protect from quick wear-and-tear (abrasion) or colour change (fading) of the print, and to prevent electrostatic charge that would interfere with the operation of processing equipment.

For the production of cards the so-called UV varnishing is most suitable, mainly from face protection aspects. UV-varnish layers can equally be glossy or matt, colourless or coloured. They can contain metal pigments (gold, silver or bronze-like), ingredients causing special effects or nacreous lustre, and micro-capsules encapsulating fragrances that release their content when touching them. They can contain substances that change their colour and character depending on the angle of view.

UV-varnish layers - unlike conventional varnish - can be very thick or can also make the application of extremely thin layers possible. Thick prints can create a 3D impression and be palpable, extending in space.

A further advantage of UV varnishing and the layers formed by it is that they do not contain solvents; therefore the varnish layer hardened upon the effect of UV radiation is perfectly dry.

Absorption of the varnish into the paper is negligible; the varnish layer has an excellent resistance to rubbing, and provides enhanced protection to the surface of the printed cards.

2. Purpose of the test

The purpose of our test was the examination of the gloss and resistance to rubbing of the selected varnishes, as well as their effect on the colour of the prints after application. Colour modification due to varnishing is known to those dealing with the subject. However, it was very important in our case to examine how the logos of card issuing companies change depending on the varnish applied, what is the colour difference that has to be taken into account in certain cases when preparing the CMS colour profile, and - in case of direct (spot) colours - in what direction should the colour of the ink be modified to achieve the desired result. This modification process is very important when producing cards, as it is essential that the colours of the company logo on publications and printed products accompanying the given card and prepared by different printing procedures on different materials be identical.

3. Test printing

For the tests a test chart was produced containing the logo colours of 20 companies (banks, insurance companies, airlines etc.) and colour fields that covered the range that could be reproduced by the CIELAB colour space in four-colour printing as much as possible.

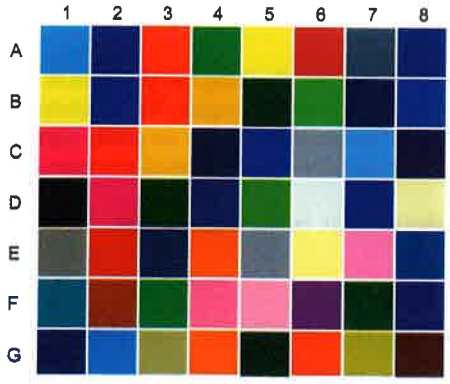

Figure 1:
The test chart

Printing was done on 250 gr/m² matt, 300 gr/m² glossy Euro Art printing papers used in card and card-mailer production, on Heidelberg Speedmaster printing machines. Varnishing was done on a screen printing machine (screen 150 l/cm). Two types of varnishes were used for our tests: Wessco UV34.238.15 and Sericol Uvibond UV371.

4. Measurements

4.1 Gloss measurement

Gloss measurement was carried out under standard conditions using a DR Lange Refo 3D glossmeter. The gloss index is a value relative to the mirror reflection of a polished black glass surface (which is considered to have a gloss of 100%). Measurement was started with 60° measurement geometry, where the range 30 - 75% was used. Here the obtained value was over 70%, so, in accordance with the measurement instructions, we changed to 20° measurement geometry. The equipment was calibrated to the polished black glass surface prior to the measurements with 60° and 20° measurement geometry. Furthermore, we checked the repeatability of the equipment, and the corrected empirical deviation was 0.2319.

According to the results, the Sericol varnish was glossier (as far as the percentage of reflection is concerned) both on the matt (78%) and on the glossy (77.6%) cardboard, examining a specific field. The reflection value of the Wessco matt varnish was 69.5%, while that of the glossy type was 64.1%. Irrespective of the varnish used, a higher gloss value was achieved on the matt print carrier than on the glossy cardboard.

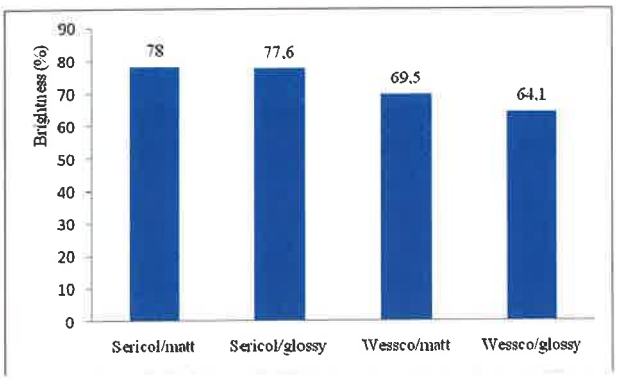

Figure 2:
Gloss values of the samples

4.2 Abrasion test

Abrasion resistance was tested under standard conditions using a Prüfbau Quartant abrasion tester. The device was set to a stroke number of 2.000. With this stroke number, change was now measurable. We used a piece cut out from the same sample sheet on the counter boards as well, modelling the processing phase and the anticipated use of the cards.

Main technical parameters of the equipment:
Stroke number: 1 - 9.999 (1 stroke = 1 go and 1 return move)
Abrasion pressure: 0.5 N/cm2
Sample size: 50 x 112 mm (on the base board) Ø45 mm on the counter board.

The samples were weighed before and after abrasion. Abrasion resistance was described in terms of mass difference, i.e. the quantity of varnish that had been rubbed off. Based on the results, we established that the abrasion resistance of the Sericol varnish is better both on the matt (1.225 mg) and on the glossy (3.475 mg) cardboard. The quantity of abraded varnish was 2.975mg for matt and 3.675 mg for glossy Wessco varnish. The glossy cardboard was more susceptible to abrasion with both types of varnish.

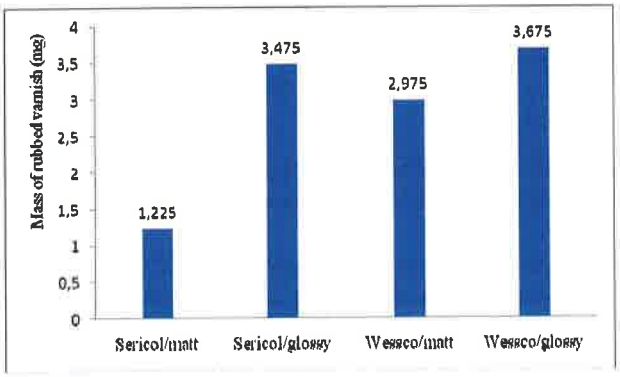

Figure 3:
Mass of varnish rubbed off from the samples

4.3 Colour measurements

The effect of surface treatment on the colour of samples was tested by means of colour stimulus measurement. The measurements were carried out using a GretagMacbeth SpectroEye colorimeter/spectrophotometer, with D50 illumination, 45/0° measurement geometry and 2° observer.

The CIELAB colour stimulus coordinates of the test fields were measured on the samples, first on prints without varnish, then with varnish. Based on the results, L^*, a^*, b^*, C^*_{ab}, h°_{ab}, ΔE^*_{ab} colour difference and differences in colour stimulus characteristics (ΔL^*, ΔC^*_{ab}, ΔH^*_{ab}) were calculated.

Besides the CIE ΔE^*_{ab} formula, the CIE ΔE_{00} formula was also used because this colour stimulus determination method takes into account local distortions in various parts of the colour space, combining the advantages of the CIE 94 and CMC formulas, and therefore the colour stimulus differences calculated with the formula more

4.3.1 Colour difference

We found that both types of varnish change their colours depending on the print carrier. With both types of varnish, there were smaller colour stimulus differences on the glossy cardboard than on the matt print carrier. This is explained by the fact that the colour saturation effect of the varnish coating is already initially less noticeable on glossier surfaces.

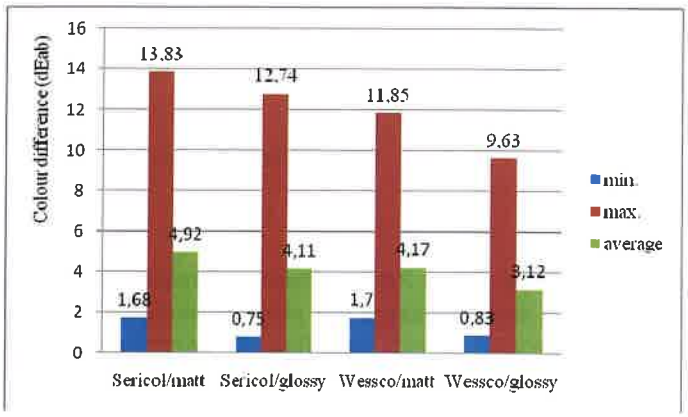

Figure 4:
Minimum, maximum and average colour changes of test prints based on the ΔE^*_{ab} formula

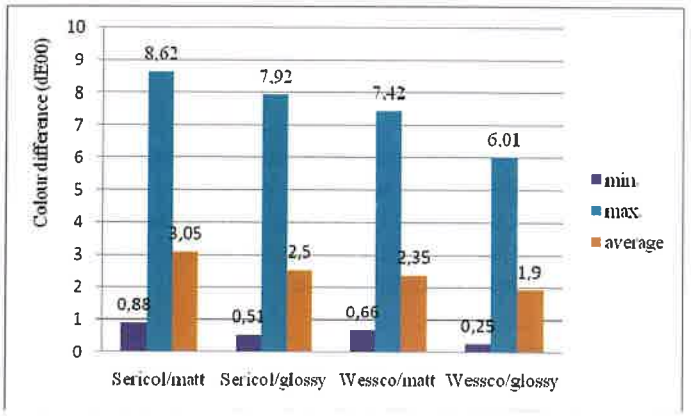

Figure 5:
Minimum, maximum and average colour changes of test prints based on the ΔE_{00} formula

The order of samples based on average colour stimulus difference was unchanged with the ΔE_{00} formula, with the Sericol/matt sample showing the biggest and the Wessco/glossy sample showing the smallest variation.

The colour stimulus difference of 75% of the samples falls in the category "visible colour change" (ΔE_{00} 1.5 - 3.0) in the case of the Wessco varnish. The colour stimulus differences represented by the Sericol varnish are substantially larger. Examining the fields showing a large colour stimulus difference, we found that they appeared in the same colour fields, virtually irrespective of print carrier or varnish.

Table I: Colour differences of basic colours and secondary colours

	Sericol/matt		Sericol/glossy		Wessco/matt		Wessco/glossy	
Field	ΔE^*_{ab}	ΔE_{00}	ΔE^*_{ab}	ΔE_{00}	ΔE^*_{ab}	ΔE_{00}	ΔE^*_{ab}	ΔE_{00}
C	5,9	1,16	1,37	1,2	2,03	1,2	0,97	0,7
Y	4,5	1,63	3,24	0,73	5,74	1,15	2,39	0,49
M	4,23	3,08	4,19	1,6	4,14	1,39	3,14	1,16
K	2,07	1,59	1,75	1,46	4,5	3,21	1,03	0,93
K50%	13,83	4,43	8,96	7,92	8,13	7,02	6,87	6,01
Y50%	11,7	6,05	12,74	3,84	11,85	3,88	9,63	2,93
M50%	9,88	8,62	10,53	5,74	10,16	5,23	8,86	4,66
G	3,58	1,17	0,75	0,62	2,49	0,66	1,03	0,25
R	2,21	0,88	2,23	0,73	3,38	1,15	1,85	0,57
B	2,58	1,89	1,75	1,28	3,25	1,73	1,67	1,22

Looking at the results indicated in the table, it is apparent that, with the exception of cyan, basic colours significantly changed, and that their 50% fields showed more than double colour stimulus difference. At the same time, colour stimulus differences determined using the ΔE_{00} formula only reflect a significant change at the 50% tonal value, which corresponds to visual experience.

*4.3.2 Colour shifting in the a*b* colour space*

The unvarnished and varnished values of all samples are represented in the a*b* coordinate system, where the direction of shifting due to the application of varnish is well noticable.

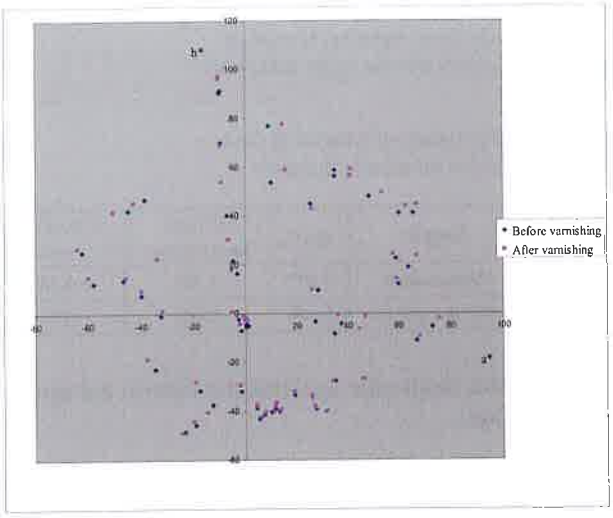

Figure 6:
*Colour shifting of samples in the a*b* colour space after varnishing*

Minor shifts do not reach a level that would be noticeable in print runs, so it is recommended to neglect such shifts during the study of the colour changing effect of varnish. Accepted levels of colour fluctuation for print runs are between ΔE^*_{ab} 2 - 2.5. In our study, eight samples showed a value around this figure of maximum 3. We disregarded those samples in further evaluations.

4.3.3 Metric chroma difference

Metric chroma variation was examined in relation to the lightness of samples. The figure shows the points of the selected systems and the corresponding regression lines. We observed that saturation changes of varnish are also influenced by the surface characteristics of the print carrier. Differences on matt print carriers are larger than those on glossy ones, and the two types of varnish also show a difference.

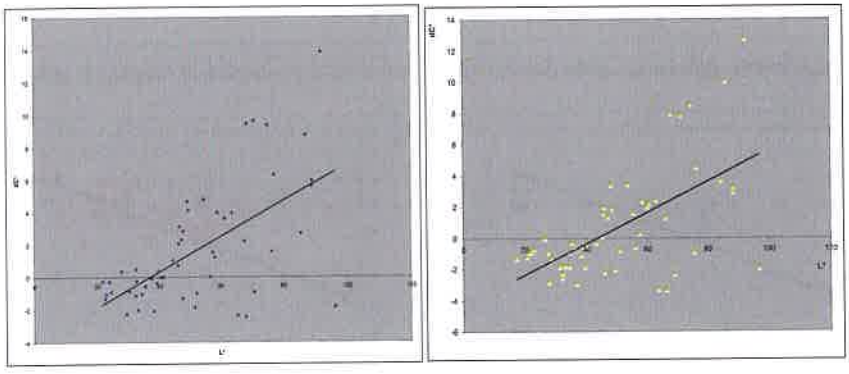

Figure 7: Metric chroma changes in relation to lightness in case of Sericol varnish on matt (on the left) and glossy (on the right) substrates

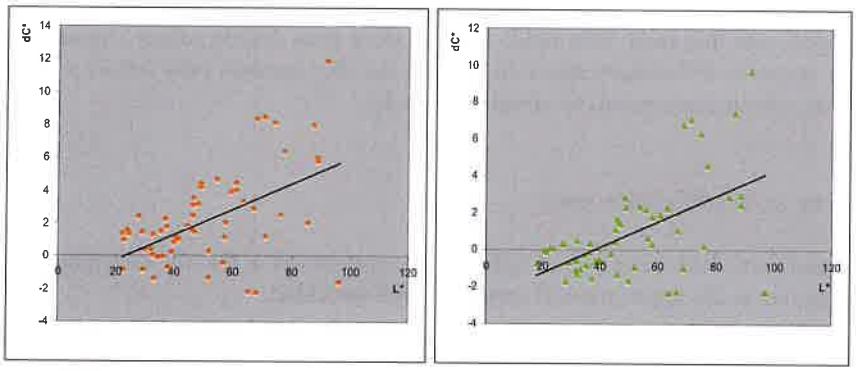

Figure 8: Metric chroma changes in relation to lightness in case of Sericol varnish on matt (on the left) and glossy (on the right) substrates

Table II: Regression lines and correlation values of samples in case of metric chroma changes represented in relation to lightness

Sample	*tg(α)*	*dC* axis intersection*	*Correlation (r2)*	*Sample*	*tg(α)*	*dC* axis intersection*	*Correlation (r2)*
Sericol/matt	0,109	-4,04	0,618	Wessco/matt	0,077	-1,761	0,531
Sericol/glossy	0,1	-4,368	0,603	Wessco/glossy	0,069	-2,603	0,556

Furthermore, we found that changes in the saturation of colour fields after applying the varnish are smaller for fields that are initially characterized by lower colour saturation.

From among the examined samples, this occurred with samples printed on matt coated cardboard varnished with the Wessco varnish. Even though the variation of points is relatively large, there is an obvious link between changes in brightness and colour saturation.

4.3.4 Lightness difference

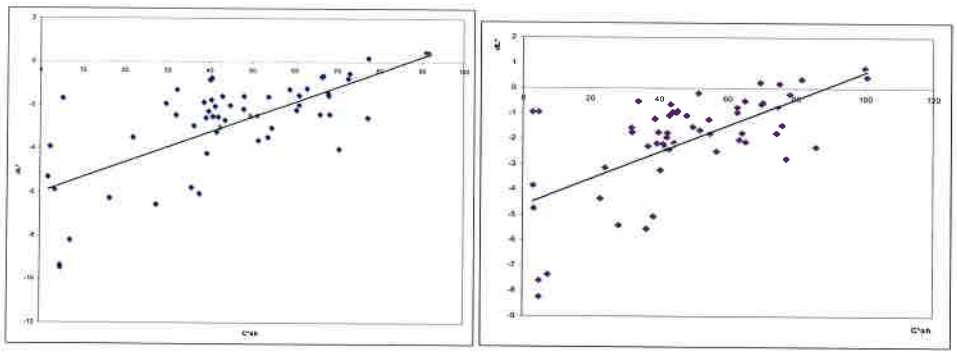

Figure 9: Lightness differences of the Sericol/matt, Sericol/glossy samples in relation to metric chroma

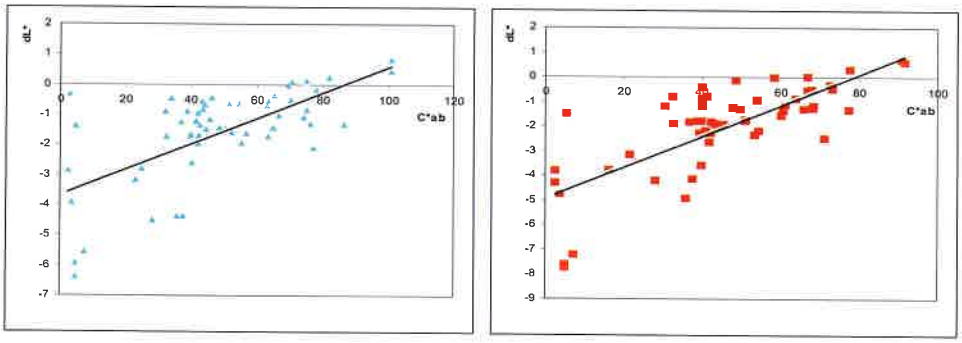

Figure 10: Lightness differences of the Wessco/matt, Wessco/glossy samples in relation to metric chroma

Our continued research into the SM system revealed that all samples except for two darkened due to the application of varnish. By representing lightness differences between varnished and unvarnished colour fields in relation to metric chroma, and using regression lines, it is possible to determine the saturation level above which colours become lighter due to the application of varnish. This is caused by the difference between the refraction coefficients of varnish and ink. According to professional literature, if the refraction coefficient of the varnish is higher than that of the ink underneath, the colour will get darker, while in the opposite case, it will get lighter.

Table III: Regression lines and correlation values of samples in case of brightness differences represented in relation to colour saturation

Sample	*tg(α)*	*dC* axis intersection*	*Correlation (r2)*
Sericol/matt	0,069	-6,022	0,704
Sericol/glossy	0,052	-4,624	0,644
Wessco/matt	0,063	-4,948	0,753
Wessco/glossy	0,042	-3,665	0,659

Based on our measurement results, it is apparent that, on the one hand, the lighter the sample, the more saturated it becomes, on the other hand, the more saturated the colour, the higher degree of darkening is caused by the varnish.

4.3.5 Hue difference

Hue differences in relation to hue angle may be positive or negative in the hue angle regions. The ΔH^*_{ab} value changes sign at 40°, 100°, 150° and 275°. For Sericol/matt samples, ΔH^*_{ab} values are positive between 0°-40°, negative between 40°-100°, at 100° there is a degree of uncertainty as for the direction of deviation, then positive between 100°-150°, negative again between 150°-275°, and there is a positive change between 275°-360°. This means that the colour of samples shifts towards red and green, in accordance with the ΔH^*_{ab} value.

The application of varnish causes similar changes in other systems (S/G, W/M, W/G) as well. However, with glossy print carriers, besides positive changes, significant negative changes can also be observed around 360°. In this case, unvarnished measurement values started at 375°; however, the varnished sample was within the 2° range.

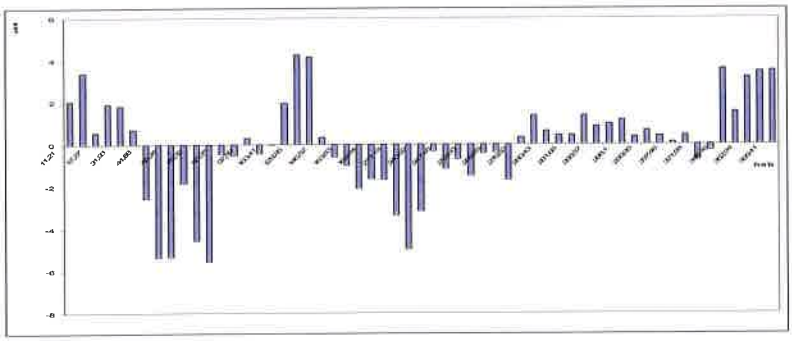

Figure 11: Hue differences in the Sericol/matt system in relation to hue angle

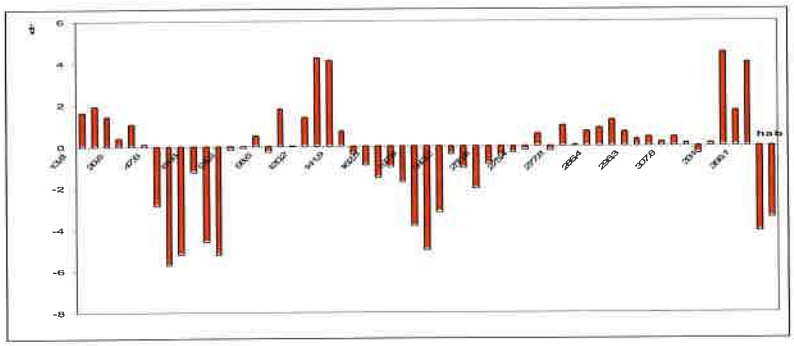

Examining the hue difference in the a*b* coordinate system, we found that the plane of the coordinate system is divided into two half-planes by the 100° and 275° half-lines, counted from the a* axis. The values left of these are directed towards 150°, while those on the right are directed towards 40°. These hue angle values correspond to green and red, which is a proof of the yellowing effect of varnish on the print in case lots of colours. This applies to each examined varnish/print carrier system.

5. Conclusions

5.1 Brand colours

It was determined that - irrespective of the varnish selected - in case of brand colours it is better to print on print carriers with a glossy surface, in order to obtain proper colour reproduction. These systems show an even smaller colour difference with Wessco and Sericol varnishes than in case of matt print carriers.

Table III: Brand colours with 3< ΔE_{00} colour difference

Colour	*Field*	*Company*	ΔE_{00}
P660C	C5	UPC	3,01
P308C	E8	UPC	3,13
P104C	G7	CIB	3,22
P321C	F1	UPC	3,47
P160C	F2	UNIQA	3,78
P130C	B4	Burger King	3,83
P165C	E4	ING	3,99
P298C	C7	Pannon	4,02
P158C	G4	UPC	4,02
P1235C	C3	Lufthansa	4,16
P616C	D8	Volksbank	4,59
P441C	D6	Malév	5,48
P451C	D8	CIB Corporate	5,63
P211C	D6	Szerencsejáték	6,25
P1905C	F5	Szerencsejáték	6,54
P Cool Gray 7C	C6	Lufthansa	8,25
P431C	A7	LG	8,35

The P431C grey (ΔE_{00} 8,35) in the LG logo produced the biggest change, almost as big as the Cool grey of Lufthansa (ΔE_{00} 8,25). The P1905C pink of Szerencsejáték Zrt. showed a smaller but quite big difference with ΔE_{00} = 6,54. Out of 20 brand colours 17 colours have more than ΔE_{00}=3 units falling into the "fully visible" (ΔE_{00} 3.0 - 6.0) or "big" (ΔE_{00} > 6) categories.

The average colour difference belongs also to the "fully visible" category. Several of the tested sample pairs resulted in colour differences bigger than ΔE_{00} 6 units which corresponds to a "big" colour difference. The majority of these were detected at the changes of secondary colours too.

5.2 Basic (primary) and secondary colours

There are only insignificant changes regarding lightness and saturation at the basic colours. The main component of colour difference is the chroma change, which is bigger at the yellow and magenta colours, but is determinant at cyan also. On average, the following can be stated for the colour modification effect of varnishing:

- the average colour difference belongs also to the „fully visible" category,
- metric chroma change is determinant in colour change.

The purpose of the examination of the secondary colours was to find out if any conclusion can be drawn for the given secondary colour which arises out of the common features of the two primary colours producing the secondary colour.

The biggest average colour difference was measured for the green colour, and the smallest for the red, but all three colour differences fall into the "fully visible" range. It can be stated that the order of average colour differences was the same as with primary colours.

The change of brightness values does not reach the upper limit of the "hardly noticeable" range. However, the deviation from the results obtained for primary colours is that the saturation of all three colours increased, and the change of the red and green colours reached the visually "noticeable" range. Changes of hue (a determinant factor here also) was for green, blue and red - in order of priority from the biggest to smallest - but the average values are smaller than that of the basic (prime) colours.

The following can be stated:

- the average colour difference of secondary colours falls into the "fully visible" category,
- on average the colours became more unsaturated,
- saturation is noticeably higher,
- metric chroma changes are smaller than in case of basic (prime) colours.

6. Proposals

Summarising our test-results the followings were determined regarding varnishing:

- colour changes that occur during varnishing belong to the "fully visible" category from the point of visual judgement,
- as an effect of varnishing it is mainly the tone that changes,
- bigger colour change occurs when applying matt paper at the varnishing than with glossy one at the varnishing.

Based on it we propose:

- to take back from the yellow colour when preparing the printing plates,
- to take into account the considerable darkening effect of varnish on unsaturated bright colours,
- for brand colours printed with direct colours corrections have to be made in the contrary direction than is the direction of the colour change when making special brand colour inks,
- to prepare a collection of varnished and unvarnished standard pairs for the printing workshop in case of brand colours.
- to follow the examination in the direction of other printing substrates and types of varnish.

Acknowledgements

Special thanks to Dr Péter Schulz and Mr Péter Rauscher for contributing in measurements and taking part in our work.

References

1. Malacara, D., 2002, *Color Vision and Colorimetry, Theory and applications, SPIE Press, Bellingham, Washington*
2. Michael, J., Penny, A., 2002, *Printing technology, Online Companion, Columbia*
3. -, 2004, *Colour Change due to a varnish layer, Colour research and application, France, 2004.3/29 p.196*
4. Schulz, P., 2002, *Vizuális kommunikáció. Színek a grafikai iparban, Papír-Press Egyesülés, Budapest*
5. www.sericol.hu
6. www.schmidt-thyner.ch
7. www.brucelindbloom.com
8. www.knt.vein.hu



The print of the double picture and INFRAREDESIGN in the space of the security graphics

Ivana Žiljak[1], Klaudio Pap[1], Jana Žiljak Vujić[2]

[1]Faculty of Graphic Arts
Getaldićeva 2, HR-10000 Zagreb, Croatia
E-mails: ivana.ziljak@vip.hr, klaudio.pap@zg.t-com.hr

[2] Polytechnic of Informatics and Design
Vrbik 8, HR-10000 Zagreb, Croatia
E-mail: janazv@tvz.hr

Abstract

The development of printing graphics with two images of which one is observed under IR light and the other in daylight is becoming a reality in graphic product protection [Žiljak V., Pap K., Žiljak I., 2008]. If we look back into history, up till now there have been two methods for producing double images: on basis of the lenticular method or with the help of holography. Both of the methods require a carrier with specific characteristics in respect to micro lens use or a highly embossed master on special material. In comparison with the mentioned methods infrared graphics are not limited with dimension characteristics. Infrared design is a method independent of material, and all kinds of paper may be used, even silk and textile. In the same way that holograms require specific conditions such as (monochromatic) light sources, infrared design recognizes two images in two different wavelength areas. For instance, any video camera today has the possibility of using the IR area along with the daylight area owing to CCD technology development. This is why the INFRAREDESIGN method can be checked easily, introduced into production and set as the simplest printing method in the graphic securities area.

Keywords: Security, infrared, steganography, printing

1. Introduction

The paper shows the algorithm as the basis for obtaining an image with an unlimited tone number in one and the same print. The previously published double separation method [Žiljak I., Žiljak-Vujić J., Pap K., 2008] is extended to abstract images created on basis of algorithms as the carrier of information hiding in the double DL/IR (daylight/infrared) image. Research results are presented that include the factor of our eye sensitivity when there is an enormous number of saturated pixels in the print where individual borderl separation conditions have been applied for each. Conventional separation is based on color setting specific for each printing ink type, paper type and printing techniques. The procedure of translation into CMYK is carried out for the RGB image according to set parameters of the UCR, GCR and UCA methods that apply to all pixels equally. Only one value of carbon K black intensity is determined for each color tone on basis of an internal algorithm program that carries out separation and for this value are calculated values of CMY tones [Žiljak I., Pap K., Žiljak V., 2008]. If compared with existing conventional methods the difference in CMYKIR separation is that a whole range of K values is used for each color tone because K is determined from the outside.

2. Methods

The basic method uses two entry input images, each with extra information: one for observing in daylight and the other for IR light. In further software development a solution was included that enables to include more images controlling the IR image selectively for certain wavelength areas. The interesting areas are image selections appearing only in near IR wavelengths ranging from 600 to 750 nm and disappearing in the remaining wavelengths.

Application is vast if taken into account that scanner and photo techniques most often used in counterfeiting have been developed for producing good quality images in detection area ranging from 400 to 700 nm. The

INFRAREDESIGN method has offered a large number of approaches to individualization. The method is shown for generating one's own algorithm of a randomly generated image through congruency. This is why discussion is held for different types of merging three graphic types: pixel graphics, vector graphics and algorithm graphics [Žiljak I., Pap K., Žiljak-Vujić J., 2008]. The last listed type is becoming the most important one in designs for security graphics, especially due to the fact that it is generated in the process of image exporting for printing. Many parameters for individualized solutions may be added through this „algorithm graphics".

As announced previously, INFRAREDESIGN is incorporated into all printing techniques. Therefore, it is necessary to set up color settings for many types of inks and materials. In this part we are demonstrating color setting differences through four opposite applications starting from newspaper printing to digital printing for one and the same color tone. Application of CMYKIR separation is subject to the color setting used here and shown grading appearing infrared image for one color V1 (Fig. 1).

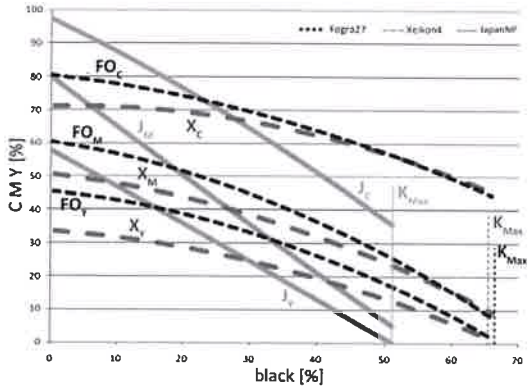

Figure 1: Dark green color in different color setting separations for the color V_1

We set the formality of the description of the colour's ton and formality of the separation with intention to set the double picture: DL (daylight) and IR (infared) graphics.

The tone of the same hue of color in the visibility (V) of human eye (not dependent on color setting) is:

$$V=\begin{bmatrix} R & H^0 & L \\ G & S\% & a \\ B & B\% & b \end{bmatrix} \tag{1}$$

with values

$$V_1=\begin{bmatrix} 83 & 211^0 & 41 \\ 100 & 28\% & -6 \\ 115 & 45\% & -13 \end{bmatrix}. \tag{2}$$

Graph in Figure 1 shows color tone V1 through dependence CMY components of process black ink for the different printing techniques and custom colors and that corresponds to the IR image under 1000 nm. Maximum values of K_{max}, and thus the IR image, are different for each color setting. These values are:

$$X_{max}^{colorsetting}=\begin{bmatrix} C \\ M \\ Y \\ K\ max \end{bmatrix};\ X_{max}^{JapanNP}=\begin{bmatrix} 36 \\ 5 \\ 0 \\ 51 \end{bmatrix};\ X_{max}^{Fogra27}=\begin{bmatrix} 43 \\ 7 \\ 0 \\ 66 \end{bmatrix};\ X_{max}^{Xeikon32}=\begin{bmatrix} 44 \\ 9 \\ 0 \\ 66 \end{bmatrix} \tag{3}$$

For color tone V1, CMY values for K = 0 are:

$$X_0^{colorsetting}=\begin{bmatrix} C_0 \\ M_0 \\ Y_0 \end{bmatrix};\ X_0^{JapanNP}=\begin{bmatrix} 97 \\ 80 \\ 58 \end{bmatrix};\ X_0^{Fogra27}=\begin{bmatrix} 80 \\ 60 \\ 45 \end{bmatrix};\ X_0^{Xeikon32}=\begin{bmatrix} 72 \\ 50 \\ 33 \end{bmatrix}. \tag{4}$$

If the value of CMY depending on replacing the K is defined through the second degree polynomial:

$$X = X_0 - E^* \begin{bmatrix} K \\ K^2 \end{bmatrix} \quad (5)$$

then values of matrix E, for each color setting that is considered in this work are:

$$E^{JapanNP} = \begin{bmatrix} 0.9336 & 0.00548 \\ 1.4873 & 0.00 \\ 1.0624 & 0.0013 \end{bmatrix}; \quad (6)$$

$$E^{Fogra27} = \begin{bmatrix} 0.2048 & 0.00517 \\ 0.2894 & 0.00769 \\ 0.1990 & 0.00711 \end{bmatrix}; \quad (7)$$

$$E^{Xeikon32} = \begin{bmatrix} -0.0489 & 0.00669 \\ 0.22346 & 0.00609 \\ 0.13877 & 0.00538 \end{bmatrix}; \quad (8)$$

It is demonstrated that newspaper's print has a steep down fall in applying the switching of black with other printing inks, and this is comprehensible due because efforts are made to save ink use in respect to quantity. The Fogra27 system has mean values whereas digital printing is quite extravagant in color layering. Shown is a comparison in order to support claims about the necessity of measuring and determining color settings for each new application. Systems JapanNP and Fogra27 can be checked in Adobe Photoshop, because the color settings are in the standard set. Print on Xeikon, inkjet devices, Xerox and special security printing techniques, must be calculated. Measurements are possible but also necessary if you want to apply INFRAREDESIGN as a method of protection in the targeted print technique. Double image is defined with very strict demand: in daylight is visible only one image. Also, under the IR light can be seen only the second image.

3. Results of Infraredesign Steganography for X4-Xeikon32 colorsetting

Relations for the color defined by matrix V_1 and matrices $X_0^{Xeikon32}$ i $E^{Xeikon32}$, have been set in the PostScript for infraredesign steganography for X4-Xeikon32 colorsetting as follows:

/K 66 def % K maximum
/C {K K mul 0.00669 mul neg K 0.04893 mul add 70.9399 add} def
/M {K K mul 0.00609 mul neg K 0.22346 neg mul add 49.94981 add} def
/Y {K K mul 0.00538 mul neg K 0.13877 neg mul add 32.9671 add} def
/boja {C 100 div M 100 div Y 100 div K 100 div setcmykcolor} def

Parameters for C, M and Y relations have been set by the multipolar regression analyses including 18 points. Experimental security graphics and their intepretations have been performed with infrared light filters from 570 do 1000 nm (Fig. 2). Textual messages cannot be seen in the light of the visual part of wavelenghts. A steganographic proposal shows various responses by information affected by IR light. In the second part of the picture the word „IARIGAI" appears differently for each letter especially in case of the increase by 10%. The text of the year „2009" has a maximum of black color possible. In case of a tone defined by the relation K_{max} for $K^{Xeikon32}$ it presents tha coverage value of 66%. The top part of the picture shows steganography with four piecies of information: „COMPUTER GRAPHICS CONFERENCE IARIGAI". Respective values of the K channel are 40%, 20%, 55% and 66% coverage, respectively. A share of other CMY colors has been subjected to regressional relations for the tone of the V_1 color.

Colorsettings JapanNewspaper and Fogra27 are well-known and published through the Photoshop programme. Calculated relations enable checking to those who would like to use these colors to make their own four-colored steganographic application. Mutual hiding of two or more graphics has been based on the idea that a print should give the same tone in the visual part of the spectrum for various ways of shares of processing CMYK components. It is very difficult to accomplish it since the human eye recognizes a difference of only 2% variation of a single component from measured values calculated analytically by the regression analysis. Therefore it is not possible to use one relation, one model of dependancy of C,M,Y on K obtained for colorsetting Fogra27, and apply it to

e.g. Euroscale v2Co. Models proposed by this work are square equations. More precise results could be obtained by the higher degree polynom model, although the regression procedures would remain the same. One may pose a question on the analytical relations that would cover the whole spectrum of tones in the visual area. Numerous mathematical expressions have been studied in order to minimize the difference between the measured values and the final analytical relation. So far applied models resulted in opposite results for different color settings.

4. Conclusion

The contribution of this work is definition, the elaboration and application of new method of generating of the double image produced with a one pass printing process with the standard process inks. Dicussion may be expanded on materials: coated, uncoated, paper weight, penetration characteristics for various components of processing inks. The most sensitive issue are additions, especially varnish, in various shares in respective CMYK components. It leads to recognition of a steganographic picture in case when the print is observed under different angle of light. It is also the initial limitation when applying dedicated pigments in hiding micrographic, as a text separation in the digital printing. Numerous areas of marginal tones cannot be carried out with three components only. Newspaper print colors require a black component in the wider area X_0 meaning that it is impossible to obtain an invisible area in the near infrared part of the spectrum. This is the beginning of the discussion on huge and unexplored area of device dependent CMYK in the moment of studying real printing inks. Application of the INFRAREDESIGN method enables a new manner of respective research since they treat a double image, double information as a steganographic task in the printing techniques.

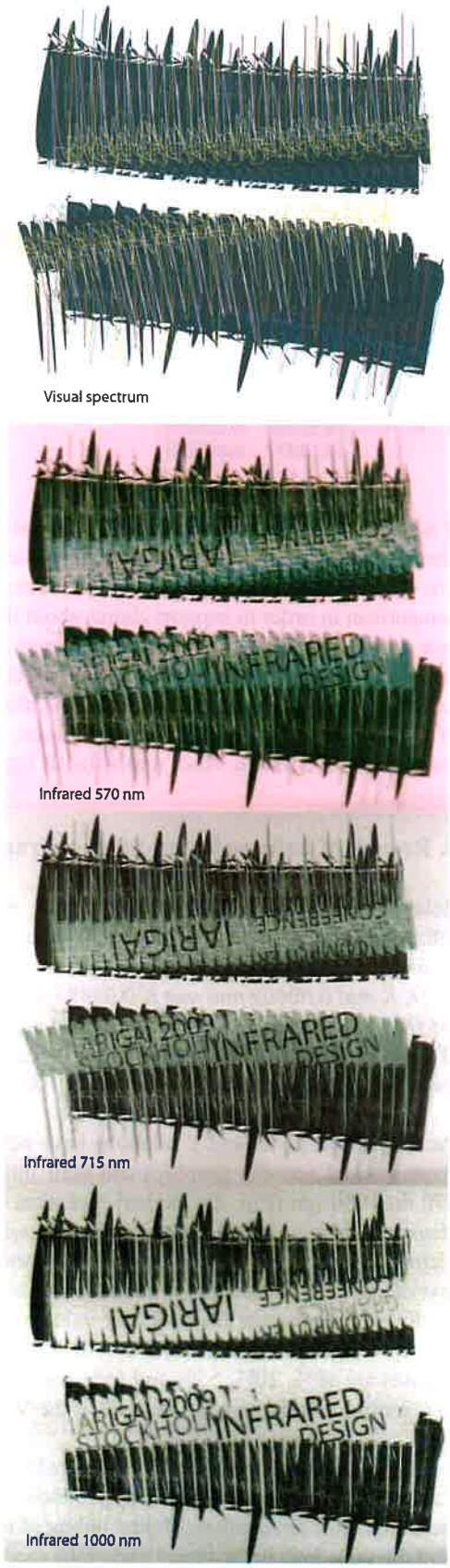

Figure 2:
Security graphic steganography

References

1. Žiljak, V., Pap, K., Žiljak, I. (2008): *CMYKIR security graphics separation in the infrared area Infrared Phyics & Technology (2009), Volume 52, Issues 2-3,* 2009, Pages 62-69
2. Žiljak, I., Žiljak-Vujić, J., Pap, K. (2008): *Colour control with dual separation for Daylight and Daylight / Infrared light, Advances in Printing and Media Technology, Vol. 35, Proceedings of the 35th International Research Conference of Iarigai, 2008,* 273-278 ISBN: 987-3-9812704-0-2
3. Žiljak, I., Pap, K., Žiljak, V. (2008): *Translation of the Infrared into a Visible Area with Double Separation // Proceedings of the 19th Central European Conference on Information and Intelling Systems / Varaždin : Faculty of Organization and Informatics , 2008, 397-400,* ISBN: 978-953-6071-04-3
4. Žiljak, I., Pap, K., Žiljak-Vujić, J. (2008): *Infraredesign, Scientific Book, Fotosoft, Zagreb, Croatia,* ISBN 978-953-7064-08-2

High volume security printing using sheet-fed offset press

Slavtcho Bonev

Epyxs Inc.
Richard-Wagner-Str. 29, D-68165 Mannheim, Germany
E-mail: s.bonev@epyxs.com

Abstract

Security printing based on *DataGrid* and *EpiCode* is a novel, very efficient anti-counterfeiting technique based on the individuality of prints. ***DataGrid*** is a **high-density halftone data storage** which forms a **unique signature** – the so called ***EpiCode*** - when it is printed. The *EpiCode* is caused by the physical interaction between printing medium (ink) and substrate (paper) and is used as a fingerprint for authentication. In sheet-fed offset printing the signature of the printing plate is a novel feature for anti-counterfeit applications.

In the presented printing tests, the influence of the substrate on the *EpiCode* and the long-term stability of the offset printing process regarding the plate signature are determined using biometrical analysis. Equal error rates (EER) better than 10^{-40} are achieved in the case of four paper grades commonly used for labels and packaging. Further, the printing plate signature has proven a stabile feature for a cluster of printed *DataGrids* and is therefore called *ClusterCode*. Authentication based on *ClusterCode* achieved equal error rates (EER) better than 10^{-10}. In addition, a recognition system using a reduced database is proposed.

Keywords: security printing, paper substrate, long-term stability, print quality control, biometrical system

1. Introduction

Each *EpiCode* is uniquely linked to a printed *DataGrid* (Figure 1). This individual print signature [Bon, 2008] comprises at least two independent components: (i) a stochastic component from the medium-substrate interaction e.g. microscopic ink smudging on the paper surface and (ii) a stochastic component from the irregularities of the printing plate. It is expected that the surface roughness will have an impact on the first component.

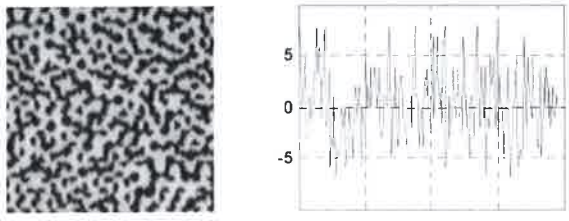

*Figure 1: Matrix code **DataGrid** (a) composed of 14 x 14 graphic symbols and its corresponding fingerprint signal **EpiCode** (b) of 196 samples with an amplitude resolution of 4 bits per sample*

The printing plate will have a systematic impact on the *EpiCodes* in a cluster. A cluster is a batch of *DataGrids* on consecutive printed sheets which originates from the same master *DataGrid* on the printing plate. So the second stochastic component, which presents the printing plate signature, is called *ClusterCode* and is comprehensively analysed here.

Marking product packaging and labels with *DataGrid* is a very effective low-cost approach for anti-counterfeit applications for mass products. The *DataGrid* is simply inserted in the package/label design before printing and carries encrypted information about the protected product and a pointer to a database. In addition the *EpiCode* is extracted from each printed *DataGrid* and is used to identify the corresponding item.

2. Methods

Fingerprint identification is based on two basic premises: (i) persistence: the basic characteristics of fingerprints do not change with time; and (ii) individuality: the fingerprint is unique to an individual [Pan, 2002]. The same assumptions are valid for an iris recognition system using the *IrisCode* [Dau, 1999]. Further, (iii) a reasonable alignment between a template (stored in the database) and the input (which needs to be identified) should be established to ensure a reliable comparison. To identify the genuine, which means to find the best match between input and template, (iv) an exhaustive search in a large data base is necessary.

The technology presented in this paper goes beyond standard fingerprint applications in two aspects. Since the *EpiCode* is adherent to the data, an exact alignment is achieved by the image preprocessing, where the code symbols are detected and used as a coordinate system to realize a repeatable measurement. Secondly, using the process specific property of sheet-fed offset printing, e.g. the systematic influence of the printing plate on the *EpiCode*, the search procedure for identification (one-to-many comparison) could be reduced to a verification (one-to-one comparison).

To analyze the influence of the paper roughness on the *EpiCode*, four different grades of paper (Figure 2) and 3.000 sheets of each paper grade were printed in the same print run. The printing process parameters and the measurement settings, including the used devices and materials, are described in detail in Table I.

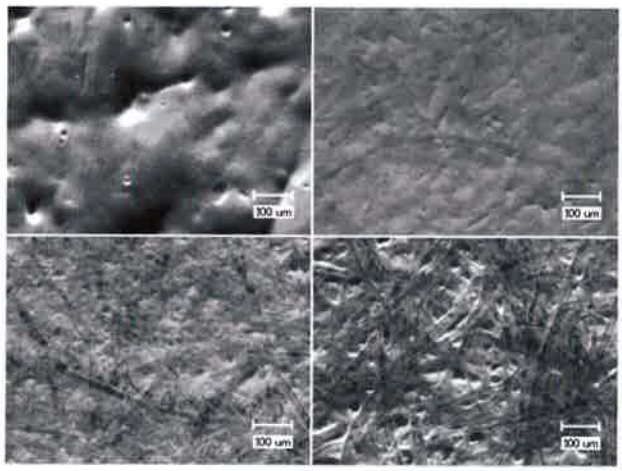

Figure 2: Microscopic images (85x) of the four paper substrates (s. Table I) made with the KEYENCE VHX-600 microscope. The surface structures are evidently different. For example, paper Nr. 2 (b) is a glossy cast-coated paper. A single printed code symbol measures 127 x 127 µm (height x width)

Table I: Detailed description of the printing process and the measurement conditions

Device/Material	Model	Comments
Platesetter	AGFA Xcalibur VLF	2400 dpi physical printing resolution, Computer-to-Plate
Printing plate	AGFA Thermostar P970	830 nm sensitive plate
Offset press	MAN ROLAND 506 LV	Six colours offset press
Printing ink	Printcom S112Y	Black fast drying ink
Coating	Printcom S204U	Dispersion coating, water based varnish
Printing unit	-	Last printing unit, no overrolling, no drying
Matrix code	DataGrid	30 x 30 graphic symbols, 3.8 x 3.8 mm (height x width)
Flatbed scanner	HP scanjet 8200	2400 dpi scan resolution is used (4800 dpi optical resolution)
Paper grades (Substrates)	Nr. 1: Twin Coat Nr. 2: ZANDERS Mega gloss Nr. 3: Niklaselect (Bekk 1200) Nr. 4: Niklakett Brilliant (4000)	Long grain, 50 x 70 cm, 350 g/m², 0.46 mm, 3000 sheets Long grain, 52 x 74 cm, 150 g/m², 0.13 mm, 3000 sheets Short grain, 52 x 74 cm, 80 g/m², 0.07 mm, 3000 sheets Short grain, 52 x 74 cm, 80 g/m², 0.07 mm, 3000 sheets

To estimate the discriminatory power of the *EpiCode* a biometrical analysis of the results is performed [Bon, 2008]. As a result of a comparisson of two different *EpiCodes*, one from the reference set (database) and one from the authentication set (probe), the cross correlation coefficient is evaluated. The higher the coefficient, the higher is the similarity between both *EpiCodes*. All possible comparisons are performed and the correlation coefficients are depicted in a histogram. Gaussian distributions are fitted to the measurements and FAR (false acceptance rate) and FRR (false rejection rate) are calculated for defined thresholds of discrimination. Finally, the EER (equal error rate) achieved is presented in a ROC (reciever operating characteristic) diagram.

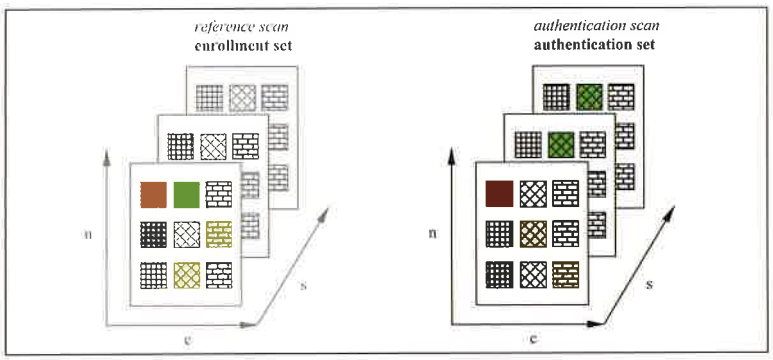

Figure 3: Experimental concept: n - code number (N = 8), c - code info (C = 8), s - sheet number (S = 8)

Short description of the constellation of comparisons in relation to the color coding is given below:
yellow: codes with different information - different plate region resp. location on sheet (*false matches*),
blue: codes with identical information - different plate region resp. location on sheet (*copies*),
green: codes with identical information - same plate region resp. location on sheet (*copies in cluster*),
red: same code - identical information, same plate region resp. location on sheet (*originals*).

3. Results

Two paper grades, Twin Coat and ZANDERS Mega gloss, are analysed and the results are presented in Figure 4. The copies in a cluster, printed by the same region of the printing plate, show high correlation values. This subset of copies contains obviously the printing plate signature which causes a systematic influence on the fingerprint signal (of the subset) called *ClusterCode*. Since only the paper substrate is changing during the printing, the influence of the paper roughness can also be validated. The stochastic influence of the substrate surface will try to reduce the correlation coefficient. Therefore the glossy paper shows higher mean value of the cluster distribution.

The recognition performances (EER) are estimated regarding *EpiCode* (print signature, red colored distribution) and *ClusterCode* (plate signature, green colored distibution) and are presented in Figure 5. As a reference, the distribution of results for printed copies (blue colored) is considered.

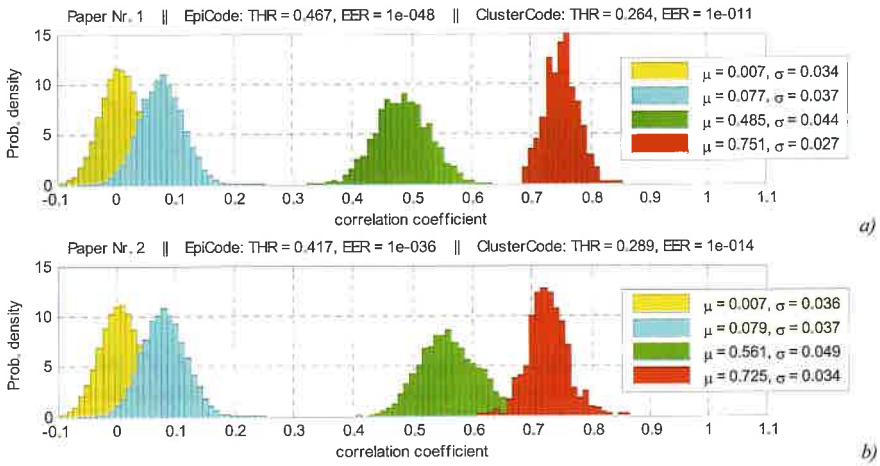

Figure 4: Results of the measurements of 8 consecutive sheets (512 EpiCodes) for paper substrates Twin Coat (a) and ZANDERS Mega gloss (b). A significant differencebetween both ClusterCodes can be observed. The EpiCode is a 900-element vector with an amplitude resolution of 4 bits per element

Using high-quality printing processes, as the experiment shows, recognition performances of around 10^{-40} using *EpiCode* and around 10^{-10} using *ClusterCode* are practically achieved.

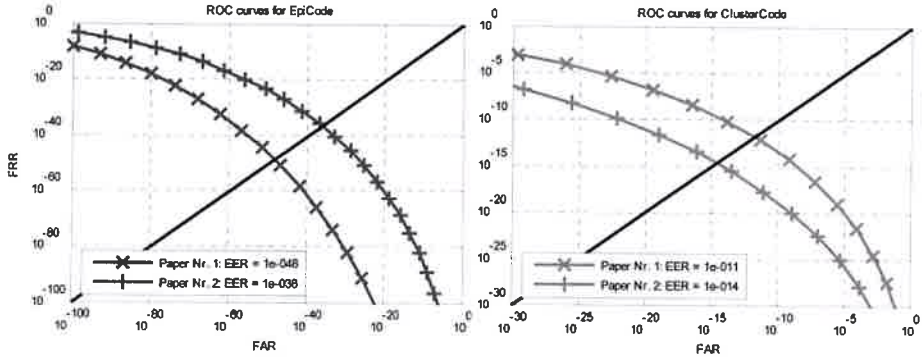

Figure 5: Estimated EER (equal error rates) using EpiCode (print signature) and ClusterCode (plate signature)

The amplitude resolution of the *EpiCode* is reduced from 4 bits/sample (optimum) to 1 bit/sample (minimum) to simulate worst-case conditions caused e.g. by defocused scan and to estimate the minimal recognition performance (Table II). This is also important if the size of the database has to be reduced to the minimum for a certain reason, for instance, improvement of storage space or search time. The corresponding EER decrease from ~10^{-40} to ~10^{-20} for *EpiCode* and from ~10^{-10} to ~10^{-6} for *ClusterCode*.

Table II: Estimated recognition performance using the printing process described in Table I

Nr.	Paper grade	Threshold / EER 4-bit EpiCode	Threshold / EER 1-bit EpiCode	Threshold / EER 4-bit ClusterCode	Threshold / EER 1-bit ClusterCode
1	Twin Coat	0.467 / 1e-048	0.315 / 1e-025	0.264 / 1e-011	0.183 / 1e-006
2	ZANDERS Mega gloss	0.417 / 1e-046	0.280 / 1e-019	**0.289 / 1e-014**	**0.202 / 1e-008**
3	Niklaselect	**0.484 / 1e-059**	**0.319 / 1e-028**	0.261 / 1e-013	0.180 / 1e-007
4	Niklakett Brilliant	0.460 / 1e-048	0.306 / 1e-025	0.256 / 1e-012	0.174 / 1e-007

The paper grade with the best behaviour regarding the *ClusterCode* (Figure 4b) is selected for the analysis of the long-term stability of the printing process and its impact on the recognition performance. A stable process would produce a constant *ClusterCode* over the whole printing cycle. For each thousand sheets a probe of four sheets is analysed (Figure 6). The cross correlation coefficients of all *EpiCodes* are compared; the distributions of results were taken into account. The measurement confirms the stability of the plate signature over 3.000 printed sheets for the high-quality printing process. An example of a low-quality printing process is given below.

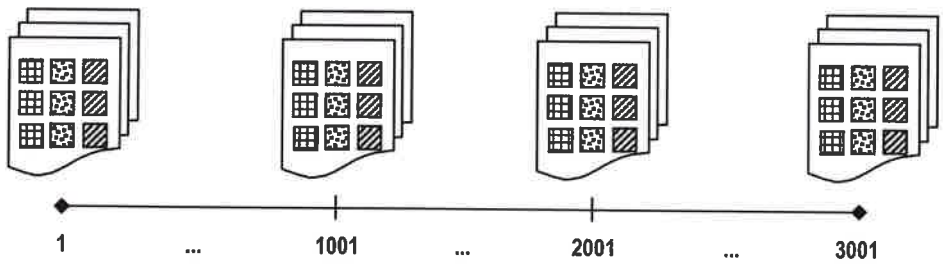

Figure 6: Constellation of the sheet sampling in the long-term stability test: A stack of 3.000 sheets is printed. After each 1.000 prints 4 sheets are extracted to measure the long-term stability of the ClusterCode

Though the *ClusterCode* remains stable over 3.000 sheets, certain decrease in EER can be observed (Figure 7). Due to slight changes of some parameters during the printing, deviations in the plate fingerprint signal occur. This is a slow process which has no impact on the *ClusterCode* measured on consecutive sheets.

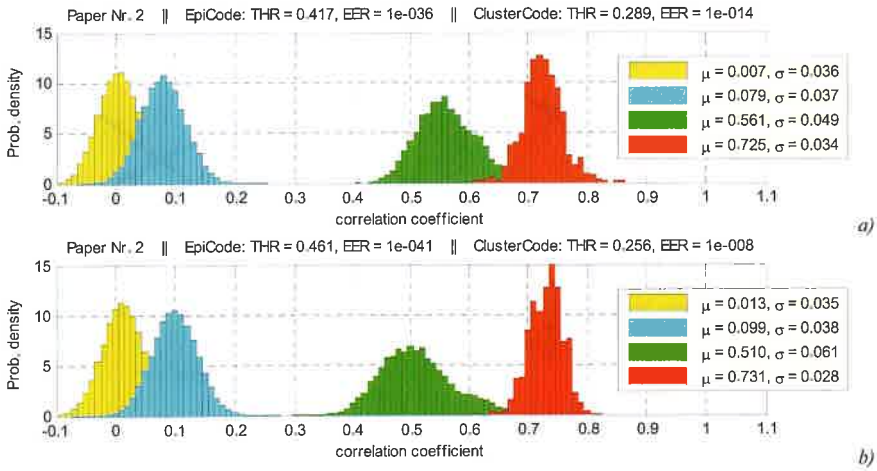

Figure 7: Long-term stability test for sheet-fed offset print on the substrate ZANDERS Mega gloss (Paper Nr. 2): Comparison of the measurements on 8 consecutive sheets (a, 512 EpiCodes) and 3000 sheets (b, 1024 EpiCodes). A slight offset and widening of the distribution of results for ClusterCode (b) can be observed due to process deviations over 3000 sheets. The ClusterCode remains stable, the EER decreases from 10^{-14} to 10^{-8}

To understand the difference between low-quality and high-quality printing processes regarding security applications, the behaviour of a quality parameter is shown in Figure 7. The quality parameter is defined according to the theory of digital communications and is a measure of the code symbol transmission quality. Its value is calculated before decoding and can also be used directly for print quality control. For critical values of the quality parameter below 2.0 the printed code is considered as non-readable and an automatic identification of the *DataGrid* is impossible.

The high-quality printing process is realized in the experimental print run described in Table I. The low-quality process is realized in an industrial print run using standard paper and ink. At each thousand printed sheets one is extracted for control measurement. Nearly 20.000 sheets are printed with 12 *DataGrids* per sheet (15 sheets measured), the high-quality process is represented with 64 *DataGrids* per sheet and only 3000 sheets (4 sheets measured). The distribution of results for the copies in a cluster, which is not presented here, shows extremely high standard deviation for the low-quality process. Generally, significant differences in mean value and standard deviation can be observed. According to this, the low-quality process will produce non-readable codes especially at the end of the print run, where the standard deviation increases visibly. This clearly shows, that not all printing processes are capable for security printing designed for the usage of automatic authentication algotrithms.

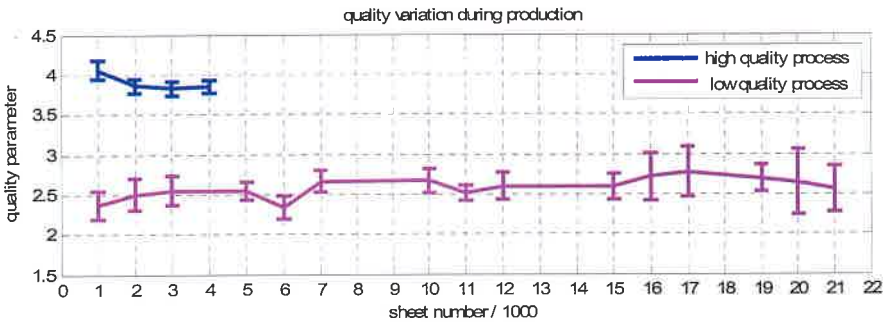

Figure 7: Comparison between estimated values of the quality paramater for high quality and low quality printing processes. The error plots show a mean value / standard deviation of 3.9 / 0.1 and 2.6 / 0.2 for the high and low quality processes, respectively. DataGrid codes with a quality parameter lower than 2.0 cannot be read due to failures in the forward error correction (FEC) algorithm

A strong decrease of the recognition performance for the low-quality process is confirmed for both recognition approaches (Figure 8). Due to the small EER for *ClusterCode* and the produced defect *DataGrids*, security

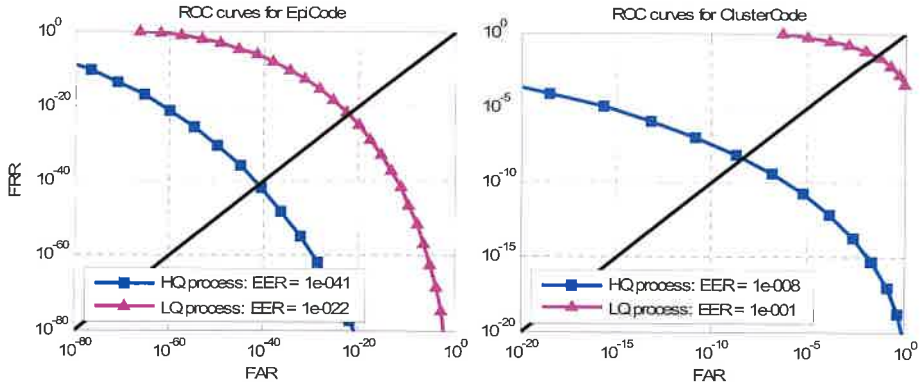

Figure 8: Comparison between estimated EER for high quality (HQ) and low quality (LQ) printing processes

4. Discussion

The quantitative comparison of the individual code properties shows a clear dependance between paper surface structure and the achieved EER. Rough paper surface will have negative impact on the *ClusterCode* and a low impact on the *EpiCode*. For a glossy paper printed with fast drying ink it could be shown, that the *ClusterCode* remains stable during thousands of prints when a high-quality process is used. Nevertheless using the introduced quality parameter, quality control can be performed on item level, also by using images from conventional print quality control devices. The long-term stability of the *ClusterCode* could be confirmed. A further investigation of the long-term behaviour over a complete production run must be done since it is known that properly developed (post-baked) printing plates may exceed run lengths of a million impressions [Wik, 2008].

The reliable detection of the plate fingerprint in printed *DataGrid* codes (*ClusterCode* approach) can be used for a new kind of security applications based on identification of original prints using reduced databases as show in Figure 9. Using scans of all printed copies on a single sheet, all product packages produced in a print run can be identified. Scanning more sheets will lead to an increase of the size of the database, but also to an increase of the authentication performance of the recognition approach.

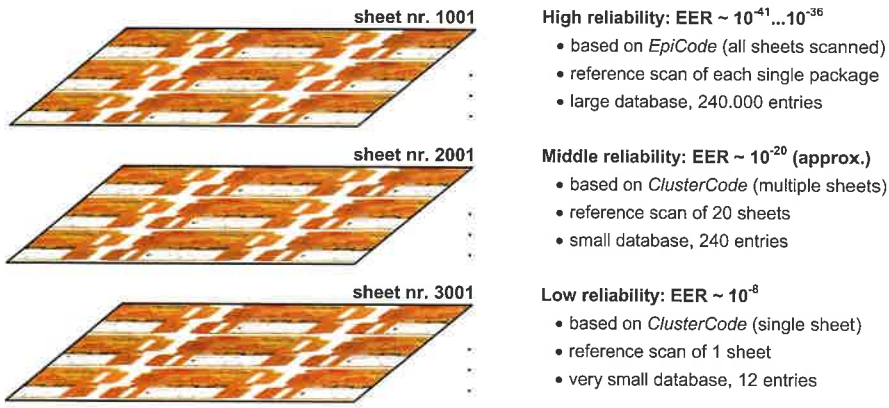

Figure 9: Principal of multilevel-security printing, based on DataGrid, for a standard print run with 20.000 printed sheets and 12 copies per sheet (240.000 product packages)

5. Conclussions and future prospects

Using the unique printing plate signature *ClusterCode* the feasibility of a novel security application has been shown. Printing processes with a long-term stability regarding to the *ClusterCode* should be identified by appropriate measurements. Industrial printing field tests will include the use of several sheet-fed offset presses with (high-durability) post-baked printing plates. Recently, new approaches for a simplified database search are implemented and tested.

Further developments are running to combine the advantages of standard mobile coding technologies with the multilevel security options of the *DataGrid* code (Mal, 2009). An example is given in Figure 10 by bicolor *DataGrids* with *DataMatrix* code for mobile applications implemented as a color overlay.

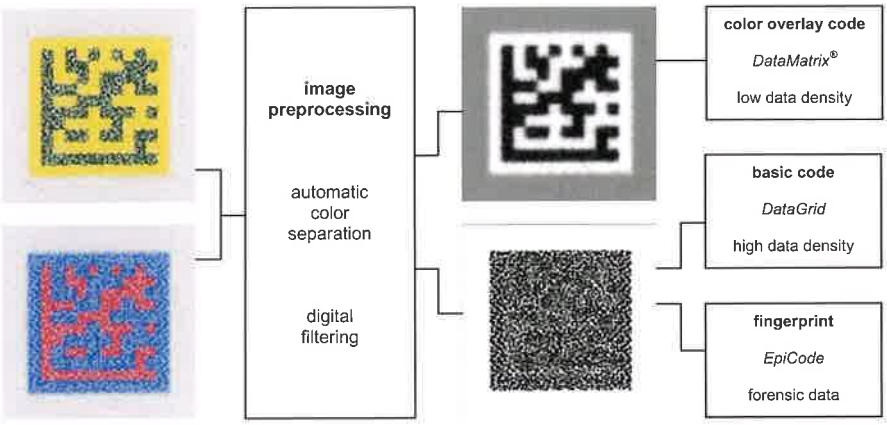

Figure 10: Bicolor DataGrids in yellow-black and cyan-magenta with implemented DataMatrix code

Acknowledgements

We gratefully acknowledge the financial support by the Federal Ministry of Education and Research of Germany (FKZ 02PU1150, OPUR project, www.opur-secure.de). We acknowledge the support of Mr. Rainer Gebhardt and Mr. Markus Jung-Diefenbach from manroland AG for performing the high-quality printing tests and providing specific information about the research. Many thanks to Mr. Thomas Buss from GEWA Etiketten GmbH for supervising the industrial field test.

References

1. Bonev, S. and Wirnitzer, B., 2008, *Security printing for product packaging in industrial printing applications*, Advances in Printing and Media Technology, 35*th* International Research Conference of IARIGAI
2. Pankanti, S., Prabhakar, S. and Jain, A. K., 2002, *On the individuality of fingerprints, IEEE Transactions on Pattern Analysis and Machine Intelligence,* 24, 8, *1010-1025*
3. Daugman, J., 1999 "Recognizing Persons by Their Iris Patterns", in Biometrics: Personal Identification in Networked Society, Jain, A. K., Bolle, R., and Pankanti, S., editors, Kluwer Academic Publishers
4. Wikipedia, 2008, http://en.wikipedia.org/wiki/Offset_printing
5. Maleshliyski, S., García, F.: Integration of anti-counterfeiting features into conventional 2D barcodes for mobile tagging, 2009, TAGA 61st Technical Conference, 15-18 March, 2009, New Orleans, USA



Index of authors

Andersson, Caisa 301
Arjas-Kauranen, Kirsti 137
Aspler, Joe 239

Bablyuk, Evgeny 315
Bjørn-Andersen, Niels 107
Blayo, Anne 407
Blohm, Erik 247
Böddicker, Alexander 207
Bohlin, Erik 301
Bolanča Mirković, Ivana 53
Bolanča, Zdenka 53
Bollström, Roger 223
Bonev, Slavtcho 449
Bould, David C. 279, 415
Bras, Julien 407

Canet, Christine 295
Cepaite, Asta 125
Chorro, Elisabeth 231
Chovancova-Lovell, Veronika 193
Chung, Robert 155
Claypole, Tim C. 279, 415
Coppel, Ludovic 301

Daneault, Claude 323
Dattner, Michael 161
de Garcia, Vicente 185, 231
Demšar, Valerija 421
Deng, Nina 239
Denneuli, Aurore 407
Dörsam, Edgar 329
Drolet, Francoise 323
Dube, Martin 323

Đorđević, Dejana 179, 273

Edström, Per 301, 373
Eleršič, Kristina 273
Endrédy, Ildikó 435
Enroth, Maria 23

Farenbrukh, Konstantin 315
Fleming, Paul D. 193
Friškovec, Mojca 429

Gane, Patrick A. C. 391
Gerstner, Philip 391
Gethin, David 415
Gilewicz, Natalia 31
Golob, Gorazd 273
Gooran, Sasan 147
Guillot, Bill 193
Gustafsson Coppel, Ludovic 83
Golob, Goraz 209, 429
Green, Phil 405
Gregor-Svetec, Diana 209
Gundlach, Mark 69

Habekost, Martin 383
Hädrich, Thomas 207
Halonen, Raisa 363
Hamel, Jean 239
Hauptman, Nina 421
Hedman, Henrik 147
Hejduk, Jiri 309
Hellén, Erkki K. O. 267
Herzau-Gerhardt, Ulrike 401
Hilscher, Frank 401
Hladnik, Aleš 179
Hoc, Miroslav 287
Hsu, Fred 155
Hübler, Arved 207
Hupp, Heike 329

Inarejos, Jesús 185, 231

Javoršek, Andrej 179
Johansson, Per-Åke 247
Junkar, Ita 273

Kaldalóns, Örn S. 107
Kaplanova, Marie 309
Kehren, Katharina 329
Kihlstedt, Annika 75
Klaman, Marianne 247
Klanjšek Gunde, Marijan 421
Klanjšek Gunde, Marta 429
Knešaurek, Nina 429
Koivumäki, Kaisa 267
Kolseth, Petter 225
Koskinen, Jorma 201
Krokan, Arne 107
Kular, Chris 31
Kulčar, Rahela 429
Kuznetsov, Yuri 345

Laine, Janne 91
Lanat, Luc 225
Leisti, Tuomas 363
Lenz, Reiner 67
Leppänen, Tapio 91
Lindberg, Siv 75, 99
Lindqvist, Ulf 107
Lindström, Annika 99
Lovreček, Mladen 273

Manfred Maciá, Juan Antonio 231
Maček, Marijan 421
Madstedt, Sandra 353
Manfred, Tony 239
Mangin, Patrice 323
Mantler, Heinz 161
Marchante, Elena 231
Marchante, Verónica 231
Martineau, Michel 295
Martínez-Verdú, F. 185, 231
Mozetič, Miran 273
Mueller, Ken 223

Nagel, Henning 401
Namedanian, Mahziar 147
Neuman, Charles 407
Norberg, Ole 373
Nors, Minna 15
Novotny, Erzsébet 435
Nurmi, Olli 91, 113
Nyström, Daniel 337

Oittinen, Pirkko 5, 363
Otero, Susana 185, 231

Pajula, Tiina 15
Panak, Ondrej 309
Pap, Klaudio 445
Parent, Frédéric 239
Passoja, Soile 201
Pauler, Nils 373
Pekarovicova, Alexandra 193
Perales, Esther 185, 231
Persson, Christian 107
Pihkola, Hanna 15
Politis, Anastasios E. 41

Rasmussen, Leif Bloch 107
Rasmussen, Soley 107
Rat, Blaž 61
Riordan, Michael 119
Rodriguez-Giles, Jorge 161
Roozeman, Robert 201

Saari, Juha 223
Sangmule, Sangmeshwar. L 193
Sävborg, Örjan 255
Schadenko, Andrey 345
Schlegel, Gert 207
Seisto, Anu 137
Sharma, Abhay 383
Solli, Martin 67
Sretentseva, Tatiana 217
Ström, Göran 353
Stúr, Elisabeth 125
Sušin, Barbara 429

Thieme, Robert 207
Timchenko, Julia 217
Toivakka, Martti 223
Tsigonias, Marios K. 41

Urban, Peter 161
Urbas, Raša 421

Vigne, Valériane 295
Vlachopoulos, Georgios 279
Vukić, Zvjezdana 53

Wozniak, Günter 207
Wu, Yu Ju 193

Yang, Li 171, 337

Žiljak Vujić, Jana 445
Žiljak, Ivana 445
Žveglič, Maša 421